MESON PHYSICS

BY ROBERT E. MARSHAK

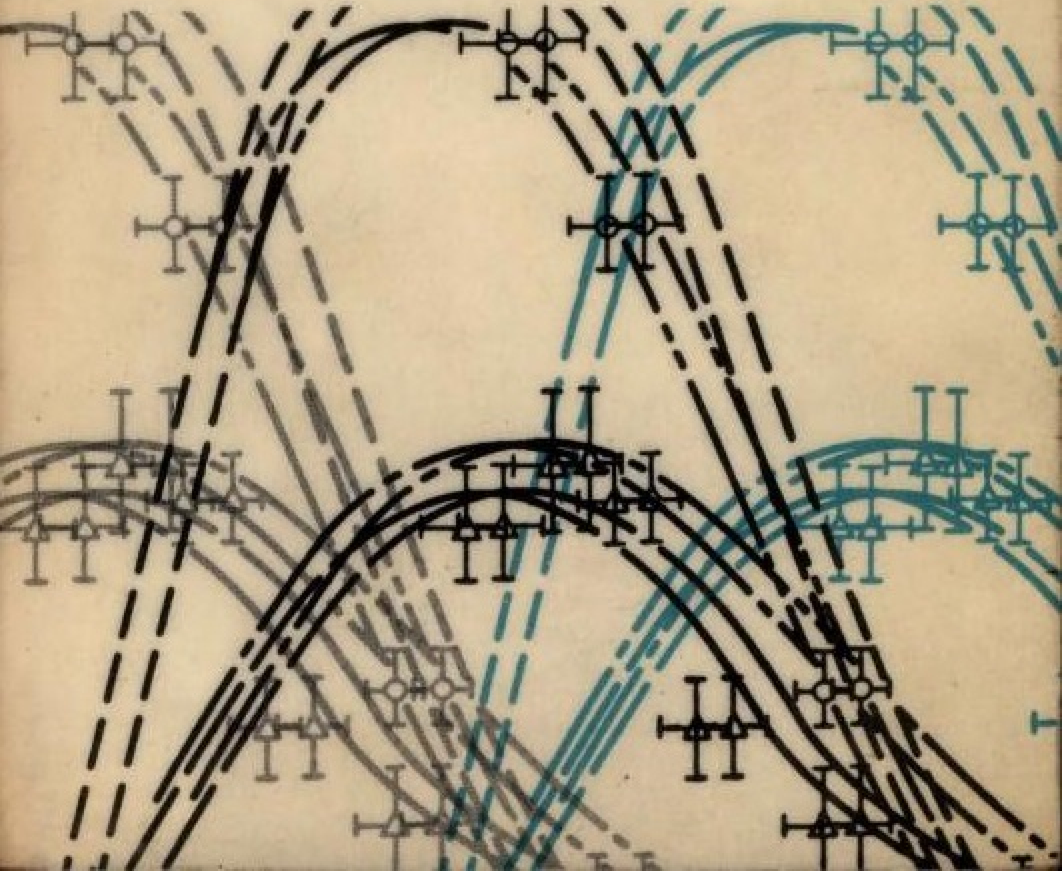

Pure Mathematical Physics

MESON PHYSICS

Robert E. Marshak
University of Rochester

DOVER PUBLICATIONS, INC.
NEW YORK

Copyright © 1952 by Robert E. Marshak

All rights reserved under Pan American and International copyright conventions.

This new Dover edition first published in 1958 is an unabridged and unaltered republication of the first edition. The publisher and author are grateful to the McGraw Hill Book Company for their cooperation in making this inexpensive edition available.

Library of Congress Catalog Card Number: 58-59927

Manufactured in the United States of America

Dover Publications, Inc.
180 Varick Street
New York 14, N. Y.

Pure Mathematical Physics

PREFACE

This volume on meson physics had its inception in a series of lectures delivered on the subject first at the University of Rochester (spring, 1950) and then at Columbia University (summer, 1950). Meson physics has been developing rapidly during the past few years, and the body of experimental knowledge in the field will no doubt grow even more rapidly in the years ahead as new meson-producing accelerators swing into action and as cosmic-ray workers take increasing advantage of the latest experimental techniques. The theoretical situation in meson physics is even less encouraging for book writing: no genuine meson theory exists but only plausible conjectures which occasionally illumine the complexities of the experimental material. Despite these formidable obstacles, the task of surveying the essential results of recent meson experiments with particular emphasis on their theoretical significance has been undertaken for two reasons. First, since the discovery of the π meson in 1947, many indisputable facts concerning π and μ mesons have been established, and these seem worth recording both for their own sake and in order to suggest promising lines of future experimentation. Secondly, by restricting ourselves to real meson processes and omitting consideration of all nuclear phenomena which involve mesons only as virtual transitions (*e.g.*, nuclear forces), we have eliminated the most speculative and least satisfactory predictions of meson theory. The theory of real meson processes, while admittedly plagued by many of the defects of virtual meson theory, nevertheless possesses on the whole a qualitative content which is in surprising accord with experiment. This agreement will have to be explained by the future quantitatively correct theory.

An attempt is made to capture some of the drama of the meson story by a suitable arrangement of chapters. The first four chapters are devoted exclusively to an elucidation of the behavior of charged and neutral π mesons at nonrelativistic nucleon energies, with special attention being given to the accelerator experiments. It is shown how the experiments become increasingly more incisive in their determination of the properties of the π mesons. Chapter 5 is a transition chapter which focuses on the striking contrast between π and μ mesons as regards their ability to interact with nuclei. Chapter 6 elaborates further on this point and on other properties of the μ meson. Chapter 7 returns to the π meson and delineates the boundary of our present knowledge concerning the nuclear interaction of π mesons. Chapter 8 moves on to a discussion of π meson production phenomena at relativistic nucleon energies, still the monopoly of cosmic-ray research, and touches on the fields of speculation outside the domain of single meson theory which are necessitated by the experimental results. Finally, Chap. 9 presents the evidence for new classes of particles and attempts to indicate the further theoretical difficulties which are created by the latest discoveries.

It is hoped that this book will be useful to research workers in meson physics. For this reason, references are given to many of the original papers of the past four years; apologies are offered for unfortunate omismissions. Most of the earlier meson references will be found in Tiomno and Wheeler's Guide to the Literature of Elementary Particle Physics (*American Scientist*, April and July, 1949). It is conceivable that this book may also serve as a primary or secondary text in a course on meson or high-energy physics. To facilitate such use, the theory is sketched in some detail in Chaps. 1 and 2 so that the student becomes acquainted at the start with the characteristic methods and limitations of present-day meson field theory. A course in quantum mechanics and some familiarity with the equivalent contents of Heitler's "Quantum Theory of Radiation" (Oxford University Press, 1947) and the early chapters of Wentzel's "Quantum Theory of Fields" (Interscience Publishers, 1949) are presupposed.

I am deeply grateful to the many graduate students at the University of Rochester whose loyal cooperation made this book possible: to Warren Cheston, Norman Francis, Lionel Goldfarb, and Albert Simon, who wrote up the original lectures on which this book is based and who performed many needed calculations along the way; to Richard Grover and Albert Petschek, who performed computations and drew graphs; and to Albert Messiah, who checked over several chapters. I am also indebted to Marilyn Petschek and John Leone for assistance with the graphs. H. Pierre Noyes was kind enough to read over the entire manuscript in a critical fashion. Finally, I wish to acknowledge with thanks the secretarial help provided by Elizabeth Ahnfeldt, Helen Lewandoski, and Phyllis Perry.

R. E. Marshak

ROCHESTER, N.Y.
JULY, 1952

CONTENTS

Preface v

CHAPTER 1 Single Production of π Mesons in Photon-Nucleon Collisions. 1

1. Introduction 1
2. Kinematics of Single Meson Production in Photon-Nucleon Collisions 3
3. Weak Coupling Theory of Photomesic Production 4
4. Classical Theory of Photomesic Production 21
5. Comparison of Theory with Experiment 27
6. Electron Production of π Mesons 38

CHAPTER 2 Single Production of π Mesons in Nucleon-Nucleon Collisions 41

1. Introduction 41
2. Kinematics of Single Meson Production in Nucleon-Nucleon Collisions 41
3. Weak Coupling Theory of Single π Meson Production in Nucleon-Nucleon Collisions 44
4. Comparison of Theory with Experiment 63

CHAPTER 3 Nuclear Production of Single π Mesons 72

1. Introduction 72
2. Kinematics of Nuclear Production of π Mesons 72
3. Nuclear Effects 77
4. Production of Charged π Mesons in Photon-Nucleus Collisions . 98
5. Production of π° Mesons in Photon-Nucleus Collisions. . . . 107
6. Production of Charged π Mesons in Nucleon-Nucleus Collisions . 109
7. Production of π° Mesons in Nucleon-Nucleus Collisions . . . 119

CHAPTER 4 Properties of π Mesons. 130

1. Introduction 130
2. Masses of the π Mesons 130
3. Decay of the π Mesons 134
4. Spins, Statistics, and Parities of the π Mesons 144

CHAPTER 5 The Capture and Absorption of Slow Negative Mesons 166
1. Introduction 166
2. Capture of Slow Negative Mesons 167
3. Structure of Mesic Atoms 172
4. Nuclear Absorption of Slow π^- Mesons 180
5. Decay and Absorption of Slow μ^- Mesons 191

CHAPTER 6 Properties of the μ Meson. 202
1. Introduction 202
2. Mass of the μ Meson 203
3. Decay of the μ Meson 204
4. Spin of the μ Meson 219
5. Nuclear Interaction of μ Mesons 226

CHAPTER 7 Nuclear Interaction of Fast π Mesons . 236
1. Introduction 236
2. Interaction of π Mesons with Protons 238
3. Interaction of π Mesons with Deuterons. 249
4. Interaction of π Mesons with Heavy Nuclei at Moderate Energies 258
5. Interaction of π Mesons with Heavy Nuclei at High Energies . 268

CHAPTER 8 Production of π Mesons at Relativistic Nucleon Energies 273
1. Introduction 273
2. Theory of Plural Production of π Mesons 276
3. Theories of Multiple Production of π Mesons 282
4. Kinematics of Multiple Meson Production 296
5. Experimental Evidence for Plural Production of π Mesons . . 308
6. Experimental Evidence for Multiple Production of π Mesons . 324
7. Auger Showers 333

CHAPTER 9 New Particles and New Processes . . 337
1. Introduction 337
2. Production and Annihilation of Antinucleons 338
3. Heavy Mesons 344
4. V Particles 351
5. Theoretical Interpretation of the V Particles 359

Name Index. 363

Subject Index 369

CHAPTER 1

SINGLE PRODUCTION OF π MESONS IN PHOTON-NUCLEON COLLISIONS

1. Introduction

We start our discussion of mesons with an analysis of the single production of π mesons in photon-nucleon collisions. The photonic production of π mesons in collisions with nucleons, which is considered in this chapter, is one of two fundamental mechanisms for the production of π mesons, the other being their production in nucleon-nucleon collisions. This second mode of production of π mesons is treated in Chap. 2. Apart from the fact that there exist no experimental results bearing on the production of π mesons in electron-nucleon collisions, it can be shown that the electronic production of π mesons reduces essentially to the case of photonic production; consequently, this possible mechanism for π meson production will be discussed rather briefly in this chapter. The evidence for the production of π mesons in π meson-nucleon collisions (and also in μ meson-nucleon collisions) is also extremely scanty and will therefore only be touched upon in Chaps. 6 and 7. In virtue of the extremely weak coupling of μ mesons to nucleons, it is not expected that μ mesons will be produced directly in photon-nucleon collisions except in the process which is the complete analogue of electron-positron production. The production of $\mu^+ - \mu^-$ pairs in a material with atomic number Z should take place with a cross section $\sim Z^2(e^2/\hbar c)(e^2/m_\mu c^2)^2 \approx Z^2 \times 10^{-32}\ \text{cm}^2$ (down by a factor of $\frac{1}{m_\mu^2}$—m_μ is the μ meson mass—compared with electron-pair production) although no experimental evidence for this process exists up to the present time.[1] We shall see that μ mesons are produced indirectly, as a result of the spontaneous decay of the π meson. Presumably, τ mesons (and possibly other types of mesons—cf. Chap. 9) will be produced in photon-nucleon collisions at sufficiently high energy. However, there are no experiments to support this supposition and the theory should follow immediately from the theoretical considerations presented below.

Although the soft component (γ rays and electrons) of the cosmic radiation certainly produces π mesons, no clear-cut cosmic-ray measurements have been made of the photon production process. Our discussion of the photonic production experiments will therefore be limited to those carried out with the electron accelerators already in existence. Since the highest electron energy (and hence photon energy) thus far attained by artificial means is about 335 Mev, comparison of the experimental results with theory will necessarily be restricted to π meson energies below about 150 Mev. This is no real restriction since the crude theories which have been advanced to explain the photonic meson production can certainly not be trusted at relativistic nucleon energies. Even under the most optimistic assumptions, one can only hope that the qualitative theoretical predictions of weak and strong coupling theory will make sense at nonrelativistic nucleon energies.

---

[1] Cf. Mather, Martinelli, and Jarmie, *Phys. Rev.*, **82**: 973 (1951).

The reasons for discussing the photonic production of π mesons prior to the nucleonic production are at least three in number: (1) the photon-nucleon production mechanism involves only one nucleon and is a first-order process (*i.e.*, the cross section is proportional to g^2 where g is the π meson-nucleon coupling constant) in contrast to nucleon-nucleon production which involves two nucleons and is a third-order process if a consistent field-theoretic viewpoint is adopted. This results in less uncertainty about the magnitudes predicted by the theory of photon-nucleon production. (2) A perturbation calculation of π meson production in nucleon-nucleon collisions requires some assumption concerning the character of the virtual meson field to which the nucleon-nucleon interaction is ascribed. Thus it matters whether it is assumed that π mesons alone are responsible for nuclear forces or whether it is assumed that other meson fields in addition to the π meson field contribute to the nuclear interaction. In lowest order perturbation theory, the photonic production of π mesons only involves the π meson field, and this is a great advantage if higher order corrections can be neglected. (3) The photon is absorbed in the meson production process so that the final state consists of a nucleon and a meson, yielding a simple two-body problem instead of the more complicated three-body problem of nucleonic production. Moreover, in nucleon-nucleon production, the strong interaction of the two nucleons in the final state distorts the high-energy end of the π meson spectrum and thereby obscures the comparison between theory and experiment. For all these reasons, the photonic production experiments should be more amenable to theoretical interpretation than the nucleonic experiments.

In practice, the photonic production experiments are carried out with γ rays produced in a synchrotron or betatron through the impact of the circulating electrons with a high Z material. Consequently, although the electrons are monoenergetic, the γ rays are not, and one must deal with the $d\omega/\omega$ (ω is the energy of the γ ray) spectrum characteristic of bremsstrahlung radiation. This is not so disadvantageous as it appears, since the two-body character of the process enables the experimental results to be expressed in terms of unique photon energies once the energies and angles of emission of the π mesons or recoil nucleons are measured. We shall therefore assume, unless stated otherwise, that we are dealing with monoenergetic photons. Finally, we note that the term π meson includes both charged and neutral π mesons; we shall write π^+, π^-, π^0 to denote the π meson of appropriate charge.

2. Kinematics of Single Meson Production in Photon-Nucleon Collisions

It is useful to start our discussion with a brief review of the kinematics of meson production in a photon-nucleon collision. If a photon of energy ω is incident upon a nucleon of mass M at rest, the kinetic energy T of the photon and nucleon in the center-of-mass system (*i.e.*, the system in which the target nucleon and the incident photon have equal and opposite momenta) is (we set $\hbar = c = 1$ in the kinematical formulas)

$$T = \sqrt{M^2 + 2M\omega} - M \tag{1}$$

At threshold, the kinetic energy of the produced meson with mass μ (the character of the meson is not specified for these kinematical considerations) must be zero so that $T = \mu$. It follows that the threshold photon energy ω_t is

$$\omega_t = \mu\left(1 + \frac{\mu}{2M}\right) \tag{1a}$$

If $\omega > \omega_t$, the meson energy $\bar{\epsilon}$ (including the rest mass) in the center-of-mass system is given by

$$\bar{\epsilon} = \frac{\mu^2 + 2M\omega}{2\sqrt{M^2 + 2M\omega}} \tag{2}$$

The corresponding value of the meson energy ϵ in the laboratory system at an angle θ with respect to the incident photon direction is

$$\epsilon = \bar{\gamma}(\bar{\epsilon} + \bar{\beta}\bar{q}\cos\bar{\theta}) \tag{3}$$

where

$$\bar{\gamma} = \frac{\omega + M}{\sqrt{M^2 + 2M\omega}}, \qquad \bar{\beta} = \frac{\sqrt{\bar{\gamma}^2 - 1}}{\bar{\gamma}}, \qquad \bar{q} = \sqrt{\bar{\epsilon}^2 - \mu^2} \tag{3a}$$

$$\cos\bar{\theta} = \frac{-\bar{\beta}\bar{\epsilon}\bar{\gamma}^2 \sin\theta\tan\theta + \sqrt{\bar{q}^2 - \bar{\beta}^2\mu^2\bar{\gamma}^2\sin^2\theta}}{\bar{q}\cos\theta(1 + \bar{\gamma}^2\tan^2\theta)} \tag{3b}$$

or alternatively

$$\cos\bar{\theta} = \frac{\cos\theta - (\omega/M)[(\omega + M)/(2\omega + M)]\sin^2\theta}{1 + (\omega/M)[\omega/(2\omega + M)]\sin^2\theta} \tag{3c}$$

It can easily be shown that Eqs. (3), (3a), and (3b) lead to the following simple formulas for $\epsilon(0°)$ and ϵ (180°):

$$\epsilon\begin{pmatrix}0^\circ\\180^\circ\end{pmatrix} = \frac{(M+\omega)[M\omega+(\mu^2/2)] \pm M\omega A}{M^2+2M\omega} \tag{3d}$$

where $A = \sqrt{(\omega+\omega')(\omega-\omega_t)}$ and $\omega' = \mu\left(1-\frac{\mu}{2M}\right)$

Note that, if the target nucleon is assumed infinitely heavy ($M \to \infty$), $\bar{\epsilon} = \omega$, $\bar{\gamma} = 1$, $\bar{\beta} = 0$, as is to be expected. In Fig. 1 are plotted graphs for the kinetic energy of the charged π meson in the laboratory system as a function of the angle of emission for values of ω from 200 to 500 Mev; the mass of the charged π meson is taken as $276m_e$ (m_e is the electron mass—cf. Chap. 4).

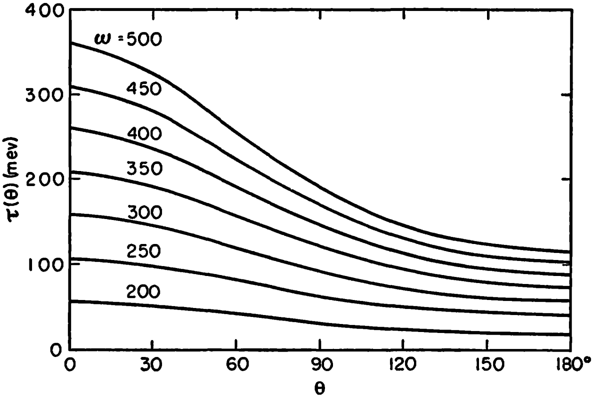

FIG. 1. Kinetic energy $\tau(\theta)$ of the charged π meson in the laboratory system as a function of the angle of emission θ of the meson with respect to the photon beam; ω is the photon energy.

It is also worth recording the relation between the differential cross section $(d\sigma/d\Omega)_{\text{lab}}$ and $(d\sigma/d\Omega)_{\text{c.m.}}$, namely,

$$\left(\frac{d\sigma}{d\Omega}\right)_{\text{lab}} = \frac{M(M+2\omega)[\omega(1+\cos\theta)+M]^2}{[(\omega+M)^2-\omega^2\cos^2\theta]^2}\left(\frac{d\sigma}{d\Omega}\right)_{\text{c.m.}} \tag{4}$$

3. Weak Coupling Theory of Photomesic Production

Before discussing the experiments dealing with the production of π mesons in photon-nucleon collisions, it is illuminating to present the theoretical predictions for the process. Despite the fact that photomesic production is about the simplest meson process which can be calculated, none of the calculations which have been performed until now can really be trusted. There are equally valid reasons for doubting the correctness of both the weak[2] and strong[3] coupling approximations in meson theory, and even the intermediate coupling theory first developed by Tomonaga[4] does not rest on a solid foundation. All these approximations have been used to calculate the cross sections for the photomesic production processes in question.[5] Since almost all the meson processes which will be considered in later chapters have been calculated exclusively in the weak coupling approximation, we shall concentrate on the weak coupling treatment of photomesic production in this chapter. In this fashion, a homogeneous theoretical framework will be provided for the most varied meson phenomena and it will be possible to decide whether weak coupling theory leads to a self-consistent set of *qualitative* predictions and what features must be discarded in the future correct theory. The strong coupling predictions for photomesic production will also be presented briefly to show the similarities and differences between them and the weak coupling predictions.

It is well known that weak coupling theory leads to excellent experimental agreement for electromagnetic radiation processes;[2] it is not at all clear, however, why a similar treatment of meson radiation processes should bear any semblance to reality. The larger size of $g^2/\hbar c$ compared with $e^2/\hbar c$, the dependence of the π meson-nucleon interaction on the spin and isotopic spin of the nucleon, the failure of the higher order meson radiative corrections to converge[6] upon application of the usual methods of charge and mass renormalization—to mention only several differences—make dubious the application of weak coupling theory to meson problems. Nevertheless, for the reasons stated above, we shall present the predictions of weak coupling meson theory and start first with the photomesic production processes.

A weak coupling calculation of photomesic production can be carried out in either of two ways: (1) quantum mechanically as a first-order process in the π meson-nucleon coupling constant or (2) classically, neglecting the reaction of the meson field on the nucleonic source (assumed infinitely heavy). The two methods yield identical results under the same assumptions and we proceed to discuss each in turn; the quantum-mechanical calculation will be presented in this section and the classical in the next.

---

[2] Cf. W. Heitler, "Quantum Theory of Radiation," Oxford University Press, 1947.

[3] Cf. W. Pauli, "Meson Theory of Nuclear Forces," Interscience Publishers, 1946.

[4] Tomonaga, *Prog. Theor. Phys.*, **2**: 6 (1947).

[5] *Weak coupling*: cf. Benoist-Guental, Prentki, and Ratier, *Compt. rend.*, **230**: 1146 (1950); G. Araki, *Prog. Theor. Phys.*, **5**: 507 (1950); K. A. Brueckner, *Phys. Rev.*, **79**: 641 (1950); M. F. Kaplon, *Phys. Rev.*, **83**: 712 (1951). *Strong coupling*: R. Serber, *Univ. Mich. Notes*, 1950; K. Brueckner and K. Case, *Phys. Rev.*, **83**: 1141 (1951); S. D. Drell, *Phys. Rev.*, **83**: 555 (1951); Y. Fujimoto and H. Miyazawa, *Prog. Theor. Phys.*, **5**: 1052 (1950). *Intermediate coupling*: K. Watson and E. Hart, *Phys. Rev.*, **79**: 918 (1950).

[6] The scalar theory (with scalar coupling) and the pseudoscalar theory (with pseudoscalar coupling) can be made to converge through the introduction of ϕ^3 and ϕ^4 terms (ϕ is the meson wave function) into the Hamiltonian [cf. A. Salam, *Phys. Rev.*, **82**: 217 (1951)].

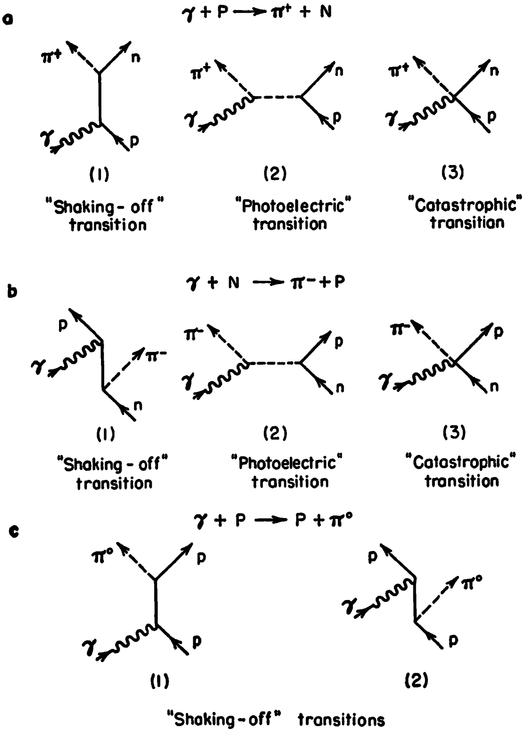
a
γ + P ⟶ π⁺ + N
π⁺
n
γ
p
(1)
"Shaking-off" transition
(2)
"Photoelectric" transition
(3)
"Catastrophic" transition
b
γ + N ⟶ π⁻ + P
p
π⁻
n
(1)
"Shaking-off" transition
(2)
"Photoelectric" transition
(3)
"Catastrophic" transition
c
γ + P ⟶ P + π°
π°
p
(1)
(2)
"Shaking-off" transitions

FIG. 2. Feynman diagrams for the photoproduction of charged and neutral π mesons. (*a*) $\gamma + P \rightarrow N + \pi^+$; (*b*) $\gamma + N \rightarrow P + \pi^-$; (*c*) $\gamma + P \rightarrow P + \pi^0$.

The matrix elements which enter into a weak coupling quantum-mechanical calculation of the cross section for photomesic production may best be classified in terms of the Feynman diagrams.[7] In the Feynman diagrams of Fig. 2, a solid line represents the nucleon (its specific identity indicated by either a *p* for proton or an *n* for neutron), a dotted line represents the π meson, and a wavy line represents the photon. Figures 2*a*, 2*b*, and 2*c* contain the relevant diagrams for the photoproduction of π^+, π^-, and π^0 mesons, respectively, neglecting the anomalous magnetic moments of proton and neutron. In the case of π^+ production, diagram 1 represents the proton absorption of the γ ray and the subsequent emission of the π^+ meson; this transition may be pictured as a "shaking-off" of the meson and is so named. Diagram 2 represents the absorption of the photon by the π^+ meson which is subsequently removed from the nucleon; this transition is called the "photoelectric" transition in analogy to the ordinary photoelectric effect. In Feynman's method, the "photoelectric" transition includes both the meson pair production by the photon with the subsequent absorption of the π^- meson by the proton and the emission of the π^+ meson and the subsequent scattering of the photon by the π^+ meson. Diagram 3 represents the simultaneous absorption of the photon and the emission of the π^+ meson; this transition is called the "catastrophic" transition. The "catastrophic" transition occurs in spin 0 meson theories with derivative couplings and in all spin 1 theories (all spin 1 theories contain derivatives of the meson wave function either implicitly or explicitly). It results from the requirement of gauge invariance for the theory; we shall speak more of this term later.

---

[7] R. P. Feynman, *Phys. Rev.*, **76**: 784 (1949).

Figure 2*b* shows the diagrams which arise in connection with a calculation of π^- production. While the production of π^- mesons in photon-neutron collisions takes place only for bound neutrons, it is useful to present the story for a free neutron since some nuclei, like those of deuterium and beryllium, contain very loosely bound neutrons. Moreover, the cross section for the inverse reaction $\pi^- + P \rightarrow N + \gamma$ can be measured (cf. Chap. 7) and, by detailed balancing, would yield a cross section for the production of π^- mesons in photon-neutron collisions. Two of the three diagrams (the "photoelectric" and "catastrophic" transitions) for π^- production are very similar to the corresponding diagrams for π^+ production. The "shaking-off" transition (diagram 1) is somewhat different since the π^- meson is first emitted by the neutron and the photon subsequently absorbed by the final proton. The "shaking-off" transition contributes appreciably to π^- production, at least in the usual formulation of the theory, whereas it gives a negligible contribution to π^+ production; this is due to the sizable recoil velocity of the proton in the former case. The correct quantitative estimate can be obtained by means of a simple classical argument (cf. Sec. 4).

In the case of π^0 production, neither the "photoelectric" nor the "catastrophic" transition is present because of the neutral charge of the meson. If the neutral meson were to possess spin 1, the presence of an anomalous magnetic moment would lead to a "photoelectric" type of transition. However, since the neutral π meson possesses spin 0 (since it decays into two γ rays, which is strictly forbidden for spin 1—cf. Chap. 4), the possibility of an anomalous magnetic moment is excluded and the only type of transition which can yield π^0 mesons is the "shaking-off" transition. There are now two "shaking-off" diagrams since the π^0 emission may precede the interaction of a photon with the proton or may follow it.

Before writing down the cross sections which result from the Feynman diagrams in Fig. 2, we shall take a closer look at the interaction terms in the total Hamiltonian for nucleon, meson, and photon. The interaction of the electromagnetic field with the proton H_{NR} is given by (we set $\hbar = c = 1$ unless otherwise noted)

$$H_{NR} = \mathbf{j} \cdot \mathbf{A} = -e\psi^*\boldsymbol{\alpha} \cdot \mathbf{A}\psi \tag{5}$$

where $\mathbf{A}$ is the vector potential,[8] $\mathbf{j}$ is the proton current, and $(\psi^*\boldsymbol{\alpha}\psi)$ its Dirac representation (ψ is the Dirac wave function for the proton and $\boldsymbol{\alpha}$ the well-known Dirac operator); as stated above, the interaction of the electromagnetic field with the anomalous magnetic moments of proton and neutron is neglected, an omission which will be rectified later (cf. below). Equation (5) makes it apparent why the "shaking-off" transition gives a negligible contribution to π^+ production whereas it contributes appreciably to π^- production: in π^+ production, the absorbing proton is at rest, whereas in π^- production, the proton has a sizable recoil velocity.

The interaction of the electromagnetic field with the π meson depends on its spin but not on its parity. Since the π meson is a boson (cf. Chap. 4), we consider only the interaction of the electromagnetic field with mesons of integral spin, in particular spin 0 and spin 1 (the theory becomes very complicated for spin values greater than 1). It will actually turn out that the spin of the π meson is 0 (cf. Chap. 4); nevertheless, we present the theoretical predictions for photonic production of spin 1 mesons because comparison of these predictions with the π meson production experiments provides evidence, albeit somewhat less direct than that cited in Chap. 4, against the vector character of the π meson field. Besides, it is possible that spin 1 mesons heavier than the π meson exist and will be observed when sufficiently energetic photon beams are available (cf. Chap. 9). If the meson spin is 0, the interaction H_{MR} is given by

$$H_{MR} = ie\mathbf{A} \cdot (\phi^*\nabla\phi - \phi\nabla\phi^*) \tag{6a}$$

where ϕ is the one-component meson wave function. If the meson spin is 1, H_{MR} is given by

---

[8] The gauge is chosen so that the fourth component of the electromagnetic four-potential is zero.

$$H_{MR} = ie\mathbf{\Gamma}\cdot\mathbf{A} \tag{6b}$$

where $\Gamma = \frac{1}{\mu^2}[\boldsymbol{\chi}(\nabla\cdot\boldsymbol{\chi}^*) - \boldsymbol{\chi}^*(\nabla\cdot\boldsymbol{\chi})] - [\boldsymbol{\phi}\times(\nabla\times\boldsymbol{\phi}^*) - \boldsymbol{\phi}^*\times(\nabla\times\boldsymbol{\phi})]$

and $\boldsymbol{\chi}$ is the canonically conjugate vector to $\boldsymbol{\phi}$, the four-component meson wave function.

The interaction Hamiltonian H_{NM} between meson and nucleon depends not only on the spin of the meson but also on its parity and on the character of its coupling to the nucleon. Thus, since we treat the two possibilities of spin 0 and 1, since the parity may be even or odd, and since, finally, the coupling may or may not involve the derivative of the meson wave function, there are eight possible H_{NM}'s, namely,[9]

$S(S)$: $$H_{NM} = g(\psi^*\beta\psi)\phi \tag{7}$$

$S(V)$: $$H_{NM} = \frac{f}{\mu}(\psi^*\beta\gamma_\nu\psi)(\partial_\nu\phi) \tag{8}$$

$PS(PS)$: $$H_{NM} = g(\psi^*\beta\gamma_5\psi)\phi \tag{9}$$

$PS(PV)$: $$H_{NM} = \frac{f}{\mu}(\psi^*\beta\gamma_5\gamma_\nu\psi)(\partial_\nu\phi) \tag{10}$$

$V(V)$: $$H_{NM} = g(\psi^*\beta\gamma_\nu\psi)\phi_\nu \tag{11}$$

$V(T)$: $$H_{NM} = \frac{f}{\mu}(\psi^*\beta\gamma_\nu\gamma_{\nu'}\psi)\,(\partial_{\nu'}\phi_\nu - \partial_\nu\phi_{\nu'}) \tag{12}$$

$PV(PV)$: $$H_{NM} = g(\psi^*\beta\gamma_5\gamma_\nu\psi)\phi_\nu \tag{13}$$

$PV(DT)$: $$H_{NM} = \frac{f}{\mu}(\psi^*\beta\gamma_5\gamma_\nu\gamma_{\nu'}\psi)\,(\partial_\nu\phi_{\nu'} - \partial_{\nu'}\phi_\nu) \tag{14}$$

In these equations, $S(V)$ is an abbreviation for scalar meson with vector coupling to the nucleon, etc.; the standard notation is employed for the coupling constants where g and f are associated with direct and derivative couplings, respectively. The β and γ operators are the standard Dirac operators[9] and ∂_ν is the four-component derivative; μ is the meson mass.

There is one important effect which has not yet been taken into account. When an electromagnetic field as well as a meson field is involved in a process, an additional term appears in the Hamiltonian for any theory with derivative coupling; this additional term is required by gauge invariance and arises when the ∇ operator is replaced by $(\nabla - e\mathbf{A})$. This "catastrophic" term—as we have called it and which we now label as H_{NMR}—leads to the simultaneous absorption of a photon and the emission of a meson. The $V(V)$ and $PV(PV)$ theories, despite the appearance of expressions (11) and (13), implicitly contain derivative terms which produce "catastrophic" transitions. This follows from the fact that ϕ_4 is a function of the first three components (by virtue of the auxiliary condition)[9] and is actually defined in terms of derivatives of these quantities. This can also be seen from the Feynman notation where the interaction contains an additional term which is a gradient operator.[7]

---

[9] G. Wentzel, "Quantum Theory of Fields," Interscience Publishers, 1949.

We may now classify the various Feynman diagrams shown in Figs. 2*a*, 2*b*, and 2*c* in terms of H_{NR}, H_{MR}, H_{NM}, and H_{NMR}, namely,

"Shaking-off" transition:	$H_{NM}H_{NR}$
"Photoelectric" transition:	$H_{NM}H_{MR}$
"Catastrophic" transition:	H_{NMR}

Both π^+ and π^- production processes involve all three types of transitions, as can be seen from Fig. 2*a* and 2*b*, and therefore all four matrix elements H_{NR}, H_{MR}, H_{NM}, and H_{NMR}. The π^0 production process involves only the "shaking-off" type of transition and therefore only two matrix elements H_{NM} and H_{NR}. In order to obtain a differential cross section, it is necessary to add the matrix elements for the various Feynman diagrams, take the absolute square, and finally evaluate the sums and averages over spins and polarizations in the usual manner. We shall write down the differential cross sections corresponding to the $S(S)$, $PS(PV)$, $V(V)$, $PV(PV)$ theories in lowest order perturbation theory. In this order, the $S(V)$ theory leads to an identically zero cross section, and the $PS(PS)$ theory yields a differential cross section which coincides with that predicted by the $PS(PV)$ theory (provided that the substitution $g = (2M/\mu)f$ is made).[10] The derivative coupling theories for spin 1 mesons lead to differential cross sections which are different from those predicted by direct coupling theories; however, if the cross sections are averaged over the meson polarization (cf. below), the qualitative differences are not very striking, and the derivative coupling predictions are omitted here. The differential cross sections for the remaining theories are, for π^+ production,

$$S(S): \left(\frac{d\sigma^+}{d\Omega}\right)_{\text{lab}} = e^2g^2S(\theta, \omega)\left[\frac{(4M^2 - \mu^2)q^2 \sin^2\theta}{2\omega^2(\epsilon - q\cos\theta)^2} + 1 - \frac{(\epsilon - q\cos\theta)}{M}\right] \tag{15}$$

$PS(PV)$:

$$\left(\frac{d\sigma^+}{d\Omega}\right)_{\text{lab}} = e^2f^2\left(\frac{2M}{\mu}\right)^2 S(\theta, \omega)\left[\frac{-\mu^2q^2\sin^2\theta}{2\omega^2(\epsilon - q\cos\theta)^2} + 1 - \frac{(\epsilon - q\cos\theta)}{M}\right] \tag{16}$$

---

[10] This result is an illustration of the equivalence theorem for the pseudoscalar meson field [cf. K. M. Case, *Phys. Rev.*, **76**: 14 (1949)], which states that to terms of order g^2 (except for processes in which a given nucleon interacts with two mesons or two photons and provided that the integrals are convergent) the $PS(PS)$ theory may be replaced by the $PS(PV)$ theory with a new coupling constant $f = \mu g/2M$.

$$V(V)\colon \left(\frac{d\sigma^+}{d\Omega}\right)_{\text{lab}} = \frac{e^2g^2S(\theta,\omega)}{\omega^2(\epsilon - q\cos\theta)^2}\Bigg[M^2\omega^2 - 3M\omega^2(\epsilon - q\cos\theta) + \frac{15}{4}\omega^2(\epsilon - q\cos\theta)^2 - \frac{\omega^3}{2}(\epsilon - q\cos\theta)^3\left(\frac{4}{M\omega} - \frac{1}{\mu^2}\right) + \frac{q^2\sin^2\theta}{2\mu^2}(\omega^2M^2 - 2\mu^4 - 4M^2\mu^2)\Bigg] \tag{17}$$

$$PV(PV)\colon \left(\frac{d\sigma^+}{d\Omega}\right)_{\text{lab}} = \text{Eq. (17)} + \frac{2e^2g^2S(\theta,\omega)M^2}{\omega^2}\left[\frac{-\omega^2}{\mu^2} + \frac{\omega^3(\epsilon - q\cos\theta)}{\mu^4} + \frac{3q^2\sin^2\theta}{(\epsilon - q\cos\theta)^2}\right] \tag{18}$$

where the notation is the same as in Sec. 2,

$$S(\theta,\omega) = \frac{q}{4M\omega\{M + \omega[1 - (\epsilon/q)\cos\theta)]\}} \tag{19}$$

and all quantities refer to the laboratory system. In deriving Eqs. (17) and (18), the matrix elements have been summed over the directions of polarization of the outgoing mesons. If one examines the matrix elements before carrying out this summation, one finds that, just above threshold, the $V(V)$ theory predicts transversely polarized (with respect to the incident photon direction) mesons whereas the $PV(PV)$ theory predicts longitudinally polarized mesons.[11]

For the $S(S)$ and $PS(PV)$ theories, the differential cross sections for π^- and π^0 production can be very simply expressed in terms of the π^+ cross sections, namely,

$$S(S)\colon \quad \left(\frac{d\sigma^-}{d\Omega}\right)_{\text{lab}} = \left(\frac{2M\omega}{2M\epsilon - \mu^2}\right)^2\left(\frac{d\sigma^+}{d\Omega}\right)_{\text{lab}} \tag{15a}$$

$$PS(PV)\colon \quad \left(\frac{d\sigma^-}{d\Omega}\right)_{\text{lab}} = \left(\frac{2M\omega}{2M\epsilon - \mu^2}\right)^2\left(\frac{d\sigma^+}{d\Omega}\right)_{\text{lab}} \tag{16a}$$

$$S(S)\colon \quad \left(\frac{d\sigma^0}{d\Omega}\right)_{\text{lab}} = \left[\frac{2M(\omega - \epsilon) + \mu^2}{2M\epsilon - \mu^2}\right]^2\left(\frac{g_p}{g}\right)^2\left(\frac{d\sigma^+}{d\Omega}\right)_{\text{lab}} \tag{15b}$$

$$PS(PV)\colon \quad \left(\frac{d\sigma^0}{d\Omega}\right)_{\text{lab}} = \left[\frac{2M(\omega - \epsilon) + \mu^2}{2M\epsilon - \mu^2}\right]^2\left(\frac{f_p}{f}\right)^2\left(\frac{d\sigma^+}{d\Omega}\right)_{\text{lab}} \tag{16b}$$

where g_p and f_p are the π^0 coupling constants to the proton; $d\sigma^0_{S(S)}$ and $d\sigma^0_{PS(PV)}$ are identically zero for the neutron as long as the anomalous magnetic moments are neglected (cf. below). The cross sections for π^- and π^0 production corresponding to the $V(V)$ and $PV(PV)$ theories are not simply related to the π^+ cross sections and they will be omitted here; it should be stated, however, that qualitatively the $V(V)$ cross sections are similar to the $S(S)$ and the $PV(PV)$ to the $PS(PV)$.

---

[11] Cf D. Feer, *Phys. Rev.*, **76**: 306 (1949).

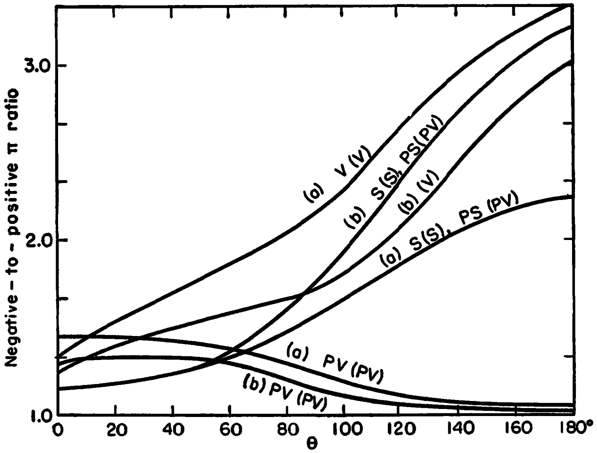

FIG. 3. π^-/π^+ production ratio predicted by the $S(S)$, $PS(PV)$, $V(V)$, and $PV(PV)$ theories as a function of the laboratory angle of emission. Curve (*a*) corresponds to 40-Mev kinetic energy for the emitted meson, (*b*) to 80 Mev.

Equations (15) to (16), (15*a*) to (16*a*), and (15*b*) to (16*b*) show the expected result that the π^- production cross section is always greater than the π^+ cross section for the spin 0 theories (the spin 1 theories lead to the same result); it is interesting to note that at threshold the π^-/π^+ ratio is predicted to be $[(M + \mu)/M]^2$. It is somewhat surprising that the π^-/π^+ ratio is the same for both spin 0 theories since the pseudoscalar theory involves negative energy states for the nucleon whereas the scalar theory does not. It is also not unexpected that the π^0/π^+ ratio is much less than 1 since the "shaking-off" (it is to be recalled that the anomalous magnetic moment has been neglected) transition, which is the only one entering the π^0 calculation, involves the much heavier nucleon in contrast to the "photo-

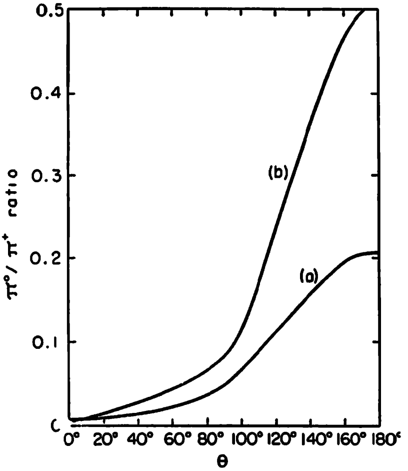

FIG. 4. π^0/π^+ production ratio in hydrogen predicted by the $S(S)$ and $PS(PV)$ theories as a function of the laboratory angle of emission. Anomalous magnetic moment of the proton is neglected and equal masses are assumed for the π^0 and π^+ mesons. Curve (*a*) corresponds to 40 Mev for the emitted meson, (*b*) to 80 Mev.

electric" and "catastrophic" transitions which enter the π^+ calculation. Since experiments are usually performed at a fixed meson energy, we plot in Fig. 3 the π^-/π^+ ratio as a function of the angle of emission (with respect to the incident photon beam) for two values of the charged π meson energy; the predictions of the $V(V)$ and $PV(PV)$ theories, as well as those of the $S(S)$ and $PS(PV)$ theories, are included. Figure 4 contains graphs of the π^0/π^+ ratio for the $S(S)$ and $PS(PV)$ theories at the same two values of the π^0 meson energy. We also give in Fig. 5 plots of $(d\sigma^+/d\Omega)_{\text{lab}}$ for the four theories corresponding to an incident photon energy $\omega = 250$ Mev. Since it will turn out that experiment strongly favors the pseudoscalar field for the π meson (see Chap. 4), we single out the pseudoscalar theory for more detailed consideration and plot in Fig. 6 the $PS(PV)$ predictions for $(d\sigma^+/d\Omega)_{\text{lab}}$ at $\omega = 200$, 250, and 300 Mev, $(d\sigma^+/d\Omega)_{\text{c.m.}}$ at $\omega = 250$ Mev, $(d\sigma^-/d\Omega)_{\text{lab}}$ at $\omega = 250$ Mev, and finally $(d\sigma^0/d\Omega)_{\text{lab}}$ at $\omega = 250$ Mev. We have included the center of mass curve for π^+ production at 250 Mev[12] in order to exhibit the kinematical effects of the forward photon momentum.

The characteristic features of the curves in Fig. 5 and curves (*a*) to (*d*) in Fig. 6 can be made more transparent by considering the limit of infinitely heavy mass for the nucleons. In this limit $\epsilon \to \omega$, the π^-/π^+ ratio becomes identically 1 and the π^0/π^+ ratio becomes identically 0 [*i.e.*, curve (*e*) coincides with curve (*b*) in Fig. 6 and curve (*f*) goes to 0]. However, the π^+ curves are not changed qualitatively and it is interesting to record the analytic expressions appropriate to the extreme nonrelativistic approximation for the nucleons. Setting $M = \infty$, Eqs. (15) to (18) reduce to[13]

$$S(S): \qquad \left(\frac{d\sigma^+}{d\Omega}\right) = \frac{e^2g^2q^3 \sin^2\theta}{2\omega^3(\omega - q\cos\theta)^2} \tag{20}$$

$$PS(PV): \qquad \left(\frac{d\sigma^+}{d\Omega}\right) = \frac{e^2f^2q}{\omega\mu^2}\left[1 - \frac{\mu^2q^2\sin^2\theta}{2\omega^2(\omega - q\cos\theta)^2}\right] \tag{21}$$

$$V(V): \qquad \left(\frac{d\sigma^+}{d\Omega}\right) = \frac{e^2g^2q\{1 + \frac{1}{2}(q^2/\mu^2)\sin^2\theta[1 - (4\mu^2/\omega^2)]\}}{4\omega(\omega - q\cos\theta)^2} \tag{22}$$

$PV(PV)$:

$$\left(\frac{d\sigma^+}{d\Omega}\right) = \text{Eq. (22)} + \frac{e^2g^2}{2\omega^3}\left[-\frac{\omega^2}{\mu^2} + \frac{\omega^3(\omega - q\cos\theta)}{\mu^4} + \frac{3q^2\sin^2\theta}{(\omega - q\cos\theta)^2}\right] \tag{23}$$

It is now clear why, for meson energies below about 100 Mev, the pseudoscalar and pseudovector theories yield essentially isotropic

---

[12] G. Araki [*Phys. Rev.*, **82**: 959 (1951)] has also calculated this curve.

[13] Equations (20) and (21) agree with the results of L. L. Foldy [*Phys. Rev.*, **76**: 372 (1949)].

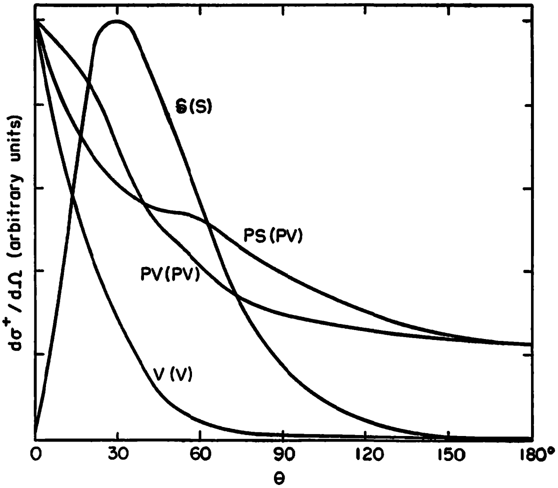

FIG. 5. Differential cross sections in the laboratory system for π^+ production at 250-Mev photon energy predicted by the $S(S)$, $S(PV)$, $V(V)$, and $PV(PV)$ theories; the curves are normalized at their maximum value.

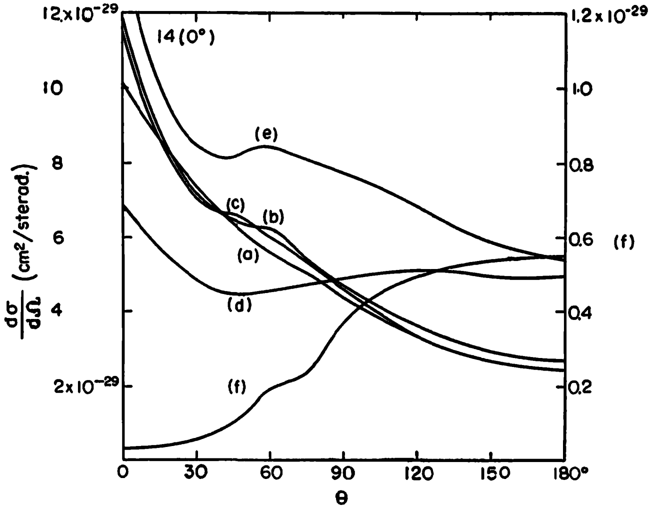

FIG. 6. Differential cross sections for π^+, π^-, and π^0 production predicted by the $PS(PV)$ theory. Curve (*a*) $d\sigma^+/d\Omega$ at $\omega = 200$ Mev, (*b*) $d\sigma^+/d\Omega$ at $\omega = 250$ Mev, (*c*) $d\sigma^+/d\Omega$ at $\omega = 300$ Mev, (*d*) $d\bar{\sigma}^+/d\bar{\Omega}$ at $\omega = 250$ Mev, (*e*) $d\sigma^-/d\Omega$ at $\omega = 250$ Mev, (*f*) $d\sigma^0/d\Omega$ at $\omega = 250$ Mev; the coupling constants are set equal to unity.

angular distributions, the scalar theory predicts a $[\sin^2 \theta/(1 - v \cos \theta)^2]$ distribution (v is the meson velocity), and the vector theory yields a strong forward maximum. The reasons are as follows: in the scalar theory, the chief transition is the "photoelectric" transition which leads to the characteristic dipole behavior, $\sin^2 \theta$; however, the $\sin^2 \theta$ distribution is strongly distorted forward by the term $[1/(1 - v \cos \theta)^2]$ which appears because of the retardation effects in the interaction of the meson charge with the photon. The "shaking-off" transition is unimportant because the proton is at rest and the scalar interaction H_{NM} couples only positive energy states of the nucleon. This can be expressed in another way by saying that, in the scalar theory, the meson cloud extends about the nucleon to distances of the order of the meson Compton wave length $\hbar/\mu c$ and is responsible for the "photoelectric" transition; the circulating currents associated with the magnetic moment of the nucleon are distributed over distances of the order $(\hbar/Mc)$ and therefore contribute in the ratio $(\mu/M)^2$. The scalar theory predicts a q^3 behavior for the differential cross section just above threshold—one q coming from the statistical factor and the other two from H_{MR}, the interaction term which is also responsible for the $\sin^2 \theta$ angular dependence.

In the $PS(PV)$ theory, the "photoelectric" and "shaking-off" transitions still occur but the new "catastrophic" transition is dominant. The relative unimportance of the "photoelectric" transition is due to the close binding of the pseudoscalar meson cloud to the nucleon so that the probability of finding the meson at the meson Compton wave length $\hbar/\mu c$ is small. However, the photon is strongly coupled to the nucleon through the triple term H_{NMR}, and the isotropic behavior and the q dependence of the differential cross section above threshold are explained in an obvious manner. As the photon energy increases, the photon wave length decreases and becomes comparable with the extension of the meson cloud so that deviations from isotropy set in.

The spin 1 theories also lead to very different predictions for the meson angular distribution. The $V(V)$ theory predicts a strong forward maximum whereas the $PV(PV)$ theory predicts a more nearly isotropic angular distribution. In both theories, the "photomagnetic" transition associated with the intrinsic magnetic moment of the meson dominates; because of the q dependence of the matrix element for the photon coupling with the meson magnetic moment, both theories exhibit a rapid increase of cross section with meson momentum above the threshold.

When we come to the total cross sections, it should be stated at once that it is not difficult to derive total cross sections[14] based on the rigorous relativistic differential cross sections [*i.e.*, Eqs. (15) to (18)]; however, the expressions are long and, since weak coupling theory can, at best, be trusted only qualitatively in the nonrelativistic nucleon energy region, we shall not record these expressions.

---

[14] Cf. Benoist-Gueutal, Prentki, and Ratier, *loc. cit.*; and Araki, *loc. cit.*

It is much more straightforward to derive the total cross sections from the approximate differential cross sections (20) to (23); one finds

$$S(S): \quad \sigma^{\pm} = \frac{2\pi e^2 g^2 q}{\omega^3}\left[\frac{\omega}{q}\ln\left|\frac{\omega+q}{\omega-q}\right| - 2\right] \tag{24}$$

$$PS(PV): \quad \sigma^{\pm} = \frac{2\pi e^2 f^2}{\mu^2\omega^3}\left[2q(\omega^2+\mu^2) - \mu^2\omega\ln\left|\frac{\omega+q}{\omega-q}\right|\right] \tag{25}$$

$$V(V): \quad \sigma^{\pm} = \frac{\pi e^2 g^2}{2\mu^2\omega^3}\left[8q\mu^2 + \omega(\omega^2-4\mu^2)\ln\left|\frac{\omega+q}{\omega-q}\right|\right] \tag{26}$$

$$PV(PV): \quad \sigma^{\pm} = \frac{\pi e^2 g^2}{2\mu^2\omega^3}\left[\omega(\omega^2+8\mu^2)\ln\left|\frac{\omega+q}{\omega-q}\right| - 16q\mu^2 + \frac{4\omega^2 q^3}{\mu^2}\right] \tag{27}$$

Equations (24) to (27) are approximately valid (within a factor 2) for $\omega < 400$ Mev and are plotted in Fig. 7 as a function of ω; there is no need to distinguish between π^+ and π^- production. For comparison, the relativistic total π^+ and π^- production cross sections are plotted in Fig. 8 for both the $S(S)$ and $PS(PV)$ theories.

The photomesic cross sections have all been calculated on the assumption that the anomalous magnetic moments of the nucleons may be neglected. Since the π^0/π^+ ratio turns out to be so extremely small even in the relativistic theory (we have already remarked that it is zero in the $M \to \infty$ approximation), one might inquire whether larger π^0 production cross sections will be predicted if the anomalous magnetic moments of the nucleons are taken into account. Kaplon[15] has answered this question in the affirmative, and his calculations are now briefly discussed. It is well known that, in the case of the photodisintegration of the deuteron, the photomagnetic part dominates over the photoelectric part at threshold and that a phenomenological treatment of the interaction of the electromagnetic field with the anomalous magnetic moments of the nucleons provides a correct description of the disintegration process. Similarly, although the interaction of the electromagnetic field with the electric current of the proton yields an extremely small cross section for π^0 production compared with π^+ production (at energies not far from the meson threshold), the photon interaction with the proton's anomalous magnetic moment leads to a π^0 cross section comparable with the π^+ cross section, at least in the $PS(PV)$ theory.

The above conclusion is arrived at by treating the interaction of the

---

[15] Kaplon, *loc. cit.*

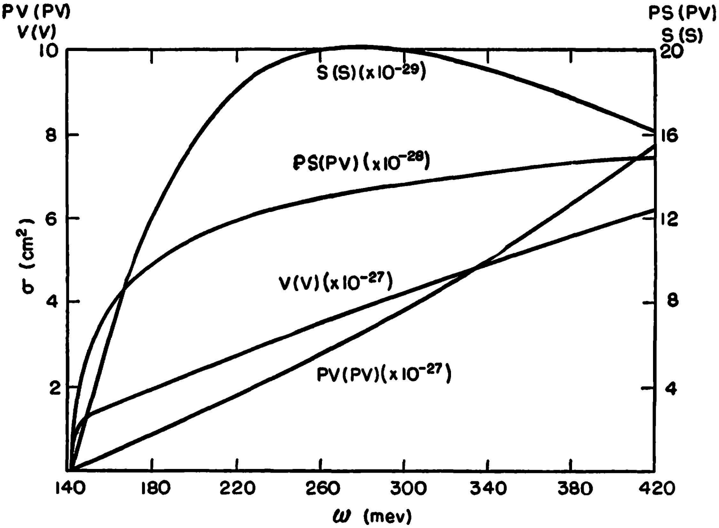

FIG. 7. Total charged π meson production cross sections (in the $M \to \infty$ limit) predicted by the $S(S)$, $PS(PV)$, $V(V)$, and $PV(PV)$ theories; the coupling constants are set equal to unity.

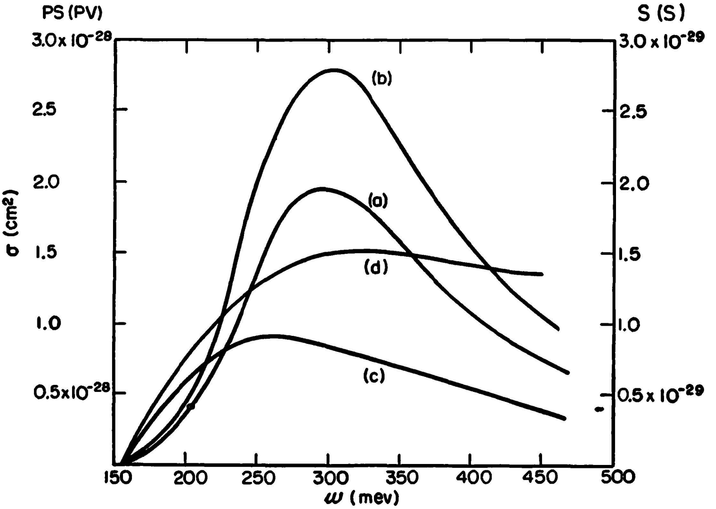

FIG. 8. Rigorous total π^+ and π^- production cross sections predicted by the $S(S)$ and $PS(PV)$ theories. Curve (a) $\sigma^+[S(S)]$; (b) $\sigma^-[S(S)]$; (c) $\sigma^+[PS(PV)]$; (d) $\sigma^-[PS(PV)]$; the coupling constants are set equal to unity.

electromagnetic field with the proton's anomalous magnetic moment as a Pauli-like term in the Hamiltonian [*i.e.*, a term of the form $(\gamma_\nu \gamma_{\nu'} F_{\nu\nu'})$ where $F_{\nu\nu'}$ is the electromagnetic field tensor and γ_ν is the Dirac γ operator] and by assuming that the static value of the anomalous magnetic moment is maintained at photon energies of several hundred Mev. In Fig. 2*c*, the Feynman diagrams can be taken over as indicated except that the Pauli interaction must now be included in the computation of the matrix element of H_{NR}. Kaplon has derived a rigorous relativistic expression for the cross section for π^0 production in photon-proton collisions, including both the electric current and magnetic moment terms in addition to the interference term. He finds that the introduction of the Pauli interaction does not alter the small cross section for π^0 production predicted by the scalar theory; this is due to the fact that the cancellation of the two matrix elements associated with the two Feynman diagrams of Fig. 2*c* is unchanged by the inclusion of the Pauli term as long as the meson field is scalar. In the case of the pseudoscalar meson field, the nucleon spin flips over and the cancellation becomes an addition, with the result that the π^0 production cross section is markedly increased in both the *PS*(*PS*) and *PS*(*PV*) theories (we now distinguish between *PS* and *PV* coupling because the inclusion of the anomalous magnetic moment causes a breakdown of the equivalence theorem between the two types of coupling—cf. above). We shall not record Kaplon's rigorous expressions for the π^0 cross sections but merely the extreme nonrelativistic approximation to his[16] *PS*(*PS*) and *PS*(*PV*) results. In this $M \to \infty$ approximation, only the Pauli moment term contributes (the electric current of the proton vanishes) and one finds

PS(*PS*):

$$\left(\frac{d\sigma^0}{d\Omega}\right) = e^2 g_p^2 \mu_p^2 \left(\frac{\mu}{2M}\right)^2 \frac{q}{M^2\omega}\left[\frac{\omega}{\mu}\left(\frac{\omega}{\mu} - \frac{2q}{\mu}\cos\theta\right) + \frac{1}{2}\left(\frac{q}{\mu}\right)^2 (1 + \cos^2\theta)\right] \tag{28}$$

PS(*PV*):

$$\left(\frac{d\sigma^0}{d\Omega}\right) = e^2 f_p^2 \mu_p^2 \frac{q^3}{2\mu^2 M^2 \omega}(1 + \cos^2\theta) \tag{29}$$

where μ_p is the anomalous magnetic moment of the proton. Figure 9 contains plots of $(d\sigma^0/d\Omega)$ as a function of the angle of emission (with respect to the incident photon beam) for the two pseudoscalar theories at three photon energies; for comparison, Kaplon's rigorous curves for $(d\sigma^0/d\Omega)_{\text{lab}}$ at $\omega = 250$ Mev are given as curves (*a*) and (*b*) in Fig. 10. The total cross sections for π^0 production in photon-proton collisions

---

[16] Strictly speaking, in the $M \to \infty$ limit, the *PS*(*PS*) cross section vanishes; however, we regard the common factor $(\mu g/2M)^2$ as a finite constant.

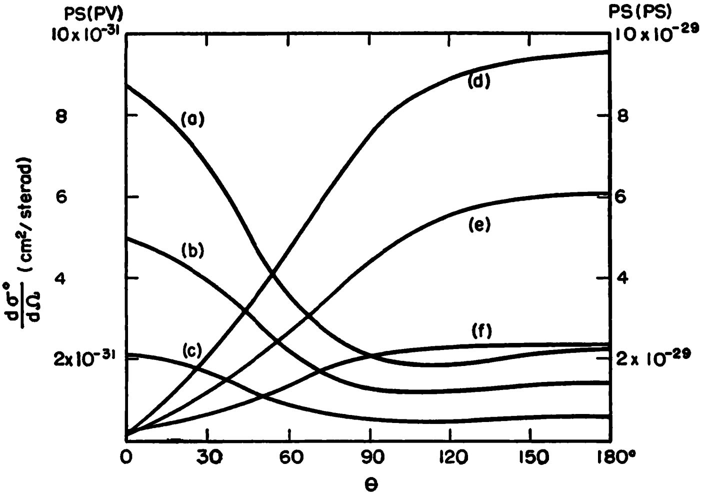

FIG. 9. Nonrelativistic differential π^0 production cross sections in hydrogen (arising from the anomalous magnetic moment of the proton) predicted by the *PS*(*PS*) and *PS*(*PV*) theories. Curve (*a*) *PS*(*PV*) cross section at 300-Mev incident photon energy, (*b*) *PS*(*PV*) at 250 Mev, (*c*) *PS*(*PV*) at 200 Mev, (*d*) *PS*(*PS*) at 300 Mev, (*e*) *PS*(*PS*) at 250 Mev, (*f*) *PS*(*PS*) at 200 Mev; the coupling constants are set equal to unity.

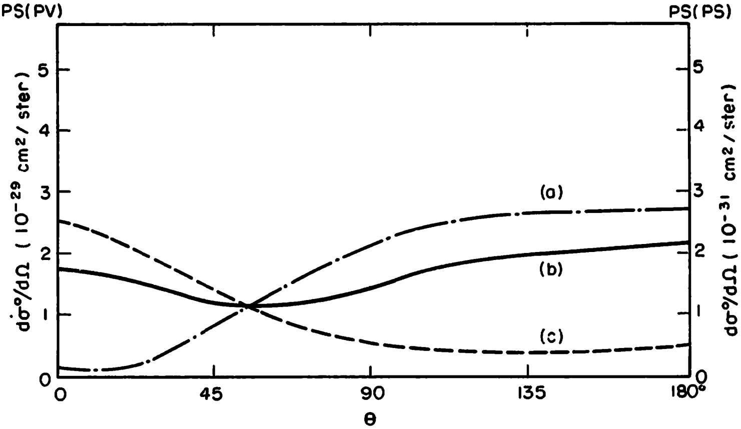

FIG. 10. Relativistic differential π^0 production cross sections in the laboratory system predicted by the *PS*(*PS*) and *PS*(*PV*) theories at a photon energy of 250 Mev. Curve (*a*) *PS*(*PS*) theory for the proton, (*b*) *PS*(*PV*) theory for the proton, (*c*) *PS*(*PV*) theory for the neutron; the coupling constants are set equal to unity.

can readily be derived from the differential cross sections; we write down the nonrelativistic expressions derived from Eqs. (28) and (29):

$$PS(PS): \qquad \sigma^0 = 4\pi e^2 g_p^2 \mu_p^2 \left(\frac{\mu}{2M}\right)^2 \frac{q(\omega^2 + \frac{2}{3}q^2)}{\mu^2 M^2 \omega} \tag{30}$$

$$PS(PV): \qquad \sigma^0 = \frac{8\pi}{3}\, e^2 f_p^2 \mu_p^2 \,\frac{q^3}{\mu^2 M^2 \omega} \tag{31}$$

While it has been shown that, in the pseudoscalar theory, the cross section for π^0 meson production is increased markedly by taking account of the anomalous magnetic moments of the nucleons, the question still remains whether the theoretical predictions for charged π meson production are affected by postulating that the photon interacts with the anomalous magnetic moments. The answer is in the negative, as can readily be seen on qualitative grounds from the fact that if, for example, the proton emits a π^+ meson instead of a π^0 meson the spin flip associated with the anomalous magnetic moment of the proton now leads to a cross section proportional to $(\mu_p + \mu_n)^2$ instead of $(\mu_p + \mu_p)^2$; the anomalous magnetic moment contribution to the π^+ production is therefore an order of magnitude smaller. Similarly, the inclusion of the anomalous magnetic moments affects only slightly the weak coupling predictions for π^- meson production. No calculations have been performed for spin 1 neutral mesons since the π^0 meson definitely does not possess spin 1 (the π^0 meson decays into two γ rays—see below).

A finite cross section for the production of spin 0 π^0 mesons on neutrons can arise only if the photon interacts with the anomalous magnetic moment of the neutron. The nonrelativistic cross sections for π^0 production in photon-neutron collisions follow immediately from Eqs. (28) and (29) by replacing g_p by g_n (the coupling constant of the π^0 meson to the neutron) and μ_p by μ_n (the anomalous magnetic moment of the neutron) in these equations. Similarly, the nonrelativistic neutron curves are obtained from the proton curves in Fig. 9 by multiplying the ordinate by $(g_n\mu_n/g_p\mu_p)^2$ or $(f_n\mu_n/f_p\mu_p)^2$, as the case may be. The relativistic neutron curves are not obtained so simply since the neutron, in contrast to the proton, does not carry an electric current; for comparison, we have therefore included in Fig. 10 [as curve (*c*)] Kaplon's rigorous curve for the *PS*(*PV*) cross section for π^0 production in photon-neutron collisions at a photon energy of 250 Mev. The theoretical cross sections for π^0 production in photon-neutron collisions are somewhat academic since free neutrons do not exist and the inverse reaction $\pi^0 + N \rightarrow N + \gamma$ cannot take place (in contrast to the case of π^- production where the inverse reaction

$\pi^- + P \rightarrow N + \gamma$ can take place). However, Francis[17] has shown that a study of the production of π^0 mesons in photon-deuteron collisions should decide whether the anomalous magnetic moment of the neutron contributes to π^0 production. For example, he has found that, at photon energies not too near threshold and at small angles, the cross section for π^0 production in the reaction $\gamma + D \rightarrow D + \pi^0$ is essentially proportional to $(g_p\mu_p + g_n\mu_n)^2$ (in the same units, the cross section for π^0 production in the reaction $\gamma + P \rightarrow P + \pi^0$ is proportional to $\frac{3}{2}(g_p\mu_p)^2$). Hence, since $\mu_n \approx -\mu_p$, the deuteron cross section should be appreciably larger than the proton cross section if $g_n = -g_p$ ("symmetrical" meson theory)[18] and much smaller if $g_n = g_p$ ("neutral" meson theory).

4. Classical Theory of Photomesic Production

Before presenting the experimental data on the photomesic process and making a comparison with the predictions of weak coupling theory, it is illuminating to present a classical derivation of the weak coupling predictions for the spin 0 theories. In a classical treatment of photomesic production, the meson is treated as a classical field and the nucleon as its infinitely heavy source. If the reaction of the meson field back upon the nucleon is neglected, the resulting "weak coupling" cross sections coincide with those derived quantum mechanically using the lowest order perturbation theory under the same assumption about the nucleon mass (that is, $M \rightarrow \infty$). We consider the classical method in some detail because of its simplicity, its clear-cut physical interpretation, and its ready generalization to other types of theories (*e.g.*, strong coupling theory—cf. below).

We first examine the scalar theory with scalar coupling to the nucleon. Suppose $U(\mathbf{r})$ is the shape function of the infinitely heavy nucleon, then the classical wave equation for the meson field ϕ interacting both with the nucleon source $U(\mathbf{r})$ and the electromagnetic potential **A** is[19]

$$(\nabla + \sqrt{4\pi}\, ie\mathbf{A})^2\phi - \frac{\partial^2\phi}{\partial t^2} - K^2\phi = \sqrt{4\pi}\, g\tau_\pm U(\mathbf{r}) \tag{32}$$

where K^{-1} is the meson Compton wave length ($K = \mu$ if $\hbar = c = 1$) and g is the meson-nucleon coupling constant as before. The quantity $\tau_\pm$ is the isotopic spin of the nucleon which is treated as a classical vector satisfying the correct commutation relations; $\tau_\pm$ denotes whether a neutron is converted into a proton with the emission of a π^- meson or a proton into a neutron with the emission of a π^+ meson. It is clear from the above equation that, if the meson is neutral, no photoproduction will occur since the term coupling the photon to the meson disappears when we set $e = 0$. It is also clear that Eq. (32) will yield identical cross sections for π^+ and π^- production. These conclusions agree with the nonrelativistic approximations to the quantum-mechanical cross sections (cf. Sec. 3).

---

[17] N. Francis, private communication; cf. N. Francis and R. Marshak, *Phys. Rev.*, **85**: 496 (1952), and Heckrotte, Henrich, and Lepore, *Phys. Rev.*, **85**: 490 (1952).

[18] L. Rosenfeld, "Nuclear Forces," North Holland Publishing Co., 1948.

[19] Cf. Serber, *loc. cit.;* several numerical errors in this reference have been corrected.

Equation (32) can be integrated immediately if we set $e = 0$; let us write **A** in the form ($\boldsymbol{\varepsilon}$ is the polarization)

$$\mathbf{A} = \sqrt{\frac{1}{2\omega}}\, \boldsymbol{\varepsilon} e^{i(\mathbf{k}\cdot\mathbf{r}-\omega t)} \tag{33}$$

which corresponds to unit incident photon flux, and

$$\phi = [(\phi_0 + \phi_1 e^{-i\omega t}) + \text{c.c.}]$$

where ϕ_0 is time independent and ϕ_1 is time independent and of order e. The equation for ϕ_0 then follows at once:

$$(\nabla^2 - K^2)\phi_0 = \sqrt{4\pi}\, g\tau_\pm U(\mathbf{r}) \tag{34}$$

whose solution is

$$\phi_0 = \frac{-g\tau_\pm}{\sqrt{4\pi}} \int U(\mathbf{r}')Y(\mathbf{r} - \mathbf{r}')d\mathbf{r}' \tag{35}$$

where $Y(\mathbf{r})$ is the Yukawa potential e^{-Kr}/r. If we choose $U(\mathbf{r})$ as the Dirac δ function, we find that the equation for ϕ_1 becomes

$$(\nabla^2 + q^2)\phi_1 = 2ieg\,\tau_\pm \mathbf{A} \circ \nabla Y(r) \tag{36}$$

where q is the wave number of the emitted meson wave. In order to compute the cross section for photomesic production, it is necessary to find the asymptotic solution of Eq. (36), namely,

$$\phi_1 = \frac{eg\tau_\pm}{\omega^2} \sqrt{\frac{1}{2\omega}}\, \frac{e^{iqr}}{r}\, \frac{\mathbf{q}\cdot\boldsymbol{\varepsilon}}{1 - v\cos\theta} \tag{37}$$

where v is the velocity of the meson emitted at the angle θ and to note that the energy density of the meson field is

$$\frac{\partial\phi^*}{\partial t}\frac{\partial\phi}{\partial t} + \phi^*(K^2 - \nabla^2)\phi \tag{38}$$

If one denotes by B the coefficient of e^{iqr}/r in Eq. (37), the differential cross section becomes

$$\frac{d\sigma}{d\Omega} = 2q(BB^* + B^*B) \tag{39}$$

which, averaging over the photon polarization vector $\boldsymbol{\varepsilon}$, yields

$$\frac{d\sigma}{d\Omega} = \frac{1}{2}e^2g^2\frac{q^3}{\omega^5}\frac{\sin^2\theta}{(1 - v\cos\theta)^2}(\tau_-\tau_+ + \tau_+\tau_-) \tag{40}$$

Equation (40) is identical with Eq. (20), the perturbation-theoretic result.

The classical theory for the photoproduction of pseudoscalar mesons is somewhat more complicated than for scalar mesons. One must now work with two equations of motion, one for the meson field ϕ and one for the nucleon spin $\boldsymbol{\sigma}$ treated as a classical vector. Only the $\boldsymbol{\sigma}\cdot\nabla$ part of the pseudovector interaction operator remains on the assumption of an infinitely heavy nucleon [the $\gamma_5(\partial/\partial t)$ part of the pseudovector operator and the pseudoscalar operator $\beta\gamma_5$ giving zero contributions]. As in the quantum-mechanical calculation, it is possible to obtain a finite cross section for the photoproduction of π^0 mesons despite the infinite mass assumption if the photon is allowed to interact with the anomalous magnetic moment of the nucleon.

Let us discuss the production of neutral pseudoscalar mesons. If we let $\bar{\mu}$ denote the nucleon magnetic moment, $U(\mathbf{r})$ the shape function of the magnetic moment of the nucleon, and $\bar{f}/\mu$ the neutral meson-nucleon pseudovector coupling constant, then the equations of motion for neutral meson production become

$$\left(\nabla^2 - \frac{\partial^2}{\partial t^2} - K^2\right)\phi = \sqrt{4\pi}\,\frac{\bar{f}}{\mu}\,\boldsymbol{\sigma}\cdot\nabla U(\mathbf{r}) \tag{41a}$$

$$\dot{\boldsymbol{\sigma}} = 2\bar{\mu}\boldsymbol{\sigma}\times\int\mathbf{H}(\mathbf{r})U(\mathbf{r})d\mathbf{r} \tag{41b}$$

where $H(\mathbf{r})$ is the magnetic field of the photon. If we write

$$\mathbf{H}(\mathbf{r}) = i\sqrt{\frac{\omega}{2}}\,\boldsymbol{\varepsilon}e^{i(\mathbf{k}\cdot\mathbf{r}-\omega t)} \tag{42a}$$

and for $\boldsymbol{\sigma}$

$$\boldsymbol{\sigma} = \boldsymbol{\sigma}_0 + \boldsymbol{\sigma}_1 e^{-i\omega t} + \text{c.c.} \tag{42b}$$

where $\boldsymbol{\sigma}_0$ is time independent and independent of $\bar{\mu}$ and $\boldsymbol{\sigma}_1$ is time independent and of first order in $\bar{\mu}$, then the equation of motion for $\boldsymbol{\sigma}$ leads to the following solution for $\boldsymbol{\sigma}_1$:

$$\boldsymbol{\sigma}_1 = -\sqrt{\frac{1}{2\omega}}\,\bar{\mu}(\boldsymbol{\sigma}_0\times\boldsymbol{\varepsilon})\int U(\mathbf{r})e^{i\mathbf{k}\cdot\mathbf{r}}\,d\mathbf{r} \tag{43}$$

If this value of $\boldsymbol{\sigma}_1$ is substituted into the equation of motion for ϕ, the radiated meson field ϕ_1 can be solved for as before and the differential cross section for neutral meson production, averaged over the directions of $\boldsymbol{\sigma}_0$, turns out to be

$$\frac{d\sigma^0}{d\Omega} = \frac{1}{2} e^2 \bar{f}^2 \bar{\mu}^2 \left(\frac{q^3}{\mu^2 M^2 \omega}\right) \frac{\sigma_0^2}{3} (1 + \cos^2 \theta) \tag{44}$$

Equation (44) coincides with Eq. (29) if σ_0^2 is set equal to 3 (which is the correspondence-theoretic value) and $\bar{\mu} = \mu_p$, $\bar{f} = f_p$.

The interaction of the electromagnetic field with the magnetic moment of the nucleon will also give rise to a finite cross section for the photoproduction of charged pseudoscalar mesons. However, a larger cross section for charged pseudoscalar meson production is derived from the interaction of the meson charge with the vector potential **A** and even more from the "catastrophic" triple source term $\boldsymbol{\sigma} \cdot \mathbf{A}\phi$ which results from the condition of gauge invariance. In other words, one can omit the interaction of the electromagnetic field with the magnetic moment of the nucleon and therefore the equation of motion for the nucleon spin. One need only work with the equation of motion of the meson field, namely,

$$(\nabla + \sqrt{4\pi}\, ie\mathbf{A})^2 \phi - \frac{\partial^2 \phi}{\partial t^2} - K^2 \phi = -\sqrt{4\pi}\, \frac{f}{\mu}\, \tau_{\pm} (\nabla + \sqrt{4\pi}\, ie\mathbf{A}) \cdot \boldsymbol{\sigma} U(\mathbf{r}) \tag{45}$$

and solve this equation in precisely the same way as the scalar Eq. (32); one finds

$$\phi_1 = \frac{ief\tau_{\pm}}{\mu} \sqrt{\frac{1}{2\omega}}\, \frac{e^{iqr}}{r} \left[\boldsymbol{\sigma} \cdot \boldsymbol{\varepsilon} + \frac{\boldsymbol{\sigma} \cdot (\mathbf{k} - \mathbf{q})\mathbf{q} \cdot \boldsymbol{\varepsilon}}{\omega^2 (1 - v \cos \theta)}\right] \tag{46}$$

and, for the differential cross section,

$$\frac{d\sigma}{d\Omega} = e^2 f^2 \left(\frac{q}{\mu^2 \omega}\right) \frac{\sigma_0^2}{3} (\tau_- \tau_+ + \tau_+ \tau_-) \left[1 - \frac{\mu^2 q^2 \sin^2 \theta}{2\omega^4 (1 - v \cos \theta)^2}\right] \tag{47}$$

Again, Eq. (47) coincides with the nonrelativistic approximation to the quantum-mechanical weak coupling result [cf. Eq. (21)].

The assumption of an infinite mass for the nucleon requires the π^-/π^+ production ratio to be unity. We have seen that in the quantum weak coupling theory the π^-/π^+ ratio is greater than 1 for a finite mass nucleon. A simple classical derivation can also be given of this ratio[20] and as an illustration we derive the classical π^-/π^+ ratio for spin 0 mesons. The classical calculation proceeds on the assumption that the cross section for meson production depends on the amount of electromagnetic energy which can be absorbed by the neutron-π^+ system which constitutes the proton and by the proton-π^- system which constitutes the neutron.

---

[20] Cf. Brueckner, *loc. cit.*

Thus, if a free proton at rest emits a π^+ meson with velocity V_+ and is converted into a recoil neutron with velocity V_n, the cross section for π^+ production is proportional to E_+^2 where

$$E_+ = \int\int \mathbf{j}_+ \cdot \mathbf{A}\, d\mathbf{r}\, dt, \qquad \mathbf{j}_+ = e\mathbf{V}_+\delta[\mathbf{r} - \mathbf{r}(t)] \tag{48}$$

and the integral is taken over all space and time. There is no contribution from the neutron current because the charge of the neutron is zero (magnetic effects are disregarded, although these can be included). If a neutron at rest emits a π^- meson with velocity V_- and is converted into a recoil proton with velocity V_p, the cross section for π^- production is proportional to E_-^2 where

$$E_- = \int\int (\mathbf{j}_- + \mathbf{j}_p) \cdot \mathbf{A}\, d\mathbf{r}\, dt \tag{49}$$

and $\mathbf{j}_-$ and $\mathbf{j}_p$ are the π^- and proton currents, respectively. In each case, the current is represented by the expression $e\mathbf{V}\delta[\mathbf{r} - \mathbf{r}(t)]$ where $\mathbf{r}(t)$ is the position of the particle in question at time t, $\mathbf{V}$ is the velocity, and δ is the Dirac δ function. The quantities E_- and E_+ can be calculated immediately if it is assumed that V changes from 0 to its final value V_+, V_-, or V_p, whatever the case may be, in a time short compared with the period of the photon. One finds E_+ is equal to

$$E_+ = \frac{e}{i\mu^2}\frac{\boldsymbol{\varepsilon} \cdot \mathbf{V}_+}{1 - \boldsymbol{\varepsilon} \cdot \mathbf{V}_+} \tag{50a}$$

and E_- is equal to

$$E_- = \frac{e}{i\mu^2}\left(\frac{\boldsymbol{\varepsilon} \cdot \mathbf{V}_p}{1 - \boldsymbol{\varepsilon} \cdot \mathbf{V}_p} - \frac{\boldsymbol{\varepsilon} \cdot \mathbf{V}_-}{1 - \boldsymbol{\varepsilon} \cdot \mathbf{V}_-}\right) \tag{50b}$$

where $\boldsymbol{\varepsilon}$ is the polarization vector of the photon. If one now inserts the energy and momentum conservation laws, the ratio of the cross sections for π^- to π^+ production becomes (v is the velocity of the meson of either charge and θ is the angle between the emitted meson and the incident photon)

$$\frac{(d\sigma^-/d\Omega)_{\text{lab}}}{(d\sigma^+/d\Omega)_{\text{lab}}} = \left[1 - \frac{\epsilon}{M}(1 - v\cos\theta)\right]^{-2} \tag{51}$$

in agreement with the previous results [cf. Eqs. (15a) and (16a)]. It is interesting to note that, if it is assumed that the electromagnetic field interacts only with the anomalous magnetic moment of the nucleon and that this magnetic interaction dominates over all electric interactions, the π^-/π^+ production ratio is changed into

$$\frac{(d\sigma^-/d\Omega)_{\text{lab}}}{(d\sigma^+/d\Omega)_{\text{lab}}} = \left[1 - \left(\frac{\mu_p + \mu_n}{\mu_p - \mu_n}\right)\frac{\epsilon}{M}(1 - v\cos\theta)\right]^{-2} \tag{51a}$$

It is clear that Eq. (51a) predicts a ratio much closer to unity than does Eq. (51) since $[(\mu_p + \mu_n)/(\mu_p - \mu_n)] \approx 0.2$.

It is not at all surprising that the classical derivation of Eq. (51) agrees with the quantum-mechanical derivation for the scalar theory where only positive energy states are important; it is not so clear why it holds for the pseudoscalar theory where the negative energy states and the "catastrophic" triple term (for *PV* coupling) play such important roles. Presumably there are accidental cancellations which finally lead to exactly the same result as does the scalar theory. For spin 1 theories the interaction of the photon with the intrinsic magnetic moment of the meson is important and alters the π^-/π^+ ratio from that predicted by Eq. (51): the vector theory predicts an even larger π^-/π^+ ratio than do the spin 0 theories, whereas the pseudovector theory predicts a ratio close to unity (cf. Fig. 3).

We have seen that the essential weak coupling predictions for photomesic production can be derived in two ways: by means of the lowest order quantum-mechanical perturbation theory or by solving the classical equations of motion for the meson field. The classical method has the advantage that it can be generalized rather easily to strong or intermediate coupling. Strong coupling theory, which takes account of the reaction of the meson radiation on the motions of the nucleonic spin and isotopic spin, is discussed in Chap. 9 in connection with the apparent existence of metastable isobaric states of nucleons. For our present purposes, it suffices to quote the classical strong coupling cross sections for the production of pseudoscalar mesons. Assuming "symmetrical" pseudovector coupling, the classical strong coupling cross section for charged π meson production is found to be identical with the weak coupling result [cf. Eq. (21)] except for a factor $\frac{2}{9}$ which arises from the classical averaging over the spin and isotopic spin variables.[21] The cross section for π^0 production in the strong coupling limit becomes:

$$\frac{d\sigma^0}{d\Omega} = \frac{7}{100}\left(\frac{\mu_p - \mu_n}{2}\right)^2\left(\frac{ae}{f}\right)^2\left(\frac{q}{\omega}\right)^3\left(1 + \frac{7}{2}\sin^2\theta\right) \qquad (52)$$

where $\mu_{p,n}$ is the magnetic moment of the proton or neutron and a represents the linear size of the nucleonic magnetic moment distribution (a is related to the nucleon "spin inertia," *i.e.*, the intrinsic moment of inertia which the nucleon possesses as a result of its coupling to the meson field). Comparison of Eq. (52) with the weak coupling cross section [cf. Eq. (29)] shows that while the absolute magnitude is comparable and the dependence on the meson momentum is the same, the angular distribution is completely different. Both Eqs. (52) and (29), as we shall see, have the wrong angular dependence when comparison is made with experiment

---

[21] Cf. Brueckner and Case, *loc. cit.*

(cf. Sec. 5). It will turn out that the angular dependence predicted by the quantum strong coupling version of the theory most nearly approximates the experimental angular distribution of π^0 mesons. Thus, a quantum mechanical, strong coupling calculation[22] of the cross section for the photoproduction of π^0 mesons leads to an expression which is identical with Eq. (52) except that the angular factor[22a] $(2 + 3 \sin^2 \theta)$ replaces $(1 + \frac{7}{2} \sin^2 \theta)$. However, it should be remarked that a classical intermediate coupling theory can achieve an angular dependence of the desired form $(2 + 3 \sin^2 \theta)$—by a suitable choice of coupling constant—since the angular function $(2 + 3 \sin^2 \theta)$ is intermediate between the $(1 + \cos^2 \theta)$ angular dependence predicted by weak coupling theory and the $(1 + \frac{7}{2} \sin^2 \theta)$ angular dependence predicted by classical strong coupling theory.

Several other more or less classical calculations of photomesic production have been carried out, a special effort being made in each case to obtain a π^0 meson cross section comparable with the π^+ cross section, a result required by experiment (see Sec. 5). For example, Drell[23] has performed a Bloch-Nordsieck type of calculation in which the nucleon mass is taken as infinite and its spin and charge are treated as classical vectors. The ability of all these calculations to predict comparable cross sections for neutral and charged meson production resides in their implicit or explicit postulation of a strong *virtual* excitation of the charged meson field by the photon as the mechanism for π^0 production. Since the virtually excited charged meson field gives rise, at the same time, to the anomalous magnetic moment of the nucleon, one can understand the equivalent prediction of weak coupling theory for π^0 production wherein the anomalous magnetic moment of the nucleon is treated phenomenologically and is assumed to interact directly with the electromagnetic field. It is to be expected that the various theoretical models will differ in such details as the predicted angular distribution of the π^0 mesons.

5. Comparison of Theory with Experiment

Under actual experimental conditions, the photon beam is not monoenergetic but consists of a bremsstrahlung spectrum with a cutoff energy corresponding to the electron energy in the accelerator. The bremsstrahlung spectrum has the form $F(\omega)(d\omega/\omega)$ where $F(\omega)$ can be calculated and has also been measured;[24] $F(\omega)$ is close to unity over most of the photon energy region. In view of the continuous distribution of photon energies, one will observe in a meson production experiment a distribution of meson angles for a fixed meson energy and conversely a distribution of meson energies at a fixed angle. The theoretical cross sections have been calculated for a specified photon energy so that, if one wishes to compare the theoretical cross sections directly with experiment, one must measure only those mesons whose energies and angles are related, for a given ω, by the equation

---

[22] Fujimoto and Miyazawa, *loc. cit.*

[22a] It can be shown that the angular dependence $(2 + 3 \sin^2 \theta)$ is due to an implicit resonance with the lowest nucleon isobar (possessing $I = \frac{3}{2}$, $J = \frac{3}{2}$—I is the isotopic spin, J the ordinary spin) predicted by the quantum strong coupling theory. Strictly speaking, neither the quantum nor classical strong coupling theory predicts a sufficiently large absolute magnitude for π^0 production except in the neighborhood of resonance with a metastable nucleon isobar (implying intermediate coupling—cf. references 21 and 22).

[23] Drell, *loc. cit.*

$$\omega = \frac{M\epsilon - \mu^2/2}{M - \epsilon + q\cos\theta} \tag{53}$$

This type of measurement can be carried out and has been carried out (*e.g.*, at $\omega = 250$ Mev for π^+ mesons—cf. below); however, thus far, the statistical accuracy has been poor compared with the type of measurement in which the meson energy or the meson angle is fixed and one works with the photon spectrum emerging from the electron accelerator. Therefore, for most experiments, to compare with theory, it is necessary to integrate the theoretical cross section over the bremsstrahlung spectrum.

In order to derive the angular distribution corresponding to a fixed meson energy ϵ_0, we take the differential cross section per unit solid angle, write it in the form $d\sigma/d\Omega = f(\theta, \epsilon)$, and integrate over the bremsstrahlung spectrum; we get

$$\frac{d\sigma}{d\Omega\, d\epsilon_0} = \frac{f(\epsilon_0, \theta)}{\omega(\epsilon_0, \theta)} \frac{\partial\omega}{\partial\epsilon_0} (\epsilon_0, \theta) F(\omega) \tag{54}$$

where

$$\frac{\partial\omega}{\partial\epsilon} = \frac{q(\omega + M) - \omega\epsilon\cos\theta}{q(M - \epsilon + q\cos\theta)} \tag{54a}$$

The meson spectrum corresponding to a fixed angle θ_0 becomes

$$\frac{d\sigma}{d\epsilon\, d\Omega_0} = \frac{f(\epsilon, \theta_0)}{\omega(\epsilon, \theta_0)} \frac{\partial\omega}{\partial\epsilon} (\epsilon, \theta_0) F(\omega) \tag{55}$$

In Eq. (55), the range of photon energies which contribute to a specified meson energy ϵ is determined by the formula

$$\omega_{\substack{\max\\ \min}} = \frac{2M\epsilon - \mu^2}{2(M - \epsilon \mp q)} \tag{55a}$$

Figures 11 to 14 contain plots of the predicted angular distribution in the laboratory system of π^+ mesons produced in photon-proton collisions at

---

[24] Powell, Hartsough, and Hill, *Phys. Rev.*, **81**: 213 (1951).

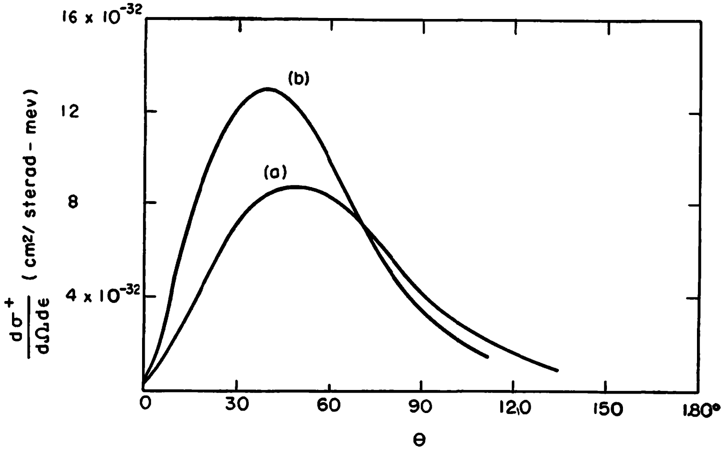

FIG. 11. Theoretical laboratory angular distribution for π^+ mesons predicted by the $S(S)$ theory for a bremsstrahlung photon spectrum with $\omega_{\max} = 300$ Mev. Curve (*a*) corresponds to 40-Mev kinetic energy for the emitted meson, (*b*) to 80 Mev; the coupling constants are set equal to unity.

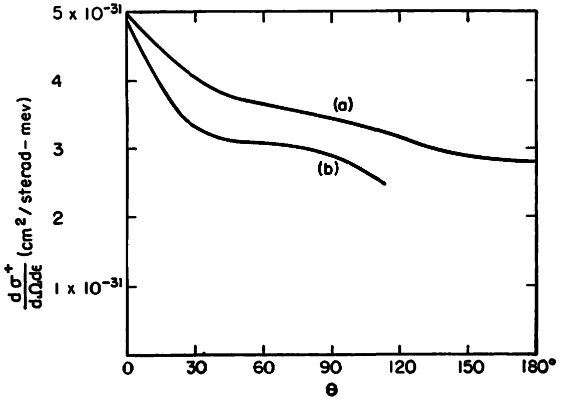

FIG. 12. Theoretical laboratory angular distribution for π^+ mesons predicted by the $PS(PV)$ theory for a bremsstrahlung photon spectrum with $\omega_{\max} = 300$ Mev. Curve (*a*) corresponds to 40-Mev kinetic energy for the emitted meson, (*b*) to 80 Mev; the coupling constants are set equal to unity.

two energies: $\epsilon = 180$ Mev and $\epsilon = 220$ Mev, assuming $F(\omega) \equiv 1$ and $\omega_{\max} = 300$ Mev; the figures represent, respectively, the four theories: $S(S)$, $PS(PV)$, $V(V)$, and $PV(PV)$ and are based on the relativistic expressions for $f(\theta, \epsilon)$ [cf. Eqs. (15) to (18)] inserted into Eq. (53). Figure 15 contains plots of the predicted π^+ meson spectra at an angle of 90°

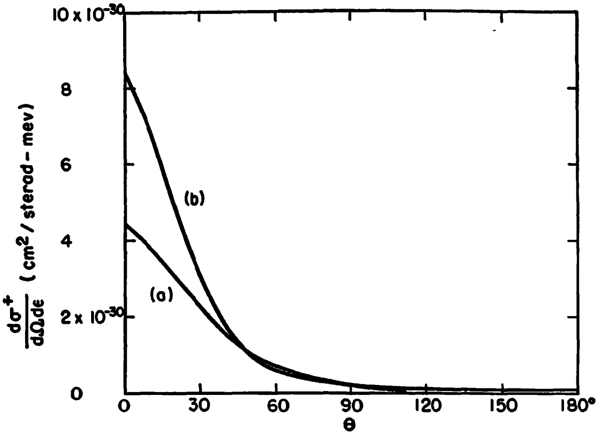

FIG. 13. Theoretical laboratory angular distribution for π^+ mesons predicted by the $V(V)$ theory for a bremsstrahlung photon spectrum with $\omega_{\max} = 300$ Mev. Curve (a) corresponds to 40-Mev kinetic energy for the emitted meson, (b) to 80 Mev; the coupling constants are set equal to unity.

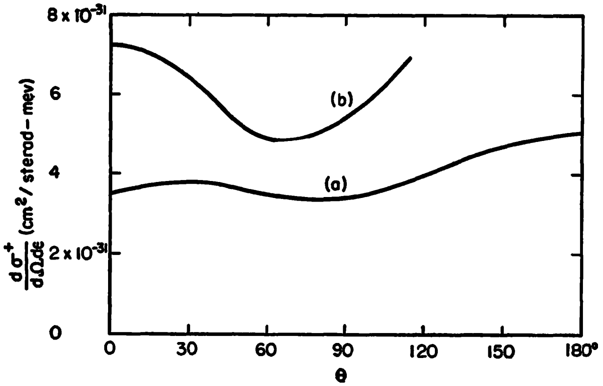

FIG. 14. Theoretical laboratory angular distribution for π^+ mesons predicted by the $PV(PV)$ theory for a bremsstrahlung photon spectrum with $\omega_{\max} = 300$ Mev. Curve (a) corresponds to 40-Mev kinetic energy for the emitted meson, (b) to 80 Mev; the coupling constants are set equal to unity.

in the laboratory system for each of the four theories, again assuming $F(\omega) = 1$ and $\omega_{\max} = 300$ Mev.

For π^0 meson production in photon-proton collisions, the angular distribution predicted by the weak coupling pseudoscalar theories (the only weak coupling theories which have relevance for π^0 mesons since the π^0 meson possesses spin 0 and the weak coupling scalar theory predicts much too small a cross section) is $(1 + \cos^2 \theta)$ at all meson energies in the

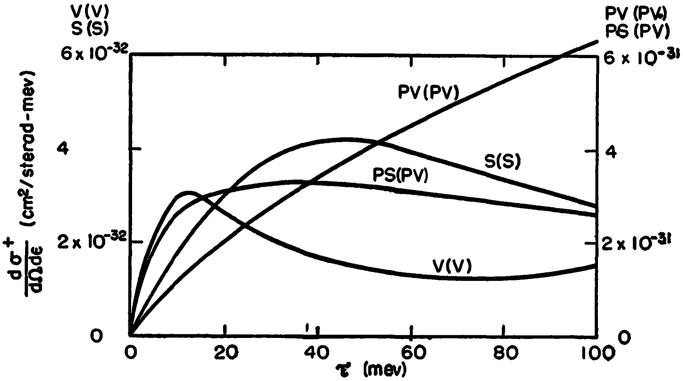

FIG. 15. Theoretical energy spectra of π^+ mesons at 90° in the laboratory system with respect to the incident photon beam predicted by the $S(S)$, $PS(PV)$, $V(V)$, and $PV(PV)$ theories; the bremsstrahlung photon spectrum has $\omega_{\max} = 300$ Mev, and the coupling constants are set equal to unity.

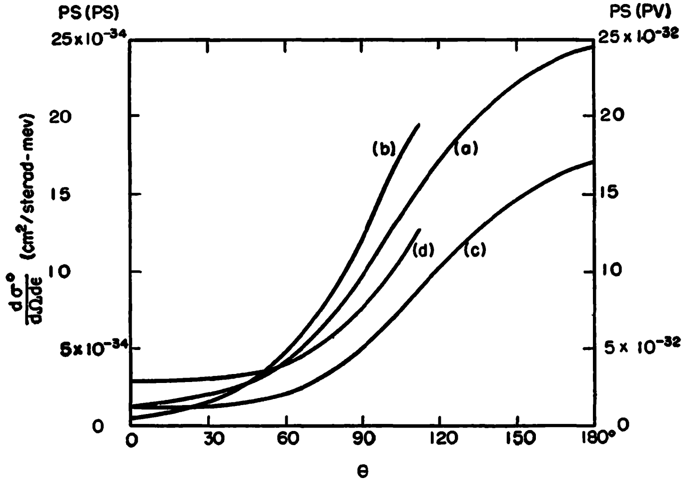

FIG. 16. Theoretical laboratory angular distribution for π^0 mesons for a bremsstrahlung photon spectrum with $\omega_{\max} = 300$ Mev. Curve (*a*) corresponds to 40-Mev kinetic energy for the emitted meson in the $PS(PS)$ theory, (*b*) to 40-Mev kinetic energy in the $PS(PV)$ theory, (*c*) to 80-Mev kinetic energy in the $PS(PS)$ theory, (*d*) to 80-Mev kinetic energy in the $PS(PV)$ theory; the coupling constants are set equal to unity.

$M \rightarrow \infty$ approximation. Figure 16 contains a plot of the π^0 angular distributions in the laboratory system, computed on the basis of Kaplon's rigorous relativistic $PS(PS)$ and $PS(PV)$ cross sections for $\epsilon = 180$ Mev and 220 Mev when $\omega_{\max} = 300$ Mev. In analogy to Fig. 14, Fig. 17 shows the π^0 meson spectra at 90° predicted by the $PS(PS)$ and $PS(PV)$

theories. Similar curves can readily be derived for the "symmetrical" *PS(PV)* strong coupling theories assuming that Eq. (52) and its quantum analogue [yielding the angular factor $(2 + 3\sin^2\theta)$ instead of $(1 + \frac{7}{2}\sin^2\theta)$—cf. above] represent differential π^0 cross sections in the center of mass system (in the $M \to \infty$ approximation there is, of course, no distinction between the barycentric and laboratory systems).

Let us now turn to the actual experiments on the photonic production of π^+, π^-, and π^0 mesons. Some preliminary measurements have been made of the π^+ and π^0 production cross sections in photon-proton collisions; however, the cross section for the process $\pi^- + P \to N + \gamma$ has not been measured as yet so that the π^- production cross section must be inferred from experiments with heavier nuclei and is therefore less certain. The first experiment on π^+ production in hydrogen was carried out at Berkeley[25] using a subtraction technique (*i.e.*, taking the difference between paraffin and carbon to find the cross section due to hydrogen) and a bremsstrahlung spectrum of 330-Mev maximum energy. The π^+ mesons were detected in scintillation counters in which they stopped after passing through appropriate amounts of absorber. In a later experiment,[26] liquid hydrogen was used; Fig. 18 (*a*) shows the π^+ spectrum measured at 90° in the laboratory system with respect to the incident photon direction. Dividing the meson spectrum by the bremsstrahlung photon spectrum [shown as Fig. 18 (*b*)], one obtains an excitation function at 90° which is plotted up as curve (*a*) of Fig. 19; curve (*b*) of Fig. 19 is the excitation function which results if it is assumed that the π^+ meson has a nuclear interaction cross section equal to the nuclear area (cf. Chap. 7) in the absorber; it is clear that the higher the meson energy, the larger the amount of absorber which must be traversed and the larger the correction. By using appropriate thicknesses of absorber, the angular distribution of π^+ mesons produced by 250-Mev photons was also measured, and the center-of-mass distribution is shown in Fig. 20. For all these curves, the absolute scale is uncertain by a factor 1.5 although, according to the authors, the relative numbers are correct to within the statistical accuracy shown.[26a]

Comparison of these experimental results, incomplete though they are, with theory argues against the scalar and vector fields for the charged π meson. The angular distribution of the π^+ mesons at a γ ray energy of 250 Mev (cf. Fig. 20) is roughly isotropic and is therefore consistent with

---

[25] J. Steinberger and A. Bishop, *Phys. Rev.*, **78**: 494 (1950).

[26] Bishop, Steinberger, and Cook, *Phys. Rev.*, **80**: 291 (1950).

[26a] A recent paper by J. Steinberger and A. Bishop [*Phys. Rev.*, **86**: 171 (1952)] confirms the essential correctness of these preliminary experiments and leads to a total π^+ cross section of $1.9 \pm 0.3 \times 10^{-28}$ cm² at a photon energy of 255 Mev (cf. below).

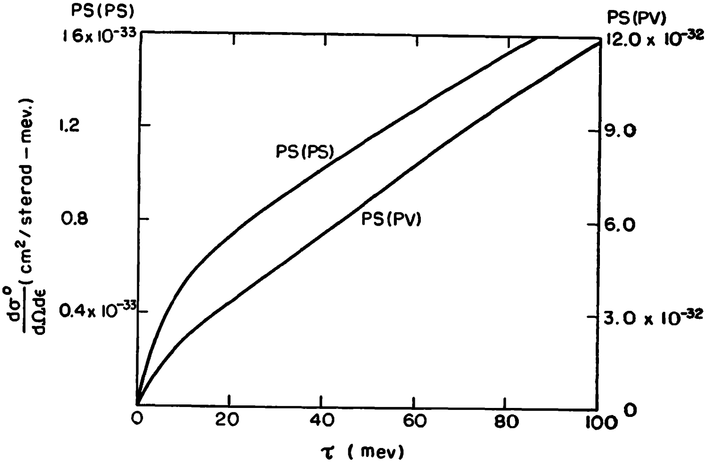

FIG. 17. Theoretical energy spectra of π^0 mesons at 90° in the laboratory system with respect to the incident photon beam predicted by the $PS(PS)$ and $PS(PV)$ theories; the bremsstrahlung photon spectrum has $\omega_{\max} = 300$ Mev, and the coupling constants are set equal to unity.

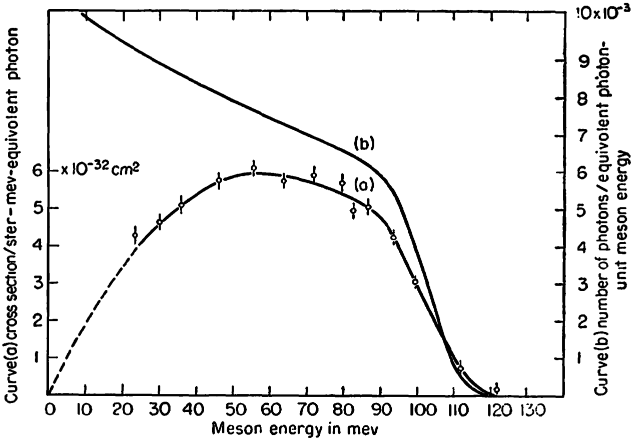

FIG. 18. Curve (a) represents the measured energy spectrum of π^+ mesons from hydrogen at 90° in the laboratory system for a bremsstrahlung spectrum with $\omega_{\max} = 330$ Mev; curve (b) represents the measured photon spectrum. An equivalent photon is defined as the ratio of the energy in the γ-ray beam to the maximum photon energy.

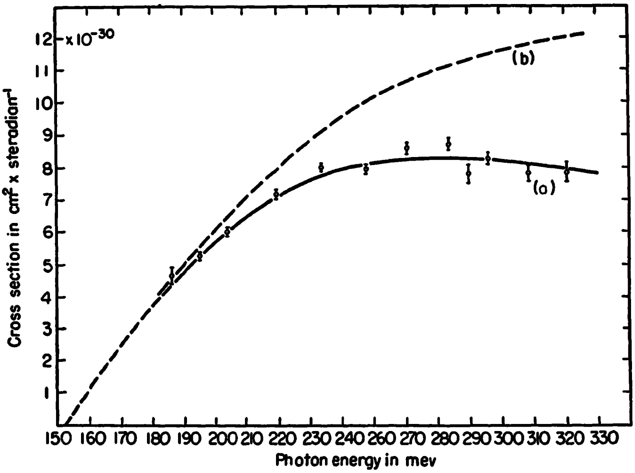

FIG. 19. Excitation function for π^+ mesons from hydrogen at 90° in the laboratory system. Curve (*a*) without correction for nuclear absorption, (*b*) with correction for nuclear absorption.

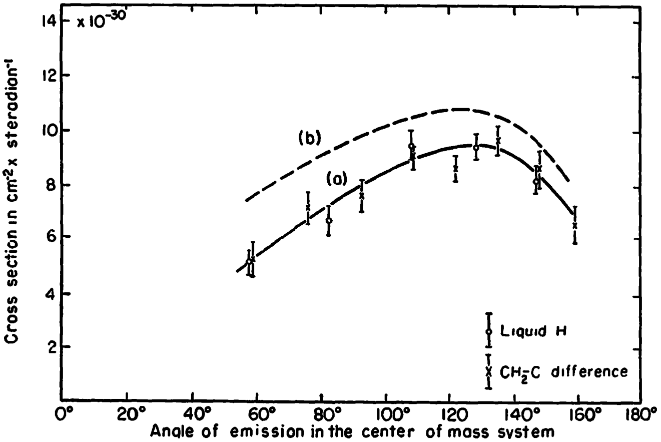

FIG. 20. Measured center-of-mass angular distribution of π^+ mesons from hydrogen at an incident photon energy of 250 Mev. Curve (*a*) without correction for nuclear absorption, (*b*) with correction for nuclear absorption.

the pseudoscalar and pseudovector theories (cf. Figs. 5 and 6) but in definite disagreement with the scalar and vector theories. The meson spectrum at 90° with respect to the photon-beam direction shown in Fig. 19 does not decide between the pseudoscalar and pseudovector weak coupling theories in view of some uncertainty in the interaction cross section of π^+ mesons in the energy region under consideration (cf. Chap. 7) and the experimental errors in the measurements. When more accurate meson spectra are measured and when our knowledge of the π^+ meson interaction cross section is more certain, a decision between the pseudoscalar and pseudovector theories might be possible on the basis of the hydrogen production experiment. If the curve in Fig. 19 is integrated over all angles, one arrives at a value of 1.5×10^{-28} cm^2 for the total π^+ cross section at a photon energy of 250 Mev; this value should be correct to within a factor 2 (cf. footnote 26*a*). Using this value of the π^+ production cross section, the charged meson coupling constant can be evaluated for the various weak coupling theories by integrating over the appropriate theoretical curves in Fig. 5; one finds

$S(S)$: $\quad \dfrac{g^2}{\hbar c} = 1.2$

$PS(PV)$: $\quad \dfrac{f^2}{\hbar c} = 0.23$

$V(V)$: $\quad \dfrac{g^2}{\hbar c} = 0.65$

$PV(PV)$: $\quad \dfrac{g^2}{\hbar c} = 0.13$

We give these numbers [including the $S(S)$ and $V(V)$ numbers even though the theoretical angular distributions fit badly] for purposes of reference, not because any reliance can be placed upon them.

Some apparent evidence that free neutrons are more efficient in producing π^- mesons than are protons in producing π^+ mesons has been obtained by Littauer and Walker[27] with the Cornell synchrotron. Using a coincidence counter system, they measured the π^-/π^+ ratio at 50 Mev for mesons emitted from Be^9 at 135° with respect to the incident photon direction. The excess neutron in Be^9 is bound by only 1.65 Mev, and therefore it would be presumed that conditions approximate the free neutron state. The ratio was found to be 2.25 ± 0.11, which agrees well with the ratio predicted for spin 0 theories by Eqs. (15*a*) and (16*a*), after correcting for the higher neutron to proton ratio in the beryllium nucleus. However, one would expect a similar result for the π^-/π^+ ratio in deuterium since the neutron binding energy is only 0.6 Mev greater compared with Be^9. Unfortunately, in the case of deuterium, the measured π^-/π^+ ratio for 50 Mev mesons emitted at 135° is 1.19 ± 0.12, which is much smaller than the beryllium ratio. This somewhat disconcerting result makes it appear that the large π^-/π^+ ratio in Be^9 has some other cause

---

[27] R. Littauer and D. Walker, *Phys. Rev.*, **82**: 746 (1951); cf. also H. A. Medicus, *Phys. Rev.*, **83**: 662 (1951).

(cf. Chap. 3) and that the agreement with the prediction of the spin 0 theories is accidental. The π^-/π^+ ratio in D should be more clearly interpretable in terms of the free nucleon predictions, and its low value may imply an incorrect treatment of the negative energy states (for the nucleons) in the weak coupling pseudoscalar theory.[28] A direct measurement of the cross section for π^- production in photon-neutron collisions (via the inverse reaction $\pi^- + P \rightarrow N + \gamma$—cf. above) would be very desirable.

The π^0 meson production experiments argue against the scalar and both spin 1 fields for the π^0 meson. The detection of π^0 turns out to be relatively simple because of its extremely rapid decay (its lifetime is about 10^{-14} sec—cf. Chap. 4) into two high-energy γ rays (the very fact that two decay rays are emitted excludes spin 1 for the π^0 meson). As a matter of fact, the existence of the neutral π meson was first definitely established by observing with scintillation counter telescopes the coincidences between γ rays resulting from the impact of the photon beam with target nuclei like carbon and beryllium[29] (for more detail, see Chap. 3). The same method was used with a liquid hydrogen target placed in front of the 330-Mev photon beam from the Berkeley synchrotron.[30] The variation of the counting rate with the angle between the two telescopes was measured at 45 and 90° with respect to the incident photon direction. When it is recognized that the observed coincidences are due to neutral mesons, it is possible to interpret the coincidence counting rates in terms of energy spectra for the π^0 meson; this interpretation is simplified by the fact that the kinematics of the two-photon decay of the π^0 meson strongly favors the emission of two photons of almost equal energy (cf. Chap. 3). In this manner, the Berkeley workers found that the π^0 cross section at 90° in the laboratory system and at 250-Mev photon energy is about one-third of the π^+ cross section and that the differential cross section at 45° is roughly twice that at 90°.

An independent experiment on the photoproduction of π^0 mesons in hydrogen has been carried out with the 310-Mev Cornell synchrotron by Silverman and Stearns.[31] The Cornell group measured the π^0 production cross section by detecting coincidences between the recoil proton and one of the decay γ rays from the π^0 meson. By measuring the energy and angle of the recoil proton, they were able to determine the energy of the incident γ ray and the energy and angle of the π^0 meson. Figure 21 shows the excitation function for π^0 production obtained by Silverman and Stearns at 90° in the laboratory system; the experimental curve can be fitted by the power law $d\sigma^0/d\Omega(90°) = k(\omega - \mu)^{1.8\pm0.5}$ where k is a constant. Silverman and Stearns also made a preliminary measurement of

---

[28] N. Francis (private communication) has shown that the *PS*(*PV*) theory predicts a π^-/π^+ ratio close to unity if only the $(\boldsymbol{\sigma} \cdot \nabla)$ part of the π meson-nucleon interaction operator is employed and the negative energy states are disregarded. It is evident that equality of π^- and π^+ production will follow from a suppression of the nucleon current contribution to the cross section.

[29] Steinberger, Panofsky, and Steller, *Phys. Rev.*, **78**: 802 (1950).

[30] J. Steller and W. Panofsky, *Phys. Rev.*, **81**: 649 (1951); cf. also Panofsky, Steinberger, and Steller, *Phys. Rev.*, **86**: 180 (1952).

[31] A. Silverman and M. Stearns, *Phys. Rev.*, **83**: 853 (1951).

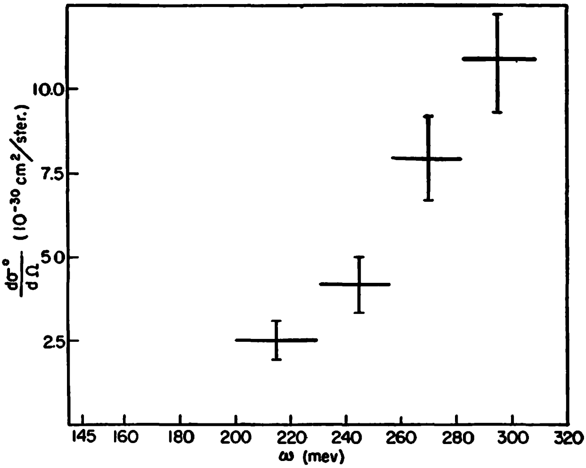

FIG. 21. Excitation function for π^0 mesons from hydrogen at 90° in the laboratory system.

the ratio of cross sections at 60 and 90° (in the laboratory system) for 250- to 310-Mev incident γ rays with the result:

$$(d\sigma^0/d\Omega)(60°)/(d\sigma^0/d\Omega)(90°) = 1.50 \pm 0.25$$

In the center-of-mass system this ratio becomes

$$(d\sigma^0/d\Omega)(76°)/(d\sigma^0/d\Omega)(112°) = 1.10 \pm 0.20$$

A recent experiment at Cornell[31a] appears to provide evidence for a $(2 + 3 \sin^2 \theta)$ angular distribution in the center-of-mass system for π^0 mesons produced by photons with energies in the neighborhood of 300 Mev.

The experimental results on π^0 meson production in hydrogen are very preliminary at the present time. However, it seems definitely established that the π^0 production cross section is comparable with the π^+ production cross section and that the excitation function for π^0 production is steeper

[31a] G. Cocconi and A. Silverman, private communication.

than for π^+ production. These features fit reasonably well the various theories which attribute the π^0 production to the interaction of the photon with the anomalous magnetic moment of the proton or its equivalent the "virtually excited charged meson" (cf. above). The magnetic moment theories predict the observed ratio ($\frac{1}{3}$—cf. Figs. 19 and 21) of the π^0 to π^+ cross section at 90° and 250 Mev incident photon energy for approximately equal values of the neutral and charged meson coupling constants. The magnetic moment theories also predict a q^3 excitation function above threshold for π^0 production (in contrast to the q excitation function for π^+ production). These predictions are qualitatively in agreement with experiment, and it would be very surprising indeed if they were accidental. It should be noted that the strong coupling versions of the magnetic moment theory appear to predict a more correct angular distribution for the π^0 mesons than does the weak coupling version. Further support for the magnetic moment explanation for π^0 production could be derived, as has already been remarked, from experiments on π^0 production in deuterium.[31b]

6. Electron Production of π Mesons

Closely related to the photoproduction of π mesons is the production of π mesons in electron-nucleon collisions. Since fairly monoenergetic beams of electrons can be made available from accelerators, it would appear at first sight that experiments with monoenergetic electrons would be preferable to experiments with continuous bremsstrahlung photon beams. However, we have already pointed out that this advantage is only apparent because the energy and momentum conservation laws permit the establishment of a direct correlation between the angle and energy of the produced meson and the incident photon energy. Moreover, the cross section for meson production by electrons is down by a factor of the order of the fine structure constant compared with the photoproduction cross section. Nevertheless, it seems worth while to record the weak coupling cross sections which have been computed for the production of spin 0 π mesons (both charged and neutral) in electron-nucleon collisions for possible comparison with future experiments.

It can readily be shown, as in the photoproduction case, that the $S(V)$ theory leads to a vanishing result in the lowest order of perturbation theory and that the equivalence theorem holds between pseudoscalar and pseudovector coupling in the pseudoscalar theory. Consequently, we consider only the $S(S)$ and $PS(PV)$ theories. Figure 22 contains the Feynman diagrams for the process in question; the first two diagrams in each case are required for both theories whereas the third diagram (corresponding to the catastrophic production transition in photoproduction) is also required for the $PS(PV)$ theory. When the matrix elements corresponding to these Feynman diagrams are written down, it is possible to separate the terms representing the interaction of the virtual transverse electromagnetic field of the electron with the charged mesons and nucleons and the terms representing the virtual longitudinal field. If it is assumed that the electron does not suffer a large deflection as a result of the meson production act, it can be shown that the transverse part of the electromagnetic field gives the major contribution to the cross section. Making this assumption, and neglecting in addition the nucleon recoil

---

[31b] Recent preliminary experiments by Cocconi and Silverman at Cornell (private communication) indicate that the deuteron is twice as efficient as the proton in producing π^0 mesons in the angular range 45–90° (in the laboratory) and in the photon energy range 250–300 Mev; this would favor the magnetic moment theory.

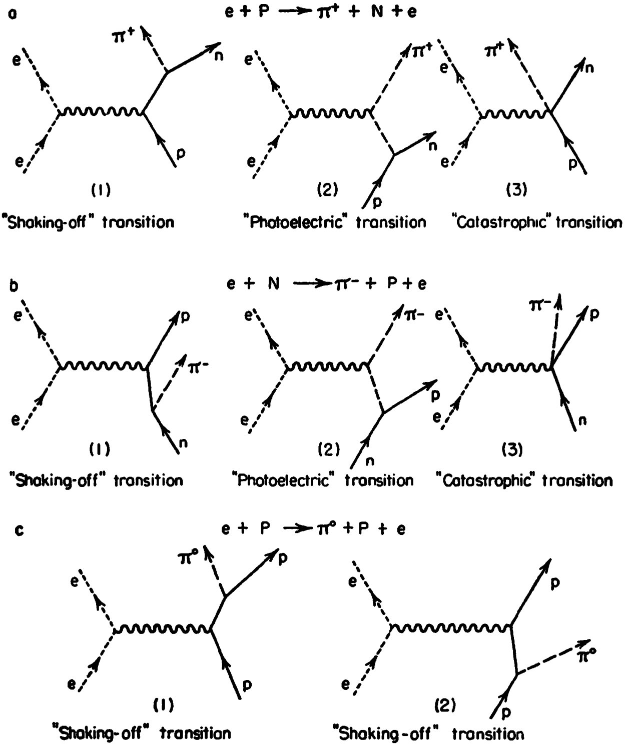
a
e + P ⟶ π⁺ + N + e
e
π⁺
n
p
(1)
"Shaking-off" transition
π⁺
(2)
"Photoelectric" transition
(3)
"Catastrophic" transition
b
e + N ⟶ π⁻ + P + e
π⁻
"Shaking-off" transition
"Photoelectric" transition
"Catastrophic" transition
c
e + P ⟶ π⁰ + P + e
π⁰
"Shaking-off" transition
"Shaking-off" transition

FIG. 22. Feynman diagrams for the electron production of charged and neutral π mesons. (*a*) $e + P \rightarrow N + \pi^+ + e$; (*b*) $e + N \rightarrow P + \pi^- + e$; (*c*) $e + P \rightarrow P + \pi^0 + e$.

(*i.e.*, setting $M = \infty$), the cross sections predicted by the weak coupling $S(S)$ and $PS(PV)$ theories can be written as follows:

$$S(S): \qquad \frac{d\sigma^+}{d\epsilon\, d\Omega} = \frac{e^4 g^2 A q^3 \sin^2 \bar{\theta}}{\pi \epsilon^4 (\epsilon - q \cos \theta)^2} \tag{56}$$

$$PS(PV): \qquad \frac{d\sigma^+}{d\epsilon\, d\Omega} = \frac{2e^4 f^2 A q}{\pi \epsilon^2 \mu^2} \left[1 - \frac{q^2 \mu^2 \sin^2 \bar{\theta}}{2\epsilon^2 (\epsilon - q \cos \theta)^2} \right] \tag{57}$$

$$\text{where} \quad A = \left[\left(\frac{E_0^2 + E^2}{E_0^2} \right) \log \left(\frac{2E_0 E}{m_e \epsilon} \right) - \frac{E}{E_0} - \frac{(E_0 + E)^2}{2E_0^2} \log \left(\frac{E_0 + E}{\epsilon} \right) \right],$$

$(\mathbf{q}, \epsilon)$ are the momentum-energy four-vector of the meson, $(\mathbf{p}_0, E_0)$, $(\mathbf{p}, E)$ the initial and final momentum-energy four-vectors of the electron, respectively, θ the angle between $\mathbf{q}$ and $(\mathbf{p}_0 - \mathbf{p}')$, and

$$\sin^2 \bar{\theta} = \sin^2 \theta + \frac{E^2 (\cos^2 \theta - \sin^2 \theta/2)}{2E_0^2}$$

For not too great incident electron energies, that is, $E_0 < 300$ Mev, $(E/E_0)^2 < \frac{1}{4}$, and $\sin^2 \bar{\theta} \approx \sin^2 \theta$. With the latter replacement, the relation of Eqs. (56) and (57) to Eqs. (20) and (21) becomes obvious, and it is clear that the cross section for the production of mesons by electrons is lower than the photoproduction at the some incident energy by a factor of the order of $e^2/\hbar c \approx \frac{1}{137}$. These expressions have been derived by Kaplon.[32]

In the above approximation, the π^-/π^+ and π^0/π^+ ratios are identical with those which are predicted for photomesic production. By the same token, the neutral π meson production by electrons can be raised relative to the charged π meson production by including the anomalous magnetic moments of the nucleons in the interaction Hamiltonian. All these considerations depend on the existence of a close connection between the electron and photon mechanisms for the production of π mesons in collision with nucleons. It is conceivable that a nonelectromagnetic interaction between electrons and nucleons may take hold at close distances of approach and give an additional contribution to π meson production. In order to throw light on this possibility, it will be necessary to carry out experiments at large angles of deflection (of the electrons) and large kinetic energies of the mesons.

[32] M. F. Kaplon, Ph.D. Thesis, University of Rochester, 1951; the papers of Sneddon and Touschek [*Proc. Roy. Soc.*, **199A**: 352 (1949)] and E. Strick (Technical Report III, Purdue University, 1950) contain slight errors which have been corrected in Kaplon's work.

CHAPTER 2

SINGLE PRODUCTION OF π MESONS IN NUCLEON-NUCLEON COLLISIONS

1. Introduction

In Chap. 1, we discussed the single production of π mesons in photon-nucleon collisions. From a comparison of experiment with theory, it was possible to argue that the neutral π meson possesses spin zero and odd parity (pseudoscalar) and the charged π meson spin zero and odd parity (pseudoscalar) *or* spin one and even parity (pseudovector). The experimental data on the nucleon-nucleon production of π mesons are, on the whole, less conclusive (it should be noted, however, that the nucleonic production experiments can discriminate between the $PS(PS)$ and $PS(PV)$ theories, whereas the photonic production experiments cannot—cf. below) and, although consistent with the above possibilities, do not require them. There are at least two reasons for the greater ambiguity in the interpretation of the nucleonic production experiments, both of which have already been mentioned: (1) the production of π mesons in nucleon-nucleon collisions requires knowledge of the potential between two nucleons, and this is not so well known as the interaction between the electromagnetic field and nucleons or mesons; and (2) the interaction of the two nucleons in the final state strongly influences the energy spectrum of the produced π mesons; in particular, the interaction may be so strong between a neutron and proton in the final state that a deuteron is formed and the meson is emitted with a discrete spectrum. Despite these handicaps to the interpretation of experiments on the production of π mesons in nucleon-nucleon collisions, we shall discuss the nucleonic production problem in some detail because of its intrinsic interest and because comparison between theory and experiment does throw considerable light on the nature of the π meson.

2. Kinematics of Single Meson Production in Nucleon-Nucleon Collisions

Just as for photonic production, it is useful to start by writing down the important kinematical formulas bearing on the single production of mesons in nucleon-nucleon collisions. It will be seen that there are some striking contrasts in the momentum-energy relations for nucleonic production as compared with photonic production; these are, of course, due to the zero rest mass of the photon in contrast to the finite rest mass of the incident nucleon. For example, the threshold energy for the production of a meson in a nucleon-nucleon collision is about double the value in a photon-nucleon collision; more exactly, if nucleon 1 is incident upon nucleon 2 at rest and the final two nucleons are unbound, the "unbound" threshold energy (including the nucleon rest mass) is[1]

$$E_t^u = \mu\left(\frac{M_1 + M_2}{M_2} + \frac{\mu}{2M_2}\right) + M_1 \tag{1}$$

where M_1 and M_2 are the nucleon masses and μ is the meson mass. Assuming equal masses for the nucleons, *i.e.*, $M_1 = M_2 = M$, Eq. (1) reduces to

$$E_t^u = \mu\left(2 + \frac{\mu}{2M}\right) + M \tag{1a}$$

If the final two nucleons are bound in a deuteron, the "bound" threshold energy is

$$E_t^b = \frac{(M_D + \mu)^2 - (M_1 + M_2)^2}{2M_2} + M_1 \tag{2}$$

where M_D is the deuteron mass; it is obvious that $E_t^b < E_t^u$.

If the energy of the incident nucleon $E > E_t$ and the final two nucleons are unbound, the maximum energy of the meson (including its rest mass) in the center-of-mass system is

$$\bar{\epsilon}_m = \frac{\mu^2 + 2(\gamma_1 - 1)M_1M_2}{2(M_1^2 + 2M_1M_2\gamma_1 + M_2^2)^{1/2}} \tag{3}$$

or, for equal masses,[2]

$$\bar{\epsilon}_m = \frac{\mu^2/M + 2(\gamma - 1)M}{2\sqrt{2(1 + \gamma)}} \tag{3a}$$

where $E = \gamma M$ with $\gamma = (1 - \beta^2)^{-1/2}$ and β = velocity of M. Since there are two nucleons and one meson in the final state, the energy $\bar{\epsilon}$ of the meson in the center-of-mass system can take on a continuum of values from μ to $\bar{\epsilon}_m$. The maximum energy of the meson in the laboratory system emitted at an angle θ with respect to the direction of the incident nucleon may be obtained from the following two relationships between the center-of-mass variables and the laboratory variables:

$$\epsilon_m(\theta) = \bar{\gamma}(\bar{\epsilon}_m + \bar{\beta}\bar{p}_m \cos \bar{\theta}) \tag{4a}$$

$$\tan \theta = \frac{\sin \bar{\theta}}{\bar{\gamma}(\cos \bar{\theta} + \bar{\beta}/\bar{\beta}_m)} \tag{4b}$$

---

[1] We again set $\hbar = c = 1$.

[2] Unless stated otherwise, we shall assume henceforth that in the unbound case $M_1 = M_2 = M$ (proton mass).

where $\bar{\gamma} = \sqrt{(\gamma + 1)/2}$, $\bar{\beta} = \sqrt{\bar{\gamma}^2 - 1}/\bar{\gamma}$, and $\bar{p} = \sqrt{\bar{\epsilon}^2 - \mu^2}$. Figure 1 contains the values of $\tau_m(\theta) = [\epsilon_m(\theta) - \mu]$ ranging from 0 to 180° for several incident nucleon kinetic energies (T = 300, 350, 400, and 450 Mev); also indicated are the values of $\bar{\tau}_m$. At each θ, the range of meson kinetic energies extends from 0 to $\tau_m(\theta)$.

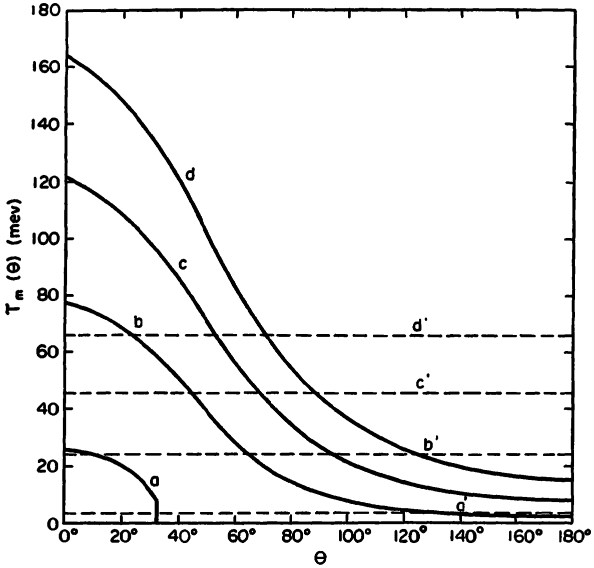

FIG. 1. Maximum kinetic energies $\tau_m(\theta)$ of the charged π meson as a function of the angle of emission θ in the laboratory system with respect to the incident nucleon direction. Curve (*a*) T = 300 Mev, (*b*) T = 350 Mev, (*c*) T = 400 Mev, (*d*) T = 450 Mev; the value of $\bar{\tau}_m$ is indicated in each case by the dashed line.

If $E > E_t$ and the final neutron and proton are bound in a deuteron, the unique energy of the meson in the center-of-mass system is

$$\bar{\epsilon}_D = \frac{1}{2}\left[\frac{(M_1^2 + M_2^2 + 2\gamma_1 M_1 M_2 + M_D^2 - \mu^2)^2}{M_1^2 + M_2^2 + 2\gamma_1 M_1 M_2} + 4\mu^2 - 4M_D^2\right]^{\frac{1}{2}} \quad (5)$$

In the laboratory system, the energy at an angle θ with respect to the incident nucleon direction is

$$\epsilon_D(\theta) = \frac{\begin{aligned}(\gamma_1 M_1 + M_2)A + \{A^2(\gamma_1 M_1 + M_2)^2 - [(\gamma_1 M_1 + M_2)^2 \\ - M_1^2(\gamma_1^2 - 1)\cos^2\theta] \times [A^2 + 4\mu^2 M_1^2(\gamma_1^2 - 1)\cos^2\theta]\}^{\frac{1}{2}}\end{aligned}}{2[(\gamma_1 M_1 + M_2)^2 - M_1^2(\gamma_1^2 - 1)\cos^2\theta]} \quad (6)$$

where $$A = M_1^2 + M_2^2 + 2\gamma_1 M_1 M_2 + \mu^2 - M_D^2. \quad (6a)$$

It is seen from Eq. (6) that $\epsilon_{\mathrm{D}}(\theta)$ is always greater than $\epsilon_m(\theta)$ (cf. Table 1 of Chap. 3).

The Jacobian relating the center of mass and laboratory cross sections [that is, $(d\sigma/d\Omega)_{\mathrm{lab}} = J(d\sigma/d\Omega)_{\mathrm{c.m.}}$] is

$$J = \frac{\bar{\gamma}^2[\bar{\beta}/\bar{\beta}_m + \sqrt{1 - \alpha^2(\bar{\beta}^2/\bar{\beta}_m^2 - 1)}]^2}{\cos^3 \theta(\alpha^2 + 1)^2 \sqrt{1 - \alpha^2(\bar{\beta}^2/\bar{\beta}_m^2 - 1)}} \tag{7}$$

where $\bar{\gamma} = (\gamma_1 M_1 + M_2)/\sqrt{M_1^2 + M_2^2 + 2\gamma_1 M_1 M_2}$ and $\alpha = \bar{\gamma} \tan \theta$.

3. Weak Coupling Theory of Single π Meson Production in Nucleon-Nucleon Collisions

The kinematics of meson production tells us what the threshold nucleon energies are and what ranges of meson energy are possible at each angle; we are not told what meson spectra and angular distributions will actually be observed. It is the function of a correct theory to predict these spectra and angular distributions and in addition the absolute cross sections. Unfortunately, contrary to the case of photomesic production, the only approach which has led to any detailed predictions regarding single meson production in nucleon-nucleon collisions[3] is weak coupling theory. Even granting the weak coupling approximation, there are still two possible methods for calculating the nucleonic production of π mesons: the field-theoretic method and the phenomenological method.

The differences between the field-theoretic and phenomenological methods can be elucidated by comparing the production of meson quanta in nucleon-nucleon collisions with the production of light quanta in electron-nuclei collisions (ordinary bremsstrahlung). In the latter process the electron which carries along a virtual photon field cannot radiate this field unless there is a transfer of momentum to another particle, *e.g.*, a nucleus, via some interaction, *e.g.*, the Coulomb force. Analogously, the nucleon carries along a virtual meson cloud which can be radiated only upon interaction with another particle, *e.g.*, a second nucleon via the specifically nuclear interaction. The short-range character of the nuclear force in contrast to the long-range Coulomb force and the change in nucleon charge resulting from charged meson emission in contrast to conservation of charge associated with photon emission merely express the fact that charged quanta of finite rest mass are involved in one process whereas neutral quanta of zero rest mass are involved in the other.

Now it is well known that Coulombic bremsstrahlung can be treated as a second-order or third-order process in the sense of perturbation theory:[4] as a second-order process if the Coulomb potential is employed for the interaction between the electron and nucleus or as a third-order process if a consistent field-theoretic approach is adopted and the Coulomb interaction is treated as the consequence of the virtual emission and reabsorption of "longitudinal" light quanta by the electron and nucleus. The two methods of treatment are completely equivalent, although the second-order calculation is the one which is usually performed since it is simpler to carry out. In the case of nucleonic meson production, it is again simpler to perform a second-order calculation on the basis of a phenomenological nuclear potential but its equivalence to a consistent third-order field-theoretic calculation is not so obvious. As a matter of fact, if the virtual mesons responsible for the nucleon-nucleon interaction are not exclusively π mesons, the two treatments will certainly not be equivalent if only π mesons are considered in the third-order calculation. In the present state of our knowledge, both the phenomenological and field-theoretic methods possess definite advantages, and it therefore seems worth while to present both methods and to compare their theoretical predictions with each other and with experiment.

---

[3] There are alternative and almost certainly more fruitful approaches to the problem of multiple meson production in nucleon-nucleon collisions (cf. Chap. 8).

A. Field-theoretic Method. The field-theoretic method is most suitable for calculating nucleonic meson production when the two final nucleons are left in the continuum and plane waves can be taken for the unbound nucleons. If the two nucleons are left in a bound state (*i.e.*, neutron and proton as a deuteron—two like nucleons are always unbound), the phenomenological treatment is more convenient (cf. below). Consequently, it is understood that the discussion of the field-theoretic method which follows is restricted to processes which leave the nucleons unbound. If we assume that π mesons (both charged and neutral) are solely responsible for the interaction between two nucleons, it is a straightforward procedure to calculate the weak coupling cross sections for π meson production.

Let H_{NM} be the meson-nucleon interaction Hamiltonian as before; then all the matrix elements for the meson production process involve transitions which can be written symbolically in the form $H_{NM}\,H_{NM}\,H_{NM}$ (cf. Chap. 1). In general, there are eight such matrix elements when the transitions are expressed in terms of Feynman diagrams; the eight diagrams are indicated schematically in Fig. 2. In each diagram, a charged or neutral π meson is emitted by one of the nucleons in the initial or final state and a virtual π meson is exchanged between the two nucleons. The eight possibilities arise from the four possible choices of the nucleon which emits the real meson and the four possible interchanges of the two initial or two final nucleons.[5] These eight matrix elements are still smaller in number than the number which would arise in the conventional perturbation-theoretic treatment where, for example, a distinction is made between an exchange matrix element (corresponding to the sequence: virtual meson emitted → real meson emitted → virtual meson reabsorbed) and an "ordinary" matrix element (corresponding to the sequence: real meson emitted → virtual meson emitted → virtual meson reabsorbed or the sequence: virtual meson emitted → virtual meson

---

[4] Cf. W. Heitler, "The Quantum Theory of Radiation," Oxford University Press, 1947.

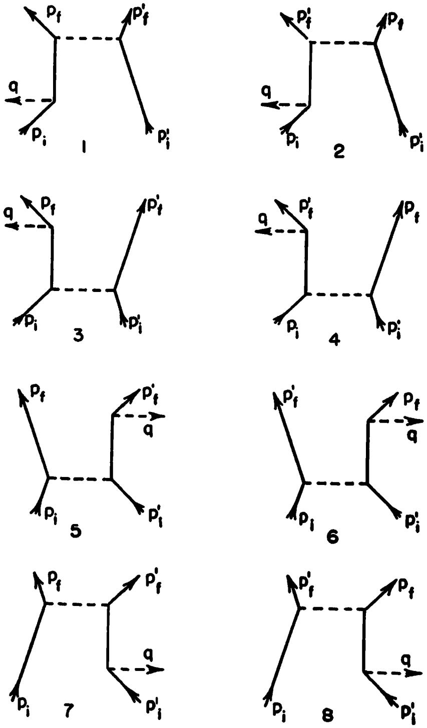

FIG. 2. Feynman diagrams for charged and neutral π meson production in a general nucleon-nucleon collision. Solid line denotes the nucleon with p_i and p'_i representing the four momenta of the initial nucleons and p_f and p'_f the four momenta of the final nucleons. Broken line denotes the π meson and q represents the four momentum of the emitted π meson.

---

[5] An alternative approach is to antisymmetrize the total wave functions of both the initial and final states of the two-nucleon system: there are then only four Feynman diagrams.

reabsorbed → real meson emitted); the Feynman method combines the "exchange" and "ordinary" terms into one diagram since the above type of ordering loses its meaning.

As an illustration of the Feynman technique, let us consider the first diagram and assume that the two colliding nucleons are a proton and a neutron and that a π^+ meson is produced. We furthermore assume that both the charged and neutral π mesons are pseudoscalar and are coupled to the nucleon through pseudoscalar coupling—the charged π meson with strength g, the neutral π meson with strength g_P or g_N depending on whether the nucleon is a proton or neutron, respectively.[6] The H_{NM} for the charged and neutral mesons are

$$\begin{aligned} H_{NM} &= g[(\psi_N^*\beta\gamma_5\psi_P)\phi_{\pi^+} + \text{c.c.}] && (\pi^\pm\text{—nucleon interaction}) \\ H_{NM} &= g_P(\psi_P^*\beta\gamma_5\psi_P)\phi_{\pi^0} && (\pi^0\text{—proton interaction}) \\ H_{NM} &= g_N(\psi_N^*\beta\gamma_5\psi_N)\phi_{\pi^0} && (\pi^0\text{—neutron interaction}) \end{aligned}$$

The other diagrams which contribute to π^+ production in neutron-proton collisions are diagrams 2 to 6. When the matrix elements corresponding to the six diagrams are added together, squared, summed, and averaged over the spins of the nucleons, the rigorous differential cross section follows immediately.[7] However, since the expression is complicated and an important effect has been neglected, *viz.*, the distortion of the final wave function by the nuclear force,[8] we merely record the nonrelativistic approximation to the cross section (which is correct to first order in the velocities of both meson and nucleons) in order to indicate the qualitative behavior for nucleon energies close to threshold and meson energies not too near the upper limit $\bar{\epsilon}_m$. In the nonrelativistic approximation, the $PS(PS)$ differential cross section in the center-of-mass system turns out to be

$$PS(PS): \qquad \frac{d\bar{\sigma}}{d\bar{\Omega}\,d\bar{\tau}} = \frac{\sqrt{\bar{\tau}(\bar{\tau}_m - \bar{\tau})}}{8\sqrt{2}\,\pi\mu M^3}\,A(n_1, n_2; S) \tag{8}$$

where $\bar{\tau} = \bar{\epsilon} - \mu$ = kinetic energy of meson in the center-of-mass system; $\bar{\tau}_m = \bar{\epsilon}_m - \mu$ = maximum kinetic energy of meson in the center-of-mass system; and $A(n_1, n_2; S)$ is a function of g, g_P, and g_N. $A(n_1, n_2; S)$

---

[6] The π^+ and π^- must both be coupled with the same strength because of gauge invariance; the π^0 nucleon coupling constant can be different for the proton and neutron. We consider the most general case where g, g_P, and g_N may all differ in both magnitude and sign although it is assumed that π^+, π^-, and π^0 possess equal masses ($\approx$ 140 Mev).

[7] Cf. M. F. Kaplon, Ph.D. Thesis, University of Rochester, 1951; cf. C. Morette, *Phys. Rev.*, **76**: 1432 (1949).

[8] Cf. K. A. Brueckner, *Phys. Rev.*, **82**: 598 (1951).

depends on the charges of the two initial nucleons ($n = \frac{1}{2}$ for proton, $n = -\frac{1}{2}$ for neutron—strictly speaking, n should be written as τ_z, the z component of the isotopic spin) and the charge of the emitted meson ($S = +1, 0, -1$ for π^+, π^0, π^-, respectively) and is given in Table 1; in the specific illustration of π^+ production in N-P collisions,

$$A(\tfrac{1}{2}, -\tfrac{1}{2}; 1) = \tfrac{1}{2}[g^6 + g_N^2(g_P + g_N)^2 g^2 + 2g^4 g_N(g_P + g_N)].$$

TABLE 1. $A(n_1, n_2; S)$ IN $PS(PS)$ THEORY

	P-P collision ($n_1 = n_2 = \frac{1}{2}$)	N-N collision ($n_1 = n_2 = -\frac{1}{2}$)	N-P collision ($n_1 = \pm\frac{1}{2}$ $n_2 = \mp\frac{1}{2}$)
π^+ ($S = 1$)	$[3g^6 + 3g^2 g_P^2(g_P + g_N)^2 - 2g^4 g_P(g_P + g_N)]$	0	$\frac{1}{2}[g^6 + g_N^2(g_P + g_N)^2 g^2 + 2g^4 g_N(g_P + g_N)]$
π^0 ($S = 0$)	$8g_P^6$	$8g_N^6$	$[4g_N^2 g_P^2(g_P^2 + g_N^2) + 2g^4(g_P + g_N)^2]$
π^- ($S = -1$)	0	$[3g^6 + 3g^2 g_N^2(g_P + g_N)^2 - 2g^4 g_N(g_P + g_N)]$	$\frac{1}{2}[g^6 + g^2 g_P^2(g_P + g_N)^2 + 2g^4 g_P(g_P + g_N)]$

Similar calculations have been performed for the $S(S)$, $PS(PV)$[9], $V(V)$, and $PV(PV)$ theories with the following results:

$$S(S): \qquad \frac{d\bar{\sigma}}{d\bar{\Omega}\,d\bar{\tau}} = \frac{\sqrt{2\bar{\tau}(\bar{\tau}_m - \bar{\tau})}}{\pi\mu^2 M^2} A(n_1, n_2; S) \tag{9}$$

where $A(n_1, n_2; S)$ is given by Table 2.

TABLE 2. $A(n_1, n_2; S)$ IN $S(S)$ THEORY

	$n_1 = n_2 = \frac{1}{2}$	$n_1 = n_2 = -\frac{1}{2}$	$n_1 = \pm\frac{1}{2}$, $n_2 = \mp\frac{1}{2}$
$S = 1$	$g^2(g^2 + g_N g_P - g_P^2)^2$	0	$\frac{1}{2}[g^2(g^2 + g_N g_P - g_N^2)^2]$
$S = 0$	0	0	0
$S = -1$	0	$g^2(g^2 + g_N g_P - g_N^2)^2$	$\frac{1}{2}[g^2(g^2 + g_N g_P - g_P^2)^2]$

$$PS(PV): \qquad \frac{d\bar{\sigma}}{d\bar{\Omega}\,d\bar{\tau}} = \frac{2M^2\bar{\tau}\sqrt{2\bar{\tau}(\bar{\tau}_m - \bar{\tau})}}{\pi\mu^7} A(n_1, n_2; S) \tag{10}$$

---

[9] The equivalence theorem for pseudoscalar fields no longer holds for nucleonic production of π mesons since the meson is emitted more than once (cf. Chap. 1); comparison of Eqs. (8) and (10) shows that PS and PV coupling lead to completely different meson spectra.

where $A(n_1, n_2; S)$ is given[10] by Table 3 (for simplicity in this section we replace f by g).

TABLE 3. $A(n_1, n_2; S)$ IN $PS(PV)$ THEORY

	$n_1 = n_2 = \frac{1}{2}$	$n_1 = n_2 = -\frac{1}{2}$	$n_1 = \pm\frac{1}{2},\quad n_2 = \mp\frac{1}{2}$
$S = 1$	$g^2[(g^2 - g_N g_P)^2 + g_P^4 + 2(2\cos^2\bar{\theta} - 1)g_P^2 \times (g_N^2 - g_N g_P)]$	0	$\frac{1}{2}g^2[(g^2 - g_N g_P)^2 + g_N^4 + 2(2\cos^2\bar{\theta} - 1)g_N^2 \times (g^2 - g_N g_P)]$
$S = 0$	0	0	$2\{(g_N^2 + g_P^2)(g^4 + g_P^2 g_N^2) - g^2 g_P g_N (g_N + g_P)^2 + (2\cos^2\bar{\theta} - 1) \times [(g_N + g_P)^2 g^2 g_P g_N - g_P^2 g_N^2 \times (g_P^2 + g_N^2) - 2g^4 g_P g_N]\}$
$S = -1$	0	0	$\frac{1}{2}g^2[(g^2 - g_N g_P)^2 + g_P^4 + 2(2\cos^2\bar{\theta} - 1)g_P^2 \times (g^2 - g_N g_P)]$

In the $V(V)$ and $PV(PV)$ theories, both longitudinal and transverse mesons are produced (with respect to the incident nucleon direction), and the cross sections predicted by the two theories can be separated into their longitudinal and transverse parts.[7] We write, for the $V(V)$ theory,

$$d\bar{\sigma} = d\bar{\sigma}_{\text{long}} + d\bar{\sigma}_{\text{trans}} \tag{11}$$

where $\dfrac{d\bar{\sigma}_{\text{long}}}{d\bar{\Omega}\, d\bar{\tau}} = \dfrac{\sqrt{2\bar{\tau}(\bar{\tau}_m - \bar{\tau})}}{\pi\mu^3 M}\cos^2\bar{\theta}\, A(n_1, n_2; S)$ with A given by Table 4 and $\dfrac{d\bar{\sigma}_{\text{trans}}}{d\bar{\Omega}\, d\bar{\tau}} = \dfrac{\sqrt{2\bar{\tau}(\bar{\tau}_m - \bar{\tau})}}{\pi\mu^3 M}\sin^2\bar{\theta}\, A(n_1, n_2; S)$ with A also given by Table 4. It is obvious that the total differential cross section is independent of $\bar{\theta}$.

TABLE 4. $A(n_1, n_2; S)$ IN $V(V)$ THEORY

	$n_1 = n_2 = \frac{1}{2}$	$n_1 = n_2 = -\frac{1}{2}$	$n_1 = \pm\frac{1}{2},\quad n_2 = \mp\frac{1}{2}$
$S = +1$	$g^2(3g^4 - 6g^2 g_P g_N + 4g_P^2 g_N^2)$	0	$\frac{1}{2}g^2 g_N^4$
$S = 0$	0	0	$(g_N - g_P)^2(g^4 - g^2 g_P g_N + g_P^2 g_N^2)$
$S = -1$	0	$g^2(3g^4 - 6g^2 g_P g_N + 4g_P^2 g_N^2)$	$\frac{1}{2}g^2 g_P^4$

---

[10] $A(n_1, n_2; S)$ is a function of $\bar{\theta}$ (the angle of meson emission in the center-of-mass system) in the $PS(PV)$ and $PV(PV)$ theories (cf. Tables 5a and 5b).

DAVID J. LANGFORD
Pure Mathematical Physics

We write the cross section predicted by the $PV(PV)$ theory in the same way as for the $V(V)$ theory, namely,

$$d\bar{\sigma} = d\bar{\sigma}_{\text{long}} + d\bar{\sigma}_{\text{trans}} \tag{12}$$

where $\dfrac{d\bar{\sigma}_{\text{long}}}{d\bar{\Omega}\, d\bar{\tau}} = \dfrac{M^2 \sqrt{\bar{\tau}(\bar{\tau}_m - \bar{\tau})}}{2\sqrt{2}\,\pi\mu^4} A_{\text{long}}(n_1, n_2; S)$ with A_{long} given by Table 5a and $\dfrac{d\bar{\sigma}_{\text{trans}}}{d\bar{\Omega}\, d\bar{\tau}} = \dfrac{M^2 \sqrt{\bar{\tau}(\bar{\tau}_m - \bar{\tau})}}{2\sqrt{2}\,\pi\mu^4} A_{\text{trans}}(n_1, n_2; S)$ with A_{trans} given by Table 5b. The total differential cross section is independent of $\bar{\theta}$ just as in the $V(V)$ theory. This statement would no longer hold for the vector or pseudovector theories if gradient coupling were employed.

TABLE 5a. $A_{\text{long}}(n_1, n_2; S)$ IN $PV(PV)$ THEORY

	$n_1 = n_2 = \frac{1}{2}$	$n_1 = n_2 = -\frac{1}{2}$	$n_1 = \pm\frac{1}{2}, \quad n_2 = \mp\frac{1}{2}$
$S = +1$	$4g^2[(g^2 - g_Pg_N)^2 + g_P^4 + 4g_P^2(g^2 - g_Pg_N)\cos^2\bar{\theta}]$	0	$2g^2[(g^2 - g_Ng_P - g_N^2)^2 + 4g_N^2(g^2 - g_Pg_N)\cos^2\bar{\theta}]$
$S = 0$	0	0	$8[(g_P + g_N)^2(g^2 - g_Pg_N)^2 + g_P^2g_N^2(g_P - g_N)^2 + 2\cos^2\bar{\theta}g_Pg_N \times (g^2 - g_Ng_P) \times (g_N^2 + g_P^2 - 2g^2)]$
$S = -1$	0	$4g^2[(g^2 - g_Pg_N)^2 + g_N^4 + 4g_N^2(g^2 - g_Pg_N)\cos^2\bar{\theta}]$	$2g^2[(g^2 - g_Ng_P - g_P^2)^2 + 4g_P^2(g^2 - g_Pg_N)\cos^2\bar{\theta}]$

TABLE 5b. $A_{\text{trans}}(n_1, n_2; S)$ IN $PV(PV)$ THEORY

	$n_1 = n_2 = \frac{1}{2}$	$n_1 = n_2 = -\frac{1}{2}$	$n_1 = \pm\frac{1}{2}, \quad n_2 = \mp\frac{1}{2}$
$S = +1$	$8g^2[(g^2 - g_Pg_N)^2 + g_P^4 - 2g_P^2(g^2 - g_Pg_N)\cos^2\bar{\theta}]$	0	$4g^2[(g^2 - g_Ng_P - g_N^2)^2 - 2g_N^2(g^2 - g_Pg_N)\cos^2\bar{\theta}]$
$S = 0$	0	0	$16[(g_P + g_N)^2 (g^2 - g_Pg_N)^2 + g_P^2g_N^2(g_P - g_N)^2 - \cos^2\bar{\theta}g_Pg_N(g^2 - g_Ng_P) \times (g_N^2 + g_P^2 - 2g^2)]$
$S = -1$	0	$8g^2[(g^2 - g_Pg_N)^2 + g_N^4 - 2g_N^2(g^2 - g_Pg_N)\cos^2\bar{\theta}]$	$4g^2[(g^2 - g_Ng_P - g_P^2)^2 - 2g_P^2(g^2 - g_Pg_N)\cos^2\bar{\theta}]$

Examination of Tables 1 to 5 reveals several interesting qualitative features which are worth noting. First, the meson spectrum predicted by a given theory depends on whether or not a gradient operator (operating on the meson wave function) is present in the meson-nucleon interaction Hamiltonian H_{NM}. Those theories which do not involve a gradient operator, such as the $S(S)$, $PS(PS)$, $V(V)$, and $PV(PV)$ theories, predict a $\bar{\tau}^{\frac{1}{2}}$ energy spectrum, whereas those theories which do involve a gradient operator, such as the $PS(PV)$ theory, predict a $\bar{\tau}^{\frac{3}{2}}$ energy spectrum. The direct coupling theories give rise to a $\bar{\tau}^{\frac{1}{2}}$ spectrum because of the presence of this term in the statistical factor occurring in the transition probability. The $\bar{\tau}^{\frac{3}{2}}$ dependence arises in the $PS(PV)$ theory because the gradient operator brings down the first power of the meson momentum in the matrix element and therefore an extra $\bar{\tau}$ in the cross section.

The second point to notice is the different angular distributions for the emitted mesons (in the center-of-mass system) predicted by the various theories. The $S(S)$ theory predicts an isotropic angular distribution, which is not surprising since this theory leads to a central force between nucleons in the lowest order of perturbation theory (cf. Table 6 below). On the other hand, the $PS(PV)$ theory predicts an anisotropic angular distribution, consistent with the fact that it yields a noncentral nuclear force in the second-order approximation. The isotropic angular distribution predicted by the $PS(PS)$ theory has no simple explanation; on the one hand, the equivalence theorem holds between the $PS(PS)$ and the $PS(PV)$ theories in so far as the nuclear force is concerned; on the other hand, the equivalence theorem breaks down for the third-order meson production process (cf. footnote 9) and presumably the anisotropic terms in the $PS(PS)$ theory are canceled out by the contributions of transitions to the negative energy states. As far as the spin 1 theories are concerned, both the $V(V)$ and the $PV(PV)$ theories lead to central nuclear forces,[11] and this is reflected in the isotropic angular distributions predicted for the sum of the longitudinal and transverse cross sections in both theories [cf. Eqs. (11) and (12)]. The dominant terms of the nucleon interaction potentials for the $S(S)$, $PS(PV)$, $V(V)$, and $PV(PV)$ theories are recorded in Table 6 [$Y(r) = e^{-Kr}/r$, $K = \mu c/\hbar$]; in writing down Table 6 it has been assumed that $g \neq g_P \neq g_N$, and the notation $\tau'_x = g\tau_x$, $\tau'_y = g\tau_y$, $\tau'_z = \begin{pmatrix} g_N & 0 \\ 0 & g_P \end{pmatrix} \tau_z$ [where τ_x, τ_y, and τ_z are the components of the ordinary isotopic spin vector and g replaces f in the

---

[11] The $PV(PV)$ theory appears to lead to a $-(\boldsymbol{\sigma}_1 \cdot \nabla)(\boldsymbol{\sigma}_2 \cdot \nabla)Y(r)$ term in addition to the central interaction: $-\boldsymbol{\sigma}_1 \cdot \boldsymbol{\sigma}_2 Y(r)$ (cf. L. Rosenfeld, "Nuclear Forces," North Holland Publishing Co., 1948); however, the noncentral term is of order $(v/c)^2$ (v is the nucleon velocity) compared with the central part and, for consistency with the assumptions underlying Tables 5a and 5b, should be neglected. In the $PS(PV)$ theory, the interaction $(\boldsymbol{\sigma}_1 \cdot \nabla)(\boldsymbol{\sigma}_2 \cdot \nabla)Y(r)$ is the only term and so must be retained.

$PS(PV)$ theory] has been employed. The operators $\boldsymbol{\sigma}_1$ and $\boldsymbol{\sigma}_2$ are the usual spin operators for the two nucleons.

TABLE 6. MESON THEORIES OF NUCLEAR FORCES

Theory	Nucleon-Nucleon Interaction
$S(S)$	$-\boldsymbol{\tau}_1' \cdot \boldsymbol{\tau}_2' Y(r)$
$PS(PV)$	$-\dfrac{\boldsymbol{\tau}_1' \cdot \boldsymbol{\tau}_2'}{\mu^2} (\boldsymbol{\sigma}_1 \cdot \nabla)(\boldsymbol{\sigma}_2 \cdot \nabla) Y(r)$
$V(V)$	$\boldsymbol{\tau}_1' \cdot \boldsymbol{\tau}_2' Y(r)$
$PV(PV)$	$-\boldsymbol{\tau}_1' \cdot \boldsymbol{\tau}_2' \boldsymbol{\sigma}_1 \cdot \boldsymbol{\sigma}_2 Y(r)$

The third important feature of Tables 1 to 5 worth noting is the relative yield predicted by the different theories for the production of positive, neutral, and negative mesons in the various types of nucleon-nucleon collisions. Interestingly enough, the $S(S)$ theory predicts zero cross section (in the nonrelativistic approximation) for the production of neutral mesons in both unlike-nucleon (neutron-proton) and like-nucleon (proton-proton and neutron-neutron) collisions, independent of the relative magnitudes and signs of g, g_P, and g_N. The $PS(PV)$ and $PV(PV)$ theories predict zero cross sections for neutral meson production in like-nucleon collisions. All other cross sections are finite in general, and the relative values depend upon the choice of the three coupling constants and can, in principle, be made completely arbitrary. The ratios of the cross sections determined by one particular choice of the three coupling constants merits special attention, *viz.*, the choice required by the so-called charge-independent hypothesis of nuclear forces. According to this hypothesis, the force between two nucleons is independent of the electric charges of the nucleons, *i.e.*, the *N-P*, *P-P*, and *N-N* forces are identical in those states allowed to all pairs of nucleons by the Pauli exclusion principle. If, in addition to the charge-independence hypothesis, it is assumed that nuclear forces are given by the lowest order (*i.e.*, second) of a correct meson-theoretic calculation,[12] then the coupling constants would be related as follows:[13] $g_N = -g_P = (1/\sqrt{2})g$. With this choice of the g's, Tables 1 to 5 reduce to expressions multiplying g^6; the results are given in a compact form in Table 7 where all quantities are expressed in units of g^6. Especially noteworthy is the zero cross section (in the nonrelativistic approximation) for π^0 production in like-nucleon collisions for all except the $PS(PS)$ theory. The nuclear potentials predicted by the various theories for the symmetrical choice of coupling constants are derived from those listed in Table 6 by replacing $\tau_1' \cdot \tau_2'$ by $g^2\tau_1 \cdot \tau_2$.

---

[12] Unfortunately, a correct theory of this character does not exist as yet.

[13] A simple way to see these relations is to recall that the *N-P* force is produced by one transfer of a π^+ from P to N, one transfer of a π^- from N to P and two transfers of π^0 between N and P; these three types of virtual meson exchange carry relative weights g^2, g^2, and $2g_Pg_N$ and a total weight $2g^2 + 2g_Pg_N$. The *P-P* force is due exclusively to two exchanges of π^0 with the weight $2g_P^2$ while the weight corresponding to the *N-N* force is $2g_N^2$. Equating the weights for the *N-P*, *P-P*, and *N-N* forces, *i.e.*, setting $2g^2 + 2g_Pg_N = 2g_P^2 = 2g_N^2$, we find $g_N = -g_P = 1/\sqrt{2}\,g$.

TABLE 7. $A(n_1, n_2; S)$ FOR SYMMETRICAL CHOICE OF COUPLING CONSTANTS

		$n_1 = n_2 = \frac{1}{2}$	$n_1 = n_2 = -\frac{1}{2}$	$n_1 = \pm\frac{1}{2},\ n_2 = \mp\frac{1}{2}$
$S = 1$	$S(S)$	0	0	0
	$PS(PS)$	3	0	$\frac{1}{2}$
	$PS(PV)$	$(3\cos^2\bar{\theta} + 1)$	0	$\frac{1}{2}(3\cos^2\bar{\theta} + 1)$
	$V(V)$	7	0	$\frac{1}{8}$
	$PV(PV)$	42	0	21
$S = 0$	$S(S)$	0	0	0
	$PS(PS)$	1	1	2
	$PS(PV)$	0	0	$(3\cos^2\bar{\theta} + 1)$
	$V(V)$	0	0	$\frac{1}{2}$
	$PV(PV)$	0	0	30
$S = -1$	$S(S)$	0	0	0
	$PS(PS)$	0	0	$\frac{1}{2}$
	$PS(PV)$	0	$(3\cos^2\bar{\theta} + 1)$	$\frac{1}{2}(3\cos^2\bar{\theta} + 1)$
	$V(V)$	0	7	$\frac{1}{8}$
	$PV(PV)$	0	42	21

B. Phenomenological Method. We have already pointed out that the nucleonic production of π mesons can be calculated as a second-order process if the force between two nucleons is represented by an empirical potential. This so-called phenomenological approach may not compare too unfavorably with the field-theoretic approach for the following reasons: (1) The π meson by itself has not yet led to a correct theory of nuclear forces, and one cannot rely too heavily on a field-theoretic calculation which uses the π meson alone to account for the momentum transfer between the nucleons. (2) The phenomenological treatment includes the large terms of the more rigorous method in all theories considered [except the $PS(PS)$ theory]; only the small[14] so-called "exchange" terms (*i.e.*, the terms which involve the emission of the real meson in the second step of the process) are neglected.

The phenomenological approach may actually possess several advantages over the field-theoretic approach: (1) the nuclear potential may be chosen so as to give the best fit to those high-energy scattering experiments which involve the large momenta transfer coming into play in the meson production process, (2) the cross section depends only on the square of the meson-nucleon constant rather than on the sixth power so that the correct value of the coupling constant is not so crucial, and (3) effects like the interaction between the nucleons in the final state can be calculated more readily (cf. below).

---

[14] The "exchange" terms are of order (μ/M) compared with the ordinary terms just above threshold except for the $PS(PS)$ theory where they dominate; the $PS(PS)$ theory is an exception because transitions to negative energy states play an essential role (cf. Brueckner, *loc. cit.*).

The Feynman diagrams for the phenomenological theory are obtained from those of Fig. 3 by collapsing the virtual meson line in each case into a point so that the two nucleons scatter each other (and thereby conserve energy and momentum) via the empirical potential. In the electron bremsstrahlung, the photon emission takes place through the interaction function $-e(\psi^*\boldsymbol{\alpha}\psi)\cdot\mathbf{A}$ (where $\boldsymbol{\alpha}$ is the Dirac operator of the electron, ψ its Dirac wave function, and $\mathbf{A}$ the electromagnetic vector potential with the gauge chosen so that the scalar potential is zero) and the electron-nucleus scattering through the Coulomb potential $(-Ze^2)/r$. In the nucleonic production of π mesons, the π emission takes place through H_{NM} (where the form of H_{NM} depends on the particular choice of meson field and coupling) and the nucleon-nucleon scattering through the static potential interaction chosen to fit the high-energy scattering experiments. Since the concept of a static potential is intrinsically nonrelativistic in character, the phenomenological method for calculating meson production by nucleons is essentially a nonrelativistic method. Consequently, the phenomenological method can be applied only to those theories of meson-nucleon interaction wherein the transitions to negative energy states are relatively unimportant and the nonrelativistic approximation to H_{NM} can be used. This is another way of saying that the phenomenological method is applicable to those theories in which the exchange terms are small compared with the ordinary terms in the field-theoretic sense (cf. footnote 14). Thus the $S(S)$, $PS(PV)$, $V(V)$, and $PV(PV)$ theories can be treated phenomenologically whereas the $PS(PS)$ theory cannot.

Once H_{NM} is fixed, the phenomenological method consists of writing down the most general static potential between two nucleons consistent with the charge independence of nuclear forces, namely,

$$V(r) = J_1(r) + \boldsymbol{\sigma}_1\cdot\boldsymbol{\sigma}_2 J_2(r) + \boldsymbol{\tau}_1\cdot\boldsymbol{\tau}_2 J_3(r) + (\boldsymbol{\sigma}_1\cdot\boldsymbol{\sigma}_2)(\boldsymbol{\tau}_1\cdot\boldsymbol{\tau}_2)J_4(r) + S_{12}J_5(r) + \boldsymbol{\tau}_1\cdot\boldsymbol{\tau}_2 S_{12}J_6(r) \quad (13)$$

where the J_i contain the radial dependence of the force (and may all be distinct), $\boldsymbol{\sigma}$ and $\boldsymbol{\tau}$, as before, are the spin and isotopic spin operators, and $S_{12} = [3(\boldsymbol{\sigma}_1\cdot\mathbf{r})(\boldsymbol{\sigma}_2\cdot\mathbf{r})/\mathbf{r}^2] - \boldsymbol{\sigma}_1\cdot\boldsymbol{\sigma}_2$ is the tensor operator; the J_i are then chosen to give the best fit to the high-energy neutron-proton and proton-proton scattering experiments.

In order to understand more clearly the power and limitation of the phenomenological method, we discuss first the results of calculations of the nucleonic meson production cross sections which can be compared directly with the cross sections derived by means of the field-theoretic method. If we examine Table 6, it is seen that the $S(S)$, $V(V)$, and $PV(PV)$ theories contain terms of types J_1–J_4 and the $PS(PV)$ theory contains terms of types J_5 and J_6. If the charge-independence hypothesis is adopted,[14a] the $S(S)$, $V(V)$, and $PV(PV)$ theories involve only J_3 and J_4 and the $PS(PV)$ theory only J_6. If now the nonrelativistic approximations to the corresponding H_{NM}'s are used, it turns out, not unexpectedly, that the resulting cross sections are identical with the field-theoretic expressions. The fact that the phenomenological method leads to the same meson energy spectra, angular distributions, and relative ratios of charge and neutral meson production as does the nonrelativistic field-theoretic method is extremely useful to know. On the basis of this result, it seems justified to employ the phenomenological method for more complicated meson problems (*e.g.*, for nuclei heavier than the proton) and to study the nucleon-nucleon meson production process with J's giving a more satisfactory fit of the high-energy nucleon-nucleon scattering experiments than do any of the nuclear potentials listed in Table 6.

It is soon realized that the phenomenological method will lead to an isotropic angular distribution for the mesons in the center-of-mass system as long as the nuclear force has no noncentral component (*i.e.*, independent of the relative contributions of J_1, J_2, J_3, and J_4). This is the reason why the first phenomenological calculations of the nucleonic meson production carried out by Foldy and Marshak[15] for the symmetric $PS(PV)$ theory led to an isotropic angular distribution for the mesons; a central nucleon-nucleon potential was fitted at that time to the high-energy neutron-proton experiments since the proton-proton experiments had not yet been performed. However, the phenomenological method leads to an anisotropic angular distribution for the mesons in the center-of-mass system as soon as a noncentral force is assumed to operate between the nucleons.[16] This is in agreement with the anisotropic angular distributions predicted by the phenomenological $PS(PV)$ theory on the basis of the noncentral static potential listed in Table 6. It should be remarked that even a purely central force between nucleons will lead to an anisotropic angular distribution for the mesons provided that the nonrelativistic approximation is not made for both mesons and nucleons but only for the nucleons, *i.e.*, provided that the meson momentum q is not assumed small compared with the nucleon momentum p. As soon as q becomes comparable with p, that is, as one moves away from threshold, a new direction is provided and deviations from isotropy will set in even for a pure central nuclear force.

[14a] Table 6 assumes only one kind of π^0 meson; it is possible to assume the existence of a second kind of neutral meson which is coupled to proton and neutron with the same sign of mesic charge and which leads to charge-independent forces of the type J_1, J_2, or J_5.

[15] L. Foldy and R Marshak, *Phys. Rev.*, **85**: 1493 (1949); cf. also C. Morette, Thèse de doctorat, Sorbonne, 1947.

[16] Cf. "Note added in proof" in the first reference of footnote 15.

Unfortunately, none of the static potentials listed in Table 6 can explain *both* the high-energy neutron-proton and proton-proton scattering experiments. Thus the strongly singular tensor force predicted by the $PS(PV)$ theory can explain the large absolute cross section and isotropic angular distribution for proton-proton scattering at high energies ($\boldsymbol{\tau}_1' \cdot \boldsymbol{\tau}_2' = g_P^2$ for two protons). On the other hand, the $PS(PV)$ symmetric static potential cannot explain, at least in its weak coupling formulation, the relatively small absolute cross section and symmetrical behavior (about 90° in the center-of-mass system) for neutron-proton scattering at high energies. A good fit of the neutron-proton high-energy scattering data is obtained with a static potential of the form[17]

$$V(r) = -g_{NP}^2 \frac{(1 + P_M)}{2} Y(r) \tag{14}$$

where P_M is the Majorana operator. Consequently, if one wishes to carry out a realistic nucleonic meson production calculation on the basis of the phenomenological method, one may relinquish the charge-independent nuclear force hypothesis and use the $PS(PV)$ potential for the P-P interaction and Eq. (14) for the N-P interaction. This choice of the N-P and P-P interactions is certainly not unique, but it does provide a reasonably good fit of the high-energy scattering experiments. Brueckner[8] has computed the meson production cross section on the basis of these interactions and a symmetric H_{NM} for the meson-nucleon interaction and finds that charged meson production cross sections no longer vanish for the $S(S)$ theory (cf. Table 7), although the vanishing cross sections for π^0 production in like-nucleon collisions continue to vanish. All cross sections which do not vanish on the charge-independent hypothesis stay finite, although in some cases the values change.

Both the field-theoretic and phenomenological cross sections thus far considered are based on the plane-wave approximation for the two final nucleons. However, before comparing with experiment, it is necessary to take account of the interaction between the two final nucleons, *i.e.*, to consider the distortion of the plane-wave function by the nuclear potential. It is clear that, for a given initial nucleon energy, the distortion will be greater, the lower the relative energy of the two final nucleons, *i.e.*, the greater the energy of the emitted meson. For this reason, it suffices to take into account the effect of the nuclear potential on the triplet S and singlet S state of the two final nucleons (of course, if the two final nucleons are identical, only the singlet S state need be considered). For initial nucleon energies reasonably close to threshold, it is a good approximation to regard the meson as emitted in the center-of-mass system with relative orbital angular momentum $l = 0$ or 1. Assuming that the two final nucleons are emitted in an S state and the mesons

---

[17] R. Christian and E. Hart, *Phys. Rev.*, **77**: 441 (1950).

TABLE 8. TRANSITIONS ALLOWED FOR THE REACTION $P + P \rightarrow N + P + \pi^+$ NEAR THRESHOLD

Meson field	Meson in s state	Meson in p state
Scalar.................	${}^1S_0 \rightarrow {}^1S_0$	${}^3P_1 \rightarrow {}^1S_0$ ${}^3P_{0,1,2} \rightarrow {}^3S_1$
Pseudoscalar...........	${}^3P_0 \rightarrow {}^1S_0$ ${}^3P_1 \rightarrow {}^3S_1$	${}^1S_0,\ {}^1D_2 \rightarrow {}^3S_1$
Vector.................	${}^3P_1 \rightarrow {}^1S_0$ ${}^3P_{0,1,2} \rightarrow {}^3S_1$	${}^1S_0,\ {}^1D_2 \rightarrow {}^3S_0$ ${}^1S_0,\ {}^1D_2 \rightarrow {}^3S_1$
Pseudovector..........	${}^1S_0,\ {}^1D_2 \rightarrow {}^3S_1$	${}^3P_{0,1,2} \rightarrow {}^1S_0$ ${}^3P_{0,1,2},\ {}^3F_{2,3} \rightarrow {}^3S_1$

TABLE 9. TRANSITIONS ALLOWED FOR THE REACTION $P + P \rightarrow P + P + \pi^0$ NEAR THRESHOLD

Meson field	Meson in s state	Meson in p state
Scalar..........................	${}^1S_0 \rightarrow {}^1S_0$	${}^3P_1 \rightarrow {}^1S_0$
Pseudoscalar...................	${}^3P_0 \rightarrow {}^1S_0$	Forbidden
Vector..........................	${}^3P_1 \rightarrow {}^1S_0$	${}^1S_0,\ {}^1D_2 \rightarrow {}^1S_0$
Pseudovector..................	Forbidden	${}^3P_{0,1,2} \rightarrow {}^1S_0$

TABLE 10. TRANSITIONS ALLOWED FOR THE REACTIONS $N + P \rightarrow N + N + \pi^+$, $N + P \rightarrow P + P + \pi^-$ NEAR THRESHOLD

Meson field	Meson in s state	Meson in p state
Scalar................	${}^1S_0 \rightarrow {}^1S_0$	${}^1P_1,\ {}^3P_1 \rightarrow {}^1S_0$
Pseudoscalar........	${}^3P_0 \rightarrow {}^1S_0$	${}^3S_1,\ {}^3D_1, \rightarrow {}^1S_0$
Vector................	${}^1P_1,\ {}^3P_1 \rightarrow {}^1S_0$	${}^1S_0,\ {}^3S_1,\ {}^1D_2,\ {}^3D_{1,2} \rightarrow {}^1S_0$
Pseudovector.........	${}^3S_1,\ {}^3D_1 \rightarrow {}^1S_0$	${}^1P_1,\ {}^3P_{0,1,2},\ {}^3F_2 \rightarrow {}^1S_0$

TABLE 11. TRANSITIONS ALLOWED FOR THE REACTION $N + P \rightarrow N + P + \pi^0$ NEAR THRESHOLD

Meson field	Meson in *s* state	Meson in *p* state
Scalar	${}^1S_0 \rightarrow {}^1S_0$	${}^1P_1,\ {}^3P_1 \rightarrow {}^1S_0$
	${}^3S_1,\ {}^3D_1 \rightarrow {}^3S_1$	${}^1P_1,\ {}^3P_{0,1,2},\ {}^3F_2 \rightarrow {}^3S_1$
Pseudoscalar	${}^3P_0 \rightarrow {}^1S_0$	${}^3S_1,\ {}^3D_1 \rightarrow {}^1S_0$
	${}^1P_1,\ {}^3P_1 \rightarrow {}^3S_1$	${}^1S_0,\ {}^3S_1,\ {}^1D_2,\ {}^3D_{1,2} \rightarrow {}^3S_1$
Vector	${}^1P_1,\ {}^3P_1 \rightarrow {}^1S_0$	${}^1S_0,\ {}^3S_1,\ {}^1D_2,\ {}^3D_{1,2} \rightarrow {}^1S_0$
	${}^1P_1,\ {}^3P_{0,1,2},\ {}^3F_2 \rightarrow {}^3S_1$	${}^1S_0,\ {}^3S_1,\ {}^1D_2,\ {}^3D_{1,2,3} \rightarrow {}^3S_1$
Pseudovector	${}^3S_1,\ {}^3D_1 \rightarrow {}^1S_0$	${}^1P_1,\ {}^3P_{0,1,2},\ {}^3F_2 \rightarrow {}^1S_0$
	${}^1S_0,\ {}^3S_1,\ {}^1D_2,\ {}^3D_{1,2} \rightarrow {}^3S_1$	${}^1P_1,\ {}^3P_{0,1,2},\ {}^1F_3,\ {}^3F_{2,3} \rightarrow {}^3S_1$

in an $l = 0$ or $l = 1$ state, Tables 8 to 11 list,[18] on the basis of angular momentum and parity considerations, what transitions contribute to the various production processes for each of the four fields (these transitions do not depend on whether the coupling is direct or derivative).

Tables 8 to 11 reveal some interesting selection rules for π meson production near threshold. For example, in the reaction $P + P \rightarrow P + N + \pi^+$, if mesons are emitted only into the *s* state, the scalar field would allow transitions only into the singlet *S* state for the final neutron and proton, whereas the pseudovector theory would allow transitions only to the triplet *S* state for the final neutron-proton system. On the other hand, if in the same reaction mesons are emitted only into the *p* state, the pseudoscalar theory would allow transitions only to the triplet *S* state for the final neutron-proton system. Even stronger selection rules emerge for the reaction $P + P \rightarrow P + P + \pi^0$ where the transition is completely forbidden for the pseudovector field if mesons are emitted into the *s* state and is forbidden for the pseudoscalar field if mesons are emitted exclusively into the *p* state. It is clear that the same reaction involves transitions only to the singlet *S* state for the final proton-proton system because of the operation of the Pauli exclusion principle. None of the transitions for the reaction $N + P \rightarrow N + N + \pi^+$ and $N + P \rightarrow P + P + \pi^-$ are forbidden for any of the four fields although again the Pauli exclusion principle permits transitions only to the singlet *S* state for the two final nucleons. Finally, no transitions are excluded for the reaction $N + P \rightarrow N + P + \pi^0$ because of the operation of the Pauli exclusion principle or by angular momentum and parity conservation. The selection rules which appear in Tables 8 to 11 exclude certain transitions independent of whether the meson-nucleon interaction is via direct or gradient coupling. However, over and above these selection rules are such effects as the cancellation of matrix elements associated with a particular type of coupling and the character of the nonrelativistic approximation to H_{NM}. This explains why Tables 1 to 5 contain many more vanishing cross sections than are required by the selection rules implied in Tables 8 to 11 [*e.g.*, the vanishing of the π^0 cross sections in the $S(S)$ theory, the vanishing of the π^0 cross sections in like-nucleon collisions for the $V(V)$ theory, etc.] and why the $PS(PS)$ theory leads to a finite cross section for π^0 production in like-nucleon collisions whereas the $PS(PV)$ theory leads to a zero cross section (pseudovector coupling yields mesons in p states, whereas pseudoscalar coupling yields s-state mesons).

---

[18] Cf. K. Watson and K. Brueckner, *Phys. Rev.*, **83**: 1 (1951).

In all cases where the meson production processes involve transitions either to the singlet S or triplet S state (as indicated by Tables 8 to 11) for the two final nucleons, there is a simple way for obtaining a good estimate of the effect of the nuclear force. Assuming a square well potential between the two final nucleons—a triplet well of magnitude V_t and a singlet well of magnitude V_s, both of range a—the plane-wave cross sections should be multiplied by the factor[19]

$$\frac{p^2 + MV_{t,s}}{p^2 + MV_{t,s}\cos^2\left(a\sqrt{p^2 + MV_{t,s}}\right)} \tag{15}$$

where p is the relative momentum of the two nucleons in the center-of-mass system and the triplet potential is used for transitions to triplet S states and the singlet potential correspondingly. If a particular reaction involves transitions which go to both singlet S and triplet S states for the final two nucleons, it is necessary to break up the total matrix element into its component singlet and triplet parts and to multiply each component by the appropriate correction factor. It is clear from Eq. (15) that the corrected cross sections will be larger than the uncorrected "plane-wave" cross sections, the more so the lower the kinetic energies of the final nucleons. Equation (15) is actually proportional to the square of the continuum wave function $\psi_c(0)$ for the two final nucleons in the center-of-mass system evaluated at zero relative distance.

We have been discussing the five possible reactions involving the collision of two free nucleons which may lead to the production of π mesons. Of these five reactions, two, *viz.*, the production of π^+ mesons in proton-proton collisions and the production of π^0 mesons in neutron-proton collisions, lead to a neutron and proton in the final state. Since for initial nucleon energies reasonably close to threshold, the triplet S interaction between the final neutron and proton is very strong, the question naturally arises whether the reactions $P + P \rightarrow D + \pi^+$ and $N + P \rightarrow D + \pi^0$

---

[19] Cf. E. Fermi, "Elementary Particles," Yale University Press, 1951.

seriously compete with the reactions $P + P \rightarrow P + N + \pi^+$ and $N + P \rightarrow N + P + \pi^0$, respectively. The question was first answered in the affirmative by Brueckner[8] for the proton-proton reaction leading to π^+ production by inserting the value of the deuteron function at the origin, *i.e.*, $\psi_D(0) = \sqrt{MV_t}(\sqrt{M\epsilon_t}/2\pi)^{\frac{1}{2}}$ (ϵ_t is the deuteron binding energy) in place of the continuum function $\psi_c(0)$ [cf. Eq. (15)], and changing the statistical factor to take account of the fact that two particles are now emitted (D and π^+) instead of three (N, P, and π^+). However, Brueckner's oversimplified treatment of the process predicts an isotropic angular distribution for the π^+ mesons in the center-of-mass system, and this prediction is in sharp disagreement with the available experimental material (cf. Sec. 4 below).

An improved calculation of the cross section for the reaction $P + P \rightarrow D + \pi^+$ has been carried out by Cheston[20] for each of the four theories $S(S)$, $PS(PV)$, $V(V)$, and $PV(PV)$. Cheston restricts himself to initial proton energies less than 500 Mev (and therefore to meson energies in the center-of-mass system less than 100 Mev) so that it is a reasonable approximation to treat the nucleons nonrelativistically. The matrix element for the reaction, regarded as a first-order process, is written in the form

$$M = \sum_{j=1}^{2} \int \Psi_f^*(\mathbf{r}_j, \boldsymbol{\sigma}_j, \boldsymbol{\tau}_j) 0 \Psi_i(\mathbf{r}_j, \boldsymbol{\sigma}_j, \boldsymbol{\tau}_j) d\mathbf{r}_1\, d\mathbf{r}_2 \tag{16}$$

where $\mathbf{r}_j$, $\boldsymbol{\sigma}_j$, and $\boldsymbol{\tau}_j$ represent the space, spin, and isotopic spin of the jth nucleon, 0 is the operator which is responsible for the emission of the π^+ meson and takes the two initial protons into the final deuteron, and Ψ_i and Ψ_f are the wave functions of the initial and final states of the two-nucleon system. Since the calculation is phenomenological, it is necessary to use nonrelativistic expressions for the meson-nucleon interaction Hamiltonian which are valid to first order in the velocity of the nucleons but completely accurate as far as the mesons are concerned. Such nonrelativistic approximations follow immediately for those interactions which contain only even operators, *i.e.*, the $S(S)$ and $PV(PV)$ theories, but can also be derived for those interactions which contain odd operators, *i.e.*, the $PS(PV)$ and $V(V)$ theories, by means of a method due to Foldy and Wouthuysen.[21] The nonrelativistic meson-nucleon interactions corresponding to the four theories are listed in Table 12 where the symbols are defined as follows: ϕ is the meson wave function (outgoing plane wave), $\mathbf{q}$ the meson momentum, ϵ is the meson energy, and $\mathbf{p}_i$ and $\mathbf{p}_f$ are the initial and final nucleon momenta. The expressions in Table 12 are more accurate—to one order in the nucleon velocity—than those employed in deriving Tables 2 to 5.

---

[20] W. B. Cheston, *Phys. Rev.*, **83**: 1118 (1951); cf. also Gunn, Power, and Touschek, *Phys. Rev.*, **81**: 277 (1951).

[21] L. Foldy and S. Wouthuysen, *Phys. Rev.*, **78**: 29 (1950). The Foldy-Wouthuysen technique can also be applied to the $PS(PS)$ theory, but a phenomenological calculation is very questionable because of the importance of the negative energy states (cf. footnote 8).

TABLE 12. MESON-NUCLEON INTERACTION OPERATORS AND THEIR NONRELATIVISTIC APPROXIMATIONS

Theory	Interaction operator	Nonrelativistic approximation
$S(S)$	$g\beta\phi$	$g\phi$
$PS(PV)$	$i\frac{f}{\mu}\beta\gamma_5\gamma_\nu\frac{\partial\phi}{\partial x_\nu}$	$-\frac{f}{\mu}\left[\boldsymbol{\sigma}\cdot\mathbf{q}-\frac{\epsilon}{2M}\boldsymbol{\sigma}\cdot(\mathbf{p}_i+\mathbf{p}_f)\right]\phi$
$V(V)$	$ig\beta\gamma_\nu\phi_\nu$	$\frac{g}{2M}\left[\left(\mathbf{p}_i+\mathbf{p}_f-\frac{2M}{\epsilon}\mathbf{q}\right)\cdot\boldsymbol{\phi}+i\boldsymbol{\sigma}\cdot(\mathbf{p}_f-\mathbf{p}_i)\times\boldsymbol{\phi}\right]$
$PV(PV)$	$ig\beta\gamma_5\gamma_\nu\phi_\nu$	$g\boldsymbol{\sigma}\cdot\boldsymbol{\phi}$

Let us consider the angular distributions (in the center-of-mass system) which would be expected on qualitative grounds for the emitted π^+ mesons for each of the four theories. Examination of Table 12 reveals that at least to first order in the nucleon velocity, the nonrelativistic approximations to all four theories allow emission of s-state mesons. Now just at threshold, the π^+ meson must be emitted in an s state, and Table 8 shows that the initial state of the two-proton system from which transitions can take place are for the four theories:

$$\begin{aligned} S(S)\colon\ & \text{none} & V(V)\colon\ & {}^3P_{0,1,2} \\ PS(PV)\colon\ & {}^3P_1 & PV(PV)\colon\ & {}^1S_0 \text{ and } {}^1D_2 \end{aligned} \tag{17}$$

Consequently, we would expect an isotropic distribution of π^+ mesons for the pseudoscalar, vector, and pseudovector theories at threshold since there is no reference axis to fix the direction of the meson. On the other hand, since no transition exists which leads to the emission of a scalar π^+ meson in an s state, the emission of scalar mesons must take place into p states or higher. This supplies for scalar mesons a final-state reference axis and yields an angular distribution for the mesons which vanishes at 90° with respect to the incident proton beam. (By the same token, the cross section for the emission of scalar mesons will start out at a much smaller value near threshold than the cross section for the emission of pseudoscalar, vector, or pseudovector mesons—cf. below.) As the incident proton energy increases above the threshold value, the π^+ meson begins to be emitted into a p state. In the case of the pseudoscalar and vector theories, it is seen from Table 12 that p-

state meson emission soon competes with *s*-state meson emission; this is not the case for the scalar and pseudovector theories where *s*-state meson emission continues to be predominant. However, in order to achieve anisotropy in the angular distribution of mesons, it is not only necessary to emit the mesons into a nonsymmetric state, but it is also necessary that the initial and final two-nucleon systems exist in nonsymmetric states. Reexamination of Table 8 shows that the initial states of the di-proton system from which transitions can lead to *p*-state meson emission are the $^1S_0$ and $^1D_2$ states. Therefore, despite the fact that in the pseudoscalar and vector theories *p*-state meson emission originates in a nonsymmetric two-proton state, *viz.*, the $^1D_2$, it also arises from the symmetric $^1S_0$ state. Thus, if one uses plane waves for the di-proton system and a $^3S_1$ wave function for the final deuteron, one would not expect an appreciably greater anisotropy in the angular distribution for the pseudoscalar and vector theories than for the pseudovector theory (the anisotropy will be very marked for the scalar theory since *p*-state meson emission—which is required by the Pauli exclusion principle although the interaction operator allows *s*-state emission—originates in a triplet *P* state of the initial di-proton system). These remarks are verified by the curves shown in Fig. 3, where the angular distribution of the emitted π^+ mesons (in the center-of-mass system) is plotted up for each of the four theories at an incident proton energy of 340 Mev. Of course, the anisotropy in the meson angular distribution would be greatly increased if the *N-P* and *P-P* potentials were very singular at small distances and somehow the high Fourier components of the $^3D_1$ part of the deuteron wave function and the $^1D_2$ state of the di-proton system were weighted very heavily compared with the $^3S_1$ and $^1S_0$ states, respectively. We shall see in Sec. 4 that there is indeed experimental evidence for this necessity.

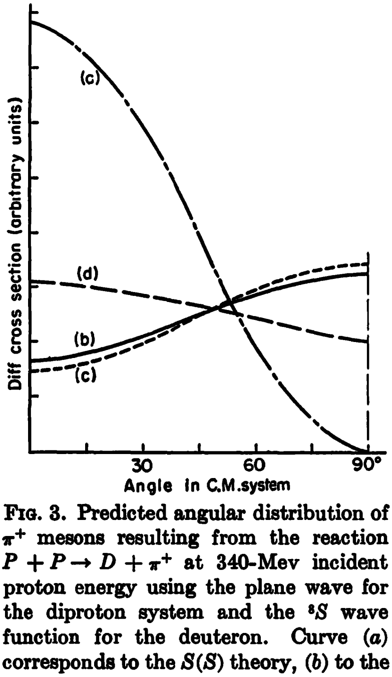

FIG. 3. Predicted angular distribution of π^+ mesons resulting from the reaction $P + P \rightarrow D + \pi^+$ at 340-Mev incident proton energy using the plane wave for the diproton system and the ^3S wave function for the deuteron. Curve (*a*) corresponds to the *S*(*S*) theory, (*b*) to the *PS*(*PV*) theory, (*c*) to the *V*(*V*) theory, (*d*) to the *PV*(*PV*) theory.

While the angular distribution of the π^+ mesons produced in the reaction $P + P \rightarrow D + \pi^+$ may be altered by a more careful treatment of the nucleon-nucleon interaction effects, it seems worth while to list in Table 13 the total cross sections predicted by each of the four theories on the basis of the plane wave approximation for the initial di-proton system and the ^3S character of the final deuteron state. Values are given for four incident proton energies, and it is thought that the variation of the cross sections with energy may be significant even if the absolute values may be somewhat in question. Examination of Table 13 reveals some interesting qualitative trends for the four theories: the spin 1 theories show a very small increase (no more than a factor 2) over the entire energy region 300 to 500 Mev for the incident proton. On the other hand, the spin zero theories exhibit a more rapid increase in cross section over the same energy region, by at least a factor 4 (although the absolute values of the scalar cross sections are down by a factor 10 compared with the pseudoscalar cross sections for the reason cited above).

TABLE 13. TOTAL CROSS SECTION FOR REACTION $P + P \rightarrow D + \pi^+$
(In units of 10^{-28} cm^2)

Theory	Proton → energy	302 Mev	340	394	494
$S(S)$	$\times g^2/\hbar c$	0.15	1.14	2.4	2.8
$PS(PV)$	$\times f^2/\hbar c$	2.2	5.3	7.9	8.6
$V(V)$	$\times g^2/\hbar c$	0.85	1.1	0.75	0.47
$PV(PV)$	$\times g^2/\hbar c$	6.1	10.8	11.2	11.8

Similar calculations can be carried out for the reaction $N + P \rightarrow D + \pi^0$, although the qualitative differences between the various theories will not be so striking because no states are excluded (by the Pauli principle) for the initial neutron-proton system.[21a]

4. Comparison of Theory with Experiment

Despite obvious deficiencies in the experimental data on the nucleon-nucleon production of π mesons at the present time, the data which do exist are so striking that some important insights are gained into the mechanism of nucleonic production of π mesons. The only nucleon-nucleon experiments which have been carried out thus far deal with the production of π^+ and π^0 mesons in P-P collisions. In the future, it should be possible to perform experiments on the production of π^+, π^-, and π^0 mesons in *N*-*P* collisions.

[21a] A. M. L. Messiah [*Phys. Rev.*, **86**: 430 (1952)] has recently shown that if the charge independence hypothesis holds for nucleons and π mesons, the cross section for the reaction $N + P \rightarrow D + \pi^0$ will be exactly one-half of the cross section for the reaction $P + P \rightarrow D + \pi^+$ at all energies and angles. The same charge independence hypothesis leads to a general relation among the total cross sections for π^0 and π^+ production in P-P and N-P collisions, namely: $\sigma_{NP}(\pi^0) + \sigma_{PP}(\pi^0) = \sigma_{NP}(\pi^+) + \frac{1}{2}\sigma_{PP}(\pi^+)$.

Several experiments have been performed at Berkeley on the π^+ production in *P*-*P* collisions. Richman and Wilcox,[22] Cartwright,[23] and most recently Whitehead and Richman[24] have used a subtraction technique (subtracting the π^+ production in proton-carbon collisions from the corresponding numbers in proton-polyethylene collisions) and Peterson[25] and Peterson *et al.*[26] have used liquid hydrogen. In both sets of experiments, the π^+ mesons were detected by means of photographic plates and the incident proton energy was 340 Mev. The π^+ spectrum was first obtained by Richman and Wilcox at 0° with respect to the incident proton direction on the basis of 1137 mesons; by integrating under their curve, Richman and Wilcox derived an approximate value of 1.5×10^{-28} cm^2/ster for $(d\sigma/d\Omega)_{\text{lab}}$ at 0°. Peterson then took two runs in his experiment at 30°, one with a "line source" of liquid hydrogen and the other with a "point" source; although the statistics were poor—115 and 487 mesons in the respective runs—it was apparent that the

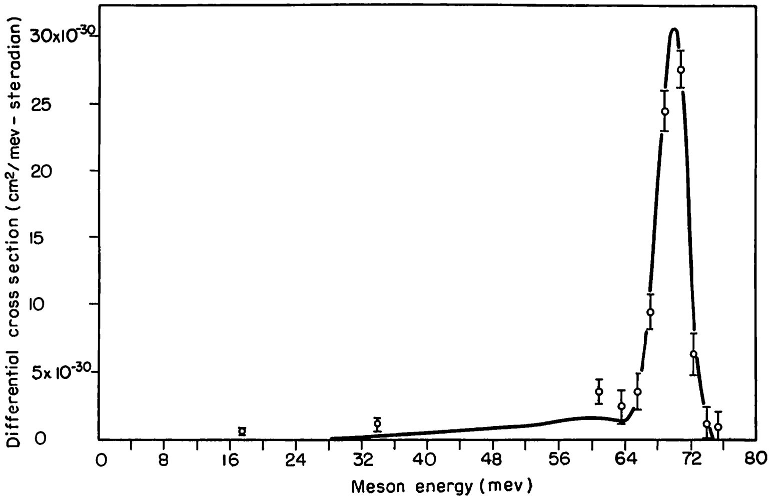

FIG. 4. Measured π^+ spectrum from hydrogen at 0° in the laboratory system for 340-Mev incident protons. Solid curve is the theoretical curve calculated on the assumption that the π^+ meson is emitted into a *p* state and the nucleons into a ^3S state.

---

[22] Cartwright, Richman, Whitehead, and Wilcox, *Phys. Rev.*, **78**: 823 (1950).

[23] W. F. Cartwright, Ph.D. Thesis, University of California, 1951.

[24] W. Whitehead and C. Richman, *Phys. Rev.*, **83**: 855 (1951).

[25] V. Z. Peterson, *Phys. Rev.*, **79**: 407 (1951).

[26] Peterson, Iloff, and Sherman, *Phys. Rev.*, **84**: 372 (1951).

cross section was down by a factor of at least 2 compared with 0°. More recently, Peterson *et al.* have measured the π^+ spectrum at laboratory angles of 18, 30, and 64° with a point source of liquid hydrogen and have found cross sections of $1.6^{+0.3}_{-0.2} \times 10^{-28}$ cm^2/ster (based on 885 mesons), $0.58^{+0.12}_{-0.06} \times 10^{-28}$ cm^2/ster (based on 482 mesons), and $0.07^{+0.04}_{-0.02} \times 10^{-28}$ cm^2/ster (based on 22 mesons), respectively. Whitehead and Richman also measured the π^+ spectrum at 60° and found a cross section of about 0.08×10^{-28} cm^2/ster. The most accurate π^+ spectrum which has been measured up to the present is the remeasurement of the π^+ spectrum carried out by Cartwright at 0°. His results are given in Table 14: column 1 lists the energies of the π^+ mesons (obtained from a knowledge of the thickness of aluminum-copper absorber traversed by the group of mesons in question), column 2 the uncorrected differential cross section with the statistical probable error, and column 3 the differential cross section corrected for nuclear absorption of the π^+ mesons by the aluminum-copper absorber (assuming nuclear area for the meson absorption cross section). The points in Fig. 4 are the experimental points corresponding to the corrected differential cross section as a function of meson energy, whereas the solid curve in Fig. 4 is a theoretical curve computed on the assumption that the π^+ meson is emitted into a p state and that the neutron and proton leave in a ^3S state (either bound or unbound—cf. below).

TABLE 14. DIFFERENTIAL CROSS SECTION AT 0° FOR π^+ MESON PRODUCTION AT 340-MEV INCIDENT PROTON ENERGY

Meson energy, Mev	$\frac{d\sigma}{d\Omega\, d\tau}$ (in units of 10^{-30} cm^2/Mev/ster)	$\left(\frac{d\sigma}{d\Omega\, d\tau}\right)_{\text{corr}}$
17.5	0.6 ± 0.3	0.6
34.0	1.1 ± 0.4	1.2
60.9	2.0 ± 0.9	2.4
63.8	1.3 ± 1.0	1.6
65.7	2.4 ± 1.3	2.9
67.2	7.4 ± 1.3	9.0
68.8	20.0 ± 1.4	24.3
70.7	22.3 ± 1.5	27.7
72.3	5.1 ± 1.4	6.5
73.5	1.2 ± 1.2	1.5
75.6	1.0 ± 1.2	1.4

The integral over the solid curve in Fig. 4 yields a cross section

$$\left(\frac{d\sigma}{d\Omega}\right)_{\text{lab}} = 2.0 \pm 0.4 \times 10^{-28}\ \text{cm}^2/\text{ster at } 0^\circ$$

Table 15 lists the measured cross sections at the four angles together with the statistical errors.[27]

TABLE 15. TOTAL DIFFERENTIAL CROSS SECTION FOR π^+ MESON PRODUCTION AS A FUNCTION OF ANGLE AT 340-MEV INCIDENT PROTON ENERGY

Lab Angle°	$\left(\frac{d\sigma}{d\Omega}\right)_{\text{lab}}$ (in units of 10^{-28} cm²/ster)
0	2.00 ± 0.40
18	$1.6\ {}^{+0.3}_{-0.2}$
30	$0.58\ {}^{+0.12}_{-0.06}$
60	$0.07\ {}^{+0.04}_{-0.02}$

None of the field-theoretic or phenomenological theories can explain the shape of the π^+ spectrum shown in Fig. 4 as long as it is assumed that the process which takes place is $P + P \rightarrow P + N + \pi^+$ and plane waves are used for the final neutron and proton. Thus neither the $\bar{\tau}^{\frac{1}{2}}$ spectrum predicted by the $S(S)$, $PS(PS)$, $V(V)$, and $PV(PV)$ theories nor even the $\bar{\tau}^{\frac{3}{2}}$ spectrum predicted by the $PS(PV)$ theory yields the tremendous high-energy peak in the π^+ spectrum. Since, at an incident proton energy of 340 Mev, the kinetic energy available in the center-of-mass system is approximately 20 Mev, most of which is taken up by the π^+ meson, the proton and neutron share only several Mev together. At such low proton and neutron energies, the N-P scattering cross section is known to be large (*i.e.*, several barns) and consequently implies a strong N-P interaction which favors the emission of high-energy π^+ mesons. It is precisely this effect which was taken into account by Eq. (15), although it can be shown that the enhancement predicted by Eq. (15) is not sufficient to explain the high-energy peak. If it is recalled that the same considerations which enhance the high-energy π^+ production in the reaction (*a*) $P + P \rightarrow P + N + \pi^+$ predict larger cross sections for the reaction (*b*) $P + P \rightarrow D + \pi^+$, it follows that the measured π^+ spectrum is a combination of the spectra associated with both reactions (*a*) and (*b*). Now, reaction (*b*) leads, at an incident proton energy of 340 Mev and a laboratory angle of 0°, to a high-energy π^+ line displaced by 4 Mev with respect to the upper end of the continuous π^+

---

[27] There is one preliminary measurement of the cross section for π^+ production in P-P collisions at Columbia by Block, Passman, and Havens [*Phys Rev.*, **83**: 167 (1951)]; their result is $(d\sigma/d\Omega)_{\text{lab}}$ (90°) $= 5.0 \pm 1\ 2 \times 10^{-29}$ cm²/ster corresponding to an incident proton energy of 381 Mev. If it is assumed that the angular distribution of the π^+ mesons is the same at 381 Mev as at 340 Mev (*i.e.*, essentially $\cos^2 \bar{\theta}$) and that two-thirds of the cross section (cf. below) is due to the reaction $P + P \rightarrow D + \pi^+$, the above value at 90° implies a total cross section for the reaction $P + P \rightarrow D + \pi^+$ of $4.8 \pm 1.6 \times 10^{-28}$ cm² at 381 Mev compared with $1.6 \pm 0.5 \times 10^{-28}$ cm² at 340 Mev (cf. below). The ratio is 3 ± 1 and is somewhat greater than the simple $PS(PV)$ theory (cf. Table 13) would predict.

spectrum resulting from reaction (*a*). Since Cartwright's apparatus has finite resolving power, the discrete spectrum of π^+ mesons from reaction (*b*) merges with the continuous spectrum from reaction (*a*); the solid curve in Fig. 4 shows the predicted π^+ spectrum from reactions (*a*) and (*b*) taking account of this finite resolution (cf. above). It is seen that the agreement with the experimental points is excellent, thereby providing strong evidence that the high-energy peak in the π^+ spectrum is due primarily to reaction (*b*).[28]

Using the solid curve in Fig. 4, it is possible to estimate fairly accurately what fraction of the cross section at 0° is due to reaction (*b*). It turns out that, of the total cross section of $2.0 \pm 0.4 \times 10^{-28}$ cm^2/ster at 0° due to reactions (*a*) and (*b*), two-thirds (to be exact, $1.3 \pm 0.26 \times 10^{-28}$) is due to reaction (*b*). A similar analysis of the π^+ spectrum measured at 18° leads to a partial yield for reaction (*b*) of 55 ± 10 per cent (cf. footnote 26). The total differential cross sections at 30 and 60° are too low to allow determinations of the partial yields of reactions (*a*) and (*b*). However, even if the total differential cross sections at 30 and 60° are ascribed to reaction (*b*), it is clear that the angular dependence of the differential cross section for reaction (*b*) is strongly anisotropic. Assuming that reaction (*b*) contributes a constant fraction of $\frac{2}{3}$ to the cross sections listed in Table 15, one can write the following formula for the differential cross section for reaction (*b*) ($\bar{\theta}$ is the angle of emission of the meson with respect to the incident proton direction in the center-of-mass system):

$$\left(\frac{d\bar{\sigma}}{d\bar{\Omega}}\right)_{\text{c.m.}} = (3.2 \pm 0.8)(0.08 \pm 0.08 + \cos^2 \bar{\theta}) \times 10^{-29} \text{ cm}^2/\text{ster} \quad (18)$$

Equation (18) suggests that the π^+ mesons are emitted almost entirely in *p* states as far as reaction (*b*) is concerned. The total cross section, obtained by integrating Eq. (18) over $d\bar{\Omega}$, for reaction (*b*) at 340-Mev incident proton energy is therefore $1.6 \pm 0.5 \times 10^{-28}$ cm^2.

A preliminary experiment on the production of π^0 mesons in proton-proton collisions has been performed by Knable,[29] using the deflected 340-Mev proton beam of the Berkeley cyclotron. Knable attempted to detect the decay photons from the π^0 mesons with a new type of "pair-scattering detector" at 135° with respect to the incident proton direction. He obtained a negative result and was able to place an upper limit on the

---

[28] Crawford, Crowe, and Stevenson [*Phys. Rev.*, **82**: 97 (1951)] have demonstrated directly that reaction (*b*) takes place by counting the deuteron and π^+ meson in coincidence.

[29] N. Knable, *UCRL* No. 1444; cf. Hales, Hildebrand, Knable, and Moyer, *Phys. Rev.*, **85**: 373 (1952).

π^0 yield in *P-P* collisions of 1 ± 1 per cent of the yield from proton-carbon collisions and 8 ± 8 per cent of the yield from proton-deuteron collisions, all measurements performed at 135°. When these results are combined with the roughly equal yields of π^+ and π^0 mesons in proton-carbon collisions at 340 Mev (cf. Chap. 3), it is possible to state that at 340 Mev the cross sections for π^0 production in *N-P* collisions and π^+ production in *P-P* and *N-P* collisions are approximately equal (and of the order of 10^{-28} cm^2), whereas the cross section for π^0 production in *P-P* collisions is lower by at least a factor of 10.[29a]

The experimental data available thus far on π^+ and π^0 production in nucleon-nucleon collisions are already sufficient to argue against some of the theories discussed in Sec. 3. The sizable cross section observed for the reaction $P + P \rightarrow D + \pi^+$ ($1.6 \pm 0.5 \times 10^{-28}$ cm^2 at 340 Mev, to be exact) argues against the $S(S)$ theory which predicts a cross section of $g^2/\hbar c \times 10^{-28}$ cm^2 at 340 Mev (cf. Table 13); theory and experiment will match if $g^2/\hbar c$ is equal to 1.5, a value which is too large.[30] Curiously enough, the $S(S)$ theory predicts a $\cos^2 \bar{\theta}$ angular distribution for the mesons in the center-of-mass system—in excellent accord with experiment; this is due to the fact, previously noted, that a scalar π^+ meson with orbital angular momentum $l = 0$ cannot be emitted because of the operation of the Pauli principle for the two initial protons (cf. Table 8). The selection rule which leads to a $\cos^2 \bar{\theta}$ angular distribution leads, at the same time, to much too small an absolute cross section. Another argument against the $S(S)$ theory is the fact that it predicts a zero cross section (in the nonrelativistic approximation) for π^0 production in *N-P* collisions; this contradicts the experimental fact that π^0 production in *N-P* collisions (cf. above) is comparable with charged π meson production in *N-P* collisions. These remarks apply to both the field-theoretic and phenomenological versions of the $S(S)$ theory.

The $PS(PS)$ theory has been calculated only field-theoretically because of the importance of the negative energy states for the nucleons; this feature of the theory makes very dubious the application of any type of phenomenological approach. Comparison of the $PS(PS)$ theory with the experimental data on π^+ production is therefore questionable, although it should be noted that the theory predicts a cross section for π^0 production in *P-P* collisions comparable with that for π^+ production (for comparable values of the neutral meson and charged meson coupling constant—a statement which appears justified by the approximate equality of π^0 production and π^+ production in *N-P* collisions) in contradiction to the experimental result. It is, of course, possible that higher order corrections to the *PS*(*PS*) theory would appreciably reduce the cross section for π^0 production without altering the cross section for π^+ production.

[29a] Recently, Marshall, Marshall, Nedzel, and Warshaw (*Phys. Rev.*, in press) have measured the cross section in the forward direction for π^0 production in *P-P* collisions at 430-Mev incident proton energy (from the Chicago cyclotron) with the result 2×10^{-28} cm^2/ster. This value is comparable to the π^+ cross section at 340 Mev (cf. above). The small relative cross section for π^0 production (compared to π^+) in *P-P* collisions near threshold is easily explained by the predominance of p-emission and therefore odd parity for the π^0 meson (cf. Table 9).

[30] Matching the other theories (cf. Table 13) with the experimental value leads to the following values for the coupling constants: $PS(PV)$: $f^2/\hbar c = 0.3$, $V(V)$: $g^2/\hbar c = 1.5$, $PV(PV)$: $g^2/\hbar c = 0.15$.

The field-theoretic versions of the spin 1 theories have a rather academic interest for π^0 production because the π^0 meson cannot possess spin 1 (cf. Chap. 4) and the π^0 meson has been included among the virtual transitions in the charged π meson production calculations. As regards the phenomenological spin 1 theories for the charged π meson, the anisotropic angular distribution of the π^+ mesons produced in *P-P* collisions provides some evidence against the *V*(*V*) and *PV*(*PV*) theories, both of which predict a fairly isotropic distribution (cf. above). Moreover, the *V*(*V*) theory appears to require too large a coupling constant (cf. footnote 30). The coupling constant required by the *PV*(*PV*) theory is reasonable, although it should be recalled that the *PV*(*PV*) theory leads to a repulsive static potential between nucleons (cf. Table 6). One would be inclined to argue against the spin 1 theories on the basis of the π meson production experiments.

The most promising description of the π meson field is provided by the *PS*(*PV*) theory, in both its field-theoretic and phenomenological versions. The *PS*(*PV*) theory predicts zero cross section (in the nonrelativistic approximation) for π^0 production in *P-P* collisions, independent of the magnitudes and signs of f, f_P, and f_N in the field-theoretic calculation and independent of the assumed empirical potential between nucleons in the phenomenological calculation. The *PS*(*PV*) theory predicts a reasonable value for the total cross section for π^+ production and an anisotropic angular distribution in the field-theoretic version. Actually, the *PS*(*PV*) field-theoretic calculation predicts a much more anisotropic angular distribution for π^+ production in *P-P* collisions than does the phenomenological calculation; for example, the *PS*(*PV*) field theory predicts a $(3\cos^2\bar{\theta} + 1)$ distribution for the symmetrical choice of coupling constants, that is, $f_P = -f_N = f/\sqrt{2}$ in contrast to an almost isotropic distribution predicted by the phenomenological *PS*(*PV*) theory. This difference can be understood if it is recalled that the symmetric *PS*(*PV*) field theory predicts a static potential between two nucleons of the form

$$-f^2(\boldsymbol{\sigma}_1 \cdot \nabla)(\boldsymbol{\sigma}_2 \cdot \nabla)Y(r) \tag{19}$$

This singular tensor force can satisfactorily explain the high-energy proton-proton scattering experiments but not the high-energy neutron-proton experiments. In the phenomenological calculation, plane waves were used for the initial two-proton system, and the deuteron wave function was taken as $^3S_1$; both these approximations resulted in a rather isotropic angular distribution for the π^+ mesons from the reaction $P + P \rightarrow D + \pi^+$.

The angular distribution predicted by the phenomenological *PS*(*PV*) theory can be made much more anisotropic by suitable assumptions about the character of the proton-proton and neutron-proton forces and by taking account of the distortions introduced into the states of the di-proton and deuteron systems by the postulated interactions. Chew *et al.*[31] have performed a calculation of this sort after adding the further simplification that the nonrelativistic *PS*(*PV*) meson-nucleon interaction operator is $[-(f/\mu)\boldsymbol{\sigma} \cdot \mathbf{q}]$ $\{$*i.e.*, dropping the $[(f/\mu)(\epsilon/2M)\boldsymbol{\sigma} \cdot (\mathbf{p}_i + \mathbf{p}_f)]$ term, which is of first order in the nucleon velocity—cf. Table 12$\}$. They find that the square of the matrix element (suitably summed and averaged) corresponding to the reaction $P + P \rightarrow D + \pi^+$ is

$$\frac{f^2}{3\mu^2} q^2 \left[F_0^2 + \sqrt{2} \cos (\delta_0 - \delta_2) F_0 F_2 (3 \cos^2 \bar{\theta} - 1) + \frac{F_2^2}{2} (3 \cos^2 \bar{\theta} + 1) \right] \tag{20}$$

where $$F_0 = \int_0^\infty u_f(r) u_i(r)\, dr, \qquad F_2 = \int_0^\infty w_f(r) w_i(r)\, dr$$

with u_i and w_i the radial parts of the deuteron *S* and *D* wave functions respectively and u_f and w_f the radial parts of the di-proton *S* and *D* wave functions, normalized asymptotically to $\sin (kr + \delta_0)$ and $\sin (kr + \delta_2 - \pi)$, respectively. Equation (20) enables one to write down immediately the ratio of the differential cross sections at 0 and 90° (in the center-of-mass system), namely,

$$\Re = \frac{d\bar{\sigma}(0^\circ)}{d\bar{\sigma}(90^\circ)} = \frac{x^2 + 4x \cos (\delta_0 - \delta_2) + 4}{x^2 - 2x \cos (\delta_0 - \delta_2) + 1} \tag{21}$$

where $x = \sqrt{2}\, F_0/F_2$.

The values of x, δ_0, and δ_2 depend on the particular choice of nucleon-nucleon force, and it is clear that $\Re$ can be much larger than unity (to agree with experiment) if this choice is properly made. As an illustration, if it is assumed that the central part of the triplet *N*-*P* force is identical with the singlet *P*-*P* force, it follows that F_0 (and therefore x) vanishes so that $\Re = 4$. As a matter of fact, if it assumed that the triplet *N*-*P* force consists of a central [with its Fourier transform denoted by $^3(NP)_{\text{central}}$] and a tensor part (with its Fourier transform denoted by $^3(NP)_{\text{tensor}}$) and if the Fourier transform of the singlet *P-P* force is denoted by $^1(PP)$, it can be shown that x can be written in the alternative form

---

[31] Chew, Goldberger, Steinberger, and Yang, *Phys. Rev.*, in press; cf. also K. Watson and C. Richman, *Phys. Rev.*, **83**: 1256 (1951).

$$x = \frac{3}{2} \frac{[^3(NP)_{\text{central}} - {}^1(PP)]}{^3(NP)_{\text{tensor}}} \tag{22}$$

Since the available high-energy scattering data still allow considerable freedom in the choice of the *P-P* and *N-P* forces, the value of x can be varied within rather wide limits and presumably can be chosen so as to fit the experimentally measured angular distribution of the π^+ mesons produced in the $P + P \rightarrow D + \pi^+$ reaction. This is seen by examining Fig. 5 where $\mathfrak{R}$ is plotted as a function of x for two values of $(\delta_0 - \delta_2)$, namely, 0 and 60°.

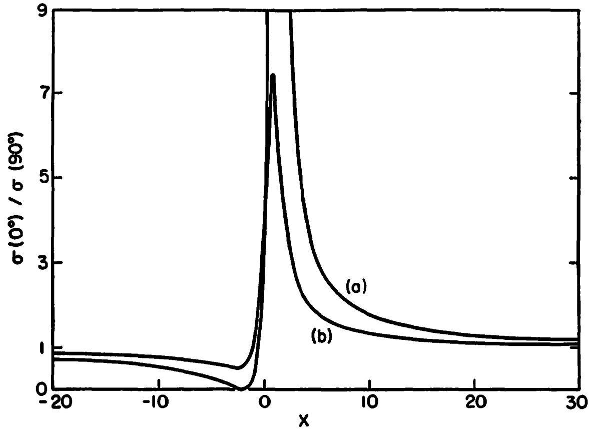

FIG. 5. Ratio of the theoretical cross sections for the reaction $P + P \rightarrow D + \pi^+$ at 0° and 90° as a function of x (defined in text) for two values of $(\delta_0 - \delta_2)$. Curve (*a*) corresponds to $(\delta_0 - \delta_2) = 0°$; (*b*) to $(\delta_0 - \delta_2) = 60°$.

When the above conclusions are considered in conjunction with those drawn from the photonic production experiments, the *PS*(*PV*) theory emerges as the most promising description of the π meson field (with a symmetrical type choice of coupling constants, that is, $f_P \approx -f_N$ and both of the order of f although not necessarily equal to $f/\sqrt{2}$). This statement must be strongly qualified because of the reliance which is being placed on the qualitative correctness of the weak coupling theory for the interpretation of the experiments on π meson production in nucleon-nucleon collisions.

CHAPTER 3

NUCLEAR PRODUCTION OF SINGLE π MESONS

1. Introduction

In Chaps. 1 and 2, we treated at some length the two fundamental mechanisms for the production of π mesons: photon-nucleon collisions and nucleon-nucleon collisions. The comparison of the theoretical predictions bearing on these π production mechanisms with the existing experimental data shed considerable light on the nature of the π meson and its coupling with nucleons. Much more experimental information has been accumulated concerning the production of π mesons resulting from collisions of photons and nucleons with complex nuclei. Unfortunately, the presence of more than one nucleon in a nucleus (except possibly for the deuteron) so complicates the physical situation that a study of production processes in complex nuclei reveals relatively little about the π meson field. The distinctive features of the different theories of photon-nucleon and nucleon-nucleon production of π mesons are quickly lost as the number of nucleons increases. The interactions among the nucleons in a nucleus are sufficiently strong so that, for incident photon and nucleon energies of several hundred Mev (available with the accelerators now in operation), it is these interactions which determine the characteristic phenomena which are observed. Consequently, a study of π meson production in nuclei reveals more about the behavior of nucleons in nuclei than it does about the π meson-nucleon interaction. Nevertheless, it does seem worth while to discuss the production of single π mesons in nuclear collisions and to show how the observational data can be correlated and understood in terms of such simple concepts as the Pauli exclusion principle, the Coulomb field, etc.

2. Kinematics of Nuclear Production of π Mesons

One of the most striking features observed in connection with nucleon-nuclei production of π mesons is the sharp reduction in threshold compared with nucleon-nucleon production. Instead of requiring 290 Mev for the incident nucleons (cf. Chap. 2), π mesons can be produced in nuclei heavier than helium by incident nucleons possessing energies as low as 180 Mev. McMillan and Teller[1] were the first to predict this reduction in threshold on the basis of the Fermi gas model of the nucleus. These authors showed that, if T is the incident kinetic energy of a nucleon, the following crude relation can be used to estimate the threshold energy for π meson production:

---

[1] W. McMillan and E. Teller, *Phys. Rev.*, **72**: 1 (1947).

$$T_t = \mu + T_F + V \tag{1}$$

where μ is the rest mass of the π meson, T_F is the Fermi energy (≈ 20 to 25 Mev), and V is the average potential energy of a nucleon in the nucleus. Equation (1) tells us that a nucleon must possess, in the laboratory system, a kinetic energy equal to μ plus the binding energy $(T_F + V) \approx -8$ Mev of a nucleon in the nucleus in order to produce a π meson. Although many approximations have been made in writing down Eq. (1), it does predict the correct order of magnitude for the reduction in threshold energy.

The above manner of estimating the threshold energy for π meson production assumes that the π meson is produced in a collision of the incident nucleon with *one* of the nucleons in the Fermi gas; this seems justified since the de Broglie wave length of the incident nucleon even at ≈ 150 Mev is small compared with the range of nuclear forces. Barkas[2] has pointed out that there is an *absolute* threshold energy for the production of π mesons which is obtained by treating the production process as if the entire target nucleus participates as a unit in the collision with the incident nucleon. Thus, if a particle of mass M_1 (say a nucleon), moving with a velocity β_1 in the laboratory system, and energy

$$E_1 \left(E_1 = M_1\gamma_1,\ \gamma_1 = \frac{1}{\sqrt{1 - \beta_1^2}} \right)$$

is incident upon a particle of mass M_2 (say a nucleus) at rest, it can be shown that the energy $\bar{E}$ of the two particles in the center-of-mass system is

$$\bar{E} = \sqrt{(M_1 + M_2)^2 + 2M_2T_1}$$

If M_i represents the total final mass of the colliding particles, one may define the quantity Q_i in the usual sense of the Q value of the reaction as $Q_i = (M_1 + M_2) - (\mu + M_i)$, where μ is the mass of the meson produced in the collision. At threshold, *i.e.*, when all final kinetic energies vanish in the center-of-mass system, $\bar{E} - (M_1 + M_2) = -Q_i$ and, solving for the threshold kinetic energy T_t, $(T_t = E_t - M_1)$, one finds

$$T_t = \frac{(\mu + M_i)^2 - (M_1 + M_2)^2}{2M_2} \tag{2}$$

Table 1 lists the threshold kinetic energies computed on the basis of Eq. (2) for typical nuclei chosen as targets. The results are listed for

---

[2] W. H. Barkas, *Phys. Rev.*, **75**: 1109 (1949).

TABLE 1*a*. ABSOLUTE THRESHOLDS FOR π MESON PRODUCTION BY PROTONS

Target	π^+		π^-		π^0	
	Product	E_t	Product	E_t	Product	E_t
${}_{1}\mathrm{H}^{1}$	${}_{1}\mathrm{H}^{2}$	290.8			$2\,{}_{1}\mathrm{H}^{1}$	280.5
${}_{1}\mathrm{H}^{2}$	${}_{1}\mathrm{H}^{3}$	209.1	$3\,{}_{1}\mathrm{H}^{1}$	218.1	${}_{2}\mathrm{He}^{3}$	199.5
${}_{2}\mathrm{He}^{4}$	${}_{2}\mathrm{He}^{4} + {}_{0}n^{1}$	180.8	${}_{2}\mathrm{He}^{3} + 2\,{}_{1}\mathrm{H}^{1}$	204.0	${}_{2}\mathrm{He}^{4} + {}_{1}\mathrm{H}^{1}$	171.9
${}_{3}\mathrm{Li}^{7}$	${}_{3}\mathrm{Li}^{8}$	162.1	${}_{4}\mathrm{Be}^{7} + {}_{1}\mathrm{H}^{1}$	163.4	$2\,{}_{2}\mathrm{He}^{4}$	136.3
${}_{4}\mathrm{Be}^{9}$	${}_{4}\mathrm{Be}^{10}$	152.1	${}_{6}\mathrm{C}^{10}$	155.2	${}_{5}\mathrm{B}^{10}$	145.2
${}_{5}\mathrm{B}^{11}$	${}_{5}\mathrm{B}^{12}$	153.5	${}_{7}\mathrm{N}^{12}$	156.5	${}_{6}\mathrm{C}^{12}$	131.1
${}_{6}\mathrm{C}^{12}$	${}_{6}\mathrm{C}^{13}$	150.1	${}_{7}\mathrm{N}^{12} + {}_{1}\mathrm{H}^{1}$	172.9	${}_{7}\mathrm{N}^{13}$	145.8
${}_{7}\mathrm{N}^{14}$	${}_{7}\mathrm{N}^{15}$	141.7	${}_{8}\mathrm{O}^{14} + {}_{1}\mathrm{H}^{1}$	156.9	${}_{8}\mathrm{O}^{15}$	138.1
${}_{8}\mathrm{O}^{16}$	${}_{8}\mathrm{O}^{17}$	147.6	${}_{8}\mathrm{O}^{15} + 2\,{}_{1}\mathrm{H}^{1}$	165.9	${}_{9}\mathrm{F}^{17}$	144.0
${}_{13}\mathrm{Al}^{27}$	${}_{13}\mathrm{Al}^{28}$	139.8	${}_{14}\mathrm{Si}^{27} + {}_{1}\mathrm{H}^{1}$	151.0	${}_{14}\mathrm{Si}^{28}$	129.8
${}_{29}\mathrm{Cu}^{63}$	${}_{29}\mathrm{Cu}^{64}$	135.9	${}_{31}\mathrm{Ga}^{64}$	137.6	${}_{30}\mathrm{Zn}^{64}$	129.1
Competing Reactions (Nearest)						
${}_{2}\mathrm{He}^{4}$	${}_{2}\mathrm{He}^{4} + {}_{0}n^{1}$	180.8	${}_{2}\mathrm{He}^{3} + 2\,{}_{1}\mathrm{H}^{1}$	204.0	${}_{2}\mathrm{He}^{4} + {}_{1}\mathrm{H}^{1}$	171.9
	${}_{1}\mathrm{H}^{2} + {}_{1}\mathrm{H}^{3}$	203.6	${}_{1}\mathrm{H}^{2} + 3\,{}_{1}\mathrm{H}^{1}$	211.0	${}_{2}\mathrm{He}^{3} + {}_{1}\mathrm{H}^{2}$	195.2
${}_{4}\mathrm{Be}^{9}$	${}_{4}\mathrm{Be}^{10}$	152.1	${}_{6}\mathrm{C}^{10}$	155.2	${}_{5}\mathrm{B}^{10}$	145.2
	${}_{2}\mathrm{He}^{4} + {}_{2}\mathrm{He}^{6}$	160.3	$2\,{}_{2}\mathrm{He}^{4} + 2\,{}_{1}\mathrm{H}^{1}$	158.2	$2\,{}_{2}\mathrm{He}^{4} + {}_{1}\mathrm{H}^{2}$	150.9
${}_{6}\mathrm{C}^{12}$	${}_{6}\mathrm{C}^{13}$	150.1	${}_{7}\mathrm{N}^{12} + {}_{1}\mathrm{H}^{1}$	172.9	${}_{7}\mathrm{N}^{13}$	145.8
	${}_{6}\mathrm{C}^{12} + {}_{0}n^{1}$	154.1	${}_{6}\mathrm{C}^{11} + 2\,{}_{1}\mathrm{H}^{1}$	173.0	${}_{6}\mathrm{C}^{12} + {}_{1}\mathrm{H}^{1}$	147.6

TABLE 1*b*. ABSOLUTE THRESHOLDS FOR π MESON PRODUCTION BY NEUTRONS

Target	π^+		π^-		π^0	
	Product	E_t	Product	E_t	Product	E_t
${}_{1}\mathrm{H}^{1}$	$2\,{}_{0}n^{1}$	295.5	$2\,{}_{1}\mathrm{H}^{1}$	289.9	${}_{1}\mathrm{H}^{2}$	252.2
${}_{1}\mathrm{H}^{2}$	$3\,{}_{0}n^{1}$	222.2	${}_{2}\mathrm{He}^{3}$	206.3	${}_{1}\mathrm{H}^{3}$	198.2
${}_{2}\mathrm{He}^{4}$	${}_{1}\mathrm{H}^{3} + 2\,{}_{0}n^{1}$	206.4	${}_{2}\mathrm{He}^{4} + {}_{1}\mathrm{H}^{1}$	177.6	${}_{2}\mathrm{He}^{4} + {}_{0}n^{1}$	172.0
${}_{3}\mathrm{Li}^{7}$	${}_{2}\mathrm{He}^{6} + 2\,{}_{0}n^{1}$	176.1	$2\,{}_{2}\mathrm{He}^{4}$	141.2	${}_{3}\mathrm{Li}^{8}$	154.0
${}_{4}\mathrm{Be}^{9}$	${}_{3}\mathrm{Li}^{8} + 2\,{}_{0}n^{1}$	178.4	${}_{5}\mathrm{B}^{10}$	149.3	${}_{4}\mathrm{Be}^{10}$	144.3
${}_{5}\mathrm{B}^{11}$	${}_{4}\mathrm{Be}^{10} + 2\,{}_{0}n^{1}$	168.9	${}_{6}\mathrm{C}^{12}$	135.9	${}_{5}\mathrm{B}^{12}$	145.9
${}_{6}\mathrm{C}^{12}$	${}_{5}\mathrm{B}^{12} + {}_{0}n^{1}$	169.9	${}_{7}\mathrm{N}^{13}$	150.5	${}_{6}\mathrm{C}^{13}$	142.4
${}_{7}\mathrm{N}^{14}$	${}_{6}\mathrm{C}^{14} + {}_{0}n^{1}$	152.7	${}_{8}\mathrm{O}^{15}$	142.7	${}_{7}\mathrm{N}^{15}$	134.3
${}_{8}\mathrm{O}^{16}$	${}_{7}\mathrm{N}^{17}$	156.2	${}_{9}\mathrm{F}^{17}$	148.6	${}_{8}\mathrm{O}^{17}$	140.2
${}_{13}\mathrm{Al}^{27}$	${}_{12}\mathrm{Mg}^{27} + {}_{0}n^{1}$	150.0	${}_{14}\mathrm{Si}^{28}$	134.3	${}_{13}\mathrm{Al}^{28}$	132.6
${}_{29}\mathrm{Cu}^{63}$	${}_{28}\mathrm{Ni}^{64}$	125.0	${}_{30}\mathrm{Zn}^{64}$	133.5	${}_{29}\mathrm{Cu}^{64}$	128.9
Competing Reactions (Nearest)						
${}_{2}\mathrm{He}^{4}$	${}_{1}\mathrm{H}^{3} + 2\,{}_{0}n^{1}$	206.4	${}_{2}\mathrm{He}^{4} + {}_{1}\mathrm{H}^{1}$	177.6	${}_{2}\mathrm{He}^{4} + {}_{0}n^{1}$	172.0
	${}_{1}\mathrm{H}^{2} + 3\,{}_{0}n^{1}$	215.1	${}_{2}\mathrm{He}^{3} + {}_{1}\mathrm{H}^{2}$	201.3	${}_{1}\mathrm{H}^{3} + {}_{1}\mathrm{H}^{2}$	194.7
${}_{4}\mathrm{Be}^{9}$	${}_{3}\mathrm{Li}^{8} + 2\,{}_{0}n^{1}$	178.4	${}_{5}\mathrm{B}^{10}$	149.3	${}_{4}\mathrm{Be}^{10}$	144.3
	${}_{2}\mathrm{He}^{6} + {}_{1}\mathrm{H}^{3} + {}_{0}n^{1}$	182.6	$2\,{}_{2}\mathrm{He}^{4} + {}_{1}\mathrm{H}^{2}$	155.8	${}_{2}\mathrm{He}^{4} + {}_{2}\mathrm{He}^{6}$	152.6
${}_{6}\mathrm{C}^{12}$	${}_{5}\mathrm{B}^{12} + {}_{0}n^{1}$	169.9	${}_{7}\mathrm{N}^{13}$	150.5	${}_{6}\mathrm{C}^{13}$	142.4
	${}_{4}\mathrm{Be}^{10} + {}_{1}\mathrm{H}^{3}$	176.0	${}_{6}\mathrm{C}^{12} + {}_{1}\mathrm{H}^{1}$	152.3	${}_{6}\mathrm{C}^{12} + {}_{0}n^{1}$	147.6

protons and neutrons corresponding to the production of either positive, negative, or neutral π mesons. The masses used for the charged and neutral π mesons are $276m_e$ and $265m_e$, respectively (m_e is the electron mass). In Table 1 are also listed the thresholds for the nearest competing reactions for several of the more interesting target nuclei, namely, He^4, Be^9, and C^{12}.

For an incident nucleon kinetic energy T greater than T_t, we can obtain the *maximum* meson energy $\bar{\epsilon}_m$ in the center-of-mass system (*i.e.*, the system in which the target nucleus and incident nucleon have equal and opposite momenta), by making use of the energy and momentum conservation equations; for this purpose, it is a sufficiently good approximation to assume that $M_i = M_1 + M_2$. We find, using the same notation as before,

$$\bar{\epsilon}_m = \frac{\mu^2 + 2(\gamma_1 - 1)M_1M_2}{2\sqrt{M_1^2 + 2M_1M_2\gamma_1 + M_2^2}} \tag{3}$$

[the threshold energy T_t follows from Eq. (3) by setting $\bar{\epsilon}_m = \mu$]. The values of ϵ_m in the laboratory system may be found by means of the Lorentz transformation

$$\epsilon_m(\theta) = \bar{\gamma}_2(\bar{\epsilon}_m + \bar{\boldsymbol{\beta}}_2 \cdot \bar{\mathbf{p}}_m) \tag{4}$$

where

$$\bar{\beta}_2 = \frac{\beta_1 M_1 \gamma_1}{\gamma_1 M_1 + M_2} \qquad \text{and} \qquad \bar{\gamma}_2 = \frac{\gamma_1 + M_2/M_1}{\sqrt{1 + 2(M_2/M_1)\gamma_1 + (M_2/M_1)^2}}$$

It is clear that once M_1, M_2, and γ_1 are known, Eq. (3) yields $\bar{\epsilon}_m$ and thus $\bar{p}_m(\bar{p}_m = \sqrt{\bar{\epsilon}_m^2 - \mu^2})$; hence ϵ_m can be determined. Table 2 lists the values of ϵ_m (0°), ϵ_m (90°), and ϵ_m (180°) for three target nuclei (H^1, H^2, C) corresponding to incident nucleon energies from 250 to 400 Mev.

TABLE 2. MAXIMUM π MESON KINETIC ENERGIES (MEV) AT THREE ANGLES IN THE LABORATORY SYSTEM FROM THREE TARGET NUCLEI AS A FUNCTION OF PROTON ENERGY

T, Mev	H			D			C		
	0°	90°	180°	0°	90°	180°	0°	90°	180°
250				47	20	8	102	90	80
300	20			90	40	24	150	134	119
350	61	12	0.1	131	74	40	198	177	158
400	95	29	8	171	100	54	247	221	197
450	128	46	14	212	125	171	289	264	234

Let us now consider the kinematics of π meson production in photon-nucleus collisions. Assuming again that photonic meson production

DAVID J. LANGFORD
Pure Mathematical Physics

involves the nucleus as a unit, the absolute threshold energy ω_t for single meson production, using the above notation, is

$$\omega_t = \frac{(\mu + M_i)^2 - M_2^2}{2M_2} \tag{5}$$

Equation (5) follows from Eq. (2) recalling that the photon possesses zero rest mass; in general, Eq. (5) results in a lower threshold than does Eq. (2). This is best illustrated in Table 3, which lists the thresholds for π^+ and π^- and π^0 production by an incident γ ray, for the same choice of target nuclei as in Table 1. Again, in Table 3 are listed the thresholds for the nearest competing reactions for the same target nuclei: He^4, Be^9, and C^{12}.

TABLE 3. ABSOLUTE THRESHOLDS FOR π MESON PRODUCTION BY PHOTONS

Target	π^+		π^-		π^0	
	Product	E_t	Product	E_t	Product	E_t
${}_1H^1$	${}_0n^1$	153.1			${}_1H^1$	145.1
${}_1H^2$	$2{}_0n^1$	149.9	$2{}_1H^1$	147.1	${}_1H^2$	140.3
${}_2He^4$	${}_1H^3 + {}_0n^1$	165.5	${}_1H^1 + {}_2He^3$	163.6	${}_2He^4$	137.9
${}_3Li^7$	${}_2He^6 + {}_0n^1$	154.2	${}_4Be^7$	143.0	${}_3Li^7$	136.8
${}_4Be^9$	${}_3Li^8 + {}_0n^1$	160.6	$2{}_2He^4 + {}_1H^1$	142.4	${}_4Be^9$	136.5
${}_5B^{11}$	${}_4Be^{10} + {}_0n^1$	154.8	${}_6C^{11}$	143.6	${}_5B^{11}$	136.3
${}_6C^{12}$	${}_5B^{12}$	156.8	${}_7N^{12}$	159.5	${}_6C^{12}$	136.2
${}_7N^{14}$	${}_6C^{14}$	142.5	${}_8O^{14}$	146.1	${}_7N^{14}$	136.1
${}_8O^{16}$	${}_7N^{16}$	150.7	${}_8O^{15} + {}_1H^1$	156.1	${}_8O^{16}$	136.0
${}_{13}Al^{27}$	${}_{12}Mg^{27}$	144.6	${}_{14}Si^{27}$	145.6	${}_{13}Al^{27}$	135.8
${}_{29}Cu^{63}$	${}_{28}Ni^{62} + {}_0n^1$	142.8	${}_{30}Zn^{63}$	144	${}_{29}Cu^{63}$	135.6
Competing Reactions (Nearest)						
${}_2He^4$	${}_1H^3 + {}_0n^1$	165.5	${}_1H^1 + {}_2He^3$	163.6	${}_2He^4$	137.9
	${}_1H^2 + 2{}_0n^1$	172.0	${}_1H^2 + 2{}_1H^1$	169.3	${}_1H^3 + {}_1H^1$	158.3
${}_4Be^9$	${}_3Li^8 + {}_0n^1$	160.6	$2{}_2He^4 + {}_1H^1$	142.4	${}_4Be^9$	136.5
	${}_3Li^7 + 2{}_0n^1$	162.6	${}_3Li^6 + {}_2He^3$	159.6	$2{}_2He^4 + {}_0n^1$	138.0
			${}_4Be^7 + {}_1H^2$	159.6		
${}_6C^{12}$	${}_5B^{12}$	156.8	${}_7N^{12}$	159.5	${}_6C^{12}$	136.2
	${}_5B^{11} + {}_0n^1$	159.3	${}_6C^{11} + {}_1H^1$	159.6	$3{}_2He^4$	143.6

For an incident photon energy ω greater than ω_t, the meson energy in the center-of-mass system (*i.e.*, the system in which the target nucleus and incident photon have equal and opposite momenta) is given by (there is only one meson energy if a final stable nucleus is produced)

$$\bar{\epsilon} = \frac{(\mu^2 + 2M_2\omega)}{2\sqrt{2\omega M_2 + M_2^2}} \tag{6}$$

where ω is the energy of the incident photon in the laboratory system and we have assumed $M_i = M_2$. The energy of the meson in the laboratory system as a function of the angle of emission can be derived, as before, using the Lorentz transformation

$$\epsilon(\theta) \doteq \bar{\gamma}_2(\bar{\epsilon} + \bar{\boldsymbol{\beta}}_2 \cdot \bar{\mathbf{p}}) \tag{7}$$

where now $\bar{\beta}_2 = \dfrac{\mathbf{k}}{\omega + M}$ and $\gamma_2 = \dfrac{\omega + M}{\sqrt{2\omega M + M^2}}$

with **k** the momentum of the incident photon. Equations (5) to (7) can be derived from the corresponding Eqs. (2) to (4) by writing $M_1 = 0$, $M_2 = M$, and $M_1\gamma_1 = \omega$. Note that, if the target nucleus is infinitely heavy, then $\bar{\epsilon} = \omega$, $\bar{\gamma}_2 = 1$, $\bar{\boldsymbol{\beta}}_2 = 0$, and $\epsilon = \bar{\epsilon}$, as is to be expected. Table 4 lists ϵ (0°), ϵ (90°), and ϵ (180°) for incident γ ray energies ranging from 250 to 450 Mev; the target selection is the same as for Table 2.

3. Nuclear Effects

The kinematics of meson production, assuming that the entire nucleus participates in the collision, tells us only what the absolute thresholds are in nucleon-nucleus and photon-nucleus collisions and what are the upper limits on the energy of the produced meson at a specified angle; Tables 1 to 4 are useful in this sense. However, the actual thresholds, *i.e.*, the lowest energies at which mesons will in practice be observed, will in general be higher because the nucleus almost certainly does not interact as a unit with the incident nucleon or photon; instead, as mentioned earlier, the production probably takes place in a nucleon-nucleon collision or a photon-nucleon collision and the threshold is lowered by the momentum distribution of the target nucleons in the nucleus. The behavior of the meson production cross section directly above threshold, particularly

TABLE 4. MAXIMUM π MESON KINETIC ENERGIES (MEV) AT THREE ANGLES IN THE LABORATORY SYSTEM FROM THREE TARGET NUCLEI AS A FUNCTION OF PHOTON ENERGY

ω, Mev	H			D			C		
	0°	90°	180°	0°	90°	180°	0°	90°	180°
250	107	65	42	109	84	66	109	104	99
300	158	94	60	159	122	96	159	152	146
350	208	122	77	209	158	123	209	199	191
400	259	147	92	259	183	149	259	246	234
450	309	173	105	309	226	166	309	292	277

for nucleon-nucleus collisions, lends support to this hypothesis, as we shall see below.

The chief effect of the finite momenta of the nucleons in the nucleus is to lower appreciably the threshold for meson production in nucleon-nucleus collisions and to lead to higher meson energies. For photon-nucleus collisions, the effective thresholds are lowered by only a negligible amount compared with photon-nucleon collisions. For both photon-nucleus and nucleon-nucleus collisions, the finite momenta of the protons and neutrons in a nucleus markedly influence the excitation function and the angular distribution and energy spectra of the produced mesons.

Further effects follow from the fact that nucleons obey the Pauli exclusion principle: the cross section per nucleon for a given meson production process in a complex nucleus is smaller than the free nucleon cross section provided that the individual nucleon cross section does not increase appreciably with energy. If there is a rapid increase in the individual cross section with energy, the Pauli principle suppression of some of the available phase space may be overcompensated by the larger cross section associated with the moving nucleons in the nucleus. Further, the Pauli principle has a marked effect on the relative cross sections for the production of π^+, π^-, and π^0 mesons near threshold because different numbers of protons and neutrons must be accommodated in the available cells of phase space; in general, the greater the unbalance in the number of nucleons of the same kind in the final nucleus, the greater is the reduction in the cross section.

In addition to these effects, there are the effect of the Coulomb field on the energy spectrum and the effect of the interaction of the outgoing mesons with nucleons on the production cross section. Both these effects become increasingly more important for the heavier nuclei. The Coulomb field seriously modifies the low-energy end of the meson spectrum, tending to inhibit the number of positive mesons and to enhance the number of negatives; it will not, of course, act on the neutral mesons. The interaction of mesons with nucleons will tend to reduce the number of mesons if the interaction cross section is large (*i.e.*, close to geometrical) as it appears to be (cf. Chap. 7). We proceed to discuss these various points in greater detail before turning to the experimental material; the experimental findings will hang together somewhat more closely if the beginnings of a theoretical understanding are established.

A. Effects of Finite Nucleon Momenta. We have stated that the finite momenta of the nucleons in a complex nucleus: (1) decrease the threshold for meson production, markedly for incident nucleons, less so for incident photons; (2) modify the variation of cross section with the energy of the incident nucleon or proton; and (3) alter the energy spectrum and angular distribution of the produced mesons as compared with those resulting from collisions with free nucleons used as targets. Let us give more substance to these statements on the basis of some assumed distribution function for the nucleon momenta in a nucleus. For heavy nuclei, it appears reasonable to employ a degenerate Fermi gas distribution for the nucleons in the nucleus. For light nuclei, the Fermi gas model should be a rather poor approximation, and a more long-tailed distribution than is provided by the Fermi model should be more suitable.

1. For the purposes of estimating the meson production threshold, we apply the Fermi gas model in the crude form originally proposed by McMillan and Teller.[1] If we let $\mathbf{p}_i$ be the momentum of the incident nucleon, $\mathbf{p}_n$ the momentum of a nucleon in the target nucleus, and the primes denote the postcollision state, then

$$\frac{p_i^2}{2M} + \left(\frac{p_n^2}{2M} + V\right) = \mu + \left(\frac{p_i'^2}{2M} + V\right) + \left(\frac{p_n'^2}{2M} + V\right) \tag{8}$$

where

$$\frac{p_n^2}{2M} \le T_F \begin{array}{l} \le \dfrac{p_i'^2}{2M} \\ \le \dfrac{p_n'^2}{2M} \end{array}$$

The Fermi kinetic energy T_F is given by

$$T_F = \frac{\pi^2}{2M}\left(\frac{3N}{\pi\Omega}\right)^{\frac{2}{3}} \tag{9}$$

where N is the number of neutrons or of protons, each of mass M, in the nuclear volume Ω. Choosing the nuclear radius $R = 1.5 \times 10^{-13}A^{\frac{1}{3}}$ and $A = 2Z$, the same value of T_F is found for the neutron and proton gas, namely, $T_F \approx 22$ Mev. Equation (8) states that the incident nucleon not only must produce the meson but also must leave the final nucleons above the Fermi sea, in addition to balancing the potential energies. Equation (8) yields, for the threshold kinetic energy T_t,

$$T_t = \mu + T_F + V \tag{10}$$

a result previously quoted. In the same approximation, the equation for the photon production becomes

$$\omega + \left(\frac{p_n^2}{2M} + V\right) = \mu + \left(\frac{p_n'^2}{2M} + V\right) \tag{11}$$

where ω is the photon energy; hence $\omega_t \approx \mu$.

Barkas[2] has pointed out that the threshold energy predicted by Eq. (10) is lower than the absolute minimum thresholds listed in Table 1. The discrepancy is due, of course, to the approximations made by McMillan and Teller, which include the use of nonrelativistic mechanics and the assumption that the threshold state is the one in which the meson has zero kinetic energy in the laboratory system. A more serious objection arises from the fact that $(T_F + V)$ may not represent the binding energy of a nucleon to the nucleus and may deviate widely from 8 Mev, especially in the lighter nuclei. A more realistic estimate of the threshold may be obtained by adding to the right-hand sides of Eqs. (8) and (11) the difference in nuclear energy between the final and initial nuclei. This would explain the difference in thresholds for π^+ and π^- production in the same nucleus which is observed (cf. Sec. 4).

2. McMillan and Teller[1] have also shown that the distribution of nucleon momenta in a Fermi gas leads, in the vicinity of threshold, to a modification of the differential nucleon-nucleon meson production cross section $\sigma_0(\tau)d\tau$ (τ is the kinetic energy of the meson in the laboratory system) by the approximate factor $(\tau_m - \tau)^2/T_F^{\frac{3}{2}}T_t^{\frac{1}{2}}$ where τ_m is the maximum kinetic energy of the meson in the laboratory system. To a first approximation, therefore, the Fermi gas model makes the following prediction for the nuclear cross section $\sigma(\tau)$:

$$\sigma(\tau)d\tau \approx \frac{(\tau_m - \tau)^2}{T_F^{\frac{3}{2}}T_t^{\frac{1}{2}}}\,\sigma_0(\tau)d\tau \tag{12}$$

Ter Haar[3] has made a similar estimate for photonic meson production in complex nuclei and finds that the photon-nucleon cross section is modified by a factor $\sqrt{\tau\mu/T_FM}\,[(\tau_m - \tau)/T_F]$ in the neighborhood of the threshold energy.

3. McMillan and Teller's and Ter Haar's simplified Fermi gas calculations are useful for estimating the variation of total meson production cross section with the energy of the incident nucleon or photon (cf. below). If it is desired to compare the theoretical predictions with the experimental data on meson spectra and angular distributions, it is necessary to carry out more rigorous Fermi gas calculations for the heavy nuclei and to use a more realistic model for the light nuclei.

The first attempt at a more rigorous calculation of nucleonic meson production on the basis of the Fermi gas model was undertaken by Taylor.[4] He assumes that the nucleon-nucleon matrix element for π production is constant in the laboratory system[5] and writes, for the differential cross section,

---

[3] D. Ter Haar, *Science*, **108**: 57 (1948).

[4] Private communication from R. Serber.

[5] The prediction of the $S(S)$, $PS(PS)$, $V(V)$, and $PV(PV)$ theories is a constant matrix element in the center-of-mass system (cf. Chap. 2); such a calculation has also been performed (cf. below), but Taylor's calculation is discussed in detail because it provides a simple illustration of the method.

$$d\sigma_0 = \frac{K}{v} \frac{q^2\, dq\, d\Omega_q\, p^2\, dp\, d\Omega_p}{dW_f} \tag{13}$$

where K is a constant, v is the velocity of the incident nucleon, **q** and **p** are the momenta in the laboratory system of the meson and one of the final nucleons, respectively, and W_f is the final energy. The integration over $d\Omega_p$ can be performed easily:

$$d\sigma_0 = \frac{2\pi K}{v} \left[\int_{p_{\min}}^{p_{\max}} (W' - \sqrt{M^2 + p^2}) p\, dp \right] \frac{q^2\, dq\, d\Omega_q}{p'} \tag{14}$$

where $\mathbf{p}' = \mathbf{p}_0 - \mathbf{q}$ with $\mathbf{p}_0 =$ the momentum of the incident nucleon, $W' = T_0 - \epsilon + 2M$, and ϵ is the energy of the meson (including its rest mass). The limits on the integral are

$$p_{\substack{\max \\ \min}} = \frac{1}{2} \left[p' \pm W' \sqrt{1 - \frac{4M^2}{W'^2 - p'^2}} \right] \tag{14a}$$

Assuming that $p \ll M$, the integral in Eq. (14) can be evaluated simply and one finds

$$d\sigma_0 = \frac{\pi K}{v} (T_0 - \epsilon + M) \left[1 + \frac{|\mathbf{p}_0 - q|^2}{2(T_0 - \epsilon + 2M)^2} \right] \times \sqrt{(T_0 - \epsilon)^2 + 4M(T_0 - \epsilon) - |\mathbf{p}_0 - q|^2}\; q\epsilon\, d\epsilon\, d\Omega_q \tag{15}$$

where T_0 is the kinetic energy of the incident nucleon.

In order to determine the meson production cross section for a complex nucleus, it is necessary to average Eq. (15) over the target nucleons in the nucleus, assuming that they constitute a Fermi gas. The condition $p^2/2M > T_F$ follows from the Fermi gas model and requires that $p_{\max} = \sqrt{(W' - E_F)^{-2} M^2}$ and $p_{\min} = \sqrt{2MT_F}$ ($\mathrm{E}_F = T_F + M$) when the product ($p_{\min} \times p_{\max}$) is greater than that calculated from Eq. (14*a*). In taking the average over the Fermi sphere, only the components of the target nucleon momenta parallel[6] to the incident beam are considered; this introduces a considerable simplification and not too great an error since the transverse momentum of a nucleon in the Fermi gas is small compared with the total parallel momentum of the incident and target nucleons. Thus, taking for the momentum distribution in the Fermi gas the expression ($P_F = \sqrt{2MT_F}$)

$$\rho(P_\parallel) dP_\parallel = \frac{3}{4P_F^3} (P_F^2 - P_\parallel^2) dP_\parallel \tag{16}$$

---

[6] This assumption leads, near threshold, to a dependence of $\sigma(\tau)$ on $(\tau_n - \tau)^3$ in contrast to $(\tau_m - \tau)^2$ for the correct Fermi distribution of momenta.

one derives the following cross section for the production of a π meson in the collision of a nucleon with a Fermi gas of nucleons:

$$\sigma(\tau)d\tau = \frac{K}{v}\, q\epsilon\, d\tau\, d\Omega_q \int_{(p_\parallel)_{\min}}^{(p_\parallel)_{\max}} (P_F^2 - P_\parallel^2)\left(T_0 + \frac{P_\parallel^2}{2M} - \epsilon + M\right)\begin{Bmatrix} F_1 \\ F_2 \end{Bmatrix} dP_\parallel \tag{17}$$

where F_1 is used when $F_1 < F_2$ and

$$F_1 = \left[1 + \frac{(\mathbf{p}_0 - \mathbf{P}_\parallel - \mathbf{q})^2}{2(W_1' + 2M)^2}\right](W_1'^2 + 4MW_1' - |\mathbf{p}_0 - \mathbf{P}_\parallel - \mathbf{q}|^2)^{\frac{1}{2}} \tag{17a}$$

$$F_2 = \frac{(W_1' + 2M)(W_1' - 2T_F)}{|\mathbf{p}_0 - \mathbf{P}_\parallel - \mathbf{q}|} \tag{17b}$$

with $W_1' = W' + P^2/2M$. The meson spectra predicted by Taylor on the basis of Eq. (17) for an incident nucleon energy of 350 Mev are plotted in Fig. 1 for several angles. Daitch[7] has performed an identical calculation to Taylor's at 250 Mev, and his curves are plotted in Fig. 2.

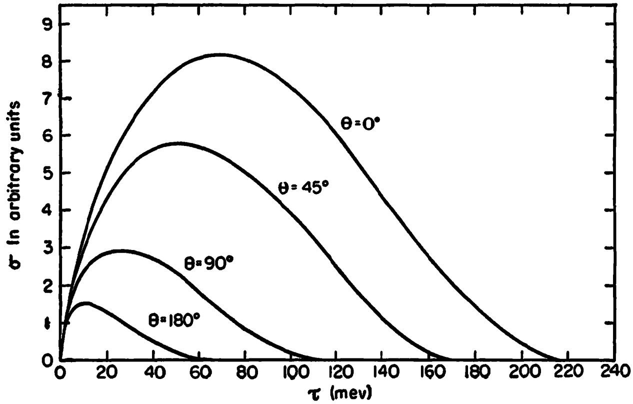

FIG. 1. Meson spectra at several laboratory angles predicted by the Fermi gas model for a constant matrix element in the laboratory system; the incident nucleon energy is 350 Mev.

Improved calculations of nucleonic production of π mesons in complex nuclei have been performed by Henley and Huddlestone[8] and by Passman *et al.*[9] The former authors have not only calculated the theoretical π^+ meson spectra corresponding to a more realistic representation of the constant matrix element theories (*i.e.*, constant matrix element in the center-of-mass system—cf. footnote 5) but have also calculated meson spectra on the assumption that the matrix element is proportional to $\bar{q}$ cos $\bar{\theta}$[10] (where $\bar{q}$ and $\bar{\theta}$ are the meson momentum and angle of emission in the center-of-mass system, respectively). Moreover, they have not restricted themselves to the Fermi gas model—which should be poor for light nuclei—but have also treated the Gaussian and the modified Chew-Goldberger momentum distributions. The Fermi gas, Gaussian, and original and modified Chew-Goldberger momentum distributions are plotted in Fig. 3. The equations for the four distributions are

---

[7] P. Daitch, private communication.

[8] E. Henley and R. Huddlestone, *Phys. Rev.*, **82**: 754 (1951); cf. also E. M. Henley, *Phys. Rev.*, **85**: 204 (1952).

[9] Passman, Block, and Havens, *Phys. Rev.*, **83**: 167 (1951); cf. also M. Block and S. Passman, Ph.D. Thesis, Columbia University, 1951.

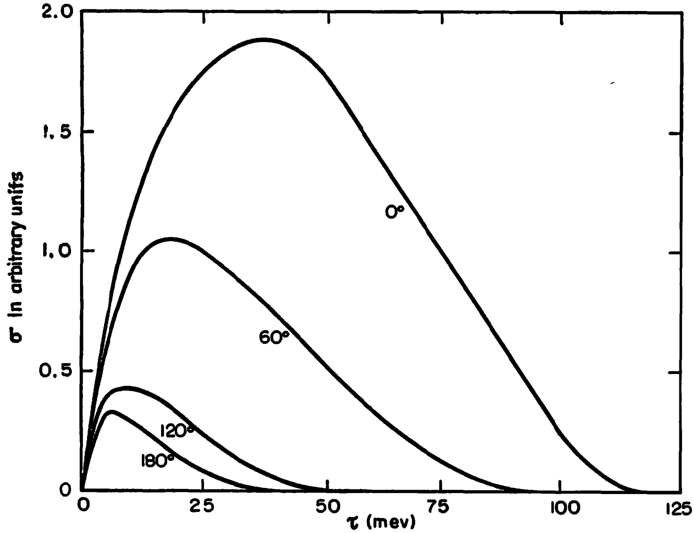

FIG. 2. Meson spectra at several laboratory angles predicted by the Fermi gas model for a constant matrix element in the laboratory system; the incident nucleon energy is 250 Mev.

Fermi gas distribution

$$\rho(\mathrm{P})d\mathrm{P} = \frac{3}{4\pi P_F^3}\,d\mathrm{P} \qquad 0 \le P \le P_F \tag{18a}$$

$$= 0 \qquad P > P_F \tag{18b}$$

where P_F is chosen as 200 Mev/c.

---

[10] A dependence which the *PS*(*PV*) theory is capable of predicting (cf. Chap. 2); a dependence of the matrix element on $\bar{q}$ implies emission of the meson into a *p*-state, whereas a constant matrix element implies *s*-state emission (cf. Chap. 2).

Gaussian distribution

$$\rho(\mathbf{P})d\mathbf{P} = \left(\frac{\alpha^{\frac{3}{2}}}{\pi^{\frac{3}{2}}}\right) e^{-\alpha P^2}\, d\mathbf{P} \tag{19}$$

the quantity α is chosen so that the average kinetic energy of the nucleons in the nucleus is 19.3 Mev, thereby giving a reasonable fit to the deuteron pickup data of York.[11]

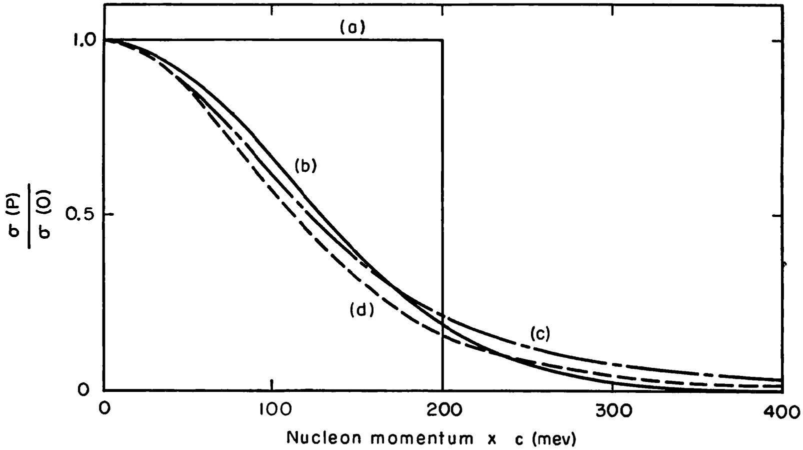

FIG. 3. Some possible nucleon momentum distributions in a complex nucleus. Curve (*a*) corresponds to the Fermi gas distribution, (*b*) to the Gaussian distribution, (*c*) to the original Chew-Goldberger distribution, (*d*) to the modified Chew-Goldberger distribution (defined in text).

Original Chew-Goldberger distribution[12]

$$\rho(\mathbf{P})d\mathbf{P} = \frac{\alpha}{\pi^2(\alpha^2 + P^2)^2}\, d\mathbf{P} \tag{20}$$

where α corresponds to an energy of 18 Mev. Equation (20) yields an infinite average kinetic energy, indicative of too long a tail as far as the meson production experiments are concerned (cf. below) although providing a fairly good fit of the deuteron data.[11]

Modified Chew-Goldberger distribution

$$\rho(\mathbf{P})d\mathbf{P} = \frac{\beta(\beta + \alpha)^2}{\pi^2(\alpha^2 + P^2)(\beta^2 + P^2)^2}\, d\mathbf{P} \tag{21}$$

---

[11] H. F. York, *Phys. Rev.*, **75**: 1467 (1949).

[12] G. Chew and M. Goldberger, *Phys. Rev.*, **77**: 470 (1950).

where $\beta = 2.5\alpha$ and yields an average kinetic energy of 48.1 Mev. Equation (21) represents the square of the Fourier transform of the Hulthen wave function $(e^{-\alpha r} - e^{-\beta r})/r$ and also fits the deuteron data fairly well. Figure 4 shows the theoretical π^+ meson spectra at 90° with respect to an incident beam of 345-Mev protons for each of the four momentum distributions derived on the assumption that the matrix element for meson production in a free nucleon-nucleon collision is proportional to $\bar{q} \cos \bar{\theta}$ in the center-of-mass system. Figure 5 contains curves for 90° emission at 345-Mev incident proton energy corresponding to the first, second, and fourth momentum distributions (since the original Chew-Goldberger distribution gives such an unreasonable meson spectrum, as we shall see below) on the assumption of a constant matrix element (in the center-of-mass system). The first, second, and fourth momentum distributions are again represented in Figs. 6 and 7 where the theoretical π^+ spectra are given for 0° emission at the same incident proton energy corresponding to matrix elements proportional to $\bar{q} \cos \bar{\theta}$ and constant, respectively.

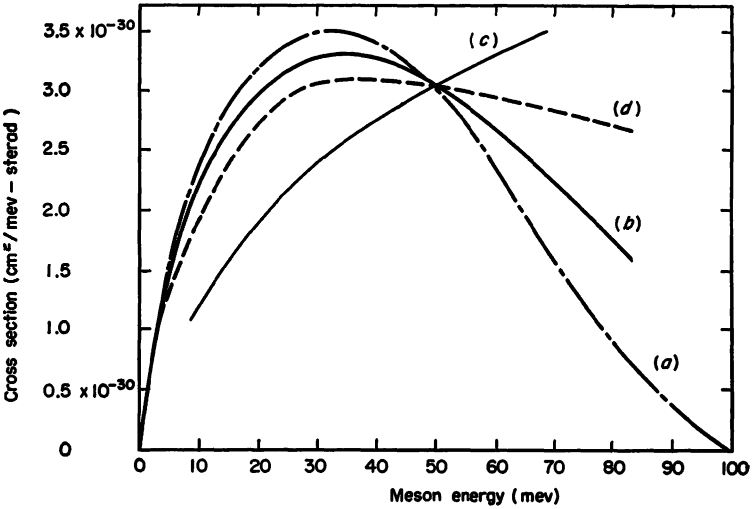

FIG. 4. Theoretical π^+ meson spectra at 90° with respect to an incident beam of 345-Mev protons; the matrix element is porportional to $\bar{q} \cos \bar{\theta}$ (defined in text). Curve (*a*) corresponds to the Fermi gas distribution, (*b*) to the Gaussian distribution, (*c*) to the original Chew-Goldberger distribution, (*d*) to the modified Chew-Goldberger distribution; the normalization is such that the modified Chew-Goldberger distribution fits the 90° experimental data for carbon at 50 Mev.

There are several interesting points to note about Figs. 4 to 7. The calculated spectrum at 90° from a complex nucleus does not depend strongly on the free nucleon matrix element which is used, *i.e.*, whether it is taken as a constant or proportional to $\bar{q} \cos \bar{\theta}$. However, it does depend appreciably on the momentum distribution which is chosen for the nucleons in the nucleus with the Chew-Goldberger distribution giving the highest meson energies, the Gaussian lower energies, and the Fermi gas distribution the lowest energies. On the other hand, at 0° the meson spectrum is relatively independent of the nucleon momentum distribution in the nucleus but is rather sensitive to the free nucleon matrix element. The essential difference between 0° and 90° is that at 90° the upper limit to the meson energy resulting from nucleon-nucleon collisions is approximately 10 Mev, whereas at 0° it is 70 Mev; consequently, the detailed behavior of the nucleon momentum distribution must influence the meson spectrum much more at 90° than at 0°.

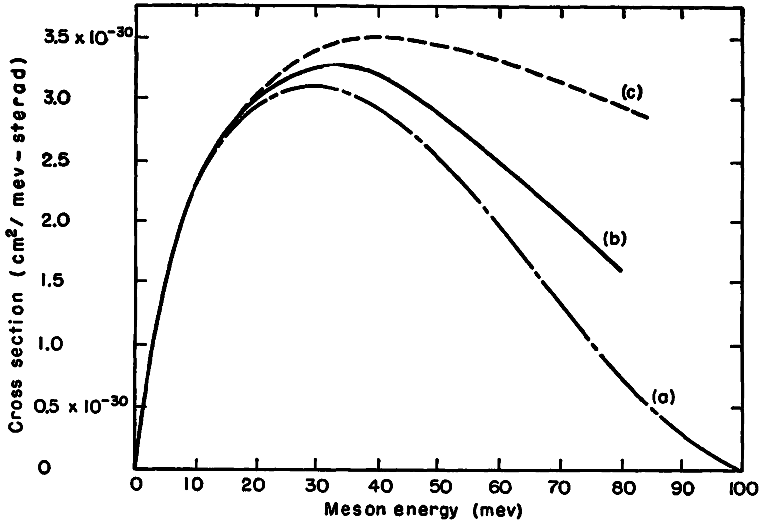

FIG. 5. Theoretical π^+ meson spectra at 90° with respect to an incident beam of 345-Mev protons; the matrix element is constant in the center-of-mass system. Curve (*a*) corresponds to the Fermi gas distribution, (*b*) to the Gaussian distribution, (*c*) to the modified Chew-Goldberger distribution; the normalization is the same as for Fig. 4.

The calculations of Passman *et al.* are different from those of Henley and Huddleston. Apart from calculating the π^+ meson spectra corresponding to an incident proton energy of 381 Mev (the energy of the Columbia cyclotron), Passman *et al.* assume that the meson which is produced receives all the available kinetic energy $\bar{\tau}_m$ in the center-of-mass system of the incident and target nucleons. That is, they regard the two final nucleons as moving off together and choose for the density of final states a term proportional to $\sqrt{\bar{\tau}_m}$; this is to be compared with the usual statistical factor $\sqrt{\bar{\tau}(\bar{\tau}_m - \tau)}$ corresponding to the three-body final state (two nucleons plus a meson). The argument in favor of $\sqrt{\bar{\tau}}$ is that the reaction $P + P \rightarrow D + \pi^+$ dominates over the reaction $P + P \rightarrow P + N + \pi^+$ in free proton-proton collisions. Passman *et al.* retain

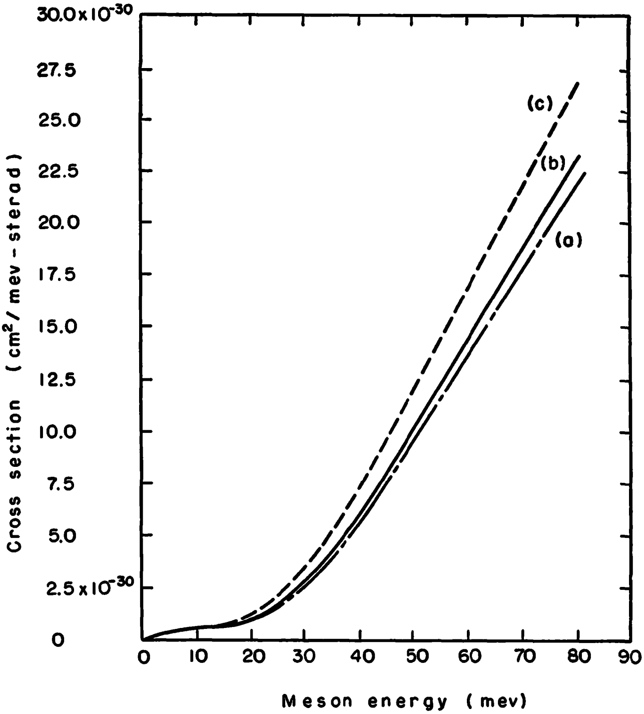

FIG. 6. Theoretical π^+ meson spectra at 0° with respect to an incident beam of 345-Mev protons; the matrix element is proportional to $q \cos \bar{\theta}$ (defined in text). Curve (*a*) corresponds to the Fermi gas distribution, (*b*) to the Gaussian distribution, (*c*) to the modified Chew-Goldberger distribution; the normalization is the same as for Fig. 4.

this feature of the free nucleon production in their calculations on the production of π mesons in nucleon-nuclei collisions, although it is quite possible that the presence of the other nucleons in the nucleus will suppress appreciably the interaction between the two final nucleons involved in the particular meson production act. For example, this suppression may occur by virtue of the Pauli exclusion principle which requires that the two final nucleons possess kinetic energies higher than the Fermi energy (about 22 Mev); the nucleon-nucleon interaction is reduced

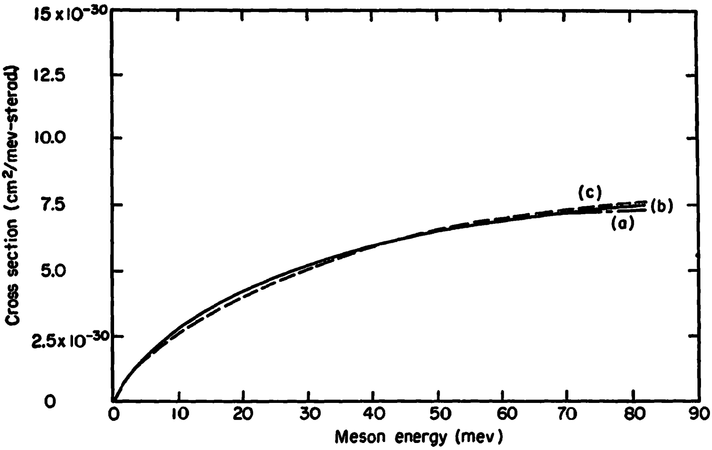

FIG. 7. Theoretical π^+ spectra at 0° with respect to an incident beam of 345-Mev protons; the matrix element is constant in the center-of-mass system. Curve (*a*) corresponds to the Fermi gas distribution, (*b*) to the Gaussian distribution, (*c*) to the modified Chew-Goldberger distribution; the normalization is the same as for Fig. 4.

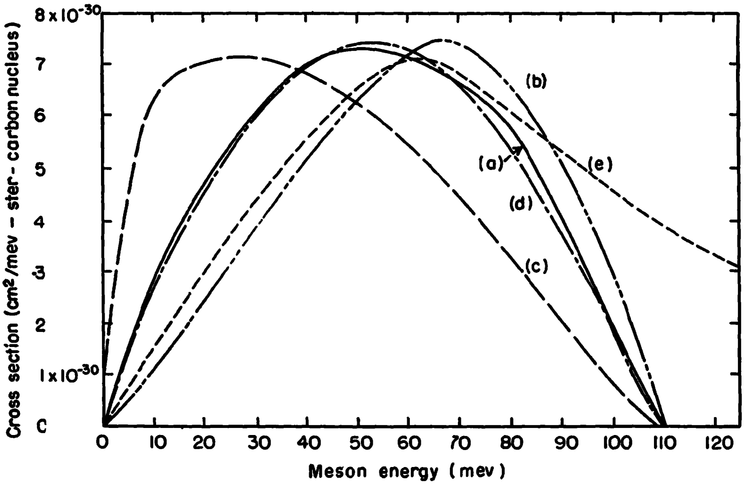

FIG. 8. Theoretical π^+ spectra at 90° with respect to an incident beam of 381-Mev protons assuming an equivalent two-body final state. Curve (*a*) corresponds to the Fermi gas distribution, matrix element ME = constant; (*b*) to the Fermi gas distribution, $ME \sim \bar{q}_m$; (*c*) to the Fermi gas distribution, $ME \sim \cos\bar{\theta}$; (*d*) to the Fermi gas distribution, $ME \sim \bar{q}_m \cos\bar{\theta}$; (*e*) to the Chew-Goldberger distribution, $ME \sim \bar{q}_m$ ($\bar{q}_m$, $\bar{\theta}$ defined in text); the theoretical curves are normalized so that their integrated areas are equal to the integrated area under the experimental spectrum from carbon at 381 Mev.

appreciably at this energy and the equivalent two-body final state may not compete at all favorably with the three-body final state. Nevertheless, it seems worth while to explore this type of approach, and the theoretically calculated curves of Passman *et al.* are shown in Fig. 8. Curve (*a*) is the Fermi gas curve for a matrix element independent of energy and angle in the center-of-mass system, curve (*b*) is the Fermi gas curve predicted on the assumption that the matrix element is proportional to $\bar{q}_m$ and isotropic in the center-of-mass system, curve (*c*) is the predicted meson spectrum corresponding to a constant matrix element and a $\cos \bar{\theta}$ angular dependence, curve (*d*) is the meson spectrum corresponding to a matrix element proportional to $\bar{q}_m \cos \bar{\theta}$, and finally curve (*e*) is the theoretical meson spectrum using the Chew-Goldberger momentum distribution and assuming that the matrix element is proportional to $\bar{q}_m$ and isotropic in the center-of-mass system. All these curves are calculated for π^+ mesons emitted at 90° with respect to an incident beam of 381-Mev protons and are based on the assumption of an equivalent two-body final state.

Theoretical calculations of charged π meson production in complex nuclei by γ rays have also been performed. Hayakawa[13] has set up the calculation in a general form by writing, for the free nucleon cross section,

$$\sigma_0(\mathbf{P}) = 4\pi^2\lambda_0^2 \int \frac{d\mathbf{q}}{q_0} \int \frac{d\mathbf{p}}{p_0} f(\mathbf{k}, \mathbf{P}, \mathbf{q})\delta(\mathbf{p} + \mathbf{q} - \mathbf{P} - \mathbf{k}) \qquad \delta(p_0 + q_0 - P_0 - k_0) \quad (22)$$

where $\lambda_0 = [(\mathbf{k}P_0 - k_0\mathbf{P})^2 - (\mathbf{k} \times \mathbf{P})^2]^{-\frac{1}{2}} \equiv k_0P_0(1 - \beta \cos \theta)(\beta = |\mathbf{P}|/P_0)$ is an invariant quantity which contains as a factor the relative velocity between the incident photon and the target nucleon, f is the invariant matrix element, and the following notation is used:

	Incident photon	Target nucleon	Meson	Recoil nucleon
Momentum............	$\mathbf{k}$	$\mathbf{P}$	$\mathbf{q}$	$\mathbf{p}$
Energy (total).........	k_0	P_0	q_0	p_0
Mass.................	0	M	μ	M

In terms of the above formulation of the free nucleon cross section, the cross section for meson production in a complex nucleus by a photon can be written

$$\sigma = \frac{4\pi^2 Z}{k_0 M} \int \frac{d\mathbf{q}}{q_0} \int \frac{d\mathbf{p}}{p_0} \int d\mathbf{P}\rho(\mathbf{P}) f(\mathbf{k}, \mathbf{P}, \mathbf{q})\delta(\mathbf{p} + \mathbf{q} - \mathbf{P} - \mathbf{k}) \qquad \delta(p_0 + q_0 - P_0 - k_0 + \Delta B) \quad (23)$$

---

[13] S. Hayakawa, *Phys. Rev.*, in press; cf. also J. Serpe, *Physica*, **16**: 890 (1950; and H. Fukuda and G. Takeda, *Prog. Theor. Phys.*, **5**: 800 (1950).

where $\rho(\mathbf{P})$ is the momentum distribution of nucleons in the nucleus. The difference in energies between the initial and final nuclei is inserted into the energy conservation law via the factor ΔB. Hayakawa now proceeds to integrate Eq. (23) under the following assumptions: (1) the nucleon momentum distribution in the nucleus is given by the Fermi gas model, (2) the invariant matrix element is a constant (in approximate agreement with the prediction of the pseudoscalar theory), (3) nonrelativistic mechanics can be used for the nucleons, and (4) the final nucleus is left in the ground state so that the nuclear energy change ΔB can be set equal to the difference between the initial and final nuclear masses. Making these assumptions, Hayakawa finds that the differential cross section for producing a meson of energy q_0 in the solid angle $d\Omega_q$ is

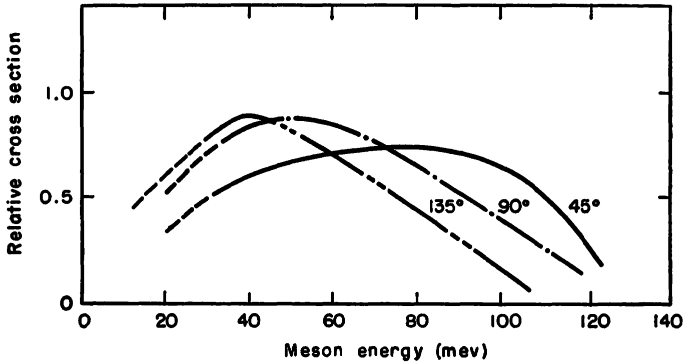

FIG. 9. Theoretical π^+ meson spectra from carbon at 45°, 90°, 135° with respect to an incident γ ray beam of 330-Mev cutoff energy based on the Fermi gas model for the nucleus.

$$\frac{d\sigma}{d\Omega_q} = \frac{3\pi^2 Zfq}{k_0 a p_0 P_F} \begin{cases} \left[1 - \left(\dfrac{b^2 - a^2}{2aP_F}\right)^2\right] & \text{for } b^2 \geq \left[P_F^2 - \left(\dfrac{b^2 - a^2}{2a}\right)^2\right] \\ \dfrac{b^2}{P_F^2} & \text{for } b^2 < \left[P_F^2 - \left(\dfrac{b^2 - a^2}{2a}\right)^2\right] \end{cases} \tag{24}$$

where $a = |\mathbf{k} - \mathbf{q}|$, $b = \sqrt{2M(k_0 - q_0 - \Delta B)}$, and P_F is the Fermi momentum. Since the usual experiment is performed with a bremsstrahlung spectrum of γ rays, Eq. (24) must be integrated over k_0 up to the maximum photon energy in order to be compared with experiment. The meson spectra predicted by Hayakawa for carbon at 45, 90, and 135° are shown in Fig. 9 corresponding to a bremsstrahlung photon spectrum with an upper limit of 330 Mev. It should be noted that taking into account the difference in nuclear energies (*i.e.*, the ΔB term in the energy conservation law) contributes to an understanding of the behavior with atomic number of the π^-/π^+ ratio in the case of mesons produced by γ rays (cf. Sec. 4). By the same token, failure to take account of the difference between the initial and final nuclear energies makes it difficult to understand at least one experiment on the production of π mesons in nucleon-nuclei collisions (cf. Sec. 6).

Lax and Feshbach[14] have carried out an independent calculation of the photonic production of mesons in complex nuclei which can be shown to be essentially equivalent to Hayakawa's. Lax and Feshbach write a cross section for meson production in a complex nucleus by a γ ray in the form

$$\sigma = 4\pi^2 Z \int d\mathbf{q} \int d\mathbf{p} \int d\mathbf{P} \rho(\mathbf{P}) |ME|^2 \delta(\mathbf{p} + \mathbf{q} - \mathbf{P} - \mathbf{k}) \\ \delta(p_0 + q_0 - M - k_0 + \Delta B) \quad (25)$$

where ME is the matrix element. If we set

$$|ME|^2 = \frac{f}{k_0 P_0 p_0 q_0} \quad (26)$$

Eqs. (23) and (25) become identical except for a slight change in the δ function expressing energy conservation. The change consists in replacing P_0 by M and reflects the fact that, whereas Hayakawa regards $\rho(\mathbf{P})$ as the momentum distribution of free nucleons inside a potential box, Lax and Feshbach consider $\rho(\mathbf{P})$ as the Fourier transform of a nuclear wave function; in the former model, a kinetic energy is assigned to the nucleon appropriate to its momentum, whereas in the latter model the target nucleon is regarded as bound in the nucleus with a specified momentum but with an energy determined by the nucleus as a whole. Since in the Fermi gas model $(P_0 - M) \leq 22$ Mev, the difference in the meson energy resulting from the difference in the two models will not be large for photon energies above 250 Mev. Lax and Feshbach use their formula for an application which is not considered by Hayakawa, *viz.*, to the Chew-Goldberger momentum distribution which is somewhat more appropriate for a light nucleus like carbon. Rewriting Eq. (25) as

$$\sigma = 4\pi^2 Z \int |ME|^2 I \, d\mathbf{q} \quad (27)$$

where $$I = \frac{2\pi(M + k_0 - q_0 - \Delta B)}{a} \int_{|a-b'|}^{a+b'} \rho(P) P \, dP$$

with $$b' = [(k_0 - q_0 - \Delta B)(2M + k_0 - q_0 - \Delta B)]^{\frac{1}{2}}$$

and inserting $$\rho(P) = \frac{\alpha}{\pi^2} \frac{1}{(\alpha^2 + P^2)^2}$$

---

[14] M. Lax and H. Feshbach, *Phys. Rev.*, **81**: 189 (1951).

one finds $$I = \frac{\alpha}{\pi} \frac{M + k_0 - q_0 - \Delta B}{a} \left[\frac{1}{\alpha^2 + p_e^2} - \frac{1}{\alpha^2 + (a + b')^2} \right] \qquad (27a)$$
where
$$\begin{aligned} p_e^2 &= a^2 - b'^2 \qquad &\text{for } a \geq b' \\ &= (b' - a)^2 \qquad &\text{for } a < b' \end{aligned}$$

The π meson spectrum is then easily computed, provided that some assumption is made about the matrix element. Choosing ME = constant [essentially the same assumption made by Hayakawa since the factor $(k_0q_0P_0p_0)$ in Eq. (26) is slowly varying], restricting the angle to 90°, and averaging over the bremsstrahlung spectrum for the photons, Lax and Feshbach obtain the π^+ meson spectrum plotted in Fig. 10.

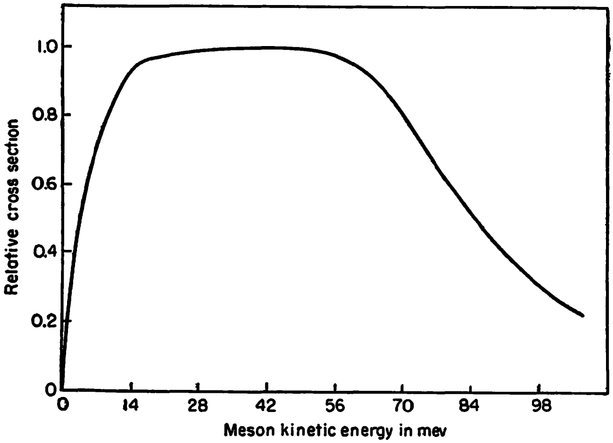

FIG. 10. Theoretical π^+ meson spectrum from carbon at 90° with respect to an incident γ ray beam of 330-Mev cutoff energy based on the Chew-Goldberger distribution.

B. Effects of the Pauli Principle. Our discussion of the effects on π meson production of the finite momenta of the nucleons in a nucleus has implicitly taken into account the Pauli exclusion principle in at least two respects: (1) the essential feature of the Fermi gas model—the filling of all states up to the Fermi energy—is fixed by the operation of the Pauli principle; and (2) the difference in nuclear energy between the initial and final nuclei, ΔB, which was fed into the energy conservation equation for the photonic production calculations reflects the operation of the Pauli principle for actual nuclei. However, it seems worth while to spell out in somewhat greater detail two connected effects of the Pauli exclusion principle: (1) the nuclear cross section for meson production per nucleon will be *less* (for incident energies not too far from threshold) than the free nucleon cross section independent of the charge of the meson, provided that the free nucleon cross section does not vary too rapidly and (2) the magnitude of the reduction will depend on the charge of the meson and of the incident particle and will be greater, the greater the change in the isotopic spin of the nucleus. These statements hold, provided that some special selection rule associated with a specific nucleus does not intervene. For both photon-nucleus and nucleon-nucleus collisions, effect (1) will exist for incident particle energies not too far from threshold (say less than twice threshold) and will in general persist to higher energies for nucleonic production than for photonic production. Qualitatively, it is expected that the magnitude of the reduction in cross section will be greatest for charged meson production by nucleons, less for neutral meson production by nucleons or charged meson production by photons, and least for neutral meson production by photons.

Let us consider in turn the efficiency for the production of charged and neutral π mesons by photons and by nucleons interacting with complex nuclei where the efficiency is defined as the ratio of the total nuclear cross section per nucleon of the appropriate kind to the total free nucleon cross section. By writing the free proton cross section in the form

$$\sigma_0 = 4\pi^2 \int |ME|^2 \, d\mathbf{q} \; \delta[\sqrt{M^2 + (\mathbf{k} - \mathbf{q})^2} + q_0 - k_0 - M] \tag{28}$$

and assuming $(\mathbf{k} - \mathbf{q}) \gg \mathbf{P}$ in Eq. (25), Lax and Feshbach have derived an expression for the efficiency for π^+ production by photons, namely,

$$\frac{\sigma^+}{Z\sigma_0} = \int_{|\mathbf{k}+\mathbf{P}| \leq d} \rho(\mathbf{P}) d\mathbf{P} \tag{29}$$

where $d = \sqrt{2M(k_0 - \Delta B_+ - \mu)}$ and ΔB_+ refers to the nuclear energy difference resulting from π^+ meson production. Equation (29) implies that the efficiency will always be smaller than unity because, consistent with energy conservation, only a part of the momentum distribution of the nucleons in a target nucleus can contribute to the nuclear cross section. Equation (29) can be evaluated by picking the distribution function; if one chooses $\rho(P) =$ the Chew-Goldberger distribution [Eq. (20)], one finds

$$\frac{\sigma^+}{Z\sigma_0} = \frac{1}{\pi}\left[\tan^{-1}\left(\frac{d - k_0}{\alpha}\right) + \tan^{-1}\left(\frac{d + k_0}{\alpha}\right)\right] + \frac{\alpha}{2\pi k_0} \log\left[\frac{\alpha^2 + (d - k_0)^2}{\alpha^2 + (d + k_0)^2}\right] \tag{30}$$

Equation (30) is plotted in Fig. 11 as a function of the photon energy after setting $\Delta B_+ = 0$.

The curve in Fig. 11 has been computed by neglecting the difference between the initial and final nuclear energies; this is satisfactory if one wishes to know the approximate variation of the efficiency with photon energy. However, if one wishes to know the π^-/π^+ production ratio from the same nucleus, the different values of ΔB_+ and ΔB_- must be taken into account. In particular, the efficiency for π^- meson production by γ rays in a complex nucleus can be written

$$\frac{\sigma^-}{(A - Z)\sigma_0} = \int_{|\mathbf{k}+\mathbf{P}| \le d} \rho(\mathbf{P})d\mathbf{P} \tag{31}$$

where $d = \sqrt{2M(k_0 - \Delta B_- - \mu)}$, ΔB_- is now the difference in nuclear energy between the initial and final nucleus resulting from π^- emission, $(A - Z)$ is the number of neutrons, and σ_0 is the free neutron cross section. The ratio of Eq. (31) to Eq. (29) will yield, for a given nucleus, the factor by which the intrinsic π^-/π^+ ratio (*i.e.*, for free nucleons) must be multiplied in order to obtain the nuclear π^-/π^+ ratio. Equations (29) and (31) allow us to obtain a quantitative estimate of the energy at which the efficiency approaches unity. It is seen that in each case the region of integration is approximately a sphere of radius

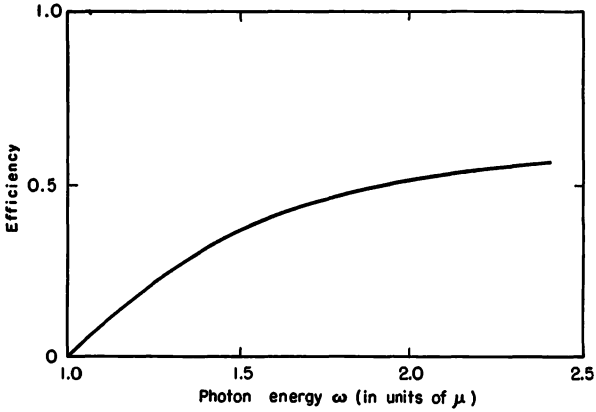

FIG. 11. Theoretical efficiency of π^+ meson production in a photon-nucleus collision based on the Chew-Goldberger distribution.

$$\sqrt{2M(k_0 - \mu)}$$

centered at $-\mathbf{k}$. However, $\rho(\mathbf{P})$ is appreciable over the sphere for $P < P_F$ and small outside; these spheres will overlap almost completely if $\sqrt{2M(k_0 - \mu)} > k_0 + P_F$. Consequently, the efficiency may be expected to approach unity at an energy $k_0 \approx 2.3\mu$, that is, 320 Mev for charged π mesons (the slow rise in efficiency indicated in Fig. 11 is due to the long tail of the Chew-Goldberger distribution which is therefore suspect).

In principle, it is possible to write down an expression for the efficiency of π^0 production in complex nuclei by photons if one knows the relative cross sections for π^0 production in photon-proton and photon-neutron collisions. Since this knowledge is incomplete at the present time, we shall refrain from writing down such an expression. It is qualitatively clear, however, and has been pointed out above, that, for a specified photon energy and nucleus, the efficiency for π^0 production should be greater than for charged π production; this follows from the fact that ΔB_0 is, in general, smaller than ΔB_+ or ΔB_-.

In the case of nucleonic meson production, expressions can be written down, though more complicated, for the efficiency of production in the complex nucleus just as for photonic production. The novel effect is the rather trivial one that the ratio of π^+ to π^- to π^0 production in a given nucleus depends on whether the incident nucleon is a proton or a neutron. If we let $\sigma^+(PP)$ be the cross section for π^+ production in P-P collisions, $\sigma^+(NP)$ the cross section for π^+ production in N-P collisions, and so on, then the a priori ratios N^+ to N^- to N^0 in a nucleon-nucleus collision (assuming $A = 2Z$) are

Proton:

$$N^+:N^-:N^0 = \sigma^+(PP) + \sigma^+(NP):\sigma^-(NP):\sigma^0(PP) + \sigma^0(NP) \tag{32}$$

Neutron:

$$N^+:N^-:N^0 = \sigma^+(NP):\sigma^-(NN) + \sigma^-(NP):\sigma^0(NN) + \sigma^0(NP) \tag{33}$$

The equality of N-N and P-P forces and the condition of gauge invariance (requiring the same coupling constant for π^+ and π^-) enable one to write[14a]

Proton: $$N^+:N^-:N^0 = \sigma_l + \sigma_u:\sigma_u:(\sigma_l^0 + \sigma_u^0) \tag{34}$$
Neutron: $$N^+:N^-:N^0 = \sigma_u:\sigma_l + \sigma_u:(\sigma_l^0 + \sigma_u^0) \tag{35}$$

where the subscripts l and u denote like and unlike nucleons, respectively. Without writing down the explicit efficiency expressions for nucleonic production, it is clear from the photonic expressions (29) and (31) that π^+ production will be favored more than π^- (or π^0) when the incident particle is a proton and that π^- production will be favored more than π^+ (or π^0) when the incident particle is a neutron. This follows if it is recalled that the efficiency is greater, the smaller the ΔB (the difference in nuclear energy between the initial and final nuclei); it is evident that, in general, ΔB will be larger for π^- production (or π^0) than for π^+ when the incident particle is a proton and conversely for the incident neutron. Consequently, the a priori ratio, which already favors π^+ production for incident protons, will be enhanced and similarly for π^- mesons when the incident particle is a neutron. From these remarks, it follows that (1) for a fixed incident proton energy and for equal like and unlike nucleon cross sections for π meson production, the positive or neutral to negative ratio should increase with meson energy; and (2) for a fixed meson energy, the positive or neutral to negative ratio should increase as the proton energy is decreased. Both statements apply to the negative or neutral to positive ratio when the incident nucleon is a neutron.

[14a] It was noted in Chap. 2 (footnote 21*a*) that if the charge independence hypothesis holds for nucleons and mesons, $\sigma_l^0 + \sigma_u^0 = \frac{1}{2}\sigma_l + \sigma_u$; if this equation is inserted into Eqs. (34) and (35), one derives the relation $N^0 = \dfrac{N^+ + N^-}{2}$ for both incident protons and neutrons. This relation is Messiah's result [cf. *Phys. Rev.*, **86**: 430 (1952)] derived on the assumption that the target nucleus possesses zero isotopic spin (the expected value for an $A = 2Z$ nucleus in its ground state).

Chew and Steinberger[15] first arrived at these conclusions by a line of argument which is essentially equivalent to the above. They pointed out that, if one regards a nucleus as consisting of alpha-particle clusters, an incident proton colliding with one of the bound nucleons in an alpha-particle cluster will yield 2 protons and 3 neutrons if a π^+ meson is produced and 4 protons and 1 neutron if a π^- meson is created. The latter situation is obviously more unfavorable than the former since the Pauli principle requires two of the final protons to possess high momenta rather than one of the final neutrons. By the same token, the production of π^0 mesons will yield 3 protons and 2 neutrons and the Pauli principle should inhibit this process (because of the equality of N-N and P-P forces) to about the same degree as the π^+ production. However, it is essentially the Pauli principle which is responsible for the large differences in ΔB depending on which type of meson is produced, and it was in terms of ΔB that the argument was presented above.

Chew and Steinberger made a rough estimate of the relative efficiency for π^+/π^- production in proton-nucleus collisions with the result

$$\frac{N^+}{N^-} = \frac{1 - (T_F/\tau_m - \tau)}{1 - (2T_F/\tau_m - \tau)} \tag{36}$$

where τ_m is the maximum kinetic energy (in the laboratory system) of the meson and τ is the kinetic energy actually observed [that is, $(\tau_m - \tau)$ is essentially the total energy available to the two final nucleons]. The dependence on the incident nucleon energy occurs through τ_m, which is a function of the nucleon energy. Equation (36) will suffice for comparison with the existing experimental data (cf. Sec. 6).

---

[15] G. Chew and J. Steinberger, *Phys. Rev.*, **78**: 497 (1950).

C. Effects of the Coulomb Field. The cross sections for charged meson production by both photons and nucleons are appreciably modified in heavy nuclei at low meson energies by the Coulomb field. Coulomb corrections are well known in the theory of β decay where the number of positrons at low energies is decreased by the Coulomb field whereas the number of electrons is enhanced. This is due to the fact that, as a result of the electric repulsion, positrons gain energy upon leaving the nucleus whereas the attractive force for the electrons leads to a finite number emitted at zero kinetic energy. In quantum-mechanical language, the positron has to overcome a Coulomb barrier whereas the electron enters a shallower well. A fairly accurate quantitative estimate of the Coulomb effect in β decay is obtained quite readily; the electron wave function ψ has the following form in the Schrodinger approximation:

$$\psi = e^{ipx/\hbar}e^{\pi\xi/2}\Gamma(1 - i\xi)\left[1 - \frac{\xi p}{\hbar}(r - x) + \cdots\right] \tag{37}$$

where $\xi = Ze^2/\hbar v$, p is the electron momentum in the direction x, v is the velocity of the electron, Z the charge on the nucleus, and r is the radial distance. At the origin, $|\psi|^2$ becomes

$$|\psi(0)|^2 = \frac{2\pi\xi}{(1 - e^{-2\pi\xi})} \tag{37a}$$

If we denote the correction factor $2\pi\xi/(1 - e^{-2\pi\xi})$ by C_- for electrons, the correction factor for positrons is

$$C_+ = \frac{2\pi\xi}{e^{2\pi\xi} - 1} \tag{38}$$

A similar calculation can be performed for the meson production problem; however, it is not expected that the correction factors C_- and C_+ will represent the meson case as well as the electron case because the de Broglie wave length of the meson is much larger and comparable with the nuclear radius [cf. the second term on the R.H.S. of Eq. (37)]. Nevertheless, we shall use C_- and C_+ to estimate the Coulomb corrections for meson production in the comparison with experiment considered below.

D. Effects of the Meson-nucleon Interaction. Thus far, we have discussed the modifications introduced into the cross sections for π meson production in photon-nucleus and nucleon-nucleus collisions by the existence of finite nucleon momenta in the nucleus, the operation of the Pauli exclusion principle, and the presence of a Coulomb field. A further modification is introduced by the fact that the cross section for the interaction of π mesons with nucleons is close to geometrical (cf. Chap. 7).

As a result, the produced meson may suffer a nuclear collision during the course of its traversal of the nucleus and may not emerge from the nucleus. It is evident that the interaction effect becomes increasingly more important for heavier nuclei. A rough quantitative estimate can be obtained at once by considering that only mesons produced on the surface of the nucleons will definitely get out; hence the cross section per nucleon in a heavy nucleus will, to a first approximation, be reduced by the factor: surface area/volume $\approx 1/A^{1/3}$. A more refined calculation can easily be carried out, assuming uniform production of the mesons inside the nuclear volume and choosing a value for the meson-nucleon interaction mean free path l. The result is[16]

$$\sigma(A) = 3A\sigma_0 \left[\frac{1}{2\eta} - \frac{1}{\eta^3} + \frac{1}{\eta^3}(1+\eta)e^{-\eta}\right] \tag{39}$$

where $\eta = 2R/l$ and $R = r_0A^{1/3}$($r_0 \approx 1.5 \times 10^{-13}$ cm) is the nuclear radius. In Eq. (39), $\sigma(A)$ is the meson production cross section for a nucleus with atomic weight A and σ_0 is the meson production cross section per free nucleon. Equation (39) has the necessary features, namely, $\sigma(A) \rightarrow A\sigma_0$ for $l \rightarrow \infty$ and $\sigma(A) \rightarrow (3l/4r_0)A^{2/3}\sigma_0$ for $l \rightarrow 0$. Even if an $A^{2/3}$ behavior is observed experimentally for the meson production cross section, conclusions concerning the meson-nucleon interaction can only be drawn provided that the total cross section for *all* processes (including meson production) for the incident photon or nucleon is not close to geometrical. If the incident particle has a geometrical cross section, *e.g.*, for star production, an $A^{2/3}$ behavior would result for meson production even if the meson-nucleon interaction were absent.

Special interest attaches to the behavior of the cross section for π^0 production. This will provide the only means for obtaining information concerning the interaction of π^0 mesons with nucleons because of the extremely short lifetime of the π^0 meson. As long as the lifetime of the π^0 meson is greater than about 10^{-23} sec (which it is—cf. Chap. 4), it will preserve its identity during its traversal of a nucleus and it will interact as a π^0 meson.

4. Production of Charged π Mesons in Photon-Nucleus Collisions

The first observations on the photonic production of charged π mesons were made in 1949 by McMillan *et al.*[17] using carbon as a target. The Berkeley synchrotron (with an upper limit of 335 Mev on the bremsstrahlung γ ray spectrum) was the source of γ rays and the charged π mesons were detected by means of photographic emulsions. A meson energy spectrum was measured at 90° with respect to the incident photon beam and a broad distribution was found with a maximum at about 40 Mev. It was also found that the π^-/π^+ ratio in the energy region 43 to 59 Mev was 1.7 ± 0.2 and that the measured angular distribution was consistent with isotropy in the center-of-mass system. Assuming isotropic production for mesons of all energies, a meson production cross section of 5×10^{-28} cm^2 per equivalent photon (an equivalent photon is defined as the integrated beam energy divided by the maximum energy of the bremsstrahlung spectrum) per carbon nucleus was derived.

---

[16] Fernbach, Serber, and Taylor, *Phys. Rev.*, **75**: 1352 (1949).

[17] McMillan, Peterson, and White, *Science*, **110**: 579 (1949).

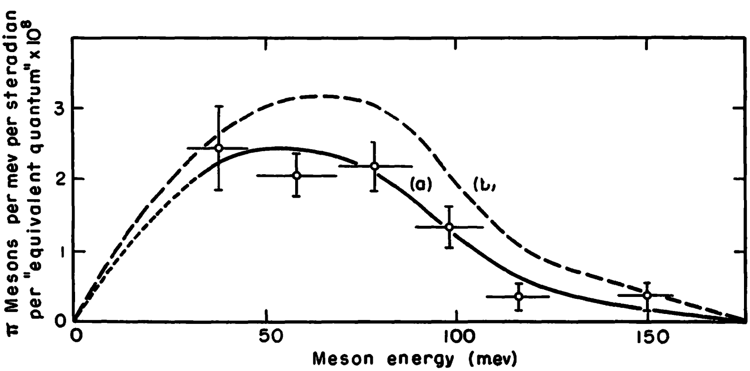

Fig. 12. Measured energy spectrum of charged π mesons from γ rays on carbon at an angle of 45° in the laboratory system with respect to the incident photon beam; the bremsstrahlung spectrum has an upper limit of 330 Mev. Curve (*a*) is uncorrected for nuclear absorption in the absorber, (*b*) is corrected for nuclear absorption.

Peterson *et al.*[18] pursued the photographic method further and obtained meson spectra from carbon at angles of 45, 90, and 135° for the same upper limit on the bremsstrahlung γ rays as before; his results are shown in Figs. 12 to 14. Peterson's absolute cross sections per steradian per nucleus per equivalent photon (for both π^+ and π^- production) are given in Table 5 on the basis of the numbers corrected for nuclear absorption in the absorber; these cross sections may contain a systematic error of 35 per

Table 5. Differential Cross Sections for Charged π Meson Production in Carbon by γ Rays with Upper Limit of 330 Mev

θ, Degrees	$\left(\frac{d\sigma}{d\Omega}\right)_{\text{lab}}$ in Units of 10^{-29} cm^2/ster
45	2.52 ± 0.22
90	3.87 ± 0.18
135	2.82 ± 0.19

---

[18] Peterson, Gilbert, and White, *Phys. Rev.*, **81**: 1003 (1951).

DAVID J. LANGFORD

cent. The total cross section deduced from the above data is 4.0 × 10^{-28} cm² ± 40 per cent per carbon nucleus per equivalent photon. Peterson also studied the π^-/π^+ ratio as a function of meson energy at the three angles; his statistical errors were so large, however, that the experimental curves are consistent with a constant ratio, and these ratios are listed in Table 6 together with the mean energy of the mesons.

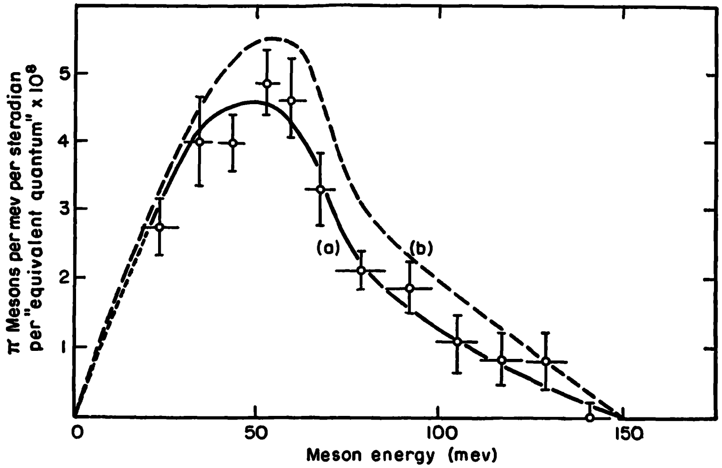

FIG. 13. Measured energy spectrum of charged π mesons from γ rays on carbon at an angle of 90° in the laboratory system with respect to the incident photon beam; the bremsstrahlung spectrum has an upper limit of 330 Mev. Curve (*a*) is uncorrected for nuclear absorption in the absorber, (*b*) is corrected for nuclear absorption.

Peterson's meson spectra at 45, 90, and 135° are to be compared with the predictions of Hayakawa's theory shown in Fig. 9 and with the theoretical curve of Lax and Feshbach shown in Fig. 10. Both theoretical curves are in sufficiently good agreement with the experimental curves to confirm the importance of the finite momentum distribution of the nucleons in the carbon nucleus. However, reliable discrimination between the two distributions is not possible because of the experimental uncertainties and the smearing-out effect produced by the bremsstrahlung

TABLE 6. π^-/π^+ RATIO FROM PHOTON-CARBON COLLISIONS AT THREE ANGLES

θ, degrees	π^-/π^+	Mean meson energy, Mev
45	1.29 ± 0.22	70
90	1.30 ± 0.12	56
135	1.34 ± 0.20	54

spectrum of the incident γ ray beam. The total cross section per carbon nucleus obtained by Peterson is only twice as large as the total cross section per free proton (cf. Chap. 1). This large drop in cross section per proton is explicable in terms of the Pauli principle and is in rough agreement with the efficiency prediction of Fig. 11 which yields 3. The π^-/π^+ ratio observed by Peterson is lower than the earlier Berkeley ratio but, as we shall see below, is still too high; hence no comparison with theory will be made at this point.

Electrical methods have also been used to detect π^+ mesons produced in photon-nucleus collisions by taking advantage of the $\pi^+ \rightarrow \mu^+ \rightarrow e^+$ sequence of decays. Thus, Steinberger and Bishop,[19] using the Berkeley synchrotron, have studied π^+ mesons produced in a carbon target in the energy range 35 to 105 Mev and in the angular range 45 to 135° and have, within statistical error, confirmed the photographic measurements. Mozley[20] has investigated the dependence on atomic number of the π^+ cross section for two specific energies, namely, 42 ± 7 and 76 ± 6 Mev, at an angle of $90 \pm 8°$ in the laboratory system and with an upper limit for the bremsstrahlung spectrum of 317 Mev. He made measurements on H, Li, Be, B, C, Al, Cu, Sn, and Pb with the results for the relative cross sections per proton in arbitrary units shown in Table 7. These numbers have not been corrected for meson absorption in the target; if the geometrical cross section for this process is taken into account, the

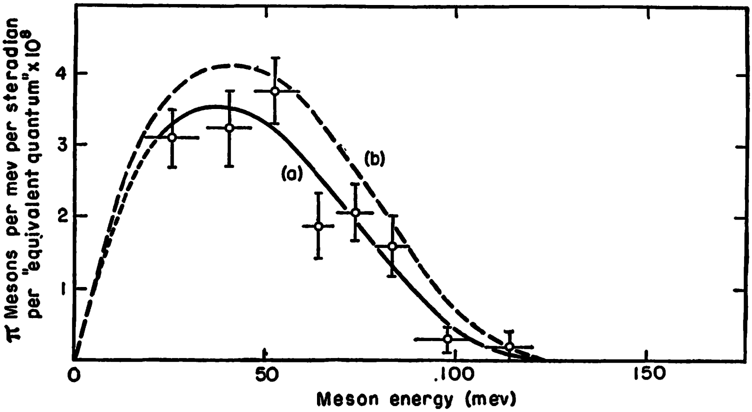

FIG. 14. Measured energy spectrum of charged π mesons from γ rays on carbon at an angle of 135° in the laboratory system with respect to the incident photon beam; the bremsstrahlung spectrum has an upper limit of 330 Mev. Curve (*a*) is uncorrected for nuclear absorption in the absorber, (*b*) is corrected for nuclear absorption.

---

[19] J. Steinberger and A. Bishop, *Phys. Rev.*, **78**: 493 (1950).

[20] R. F. Mozley, *Phys. Rev.*, **80**: 493 (1950).

correction is 8 per cent at 42 Mev and 25 per cent at 76 Mev. Table 7 shows the large drop in the cross section per proton in going from hydrogen to the light nuclei and the more gradual drop in moving up the periodic table to the heavier nuclei. The first drop can easily be explained, as before, in terms of the Pauli exclusion principle. The more gradual drop can be explained most plausibly in terms of the interaction of the outgoing π^+ meson with the nucleons in the nucleus (the energies are too high for the Coulomb barrier to be effective). As shown in Sec. 3, such a meson-nucleon interaction leads approximately to an $A^{-\frac{1}{3}}$ behavior for the cross section per proton, a result which fits quite well the numbers in Table 7. From other experiments,[21] it is known that the total cross section for all processes for photon energies of several hundred Mev is much smaller than geometrical, of the order of 10^{-28} cm^2 per nucleon, so that an $A^{\frac{2}{3}}$ behavior for the meson production cross section would not be expected if the meson-nucleon interaction were negligible [cf. Eq. (39)].

TABLE 7. RELATIVE YIELDS OF PHOTO-PRODUCED π^+ MESONS AS A FUNCTION OF ATOMIC NUMBER

Element	H	Li	Be	B	C
σ/Z at 42 Mev	6.6 ± 17%	3.32 ± 10%	2.82 ± 11%	3.02 ± 11%	2.60 ± 6%
σ/Z at 76 Mev	8.07 ± 11%	2.80 ± 11%	2.13 ± 10%	2.28 ± 15%	1.93 ± 5%

Element	Al	Cu	Sn	Pb
σ/Z at 42 Mev	2.50 ± 11%	1.92 ± 19%	1.66 ± 25%	0.51 ± 91%
σ/Z at 76 Mev	1.68 ± 9%	1.17 ± 15%	0.51 ± 55%	0.80 ± 65%

The most recent application of electrical methods to the study of photomesic production has been made by Jakobson.[22] Taking advantage of recent developments in electronic and scintillation-counter techniques, which allow the detection of the $\pi^+ \rightarrow \mu^+$ decay directly, Jakobson has studied, with the help of the Berkeley synchrotron, the photoproduction of π^+ mesons in helium. Figures 15 to 17 show the observed energy spectra from helium at 45, 90, and 135°, respectively, both with and without the correction for nuclear absorption of the emitted π^+ mesons (the 45° curve was actually measured with the emulsion technique). The other curves in Figs. 15 to 17 represent the energy spectra of π^+ mesons from hydrogen at the respective angles 45, 90, and 135°, which

---

[21] Cf. S. Kikuchi, *Phys. Rev.*, **81**: 1059 (1951); and R. D. Miller, *Phys. Rev.*, **82**: 260 (1951).

[22] M. J. Jakobson, *UCRL* No. 1317.

Jakobson also measured in order to compare directly with helium and as a check on previous work. It is interesting to note that the π^+ spectra from helium cover larger energy intervals than those from hydrogen—a result which would be expected because of the finite momenta of the nucleons in the helium nucleus. The integrated cross sections per steradian which are derived from Figs. 15 to 17, together with the total cross sections and the carbon cross sections, are given in Table 8. The decrease in cross section per proton from hydrogen to helium to carbon shows clearly the operation of the Pauli exclusion principle and the important role played by the saturated alpha-particle structure.

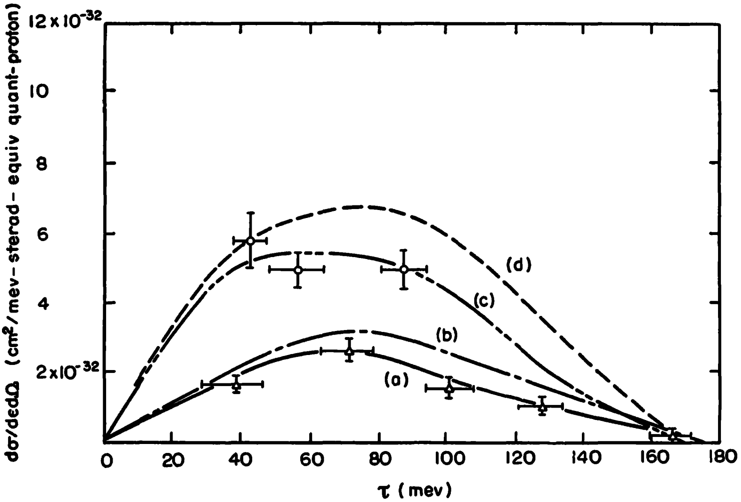

FIG. 15. Measured energy spectrum of π^+ mesons from γ rays on helium and hydrogen at an angle of 45° in the laboratory system with respect to the incident photon beam; the bremsstrahlung spectrum has an upper limit of 312 Mev. Curve (*a*) is the uncorrected curve from He, (*b*) is the corrected curve from He, (*c*) is the uncorrected curve from H, (*d*) is the corrected curve from H.

TABLE 8. DIFFERENTIAL CROSS SECTIONS PER PROTON FOR π^+ PRODUCTION BY γ RAYS IN H, He, AND C
(Corrected for nuclear absorption)

θ / Element	$45^{\circ}\,^{+17^{\circ}}_{-15^{\circ}}$ (10^{-30} cm²/ster)	90° ± 19° (10^{-30} cm²/ster)	$135^{\circ}\,^{+19^{\circ}}_{-21^{\circ}}$ (10^{-30} cm²/ster)	Total (10^{-29} cm²)
H	7.1 ± 0.7	9.1 ± 0.6	6.0 ± 0.4	9.5 ± 0.6
He	3.1 ± 0.3	4.7 ± 0.4	3.8 ± 0.3	4.8 ± 0.2
C	2.4	3.5	2.4	3.6

The most accurate measurement of the π^-/π^+ ratio has been carried out by Littauer and Walker[23] using the 300-Mev Cornell synchrotron; these authors observe the charged π mesons which are produced after they are magnetically focused onto an array of counters. Their results are summarized in Table 9 for several different targets for 50-Mev π^- and π^+ mesons emitted at 135° with respect to the incident photon direction. The last column in Table 9 lists Hayakawa's predictions for the π^-/π^+ ratios based on Eq. (24); the theoretical ratios are normalized to carbon. The agreement between theory and experiment is reasonably satisfactory for all nuclei except calcium. The discrepancy for calcium may find its explanation in the fact that the final nucleus possesses a spin of 4 whereas the spin of Ca^{40} is 0. The photomesic production process probably leads, in the majority of cases, to excited states of the final nucleus having smaller spins than 4, and it can be shown that this should decrease the π^-/π^+ ratio. The Cornell group has also measured the sum of the differential cross sections for π^- and π^+ production as a function of

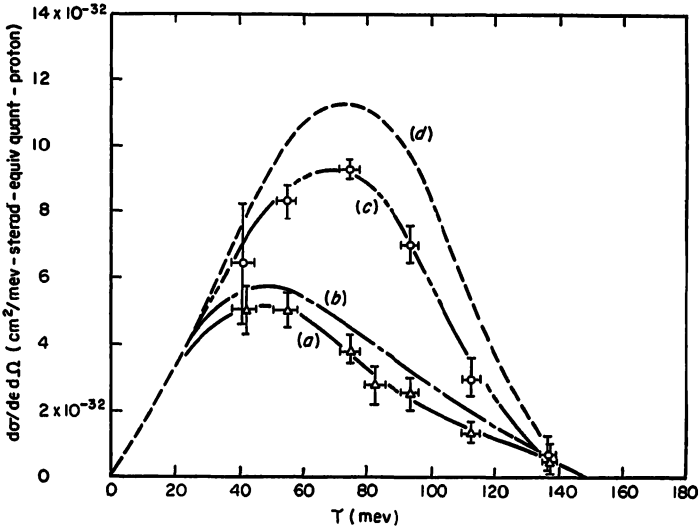

FIG. 16. Measured energy spectrum of π^+ mesons from γ rays on helium and hydrogen at an angle of 90° in the laboratory system with respect to the incident photon beam; the bremsstrahlung spectrum has an upper limit of 312 Mev. Curve (*a*) is the uncorrected curve from He, (*b*) is the corrected curve from He, (*c*) is the uncorrected curve from H, (*d*) is the corrected curve from H.

---

[23] R. Littauer and D. Walker, *Phys. Rev.*, **82**: 746 (1951); H. A. Medicus [*Phys. Rev.*, **83**: 662 (1951)] has measured the π^-/π^+ ratio from Be with the result 2.2 ± 0.25 for mesons in the energy range 30 to 70 Mev.

mass number with respect to hydrogen as the norm; their results are shown in Fig. 18 where the solid line represents the $A^{2/3}$ variation of cross section. The agreement between theory and experiment is truly remarkable (the proximity of the deuterium point to the solid line must be sheer accident) and argues strongly for a charged π meson-nucleon interaction cross section close to geometrical.

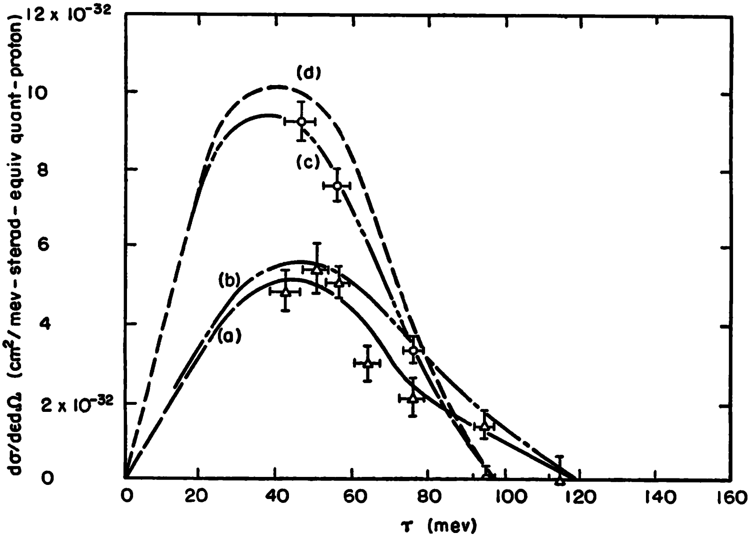

FIG. 17. Measured energy spectrum of π^+ mesons from γ rays on helium and hydrogen at an angle of 135° in the laboratory system with respect to the incident photon beam; the bremsstrahlung spectrum has an upper limit of 312 Mev. Curve (*a*) is the uncorrected curve from He, (*b*) is the corrected curve from He, (*c*) is the uncorrected curve from H, (*d*) is the corrected curve from H.

TABLE 9. π^-/π^+ RATIO FOR 50-MEV MESONS AT 135° (IN THE LABORATORY) AS A FUNCTION OF ATOMIC NUMBER

Target	Exp π^-/π^+	Theor π^-/π^+
D	1.19 ± 0.12	1.15 ± 0.02
C	1.06 ± 0.02	1.06 ± 0.02
O	1.04 ± 0.04	1.03 ± 0.02
S	0.85 ± 0.03	0.98 ± 0.02
Ca	0.58 ± 0.02	0.95 ± 0.02
Be	2.25 ± 0.11	1.84 ± 0.03
F	1.42 ± 0.05	1.28 ± 0.02
Al	1.20 ± 0.05	1.06 ± 0.02
Bi	1.32 ± 0.12	1.26 ± 0.02

Despite the reasonable agreement between Hayakawa's numbers and the experimental data for the π^-/π^+ ratio, there is one disconcerting feature of the Cornell experiments—a difficulty which is masked by normalizing the theoretical π^-/π^+ ratio to C. This difficulty stems from the fact that, for 50-Mev π mesons detected at 135° with respect to the incident photon direction, the pseudoscalar theory—which is favored by the meson production experiments with free nucleons (cf. Chaps. 1 and 2)—predicts a π^-/π^+ ratio of 2.1; it is strange that the loosely bound symmetric deuteron should lead to a π^-/π^+ ratio so different (about one-half) from the theoretically predicted value for free nucleons unless the free nucleon ratio itself is close to unity. The situation is further obscured by the fact that nuclei like Be^9, F^{19}, and Al^{27}, each with an unpaired neutron, have π^-/π^+ ratios appreciably higher than those measured from symmetric nuclei like C, O, S, and Ca since the binding-energy effect can account for the difference. If the chief contribution to charged meson production in photon-nucleon collisions comes from the interaction of the electromagnetic field with the charged meson and nucleon electric currents, the discrepancy in deuterium constitutes a real contradiction between theory and experiment. One way of obtaining a smaller π^-/π^+ ratio has already been mentioned in Chap. 1, *viz.*, to retain only the gradient part of the π meson-nucleon interaction operator in the $PS(PV)$ theory and to suppress the negative energy states of the nucleons. Another way is to assert that, for an as yet unknown reason, the contribution of the nucleon current to the charged photomesic

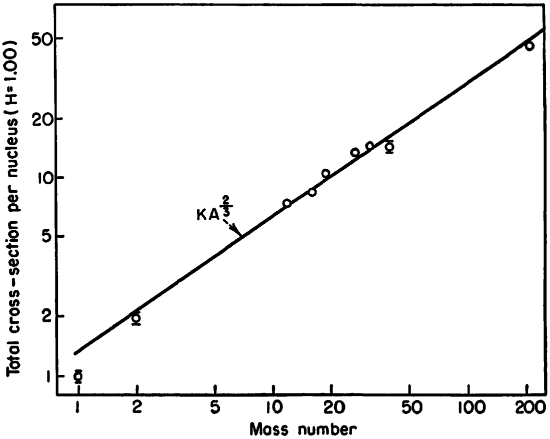

FIG. 18. Measured sum of the π^- and π^+ differential cross sections at 135° in the laboratory system for 50-Mev mesons as a function of mass number; the solid line represents the $A^{\frac{2}{3}}$ law (K is a constant).

production is suppressed. At the present time, these are, of course, only conjectures, and further experiments in deuterium at other angles are obviously desirable.

5. Production of π^0 Mesons in Photon-Nucleus Collisions

The production of π^0 mesons in photon-nucleus collisions has been studied by Steinberger *et al.*[24] using the Berkeley synchrotron. They have observed coincidences between the two γ rays into which the π^0 meson decays just as in the experiment on photon-proton production (cf. Chap. 1). As a matter of fact, it was their observation of γ ray coincidences from photon-beryllium and photon-carbon collisions which definitely established the existence of the neutral π meson. For this reason, we discuss the Berkeley experiment in some detail.

Steinberger *et al.* detected the γ rays from the π^0 meson using an apparatus consisting of two crystal telescopes operating in coincidence at a variable angle β between them; the plane of the two telescopes and the target formed a variable angle θ with respect to the incident photon direction. For a maximum photon energy of 330 Mev, the average kinetic energy of π^0 mesons (assuming the same mass as for charged π mesons—cf. Chap. 4) coming from a target like beryllium is 50 to 60 Mev (cf. Table 6) in the neighborhood of $\beta = \theta = 90°$. Consequently, the two decay photons should each possess an energy of about 100 Mev, and the coincidence counting rate of the two telescopes should reach a maximum for $\frac{1}{4}$-in. Pb converters (*i.e.*, materializers into electrons) placed before the telescopes. The Berkeley workers showed that the $\frac{1}{4}$-in. Pb converters do indeed give the maximum counting rate, that both telescopes require converters, and that $\frac{1}{4}$-in. Cu converters possess approximately the same conversion efficiency as do $\frac{1}{16}$-in. Pb converters. All these observations provide strong evidence for the photon character of the particles giving rise to the coincidences. The nuclear origin of the photons was demonstrated by showing that the coincidence rate was only six times as large (at $\theta = \beta = 90°$) for Pb compared with Be, rather than 400 times as great (Z^2 dependence); this fact proves that the photons do not have a shower (electromagnetic) origin. Finally, the beam energy was reduced to 175 Mev, and it was observed that the counting rate went down by a factor of 50 compared with the value at 330 Mev (still at $\theta = \beta = 90°$); this steep excitation function is also observed for charged π meson production and is characteristic of a phenomenon with a threshold. The fact that γ rays of about 100-Mev energy, of non-Coulombic origin, and with a threshold close to that for charged π production are observed, is overwhelming evidence for the production of a neutral π meson with a mass approximately equal to that of the charged π meson.

---

[24] Steinberger, Panofsky, and Steller, *Phys. Rev.*, **78**: 802 (1950); cf. also *Phys. Rev.*, **86**: 180 (1952).

Figure 19 contains the experimental results for the coincidence γ ray counting rates from Be as a function of β for $\theta = 45$, 90, and 135°. The shapes of these curves provide definitive evidence for the two-photon decay of the π^0 meson since the expected angular distribution for a decay into more than two photons does not show a valley for small β. Once it is recognized that the γ rays are due to neutral π mesons, it is possible to interpret the observed coincidence counting rates of Fig. 19 in terms of energy spectra for the π^0 mesons. This interpretation is simplified by the fact that the kinematics of the two-photon decay of a moving π^0 meson strongly favors the emission of two photons of almost equal energy close to the minimum angle

$$\beta_{\min} = 2 \sin^{-1} (\mu_0/\epsilon_0)$$

(μ_0 is the π^0 mass, ϵ_0 its total energy including its rest mass) which is permissible for the process.[25]

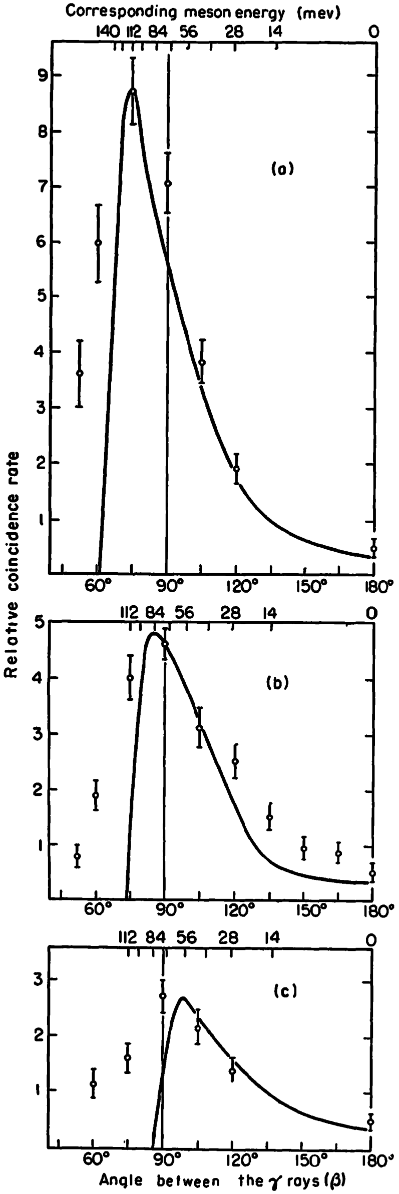

FIG. 19. Measured variation of γ ray coincidence counting rate as a function of the angle between the γ rays. Curve (*a*) corresponds to the plane of the counters at an angle of 45° (in the laboratory system) with respect to the incident photon beam, (*b*) to 90°, (*c*) to 135°; the solid curves (arbitrarily normalized for each angle) represent the γ ray distributions predicted on the assumption that the π^0 mesons are emitted with the same energy spectrum as the π^+ mesons.

---

[25] The kinematics of the two-photon decay of the π^0 meson was discussed in Chap. 1 and is further discussed in Sec. 7 below.

Thus each β in each of the three curves of Fig. 19 corresponds fairly uniquely to a specific meson energy which is so indicated; the coincidence counting rates are thereby converted into π^0 meson spectra with striking similarities to the charged π meson spectra (cf. Figs. 12 to 14). While the π^0 spectra from Be and the π^+ spectra from C are comparable as regards shape, the relative cross section for π^0 production in hydrogen and carbon at $\theta = \beta = 90°$ turns out to be 0.12 ± 0.03 in contrast to the ratio 0.5 for π^+ production. This difference can be explained partly by the fact that π^0 production does not alter the isotopic number of the carbon nucleus whereas π^+ production does: the greater number of neutrons in the latter case leads, by virtue of the Pauli principle, to a greater reduction in the available phase space than in the case of π^0 production. The π^+ production cross section per proton therefore drops suddenly in going from a free proton to a nucleus like carbon. Another reason for the greater relative cross section in carbon (with respect to hydrogen) for π^0 production compared with π^+ production lies in the fact that the neutrons in the carbon nucleus contribute to π^0 production but not to π^+ production [the neutron can produce a π^+ meson if a negatively charged isobaric nucleon is produced at the same time but presumably the cross section for this process, if it exists at all, is very small (cf. Chap. 9)]. This follows from the observation (cf. Chap. 1, Sec. 5) that the cross section for the photoproduction of π^0 mesons in deuterium is approximately twice that in hydrogen.

Preliminary measurements by Panofsky and Steller[26] on the relative yield per nucleon of 75-Mev π^0's for H, Li, Be, C, Al, Cu, and Pb show that the π^0 cross section in H is the same as the Li cross section per nucleon and that the π^0 cross section per nucleon starting at Be falls off with increasing atomic weight as does the π^+ cross section per proton. If the latter fact is confirmed, it would imply as large an interaction cross section for π^0 mesons with nuclear matter as for π^+ mesons. As was remarked earlier, this type of experiment constitutes one of the few methods available for measuring the interaction of π^0 mesons with nuclei.

6. Production of Charged π Mesons in Nucleon-Nucleus Collisions

Since the experimental data on the nucleonic production of charged π mesons in complex nuclei is rather extensive, we consider the subject under the headings: (A) excitation function, (B) energy spectrum and angular distribution, (C) π^-/π^+ ratio, and (D) dependence on atomic number.

A. Excitation Function. One of the most striking features of π meson production in nucleon-nucleus collisions is its rapid variation above threshold with the incident energy of the nucleon. Since the threshold energy T_t is pushed down to about μc^2 by the momentum distribution of the nucleons in the target nucleus (from about $2\mu c^2$ in free nucleon-nucleon collisions), the rapid variation should persist until the incident energy is at least $2T_t$. Some early measurements by Jones and White,[27] using photographic methods, confirm the rapid variation of the π^- meson excitation function. Figure 20 contains their results for π^- mesons in the energy region 2 to 10 Mev emitted from carbon within the angular range 0 to 45° with respect to the incident proton beam; the smooth curve is a plot of the function $Y(E) = k(T - T_t)^{2.3}$ ($T_t \approx 180$ Mev and k is a constant) which gives the best least-square fit of the experimental data. The exponent is, within the statistical accuracy, in agreement with the prediction of the Fermi gas model (or any one of the other models, for that matter).

---

[26] W. Panofsky and J. Steller, quoted in Mozley, footnote 20.

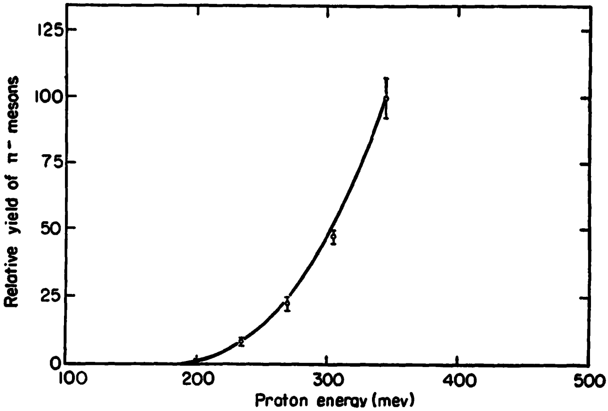

FIG. 20. Measured charged π meson excitation function for protons corresponding to a meson energy interval of 2 to 10 Mev and normalized to 100 at 345 Mev incident proton energy; the solid curve represents the function $k(T - T_t)^{2.3}$.

B. Energy Spectra. Richman and Wilcox,[28] using the Berkeley cyclotron, have measured with the emulsion technique the differential cross section for both π^+ and π^- production from a carbon target at a proton energy of 345 Mev. Their measurement was performed at an angle of 90 ± 12° with respect to the incident proton beam, and their results are shown in Fig. 21. Weissbluth[29] has carried out identical measurements with a lead target, and his results are given in Fig. 22. The curves for carbon and lead have been corrected for nuclear absorption of the emerging mesons in the absorber, assuming geometrical cross section for the nuclear absorption.[30] Several interesting points emerge from a comparison of the curves for carbon and lead: the cutoff energy is higher for π^+ production than for π^- production for both carbon and lead and is presumably due to the difference in energies between the initial and final nuclei (that is, $\Delta B_- \gg \Delta B_+$) which makes the production of high-energy π^- mesons less favorable than π^+. The suppression of low-energy π^+ mesons and the enhancement of π^- production in lead compared with carbon is to be attributed to the larger Coulomb field of the lead nucleus as is the increase in energy at which the maximum in the cross section occurs. It is to be noted that the total cross section at 90° for carbon is $2.5 \pm 0.6 \times 10^{-28}$ cm²/ster/nucleus for π^+ production and $4.5 \pm 1.3 \times 10^{-29}$ cm²/ster/nucleus for π^- production. The corresponding numbers[30a] for lead are $7.5 \pm 1.4 \times 10^{-28}$ and $4.7 \pm 2.0 \times 10^{-28}$ so that the yield per nucleon is much less in lead than in carbon. However, it is not possible to use these data to derive information concerning the

---

[27] S. Jones and R. White, *Phys. Rev.*, **78**: 12 (1950).

[28] C. Richman and H. Wilcox, *Phys. Rev.*, **78**: 496 (1950).

[29] M. Weissbluth, Ph.D. Thesis, University of California, 1950; cf. Richman, Weissbluth, and Wilcox, *Phys. Rev.*, **85**: 161 (1952). The curves given in the second reference (for both C and Pb) differ by as much as 15 per cent compared to Figs. 21 and 22 (for some points).

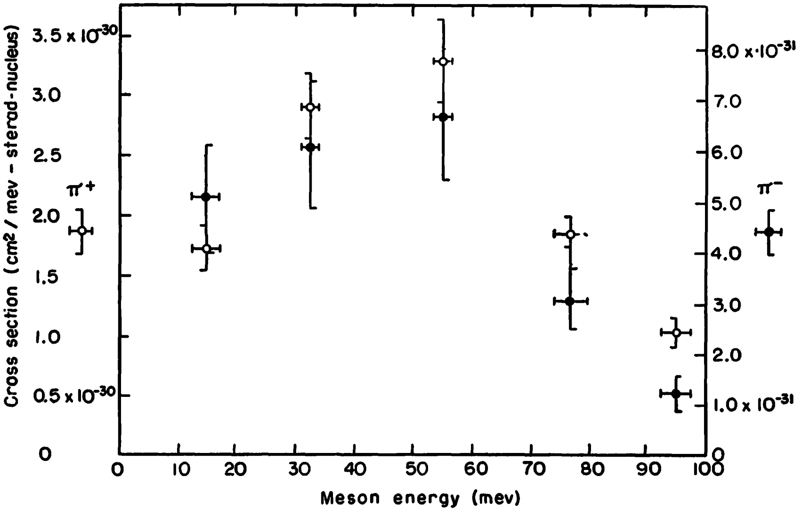

FIG. 21. Measured energy spectra of π^+ and π^- mesons at 90° in the laboratory system with respect to the beam direction produced in carbon by 345-Mev protons.

---

[30] The original curves for both C and Pb did not contain the nuclear-absorption correction, which was unknown at the time.

[30a] The corresponding numbers listed in the second reference of footnote 29 are: $\pi^+(C) = 2.3 \pm 0.5 \times 10^{-28}$, $\pi^-(C) = 4.5 \pm 1.3 \times 10^{-29}$, $\pi^+(Pb) = 7 \pm 2.1 \times 10^{-28}$, and $\pi^-(Pb) = 4.7 \pm 1.9 \times 10^{-28}$.

meson-nucleon interaction because of the large Coulomb effects for the π^+ mesons and the fact that the total cross sections for the interaction of protons with the carbon and lead nuclei are already close to geometrical (cf. Sec 3). Comparison of the experimental curves with the theoretical curves in Figs. 4 and 5 shows that the best fit is obtained with the theoretical curves 4(*b*) and 5(*b*) for carbon and the theoretical curves 4(*a*) and 5(*a*) for lead. These fits are, of course, not to be taken too seriously because of the numerous approximations made in the theoretical calculations, although the better fit of the Fermi gas model to the lead nucleus as compared with the carbon nucleus may be significant. Finally, the π^-/π^+ ratios, determined by Figs. 21 and 22, will be discussed under subheading (*C*) below. For purposes of reference, it is worth while to note the total cross sections for carbon and lead at 345 Mev, assuming an isotropic angular distribution (which may be far from the truth):

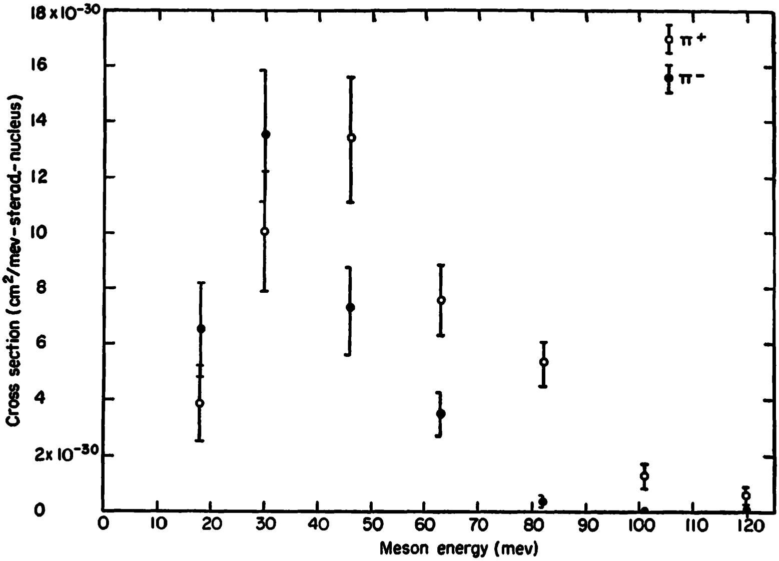

FIG. 22. Measured energy spectrum of π^+ and π^- mesons at 90° in the laboratory system with respect to the beam direction produced in lead by 345-Mev protons.

$$\sigma^+(\mathrm{C}) \approx 3.1 \times 10^{-27}\ \mathrm{cm}^2$$
$$\sigma^-(\mathrm{C}) \approx 5.7 \times 10^{-28}\ \mathrm{cm}^2$$
$$\sigma^+(\mathrm{Pb}) \approx 9.4 \times 10^{-27}\ \mathrm{cm}^2$$
$$\sigma^-(\mathrm{Pb}) \approx 5.9 \times 10^{-27}\ \mathrm{cm}^2$$

The most recent experimental work on charged meson production in nucleon-nucleus collisions has been carried out with the Columbia cyclotron by Passman *et al.*[31] These workers have measured the energy spectra for both π^+ and π^- mesons produced in a carbon target at 90° with respect to an incident proton beam of 381 Mev; their results are shown in Fig. 23. The shape of the π^+ curve in Fig. 23 is quite similar to the 345-Mev curve of Richman and Wilcox except for the expected increase in absolute cross section and shifting of the maximum to higher meson energies. Comparison of the 381-Mev curve with the theoretical curve in Fig. 8 shows that the best fit is obtained with Fig. 8*c* or 8*e*. The π^- energy spectrum at 381 Mev is surprising in that the absolute cross section is identical with the result obtained at 345 Mev; it is difficult to understand the reason for this constancy unless the experiment is in error.[31a] The total π^- production cross section at 90° integrated over energy turns out to be $4.6 \pm 1.8 \times 10^{-28}$ cm²/ster/nucleus at 381 Mev compared with $4.5 \pm 1.3 \times 10^{-29}$ cm²/ster/nucleus at 345 Mev. The corresponding π^+ numbers are $5.2 \pm 1.3 \times 10^{-28}$ cm²/ster/nucleus at 381 Mev compared with $2.5 \pm 0.6 \times 10^{-28}$ cm²/ster/nucleus at 345 Mev. The increase of a factor 2.1 ± 0.6 in the cross section for π^+ production in going from 345 to 381 Mev is consistent with a matrix element proportional to the meson momentum, whereas the constancy in cross section for π^- production appears to require a constant matrix element.

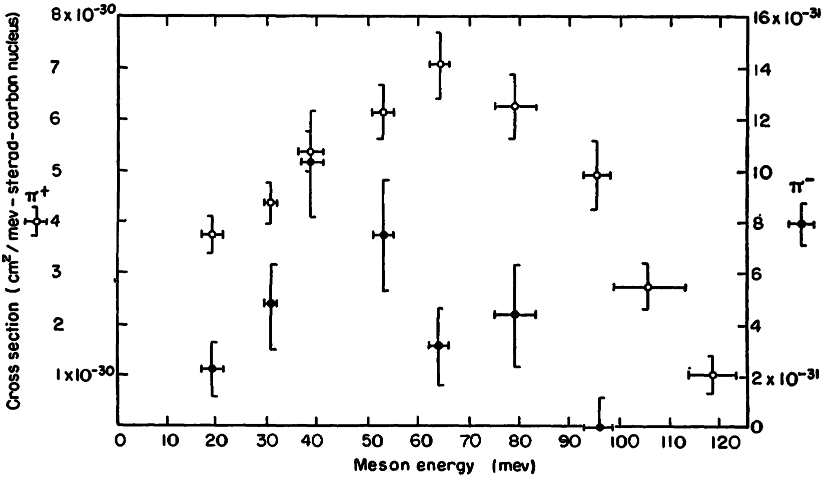

FIG. 23. Measured energy spectrum of π^+ and π^- mesons at 90° in the laboratory system with respect to the beam direction produced in carbon by 381-Mev protons.

---

[31] Passman, Block, and Havens, *Phys. Rev.*, **83**: 167 (1951).

[31a] Or unless the unlike nucleon charged π meson production cross section increases less rapidly with energy than the like nucleon cross section.

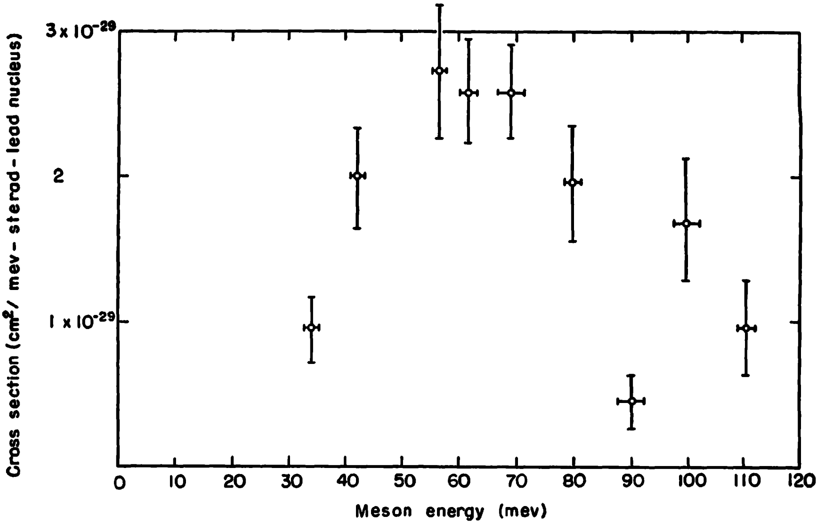

FIG. 24. Measured energy spectrum of π^+ mesons at 90° in the laboratory system with respect to the beam direction produced in lead by 381-Mev protons.

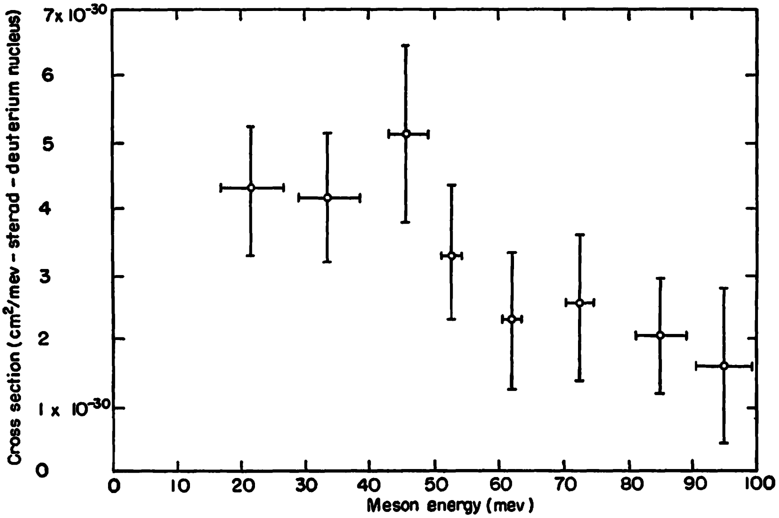

FIG. 25. Measured energy spectrum of π^+ mesons at 90° in the laboratory system with respect to the beam direction produced in deuterium by 381-Mev protons.

This has the strange consequence that the π^-/π^+ ratio decreases from 345 to 381 Mev, a point which will be discussed further below.

Passman *et al.* have also measured the π^+ spectrum produced in lead and deuterium targets at 90° with respect to the beam direction and at 381-Mev incident proton energy; the corresponding curves are shown in Figs. 24 and 25. Table 10 contains a summary of the 90° cross section obtained at Columbia and Berkeley for the production of π^+ and π^- mesons by protons (the numbers for π^- production in lead and deuterium at 381 Mev have been included although the curves have not been given).

TABLE 10. 90° CROSS SECTIONS FOR CHARGED π MESON PRODUCTION BY PROTONS (LABORATORY)

Element	381 Mev		345 Mev	
	$\frac{d\sigma^+}{d\Omega}$ (90°) (in 10^{-28} cm^2/ster)	$\frac{d\sigma^-}{d\Omega}$ (90°) (in 10^{-28} cm^2/ster)	$\frac{d\sigma^+}{d\Omega}$ (90°) (in 10^{-28} cm^2/ster)	$\frac{d\sigma^-}{d\Omega}$ (90°) (in 10^{-28} cm^2/ster)
H	0.50 ± 0.12			
D	2.9 ± 1.2	0.11 ± 0.09		
C	5.2 ± 1.3	0.46 ± 0.18	2.5 ± 0.6	0.45 ± 0.13
Pb	16.5 ± 3.8	3.5 ± 1.7	7.5 ± 1.4	4.7 ± 2.0

We shall not compare the deuterium results with theory[32] because of the preliminary character of the measurements.

C. π^-/π^+ Ratio. Although the π^-/π^+ ratio follows immediately from the cross sections discussed in subsection (*B*), we devote some special remarks to this aspect of the problem. The π^-/π^+ ratios for C and Pb at 345 Mev are plotted in Fig. 26. The agreement is reasonably good when comparison is made with the theoretical ratios derived from the crude theoretical formula [assuming the same energy dependence for σ_l and σ_u in Eq. (34)]:

$$\frac{N^-}{N^+} = \frac{C_-}{3C_+}\,\frac{1 - (2T_F/\tau_m - \tau)}{1 - (T_F/\tau_m - \tau)} \tag{40}$$

where C_- and C_+ are the Coulomb correction factors of Eq. (37) and the other terms are taken from Eq. (36). We have not plotted the π^-/π^+ ratio from carbon at 381 Mev because of the curious behavior of the π^- cross section. If taken seriously, the π^- result would imply that, instead of increasing with increasing proton energy, the π^-/π^+ ratio decreases; this would contradict the entire qualitative discussion of Sec. 3 unless the energy dependence of the cross sections for the production of charged π mesons in proton-proton and proton-neutron collisions are different. Such a difference could explain the anomaly since π^+ mesons are produced in both *P-P* and *P-N* collisions whereas π^- mesons are produced only in *P-N* collisions.

---

[32] H. P. Noyes, *Phys. Rev.*, **81**: 924 (1951).

In order to decide whether the π^-/π^+ ratio is reversed in favor of π^- mesons when the incident nucleon is a neutron—as theory predicts even if the *P-P* and *P-N* cross sections are different—Bradner *et al.*[33] have studied the numbers of π^- and π^+ mesons produced in the energy range 50 to 65 Mev by the 280-Mev–centered neutron beam resulting from a beam of 345-Mev protons striking an internal target in the Berkeley cyclotron. The mesons were produced in a carbon target at 90° with respect to the incident neutron beam. The π^-/π^+ ratio was found to be 12.6 ± 1.5, to be compared with a π^-/π^+ ratio of 0.2 at 90° for 345-Mev protons striking a carbon target (cf. Fig. 26). This strikingly different result follows theoretical expectation, which predicts for energetic mesons (above the Coulomb barrier) produced by incident neutrons the ratio

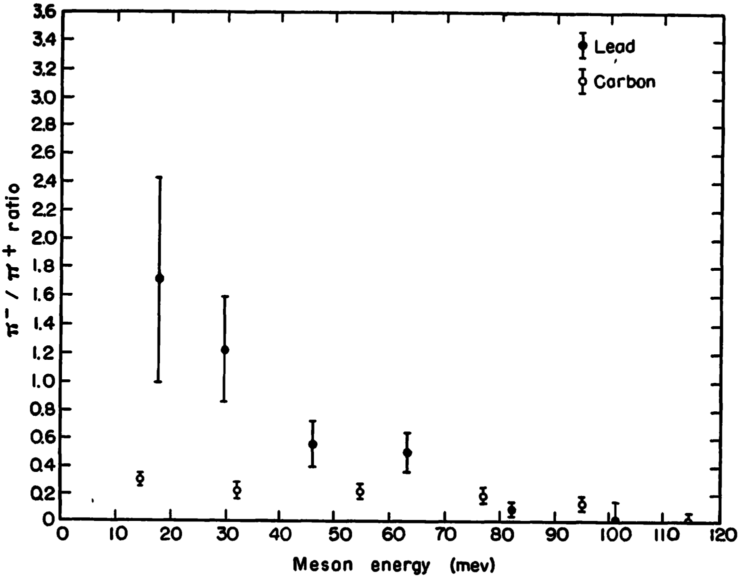

FIG. 26. Measured π^- to π^+ ratios at 90° in the laboratory system with respect to the beam direction at 345-Mev incident proton energy for carbon and lead.

$$\frac{N^-}{N^+} = \frac{3[1 - (T_F/\tau_m - \tau)]}{[1 - (2T_F/\tau_m - \tau)]} \tag{41}$$

---

[33] Bradner, O'Connell, and Rankin, *Phys. Rev.*, **79**, 720 (1950).

Inserting $T_F = 22$ Mev, $\tau_m = 100$ Mev, $\tau = 55$ Mev, one finds $\pi^-/\pi^+ \approx 15$; Eq. (41) is, as has already been remarked, the crudest sort of approximation but it does show that incident neutrons produce anomalously large π^-/π^+ ratios for meson energies close to the maximum available meson energy.

D. Dependence on Atomic Number. Hamlin *et al.*,[34] using the Berkeley cyclotron, have measured, by electrical means, the cross section for the production of 53 ± 4 Mev π^+ mesons at an angle of 0° ± 7° with respect to the incident proton beam as a function of atomic number. Their results are shown in Fig. 27 for the elements C, Al, Fe, Cu, Ag, and Pb; curve 1 is the relative yield in arbitrary units per nucleus and curve 2 the relative yield per nucleon. The gradual decrease exhibited by curve 2 for the heavier elements can, as in the case of photonic production, be explained in terms of a nuclear interaction of the outgoing mesons with the nucleons in the nucleus. However, this explanation is not unequivocal in the present instance since the total cross section for all processes for 340-Mev protons is fairly close to geometrical so that an $A^{2/3}$ behavior for the π^+ meson cross section will result without the existence of a strong meson-nucleon interaction.

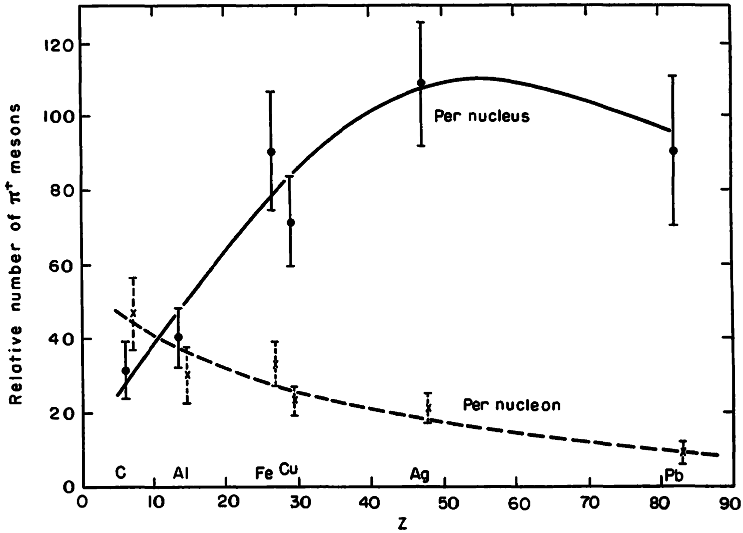

FIG. 27. The relative cross sections in arbitrary units for the production at 0° ± 7° of 53-Mev π^+ mesons by 340-Mev protons on C, Al, Fe, Cu, Ag, and Pb. The relative cross section per nucleus is shown as a solid line and the relative cross section per nucleon is shown as a dotted line.

---

[34] Hamlin, Jakobson, Merritt, and Schulz, *Phys. Rev.*, **84**: 857 (1951).

An accurate measurement of the relative yields of 40-Mev charged π mesons in Be, C, Al, Cu, Ag, W, and Pb has been performed by Clark,[35] who used the 240-Mev proton beam of the Rochester cyclotron and corrected for recirculation of the beam. The π^+ mesons were observed at 135° ± 15° (in the laboratory) with respect to the beam direction and the π^- mesons at 45° ± 15° with the results shown in Table 11. Examination of Table 11 reveals that the relative cross sections vary approximately as the geometrical cross section of the target nuclei but with significant deviations. The maximum in the cross section (per unit area; so to speak) for π^- production in the case of Cu presumably reflects the additional nuclear energy which is available in this region of the periodic table (Cu is near the minimum in the packing-fraction curve). For π^+ production, the maximum appears to occur at Al (although Cu is also a candidate within the statistical accuracy); unfortunately, there exist no theoretical calculations of nucleonic production of π mesons which take into account the difference between initial and final nuclear energies and hence can be compared with Clark's results.

TABLE 11. RELATIVE YIELDS OF 40 MEV CHARGED π MESONS

Element	Atomic weight	$\dfrac{\sigma(\pi^+)}{A^{\frac{2}{3}}}$ (arbitrary units)	$\dfrac{\sigma(\pi^-)}{A^{\frac{2}{3}}}$ (arbitrary units)
Be	9.02	0.169 ± 0.006	0.237 ± 0.019
C	12.01	0.491 ± 0.016	0.341 ± 0.014
Al	26.97	0.640 ± 0.023	0.675 ± 0.031
Cu	63.57	0.617 ± 0.025	0.927 ± 0.042
Ag	107.9	0.523 ± 0.022	0.850 ± 0.044
W	183.9	0.427 ± 0.018	0.740 ± 0.039
Pb	207.2	0.387 ± 0.017	0.703 ± 0.039

Thus far, we have considered exclusively charged π meson production in complex nuclei by artificially created photons or accelerated protons. The photons in the cosmic radiation certainly produce charged π mesons of all varieties and all energies; however, a clear-cut cosmic-ray experiment on the photonic production of charged π mesons is very difficult to perform. This is less true of the nucleonic production of charged π mesons in complex nuclei. A great number of such cosmic-ray experiments have been carried out and until now have provided our only source of information concerning such phenomena as multiple meson production and plural meson production (cf. Chap. 8). As far as single charged π meson production by nucleons is concerned, we shall make passing reference to several experiments, none of which alters the conclusions arrived at on the basis of the accelerator experiments.

---

[35] D. L. Clark, *Phys. Rev.*, in press.

One cosmic-ray experiment carried out by Occhialini *et al.*[36] showed the importance of the Coulomb field for charged π mesons of low energy. These authors observed 20 nuclear stars containing outgoing slow mesons in insensitive emulsions exposed at mountain altitudes; of these 20 mesons, 17 gave rise to further stars and only 3 ended without any visible track in the emulsion. This simple experiment provided strong evidence for the preponderance of slow π^- mesons over slow π^+ mesons and therefore for the vital role played by the Coulomb field for mesons with energies below 5 Mev. Another interesting cosmic-ray experiment was performed by Camerini *et al.*,[37] who measured the charged π meson spectrum resulting from proton-nuclei collisions in photographic emulsions; by combining scattering and grain-density measurements, this group of workers was able to discriminate between π mesons and protons for energies up to 1500 Mev. In this energy range, they found an integral energy spectrum which can be represented by $d\epsilon/\epsilon^{1.5}$ where ϵ is the total energy of the π meson including its rest mass. Finally, a third experiment was carried out by Sands,[38] who measured the intensity of μ mesons in the cosmic radiation as a function of altitude and the differential range spectrum of μ mesons at sea level. A careful analysis of these data led Sands to an integral energy spectrum for the mesons giving rise to the μ mesons, *viz.*, the π mesons, in agreement with Camerini *et al.* Unfortunately, the π meson spectrum so determined is difficult to interpret in terms of a cross section for charged π meson production in nucleon-nucleus collisions since it reflects in the main the energy spectrum of the initiating nucleons.

7. Production of π^0 Mesons in Nucleon-Nucleus Collisions

We have already pointed out that the first conclusive demonstration of the existence of the π^0 meson was provided by the observation of coincidences between γ rays resulting from the collision of photons with the nuclei of beryllium and carbon. However, the experiment with high-energy accelerators which provided the initial strong evidence for the existence of the π^0 meson was carried out by Bjorklund *et al.*[39] with the proton beam of the Berkeley cyclotron. These authors observed single high-energy γ rays resulting from the collision of protons with targets of beryllium and carbon and, by varying many different parameters, were able to establish powerful arguments for the production of π^0 mesons.

[36] G. Occhialini and C. Powell, *Nature*, **162**: 168 (1948).
[37] Camerini, Fowler, Lock, and Muirhead, *Phil. Mag.*, **41**: 413 (1950).
[38] M. Sands, *Phys. Rev.*, **77**: 180 (1950).
[39] Bjorklund, Crandall, Moyer, and York, *Phys. Rev.*, **77**: 213 (1950).

In view of the intrinsic interest of this experiment and its historical importance, we shall present the results and outline the arguments.

Bjorklund *et al.* observed the γ rays in approximately the forward and backward directions with respect to the incident proton beam for proton energies ranging from 180 to 340 Mev. In order to establish that the observed radiation actually consisted of photons, attenuation measurements were made in lead and aluminum. The total cross sections agreed with those measured by Lawson[40] and were not consistent with any other known radiation. The energy spectra of the γ rays in the forward and backward directions were measured with a pair spectrometer with the results shown in Figs. 28 and 29 for a carbon target. It is seen that the cross section varies by a factor of about 100 in the energy region under consideration for both the forward and backward directions. The Berkeley group also obtained absolute γ ray cross sections from the carbon target with the results shown in Table 12.

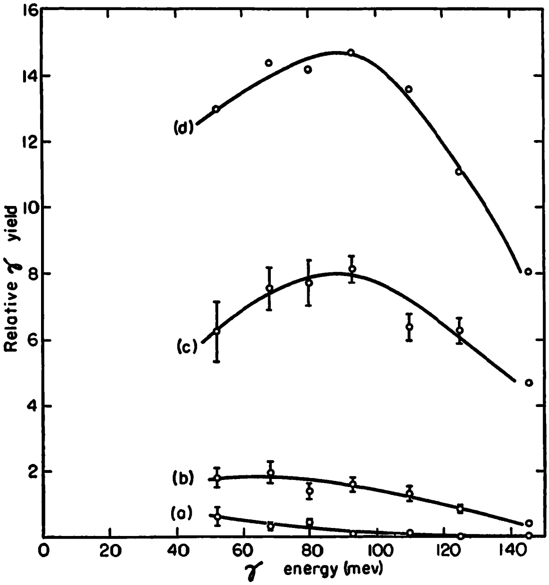

FIG. 28. Relative γ ray yield in the forward direction from a carbon target at various proton energies. Curve (*a*) $T = 180$ Mev; (*b*) $T = 230$ Mev; (*c*) $T = 290$ Mev; (*d*) $T = 340$ Mev.

The γ ray yields from a beryllium target with 340-Mev protons were measured for four different angles, and the results are shown in Fig. 30. If the photons are emitted with spherical symmetry in some coordinate

---

[40] J. Lawson, *Phys. Rev.*, **75**: 443 (1949).

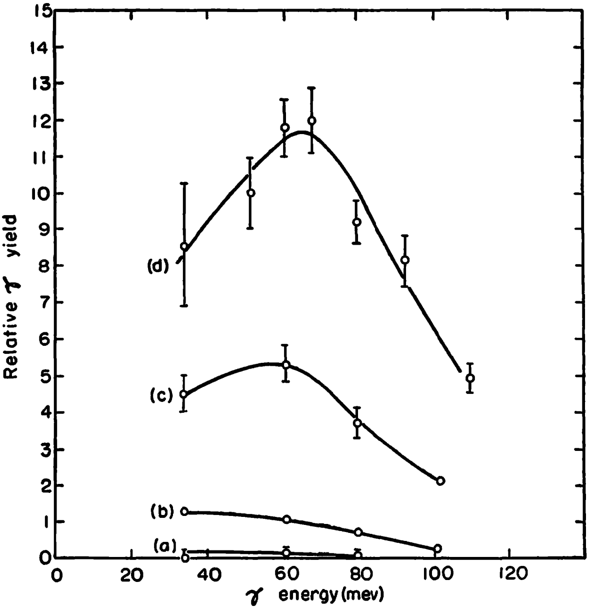

FIG. 29. Relative γ ray yield in the backward direction from a carbon target at various proton energies. Curve (*a*) $T = 180$ Mev; (*b*) $T = 230$ Mev; (*c*) $T = 290$ Mev; (*d*) $T = 340$ Mev.

system moving with velocity β, and if the spectrum of photons in that system is $I_C(\omega)$, then the spectrum in the laboratory system at an angle θ

TABLE 12. γ RAY CROSS SECTIONS PER C NUCLEUS

	Laboratory system	$\beta = 0.32$ system (see text)
$d\sigma$ (0°) at peak	1.2×10^{-30} cm²/ster/Mev	0.85×10^{-30} cm²/ster/Mev
$d\sigma$ (180°) at peak	0.6×10^{-30} cm²/ster/Mev	0.85×10^{-30} cm²/ster/Mev
Integrated σ using 0° spectrum	1.5×10^{-28} cm²/ster	0.75×10^{-28} cm²/ster
Integrated σ using 180° spectrum	0.35×10^{-28} cm²/ster	0.70×10^{-28} cm²/ster
Total σ assuming isotropy in $\beta = 0.32$ system	....	1×10^{-27} cm²

will be

$$I(\omega, \theta) = \frac{\sqrt{1 - \beta^2}}{1 - \beta \cos \theta} I_C \left[\frac{(1 - \beta \cos \theta)\omega}{\sqrt{1 - \beta^2}} \right] \tag{42}$$

where the Doppler shift and aberration effects have been taken into account. If Eq. (42) is used to transform the four 340-Mev curves of

Fig. 30 to a system moving with $\beta = 0.32$, one obtains a single consistent curve within the experimental accuracy. The value $\beta = 0.32$ is a reasonable choice for the center-of-mass system of the colliding proton and the target nucleus for the following reason: a 340-Mev proton has a β of 0.67 whereas the β of the center of mass of it and a stationary nucleon is 0.39. However, if, as Figs. 28 and 29 indicate, the production process for photons is highly energy-dependent, the major contribution to the cross section should come from nucleons moving with maximum velocity in the nucleus (of the order 22 Mev) and in approximately opposite directions to the incident proton. For such a choice of numbers, the center-of-mass velocity is in the range 0.3 to 0.35.

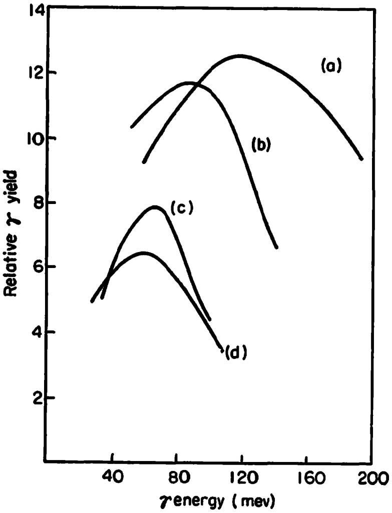

FIG. 30. Relative γ ray yield at various angles in the laboratory system from a beryllium target at 340-Mev incident proton energy. Curve (*a*) corresponds to 0°, (*b*) to 47°, (*c*) to 133°, (*d*) to 180°.

On the basis of the above data, it is possible to rule out almost all explanations for the origin of the γ rays resulting from the proton-nucleus collisions except the neutral meson hypothesis. Thus the nuclear-excitation explanation can be ruled out because of the large observed Doppler shift and the fact that alpha particles with about the same energy as the protons give a much smaller yield of γ rays. The extremely large Doppler shift also excludes the hypothesis which postulates that the γ rays arise from the decay of isobaric states of nucleons (cf. Chap. 9) for if 75 Mev, deduced from the γ ray curve in the $\beta = 0.32$ system, is the isobaric excitation energy, then the observation of 40-Mev γ rays in the forward direction would require appreciable numbers of nucleons in the nucleus with energies greater than 250 Mev, which is certainly excluded. Isobaric states of charged π mesons are ruled out by the fact that the observed γ ray threshold is in the neighborhood of 175 to 200 Mev. The most difficult hypothesis to rule out proves to be the argument that the observed γ rays are due to proton bremsstrahlung, *i.e.*, the high-energy γ rays resulting from the nuclear force between the incident proton and the neutrons in the target nucleus. It can easily be shown that the proton bremsstrahlung resulting from the Coulomb interaction between the incident proton and the target nucleus leads to a cross section down by a factor of $(m_e/M)^2$ compared with the cross section for electron bremsstrahlung, *viz.*, a cross section of the order of 10^{-32} cm² (for Be or C). Since the nuclear force is much stronger than the Coulomb interaction, the cross section for the production of γ rays via the proton-neutron interaction will be much larger. However, no reasonable theory of proton bremsstrahlung, either along phenomenological lines[41] or along field-theoretic lines,[42] predicts a cross section larger than 10^{-29} cm² per nucleus. This is to be compared with the cross section 10^{-27} cm² per nucleus observed in the Berkeley experiment. What is even more important is that the extremely rapid increase of yield which is observed as a function of incident proton energy (a factor of 100 when the proton energy is doubled) cannot be explained by the hypothesis of proton bremsstrahlung.[43]

In contrast, the neutral meson hypothesis fits all the data extremely well. Thus the excitation function for the production of high-energy γ rays is very similar to the excitation function for charged π meson production, as can be seen from Table 13, which compares the variation of yield of π^- mesons in the energy range 2 to 10 Mev (cf. Fig. 20) and the variation of γ ray yield as a function of incident proton energy (cf. Figs. 28 and 29). The agreement is manifestly excellent, though somewhat fortuitous, and shows that the mechanisms for the production of the γ rays and the π^- mesons are closely related. Furthermore, the absolute yield of γ rays is close to that for charged π mesons produced in

TABLE 13. EXCITATION FUNCTIONS FOR γ RAY AND π^- MESON PRODUCTION IN PROTON-NUCLEUS COLLISIONS

γ rays		π^- mesons	
E_0, Mev	Yield, arbitrary units	E_0, Mev	Yield, arbitrary units
340	100	345	100
290	35	306	47
230	7	269	22
180	1	233	8
		201	1
		167	0

---

[41] Cf. J. Ashkin and R. Marshak, *Phys. Rev.*, **76**: 58 (1949).

[42] Cf. A. Simon, *Phys. Rev.*, **79**: 573 (1950).

[43] Recently, R. Wilson, *Phys. Rev.*, **85**: 563 (1952) has shown that the cross section for proton bremsstrahlung at 140 Mev (below the π^0 production threshold) is indeed of the order of 10^{-29} cm².

proton-nucleus collisions, that is, 1×10^{-27} cm^2 per carbon nucleus[43a] as compared with about 3×10^{-27} cm^2 per carbon nucleus (assuming isotropic production). The occurrence of a threshold for the γ radiation at about 175 Mev and the peak of the radiation at about 75 Mev in the center-of-mass system indicate that the hypothesized π^0 meson decays into no more than two photons. The fact that the threshold for the γ radiation is about at the same energy as for charged π production and the observation that the peak in the center-of-mass system occurs at the same point (*i.e.*, 75 Mev), independent of the incident proton energy, both argue strongly that the γ rays originate from a neutral π meson with a mass roughly equal to that of the charged π meson. Theoretical calculations of the expected γ ray spectra in the forward and backward directions, assuming two-photon decay and a π^0 mass of 150 Mev (the best value is about 135 Mev—Chap. 4), fit the experimental data quite well, as can be seen from Fig. 31. The curves in Fig. 31 were computed[44] on the assumptions that (1) the π^0 production is isotropic in the center-of-mass system of the two nucleons, (2) the π^0 energy spectrum has the form

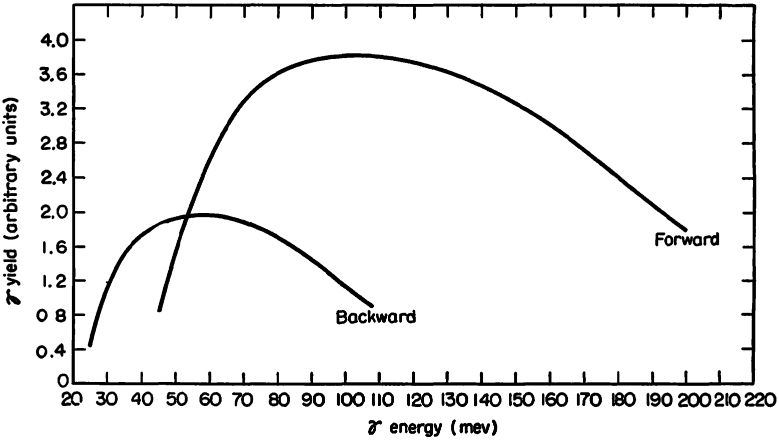

FIG. 31. Theoretical γ ray spectra from a complex nucleus in the forward and backward directions on the basis of the neutral meson hypothesis at 340-Mev proton energy; the meson mass is taken as 150 Mev.

[43a] Recently, an improved measurement of the absolute yield of π^0 mesons from 340 Mev protons on carbon has been carried out with the result: $\sigma = 1.8 \pm 0.4 \times 10^{-27}$ cm^2 (B. J. Moyer, *UCRL* No. 1811); as soon as improved measurements of the π^+ and π^- cross sections are available, the charge independence prediction:

$$\sigma^0(C) = \tfrac{1}{2}[\sigma^+(C) + \sigma^-(C)]$$

(cf. footnote 14*a*) can be tested.

[44] M. F. Kaplon, private communication.

$(\tau_m - \tau)^2$ where τ_m is the maximum kinetic energy of the π^0 mesons in the laboratory system, and (3) the γ emission is isotropic in the rest system of the π^0 meson.

More recently, Knable[45] has studied the production of π^0 mesons in nucleon-nucleus collisions with a new type of photon detector using the 341-Mev external proton beam of the Berkeley cyclotron. The measurements were carried out at an angle of 135° for several light nuclei with the results shown in Table 14. The fact that the proton yield is essentially zero has been remarked before (in Chap. 2). Further evidence that, at 340 Mev, the π^0 mesons are produced in *P-N* collisions, not in *P-P*, comes from the fact that the yield from Be^9 is the same as the yield from B^{10}, and similarly for B^{11} compared with C^{12}. Another conclusion which can be drawn from Table 14 is that there is very little nuclear absorption of π^0 mesons in the very light nuclei, a conclusion which is not incompatible with appreciable nuclear absorption in the heavy nuclei.

TABLE 14. RELATIVE CROSS SECTIONS FOR π^0 PRODUCTION BY 341-MEV PROTONS AT 135° WITH RESPECT TO THE BEAM DIRECTION

Nucleus	Cross Section, Arbitrary Units
H	0.07 ± 0.06
D	0.85 ± 0.20
Be^9	5.01 ± 0.12
B^{10}	4.99 ± 0.11
B^{11}	5.95 ± 0.13
C^{12}	6.00 ± 0.16
O^{16}	7.46 ± 0.28

This completes our account of accelerator experiments on the nucleonic production of π^0 mesons in complex nuclei. Just as in the case of the nucleonic production of single charged π mesons, there exist cosmic-ray data bearing on the production of single π^0 mesons in nucleon-nucleus collisions; and, as before, the cosmic-ray experiments, while providing interesting circumstantial evidence for the π^0 production phenomena, do not offer the possibility of as clean-cut theoretical interpretation as do the accelerator experiments.[46] Nevertheless, we shall discuss briefly some of the cosmic-ray experiments carried out with cloud chambers and photographic plates.

Quite a few cosmic-ray experimentalists[47] have performed cloud-chamber experiments either at mountain altitudes or at sea level, in which the cloud chamber is triggered by a penetrating shower. Usually, one or more lead plates is placed inside the cloud chamber and it is observed that electron cascade showers accompany the penetrating showers. Such showers are called mixed showers and find their most natural interpretation in terms of a simultaneous production of neutral and charged π mesons; the π^0 mesons decay very rapidly into γ rays, which in turn initiate soft component cascades. Support for this interpretation comes from the fact that some of these mixed showers contain double cores of electron cascade showers and the angle between the two cores and the energies of the electrons in the cores are related in such a manner as to suggest the existence of a π^0 meson decaying into two γ rays. The possibility of such a deduction stems from the fact that the angle between the two γ rays arising from a π^0 meson decay depends only on the energy of each γ ray and not on the direction of motion of the original π^0 meson. This statement can be proved by repeating the kinematical argument of Chap. 1 in a slightly altered form: consider a π^0 meson of momentum $\mathbf{q}_0$ and energy ϵ_0 (including its rest mass) decaying into two photons of momenta $\mathbf{k}_1$ and $\mathbf{k}_2$ and energies ω_1 and ω_2. By conservation of energy and momentum,

---

[45] N. Knable, *UCRL* No. 1444; cf. Hales, Hildebrand, Knable, and Moyer, *Phys. Rev.*, **85**: 373 (1952).

[46] The production of π^0 mesons at relativistic nucleon energies is, of course, another matter and will be discussed in Chap. 8.

[47] Cf. C. Y. Chao, *Phys. Rev.*, **75**: 881 (1949); W. B. Fretter, *Phys. Rev.*, **76**: 511 (1949); Gregory, Rossi, and Tinlot, *Phys. Rev.*, **77**: 299 (1950).

$$k_1 + k_2 = q_0$$
$$\omega_1 + \omega_2 = \epsilon_0$$

and solving for the angle β between $\mathbf{k}_1$ and $\mathbf{k}_2$, we find

$$\sin\frac{\beta}{2} = \frac{1}{2}\sqrt{\frac{\mu_0^2}{\omega_1\omega_2}} \tag{43}$$

(the minimum angle, $\beta_{\min}$, is equal to $\sin^{-1}(\mu_0/\epsilon_0)$, in agreement with our earlier calculation). Consequently, if a π^0 meson is the source of a double core of electron cascades, the energies ω_1 and ω_2 of the two cores and the angle β between the two cores will be related by means of Eq. (43).

As an illustration, consider some data of Fretter's[47] presented in Table 15. The first two columns indicate the number of $\frac{1}{4}$-in. lead plates penetrated by each of the two soft showers (four plates correspond to about a

TABLE 15. DOUBLE CORES OF ELECTRON SHOWERS

t_1	t_2	β_{obs}, degrees	β_{theo}, degrees
7	7	9	9
2	2	24	31
4	3	32	18
5	4	26	15
4	3	12	18

200-Mev cascade shower while eight plates correspond to about a 1-Bev shower), the third column the observed angle between the cores, and the fourth column the theoretically predicted angle on the basis of the implicit energies contained in columns 1 and 2. The agreement is not bad, considering the uncertainties of cascade shower theory and the large fluctuations inherent in small cascades. Fretter[47] has also tabulated the frequency of occurrence of mixed and unmixed showers as a function of the multiplicity of the shower, with the results shown in Table 16; here the multiplicity refers to the number of penetrating particles produced in the event. The table shows that the number of mixed showers increases in frequency with the multiplicity of the shower. This result would be expected if π^0 mesons are responsible for the mixed showers since for a shower of high multiplicity the probability is greater that one of the mesons produced is a π^0 meson and has its decay γ rays converted in the lead than for a shower of low multiplicity.

TABLE 16. FREQUENCY-SIZE DISTRIBUTION OF MIXED AND UNMIXED PENETRATING SHOWERS

Multiplicity of shower	2	3	4	5	6	7	8	9	>9
No. of unmixed showers	20	37	15	4	3	1	2	1	0
No. of mixed showers	71	87	42	21	17	7	7	3	4
Difference	51	50	27	17	14	6	5	2	4

Before we leave the question of mixed showers, it would seem appropriate to ask whether an electron pair produced directly in the original nuclear event can be responsible for the mixed showers. This question has been answered in the negative by Fowler,[48] who, using photographic plates, measured the mass of particles coming out of stars (from their multiple scattering and grain density) and found that electrons constitute less than 2 per cent of the charged particles.[48a]

We have now seen that the electron cores in mixed showers are probably due to the γ rays resulting from the decay of π^0 mesons. Another indirect proof of the existence of π^0 mesons is the rapid increase with altitude[49] of the frequency of cosmic-ray bursts (bursts are large bursts of ionization produced by large electronic cascades) under thick layers of material. Since π^0 mesons are produced in greater numbers at higher altitude, this

[48] P. H. Fowler, *Phil. Mag.*, **41**: 169 (1950).

[48a] Recent experiments [cf. Daniel, Davies, Mulvey, and Perkins, *Phil. Mag.*, **43**: 753 (1952), and M. Schein, private communication] indicate that electron pairs are closely associated with stars in small numbers and presumably arise from π^0 mesons decaying by the alternative mode: $\pi^0 \rightarrow \gamma + e^+ + e^-$ (cf. Chap. 4).

[49] H. Bridge and B. Rossi, *Phys. Rev.*, **75**: 810 (1949).

variation is easily understood on the basis of the rapid increase of the N component of the cosmic radiation with altitude, the component chiefly responsible for π meson production (cf. Chap. 6).

The most conclusive cosmic-ray evidence for the production of single π^0 mesons (apart from the multiple production evidence discussed in Chap. 8) in nucleon-nuclei collisions has been obtained with photographic methods by Carlson *et al.*[50] These authors have measured the energies of 500 electron pairs—presumably produced by γ rays—in plates exposed at 70,000 ft. The energy spectrum of the γ rays deduced from these measurements is shown in Fig. 32. Since π^0 mesons with a given energy ϵ_0 would yield a square pulse of γ rays with energies between $[(\epsilon_0 - q_0)/2]$ and $[(\epsilon_0 + q_0)/2]$ if the mesons are produced isotropically by the cosmic-ray beam and the two decay γ rays are emitted isotropically in the rest system of the π^0 meson, it follows that the minimum and maximum energies of the γ rays, $\omega_{\min}$ and $\omega_{\max}$, will obey the relation $\sqrt{\omega_{\min}\omega_{\max}} = \mu_0/2$ for each given ϵ_0 (a relation already derived for the purposes of our discussion of mixed showers—cf. above). Consequently, if $F(\epsilon_0)d\epsilon_0$ is the

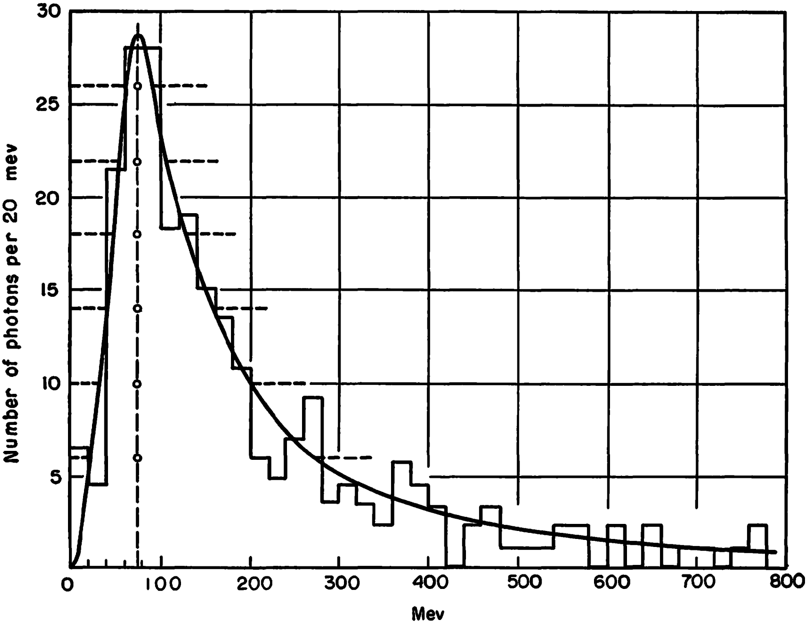

FIG. 32. Measured energy spectrum at 70,000 ft of photons observed in photographic emulsions as converted electron pairs.

---

[50] Carlson. Hooper, and King, *Phil. Mag.*, 41: 701 (1950).

differential energy spectrum of π^0 mesons produced by the cosmic-ray beam (chiefly protons) interacting with the air nuclei, it can easily be shown that the observed γ ray spectrum $N(\omega_0)$ will be related to $F(\epsilon_0)$ by means of the relation

$$N(\omega_0) = \int_{\omega_0 + \frac{\mu^2}{4\omega_0}}^{\infty} \frac{F(\epsilon_0)d\epsilon_0}{\sqrt{\epsilon_0^2 - \mu_0^2}} \tag{44}$$

Clearly, the peak of the distribution function $N(\omega_0)$ will occur when $\omega_{\text{min}} = \omega_{\text{max}}$ or ω_{peak} is equal to $\mu_0/2$. From the observed peak, Carlson *et al.* have derived the mass of the π^0 meson, which turns out to be 295 $\pm 20m_e$, in agreement with other measurements (cf. Chap. 4); and, from the observed distribution function $N(\omega_0)$, they have derived the production spectrum $F(\epsilon_0)d\epsilon_0 \approx d\epsilon_0/\epsilon_0^{1.5}$, in agreement with the charged π meson spectrum observed in cosmic-ray nucleon-nuclei collisions at the same altitude (see above).

CHAPTER 4

PROPERTIES OF π MESONS

1. Introduction

The π meson production experiments discussed in Chaps. 1 to 3 have shed considerable light on the properties of the charged and neutral π mesons. Thus the experiments on the photonic production of charged π mesons enabled us to conclude that the charged π meson is described by a pseudoscalar or pseudovector field (*i.e.*, spin zero and odd parity field or spin one and even parity field). The experiments on neutral π meson production fixed the spin of the π^0 meson as 0 (or greater than 1) and gave indications that its parity is odd. The experiments on the nucleonic production of charged and neutral π mesons were not only consistent with the above conclusions but led to rough estimates of the π meson masses (in the vicinity of 300 electron masses) and even argued for the pseudoscalar field with pseudovector coupling for both charged and neutral π mesons. In this chapter, we consider in more detail the properties of the π mesons: the most accurate mass and lifetime determinations of both the charged and neutral mesons, their modes of decay and the various experiments bearing on the determination of their spins and parities. We shall, as before, devote our chief attention to experiments with artificial meson sources, although corroborative evidence furnished by cosmic-ray experiments will be utilized wherever possible.

2. Masses of the π Mesons

A. Mass of the Charged π Meson. It is well known that in order to determine the mass of a charged particle it is necessary to measure at least two parameters among the following: radius of curvature in a magnetic field, range, multiple Coulomb scattering, grain density in a photographic emulsion, etc. Ever since the π meson was discovered in 1947,[1] attempts have been made to obtain an accurate determination of its mass by a measurement of two of the above parameters. Powell's review article[2] contains a thorough discussion of these attempts through 1949. We shall not repeat this discussion here but merely present the most accurate mass measurements which have been carried out since Powell's article appeared.

---

[1] Lattes, Occhialini, and Powell, *Nature*, **160**: 453 (1947).

[2] C. F. Powell, *Reports on Progress in Physics*, XIII: 350 (1950).

Barkas *et al.*[3] have derived an accurate value of the π^+ mass by measuring the π^+ meson to proton momentum and range ratios inside the Berkeley cyclotron. This method of mass measurement depends on the fact that, if the range ratio of two particles of equal charge is found to be equal to the momentum ratio, their velocities are equal and the common ratio is equal to their mass ratio. Hence the mass measurement becomes independent of the absolute value of the magnetic field and also of any direct dependence on a knowledge of the range-energy curve in a photographic emulsion. This conclusion follows if it is recalled that a particle of charge e and momentum p has a radius of curvature ρ in a magnetic field H given by the relation $\rho = p/eH$ and that the energy T corresponding to a specified range R for a particle of mass m can be written in the form $T = kR^n m^{1-n}$ where k and n are positive constants and depend upon the medium in question. In this manner, the Berkeley workers arrive at the following value for the mass of the π^+ meson: $277.4 \pm 1.1m_e$ (m_e is the electron mass). Another set of measurements of the π^+ meson mass has been carried through by Birnbaum *et al.*[4]: by measuring the ratio of the π^+ to μ^+ masses and the absolute momentum of the μ meson, p_μ, which it receives when the π meson decays at rest, these authors can deduce a value of the π^+ mass. The results are $m_{\pi^+}/m_{\mu^+} = 1.317 \pm 0.004$ and $p_{\mu^+} = 29.86 \pm 0.06$ Mev/c. If one assumes that the neutral decay particle from the π^+ meson is a particle of zero mass (*i.e.*, a neutrino—cf. below), one finds

$$(m_{\pi^+} - m_{\mu^+}) = 66.46 \pm 0.16m_e$$

$m_{\pi^+} = 276.1 \pm 2.3m_e$, and incidentally $m_{\mu^+} = 209.6 \pm 2.4m_e$ as absolute values with no reference to the proton as a comparison particle.

A recent indirect determination of the π^+ meson mass has come from a somewhat unexpected direction, *viz.*, from a study of the reaction $P + P \rightarrow D + \pi^+$. Using the known proton and deuteron masses, a Cerenkov radiation measurement of the proton kinetic energy, and an accurate range-energy measurement of the meson energy, Cartwright[5] was able to deduce a value of $275.1 \pm 2.5m_e$ for the mass of the π^+ meson.

As regards the π^- mass, the momentum-range method of Barkas *et al.*[3] leads to a value of $276.1 \pm 1.3m_e$ for the mass of the π^- meson. The $\pi \rightarrow \mu$ decay method is not applicable to the determination of the π^- mass because π^- mesons undergo nuclear absorption when they come to rest in matter instead of decaying as do π^+ mesons. It is also clear that the analogue of Cartwright's method will not work for π^- mesons because free neutron-neutron collisions would be necessary. However, there is one indirect method for measuring the π^- meson mass which cannot be applied to the π^+ meson; this method consists in making a careful measurement of the energy of the discrete γ ray which results from the slow meson reaction $\pi^- + P \rightarrow N + \gamma$. Since the π^- meson is absorbed from the K shell of the mesic-hydrogen atom with a binding of only 3 kev, it can be assumed that the π^- meson is absorbed while at rest and that the mass of the π^- meson is simply related to the γ ray energy by the relation

---

[3] Barkas, Smith, and Gardner, *Phys. Rev.*, **82**: 102 (1951).

[4] Birnbaum, Smith, and Barkas, *Phys. Rev.*, **83**: 895 (1951); cf. also W. H. Barkas, *UCRL* No. 1285.

[5] W. F. Cartwright, *Phys. Rev.*, **82**: 460 (1951).

$$m_{\pi^-} = \omega\left(1 + \frac{\omega}{2M}\right) \tag{1}$$

where ω is the γ ray energy and M is the nucleon mass. The energy of the γ ray has been measured with a pair spectrometer by Panofsky *et al.*[6] (a more detailed discussion of this experiment will be given in a later section), and when proper account is taken of the resolving power of the pair spectrometer, the mass of the π^- meson turns out to be $275.2 \pm 2.5m_e$. This result is in excellent agreement with the direct determination of Barkas *et al.* Within statistics, the π^- and π^+ masses are equal, a not too surprising result.

B. Mass of the π^0 Meson. The mass of the π^0 meson can be determined only indirectly because it decays into two γ rays with such an extremely short lifetime (cf. below). We have already remarked that the experiments on the production of π^0 mesons have indicated a π^0 mass roughly equal to that of the charged π meson, *viz.*, in the neighborhood of 300 electron masses. We have also cited (cf. Chap. 3) a somewhat better cosmic-ray measurement of the π^0 mass carried out by Carlson *et al.*[7], in which the π^0 mass is deduced from the measured γ ray spectrum at 70,000 ft and turns out to have a value $295 \pm 20m_e$.

None of the above determinations of the π^0 meson mass is really accurate and, in particular, it is not clear from any of these measurements whether the π^0 mass is smaller or larger than the mass of the charged π meson. A very accurate measurement of the π^0 mass is made possible by the fact that the π^0 mass is actually smaller than the π^- mass by at least the neutron-proton mass difference, *i.e.*, 1.25 Mev. With a $(\pi^- - \pi^0)$ mass difference greater than 1.25 Mev, the slow meson reaction: (*a*) $\pi^- + P \rightarrow N + \pi^0$ can compete with the reaction (*b*) $\pi^- + P \rightarrow N + \gamma$ mentioned in connection with the π^- mass determination. Reaction (*a*) has been measured with the same apparatus as reaction (*b*) since the π^0 meson quickly decays into two γ rays. The measured γ ray spectrum from reaction (*a*) must be a square pulse since the π^0 meson must emit its two γ rays isotropically in its own frame of reference. The square pulse follows from the fact that, for isotropic γ emission in the frame of reference of the π^0 meson, the angular distribution of γ rays in the laboratory system must be

---

[6] Panofsky, Aamodt, and Hadley, *Phys. Rev.*, **81**: 565 (1951).

[7] Carlson, Hooper, and King, *Phil. Mag.*, **41**: 701 (1950).

$$I(\theta)d\Omega = \frac{(1 - \beta_0 \cos \theta)^2}{\gamma_0^2}\, d\Omega \tag{2}$$

and its energy spectrum [note that $N(\omega)d\omega = I(\theta)d\Omega/4\pi$]

$$N(\omega)d\omega = \frac{1}{\beta_0\epsilon_0} \tag{3}$$

where $\epsilon_0 = \gamma_0\mu_0$ is the energy of the π^0 meson (including its rest mass), $\gamma_0 = 1/\sqrt{(1 - \beta_0^2)}$, β_0 is the velocity of the π^0 meson, ω is the energy of the γ ray in the laboratory system, and θ its angle of emission with respect to the original π^0 meson in the laboratory system. Equation (3) shows that, for a given ϵ_0, the γ ray spectrum is a square pulse for ω between $\omega_{\text{min}} = (\epsilon_0/2)(1 - \beta_0)$ and $\omega_{\text{max}} = (\epsilon_0/2)(1 + \beta_0)$; ω_{min} and ω_{max} follow immediately from the Doppler relation $\omega = \mu_0/[2\gamma_0(1 - \beta_0 \cos \theta)]$. The experimental γ ray curve, containing the contributions from both reactions (*a*) and (*b*), is shown in Fig. 1. Careful analysis of the square-pulse part of this experimental curve leads to values of ω_{min} and ω_{max} of

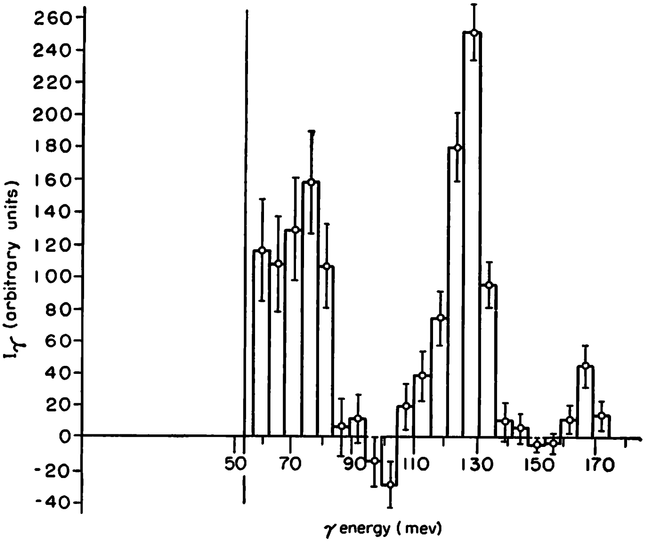

FIG. 1. Measured γ ray spectrum from the absorption of slow π^- mesons in hydrogen.

53.6 Mev and 85.0 Mev, respectively, which yield a π^0 mass of 264.6 ± $3.2m_e$ using the relation $\mu_0 = 2\sqrt{\omega_{\min}\omega_{\max}}$. This mass determination of the π^0 meson is remarkably accurate and is, of course, due to the Doppler amplification of the small mass difference between π^- and π^0—about 5 Mev—into a large energy spread for the γ rays—about 30 Mev.

3. Decay of the π Mesons

A. Decay of the Charged π Meson. The charged π meson is an unstable particle which decays much faster (by a factor of about 100) than the lighter μ meson. Actually, the μ meson is the charged decay product of the π meson, and it has been possible to observe the sequence of decays $\pi^+ \rightarrow \mu^+ \rightarrow e^+$ in a photographic plate. It was this sequence of decays, too, which was exploited to detect π^+ mesons by electronic means in the photoproduction experiments (cf. Chap. 3). Thus far, no conclusive experimental evidence exists for the direct decay of the π meson into an electron; as a matter of fact, Friedman and Rainwater[8] have shown that not more than one π^+ meson in 1400 decays into a positron. We shall first examine the experimental evidence bearing on the lifetime for π decay and then consider the nature and energies of the products resulting from this decay.

1. *Lifetime for π decay.* As is well known, the first experimental evidence for the existence of the π meson was obtained by Lattes *et al.*[1] in photographic emulsions exposed to the cosmic radiation. It was shown by Marshak and Bethe[9] that the very observation of π^+ mesons by the Bristol group enabled one to set a lower limit of 10^{-11} sec on the lifetime of the π meson. The same authors also showed that other cosmic-ray experiments, such as the small scattering cross section for cosmic-ray mesons, implied an upper limit of 10^{-7} sec on the lifetime of the π meson. More recent cosmic-ray experiments, such as the measurement of the difference in upward and downward flux of π mesons at mountain altitudes[10] and the measurement of the variation of intensity of μ mesons as a function of underground depth[11] (cf. Chap. 6), have led to rough values for the lifetime of the π meson, of the order of 10^{-8} sec.

However, it is clear, in principle, that the most accurate measurements of the lifetime for π decay must come from experiments with artificial sources of π mesons. Unfortunately, the agreement among the different accelerator measurements was at first none too good, although more recent experiments appear to be settling down to a value of about 2.6 $\times 10^{-8}$ sec for the mean lifetime. The first accelerator experiment on the π decay lifetime was carried out by Richardson,[12] who measured the number of π^- mesons produced in proton-carbon collisions as a function of angular distance in the magnetic field of the Berkeley cyclotron. The π^- mesons were detected by photographic plates placed at various path lengths from the target inside the cyclotron vacuum tank. Richardson found the value $\tau^- = 1.11^{+0.31}_{-0.22} \times 10^{-8}$ sec for the mean life. Using the same method, Martinelli and Panofsky[13] measured the mean life of the π^+ meson and found it to be $\tau^+ = 1.97^{+0.14}_{-0.17} \times 10^{-8}$ sec. The recent measurements of the π^+ lifetime have all been by electrical means. One measurement of this type was performed by Kraushaar *et al.*,[14] using π^+ mesons produced in carbon or beryllium targets by the γ rays from the MIT synchrotron. Taking advantage of the time lag between two bursts of fluorescence due to $\pi \rightarrow \mu$ decay and $\mu \rightarrow e$ decay in the same scintillation counter to identify the $\pi \rightarrow \mu$ decay process, and measuring the distribution in time of the first burst led the MIT group to a mean life of the π^+ meson of $1.65 \pm 0.33 \times 10^{-8}$ sec. An electronic measurement carried out at the same time by Chamberlain *et al.*,[15] using the π^+ mesons produced in a polyethylene target by the γ rays of the Berkeley synchrotron, led to a mean life of $2.58 \pm 0.14 \times 10^{-8}$ sec (averaging the authors' differential and integral data). While the MIT result is consistent with the time-of flight measurement whereas the Berkeley result is not, it is likely that the latter is more correct since it is based on an analysis of 1419 events whereas the MIT lifetime is based on only 57 events. Moreover, the original time-of-flight experiment was certainly not reliable because of the many geometrical corrections which had to be made. Very recently, Jakobson *et al.*[16] have made another accurate electronic measurement of the π^+ lifetime and found

---

[8] H. Friedman and J. Rainwater, *Phys. Rev.*, **81**: 644 (1951); cf. also F. M. Smith, *Phys. Rev.*, **81**: 897 (1951).

[9] R. Marshak and H. Bethe, *Phys. Rev.*, **72**: 506 (1947).

[10] Camerini, Muirhead, Powell, and Ritson, *Nature*, **162**: 433 (1948).

[11] K. Greisen, *Phys. Rev.*, **73**: 521 (1948).

$$\tau^+ = 2.54 \pm 0.11 \times 10^{-8} \text{ sec}$$

Hence the best value of the π^+ lifetime at the present time appears to be 2.55×10^{-8} sec.

It should be noted that all the electronic lifetime measurements refer to the π^+ meson, and it would be desirable to have an equally accurate measurement of the π^- lifetime. Since the π^- meson will decay only in the absence of matter, it is necessary to measure the π^- lifetime by some other method. The best value of the π^- lifetime obtained thus far is the one measured by Lederman *et al.*[17] with a cloud chamber in a magnetic field; from a study of the number of $\pi \rightarrow \mu$ decays and their energies, the Columbia group derived the value $\tau = 2.92 \pm 0.32 \times 10^{-8}$ sec. The Columbia value is more trustworthy than the old Richardson value and is compatible with equality of π^+ and π^- lifetimes.

---

[12] J. R. Richardson, *Phys. Rev.*, **74**: 1720 (1948).

[13] E. Martinelli and W. Panofsky, *Phys. Rev.*, **77**: 465 (1950).

[14] Kraushaar, Thomas, and Henri, *Phys. Rev.*, **78**: 486 (1950).

[15] Chamberlain, Mozley, Steinberger, and Wiegand, *Phys. Rev.*, **79**: 394 (1950); cf. also C. E. Wiegand, *Phys. Rev.*, **83**: 1085 (1951).

[16] Jakobson, Schulz, and Steinberger, *Phys. Rev.*, **81**: 894 (1951).

2. *Decay products.* The π^+ meson is known to give rise to a μ^+ meson at the end of its track in a photographic emulsion. As a matter of fact, it was this observation in particular which led Lattes *et al.*[1] to the discovery of the charged π meson. Since all available evidence indicates that the vast majority[18] of μ^+ mesons resulting from π^+ decay have a fixed range of about 600 microns in the photographic emulsion, the predominant mode of decay of the π^+ meson must involve the emission of only one neutral particle in addition to the μ meson. The range of the μ^+ meson observed in a photographic emulsion will not be exactly constant because of straggling, *i.e.*, variation due to the statistical nature of the ionization energy loss process. Figure 2 shows the range distribution observed by Barkas *et al.*[19] in a C2 emulsion for $163\mu^+$ meson tracks resulting from the decay of π^+ mesons at rest. The mean range turns out to be 600 microns with a standard deviation of 4.4 per cent, to be compared with the theoretical straggling of 4.0 per cent, assuming each electron in the emulsion to be free. The additional 10 per cent straggling which is observed is probably to be attributed to the small

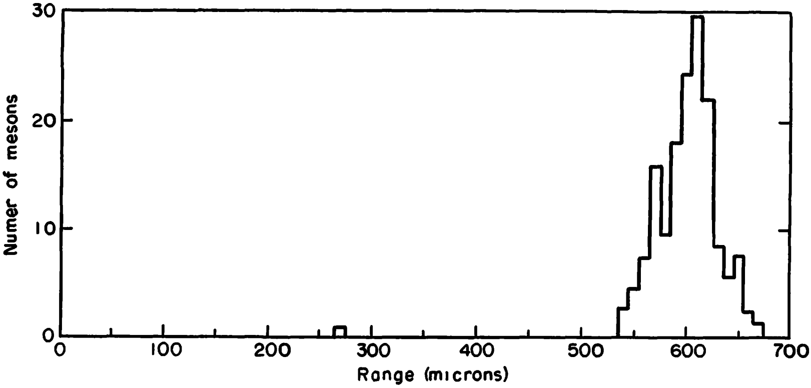

FIG. 2. Measured range distribution of μ^+ mesons from the decay of the π^+ meson.

---

[17] Lederman, Booth, Byfield, and Kessler, *Phys. Rev.*, **83**: 685 (1951).

[18] The rare exceptions will be discussed below.

[19] W. H. Barkas, *UCRL* No. 1285; cf. also footnote 2.

effect of electron binding. The energy corresponding to a range of 600 microns is 4.085 ± 0.044 Mev.

Let us therefore assume that a μ meson and a neutral particle of mass m_n are the decay products of the π meson and see what information can be deduced concerning m_n. From energy and momentum conservation, we can write

$$m_\pi = \sqrt{m_\mu^2 + p^2} + \sqrt{m_n^2 + p^2} \tag{4}$$

where p is the momentum of the decay particles. Solving this relation for m_n, one finds

$$m_n = m_\mu[(\rho - 1)^2 - 2\rho\delta]^{\frac{1}{2}} \tag{5}$$

where $\rho = m_\pi/m_\mu$, $\delta = T_\mu/m_\mu$ with T_μ the kinetic energy of the μ meson. It will be recalled that, if we choose $\rho = 1.317$ and $\delta = 0.0382$, then $m_n = 0$; this is not surprising since the value for T_μ was determined originally from Eq. (4). However, m_n is extremely sensitive to the values of ρ and δ. Thus, if we use the value of ρ allowed by the standard deviation, namely, $\rho = 1.321$, and the value of $\delta = 0.0377$ allowed by the uncertainty in the range-energy curve for μ mesons, we obtain

$$m_n = 12.3m_e.$$

Consequently, slight errors in the range-energy calibration for the μ meson and in the ratio of the π to μ masses lead to considerable uncertainty in the mass of the neutral decay particle, and the upper limit on the mass of the neutral particle is at best several electron masses. It is simplest, of course, not to invoke a new type of neutral particle and to assume that the neutral decay particle possesses zero rest mass and is a photon or a neutrino.

It is still necessary to decide whether the neutral particle associated with the π meson decay is a photon or a neutrino. If there is a theoretical connection between $\pi \rightarrow \mu$ decay and the absorption of μ^- mesons by heavy nuclei (cf. Chap. 5), then the absence of high-energy γ rays in connection with the latter[20] process would argue against a photon being the neutral decay particle. An experimental attempt has been made by O'Ceallaigh[21] to decide whether the neutral particle is a photon—with negative results. O'Ceallaigh carefully searched for electron pairs associated with $\pi \rightarrow \mu$ decays which would be produced by the 30-Mev photon moving in a direction opposite to that of the visible μ meson. In a total scan length of 38 cm in the vicinity of 250 $\pi \rightarrow \mu$ decays, not a single electron pair was found. Since, if a photon were emitted in the $\pi \rightarrow \mu$ decay process, the probability that it would fail to produce an

---

[20] Cf. O. Piccioni, *Phys. Rev.*, **74**: 1754 (1948).

[21] C. O'Ceallaigh, *Phil. Mag.*, **41**: 838 (1950).

DAVID J. LANGFORD

Pure Mathematical Physics

electron pair is 4×10^{-3} under the conditions of the experiment, the evidence is strong that the neutral particle accompanying the μ meson in the π meson decay is not a photon. It is therefore likely that the π meson decays into a μ meson plus a neutrino.

The question may be raised whether there are any other modes of decay of the π meson besides the dominant mode: $\pi \rightarrow \mu + \nu$. We have already remarked that thus far there is no evidence[8] for the decay of the π meson into an electron. Hence, since the lifetime for μ decay is 2.55×10^{-8} sec, the partial lifetime for electron decay must be greater than 3×10^{-5} sec. On the other hand, there is some evidence for an alternative mode of decay of the π meson which involves the μ meson. Several $\pi \rightarrow \mu$ decays have been observed in photographic emulsions with anomalously short μ tracks which cannot be ascribed to straggling. Thus, Fry[22] finds four anomalous μ meson tracks (260, 258, 185, 120 microns in length) in 3018 $\pi \rightarrow \mu$ decays, whereas Bramson *et al.*[22a] find one anomalous μ meson track (235 microns in length) in 1500 $\pi \rightarrow \mu$ decays. One possible explanation of these anomalously short μ meson tracks is the occurrence of the process $\pi \rightarrow \mu + \nu + \gamma$ with the γ ray taking away as much as 17 Mev, although all intermediate energies (0 to 17 Mev), and therefore kinetic energies, of the μ meson from 0 to 4 Mev are possible. This process is the analogue of internal bremsstrahlung in nuclear beta decay and a straightforward calculation[22b] leads to a ratio of probabilities for the two processes $\pi \rightarrow \mu + \nu + \gamma$ to $\pi \rightarrow \mu + \nu$ of about $(e^2/\hbar c)(T_\mu/\mu c^2) \approx \frac{1}{4000}$, a value which is somewhat too low. However, it is too early to say whether there is disagreement with experiment.[22c]

Let us return to the dominant mode of decay of the π meson and consider the nature of the coupling to the μ meson-neutrino field responsible for the decay process. From a theoretical point of view, it is noteworthy that the $\pi \rightarrow \mu$ lifetime is extremely long compared with the characteristic time τ_0 of the decay process, namely,

$$\tau_0 = \frac{\hbar}{m_\pi c^2} = 5 \times 10^{-24} \text{ sec}$$

(m_π is the π meson mass). This implies that the μ meson-neutrino field and a fortiori the electron-neutrino field is very weakly coupled to the π meson field. We may obtain an estimate of the strength of this coupling by equating the theoretical prediction for the lifetime to the experimental value. For example, suppose the π meson is scalar and is scalar coupled to the μ meson-neutrino field [*i.e.*, the $S(S)$ theory], then the interaction Hamiltonian is

---

[22] W. F. Fry, *Phys. Rev.*, **83**: 1268 (1951).

[22a] Bramson, Seifert, and Havens, quoted in Primakoff, footnote 22*b*.

[22b] A. M. L. Messiah, private communication. Cf. also H. Primakoff, *Phys. Rev.*, **84**: 1255 (1951); and T. Eguchi, *Phys. Rev.*, **85**: 943 (1952).

[22c] Recently, Fry [*Phys. Rev.*, **86**: 418 (1952)] has found the ratio of probabilities for the two processes to be $2.8 \pm 1.2 \times 10^{-4}$, which is in accord with theory.

$$H_{\pi\mu} = G_\mu \psi_\mu^* \beta \psi_\nu \phi_\pi \tag{6}$$

where ψ_μ, ψ_ν, ϕ_π represent the μ meson, neutrino, and π meson wave functions, respectively, and G_μ is the coupling constant we wish to determine. It can easily be shown that the transition probability per second for μ decay, τ_μ, is given by

$$\tau_\mu^{-1} = \frac{1}{4\tau_0} \frac{G_\mu^2}{\hbar c} \left(1 - \frac{m_\mu^2}{m_\pi^2}\right)^2 \tag{7}$$

where τ_0 is the characteristic time defined above. Formulas for the $\pi \rightarrow \mu$ decay lifetime can readily be derived for the other fields and couplings for the π meson considered in Chaps. 1 and 2, assuming always that the decay products μ and ν obey the Dirac equation. The results are[23]

$$PS(PS){:} \qquad \tau_\mu^{-1} = \frac{1}{4\tau_0} \frac{G_\mu^2}{\hbar c} \left(1 - \frac{m_\mu^2}{m_\pi^2}\right)^2 \tag{8}$$

$$PS(PV){:} \qquad \tau_\mu^{-1} = \frac{1}{4\tau_0} \frac{F_\mu^2}{\hbar c} \left(\frac{2m_\mu}{m_\pi}\right)^2 \left(1 - \frac{m_\mu^2}{m_\pi^2}\right)^2 \tag{9}$$

$$V(V){:} \qquad \tau_\mu^{-1} = \frac{1}{12\tau_0} \frac{G_\mu^2}{\hbar c} \left(2 + \frac{m_\mu^2}{m_\pi^2}\right) \left(1 - \frac{m_\mu^2}{m_\pi^2}\right)^2 \tag{10}$$

$$PV(PV){:} \qquad \tau_\mu^{-1} = \frac{1}{12\tau_0} \frac{G_\mu^2}{\hbar c} \left(1 + \frac{2m_\mu^2}{m_\pi^2}\right) \left(1 - \frac{m_\mu^2}{m_\pi^2}\right)^2 \tag{11}$$

Table 1 lists the values of the coupling constants for $\pi \rightarrow \mu$ decay derived for the different theories by setting $\tau_\mu = 2.5 \times 10^{-8}$ sec.

TABLE 1. COUPLING CONSTANTS FOR $\pi \rightarrow \mu$ DECAY

Theory	$G_\mu^2/\hbar c$[$F_\mu^2/\hbar c$ in $PS(PV)$ theory]
$S(S)$	4.1×10^{-15}
$PS(PS)$	4.1×10^{-15}
$PS(PV)$	1.8×10^{-15}
$V(V)$	4.8×10^{-15}
$PV(PV)$	5.7×10^{-15}

Equations (7) to (11) can immediately be applied to the electron decay process ($\pi \rightarrow e + \nu$) by setting m_μ equal to the electron mass m_e. Comparison of the resulting formulas with Eqs. (7) to (11) reveals the interesting point—first noted by D'Espagnat[24]—that for equal values of the μ meson and electron coupling constants (that is, $G_e = G_\mu$), τ_e is shorter for four of the theories [$S(S)$, $PS(PS)$, $V(V)$, $PV(PV)$] and longer for one of the theories [that is, $PS(PV)$]. As a matter of fact, in the $PS(PV)$ theory, τ_e/τ_μ is equal to $(m_\mu/m_e)^2 \approx 4 \times 10^4$, a value completely in accord with the experimental observations thus far. This is an agreeable result since, as we shall see (cf. Chap. 7), the $PS(PV)$ theory governs the coupling of the π meson to the proton-neutron field although there is no a priori reason for choosing $G_e = G_\mu$. Even though the $PS(PV)$ theory makes it possible to understand the branching ratio for the electron decay of the π meson, the $PS(PV)$ theory does not yield a proper understanding of nuclear β decay in terms of Yukawa's original scheme: $N \rightarrow \left\{\begin{matrix} P + \pi^- \\ N + \pi^+ + e^- + \nu \end{matrix}\right\} \rightarrow P + e^- + \nu$ either for $G_e = G_\mu$ or for any value of G_e for that matter.[25] Apart from the numerical disagreement, which is huge (a factor of 10^9), the $PS(PV)$ theory predicts a dependence of the β decay lifetime on the maximum energy W_0 of the β ray of the form W_0^7 instead of W_0^5, as required by experiment. Caianiello has actually shown that the only meson field which can qualitatively account for nuclear β decay (apart from quantitative difficulties) is a vector meson field, the one field definitely excluded for the π meson by the photonic production experiments already discussed (cf. Chap. 1) and the π meson absorption experiments still to be discussed (cf. below).

---

[23] R. Latter, Ph.D. Thesis, California Institute of Technology, 1948.

[24] B. D'Espagnat, *Compt rend.*, **228**: 744 (1949).

B. Decay of the π^0 Meson. We have already pointed out that the decay particles of the π^0 meson are two γ rays, the detection of which established the existence of the π^0 meson. We have also remarked that the lifetime for the process $\pi^0 \rightarrow 2\gamma$ is extremely short, so short, in fact, that all experiments (except one) designed to measure its value have succeeded only in placing an upper limit thereon.

For example, the experiment of Bjorkland *et al.*[26] on the γ rays arising from proton-nucleus collisions (cf. Chap. 3), which was taken as evidence for the production of π^0 mesons, led to an upper limit on the π^0 lifetime of 10^{-11} sec in virtue of the disappearance of the γ rays when the target was moved behind a fixed shield. An improved experiment of this type was later carried out by York[27] at Berkeley and led to a reduction in the upper limit to 2×10^{-13} sec. Three other values for an upper limit on the π^0 lifetime were derived from cosmic-ray experiments. The first cosmic-ray value was obtained from an analysis of a high-energy event (the so-called R star), observed by Bradt *et al.*[28] in a stack of photographic plates exposed at 95,000 ft. In this event, an alpha particle of about 10^{12} ev produces a shower of some 56 singly charged, relativistic particles, half of which are concentrated in a core of half width 1.5°. An appreciable multiplication of the number of charged particles was found in the core of the shower and was presumed due to electron pair production resulting from the decay γ rays of the π^0 mesons created in the initial alpha-nucleus interaction. From a measurement of this multiplication, the Rochester group was led to an upper limit on the π^0 lifetime of 3×10^{-13} sec. More recently, Lord *et al.*[29] observed an event similar to the *R* star, except that it was produced by a primary proton with an energy of the order of 10^{13} ev. From the observation of a single electron pair about 5000 microns from the point of collision, these workers deduced an upper limit on the π^0 lifetime of 2×10^{-15} sec. However, this value is subject to considerable doubt since it is based on one electron pair of rather low energy. The best upper limit on the π^0 lifetime was inferred by Carlson *et al.*[7] from observations on the electron pairs[30] produced by photons associated with stars emitting shower particles. These authors surveyed the area in the vicinity of stars containing at least three shower particles and obtained a distribution for the perpendicular distances from the lines passing through accompanying electron pairs. On the basis of this distribution, an upper limit of 5×10^{-14} sec was derived for the π^0 lifetime.

---

[25] Cf. E. R. Caianiello, *Phys. Rev.*, **81**: 625 (1951).

[26] Bjorkland, Crandall, Moyer, and York, *Phys. Rev.*, **77**: 213 (1950).

[27] H. F. York, private communication.

[28] Bradt, Kaplon, and Peters, *Helv. Phys. Acta*, **23**: 24 (1950); this event is discussed in greater detail in Chap. 8.

An actual, though approximate, value for the lifetime of the π^0 meson has been measured by Kaplon *et al.*[31] by means of an emulsion cloud chamber consisting of alternate layers of photographic emulsions and brass absorbers. By studying the cascade development through the brass absorbers of the soft component associated with an extremely high-energy nuclear interaction, the so-called *T* star, these authors were able to deduce a lifetime of the π^0 meson of approximately 1×10^{-14} sec. The *T* star will be described in greater detail in Chap. 8. For our present purposes, it suffices to state that the *T* star was produced by a proton having an energy of about 2×10^{13} ev and that among the 55 or so charged and neutral π mesons produced in the star were two very energetic π^0 mesons (revealed by the presence of two very energetic double-cored showers) decaying at finite distances from the initial nuclear explosion. The energies of these two mesons were 1.6×10^{12} ev and 2.4×10^{12} ev, respectively, (derived from the angular separations of the two double-cored showers which were 2.1×10^{-4} and 1.35×10^{-4} radians, respectively) and their decay distances were 2.5 and 7 cm, respectively, leading to an approximate value of 1×10^{-14} sec for the π^0 lifetime. This value must, of course, be regarded as a very preliminary one, although it is unlikely that the error is greater than, say, a factor 3 (unless the double-cored showers are incorrectly attributed to π^0 mesons).

---

[29] Lord, Fainberg, and Schein, *Phys. Rev.*, **80**: 970 (1950).

[30] Recently, a sufficient number of electron pairs directly associated with the π^0 decay in competition with the two-photon decay [cf. R. H. Dalitz, *Proc. Phys. Soc. London*, **64**: 667 (1951)] have been observed to permit a deduction of the actual π^0 lifetime in the neighborhood of 1×10^{-14} sec [cf. Daniel, Davies, Mulvey, and Perkins, *Phil. Mag.*, **43**: 753 (1952)]. Dalitz predicts that the two chief modes of decay of a spin zero π^0 meson, namely $\pi^0 \rightarrow \gamma + e^+ + e^-$ and $\pi^0 \rightarrow 2\gamma$, should occur in the ratio 1:80.

[31] Kaplon, Peters, and Ritson, *Phys. Rev.*, **85**: 900 (1952).

For purposes of theoretical comparison, we shall assume that the lifetime of the π^0 meson is 10^{-14} sec. Just as in the case of $\pi \rightarrow \mu$ decay, it is possible to regard the decay process $\pi^0 \rightarrow 2\gamma$ as due to a direct coupling between the initial and final particles. In the case of π^0 decay, the interaction Hamiltonian must be a scalar invariant containing the π^0 wave function ϕ and the wave functions for the two final photons. Since a neutral spin 1 meson cannot decay into 2γ rays[32] (and we exclude the possibility of the π^0 spin being greater than 1), the interaction Hamiltonian becomes

$$H_S = \eta_S \left(\frac{\hbar}{\mu_0 c}\right) \frac{c^2}{\sqrt{\hbar c}} \phi(E^2 - H^2) \tag{12}$$

for a scalar π^0 meson and

$$H_{PS} = \eta_{PS} \left(\frac{\hbar}{\mu_0 c}\right) \frac{c^2}{\sqrt{\hbar c}} \phi(\mathbf{E} \cdot \mathbf{H}) \tag{13}$$

for a pseudoscalar π^0 meson. In Eqs. (12) and (13), η_S and η_{PS} are the dimensionless coupling constants between the π^0 meson and the photon field, μ_0 is the π^0 mass, and **E** and **H** are the ordinary Maxwell electric and magnetic fields. The lifetime of the π^0 meson can be expressed in terms of η_S or η_{PS} by applying first-order perturbation theory, with the result

$$\tau_{\pi^0}^{-1} = \frac{\eta_S^2}{16\pi}\left(\frac{\mu_0 c^2}{\hbar}\right) \qquad \text{(scalar } \pi^0\text{)} \tag{14}$$

or

$$\tau_{\pi^0}^{-1} = \frac{\eta_{PS}^2}{64\pi}\left(\frac{\mu_0 c^2}{\hbar}\right) \qquad \text{(pseudoscalar } \pi^0\text{)} \tag{15}$$

Substituting 10^{-14} sec for τ_{π^0} into Eq. (14) and (15) leads to the values

$$\eta_S = 1.6 \times 10^{-6} \tag{16}$$

or

$$\eta_{PS} = 3.2 \times 10^{-6} \tag{17}$$

While it is certainly legitimate to regard the π^0 decay as due to a direct coupling between the π^0 meson and the electromagnetic field, one may well inquire whether it is possible to explain the decay of the π^0 meson in terms of known couplings, *i.e.*, the coupling of the π^0 meson to the nucleon field (which must exist because the π^0 meson is produced in nucleon-nucleon collisions—at least in proton-neutron collisions—cf. Chap. 2) and the coupling of the electromagnetic field to the nucleon field. As a matter of fact, it was pointed out a long time ago by Sakata and Tanikawa[33] that, if nucleons are assumed to obey the Dirac equation and exist in negative energy states, the π^0 meson should decay rapidly into 2γ rays through the virtual creation of a proton-antiproton pair, to wit,

---

[32] C. N. Yang, *Phys. Rev.*, **77**: 242 (1950); cf. also D. C. Peaslee, *Helv. Phys. Acta*, **23**: 845 (1950).

$$\pi^0 \rightarrow P + \bar{P} \rightarrow P' + \gamma_1 + \bar{P} \rightarrow \gamma_1 + \gamma_2 \tag{18}$$

where $\bar{P}$ is the antiproton. In Eq. (18), the π^0 meson produces a virtual proton-antiproton pair because of its coupling with the nucleon field.

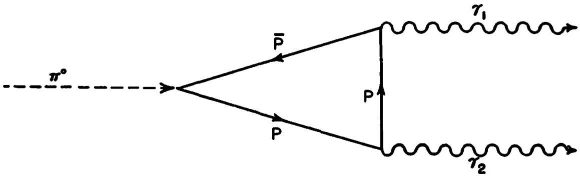

FIG. 3. Feynman diagram for the decay of the π^0 meson.

The proton pair being charged is coupled to the electromagnetic field (the anomalous magnetic moments of the neutron pair would also lead to a coupling with the electromagnetic field, but presumably this is weaker than the interaction of the proton pair with the electric field) and the two components of the proton pair annihilate each other in successive steps to produce the two final photons. The Feynman diagram corresponding to the transition scheme shown in Eq. (18) is sketched in Fig. 3. The presence of the closed loop in Fig. 3 leads to difficulties with a perturbation-theoretic calculation of the lifetime for the two-photon decay of the π^0 meson[34] unless one performs the calculation in a gauge invariant and relativistically covariant fashion. When the latter type of calculation is carried out,[35] both the $S(S)$ and $PS(PS)$ theories lead to finite results for the π^0 lifetime, and the equivalence theorem holds between the $PS(PS)$ and $PS(PV)$ theories. As a matter of fact, the third-order process visualized in Eq. (18) and Fig. 3 can be replaced by an effective interaction between the π^0 field and the electromagnetic field of the form (12) with $\eta_S = e^2\mu_0 g_S^0/3\pi\hbar c\sqrt{\hbar c}\,M$ for the $S(S)$ theory and of the form (13) with $\eta_{PS} = e^2\mu_0 g_{PS}^0/\pi\hbar c\sqrt{\hbar c}\,M$ for the $PS(PS)$ theory. The equivalence theorem between the $PS(PS)$ and $PS(PV)$ theories implies that the effective interaction Hamiltonian between a $PS(PV)$ π^0 meson and the electromagnetic field can be written in the form

---

[33] S. Sakata and Y. Tanikawa, *Phys. Rev.*, **57**: 548 (1940).

[34] Cf. R. J. Finkelstein, *Phys. Rev.*, **72**: 415 (1947); J. Steinberger, *Phys. Rev.*, **76**: 1180 (1949); H. Fukuda and Y. Miyamoto, *Prog. Theor. Phys.*, **4**: 347 (1949). The last two calculations were performed with regulator methods [cf. W. Pauli and F. Villars, *Rev. Mod. Phys.*, **21**: 433 (1949)]; however, P. T. Matthews [*Phys. Rev.*, **81**: 936 (1951)] has shown that no consistent regulator prescription exists for nonrenormalizable theories like the $PS(PV)$ theory.

[35] J. Schwinger, *Phys. Rev.*, **82**: 664 (1951).

$$H' = \frac{e^2\mu_0 f^0}{2\pi\hbar c M^2}\,\phi(\mathbf{E}\cdot\mathbf{H}) \tag{19}$$

where f^0 is the $PS(PV)$ π^0 coupling constant. The relationship between the lifetime and the coupling constant holds as before, and it is possible to deduce values for the meson-nucleon coupling constants from Eqs. (14) and (15) once the value for the π^0 lifetime is inserted; the results are shown in Table 2. Unfortunately, the pseudoscalar π^0 meson-nucleon interaction constants turn out to be much smaller than those deduced from the photonic and nucleonic production experiments. The reason for this discrepancy is not clear unless the negative energy states for the nucleons are incorrectly treated or do not exist.

TABLE 2. π^0 COUPLING CONSTANTS FROM MEASURED LIFETIME

Theory	π^0 Coupling Constant
$S(S)$	0.15
$PS(PS)$	0.10
$PS(PV)$	0.007

It should be mentioned that Primakoff[36] has deduced a lower limit on the lifetime of the π^0 meson from the experiments on the photoproduction of π^0 mesons in complex nuclei. He points out that, if an interaction of the form (12) or (13) exists between the π^0 and photon fields (and this is independent of whether there is a direct coupling or an indirect coupling through the nucleon field), then a π^0 meson can be produced in the collision of a high-energy γ ray with the Coulomb field of a nucleus. The cross section for this effect varies with Z^2 (Z is the atomic number of the nucleus) and is inversely proportional to the lifetime of the π^0 meson. From the fact that a Z^2 term has not been observed in experiments on the production of π^0 mesons in photon-nucleus collisions (cf. Chap. 3), Primakoff concludes that the lifetime for the π^0 meson must be greater than 5×10^{-16} sec.

4. Spins, Statistics, and Parities of the π Mesons

We have already stated that one may conclude immediately from the observed two-photon decay of the π^0 meson that the π^0 meson must possess spin 0 (or a spin greater than 1). It can be shown by general angular momentum arguments[34] that a spin 1 meson must decay into a minimum of three γ rays (or an electron-positron pair); this follows from the fact that, while a photon possesses spin 1, the transversality of the electromagnetic field requires that two photons carry off 0 or 2 units of angular momentum. A more detailed calculation shows that, while a vector neutral meson can decay into three γ rays (or an electron-positron pair), a pseudovector neutral meson must—by an application of Furry's theorem[34]—decay into at least four γ rays (or one γ ray plus an electron-positron pair). While the spin of the π^0 meson is not completely fixed by its two-photon decay (unless one chooses the smallest possible value, *viz.*, spin 0), the two-photon decay of the π^0 meson does establish its boson character.[36a]

---

[36] H. Primakoff, *Phys. Rev.*, **81**: 899 (1951).

The statistics of the charged π meson can also be determined more readily than its spin. For example, a study of the excitation energies associated with the absorption of slow π^- mesons by heavy nuclei[37] indicates that the π^- meson is a boson rather than a fermion, a subject which will be treated more fully in Chap. 5. In the present section, we turn our attention to the experiments on the absorption of slow π^- mesons in hydrogen and deuterium[38] since these experiments shed light not only on the statistics of the charged π meson but also on its spin and parity. Moreover, the same π^- absorption experiments in hydrogen and deuterium supply similar information concerning the neutral π meson.

A. Slow π^- Reactions in Hydrogen. We have already reproduced in Fig. 1 the γ ray spectrum which is observed to accompany the absorption of slow π^- mesons by protons. It was pointed out that accurate determinations of the masses of the charged and neutral π mesons can be derived from a knowledge of this γ ray spectrum. For our present purposes, it is necessary to treat the hydrogen absorption experiment in greater detail and then to consider the deuterium absorption experiment.

It was stated in Sec. 2 that the π^- meson is absorbed from the K shell of the mesic-hydrogen atom; this statement is not immediately obvious because Fermi and Teller's[39] slowing-down considerations (cf. Chap. 5) do not apply to an atom as light as hydrogen. Wightman[40] has investigated the slowing-down mechanism for π^- mesons in hydrogen and has shown that the moderation of a π^- meson in hydrogen takes place in four stages: (1) In this stage—from several Mev to about 1 kev—the π^- meson loses energy by ionizing and exciting the H_2 molecules; this loss of energy is adequately described by the usual stopping-power formula. (2) In this stage—from about 1 kev to capture by an H_2 molecule—the velocity of the meson drops below that of the electrons of the H_2 molecule although it continues to ionize H_2 molecules. Even at 1 ev, a π^- meson moves fast enough to cause nonadiabatic processes in the molecule because the binding energy of the last electron is so low when the meson is in the middle of the molecule. As a last step, the π^- meson is captured into an orbit about the H_2^+ molecular ion. (3) In this stage, the highly excited $\pi^-H_2^+$ system formed at the end of stage (2) rapidly decomposes into $\pi^-P + H$; the resulting π^-P atom (with the π^- meson excited to levels of principal quantum number $\sim 15 - 30$) collides with H_2 forming $\pi^-H_3^+$ which, in general, rapidly dissociates into $\pi^-P + 2H$. In each such dissociation the meson loses at least 4 ev and thereby cascades into lower orbits about the proton. (4) In the last stage, the π^- meson cascades down to the K shell of the mesic-hydrogen atom by emitting radiation and by exciting and ionizing nearby molecules via the oscillating electric field associated with its motion about the proton. Wightman estimates that a maximum time of 10^{-10} sec elapses for the π^- meson to pass through all four stages in liquid hydrogen starting at several Mev. This time is much shorter[41] than the decay time for the π^- meson which, in turn, is much shorter than the time for absorption of the π^- meson from the continuum. It can also be shown[42] that the probability for nuclear absorption of the π^- meson from a p state is appreciably smaller than the probability for a radiative transition to an s state. Consequently, slow π^- reactions in hydrogen will take place predominantly from the K shells of mesic-hydrogen atoms (or at least from s states).

[36a] W. Pauli [*Phys. Rev.*, **58**: 716 (1940)] has proved, under very general assumptions, that an elementary particle possessing integral spin must obey Bose-Einstein statistics, whereas a particle possessing half-integral spin must obey Fermi-Dirac statistics. However, in the present instance, the boson character of the π^0 meson follows immediately from the fact that the photon is a boson. Cf. also W. Pauli, *Prog. Theor. Phys.*, **5**: 526 (1950).

[37] W. Cheston and L. Goldfarb, *Phys. Rev.*, **78**: 683 (1950).

[38] These experiments are also reviewed in R. E. Marshak [*Rev. Mod. Phys.*, **23**: 137 (1951)].

Since the binding energy of the π^- meson in the K shell of the mesic-hydrogen atom is only 3 kev, the question arises as to what will happen when a π^- meson of essentially zero kinetic energy and zero orbital angular momentum is absorbed by a proton. Let us suppose that a π^- meson is absorbed by a proton: then energy and momentum conservation require that at least one neutral particle is emitted in addition to the neutron. The simplest assumption to make is that only one neutral particle Q is emitted, namely, $\pi^- + P \rightarrow N + Q$. Thus, if the π^- meson is a fermion, Q must be a fermion, *e.g.*, a neutrino. On the other hand, if the π^- meson is a boson, Q must be a neutral boson, *e.g.*, a γ ray or a neutral π meson. (As we have stated before, Q can be a π^0 meson only if the mass of the π^- meson exceeds the mass of π^0 by an amount greater than 1.25 Mev, *i.e.*, the mass difference between the neutron and proton.) The boson modes of absorption can be represented by (a) $\pi^- + P \rightarrow N + \gamma$ (radiative absorption) and (b) $\pi^- + P \rightarrow N + \pi^0$ (mesic absorption). In the case of radiative absorption, the final products will be a neutron of about 10 Mev and a discrete γ ray of about 130 Mev; whereas, if mesic absorption takes place, the final products will be a neutron of less than 1 Mev and a square pulse of γ rays centered at about 70 Mev (cf. Sec. 2B). In either case, the boson character of the π^- meson will be established if γ rays associated with reaction (a) or (b) are observed. The experimental curve shown in Fig. 1 proves that both reactions (a) and (b) do indeed take place[43] and therefore that the charged π meson is unquestionably a boson. As far as the spins and parities of the charged and neutral π meson fields are concerned, the relevant piece of experimental information in the hydrogen absorption experiment is the measurement of the relative probability of mesic to radiative absorption which yields 0.94 ± 0.20.

---

[39] E. Fermi and E. Teller, *Phys. Rev.*, **72**: 399 (1947).

[40] A. Wightman, Ph.D. Thesis, Princeton University, 1949; cf. also *Phys. Rev.*, **77**: 521 (1950).

[41] Direct experimental evidence that the vast majority of π^- mesons reach the K shell and do not decay en route has been obtained by varying the pressure of the hydrogen gas (cf. footnote 6).

[42] S. Tamor, *Phys. Rev.*, **82**: 38 (1951); cf. also Brueckner, Serber, and Watson, *Phys. Rev.*, **81**: 575 (1951).

What is the significance of this approximate equality of radiative and mesic absorption of slow π mesons in hydrogen for the spins and parities of the π meson fields? To answer this question, it is necessary to inquire into the theoretically predicted transition probabilities for radiative and mesic absorption from the K shell of a mesic-hydrogen atom. The predicted probabilities will differ, of course, depending upon the fields and nucleon couplings which are assumed to govern the charged and neutral π mesons. Some idea of relative magnitudes, however, can be obtained immediately by specifying, for any particular choice of fields and couplings, the angular momenta and parities of the γ ray and π^0 meson which can be emitted. Table 3 lists the total angular momenta and parities of the meson-proton system[44] for the four simplest fields for the π^- meson, the lowest pole of the outgoing photon (e.d. = electric dipole, m.d. = magnetic dipole) and the angular momentum state of the outgoing π^0 meson for the two possible spin zero fields (excluding a spin greater than 1—cf. above). When cognizance is taken of the low kinetic energies of the π^0 meson (3 to 4 Mev) and of the recoil neutron ($\sim \frac{1}{2}$ Mev), it is evident that the mesic absorption probability decreases rapidly as the angular momentum of the outgoing π^0 increases. Consequently, Table 3 predicts that opposite parities for the π^- and π^0 mesons will be much less favorable for mesic absorption than the same parity. For spin 1 π^- mesons, the qualification must be added that, for the same parity for the π^- and π^0 mesons, mesic absorption is only probable for the $J = \frac{1}{2}$ substate of the meson-proton system; mesic absorption from the $J = \frac{3}{2}$ substate is greatly reduced, and one would expect that at least two-thirds of the π^- mesons (each substate acts as an independent system, and the statistical weight of the $J = \frac{3}{2}$ substate is 4 compared with 2 for the $J = \frac{1}{2}$ substate) would undergo radiative absorption unless the π^0 coupling constants are inordinately large.

---

[43] A. Sachs and J. Steinberger [*Phys. Rev.*, **82**: 973 (1951)] have definitely established that the 70-Mev γ rays are due to π^0 mesons by performing a coincidence experiment between the two 70-Mev γ rays.

Because of the fundamental importance of the hydrogen absorption experiment and for the purposes of later comparison with the equally fundamental deuterium absorption experiment, we shall discuss briefly the predictions of weak coupling theory and how they bear out the qualitative features of Table 3. The weak coupling formulas for the absorption of a π^- meson from the K shell of a mesic-hydrogen atom can be derived by calculating the transition probability for the absorption by a proton of a slow π^- meson from the continuum and replacing the number of protons per cubic centimeter by $\phi^2(0)$ where $\phi(0)$ is the Coulomb wave function of the π^- meson evaluated at the position of the proton and the Schrodinger approximation can be used, namely,

$$\phi^2(0) = \frac{1}{\pi a_\pi^3}$$

where $a_\pi = \hbar^2/m_\pi e^2$. The transition probabilities for an unbound meson are readily computed with the help of the Feynman diagrams which, for the radiative absorption reaction, are merely the inverse of the photomesic production diagrams (cf. Fig. 2 in Chap. 1). Since the velocities of the initial π^- meson and proton are essentially zero, the only Feynman diagrams which contribute to the radiative absorption are the ones containing: the anomalous magnetic moments of the nucleons in the

---

[44] We shall refer to the mesic-hydrogen atom in its ground state (K shell) as the meson-proton system; J is the total angular momentum of the meson-proton system.

$S(S)$ theory, the transitions to the negative energy states in the $PS(PS)$ theory, the "catastrophic" term in the $PS(PV)$ theory, and the intrinsic magnetic moments of the meson in the spin 1 theories. The Feynman diagrams for the mesic absorption reaction are nothing more than the diagrams for charge-exchange scattering in the Thomson limit and will be enumerated in Chap. 7.

TABLE 3. SELECTION RULES FOR π^- ABSORPTION IN HYDROGEN

π^- field	Initial state	Pole of γ ray	Angular momentum of π^0	
			Scalar	Pseudoscalar
Scalar	$J = \frac{1}{2}, +$	m.d.	s	p
Pseudoscalar	$J = \frac{1}{2}, -$	e.d.	p	s
Vector	$J = \frac{1}{2}, -$	e.d.	p	s
	$J = \frac{3}{2}, -$	e.d.	p	d
Pseudovector	$J = \frac{1}{2}, +$	m.d.	s	p
	$J = \frac{3}{2}, +$	m.d.	d	p

Table 4[45] lists the transition probabilities for both radiative and mesic absorption of the π^- meson from the K shell of the mesic-hydrogen atom on the basis of the weak coupling theories considered in Chaps. 1 and 2. The transition probabilities are expressed in units of

$$\left[\alpha^3 \left(\frac{g^2}{\hbar c}\right)\left(\frac{\mu c^2}{\hbar}\right)\right] = 0.9 \times 10^{16} \frac{g^2}{\hbar c} \sec^{-1}$$

where α is the fine-structure constant, μ is the π^- mass, and g is the π^- coupling constant (g is to be replaced by f for the $PS(PV)$ theory). The abbreviations used are $\delta = \mu/M$ (M is the nucleon mass),

$$\bar{g} = g_P + g_N,$$

$\Delta g = g_P - g_N$ (g_P and g_N are the π^0 coupling constants to the proton and neutron, respectively), $\Gamma = 4.71$ = difference between proton and neutron magnetic moments (in units of the nuclear magneton), and $\beta_0 = q_0/\mu_0 c$ (q_0 and μ_0 are the recoil momentum and mass of the π^0 meson, respectively). In the first column of Table 4, $S(S)$ means the absorption of a scalar π^- meson with scalar coupling leading to the emission of a γ ray, etc.; in the remaining columns, the first designation, for example, $PS(PS)$, refers to the absorbed π^- meson and the second, for example $S(S)$, refers to the emitted π^0 meson. For reasons which will become apparent later, we list the values of the π^0 coupling constant, obtained by using the experimental numbers for P_γ/P_{π^0} (the ratio of the transition probabilities for radiative and mesic absorption) and β_0 (deduced from the $\pi^- - \pi^0$ mass difference), namely, 0.94 and 0.23, respectively, even when they belie the basic assumption of weak coupling theory. Moreover, for the $V(V)$-$PS(PS)$, $V(V)$-$PS(PV)$, and $PV(PV)$-$S(S)$ theories, we list only the π^0 coupling constants for the $J = \frac{1}{2}$ substate; the $J = \frac{3}{2}$ substate leads, in each case, to a much smaller transition probability—by at least a factor of 10^3—and to a correspondingly much larger π^0 coupling constant. Of course, comparison with experiment yields only one value of the π^0 coupling constant determined by weighting the two substates according to their statistical weights; the breakdown is emphasized because each substate acts as an independent system and yields π^0 mesons of different angular momenta (cf. Table 3).

---

[45] This table is taken from R. E. Marshak, *loc. cit.*; several entries in Table 1 of Marshak, Tamor, and Wightman [*Phys. Rev.*, **80**: 765 (1950)] have been corrected. Cf. also Aidzu, Fujimoto, Fukuda, Hayakawa, Takayanagi, Takeda, and Yamaguchi, *Prog. Theor. Phys.*, **5**: 931 (1950).

TABLE 4. ABSORPTION PROBABILITIES PER SECOND IN HYDROGEN

Radiative	Mesic		
$S(S)$ $2e^2\Gamma^2\delta^2$	$S(S)$-$S(S)$ $4\beta_0(\Delta g)^2$ $(\Delta g)^2 = 0.008$	$S(S)$-$PS(PS)$ $\beta_0^3\delta^2(\Delta g)^2$ $(\Delta g)^2 = 27$	$S(S)$-$PS(PV)$ $4\beta_0^3(\Delta g)^2$ $(\Delta g)^2 = 0.15$
$PS(PS)$ $2e^2\delta^2$	$PS(PS) - S(S)$ $\frac{\beta_0^3\delta^4}{4}(\Delta g)^2$ $(\Delta g)^2 = 210$	$PS(PS) - PS(PS)$ $\beta_0\delta^2(\bar{g})^2$ $(\bar{g})^2 = 0.06$	$PS(PS)$-$PS(PV)$ $\beta_0\delta^2(\Delta g)^2$ $(\Delta g)^2 = 0.06$
$PS(PV)$ $8e^2$	$PS(PV)$-$S(S)$ $4\beta_0^3\delta^2 g_p^2$ $(2g_p)^2 = 210$	$PS(PV)$-$PS(PS)$ $\beta_0\delta^2(\Delta g)^2$ $(\Delta g)^2 = 11$	$PS(PV) - PS(PV)$ $\beta_0\delta^2(\bar{g})^2$ $(\bar{g})^2 = 11$
$V(V)$ $\frac{2}{3}e^2$	$V(V)$-$S(S)$ $(\frac{4}{3})\beta_0^3\delta^2 g_p^2$ $(2g_p)^2 = 52$	$V(V)$-$PS(PS)$ $\left.\begin{matrix} 3\beta_0\delta^2(\Delta g)^2 \\ (\Delta g)^2 = 0.3 \end{matrix}\right\} J = \frac{1}{2}$	$V(V)$-$PS(PV)$ $\left.\begin{matrix} 3\beta_0\delta^2(\bar{g})^2 \\ (\bar{g})^2 = 0.3 \end{matrix}\right\} J = \frac{1}{2}$
$PV(PV)$ $\frac{2}{3}e^2$	$PV(PV)$-$S(S)$ $\left.\begin{matrix} 12\beta_0(\Delta g)^2 \\ (\Delta g)^2 = 0.002 \end{matrix}\right\} J = \frac{1}{2}$	$PV(PV)$-$PS(PS)$ $\frac{\beta_0^3\delta^2[(\Delta g)^2 + 2(\bar{g})^2]}{3}$ $[(\Delta g)^2 + 2(\bar{g})^2] = 52$	$PV(PV)$-$PS(PV)$ $\frac{4\beta_0^3[(\Delta g)^2 + 2(\bar{g})^2]}{3}$ $[(\Delta g)^2 + 2(\bar{g})^2] = 0.3$

Examination of Table 4 reveals mostly expected but also some strange results. For example, the ratio of the $PS(PS)$ to the $PS(PV)$ radiative probability is $\delta^2/4$, as would be expected from the equivalence theorem.

Similarly, the ratio of the *PS*(*PS*)-*S*(*S*) to the *PS*(*PV*)-*S*(*S*) mesic probability is $\delta^2/4$. The fact that, in these examples, the equivalence theorem holds for both radiative and mesic absorption explains the identical values shown for the scalar π^0 coupling constants. The ridiculously large and meaningless value for the scalar coupling constant which is listed in Table 4 is merely a manifestation of the enormous drop in the probability for mesic absorption when opposite parities are assumed for the π^- and π^0 mesons (cf. Table 3). A similar effect is exhibited for the *S*(*S*)-*PS*(*PS*) and *S*(*S*)-*PS*(*PV*) theories. If both π^- and π^0 mesons possess spin 0, the fact that the same parity leads to reasonable values of the π^0 coupling constant whereas opposite parities lead to completely unreasonable ones is to be taken as support for the former alternative. If spin 1 is assumed for the π^- meson, the two widely disparate values for the π^0 coupling constant required for the *V*(*V*)-*PS*(*PS*), *V*(*V*)-*PS*(*PV*), and *PV*(*PV*)-*S*(*S*) theories must be regarded as evidence against the same parity for the π^0 and π^- mesons since the experimental ratio of 0.94 for P_γ/P_{π^0} can be matched only by choosing, in each case, the large and unreasonable value for the π^0 coupling constant.

Surprisingly enough, opposite parities cannot be excluded for spin 1 π^- and spin 0 π^0 mesons because both substates ($J = \frac{1}{2}$ and $J = \frac{3}{2}$) of the π^- meson-proton system lead to p states for the π^0 meson, and while the π^0 emission is depressed, the π^0 coupling constants turn out to be not too unreasonable. Some unexpected results are also to be found in the fact that the ratios of the *PS*(*PS*)-*PS*(*PS*) to the *PS*(*PS*)-*PS*(*PV*) and of the *PS*(*PV*)-*PS*(*PS*) to the *PS*(*PV*)-*PS*(*PV*) mesic probabilities are unity except for the changes in the relative signs of g_P and g_N. This strange result is due to a breakdown of the equivalence theorem when the pseudoscalar field is assumed for both π^- and π^0 mesons and yields a much larger relative mesic probability for *PS* coupling as compared with *PV* coupling. When this effect is combined with the operation of the equivalence theorem for the radiative probability, we obtain the surprising inversion of the magnitudes of the *PS*(*PS*) and *PS*(*PV*) coupling constants shown in Table 4 when the same coupling is assumed for both π^- and π^0; for different couplings (and the same pseudoscalar field), the values of the coupling constants are inverted back and so are the relative signs of g_P and g_N. It should also be noted that in the *PS*(*PS*)-*PS*(*PS*) case, equal magnitudes and opposite signs for g_P and g_N would require much larger values for the π^0 coupling constants. The pseudoscalar numbers have no particular quantitative significance; however, if the pseudoscalar field governs both the π^- and π^0 mesons, then the striking diagreement of the pure coupling [that is, *PS*(*PS*)-*PS*(*PS*) and *PS*(*PV*)-*PS*(*PV*)] numbers with those obtained from other processes may be indicative of opposite neutral mesic charges for the proton and neutron, of the need for a linear combination of *PS* and *PV* coupling, or of some peculiar breakdown of the theory when negative energy states for the nucleons play an important role.[46]

To sum up, the essential conclusion to which we have been led is that the approximate equality between the mesic and radiative absorption probabilities in hydrogen argues for the same parity for π^- and π^0 mesons if both charged and neutral π mesons possess spin zero and for opposite parities if the charged meson possesses spin 1 and the neutral meson possesses spin 0.

B. Slow π^- Reactions in Deuterium. While the slow π^- absorption experiments in hydrogen provide evidence against certain combinations of spins and parities of the π mesons, the corresponding experiments in deuterium are even more clear-cut in their implications. In deuterium, energy and momentum conservation do not require the absorption of π^- mesons in deuterium to be accompanied by the emission of γ rays or π^0 mesons. It is now possible for the rest energy of the π^- meson to be completely converted into the kinetic energies ($\approx$ 70 Mev apiece) of the two final neutrons in accordance with the reaction scheme $\pi^- + D \rightarrow N + N$ (we shall term this process neutron absorption). Since the electromagnetic reaction is inherently weak and the 5-Mev mass difference between the π^- and π^0 mesons barely allows the mesic absorption to take place in deuterium (the $\pi^- - \pi^0$ mass difference must be larger than the sum of the deuteron binding energy and the neutron-proton mass difference, namely, 3.5 Mev), neutron absorption would be expected to be the dominant reaction. However, when the Pauli principle for the two final neutrons is combined with parity and angular momentum considerations, this conclusion is strongly modified for some of the possible π^- meson fields. For some fields, the reaction $\pi^- + D \rightarrow N + N + \gamma$ (radiative absorption—involving the emission of two slow neutrons and a high-energy γ ray) acquires a transition probability comparable with or even greater than that of neutron absorption, and there is even the possibility of competition from the reaction $\pi^- + D \rightarrow N + N + \pi^0$

---

[46] In the *PS*(*PV*) theory, the ($\boldsymbol{\sigma}\cdot\nabla$) part of the meson-nucleon interaction operator does not contribute to the transition probability because the π^- meson practically possesses zero momentum in the *K* shell of the mesic-hydrogen atom. The finite probability for mesic absorption comes from the $\gamma_5\, \partial/\partial t$ part of the operator, whereas for radiative absorption, the triple term ($\boldsymbol{\sigma}\cdot\mathbf{A}\phi$) gives the chief contribution; the former operator involves the negative energy states of the nucleons in an essential way, whereas the latter operator does not. It is this asymmetry in the two processes which may be responsible for the anomalously large *PS*(*PV*) value of the π^0 coupling constant which is derived by matching the weak coupling prediction for (P_γ/P_{π^c}) to experiment.

(mesic absorption—involving the emission of two slow neutrons and a π^0 meson).

Just as in hydrogen, slow π^- mesons moving through deuterium are quickly slowed down and captured into K shells of zero orbital angular momentum before they have the opportunity to decay. Once the π^- meson is in the K shell of the mesic-deuterium atom, the total angular momentum and parity of the meson-deuteron system (as of the meson-proton system—cf. footnote 4) depends on the intrinsic spin and parity of the π^- meson. Thus, suppose the π^- meson possesses spin 0 and even parity (scalar); then, since the deuteron has total angular momentum 1 and even parity, the meson-deuteron system would also possess $J = 1$ and even parity. Similarly, a π^- meson with spin 0 and odd parity (pseudoscalar) would lead to $J = 1$ and odd parity for the meson-deuteron system. On the other hand, if the π^- meson were to possess spin 1, there would be three possible values for the total angular momentum of the meson-deuteron system, namely, $J = 0, 1, 2$. The parity of the meson-deuteron system would be odd or even depending on whether the π^- meson were vector or pseudovector. We have already stated that spins greater than 1 are not considered for reasons of simplicity, although this point can be settled by an experiment on the absorption of fast π^+ mesons in deuterium (cf. below). Now, if neutron absorption is to take place, the two final neutrons, by the Pauli principle, must be in a $^1S_0, {}^3P_{0,1,2}, {}^1D_2, \ldots$ state. Consequently, a scalar π^- meson in the K shell of the mesic-deuterium atom cannot undergo neutron absorption at all. Also, neutron absorption cannot take place for pseudovector π^- mesons from the $J = 1$ substate of the meson-deuteron system. No such selection rules operate for pseudoscalar and vector mesons. There are also selection rules for radiative and mesic absorption but not absolute ones as in the case of neutron absorption. Table 5[47] lists the total angular momenta and parities of the meson-deuteron system for the four fields, the states of the two-neutron system to which neutron absorption transitions are possible, the lowest two-neutron states to which radiative absorption can take place, and finally the lowest two-neutron states to which mesic absorption is allowed (assuming that the outgoing π^0 meson is first a scalar and then a pseudoscalar particle). In the radiative column of Table 5, we have indicated the character of the outgoing electromagnetic radiation (e.d., m.d. as before—cf. Table 3—e.q. = electric quadripole, m.q. = magnetic quadripole) and in the mesic columns the angular momentum state of the outgoing π^0 meson.

---

[47] Five entries in Table 5—the $^1S_0$(c.d.), $^1S_0$(m.q.), $^1S_0(p)$, and $^3P_{1,2}(p)$ entries for the vector field and the $^3P_{1,2}(p)$ entry for the pseudovector field—differ from the corresponding entries in Table III of footnote 38 because the latter table implicitly took account of the restrictions imposed by the interaction operators which enter into the weak coupling formulation of the vector and pseudovector theories [*e.g.*, the $^3P_{1,2}(p)$ mesic absorption transitions allowed by angular momentum conservation are forbidden when the actual operators are inserted into the matrix elements].

We see from Table 5 that the absorption of a π^- meson from the *K* shell of a mesic-deuterium atom is strongly affected by the requirements of the exclusion principle applied to the final two neutrons. These effects of the exclusion principle derive from simple properties of the angular momentum and parity, and thus the chief qualitative conclusions can be drawn from a comparison of Tables 3 and 5 without having recourse to the questionable weak coupling meson theory. By the same token, the use of weak coupling theory should, as in the case of hydrogen, confirm the correctness of the selection rules and provide quantitative estimates of some interest. Tamor[48] has performed the weak coupling calculations and has computed the transition probabilities for the three competing reactions assuming, in turn, the four simplest fields for the π^- meson. Tamor's treatment of the three processes is phenomenological in character so that the relative probabilities of neutron and radiative absorption are independent of any detailed theory of nuclear forces and of the strength of the π^- meson-nucleon coupling. Tamor's mesic absorption predictions appear to require knowledge of the strength of the π^0-nucleon coupling, but actually even this arbitrariness is removed by making use of the hydrogen absorption experiment; that

TABLE 5. SELECTION RULES FOR SLOW π^- ABSORPTION IN DEUTERIUM

π meson theory	Initial state	Neutron absorption	Final states, radiative absorption	Mesic absorption	
				π^0 scalar	π^0 pseudoscalar
Scalar............	$J = 1(+)$	Forbidden	${}^1S_0$ (m.d.)	${}^3P_{0,1,2}$ (p)	${}^1S_0$ (p)
Pseudoscalar......	$J = 1(-)$	${}^3P_1$	${}^1S_0$ (e.d.)	${}^1S_0$ (p)	${}^3P_{0,1,2}$ (p)
Vector	$J = 0(-)$	${}^3P_0$	${}^3P_1$ (m.d.)	${}^3P_0$ (s)	${}^1S_0$ (s)
	$= 1(-)$	${}^3P_1$	${}^1S_0$ (e.d.)	${}^1S_0$ (p)	${}^3P_{0,1,2}$ (p)
	$= 2(-)$	${}^3P_2$, ${}^3F_2$	${}^1S_0$ (m.q.)	${}^3P_2$ (s)	${}^3P_{1,2}$ (p)
Pseudovector......	$J = 0(+)$	${}^1S_0$	${}^3P_1$ (e.d.)	${}^1S_0$ (s)	${}^3P_0$ (s)
	$= 1(+)$	Forbidden	${}^1S_0$ (m.d.)	${}^3P_{0,1,2}$ (p)	${}^1S_0$ (p)
	$= 2(+)$	${}^1D_2$	${}^1S_0$ (e.q.)	${}^3P_{1,2}$ (p)	${}^3P_2$ (s)

---

[48] S. Tamor, *loc. cit.*; cf. also S. Tamor and R. Marshak, *Phys. Rev.*, **80**: 766 (1951); and Ogawa, Yamada, and Nagahara, *Prog. Theor. Phys.*, **6**: 227 (1951); with erratum, *Prog. Theor. Phys.*, **6**: 444 (1951).

is to say, the observed ratio of radiative to mesic absorption in hydrogen can, because of the weak binding of the deuteron, be employed in a semiempirical fashion (using the π^0 coupling constants in Table 4 as numbers in a "ledger," so to speak) to predict the relative intensities of these two modes of absorption in deuterium. Thus, as an example, consider the absorption of a pseudoscalar π^- meson and the emission of a pseudoscalar π^0: in hydrogen, the radiative absorption process is electric dipole whereas the mesic absorption yields a π^0 meson in an s state (cf. Table 3). In deuterium, the radiative absorption is again electric dipole; however, the mesic absorption involves a transition to a ${}^3P_0$ state for the two neutrons and a p state for the π^0 meson. It is clear that the ratio

$$\frac{(P_{\pi^0}/P_\gamma)_D}{(P_{\pi^0}/P_\gamma)_H} \ll 1 \tag{20}$$

and inserting numbers leads to an estimated $\pi^0{:}\gamma$ ratio in deuterium in agreement with the weak coupling prediction (cf. Table 6 below).

Table 6[49] lists the theoretical probabilities for neutron and radiative absorption in deuterium for the weak coupling theories considered for hydrogen. The numbers are listed in units of $0.9 \times 10^{16} g^2/\hbar c$ sec^{-1} where $g^2/\hbar c$ is the dimensionless π^- meson-nucleon coupling constant [$f^2/\hbar c$ for the $PS(PV)$ theory]. The ratios of neutron to radiative absorption predicted by the various theories are also listed. It is interesting to note that the ratios for the $PS(PS)$ and $PS(PV)$ theories are different, owing to the breakdown of the equivalence theorem for neutron absorption. Dyson[50] has shown that the equivalence theorem breaks down when the interaction between two nucleons contains a

TABLE 6. WEAK COUPLING NEUTRON AND RADIATIVE ABSORPTION PROBABILITIES IN DEUTERIUM

π^- meson theory	$S(S)$	$PS(PS)$	$PS(PV)$	$V(V)$	$PV(PV)$
Neutron.....	0	2.7×10^{-3}	0.25	0.12 $(J = 0, 1, 2)$	2.5 $(J = 0)$ 0 $(J = 1)$ 0.05 $(J = 2)$
Radiative....	0.012	6.6×10^{-4}	0.12	2.2×10^{-3} $(J = 0, 1, 2)$	1.4×10^{-2} $(J = 0)$ 2.0×10^{-2} $(J = 1)$ 1.3×10^{-2} $(J = 2)$
Ratio........	0	4.1	2.1	55	2

---

[49] Some of Tamor's numbers have been corrected in Tables 6 and 7.

[50] F. J. Dyson, *Phys. Rev.*, **73**: 929 (1948).

charge-exchange part; as a consequence, the *PS*(*PS*) ratio actually depends upon the assumed neutron-neutron interaction potential (which is taken as a Yukawa potential) in contrast to the *PS*(*PV*) theory. Table 7[49] lists the theoretical predictions for the ratio of the probabilities of mesic absorption to radiative absorption for the various possible combinations of fields for the π^- and π^0 mesons. The mesic absorption probabilities are based on a $\pi^- - \pi^0$ mass difference of 4.75 Mev,[51] and the π^0 coupling constants, to which they are proportional, are taken from Table 4. Tables 6 and 7 show quite clearly that the relative probabilities for the three competing slow π^- meson reactions in deuterium depend strongly upon the assumed spins and parities of the π^- and π^0 mesons, in agreement with the selection rules indicated by Tables 3 and 5.

TABLE 7. RATIOS OF MESIC TO RADIATIVE ABSORPTION IN DEUTERIUM

S(*S*)-*S*(*S*)	5.5×10^{-7}	*S*(*S*)-*PS*(*PS*) or *PS*(*PV*)	1×10^{-8}
PS(*PS*)-*S*(*S*)	4.5×10^{-5}	*PS*(*PS*)-*PS*(*PS*) or *PS*(*PV*)	2.5×10^{-8}
PS(*PV*)-*S*(*S*)	8×10^{-3}	*PS*(*PV*)-*PS*(*PS*) or *PS*(*PV*)	4×10^{-6}
V(*V*)-*S*(*S*)	3×10^{-3} ($J = 0,1,2$)	*V*(*V*)-*PS*(*PS*) or *PS*(*PV*)	> 30($J = 0$)
PV(*PV*)-*S*(*S*)	> 30 ($J = 0$)	*PV*(*PV*)-*PS*(*PS*) or *PS*(*PV*)	2×10^{-3} ($J = 1$)

The theoretical predictions for slow π^- absorption in deuterium can therefore be summed up as follows: if the π^- meson possesses spin 0 and even parity (scalar), no neutron absorption should take place and most π^- mesons should undergo radiative absorption. If the π^- meson possesses spin 0 and odd parity (pseudoscalar), neutron and radiative absorption should compete on roughly comparable terms. If the π^- and π^0 mesons are both scalar or both pseudoscalar, mesic absorption should be negligible, whereas if one is scalar and the other is pseudoscalar, about 10 per cent of the π^- mesons should give rise to π^0 mesons. For a spin 1 π^- meson, the relative probabilities for the three modes of absorption depend on the particular substate ($J = 0$, 1, or 2) of the meson-deuteron system from which the transition takes place. Since each substate behaves, as far as the processes in question are concerned, as an independent system, the predicted ratios of neutron to radiative and radiative to mesic absorption must be weighted according to the statistical weight $(2J + 1)$ of each substate. Carrying out this weighting procedure, it can be shown, using Tables 6 and 7, that for a vector π^- meson (spin 1 and odd parity), neutron absorption should be much more probable (by a factor of 100) than radiative[52] absorption. On the other hand, if the π^- meson possesses spin 1 and even parity (pseudovector), the ratio of neutron to radiative absorption should be 2 (determined by the statistical weights of the $J = 0, 1, 2$ substates of the meson-deuteron system). Some competition from π^0 emission should result (of the order 10 per cent) regardless of the parity of the π^0 meson.

---

[51] The more recent value (footnote 6) is closer to 5.4 Mev, which increases the probabilities for mesic absorption by about a factor 1.5.

In view of the strikingly different theoretical predictions, the experimental results on the π^- absorption in deuterium become of great interest.

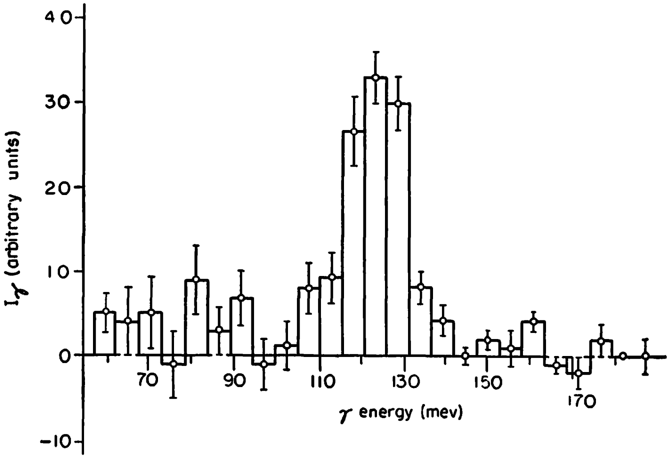

FIG. 4. Measured γ ray spectrum from the absorption of slow π^- mesons in deuterium.

Panofsky *et al.*,[6] using the same apparatus as for the hydrogen absorption experiment, have observed the γ ray spectrum given in Fig. 4. The conspicuous features of this spectrum are the peak in the neighborhood of 130 Mev (corresponding to radiative absorption) and the absence of γ rays in the middle energy region (corresponding to mesic absorption). No direct measurement of the neutron absorption probability has been made, but instead it is inferred from a comparison of the intensity of the high-energy γ ray peak with the similar peak in the hydrogen absorption experiment. In addition, a direct comparison of the middle-energy γ rays has been made by sending the slow π^- mesons first into the high-pressure hydrogen gas and then into the high-pressure deuterium gas.

---

[52] At first sight, it appears that radiative absorption should compete favorably with neutron absorption from the $J = 1$ substate since the same initial and final neutron states are involved as in the pseudoscalar theory (cf. Table 5). However, while the V and PS neutron absorption probabilities are indeed comparable, the radiative absorption probability turns out to be much lower for a vector π^- meson (compared with a pseudoscalar π^-) because of the character of its coupling to the electromagnetic field.

The respective numbers of counts are listed in Table 8. Table 8 shows that neutron absorption is about twice as probable as radiative absorption and that mesic absorption is negligible compared with both radiative and neutron absorption. These observations enable us to conclude immediately that the scalar and vector fields are excluded for the charged π meson. Both the pseudoscalar and pseudovector fields for the charged π meson are, in view of the theoretical and experimental uncertainties, consistent with the data. If the π^- meson is pseudoscalar, the absence of γ rays in the middle-energy region is some evidence against mesic absorption and for a pseudoscalar π^0 meson, although this evidence is not conclusive because of the experimental error. If the π^- meson is pseudovector, nothing can be said about the π^0 field on the basis of the deuterium absorption experiment.

TABLE 8. EXPERIMENTAL DATA ON π^- ABSORPTION IN HYDROGEN AND DEUTERIUM

Type of absorption	Hydrogen	Deuterium
Mesic	0.45 ± 0.09 c/m	-0.007 ± 0.020 c/m
Radiative	0.470 ± 0.046 c/m	0.275 ± 0.034 c/m
Neutron	....	0.65 ± 0.11 c/m

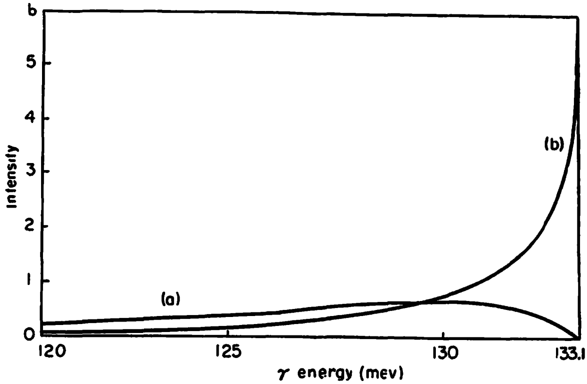

FIG. 5. Theoretical γ ray spectrum from the reaction $\pi^- + D \rightarrow N + N + \gamma$. Curve (*a*) neglects the *N*-*N* interaction; (*b*) includes the *N*-*N* interaction.

It should be mentioned that the interaction between the two final neutrons (which are chiefly in the $^1S_0$ state) affects the spectral distribution of the γ rays resulting from the radiative absorption reaction in deuterium (although not the total transition probability to any appreciable extent). If one ignores the neutron-neutron interaction, the γ ray spectrum has a peak near 130 Mev and a width of about 12 Mev.

If it is assumed that the neutron-neutron force is identical with the proton-proton force, the γ ray peak is sharpened to 2 Mev and shifted to the maximum possible energy, namely, 133.1 Mev (assuming 140 Mev for the π^- mass). The theoretical γ ray curves corresponding to the two assumptions are given in Fig. 5 assuming that the π^- meson is a pseudoscalar particle. The shapes of the γ ray spectra for scalar or pseudovector π^- mesons would be almost indistinguishable from the pseudoscalar shapes. Watson and Stuart[52a] have studied the shape of the γ ray spectrum as a function of the assumed neutron-neutron interaction. They have shown that the shape of the spectrum in the neighborhood of the peak is given, to a good approximation, by the expression $(c \sin^2 \delta)/p$ where c is a constant, p is the relative momentum of the two outgoing neutrons, and δ is the ${}^1S_0$ phase shift determined by the assumed neutron-neutron potential. The phase shift δ is related to the low-energy scattering parameters in the usual way:[53]

$$p \cot \delta = -a^{-1} + \frac{r_0}{2} p^2 \tag{21}$$

where a is the "scattering length" and r_0 the "effective range." Using Eq. (21) and comparing the theoretical predictions with the preliminary experimental curve,[54] Watson and Stuart have been led to the conclusion that the di-neutron cannot be bound, if at all, by more than 200 kev.

C. Slow π^- Reactions in Tritium. It has been shown that the relative yields of the three possible slow π^- reactions in deuterium are very sensitive to the spin and parity of the π^- meson. In fact, the order of magnitude of the branching ratios can be predicted on the basis of general angular momentum and parity selection rules (if cognizance is taken of the Pauli principle for the two final neutrons) which are independent of the weak coupling approximation. The question naturally arises whether similar selection rules hold for the relative yields of the two slow π^- reactions in tritium, namely, (*a*) $\pi^- + H^3 \rightarrow 3N$ and (*b*) $\pi^- + H^3 \rightarrow 3N + \gamma$ (the reaction $\pi^- + \mathrm{H}^3 \rightarrow 3N + \pi^0$ is excluded on energetic grounds). This question was investigated by Messiah *et al.*,[55] who arrived at the conclusion that selection rules forbidding reaction (*a*) will exist for a scalar or pseudovector π^- field provided that the ground-state wave function of H^3 is space-symmetric (since the final three-neutron system cannot be space-symmetric), no such selection rule exists for a pseudoscalar or vector field for reaction (*a*). For reaction (*b*), there appears to be no selection rule, whatever be the spin and parity of the π^- meson. Since the low-energy data (absorption of slow neutrons by deuterons,[56] etc.) favor an H^3 wave function which is predominantly space-symmetric, a measurement of the relative yields of reactions (*a*) and (*b*) should permit a distinction between the *PS* and *PV* fields, a distinction which cannot be made on the basis of the hydrogen and deuterium experiments.

[52a] K. Watson and R. Stuart, *Phys. Rev.*, **82**: 738 (1951).

[53] Cf. J. Blatt and J. Jackson, *Phys. Rev.*, **76**: 18 (1949); H. A. Bethe, *Phys. Rev.*, **76**: 38 (1949).

[54] Aamodt, Panofsky, and Phillips, *Phys. Rev.*, **83**: 1057 (1951).

[55] Messiah, Caianiello, and Basri, *Phys. Rev.*, **83**: 652 (1951).

D. Other Experiments. The slow π^- reactions in hydrogen and deuterium have taught us a great deal about the spins and parities of the π meson, but they have not fixed completely the spin of the charged π meson or the parity of the neutral π meson. One could, of course, invoke the principle of simplicity and argue that the charged and neutral π mesons should possess the same spin and parity. This would fix the fields of both charged and neutral π mesons as pseudoscalar. However, it is essential that such a conclusion be drawn on direct experimental grounds. One method[57] for measuring the spin of the charged π meson would be to attempt to produce polarized beams of π mesons in nucleon-nucleon or photon-nucleon collisions. Provided the spin of the charged π meson is greater than 0, for example, 1, the polarization effects will be maximized by producing the π mesons as close to threshold as possible.[57] Thus, if the charged π meson were vector with vector coupling to the nucleon, that is, $V(V)$, the polarization would be predominantly longitudinal [cf. Eq. (11) in Chap. 2]; if it were vector with tensor coupling to nucleon, that is, $V(T)$, the polarization would be predominantly transverse. On the other hand, Kaplon[58] has pointed out that, if the charged π meson were $PV(PV)$ or $PV(DT)$ (DT stands for dual tensor), the polarization effects would be quite unimportant in nucleon-nucleon collisions even in the neighborhood of threshold. In the case of photonic production of π mesons, Feer[59] has shown that, in the vicinity of threshold, a $V(V)$ charged π meson would be produced with transverse polarization, a $V(T)$ with a ratio of longitudinal to transverse polarization of 0.4, a $PV(PV)$ with longitudinal polarization, and a $PV(DT)$ with transverse polarization. For both photonically and nucleonically produced charged π mesons, the hypothesized polarization is measured with respect to the direction of the initial photon or nucleon beam. The argument now is that, were polarized charged π mesons, no matter how produced, to decay into μ mesons, an anisotropy in the angular distribution of the $\pi \rightarrow \mu$

---

[56] Cf. N. Austern, *Phys. Rev.*, **83**: 672 (1951).

[57] Cf. G. Wentzel, *Phys. Rev.*, **75**: 1810 (1949); cf. also *Helv. Phys. Acta*, **22**: 101 (1949).

[58] M. F. Kaplon, private communication; cf. Chap. 2.

[59] D. Feer, *Phys. Rev.*, **76**: 306 (1949).

decays would result. The anisotropy would have the form

$$N(\theta) = 1 + Av_\mu \cos 2\theta \tag{22}$$

where θ is the angle between the direction of emission of the μ meson and the polarization vector, v_μ is the velocity of the μ meson, and A lies between -1 and $+1$, depending on the degree of polarization. For a π/μ mass ratio of 1.3, v_μ is equal to 0.27 and the maximum possible anisotropy which can occur is 1.74. This value of the anisotropy would result if the charged π mesons possessed spin 1, were produced close to threshold, and enjoyed pure couplings to both the nucleon and the μ meson (plus neutrino) fields.

Several experimenters have looked for a possible anisotropy in the angular distribution of $\pi^+ \rightarrow \mu^+$ decays. In the first photonic production experiment, McMillan *et al.*[60] examined the angular distribution of $\pi^+ \rightarrow \mu^+$ decays and, within statistical error, found an isotropic distribution with respect to the incident photon direction. Powell[2] has examined the angular distribution of $\pi^+ \rightarrow \mu^+$ decays with respect to the downward flux of cosmic-ray nucleons and has also found a negative result. These results are not conclusive evidence against a spin 1 charged π meson—apart from their poor statistical accuracy—because of the possibility that large depolarization effects are at work. Peterson[61] has found a small positive effect, but the anisotropy in the angular distribution of $\pi^+ \rightarrow \mu^+$ decays which he observes is very peculiar and contrary to all theoretical expectations. One may summarize the present status of the polarization experiment by saying that the evidence is inconclusive either way.

A more promising direct method for determining the spin of the charged meson, suggested by the author[62] and Cheston[63] and independently by Johnson,[64] is to measure the cross section for the process $\pi^+ + D \rightarrow P + P$ which is the inverse of the reaction $P + P \rightarrow \pi^+ + D$ discussed in Chap. 2. If we denote the cross section for the first process by $\sigma_{1\rightarrow 2}$ and for the inverse $\sigma_{2\rightarrow 1}$, the two differential cross sections are related by the principle of detailed balancing (in the center-of-mass system) as follows:

$$\frac{d\bar{\sigma}_{2\rightarrow 1}}{d\bar{\Omega}} = \frac{3(2S+1)q^2}{2p^2}\,\frac{d\bar{\sigma}_{1\rightarrow 2}}{d\bar{\Omega}} \tag{23}$$

where S is the spin of the π^+ meson, p is the momentum of either proton, and q is the momentum of the π^+ meson or the deuteron. Thus, if both

---

[60] McMillan, Peterson, and White, *Science*, **110**, 579 (1949).

[61] V. Z. Peterson, Ph. D. Thesis, University of California, 1950.

[62] R. E. Marshak, *Phys. Rev.*, **82**: 313 (1951).

[63] W. B. Cheston, *Phys. Rev.*, **83**: 1118 (1951).

[64] M. H. Johnson, private communication.

$d\bar{\sigma}_{1\to2}/d\bar{\Omega}$ and $d\bar{\sigma}_{2\to1}/d\bar{\Omega}$ are measured for the same $\bar{\theta}$ (the angle between the meson and one proton) and the same energy in the center-of-mass system or if the total cross sections $\sigma_{1\to2}$ and $\sigma_{2\to1}$ are measured at the same center-of-mass energy, S will be determined. A π^+ meson energy of 22.7 Mev in the laboratory system corresponds to the incident proton energy of 340 Mev in the laboratory system at which the Berkeley measurements (cf. Chap. 2) of the cross section for the reaction $P + P \to \pi^+ + D$ were carried out. It will be recalled that the differential cross sections for the reaction $P + P \to \pi^+ + D$ were measured at four angles—0, 18, 30, and 60°—in the laboratory system and that these data yield a differential cross section in the center-of-mass system:[65] $d\bar{\sigma}_{2\to1}/d\bar{\Omega} = (3.2 \pm 0.8)(0.08 \pm 0.08 + \cos^2 \bar{\theta}) \times 10^{-29}$ cm²/ster. The total production cross section is $1.3_5 \pm 0.3_5 \times 10^{-28}$ cm² or $2.0 \pm 0.5 \times 10^{-28}$ cm², depending on whether the angular distribution is chosen as $\cos^2 \bar{\theta}$ or $(0.16 + \cos^2 \bar{\theta})$ (using the limits of statistical error). Since the factor $2p^2/3q^2$ in Eq. (23) is equal to 18 at a proton energy of 340 Mev, the differential cross section in the center-of-mass system for the reaction $\pi^+ + D \to P + P$ at 22.7-Mev laboratory energy for the π^+ mesons should be $(5.8 \pm 1.4)(0.08 \pm 0.08 + \cos^2 \bar{\theta}) \times 10^{-28}$ cm²/ster for $S = 0$, $(1.9 \pm 0.5)(0.08 \pm 0.08 + \cos^2 \bar{\theta}) \times 10^{-28}$ cm²/ster for $S = 1$, etc. The total cross sections, corresponding to the limits of error in the angular distribution, should be $2.4 \pm 0.6 \times 10^{-27}$ cm² or $3.6 \pm 0.9 \times 10^{-27}$ cm² for $S = 0$, $0.8 \pm 0.2 \times 10^{-27}$ cm² or $1.2 \pm 0.3 \times 10^{-27}$ cm² for $S = 1$, etc.

Clark *et al.*[66] have carried out a measurement of the total cross section for the reaction $\pi^+ + D \to P + P$, using the externally focused π^+ beam from the Rochester cyclotron. These workers measured the total cross section in question by sending a beam of 40-Mev π^+ mesons through a threefold scintillation counter telescope into a heavy-water target sufficiently thick to stop the mesons. The high-energy protons produced in the D_2O were detected in coincidence by two large NaI scintillation counters operating in coincidence with the threefold scintillation meson counter telescope. To find the cross section at 22.7 Mev, which corresponds to 340 Mev in the production experiment, the Rochester group measured the average absorption cross section from 23 to 33 Mev and from 0 to 23 Mev. Fortunately, these two average cross sections were equal within the statistical error of 10 per cent, and so it was possible to evaluate a total cross section for an energy of 23 Mev. Since the detectors, although large, did not subtend a complete solid angle, it was necessary to make a solid-angle correction, and the final result turned out to be 5 or 4.4 millibarns (with an experimental error of 20 per cent) depending on whether it was assumed that the angular dependence in the center-of-mass system for the production data was $\cos^2 \bar{\theta}$ or $(0.16 + \cos^2 \bar{\theta})$. Within experimental error, the measured absorption cross section is in much better agreement with the predicted cross section from the production experiment for $S = 0$ than for $S = 1$ or higher.

---

[65] Cf. Eq. (18) of Chap. 2.

[66] Clark, Roberts, and Wilson, *Phys. Rev.*, 83: 649 (1951).

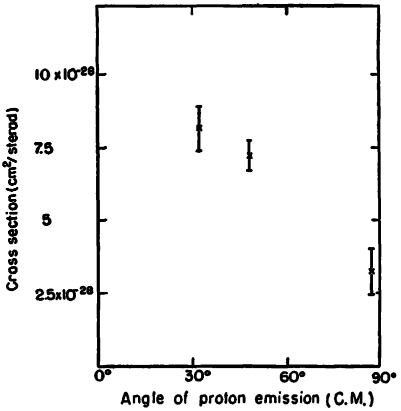

Fig. 6. Measured angular distribution of the protons from the reaction $\pi^+ + D \rightarrow P + P$ at an incident meson energy of 28 Mev in the center-of-mass system.

A similar experiment was carried out by Durbin *et al.*,[67] using the π^+ meson beam from the Columbia cyclotron which is of somewhat greater intensity and higher energy. Both these advantages made it possible for the Columbia group to measure the proton angular distribution at each energy and the absorption cross section as a function of energy at a given angle. Figure 6 shows the measured angular distribution of the protons produced in the reaction $\pi^+ + D \rightarrow P + P$ by π^+ mesons with an average energy of 28 Mev in the center-of-mass system. Figure 7 contains a plot of the measured differential cross section as a func-

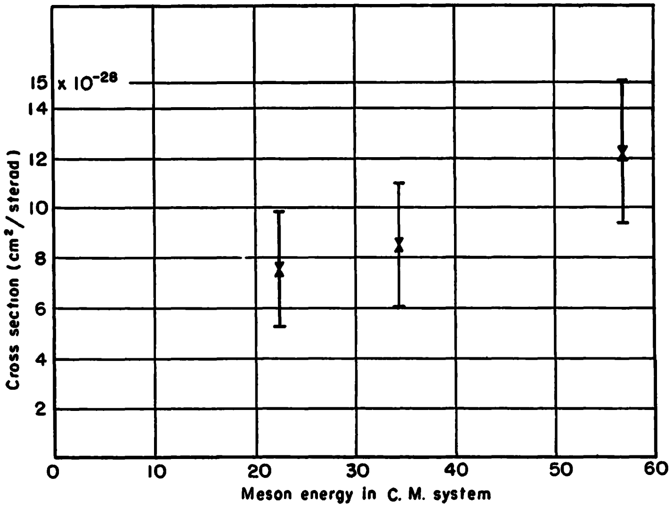

Fig. 7. Measured differential cross section at 45° in the center-of-mass system for the reaction $\pi^+ + D \rightarrow P + P$ as a function of the center-of-mass meson energy.

---

[67] Durbin, Loar, and Steinberger, *Phys. Rev.*, **83**: 646 (1951).

tion of meson energy for protons emitted at 45° in the center-of-mass system with respect to the incident π meson direction. The differential absorption cross section in Fig. 6 is in reasonably good accord with the differential production cross section corresponding to 340-Mev protons[67a] and the absolute value of the cross section is, within statistical error, in agreement with the Rochester experiment. Figure 7 seems to indicate that the absorption cross section increases with meson energy, although the precise variation is not established in view of the large statistical errors.

Both the Rochester and Columbia experiments definitely prove that the spin of the π^+ meson is 0. If we assume that the π^+ and π^- mesons possess the same spin and parity, we must conclude from the combination of the slow π^- reactions in deuterium and the fast π^+ absorption reaction in deuterium that the charged π meson is pseudoscalar. Once it is settled that the charged π meson is pseudoscalar, the evidence is then very strong from the slow π^- absorption experiment in hydrogen[67b] that the π^0 meson is also pseudoscalar. However, although the parity of the π^0 meson is fairly well established in this indirect manner, a direct method for deciding the parity of the π^0 meson would be very welcome. Yang[68] has pointed out that the relative polarization of the two decay γ rays from the π^0 meson will depend on the parity of the π^0 meson. If the π^0 meson is a scalar particle, the two γ rays resulting from its decay will have parallel polarizations while the γ rays resulting from the decay of a pseudoscalar π^0 meson will have perpendicular polarizations. In actual fact, Yang has investigated the general problem of the polarization relations which obtain for the two-photon decay of a neutral particle having a definite parity and angular momentum, and his results are given in Table 9 (the symbol $\parallel$ indicates parallel polarization and $\perp$ perpendicular polarization—J is the angular momentum). With these results in mind,

TABLE 9. POLARIZATION RELATIONS FOR TWO-PHOTON DECAY OF A NEUTRAL PARTICLE

Parity \ J	0	1	2, 4, 6, . . .	3, 5, 7, . . .
Even......	$\parallel$	Forbidden	$\parallel \geq 50\%$, $\perp \leq 50\%$	$\parallel$ 50%, $\perp$ 50%
Odd.......	$\perp$	Forbidden	$\perp$	Forbidden

[67a] Namely, essentially a $\cos^2 \bar{\theta}$ distribution; more recently, Durbin *et al.* [*Phys. Rev.*, **84**: 581 (1951)] have measured the angular distributions of the protons using π^+ mesons of 25, 40, and 53 Mev energy (in the laboratory) and have again found very closely $\cos^2 \bar{\theta}$ distributions. The total cross sections turn out to be 3.1 ± 0.3, 6.1 ± 0.6 and 7.0 ± 0.7 × 10^{-27} cm² respectively.

[67b] And from the small cross section for π^0 production in *P-P* collisions near threshold (cf. footnote 29*a* of Chap. 2).

[68] C. N. Yang, *Phys. Rev.*, **77**: 242 (1950).

Yang[69] has suggested an experiment to distinguish between the scalar and pseudoscalar fields for the π^0 meson. The apparatus is shown in Fig. 8, where M is the point at which the neutral meson decays and the two photons produce electron pairs at L and L'. Fourfold coincidence counts in symmetrically placed counters A, A', B, and B' are to be recorded, and the entire apparatus to the left of M is to be rotated through an angle ϕ. The predicted variation of counting rate with ϕ turns out to be

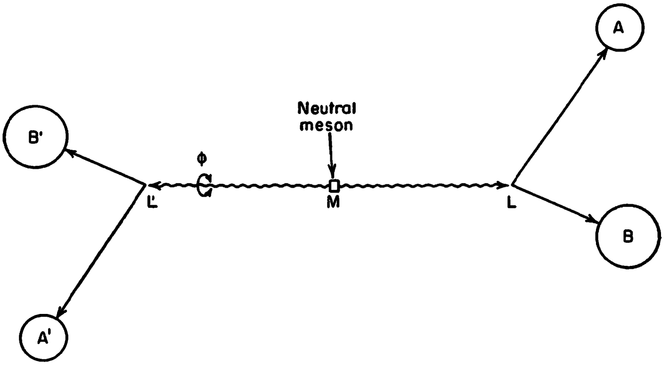

FIG. 8. Possible experimental arrangement for measuring the relative polarization of the decay γ rays from the π^0 meson (see text).

$$N = a(1 \pm b \cos 2\phi) \qquad \begin{array}{l}(+\text{ scalar } \pi^0)\\ (-\text{ pseudoscalar } \pi^0)\end{array} \tag{24}$$

where a and b are constants depending on the particular counter setup. If one assumes counters infinitesimal in size and $\sphericalangle MLA = \sphericalangle MLB$, one finds that $b = \frac{1}{18}$ and

$$\frac{N(\phi = 0°)}{N(\phi = 90°)} = \begin{array}{ll} 1.13 & (\text{scalar } \pi^0) \\ 0.88 & (\text{pseudoscalar } \pi^0) \end{array}$$

Unfortunately, Yang's experiment is a very difficult one, and a more feasible experiment may have to be thought up if the parity of the π^0 meson is to be directly measured.

[69] C. N. Yang, *Phys. Rev.*, **77**: 722 (1950).

CHAPTER 5

THE CAPTURE AND ABSORPTION OF SLOW NEGATIVE MESONS

1. Introduction

In Chap. 4 we pointed out that the large excitation energies associated with π^- meson disintegrations in heavy nuclei provide evidence for the boson character of the charged π meson. In this chapter, we shall discuss the absorption[1] of slow π^- mesons by heavy nuclei in considerably greater detail. We shall discover that, except for the information concerning the statistics of charged π mesons, the slow π^- absorption process reveals more about the mechanism of energy sharing by the nucleons of a nucleus than about the properties of π mesons. It will be recalled that a similar situation obtained for the production of π mesons in heavy nuclei (cf. Chap. 3) where the complexities of nuclear structure interfered with a straightforward interpretation of the experiments in terms of the properties of π mesons.

Apart from the real interest which attaches to an understanding of the mechanism of the slow π^- disintegration of heavy nuclei, the absorption of slow π^- mesons leads logically to the nuclear absorption of slow μ^- mesons. The contrast in the rates and products of nuclear absorption of slow π^- and μ^- mesons underlines, as does no other set of experimental facts, the striking differences between the two types of mesons as regards both their intrinsic properties and their interactions with nucleons. Our discussion of the absorption of slow μ^- mesons will serve as an introduction to a more detailed consideration of the properties of the μ meson in Chap. 6.

Despite the tremendous difference in the rates of nuclear absorption of slow π^- and μ^- mesons and the qualitatively different nuclear effects which are observed when absorption actually takes place, the slowing down and capture of slow π^- and μ^- mesons is essentially the same process for both.[2] This is due to the fact that the slowing-down and capture process depends almost exclusively upon the charge and mass of the meson, and the charges are the same and the masses differ by only 30 per cent. Even the different spins of the π^- and μ^- mesons affect only slightly (through the "fine structure") the optical and Auger transitions occurring in the mesic atoms in the final stages of the capture process. Consequently, our discussion of the capture of slow negative mesons can proceed quite generally: we need specify only the particular type of meson in order to compute the actual numbers.

---

[1] We shall restrict the term "capture" to the capture of a meson in an outer atomic orbit and use the term "absorption" when the meson actually disappears by combining with the nucleus.

[2] Similar remarks would apply to mesons heavier than the π meson, the τ^- meson, the κ^- meson, etc. (cf. Chap. 9).

We start with the capture problem and then continue with separate treatments of the absorption of slow π^- and μ^- mesons.

2. Capture of Slow Negative Mesons

Tomonaga and Araki[3] were the first to point out the importance of the Coulomb field of the nucleus for the behavior of slow charged mesons. They showed that the repulsion of a slow positive meson by the positively charged nucleus would prevent it from approaching the nucleus and compel it to wander around in matter until it decays. On the other hand, the electric attraction for a slow negative meson would enable the meson to approach very close to the nucleus and allow it to undergo nuclear absorption. However, it soon becomes clear that a negative charge on the meson is a necessary but not a sufficient condition for the occurrence of nuclear absorption. Since the charged π and μ mesons are unstable particles, we must inquire into the time taken by the mesons to slow down and be captured into Bohr orbits (from which nuclear absorption can take place[3a]) and compare this slowing-down time with the lifetime for the decay of the meson in question. Obviously, if the lifetime for decay is much shorter than the slowing-down time, the meson will rarely be absorbed by the nucleus but will rather decay. Fermi *et al.*[4] were the first to point out that the time for slowing down and capture is much shorter than the decay time of the π or μ meson. Fermi and Teller[5] then demonstrated, on the basis of a reasonable model for the electrons, why the slowing-down time is so much shorter than the decay time. We sketch briefly Fermi and Teller's description of the slowing-down and capture process, although their treatment cannot be applied to very light elements like hydrogen. It has already been pointed out in Chap. 4 that a separate demonstration is necessary to prove that the slowing-down time in hydrogen is also much shorter than the decay time of the π or μ meson. This is due to the fact that there is only one electron in hydrogen and the dominant mode of energy loss by the mesons cannot be through energy transfer to the electrons.

---

[3] Tomonaga and G. Araki, *Phys. Rev.*, **58**: 90 (1940).

[3a] Nuclear absorption can take place from the continuum, but the lifetime for continuum absorption is long compared to the slowing-down time even for geometrical cross section.

[4] Fermi, Teller, and Weisskopf, *Phys. Rev.*, **71**: 314 (1947); cf. also J. A. Wheeler, *Phys. Rev.*, **71**: 320 (1947).

[5] E. Fermi and E. Teller, *Phys. Rev.*, **72**: 399 (1947); cf. also B. Ferretti, *Nuovo cimento*, **5**: 325 (1948).

According to Fermi and Teller, the history of a slow negative meson of several Mev which is finally captured into the K shell of an atom can be split into three energy regions: (A) the normal ionization region which covers the range from the initial energy of several Mev to a meson energy corresponding to the velocity of a valence electron, say several Kev, (B) from several Kev to zero energy, and (C) from zero energy to the negative energy of the K shell of the appropriate mesic atom.

A. Energy Loss from Several Mev to Several Kev. The time taken for a meson of several Mev to slow down to a velocity corresponding to that of a valence electron is determined by the normal ionization loss formula for charged particles passing through matter. The nonrelativistic approximation to this formula may be written

$$-\frac{d\tau}{dx} = \frac{4\pi e^4 NZ}{mV^2} \ln\left(\frac{2mV^2}{I}\right) \tag{1}$$

where V = velocity of meson, τ its kinetic energy, e = charge of the electron, m = mass of the electron, N = number of atoms per cubic centimeter, Z = nuclear charge, and I = average ionization potential of the atom. By writing $V = dx/dt$, we can integrate Eq. (1) and obtain the time taken by a meson to slow down from several Mev to several Kev:

$$t = \frac{m\mu\bar{V}^3}{8\pi NZe^4}\left[Ei\left(3 \ln \frac{V_i}{V}\right) - Ei\left(3 \ln \frac{V_f}{V}\right)\right] \tag{2}$$

where μ is the meson mass, V_i and V_f are the initial and final velocities, respectively, and $\bar{V} = (I/2m)^{\frac{1}{2}}$. A crude approximation to Eq. (1) is to replace the logarithmic term by some sort of average and one then obtains the simple V^3 law, namely,[6]

$$t = \frac{m\mu(V_i^3 - V_f^3)}{12\pi e^4 NZ\langle\ln (2mV^2/I)\rangle} \tag{3}$$

The slowing-down time for a μ^- meson of 5 Mev, say, in carbon comes out to be 1.5×10^{-11} sec on the basis of Eq. (2); it can easily be seen that Eq. (3) can lead to an error of as much as a factor of 10. It is to be noted that the slowing-down time defined by Eq. (2) is of the same order of magnitude for both π and μ mesons and that it does not depend on the sign of charge of the meson under consideration.

---

[6] This formula was first derived by H. Yukawa and T. Okayama, *Papers Inst. Phys. Chem. Res.*, **36**: 385 (1939).

B. Energy Loss to a Degenerate Eleciron Gas (several Kev to zero energy). Fermi and Teller next consider the time taken for a negative meson of several Kev to be slowed down and captured into the outer orbits of a mesic atom and regard the meson as moving inside a degenerate electron gas with a velocity V much smaller than the maximum (Fermi) velocity v_0 of the electrons. Now, the meson can interact only with those electrons whose velocities are between $(v_0 - V)$ and v_0 since an electron whose velocity is below $(v_0 - V)$ cannot contribute to the energy loss because of the Pauli exclusion principle. On the basis of this model, the energy loss per unit time of the meson may be written

$$-\frac{d\tau}{dt} = n\sigma v_0 w \tag{4}$$

where n is the number of electrons per cubic centimeter which can collide with the meson, σ is the electron-meson collision cross section for large deflections, and w is the average energy transferred in collisions of this type. Rough estimates of the quantities on the R.H.S. of Eq. (4) are

$$n \sim m^3 v_0^2 \frac{V}{\hbar^3}$$
$$\sigma \sim \left(\frac{e^2}{mv_0^2}\right)^2$$
$$w \sim mv_0 V$$

so that

$$-\frac{d\tau}{dt} \sim \frac{\tau}{t_0} \tag{5}$$

where $t_0 = \mu\hbar^3/m^2e^4 = 5.08 \times 10^{-15}$ sec is the characteristic time for the process and in this approximation Eq. (5) is independent of the electron density. A more exact calculation has also been carried out by Fermi and Teller, and the times they compute for the slowing down of μ^- mesons from 2 Kev to zero energy in graphite and iron appear in the first line of Table 1. These numbers will be roughly the same for π^- mesons.

C. Cascading to the K Shell. Once the meson is reduced to zero energy, it is soon captured into a high circular Bohr orbit (the elliptical Bohr orbits have smaller l's and consequently smaller statistical weights), and from this orbit it starts to cascade down to the K shell. At first, the cascade process takes place via Auger transitions, but from the low orbits optical transitions predominate for sufficiently large Z. We shall discuss the energy levels of the mesic atom and the types of transitions which take place between levels in Sec. 3. For our present purposes, it suffices to state that Fermi and Teller have also calculated the time taken for the μ^- meson to cascade down to the K orbit in graphite and iron, with the results given in the second row of Table 1. Row 3 lists the total times spent in the "slow" range by μ mesons; they are of the same order of magnitude for π^- mesons, namely, about 10^{-13} sec. If the "slow" range time is calculated for insulators where the electrons must jump the Brillouin gaps, or for gases where the electrons cannot accept arbitrarily small amounts of energy because of the ionization potentials which must be overcome, the slowing-down time for negative mesons is increased at most by a factor of 10.[7]

TABLE 1. SUMMARY OF SLOWING-DOWN TIMES IN GRAPHITE AND IRON

	Graphite	Iron
2 Kev → 0	$5.4t_0$	$4.5t_0$
$0 \rightarrow -Ze^2/r_0$ where $r_0 = \hbar^2/Z\mu e^2$	$13.5t_0$	$8.0t_0$
Total "slow" range time	9.6×10^{-14} sec	6.4×10^{-14} sec

Therefore, the total times for μ^- or π^- mesons of several Mev to be slowed down and captured into the lowest Bohr orbits of mesic atoms are much less than the decay times of both the μ^- and π^- mesons (which are 2.1×10^{-6} and $2.5_5 \times 10^{-8}$ sec, respectively).

D. Mixtures. Thus far, we have considered the slowing down and capture of negative mesons in a single element. If negative mesons are slowed down in a homogeneous chemical mixture, the relative number of captures in different elements should, according to Fermi and Teller, be roughly proportional to Z. In photographic emulsions, the number of captures in the light and heavy elements is not proportional to Z, for either μ^- or π^- mesons; however, this is not in contradiction to the Z law. This follows from the fact that, while the gelatin itself is a homogeneous mixture of H, C, N, and O, the AgBr crystals have dimensions of thousands of atomic diameters. Therefore, the relative volumes and the relative stopping powers of the AgBr crystals and the gelatin determine the relative probabilities for capture, thereby obscuring the Z effect predicted for homogeneous mixtures.

Evidence from photographic emulsions shows that about 60 to 70 per cent of the negative meson captures occur in AgBr while 30 to 40 per cent occur in the gelatin of the emulsion. Part of this evidence is based on the α particle to proton ratios observed in connection with π^- disintegrations observed to occur in photographic plates.[8] The Coulomb barrier in elements with large Z favors emission of protons and therefore the alpha to proton ratio should be smaller than for elements of low Z. The alpha to proton ratio is about 1 for the CNO group and about 0.3 for AgBr, and from these ratios and the energies of the α particles it is possible to obtain a rough value for the relative number of π^- captures in the light and heavy elements of the emulsion. Further evidence concerning the relative capture probabilities has been derived from the relative numbers of decay electrons from the positive and negative μ mesons observed to stop in emulsions exposed at mountain altitudes. Cosyns *et al.*[9] have observed 409 μ mesons stopping in photographic plates exposed at an altitude of 8000 ft; of these 409, 257 decay and 152 are absorbed. But another experiment with the magnetic sandwich method[10] has shown that there are equal numbers of μ^+ and μ^- mesons at the same elevation. Hence, 53 of the μ^- mesons decay and since four-fifths of the μ^- mesons which are captured by the CNO group must decay (cf. below), it follows that $53/204 \times \frac{4}{5} \approx 31$ per cent of the μ^- mesons are captured by the gelatin atoms and the remainder ≈ 69 per cent, by the AgBr atoms. These percentages are in agreement with rough calculations based on the relative abundances and stopping powers of the two groups of elements.

---

[7] The subject of insulators has been rather controversial [cf. H. Frohlich, *Nature*, **160**: 255 (1947); and N. F. Mott, *Proc. Phys. Soc.*, **62A**: 136 (1949)]. The remark concerning gases is correct on the assumption of the same density as for a solid (cf. footnote 5).

The only clear-cut experiment with which the Z law could be confronted gave a negative result. This negative result can be understood because one of the elements of the mixture was hydrogen. Thus Panofsky *et al.*[11] sent slow π^- mesons into lithium hydride (LiH) and into paraffin (CH_2); the Z law would predict that in each case about one-third of the captures should occur in H. The Berkeley workers attempted to measure the relative capture of the π^- mesons in hydrogen by looking for the high-energy γ rays associated with the radiative or mesic absorption process in hydrogen (cf. Chap. 4); their results are shown in Table 2 where f = fraction of incident π^- mesons captured in H and which should be equal to one-third if the Z law is valid. It is seen that $f < 2 \times 10^{-3}$ for CH_2 and $f < 6 \times 10^{-3}$ for LiH. This apparent contradiction with Fermi and Teller's prediction is explicable if it is realized that, after the π^-

---

[8] D. H. Perkins, *Phil. Mag.*, **40**: 601 (1949).

[9] Cosyns, Dilworth, Occhialini, Schoenberg, and Page, *Proc. Phys. Soc.*, **62A**, 801 (1949); cf. also W. F. Fry, *Phys. Rev.*, **83**: 594 (1951).

[10] C. Franzinetti, *Phil. Mag.*, **41**: 86 (1950).

[11] Panofsky, Aamodt, and Hadley, *Phys. Rev.*, **81**: 565 (1951).

meson has reached a meson orbit inside the electron K shell of the hydrogen atom, it can reach the mesic K shell only via optical transitions. Since the probability for optical transitions in hydrogen is quite small (cf. below), the neutral mesic hydrogen atom will generally diffuse around and collide with the carbon or lithium nuclei before the mesic K shell in hydrogen is reached. During the course of these collisions, there is an excellent chance for the π^- meson to be transferred from the hydrogen to the heavier atom. Hence it is not surprising that the Z law for the capture of negative mesons in mixtures is contradicted by an experiment in which hydrogen is one of the elements.

TABLE 2. CAPTURE OF π^- MESONS IN MIXTURES

Compound	Energy of γ ray, Mev	Expected counts per hour	Measured counts per hour
CH_2	135	$5000f$	0 ± 2
LiH	135	$1500f$	0.5 ± 2
LiH	68	$1500f$	-1 ± 4

3. Structure of Mesic Atoms

A. Energy Levels. We shall now discuss the energy levels of a negative meson in the field of the nucleus and the competition between the different modes of transition from one energy level to another. This subject is not only of interest for estimating the capture time for negative mesons (cf. above), but experiments on the γ ray and Auger transitions should yield information concerning the electromagnetic properties of the μ and π mesons and perhaps throw some light on the distribution of nuclear charge. The first point to notice is that the radius of a Bohr orbit of the mesic atom is much smaller than the radius of a Bohr orbit of the ordinary atom, approximately in the inverse ratio of the masses. For very heavy elements, the radius of the first electron Bohr orbit is still about fifty times as large as the radius of the nucleus; consequently, in calculating the energy levels of an electron in the field of a nucleus, the nucleus may be treated as a point. For the mesic atom, however, the radius of the first Bohr orbit for very heavy elements is comparable with the nuclear radius; therefore, in calculating the energy levels for a mesic atom, one must take account of the finite extension of the nucleus.

Wheeler[12] has suggested visualizing the nucleus as a uniform spherical distribution of charge of radius R. The potential energy due to such a charge distribution is given by

---

[12] J. A. Wheeler, *Rev. Mod. Phys.*, **21**: 133 (1949).

$$
\begin{aligned}
V(r) &= -\frac{Ze^2}{R}\left(\frac{3}{2} - \frac{r^2}{2R^2}\right) \qquad (r \leq R) \\
&= -\frac{Ze^2}{r} \qquad (r > R) \qquad (6)
\end{aligned}
$$

where Ze is the total charge of the nucleus (cf. Fig. 1). For lead,

$$V(R) = -14.2 \text{ Mev}$$

and $V(0) = -21.3$ Mev. The modified potential energy function resulting from the finite extension of the nucleus not only alters the position of the energy levels but actually interchanges the order of the $2s$ and $2p$ levels, *i.e.*, the $2p$ level lies lower than the $2s$ level; the interchange of the $2s$ and $2p$ levels can be understood in terms of the greater screening experienced by the $2s$ meson because of the finite charge distribution in the nucleus.

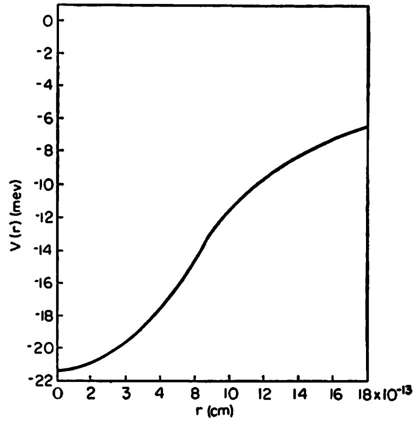

FIG. 1. Electric potential presented to a μ^- meson by a lead nucleus.

The effects of the finite nuclear extension can be seen most clearly by going to the extreme limit where it is assumed that the meson spends an inappreciable time outside the nucleus. The meson is thus assumed to exist within a parabolic potential whose force constant is represented by $k = Ze^2/R^3$. The energy difference between levels is then

$$\hbar\omega = \sqrt{\frac{8mZ}{\mu A}}\, 137mc^2 \qquad (7)$$

where $R = (e^2/2mc^2)A^{1/3}$ and μ is the meson mass. This energy difference in uranium turns out to be 8.7 Mev and 7.4 Mev for μ mesons and π mesons, respectively, to which this extreme approximation should most closely apply. These values are to be contrasted with 23.7 Mev and 18.1 Mev for the $2p$-$1s$ energy differences which are predicted by the Bohr formula

$$E_n = -\frac{\mu c^2}{2}\left(\frac{\alpha Z}{n}\right)^2 \qquad (8)$$

(α is the fine-structure constant, and n is the principal quantum number) or similar values which are predicted by the Klein-Gordon equation[13]

$$E_{nl} = +\mu c^2 \left(\left\{ 1 + \frac{(\alpha Z)^2}{[n' + \frac{1}{2} + \sqrt{(l + \frac{1}{2})^2 - (\alpha Z)^2}]^2} \right\}^{-\frac{1}{2}} - 1 \right) \qquad \left(Z < \frac{137}{2} \right) \tag{9}$$

(l is the orbital angular momentum, and $n' = n - l - 1$) or the $2p_{\frac{3}{2}} \rightarrow 1s_{\frac{1}{2}}$ values 28.2 Mev and 21.5 Mev predicted by the Dirac equation

$$E_{nj} = \mu c^2 \left(\left\{ 1 + \frac{(\alpha Z)^2}{[n' + \sqrt{(j + \frac{1}{2})^2 - (\alpha Z)^2}]^2} \right\}^{-\frac{1}{2}} - 1 \right) \tag{10}$$

where j is the total angular momentum, $n' = n - (j + \frac{1}{2})$. The wave function for the ground state in the pure harmonic potential is $e^{-\mu\omega r^2/2\hbar}$ which predicts a 50 per cent probability of finding the meson within 7.2×10^{-13} cm and 6.1×10^{-13} cm of the origin for the μ and π mesons, respectively.

Wheeler[12] has calculated more accurate values for the energy levels using the mixed Coulomb-oscillator potential. As a first orientation, he neglects the fine structure of the levels due to relativistic effects and possible spin-orbit interactions. Moreover, in view of the 10 per cent uncertainty in the nuclear radius, he calculates the energy levels by means of the W.K.B. method applied to the Klein-Gordon equation in accordance with the formula

$$n = \left(l + \frac{1}{2} \right) + \frac{1}{\pi} \int_{\rho_{\min}}^{\rho_{\max}} \left[\left(\frac{E_{nl} - V}{\mu c^2} \right)^2 - 1 - \frac{(l + \frac{1}{2})^2}{\rho^2} \right]^{\frac{1}{2}} d\rho \tag{11}$$

where $\rho = (\mu c/\hbar) r$, $\rho_{\min}$ and $\rho_{\max}$ are defined by the zeros of the integrand, and Eq. (6) is used for the potential energy. The three lowest energy levels for the μ^- and π^- mesons, derived on the basis of Eq. (11), are listed in Table 3; we have used $\mu = 210$ m and 276 m for the masses of the μ^- and π^- mesons, respectively. The inversion of the $2p$ and $2s$ levels is seen clearly; it is most evident for the large Z's where the finite size of the nucleus plays a very important role. The inversion effect makes possible radiative transitions from the $2p$ to the $1s$ level and ensures that the $2s$ level will not be metastable.

---

[13] For $Z > \frac{137}{2}$, the Klein-Gordon equation does not yield a well-defined solution corresponding to a point Coulomb field (cf. G. Wentzel, "The Quantum Theory of Fields," Interscience Publishers, 1949). However, the actual nucleus is not a point source and determines the arbitrary phase permitted by a point Coulomb field [cf. K. Case and A. Messiah, *Phys. Rev.*, **82**: 563 (1951)].

TABLE 3. THREE LOWEST IONIZATION POTENTIALS OF DIFFERENT MESIC ATOMS (IN MEV)

Z	μ^- meson			π^- meson		
	$1s$	$2p$	$2s$	$1s$	$2p$	$2s$
8	0.182	0.04576	0.04566	0.240	0.06036	0.06023
16	0.705	0.1833	0.1801	0.931	0.2418	0.2375
26	1.65	0.486	0.452	2.20	0.641	0.596
30	2.14	0.648	0.590	2.83	0.855	0.778
35	2.74	0.884	0.779	3.61	1.17	1.03
47	4.33	1.61	1.32	5.71	2.12	1.75
53	5.13	2.05	1.63	6.77	2.70	2.15
56	5.54	2.29	1.79	7.31	3.02	2.35
74	8.26	4.00	2.90	9.00	5.28	3.82
82	9.48	4.84	3.44	12.51	6.38	4.54
92	11.01	5.91	4.16	14.53	7.80	5.49

While Table 3 exhibits the gross features of the energy levels of the mesic atom, it is interesting to inquire into the uncertainties of these numbers in terms of the effects which have been neglected and our lack of precise knowledge of the nuclear radius and of the charge distribution inside the nucleus. The numbers in Table 3 have derived using the W.K.B. method; as a check on this method, Wheeler[14] has computed the lowest level in lead exactly and found 10.05 Mev for the energy value compared with 9.50; this is a 5 per cent error. The μ meson probably obeys the Dirac equation, and there will be a splitting of the $2p_{\frac{1}{2}}$-$2p_{\frac{3}{2}}$ doublet resulting from the magnetic moment associated with the μ meson spin. A rough estimate of the $2p$ doublet splitting can be obtained by means of the well-known formula

$$\Delta E = \frac{3\hbar^2}{4\mu^2c^2}\frac{1}{r}\frac{dV}{dr} \tag{12}$$

Setting $V = \mu\omega^2r^2/2$ in Eq. (12) (for the ideal heavy nucleus), one finds $\Delta E = 0.59$ Mev compared with 9.1 Mev, a 6.5 per cent effect. A more accurate formula has been given by Wheeler,[14] namely,

$$\Delta E = \left(\frac{Z}{101}\right)^4 \frac{1}{1 + 0.2\left(\dfrac{Z\mu e^2R}{\hbar^2}\right)^2} \tag{13}$$

which predicts a splitting of the same order of magnitude as Eq. (12). If the μ meson were to possess in addition an anomalous magnetic moment, $\eta(e\hbar/2\mu c)$, Eq. (13) would have to be multiplied by $(1 + 2\eta)$. The energies of the $2p_{\frac{1}{2}}$-$1s_{\frac{1}{2}}$ and $2p_{\frac{3}{2}}$-$1s_{\frac{1}{2}}$ γ rays have been plotted in Fig. 2 as a function of the atomic number,[14] assuming that the μ^- meson possesses a normal Dirac magnetic moment.

---

[14] J. A. Wheeler, private communication.

The Klein-Gordon equation is probably correct for the π^- meson since the measured spin of the π^+ meson is zero. A spin zero particle cannot carry a magnetic moment or even an anomalous magnetic moment. Even if the π^- meson possessed spin 1 and an associated magnetic moment, the fine structure of the levels of the mesic atom would be washed out by the broadening due to the nuclear absorption of the π^- mesons. Thus the broadening of the hydrogen ground state is given by $\Delta E \approx \hbar/P_\gamma$ where P_γ is determined by Table 4 of Chap. 4 and depends upon the value of $f^2/\hbar c$ [in the $PS(PV)$ theory]. Assuming the reasonable value 0.3 for $f^2/\hbar c$, one finds that ΔE is of the order of 0.1 ev, to be compared with a fine-structure splitting of the order[15] of $\alpha^4\mu c^2/2 \approx 0.5$ ev. For heavier nuclei, the transition probability (per proton) for the absorption of the π^- meson from the K shell is at least a factor of 10 greater since nuclear stars are observed from π^- absorptions and not high-energy γ rays (cf. below). Since the value of the meson wave function at the origin goes as Z^3, the absorption probability goes approximately

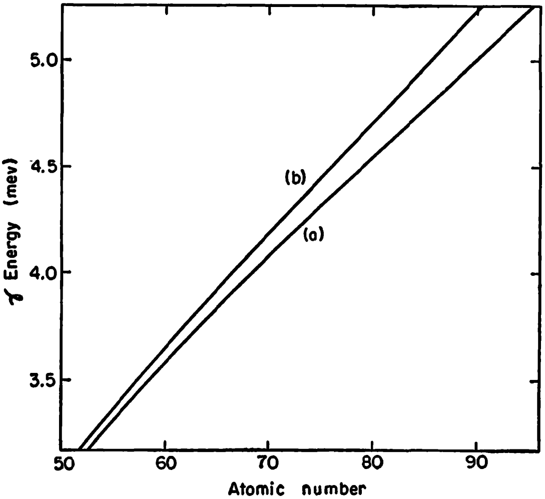

FIG. 2. Theoretical γ ray energies as a function of the atomic number of the μ mesic atom. Curve (*a*) corresponds to the $2p_{\frac{1}{2}} \rightarrow 1s_{\frac{1}{2}}$ transition, (*b*) to the $2p_{\frac{3}{2}} \rightarrow 1s_{\frac{1}{2}}$ transition.

---

[15] Cf. A. Simon, *Phys. Rev.*, **76**: 1877 (1949); cf. also Case and Messiah, *loc. cit.*

as Z^4, and this must be compared with the fine-structure splitting, which also varies as Z^4. Consequently, the fine-structure splitting would be completely smeared out by the broadening due to nuclear absorption. Apart from the broadening of the levels of the mesic atom due to nuclear absorption, the interaction of the slow π^- meson with the nucleons in the nucleus should not appreciably shift the positions of the mesic levels (since the magnitude of the π meson-nucleon interaction decreases rapidly with decreasing energy although always remaining much stronger than the μ meson-nucleon interaction—cf. Chaps. 6 and 7).

Apart from the above uncertainties in the values of Table 3, a change in the nuclear radius of 10 per cent alters, for example, the components of the lead line by about 0.4 Mev in 4.5 Mev, a 10 per cent effect. Moreover, a nonuniform charge density in the nucleus will also change the energy levels of the mesic atom; thus, if the charge density at the surface $\rho(R)$ exceeds the central density $\rho(0)$ by a factor $(1 + \delta)(\delta = 0.0022\ A$ where A is the atomic number[16]), the energy is shifted by the amount

$$\Delta E = \frac{3\delta}{20}\left\{1 + 0.6\delta\,\frac{\langle[1-(r^2/R^2)]^2\rangle}{\langle[1-(r^2/R^2)\rangle}\right\} E \tag{14}$$

where the $\langle\ \rangle$ indicates an average. Equation (14) leads to a raising of the 1*s* level by 0.14 Mev for Pb, which effect is equivalent to a 3 per cent decrease in nuclear radius. To distinguish between the effects of the nuclear radius and the nonuniformity of the charge distribution, it would be necessary to measure the 2*s*-2*p* γ rays since the 2*s* and 1*s* levels respond differently to the two influences; such a separation will be difficult to establish experimentally.

B. γ Ray and Auger Transitions. Wheeler[12] has also investigated the probabilities per unit time for the $2s \rightarrow 2p$, $2s \rightarrow 1s$, and $2p \rightarrow 1s$ transitions. He disregards the finite extension of the nucleus and uses the formulas appropriate to a point charge; for the $2p \rightarrow 1s$ γ ray transitions, he finds

$$w_\gamma(2p \rightarrow 1s) = \left(\frac{2}{3}\right)^8 \frac{Z^4}{(137)^5}\frac{\mu c^2}{\hbar} \tag{15}$$

For the $2s \rightarrow 2p$ transition, Wheeler uses the matrix element appropriate to the hydrogenic problem but inserts the correct value for the energy difference ΔE obtained from the mixed Coulomb-oscillator potential (cf. Table 3); he finds

$$w_\gamma(2s \rightarrow 2p) = \frac{4932}{Z^2}\left(\frac{\Delta E}{\mu c^2}\right)^3 \frac{\mu c^2}{\hbar} \tag{16}$$

---

[16] Cf. E. Feenberg, *Phys. Rev.*, **60**: 593 (1941).

For the Auger transition probability, he takes over the nonrelativistic Schrodinger formula and writes

$$w_{\text{Auger}}(2s \longrightarrow 1s) = \frac{2^{21}}{3^{\frac{21}{2}}} \left(\frac{m}{\mu}\right)^{\frac{1}{2}} \left(\frac{me^4}{\hbar^3}\right) \tag{17}$$

On the basis of these formulas, it is possible to calculate the competition between γ ray and Auger transitions, and the results are given in Table 4; the numbers quoted are based on a μ^- mass of 210 m and a π^- mass of 276 m.

TABLE 4. TRANSITION PROBABILITIES BETWEEN THE LEVELS OF THE MESIC ATOM

Z	μ^- meson			π^- meson		
	$w_\gamma(2s \to 2p)$	w_{Auger} $(2s \to 1s)$	$w_\gamma(2p \to 1s)$	$w_\gamma(2s \to 2p)$	w_{Auger} $(2s \to 1s)$	$w_\gamma(2p \to 1s)$
5	2.2×10^4	2.2×10^9	0.8×10^{14}	1.3×10^4	1.3×10^8	1.1×10^{14}
10	2.1×10^8	2.2×10^9	1.4×10^{15}	2.1×10^8	1.3×10^8	1.8×10^{15}
15	3.6×10^{10}	2.2×10^9	6.9×10^{15}	2.1×10^{10}	1.3×10^8	9.1×10^{15}
20	1.3×10^{12}	2.2×10^9	2.2×10^{16}	7.0×10^{11}	1.3×10^8	2.9×10^{16}
25	1.8×10^{13}	2.2×10^9	5.4×10^{16}	1.0×10^{13}	1.3×10^8	7.1×10^{16}
30	9.0×10^{13}	2.2×10^9	1.2×10^{17}	5.0×10^{13}	1.3×10^8	1.5×10^{17}
35	6.3×10^{14}	2.2×10^9	2.0×10^{17}	4.0×10^{14}	1.3×10^8	2.6×10^{17}
40	1.8×10^{15}	2.2×10^9	3.5×10^{17}	1.0×10^{15}	1.3×10^8	4.6×10^{17}
92	2.9×10^{17}	2.2×10^9	2.0×10^{18}	1.7×10^{17}	1.3×10^8	2.6×10^{18}
∞	1.0×10^{19}	2.2×10^9	5.9×10^{18}	5.7×10^{18}	1.3×10^8	7.8×10^{18}

It is evident that, for low Z, the Auger transitions are the most probable transitions from the 2s level while for high Z, γ ray transitions are the most probable. Inspection of Table 4 also clarifies the reason for the previous assertion that the μ^- or π^- meson[17] will usually reach the K shell of the mesic atom before decaying: the lifetime for the $2p \to 1s$ transition is extremely short compared with the decay time of either the μ^- or π^- meson, and it is likely that the majority of mesons will pass through the 2p rather than the 2s state since negative mesons are originally captured chiefly into high circular orbits. Even mesons reaching the $2s$ state will drop to the $1s$ state by means of an Auger transition in 10^{-9} sec for $Z \lesssim 12$ and increasingly more rapidly by the sequence of optical transitions $2s \rightarrow 2p$, $2p \rightarrow 1s$ for $Z \gtrsim 12$.

---

[17] In the case of the π^- meson, the K shell will be reached, provided that the competition from nuclear absorption is also surmounted (cf. Chap. 4). Recently, Camac, McGuire, Platt, and Schulte (*Phys. Rev.*, in press) have shown, by detecting the 100 kev γ rays associated with the $2p \to 1s$ transition, that only 13 per cent of the π^- mesons reach the K shell of carbon from the 2p level; since most mesons pass through the 2p level (rather than the 2s), this implies that the probability of nuclear absorption from the 2p level is more than six times as great as $w_\gamma(2p \to 1s)$. Actually (cf. Messiah and Marshak, *Phys. Rev.*, in press), nuclear absorption is so strong that the majority of π^- mesons will not reach the K shell for elements as light as lithium.

Thus far, the experimental evidence bearing on γ ray and Auger transitions in mesic atoms is meager and somewhat contradictory. Chang[18] and, more recently, Shanley,[19] using a cloud chamber with lead foils, have observed electrons of 1 to 5 Mev associated with μ^- mesons stopping in the lead foils. They attribute these electrons to γ rays resulting from radiative transitions between the lower lying levels of the mesic-lead atom. No such electrons were found for lower Z foils like Fe and Al, presumably because the γ rays are of lower energy (below 1 Mev) and the probability of producing photoelectrons is appreciably smaller. On the other hand, Cosyns *et al.*[9] have found evidence for Auger electrons associated with μ^- capture in the silver and bromine of the emulsion. This experiment has already been cited in connection with the relative stopping powers of the light and heavy elements in the emulsion (cf. Sec. 2 above). For our present purposes, the relevant observations are that 7.2 ± 1.3 per cent of the μ meson tracks (or 14 per cent of the μ^-) have associated slow electrons. Since only 1 per cent of these slow electrons are associated with fast decay electrons, the authors argue that most of the Auger electrons are due to capture in the heavy elements; and since only 70 per cent of the μ^- mesons are captured by the heavy nuclei, it would follow that about 20 per cent of the μ^- mesons captured by heavy nuclei are accompanied by Auger electrons. The energy-frequency distribution of the Auger electrons are given in Fig. 3. It is seen that the electron energies are quite low and must arise from Auger transitions in Ag and Br associated with principal quantum numbers in the range $n = 4$ to 8. This is consistent with the theory of Fermi and Teller[5] according to which the principal quantum numbers below which radiative transitions dominate over the Auger transitions are $n = 4.8$ for Br and $n = 5.6$ for Ag. Some of the 75- to 125-Kev electrons may be

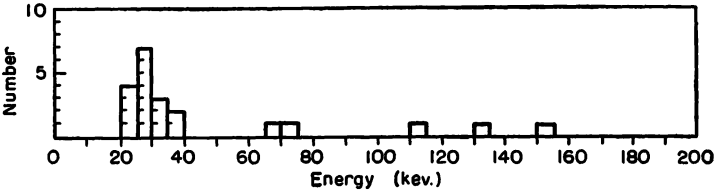

FIG. 3. Measured frequency-energy distribution of Auger electrons associated with the capture of slow μ^- mesons by the nuclei of the photographic emulsion.

[18] W. Y. Chang, *Rev. Mod. Phys.*, **21**: 166 (1949).

[19] T. J. B. Shanley, Ph.D. Thesis, Princeton, 1951.

due to the $2s \rightarrow 1s$ transitions in elements of the CNO group unless the probability of cascading through the $2s$ state is extremely small. However, the statistics are still too poor to draw any definite conclusions.[19a]

C. Dependence of K-shell Absorption on Atomic Number. Once the negative meson arrives in the K shell of the mesic atom, the probability of nuclear absorption depends sensitively upon the atomic number of the nucleus, *viz.*, approximately[20] as Z^4, at least for light nuclei. In the hydrogenic approximation, this can be seen as follows: the number of protons, with which the negative meson interacts, increases approximately linearly with Z, and the probability of finding the meson at the nucleus, namely, $\phi^2(0)$, increases[20a] as Z^3; the total increase is therefore approximately as Z^4. For heavy nuclei, the hydrogenic approximation is not justified, and the probability for absorption increases much less rapidly than Z^4. We can assert that the absorption probability is proportional to Z_{eff}^4 provided that we define Z_{eff} as

$$Z_{\text{eff}} = \left[\left(\frac{\hbar}{\mu e^2}\right)^3 \pi \sum_{\text{protons}} \phi^2\right]^{\frac{1}{4}} \tag{18}$$

Wheeler[12] has evaluated Eq. (18) exactly for I and Pb, taking $\mu = 200m_e$; he finds $Z_{\text{eff}} = 27.6$ and 31.5, respectively. For the ideal heavy nucleus where the oscillator potential governs the electric interaction with the meson, $Z_{\text{eff}} = 37.2$. A good empirical formula for Z_{eff} as a function of Z turns out to be

$$Z_{\text{eff}} = Z\left[1 + \left(\frac{Z}{37.2}\right)^{1.54}\right]^{-\frac{1}{1.54}} \tag{19}$$

Numerical values for Z_{eff} will be found in Table 9 of Sec. 5.

4. Nuclear Absorption of Slow π^- Mesons

We have seen that, as far as the slowing-down and capture phenomena are concerned, slow μ^- and π^- mesons behave rather similarly. However, once the μ^- and π^- mesons reach the K or higher shells of the same mesic atom, the rates and products of nuclear absorption are quite different for the two types. The π^- meson interacts strongly with the nucleons in the nucleus and is absorbed by all nuclei including hydrogen (cf. Chap. 4) before it decays into a μ^- meson. The μ^- meson, however, interacts very weakly with the nucleons and, for nuclei corresponding to $Z \lesssim 10$, decays into an electron before it is absorbed by the nucleus even though the lifetime for μ^- decay is about 100 times as long as the decay time of the π^- meson. For nuclei with $Z \gtrsim 10$, the rapid increase for the probability of nuclear absorption (cf. Sec. 3*C*) leads to a preponderance of nuclear absorption over decay. We first consider the absorption of π^- mesons by nuclei with $Z > 1$ (the hydrogens have already been discussed in Chap. 4). We shall then summarize in Sec. 5 the experimental material bearing on the nuclear absorption of μ^- mesons.

[19a] Cf. W. F. Fry, *Phys. Rev.*, **81**: 594 (1951).

[20] Even for pseudoscalar mesons, this is true contrary to a statement in Wheeler (footnote 12) [cf. S. Tamor, *Phys. Rev*, **77**: 412 (1950); and P. Budini, *Nuovo cimento*, **8**: 901 (1951)].

[20a] For a meson with orbital angular momentum l, the probability of finding it at the nucleus increases as Z^{3+2l}.

A. Experimental Data. In Chap. 4, we presented the experimental results on the absorption of slow π^- mesons by protons and deuterons. It was seen that, when protons absorb π^- mesons, high-energy γ rays ($\approx$ 130 Mev) and slow π^0 mesons are emitted with about equal probabilities. The deuteron absorption was found to give high-energy γ rays in about one-third of the cases; the remaining two-thirds of the π^- mesons absorbed in deuterium gave rise to two high-energy neutrons. The large amount of radiative absorption in deuterium, surprising at first sight, could be explained by the pseudovector character of the charged π meson field or by a pseudoscalar π^- meson and the absence of high nucleon momenta in the deuteron wave function. Moreover, the absence of mesic absorption (*i.e.*, emission of π^0 mesons) was explicable in terms of the requirement of the Pauli principle for the two final neutrons. For nuclei heavier than the deuteron, one would expect that the absorption of slow π^- mesons would lead, in general, to the preponderant emission of nucleons, rather than to the emission of high-energy γ rays or π^0 mesons. This follows for three reasons: (1) most nuclei are more strongly bound than the deuteron so that higher nucleon momenta are available for the π^- absorption process leading to the emission of nucleons, thereby increasing the relative probability for this process compared with radiative absorption; (2) the π^- absorption process leading to the emission of a high-energy γ ray requires only one nucleon and gives rise to a low-energy recoil nucleon whose emission, in a heavy nucleus, is suppressed by the Pauli exclusion principle; and (3) the emission of π^0 mesons is in most cases energetically forbidden for heavy nuclei, and in those cases where it is energetically allowed (for example, N^{14}, Cl^{35}), the available phase space is much smaller than for nucleon emission (because of the small amount of kinetic energy available to the π^0 meson), thereby suppressing the π^0 process compared with nucleon emission.

The expectation that the absorption of slow π^- mesons by heavy nuclei will lead chiefly to nucleon emission is borne out by experiment. Panofsky[21] has looked for high-energy γ rays from π^- mesons stopped in helium, lithium, and carbon (the latter two were in the form of LiH and CH_2, but it was pointed out earlier that hydrogen is completely ineffectual in capturing π^- mesons—cf. Sec. 2) and has in all cases found a negative effect. Panofsky's data enable him to place an upper limit of 8 per cent on the radiative absorption of slow π^- mesons in helium and of 1 per cent in heavier nuclei. The other type of experiment which has been performed by many authors is to let π^- mesons stop in a photographic emulsion and to investigate the disintegration products. It is found that about 70 per cent of the π^- mesons which end in the emulsion give rise to nuclear stars with visible prongs and that about 30 per cent end without giving rise to any observable prongs (except for occasional small blobs which are presumed to be due to nuclear recoils). In view of Panofsky's results, the starless 30 per cent must be interpreted chiefly in terms of the emission of one or more neutrons unaccompanied by charged particles.

---

[21] Footnote 11 and W. K. H. Panofsky, private communication.

We report in some detail the essential experimental results bearing on π^- stars produced in photographic emulsions and then set forth a tentative theoretical interpretation of these results. The approximate numbers of π^- meson disintegrations studied by the different authors were: Perkins[8] (100), Adelman and Jones[22] (500), Cheston and Goldfarb[23] (500), Menon *et al.*[24] (2500), and Adelman[25] (1500). Since the last two workers use the same convention for a star prong, *viz.*, any group of grains (except an electron track) leaving the terminus of a π^- meson with a well-defined direction, their data are combined to give the frequency-prong distribution shown in Table 5. The percentages which are given should be fairly reliable since they are based on more than 4000 stars. The energy spectrum of protons less than 30 Mev from one- and two-prong stars[24] is given in Fig. 4 while the energy spectrum of alpha particles less than 30 Mev from one-prong stars[24] is given in Fig. 5. The peak of

TABLE 5. FREQUENCY-PRONG DISTRIBUTION OF π^- STARS

Number of Prongs	Per Cent
0	28 ± 2
1	23.3 ± 0.7
2	23.5 ± 0.7
3	16.1 ± 0.5
4	7.6 ± 0.4
5	1.4 ± 0.2
6	0.1 ± 0.1

[22] F. Adelman and S. Jones, *Science*, **111**: 226 (1950).

[23] W. Cheston and L. Goldfarb, *Phys. Rev.*, **78**: 683 (1950).

[24] Menon, Muirhead, and Rochat, *Phil. Mag.*, **41**: 583 (1950).

[25] F. L. Adelman, Ph.D. Thesis, University of California, 1950; cf. *Phys. Rev.*, **85**: 249 (1952).

the proton spectrum is at 9.6 Mev, and it can be shown that the spectrum is fitted quite well by a theoretical distribution based on the Weisskopf evaporation model (cf. below) corresponding to an excitation energy of about 110 Mev. The alpha particle spectrum is seen to have a double peak with a transition point at about 9 Mev; it is very likely that most of the alpha particles below 9 Mev originate from the light nuclei in the emulsion (CNO) and those above 9 Mev from the heavy nuclei (Ag and Br) because of the difference in the potential barriers. If this separation is taken seriously, it is possible to deduce the α particle to proton ratio for light and heavy nuclei; it is found that this ratio is 1.0 ± 0.1 for light nuclei and 0.3 ± 0.04 for heavy nuclei, a result already quoted.

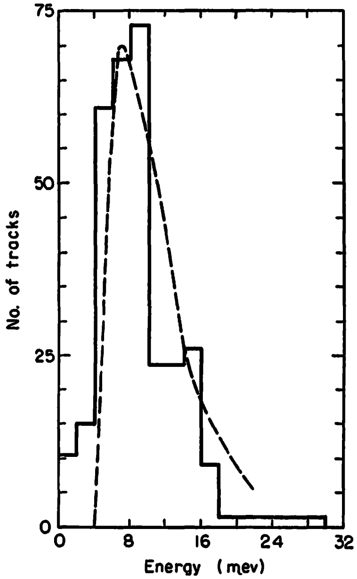

FIG. 4. Measured proton energy spectrum below 30 Mev from π^- disintegrations of the nuclei of the photographic emulsion; the dotted curve represents the prediction of the statistical theory (see text).

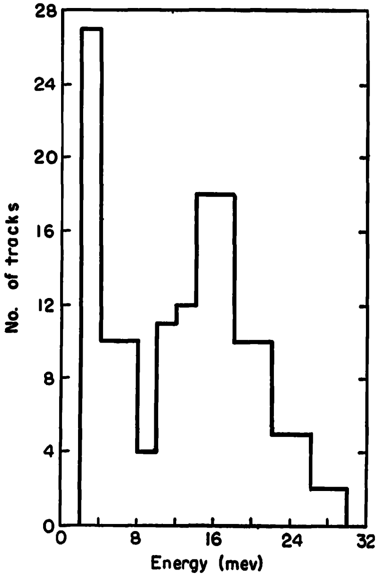

FIG. 5. Measured alpha particle energy spectrum below 30 Mev from π^- disintegrations of the nuclei of the photographic emulsion.

The separation into light and heavy nuclei on the basis of the α particle to proton ratio is not completely reliable; this is indicated by the fact that the α particle to proton ratio, determined by direct observation of π^- stars in the gelatin (sandwiched in between layers of emulsion), turns out to be 1.55 ± 0.2. It is interesting to list in Table 6 the composition of the 41 events observed[24] to originate in the gelatin which served as the basis for the 1.55 value for the α particle to proton ratio. Menon *et al.*[24]

TABLE 6. π^- STARS IN LIGHT NUCLEI

Number of charged particles ejected per star	Classification of star	Number of stars observed
1	$1p$	5
	1α	5
	$1f$*	3
2	$2p$	1
	2α	3
	1α, $1p$	5
	$1p$, $1f$	1
	$2f$	1
3	3α	1
	2α, $1p$	10
	1α, $2p$	4
	1α, $1p$, $1f$	1
4	2α, $2p$	1

* *f* means heavy fragment, which term is reserved for (*a*) heavily ionizing particles producing tracks less than 5 microns in length, (*b*) particles producing longer tracks if their ionization appears to be much greater than that produced by an α particle, and (*c*) ${}_3\mathrm{Li}^8$ nuclei which produce the characteristic "hammer" tracks.

have also observed 38 π^- mesons which appeared to end in the gelatin without giving rise to visible stars; it is possible that some of these 38 cases may contain prongs which are lost to the observer, but the majority do not, and this represents a sizable fraction of zero-prong stars for the light nuclei. Of the 41 stars listed in Table 6, certain categories can be ascribed to specific nuclei in the gelatin; thus the $2\alpha + 1p$ stars must be due to C, in accordance with the reaction scheme

$$\pi^- + {}_6\mathrm{C}^{12} \rightarrow 2\alpha + 1p + 3n \qquad (A)$$

and the 3α stars must be due to N in accordance with the reaction scheme

$$\pi^- + {}_7\mathrm{N}^{14} \rightarrow 3\alpha + 2n \qquad (B)$$

These two reactions can also be identified when the π^- mesons stop in the emulsion. A third reaction can be identified as due to O, namely,

$$\pi^- + {}_8\mathrm{O}^{16} \rightarrow 3\alpha + 1p + 3n \qquad (C)$$

Menon *et al.*[24] have measured the frequency of occurrence of reactions (A), (B), and (C) in a study of 780 stars. They find that about 15 per cent represent one of the three reactions; more precisely, 7.6 ± 1 per cent, 3.7 ± 0.7 per cent, and 4.2 ± 0.7 per cent represent reactions (*A*), (*B*), and (*C*), respectively. Since only about[26] 30 to 40 per cent of the π^- mesons are captured by the light nuclei, these three reactions represent probable modes of disintegration of the CNO group.

Once the particular light nucleus, which is disintegrated by the π^- meson, is identified, it becomes of interest to measure the α particle spectrum from such a nucleus; the results for C, N, and O are given in Fig. 6. The effect of the structure of the particular nucleus is especially to be noted: for the α particle nuclei C and O, the α particle spectrum extends to about 25 Mev, whereas for the α particle + deuteron nucleus *N* the cutoff is at about 15 Mev. This difference may perhaps be understood in terms of the extra deuteron in N^{14} which can react with the π^- meson and absorb a large fraction of its energy, leaving an excited C^{12} nucleus which disintegrates into 3α particles of rather low energy. For C^{12} and O^{16}, it is plausible to assume that the π^- meson interacts with one of the α particles which can transfer appreciable energy to the other α particles constituting the nucleus.

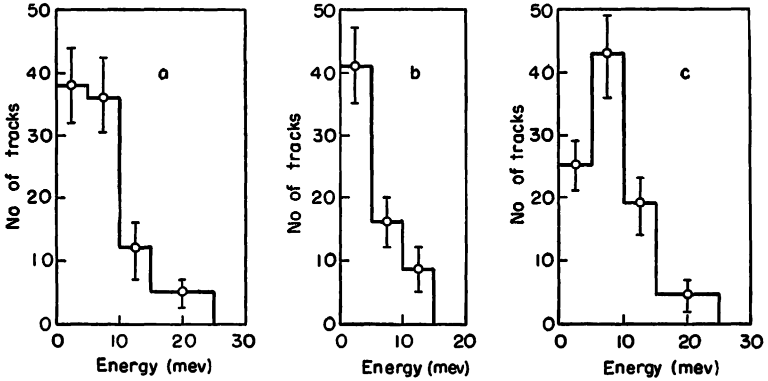

FIG. 6. Measured alpha particle energy spectra from π^- disintegrations of C, N, and O. Curve (*a*) corresponds to C, (*b*) to N, (*c*) to O.

In addition to protons less than 30 Mev (chiefly evaporation protons) associated with π^- stars, π^- stars are accompanied by an appreciable number of high-energy protons, greater than 30 Mev, which, it will turn out, cannot be explained as the high-energy "tail" of the evaporation

---

[26] The lower value 30 per cent is based on the assumption that the relative probabilities for capture of π^- mesons by light and heavy nuclei are about the same as for μ^- mesons (the evidence for 30 per cent capture of μ^- mesons by the CNO group was given in Sec. 2). Menon *et al.* argue for the larger number 40 or even 50 per cent, but, in our opinion, their arguments are not convincing.

DAVID J. LANGFORD
Pure Mathematical Physics

spectrum. The spectra which were obtained by Cheston and Goldfarb[23] and Adelman[25] for protons > 30 Mev are plotted in Fig. 7. The two sets of workers observe that the fractions of π^- absorptions which lead to high-energy protons are 10 ± 2 per cent, and 9.5 ± 1.3 per cent, respectively. In each experiment, the total number of high-energy protons observed was about 50 so that in no case were the statistics very good. In view of the difficulty of making an accurate assignment of the energy to the proton, and the somewhat different corrections made in the two experiments, it is not advisable to combine the data. The poor statistics prevent the drawing of too nice conclusions about specific models developed to explain the mechanism of absorption of slow π^- mesons, as we shall see below. It is worth remarking that some of the stars with high-energy protons exhibit visible excitation energies of the order of 100 Mev. Such high excitation energies provided the first strong evidence for the boson character of the π^- meson, conclusive proof for which is now supplied by the reaction $\pi^- + P \rightarrow N + \gamma$ (cf. Chap. 4). If the π^- meson were a fermion, a neutral particle would have to be emitted in the absorption process to conserve statistics, and the neutral particle would depart with most of the rest energy of the π^- meson—in contradiction to experiment. We shall see in Sec. 5 the striking contrast

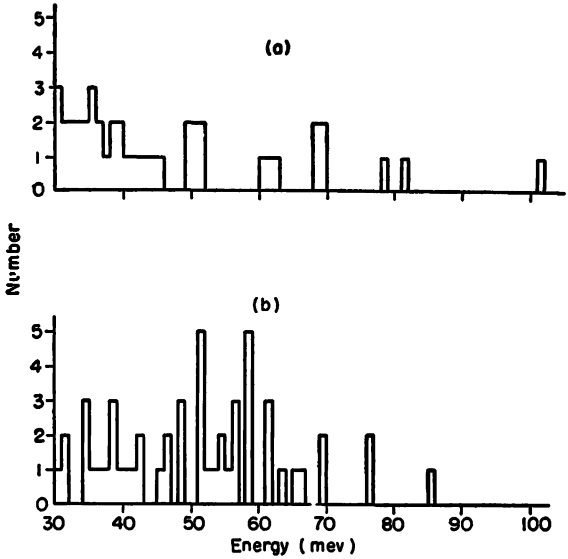

FIG. 7. Measured frequency-energy distribution of fast protons (> 30 Mev) from π^- disintegrations of the nuclei of the photographic emulsion. Histogram (*a*) represents Cheston and Goldfarb's results, (*b*) Adelman's results.

offered by μ^- mesons; the extremely small amounts of visible excitation energy associated with the nuclear absorption of μ^- mesons are indeed evidence for the fermion character of the μ^- meson.

The experimental evidence considered above has been concerned with the nuclear absorption of π^- mesons in photographic emulsions which do not contain elements heavier than silver. It is to be expected that fission will compete seriously with ordinary star production when slow π^- mesons are absorbed by very heavy elements like uranium. This follows from the fact—as we shall see below—that the absorption of a π^- meson converts a nuclear proton into a high-energy neutron (70 to 90 Mev), and the high-energy neutron readily induces fission in U and Th. Thus the measured fission cross sections for 90-Mev neutrons are[27]

Uranium: $\sigma_{\text{fission}} = 1.4 \times 10^{-24}\ \text{cm}^2$
Thorium: $\sigma_{\text{fission}} = 1.0 \times 10^{-24}\ \text{cm}^2$
Bismuth: $\sigma_{\text{fission}} = 0.03 \times 10^{-24}\ \text{cm}^2$

In the case of uranium and thorium, the fission cross sections are close to their geometrical values, whereas for bismuth the cross section is much smaller. Hence high-energy neutrons of 70- to 90-Mev energy, resulting from the absorption of slow π^- mesons, should frequently lead to fission of uranium and thorium but not of bismuth. Al-Salam[28] has observed 22 π^- fissions in photographic plates soaked in uranyl acetate and exposed to π^- mesons in the Berkeley cyclotron. This represents about 1 fission per 100 π^- mesons stopping in the emulsion and is consistent with the assumption that all the π^- mesons entering uranium nuclei (calculated as 1 in 85) cause fission. The 22 fission events are characterized by a fairly constant total track length (from 22 to 29 microns) and by ratios of the two fission-fragment track lengths varying from 1 to 1.4 (with most ratios lying below 1.2). The lengths of the fission-fragment tracks are approximately the same as the lengths of fission-fragment tracks produced by high-energy neutron bombardment of uranium[27] which, in turn, do not differ significantly from low-energy neutron bombardment. Moreover, the tendency toward symmetrical fission is in agreement with observations on the symmetrical fission of U^{238} (as against the unsymmetrical fission of U^{235}). These results are in accord with Serber's hypothesis[29] that high-energy nuclear fission first leads to the emission of a sizable number of low-energy neutrons and then goes like low-energy fission with the fission-fragment energy deriving from the electrostatic forces. It is interesting to note that three of the fission events observed by Al-Salam contain a fast particle emerging at about 90° with respect to the fission tracks. The occurrence of these fast tracks, in excess of those observed in neutron-induced fission, probably have the same origin as the excess of fast single tracks observed in connection with π^- stars.

---

[27] J. Jungerman and S. Wright, *Phys. Rev.*, **76**: 1112 (1949).
[28] S. G. Al-Salam, *Phys. Rev.*, **84**: 254 (1951).
[29] R. Serber, quoted in footnote 27.

B. Theory of π^- Disintegrations. The first attempt to understand the characteristics of π^- disintegrations of heavy nuclei was based on the evaporation model in which it was assumed that the rest energy of the π^- meson (*i.e.*, 140 Mev) is converted into excitation energy of the nucleus. In order to make predictions with the evaporation model, it is necessary to assume in addition some specific nuclear model which establishes a relationship between the temperature and the excitation energy. Fujimoto and Yamaguchi[30] adopted the Fermi gas model for this purpose while Clementel and Puppi[31] employed the liquid-drop model. Both calculations led to theoretical predictions for the heavy nuclei in the emulsion in disagreement with experiment: the Fermi model predicted too great a frequency of many-prong stars whereas the liquid-drop model predicted the wrong energy distribution for the emitted particles. A much better fit to the prong distribution, the α particle to proton ratio, and the energy spectra of the protons and α particles (below 30 Mev) from Ag and Br is obtained by choosing the excitation energy equal to about three-fourths of the rest mass of the π^- meson. The dotted curve in Fig. 4 is a plot of the probability function for silver (T is the proton energy and C is a suitably normalized constant):

$$P(T) = C(T - 4)e^{-3.16T/\sqrt{U}} \tag{20}$$

with $U = 109$ Mev and T expressed in Mev; 4 Mev is the effective Coulomb barrier of silver[32] at an excitation energy of the order of 100 Mev. Formula (20) is the probability function for the emitted protons predicted by the evaporation theory with the Fermi gas relation between temperature and excitation energy, namely, T' (temperature) $= \sqrt{10U/A}$ (A is the atomic weight). Needless to say, the evaporation theory should not be applied too strictly to the light nuclei (CNO) of the emulsion.

The fact that only about three-fourths of the total available energy of the π^- meson appears to be transformed into evaporation nucleons and the presence of a sizable number of high-energy protons ($>$ 30 Mev) in the π^- stars, which cannot be ascribed to the high-energy tail of the evaporation spectrum, raise the question as to whether the primary mechanism for the absorption of the π^- meson is really the evaporation mechanism.

---

[30] Y. Fujimoto and Y. Yamaguchi, *Prog. Theor. Phys.*, **4**: 468 (1949).

[31] E. Clementel and G. Puppi, *Nuovo cimento*, **6**: 494 (1949).

[32] K. J. LeCouteur, *Proc. Phys. Soc.*, **63A**: 259 (1950).

In an attempt to answer this question, Tamor[33] has examined the consequences of the hypothesis that the π^- meson disappears as a result of its interaction with a small number (at least two) of nucleons in the nucleus. On this assumption, the π^- rest energy of 140 Mev is shared among a small number of nucleons, and the subsequent excitation of the nucleus results from secondary collisions of these initially energetic nucleons. Tamor considers two specific models for his calculations: (*a*) the two-nucleon model which assumes that the energy release associated with the π^- absorption by a proton is shared by one other nucleon moving in the opposite direction and (*b*) the α particle model which assumes that the π^- meson is absorbed by a proton in an α particle and that the resulting neutron and triton share the energy. Model (*b*) is also called the multinucleon model since the results do not depend sensitively on whether an α particle or a somewhat different small ensemble of nucleons is chosen as the multinucleon structure. On the basis of each model, Tamor calculates the probabilities that the high-energy nucleons [two 70-Mev nucleons on model (*a*), one 93-Mev neutron on model (*b*)] undergo collisions with the other nucleons in the nucleus, correcting the elastic scattering cross sections for Fermi gas effects along the lines of Goldberger[34] and taking account of charge exchange in neutron-proton scattering.[35] When the nucleon energy is degenerated below 30 Mev, the nucleon is considered "lost" to the evaporation star. In this way, one obtains an estimate of the numbers of fast protons and neutrons of energies greater than 30 Mev and the average excitation energy per star. The results are given in Table 7 for nitrogen and silver, chosen as the

TABLE 7. THEORETICAL PREDICTIONS FOR π^- DISINTEGRATION OF NUCLEI

	Model	N	Ag
Number of fast protons per 100 π^- absorptions....	(*a*)	39	16.5
	(*b*)	10.6	8.6
Number of fast neutrons per 100 π^- absorptions...	(*b*)	77.6	49.3
Average excitation energy of evaporation star.....	(*a*)	70 Mev	101 Mev
	(*b*)	72 Mev	98 Mev

---

[33] S. Tamor, *Phys. Rev.*, **77**: 412 (1950); cf. also J. Heidmann and L. LePrince-Ringeut, *Compt. rend.*, **226**: 1716 (1948); P. Cuer and M. Morand, *Compt. rend.*, **226**: 649 (1948); and B. Bruno, *Arkiv. Mat., Astron. Fysik*, **36A**: 1 (1948).

[34] M. L. Goldberger, *Phys. Rev.*, **74**: 1269 (1948); the cross section is divided by 1.4, and the average energy loss per collision is taken as 25 Mev.

[35] The high-energy neutron-proton scattering experiments [cf. Hadley, Kelly, Leith, Segre, Wiegand, and York, *Phys. Rev.*, **75**: 350 (1949)] indicate that the "ordinary" and charge-exchange components contribute about equally.

representative light and heavy nuclei in the photographic emulsion. Table 7 differs[36] somewhat from the table given by Tamor[33] because the neutron-neutron scattering cross section was taken equal to the neutron-proton cross section (to agree with recent experiments on high-energy proton-proton scattering[37]) rather than one-fourth of the neutron-proton cross section as Tamor had done.

Examination of Table 7 reveals that the multinucleon model predicts an appreciably smaller number of fast protons than does the two-nucleon model; this is not at all surprising since in the former model, only one nucleon, *i.e.*, a neutron, is imparted high energy by the initial absorption of the π^- meson by a proton. As a matter of fact, on the multinucleon model, no fast protons would be expected if the elastic neutron-proton collisions did not possess a charge-exchange component. Assuming that one-third of the π^- captures take place in the gelatin of the emulsion, it is evident that the two-nucleon model predicts almost three times as many fast protons (24 per cent) as does the multinucleon model (9 per cent); the latter value is in excellent agreement with experiment (9 to 10 per cent).

The multinucleon model not only predicts correctly the number of fast protons but it also predicts a reasonable value for the average excitation energy of the silver nucleus. In other words, the successive collisions of the high-energy nucleons heat up the nucleus to a temperature ($\approx$ 3 Mev) corresponding to an excitation energy of about 100 Mev, and this temperature can explain the energy spectrum of the low-energy prongs which are observed. Not all low-energy nucleons ($<$ 30 Mev) need be evaporation prongs; an appreciable fraction may be "knock-on" nucleons present on the surface of the nucleus and recoiling from collisions with high-energy nucleons. As a matter of fact, Adelman[25] finds some support for this qualification in that he observes a measurable preference for low-energy protons in the backward hemisphere with respect to the fast protons.

Because of the initial prejudice for neutrons in the elementary act of absorption of a π^- meson by a proton, the multinucleon model also predicts a much larger fraction of high-energy neutrons than of high-energy protons and proportionately more for the light than for the heavy nuclei. This probably explains most of the 28 per cent of the starless π^- disintegrations seen in the emulsion and the even larger fraction of starless π^- disintegrations observed in the gelatin by Menon *et al.*[24] Many of these starless cases probably consist of one and occasionally two fast neutrons and a small number (3 to 5) of evaporation neutrons.

---

[36] The new numbers were calculated by N. Francis.

[37] Birge, Kruse, and Ramsey, *Phys. Rev.*, **83**: 274 (1951).

The fact that perhaps 50 per cent of these starless π^- disintegrations have associated blobs representing nuclear recoils responding to the emission of high-energy neutrons is further support for the multinucleon hypothesis.

5. Decay and Absorption of Slow μ^- Mesons

In contrast to slow π^- mesons which undergo nuclear absorption by all elements including hydrogen, slow μ^- mesons undergo nuclear absorption only for sufficiently large $Z \gtrsim 10$. As Z decreases below 10, nuclear absorption loses out very rapidly to decay; that is to say, at $Z \approx 10$, the lifetime for nuclear absorption is approximately equal to the lifetime for electron decay, namely, 2.1×10^{-6} sec. Since the determination of this transition point is of considerable theoretical importance, we first summarize the experiments bearing on the decay of slow μ^- mesons in light elements before turning to a consideration of the absorption of slow μ^- mesons by heavy nuclei.

The experiment of Conversi *et al.*[38] gave the first clear demonstration that a slow μ^- meson decays in an element as light as carbon ($Z = 6$) instead of being absorbed by the carbon nucleus. At the same time, these workers showed that decay electrons do not emerge from a piece of iron ($Z = 26$) when the μ^- mesons are stopped in iron. If nuclear absorption competes with decay, then the lifetime τ^- for the decay of a μ^- meson from the K shell of a mesic atom can be written as

$$\frac{1}{\tau^-} = \frac{1}{\tau^+} + \frac{1}{\tau_a} \tag{21}$$

where τ^+ = lifetime for the decay of a free μ^- meson = lifetime of a μ^+ meson, τ_a = lifetime for nuclear absorption. Now, in accordance with our discussion in Sec. 3, τ_a should be a sensitive function of the atomic number for light nuclei; in particular, τ_a should satisfy a relation of the form $1/\tau_a = kZ_{\text{eff}}^4$ where k is a constant and Z_{eff} is a function of Z, being equal to Z for small Z and approaching 37 for large Z (cf. Sec. 3). Table 8 lists the theoretical values of Z_{eff}, τ^-, and $f = \tau^-/\tau^+$ as functions of Z; τ^- and f were computed assuming $Z_0 = 10.2$ where Z_0 is defined by the relation $Z_0 = (k\tau^+)^{-\frac{1}{4}}$ so that

$$\frac{1}{\tau^-} = \frac{1}{\tau^+}\left[1 + \left(\frac{Z_{\text{eff}}}{Z_0}\right)^4\right] \tag{22}$$

It is clear from Table 8 that the lifetime for the decay of the μ^- meson is always less than τ^+ and decreases with increasing Z. The column marked

---

[38] Conversi, Pancini, and Piccioni, *Phys. Rev.*, 71, 209 (1947).

TABLE 8. THEORETICAL PARAMETERS RELATING TO THE DECAY AND NUCLEAR ABSORPTION OF SLOW μ^- MESONS

Z	4	5	6	7	8	9	11	12	13	16
Z_{eff}	3.925	4.855	5.78	6.68	7.56	8.40	10.02	10.83	11.58	13.70
$\tau^- \times 10^6\ \text{sec}^{-1}$	2.05	2.00	1.90	1.77	1.61	1.44	1.09	0.92	0.79	0.49
$f = \frac{\tau^-}{\tau^+}$	0.978	0.951	0.907	0.845	0.768	0.684	0.518	0.440	0.376	0.235

Z	26	30	35	47	53	56	74	82	92	∞
Z_{eff}	19.40	21.1	23.0	26.4	27.67	28.25	30.66	31.5	32.17	37.25
$\tau^- \times 10^6\ \text{sec}^{-1}$	0.149	0.108	0.078	0.046	0.038	0.035	0.025	0.023	0.021	0.012
$f = \frac{\tau^-}{\tau^+}$	0.071	0.052	0.037	0.022	0.018	0.017	0.012	0.011	0.010	0.006

f in this table is not merely the ratio of τ^- to τ^+ but should represent the ratio of the number of decay electrons emitted to the number of μ^- mesons stopped, *provided* nuclear absorption is the competing process. This latter statement can be seen as follows: let us write

$$dN^-(t) = N_0^- e^{-(\lambda+\Lambda)t}\lambda\, dt \tag{23}$$

where $\lambda \equiv 1/\tau^+ =$ probability per unit time for decay,

$$\Lambda \equiv \frac{1}{\tau_a} = \text{probability per unit time for absorption,}$$

$N_0^- =$ number of μ^- mesons stopping in the absorber per unit time, $N^-(t) =$ number of decay electrons at time t. Integration of Eq. (23) yields

$$N^-(t) = N_0^- \frac{\lambda}{\lambda + \Lambda}\left[1 - e^{-(\lambda+\Lambda)t}\right] \tag{24}$$

Since μ^+ mesons are not absorbed by nuclei, it is evident that

$$N^+(t) = N_0^+(1 - e^{-\lambda t}) \tag{25}$$

where the notation is obvious. Therefore, after a time long compared with the decay time of the μ meson, the ratio of Eq. (24) to Eq. (25) reduces to

$$\frac{N^-(\infty)}{N^+(\infty)} = \frac{N_0^-\lambda}{N_0^+(\lambda + \Lambda)} \tag{26}$$

If we let $\eta = N_0^-/N_0^+$ be the ratio of the intensities of μ^- to μ^+ mesons stopping in the absorber, then we may write for the ratio f' of the number of electrons from μ^- and μ^+ decay corresponding to equal fluxes of μ^- and μ^+ mesons

$$f' = \frac{1}{\eta}\frac{N^-(\infty)}{N^+(\infty)} = \frac{\lambda}{\lambda + \Lambda} \leq 1 \tag{27}$$

While the hypothesis of nuclear absorption as the process competing with the decay can explain the results of Conversi *et al.*, other hypotheses predicting a rapid decrease in the decay lifetime are not ruled out. For example, one attempt to explain the decrease of τ^- with increasing Z envisaged the decay process as accelerated[39] by the increasing electric fields of heavier nuclei. However, apart from other unrealized predictions, *e.g.*, that photons should accompany μ^+ disintegrations, the "acceleration" theory predicts one decay electron for each μ^- meson stopped, that is, $f' = 1$ although $f < 1$. If, on the other hand, nuclear absorption of the μ^- meson is the competing process, then the number of decay electrons will be less than the number of μ^- mesons stopping in the material and $f' \equiv f < 1$. This point has been settled by further experiments[40] which have measured both f' and f: the lifetime τ^- is deduced from the slope of the disintegration curve of the μ^- meson and f' is determined by extrapolating to zero time the disintegration curves of the μ^- and μ^+ mesons taken during equal time intervals (at the same time correcting for the positive excess, *i.e.*, the fact that $\eta = 0.82$). Figure 8 shows the results of the experiment on aluminum performed by Valley,[40] who found that $\tau^- = 0.70 \pm 0.06 \times 10^{-6}$ sec and $f' = 0.4$ (which is equal to $f = \tau^-/\tau^+$ within the statistical accuracy). The results of Ticho's more extensive experiments are given in Table 9. It is clear that Valley's and Ticho's results definitely favor the hypothesis of nuclear absorption as the competing process rather than accelerated decay.

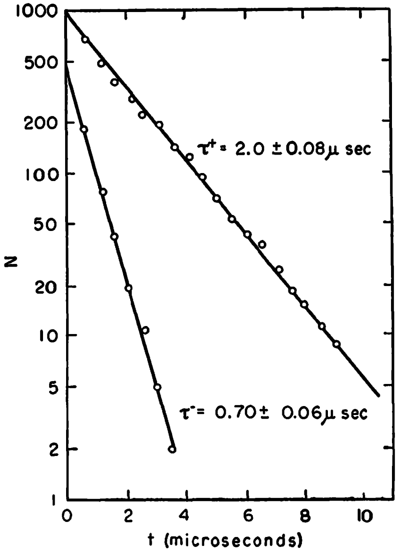

FIG. 8. Measured disintegration curves of μ^+ and μ^- mesons in aluminum; N is the number of observed electrons and t is the time.

---

[39] Cf. Epstein, Finkelstein, and Oppenheimer, *Phys. Rev.*, **73**: 1140 (1948).

[40] G. E. Valley, *Phys. Rev.*, **72**: 772 (1947); H. K. Ticho, *Phys. Rev.*, **74**: 1337 (1948).

TABLE 9. DECAY OF μ^- MESONS IN SEVERAL SUBSTANCES

Substance	Z	τ^- ($\times 10^{-6}$ sec)	$f = \tau^-/\tau^+$	f'
H_2O*	8	1.89 ± 0.15	0.877 ± 0.069	0.833 ± 0.083
NaF†	10.1	1.28 ± 0.12	0.595 ± 0.060	0.602 ± 0.060
Mg	12	0.96 ± 0.06	0.446 ± 0.032	0.558 ± 0.044
Al	13	0.75 ± 0.07	0.34 ± 0.03	0.40 ± 0.03
S	16	0.54 ± 0.12	0.25 ± 0.04	0.28 ± 0.03

* Only O is effective since the H rarely captures the μ^- meson (cf. Sec. 3)

† The effective Z is computed assuming the validity of the Z law for mixtures (cf. Sec. 3).

Recently, Harrison *et al.*[41] have employed liquid scintillation counters to measure τ^- in Cu and Sb by detecting the nonionizing radiations (γ rays and neutrons of several Mev) accompanying μ^- absorption in these two elements. Their results are: $\tau^-(\text{Cu}) = 1.22 \pm 0.14 \times 10^{-7}$ sec and $\tau^-(\text{Sb}) = 5.0 \pm 0.6 \times 10^{-8}$ sec. These numbers, together with those of Valley and Ticho, can be used to deduce τ_a^{-1} [from Eq. (21)] which is plotted in Fig. 9 as a function of Z_{eff} (taken from Table 8). The straight line which is drawn in Fig. 9 represents the equation

$$\frac{1}{\tau_a} = \frac{1}{\tau^+}\left(\frac{Z_{\text{eff}}}{10.3}\right)^4 \tag{28}$$

where $\tau^+ = 2.15 \times 10^{-6}$ sec. The agreement between theory[42] and experiment is therefore quite good and demonstrates the great importance of the finite radius of the nucleus [*e.g.*, for antimony, if $Z = 51$ were used in Eq. (28) instead of $Z_{\text{eff}} = 27$, τ_a would be reduced by a factor of 0.08].

The fact that $Z_0 \approx 10$ implies that $\tau_a \approx \tau^+ = 2.1 \times 10^{-6}$ sec for $Z \approx 10$. The long lifetime for μ^- absorption from the K shell is to be compared with a lifetime of about 10^{-19} sec[43] expected for π^- absorption from the K shell of a mesic atom with $Z \approx 10$. The enormous factor of 10^{13} in the strength of the coupling of the μ^- and π^- mesons to the proton spells out the fundamentally different properties of the two types of mesons. As a matter of fact, the striking discrepancy between the value of τ_a observed for the μ^- meson and the value which would be expected if the μ meson were responsible for nuclear forces (a discrepancy first emphasized by Fermi *et al.*[4]) led to the two-meson hypothesis[44] even before the π meson was discovered. In accordance with the two-meson hypothesis, charged π mesons are strongly coupled to nucleons and are produced with large cross sections, whereas μ mesons are decay products

---

[41] Harrison, Keuffel, and Reynolds, *Phys. Rev.*, **83**: 680 (1951).

[42] In making a more refined comparison between theory and experiment, one must make a small correction for the fact that the μ^- meson decays from the K shell of the mesic atom, *viz.*, one must decrease the decay lifetime by the factor $(Z_{\text{eff}}/137)^2$ [cf. H. Primakoff, *Phys. Rev.*, **74**: 878 (1948)].

[43] This approximate value is estimated by using a lifetime of 10^{-15} sec for the absorption of the π^- meson from the K shell of deuterium (since hydrogen leads to the emission of γ rays—cf. Chap. 4) and extrapolating in accordance with the Z_{eff}^4 law.

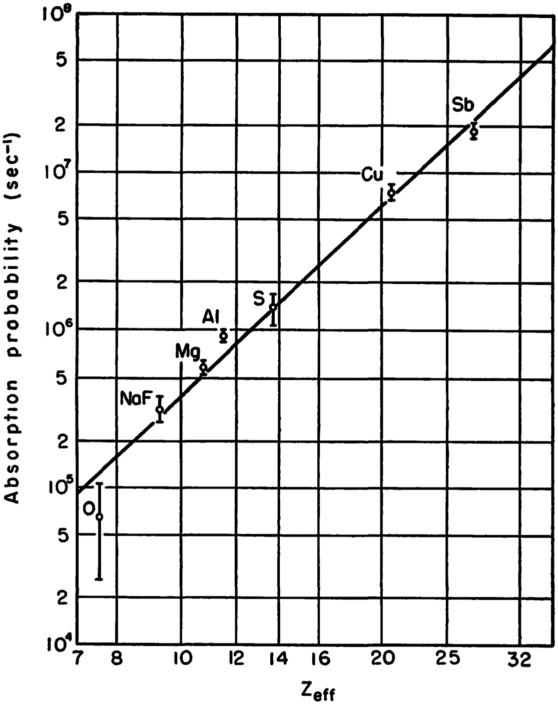

FIG. 9. Measured absorption probabilities of slow μ^- mesons as a function of Z_{eff}; the solid line represents the curve $k(Z_{\text{eff}})^4$ (k is a constant).

of π mesons and experience weak interactions with nucleons as a consequence of their weak coupling to charged π mesons. Applied to the present problem of the nuclear absorption of μ^- mesons, this hypothesis would imply that a μ^- meson is absorbed by a proton via the following two-step process:

---

[44] R. Marshak and H. Bethe, *Phys. Rev.*, **72**: 506 (1947); a two-meson theory was proposed independently by S. Sakata and T. Inoue [*Prog. Theor. Phys.*, **1**: 143 (1946)] in order to explain the low cross section for the nuclear scattering of cosmic-ray mesons and the difficulties with Yukawa's scheme of nuclear beta decay. However, since neither phenomenon was so glaringly contradictory as the observed μ^- decay in light elements, Sakata and Inoue predicted much too short a lifetime for $\pi \rightarrow \mu$ decay, that is, 10^{-21} sec instead of 10^{-8} sec.

$$\mu^- \rightarrow \left\{ \begin{matrix} \pi^- + \nu + P \\ \mu^- + \pi^+ + N \end{matrix} \right\} \rightarrow N + \nu \tag{29}$$

In other words, the μ^- may virtually create a (π^-, ν) pair and the P a (π^+, N) pair, both of which lead to the same final state of neutron plus neutrino. The probability for this indirect coupling of the μ^- meson to the proton can be calculated[44] from a knowledge of the coupling of the charged π meson to the nucleon (which may be derived from such experiments as the photonic and nucleonic production of charged π mesons) and the lifetime for the μ decay of the charged π meson.

Latter[45] has calculated the probability for the absorption of a μ^- meson by a proton in a nucleus on the basis of the hypothesis (29). Since we now know that the π meson is pseudoscalar (cf. Chap. 4) and that the μ meson very likely possesses spin $\frac{1}{2}$ (cf. Chap. 6), we record only Latter's formula corresponding to this assignment of π and μ meson spins and parities;[46] $PS(PV)$:

$$\frac{1}{\tau_a} = \frac{\pi}{3}\left(\frac{f^2}{\hbar c}\right)\left(\frac{F_\mu^2}{\hbar c}\right)\frac{E_n^2}{m_\pi c^2}\left(\frac{E_n}{Mc^2}\right)^2 \frac{|\phi(0)|^2}{(m_\pi c/\hbar)^3} \left| \sum_{\text{protons}} \int d\mathbf{r}\Psi_N^* \left(\frac{\tau_x + i\tau_y}{2}\right)\Psi_P e^{-i\mathbf{k}_n\cdot\mathbf{r}} \right|^2 \tag{30}$$

In Eq. (30), E_n is the energy of the neutrino, k_n its momentum, $\phi(0)$ is the wave function of the μ^- meson evaluated at the nucleus, Ψ_N and Ψ_P are the nucleon wave functions, f is the π meson-nucleon coupling constant, and F_μ is the $\pi \rightarrow \mu$ coupling constant. The values of $F_\mu^2/\hbar c$ are determined by the lifetime for $\pi \rightarrow \mu$ decay (*i.e.*, $2.5_5 \times 10^{-8}$ sec) in accordance with Eq. (9) of Chap. 4 and the value of $f^2/\hbar c$ is taken as 0.3 (cf. Chaps. 1 and 2). In order to derive numbers for τ_a, it is necessary to evaluate the nuclear matrix element. The evaluation of the nuclear matrix element is complicated; and in order to obtain a reasonable estimate, Latter made several simplifying assumptions, namely: (*a*) The energy imparted to the nucleus is small compared with the rest mass of the μ meson. This seems to be in accord with experiment and is expected since the light neutrino should leave with most of the available energy.[47] (*b*) Plane wave functions can be used for the π^- meson in the virtual state; this should be a good approximation since the μ^- meson is essentially at rest. (c) The nucleus can be treated as a point; this is certainly justified for Z in the neighborhood of 10. On the basis of these assumptions it turns out that a reasonable estimate of the nuclear matrix element is $Z/3$, and inserting numbers into Eq. (30), that is, $Z = 10$, etc., Latter finds $\tau_a = 2 \times 10^{-7}$ sec. This value of τ_a is a factor 10 too large; however, in view of the uncertainty in the nuclear matrix element, the π meson-nucleon coupling constant, etc., this does not necessarily constitute disagreement.

---

[45] R. Latter, Ph.D. Thesis, California Institute of Technology, 1948.

[46] The equivalence theorem holds between PS and PV coupling.

[47] In this connection it is worth recalling that the π^- absorption by a proton yields a zero-mass γ ray of about 130 Mev.

An alternative approach to the problem of the nuclear absorption of μ^- mesons was first enunciated by Pontecorvo.[48] He was impressed by the fact that the lifetime for μ^- absorption from the K shell of a mesic atom is of the same order of magnitude as the probability for an ordinary K-electron capture process when proper account is taken of the differences in available energy and in the volumes of the electron and μ^- K orbits. This analogy may be genuinely significant (cf. Chap. 6) and may imply that there is a direct interaction between the (μ, ν) fields and the (P, N) fields of the same form and with exactly the same coupling constant required by the theory of beta decay. If this is the case, the K-electron capture reaction

$$e^- + P \rightarrow N + \nu$$

is to be replaced by the μ^- absorption reaction

$$\mu^- + P \rightarrow N + \nu$$

Inserting appropriate values for the available energy and the Coulomb wave function for the μ^- meson (corresponding to $Z = 10$) into Moller's formula[49] for allowed K-electron capture, we find $\tau_a = 9 \times 10^{-7}$ sec, which is certainly consistent with the experiment value (the coupling constant has been chosen as 2×10^{-49} erg cm^3).

At the present time, it is difficult to decide whether the indirect or direct coupling theory for μ^- absorption is correct. However that may be, both theories predict that nuclear absorption of a slow μ^- meson will be accompanied by the emission of a light neutral particle, *viz.*, a neutrino. This prediction has the consequence, already referred to above, that the residual nucleus will be left in a state of low excitation energy. Rosenblueth[50] has calculated the excitation energy for a heavy nucleus (assuming equal numbers of neutrons and protons, Fermi gas model, etc.) which is expected on the basis of the absorption mechanism $\mu^- + P \rightarrow N + \nu$. His curve is plotted in Fig. 10 and shows that 15 Mev is a reasonable estimate of the mean excitation energy and that 20 Mev is essentially an upper limit. An excitation energy of the order of 15 to 20 Mev would explain the qualitatively different phenomena which are associated with nuclear absorption of μ^- and π^- mesons despite the fact that the masses of the μ^- and π^- mesons differ by only 30 per cent. When a π^- meson is absorbed by a nucleus, the prong distribution, the energy spectrum of the protons, etc., all indicate mean nuclear excitation energies of 100 Mev or so (cf. Sec. 4). On the other hand, when a μ^- meson stops in a heavy material, visible prongs are rarely observed, and other experimental evidence indicates that the mean excitation energy of the nucleus following μ^- absorption is indeed of the order of 15 to 20 Mev.

---

[48] B. Pontecorvo, *Phys. Rev.*, **72**: 246 (1950).

[49] C. Moller, *Physik. Z. Sowjetunion*, **11**: 9 (1937).

[50] M. N. Rosenblueth, *Phys. Rev.*, **75**: 532 (1949); J. Tiomno and J. Wheeler [*Rev. Mod. Phys.*, **21**: 153 (1949)] have made the same calculation with the same result. The latter authors have also calculated the excitation curve on the basis of two other models (Hartree and dipole) with similar results.

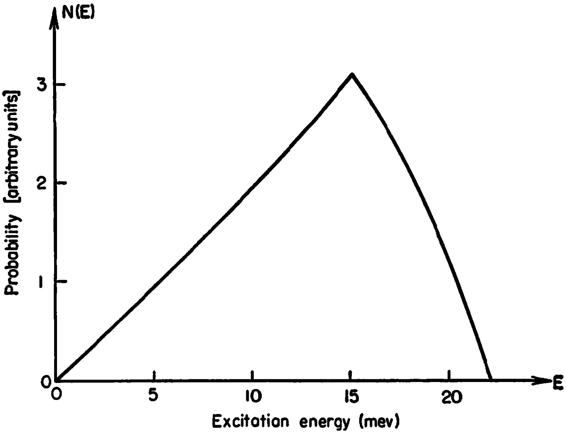

FIG. 10. Theoretical distribution of nuclear excitation energies resulting from the absorption of μ^- mesons by a complex nucleus on the basis of the Fermi gas model.

Several authors[51] have looked for charged particles accompanying nuclear absorption of slow μ^- mesons but without conclusive results. However, recently, George and Evans[52] have exposed photographic emulsions underground at a depth of 20 to 60 m.w.e. (meters of water equivalent) and have seen nuclear stars produced by slow μ^- mesons. The method of George and Evans has the advantage that π^- mesons are eliminated and most of the nuclear stars observed must be due to μ^-

---

[51] Cf. footnotes 8 and 18; also H. G. Voorhees and J. Street, *Phys. Rev.*, **76**: 1100 (1949); C. Franzinetti, *Phil. Mag.*, **41**: 86 (1950).

[52] E. George and J. Evans, *Proc. Phys. Soc.*, **64A**: 193 (1951); cf. W. F. Fry, *Phys. Rev.*, **86**: 676 (1952).

mesons. In previous experiments, whether aboveground in cosmic-ray work or with accelerators, the occasional small stars produced by μ^- mesons were obscured by the much more efficient star-forming π^- mesons. George and Evans, in their experiment, examined 250 cm^3 of emulsion and found 30 meson-induced stars, $5\pi \rightarrow \mu$ decays, and 1014 μ mesons. Since the number of π mesons deep underground must be small and consist almost equally of π^+ and π^- mesons, most of the meson-induced stars cannot be due to π^- mesons but must be due to μ^- mesons. Further support for this deduction is furnished by the prong distribution of the 30 stars which are seen; this prong distribution is given in Table 10 together with the prong distribution of 30 meson-induced stars observed at mountain altitudes. Since the meson-induced stars at mountain altitudes are known to be due primarily to π^- mesons, the discrepancy between the prong distributions in Table 10 adds strong weight to the statement that the underground stars are initiated chiefly by μ^- mesons. Finally, conclusive evidence is provided by two further observations: the marked collimation in the downward direction of the mesons producing the underground stars (in accord with a similar collimation of the fast μ mesons), in contrast to the roughly isotropic distribution of $\pi \rightarrow \mu$ decays, and the similar variation with depth (from 20 to 60 m.w.e.) of both the stars and the μ mesons. Consideration of the detailed structure of π^- induced stars (in particular the three-prong stars) leads to the assignment of 5 of the underground stars (1 one-prong, 2 two-prong, and 2 three-prong) to π^- mesons. This leaves 22 one-prong and 3 two-prong stars which are attributed to μ^- disintegrations. The 3 two-prong stars are completely atypical of π^- disintegrations because of the extremely low energy (1 to 2 Mev) of the emitted charged particles. From the measured value[53] of 1.27 for the ratio of positive to negative particles with momentum10^{10} ev/c at sea level (the momentum required by μ mesons to reach 20 to 60 m.w.e. underground), George and Evans conclude that approximately 458 out of the total of 1039 (1014 + 25) μ mesons which are observed are negative. Since about two-thirds of these are captured in Ag and Br^9 and 20 per cent of those captured in gelatin are absorbed, it follows that about 336 μ^- mesons were absorbed by nuclei. This implies that 7.5 ± 1.5 per cent of the μ^- disintegrations lead to the emis-

TABLE 10. PRONG DISTRIBUTION OF UNDERGROUND AND MOUNTAIN-ALTITUDE STARS

Number of prongs	1	2	3	4	5
Underground stars	23	5	2	0	0
Mountain-altitude stars	10	8	7	4	1

---

[53] B. Owen and J. Wilson, *Proc. Phys. Soc.*, **62**: 601 (1949).

sion of charged particles and that the mean prong number is 0.08 ± 0.02. These results can be reconciled with the earlier statement that the average excitation energy which a nucleus receives from the absorption of a μ^- meson is 15 to 20 Mev.

If absorption of slow μ^- mesons by heavy nuclei leads to an average excitation energy in the neighborhood of 15 to 20 Mev, neutron emission should be much more probable than proton emission. Indeed, a calculation of the predicted mean neutron multiplicity on the basis of the Fermi gas model for the distribution of nuclear excitations and Weisskopf's statistical theory of neutron evaporation[54] leads to a value of 0.9; this is a factor of 15 greater than the number of protons. Several authors have investigated the neutron emission resulting from the absorption of slow μ^- mesons stopped in various elements. One of the first experiments was carried out by Sard *et al.*,[55] who looked for neutrons resulting from nuclear absorption of μ^- mesons in lead. Sard *et al.* used BF_3 counters (enriched with B^{10}) embedded in paraffin to slow down the neutrons. The counters were delayed 80 microsec with respect to the μ mesons stopping in the lead, since it takes neutrons about 150 microsec to slow down in paraffin to thermal velocity so that they can be absorbed by B^{10}. With this experimental setup, Sard *et al.* found positive evidence for neutron emission accompanying nuclear absorption of μ^- mesons and determined the mean neutron multiplicity to be of the order of 2 or 3. More recent experiments have led to more accurate values of the mean neutron multiplicity: thus Groetzinger *et al.*[56] have focused negative μ mesons at sea level onto a lead absorber by means of a magnetic cosmic-ray spectrometer and have detected the neutrons with the same type of counter arrangement as Sard *et al.*; based on 5500 stopped μ^- mesons, these authors find a mean neutron multiplicity of 1.96 ± 0.72. Crouch and Sard,[57] working under 2000 g/cm² of clay and limestone and a 144 g/cm² lead filter, found that μ^- mesons absorbed in lead give rise to neutrons with a mean multiplicity of 2.16 ± 0.15. Finally, Conforto and Sard,[54] working at sea level, studied the neutron emission accompanying the nuclear absorption of μ^- mesons in lead, calcium, and magnesium. The average number of neutrons emitted per μ^- absorption was found to be 1.47 ± 0.13 in Pb, and not more than one-fifth of this value in Ca or Mg. The value of 1.47 ± 0.13 is claimed by the authors not to be incompatible with the value 2.16 ± 0.15 obtained by Crouch and Sard in the underground measurements because of certain systematic errors entering the latter experiment. The most reliable value for the mean neutron multiplicity from lead seems therefore to be close to 2; this number seems to be markedly higher than the value 0.95 predicted by the Fermi gas model and the statistical evaporation theory It is not clear at the present time whether the discrepancy reflects the approximations made in the theoretical calculation or is indicative of something more fundamental. It is also not clear why so few neutrons accompany μ^- absorption in Mg and Ca, unless the effect is associated with a special property of α particle nuclei.

---

[54] A. Conforto and R. Sard, *Phys. Rev.*, **86**: 465 (1952).

[55] Sard, Ittner, Conforto, and Crouch, *Phys. Rev.*, **74**: 97 (1948); cf. G. Groetzinger and G. McClure, *Phys. Rev.*, **74**: 341 (1948).

[56] Groetzinger, Berger, and McClure, *Phys. Rev.*, **81**: 969 (1951).

[57] M. Crouch and R. Sard, *Phys. Rev.*, **85**: 120 (1952).

In conclusion, it is worth noting that an experiment has been performed to decide whether the light neutral particle which accompanies the nuclear absorption of a μ^- meson and departs with most of the available energy (120 to 125 Mev) is a γ ray. Piccioni[58] has searched for high-energy γ rays resulting from μ^- mesons stopping in iron and has shown that there are no γ rays above 20 Mev. The evidence is therefore very strong that the nuclear absorption of a slow μ^- meson leads to the emission of some form of neutrino.

[58] O. Piccioni, *Phys. Rev.*, **74**: 1754 (1948).

CHAPTER 6

PROPERTIES OF THE μ MESON

1. Introduction

One of the most surprising developments in the field of meson physics during the past few years has been the dethroning of the μ meson—the meson most commonly observed in cosmic rays—from its former exalted position of supreme interest for an understanding of nuclear forces and cosmic-ray phenomena to its present subsidiary position with hardly any apparent reason for existing at all. When Anderson and Neddermeyer[1] and Street and Stevenson[2] discovered a particle of mass intermediate between proton and electron in the cosmic rays, this new particle, now called the μ meson, was immediately identified with Yukawa's[3] hypothetical heavy quantum which had been postulated two years earlier in order to explain the magnitude, short range, and exchange character of nuclear forces. When Yukawa's further suggestion that the heavy quantum would be unstable and decay into an electron (hypothesized to account for nuclear beta decay through the sequence of transitions:

$$N + \bar{\nu} \rightarrow \left\{ \begin{matrix} P + \mu^- + \bar{\nu} \\ N + \mu^+ + e^- \end{matrix} \right\} \rightarrow P + e^- \tag{1}$$

where $\bar{\nu}$ is the antineutrino) with a lifetime of the order of microseconds was confirmed by experiment, it was believed that an explanation of nuclear forces and of the principal features of cosmic-ray phenomena was near at hand. However, experimental data soon accumulated which implied that normal cosmic-ray mesons (*i.e.*, the μ mesons) interact weakly with nuclei at low altitudes in contradistinction to their apparent large production cross section in the high atmosphere. It was found that the nuclear scattering cross section for μ mesons at sea level was extremely small, that μ mesons penetrated to much greater depths underground than was reconcilable with their presumed strong coupling to nucleons, and so on. The final blow to the identification of the μ meson with the Yukawa particle came with the experiment of Conversi *et al.*[4] on the decay of μ^- mesons in light nuclei. Shortly thereafter, Lattes *et al.*[5] discovered the π meson, and numerous experiments soon demonstrated that it was the π meson, not the μ meson, which possessed many of the properties of the Yukawa particle. The μ meson, it turns out, is merely a decay product of the π meson, and its importance for an understanding of nuclear phenomena seems to have vanished.

---

[1] C. Anderson and S. Neddermeyer, *Phys. Rev.*, **51**: 884 (1937).

[2] C. Street and E. Stevenson, *Phys. Rev.*, **51**: 1005 (1937).

[3] H. Yukawa, *Proc. Phys.-Math. Soc. Japan*, **17**: 48 (1935).

[4] Conversi, Pancini, and Piccioni, *Phys. Rev.*, **71**: 209 (1947); this experiment is discussed in considerable detail in Chap. 5.

Despite the fact that the μ meson appears to have little bearing on nuclear forces and nuclear processes in general, we shall discuss its properties because of the illuminating contrast between them and those of the π meson. Moreover, apart from the fact that certain μ meson experiments yield information concerning the π meson, a study of the μ meson may provide a clue to a future comprehensive theory of elementary particles. With these points in mind, we shall discuss the mass, lifetime, decay, spin, statistics, electromagnetic properties, and nuclear interactions of the μ meson.

It should be remarked that no evidence has been found for the existence of a μ^0 meson. Presumably such evidence would be difficult to gather because a μ^0 meson would possess many of the properties of a neutrino (spin $\frac{1}{2}$, extremely weak interaction with matter, etc.—cf. below). Our discussion will therefore be confined to the charged μ meson.[5a]

2. Mass of the μ Meson

The numerical value of the mass of the μ meson is certainly no clue to the tremendous disparity between it and the π meson. The best "accelerator" value of the μ^+ meson mass has been derived by Barkas and coworkers[6] from a measurement of the mass ratio of the π^+/μ^+ meson (determined by magnetic curvature and range) and the value of the absolute momentum of the μ^+ meson (derived from π mesons decaying at rest—cf. Chap. 4). Barkas finds $m(\mu^+) = 209.6 \pm 2.5\, m_e$ where m_e is the electron mass. The μ^- meson possesses the same mass as the μ^+ meson within experimental error, according to a cloud-chamber measurement of Lederman *et al*;[7] by studying 75 $\pi^- \rightarrow \mu^-$ decays in flight in a 16-in. cloud chamber subjected to a magnetic field, the Columbia group derived a value $209.8 \pm 2.2m_e$ for the mass of the μ^- meson, assuming the π^- meson mass to be $276.1 \pm 1.3m_e$.[6] The best cosmic-ray measurement of the μ meson mass was carried out by Brode and coworkers,[8] using a set of cloud chambers with magnetic field and lead plates (curvature plus range method); combining the data for μ^+ and μ^- mesons, the Berkeley cosmic-ray group finds $m(\mu) = 215 \pm 4m_e$. This result is certainly consistent with the "accelerator" values.

---

[5] Lattes, Occhialini, and Powell, *Nature*, **160**: 453 (1947); cf. also O. Piccioni, *Phys. Rev.*, **77**: 1 (1950).

[5a] Cf., however, G. Uhlenbeck and C. Chang, *Phys. Rev.*, **85**: 684 (1952).

[6] W. H. Barkas, *UCRL* No. 1285.

[7] Lederman, Booth, Byfield, and Kessler, *Phys. Rev.*, **83**: 685 (1951).

[8] R. B. Brode, *Rev. Mod. Phys.*, **21**: 38 (1949); cf. also J. Retallack and R. Brode, *Phys. Rev.*, **75**: 1716 (1949).

3. Decay of the μ Meson

A. Lifetime. A great many cosmic-ray experiments have been performed to measure the lifetime for decay of the μ meson. The earliest determinations were indirect and were based on the absorption anomalies associated with the penetrating component of the cosmic radiation. Thus the penetrating particles appeared to decrease in intensity more rapidly in air than in condensed matter for the same amount of material in g/cm^2. Also, the intensity decreased more rapidly with increasing zenith angle than could be explained by merely considering the greater mass (in g/cm^2) of material traversed by the penetrating particles coming from inclined directions. Both these anomalies could be understood in terms of an instability of the μ meson; as a matter of fact, the empirical data led to a value[9] of 2.5×10^{-8} sec/Mev for the ratio of lifetime τ to rest energy of the μ meson. With a value of $210m_e$ for the μ meson mass, τ becomes 2.4×10^{-6} sec—a value fairly close to the correct value of 2.1×10^{-6} sec (cf. below). The best cosmic-ray determination of the μ^+ meson lifetime was made by Rossi and Nereson[10] by means of a method of delayed coincidences; they obtained the value $\tau^+ = 2.15 \pm 0.07 \times 10^{-6}$ sec. More recently, Alvarez *et al.*[11] have measured the lifetime of the μ^+ meson by detecting, with scintillation counters operating in delayed coincidence, the decay of the μ^+ arising from artificially produced π^+ mesons; they found $\tau^+ = 2.09 \pm 0.03 \times 10^{-6}$ sec from a curve covering an intensity variation of a factor of 10^4. The different values agree within their statistical errors, and we shall use 2.1×10^{-6} sec as the lifetime. We have already discussed in Chap. 5 the effect on the μ^- meson lifetime of competition from nuclear absorption. All evidence points to an equality of μ^- and μ^+ meson lifetimes in the absence of matter.

B. Decay Products. 1. *Experimental results.* The true nature of the decay particles resulting from the spontaneous disintegration of the μ meson has only recently been elucidated. For a long time, it was thought that the μ meson decays into an electron and a neutrino, each departing with about 50 Mev apiece. However, in 1947, Anderson *et al.*[12] obtained two cloud-chamber photographs, each showing a μ meson decaying into an electron with an energy of about 25 Mev. Soon thereafter, many experimentalists secured evidence for the nonuniqueness of the electron energy (two-particle decay should lead to a unique energy), and it is now certain that the μ meson emits a continuous spectrum of electrons. The latter fact implies that the decay of the μ meson is accompanied by the emission of at least two neutral particles in addition to an electron.

---

[9] Rossi, Hilberry, and Hoag, *Phys. Rev.*, **57**: 461 (1940).

[10] B. Rossi and N. Nereson, *Phys. Rev.*, **62**: 417 (1942).

[11] Alvarez, Longacre, Ogren, and Thomas, *Phys. Rev.*, **77**: 752 (1950).

[12] Anderson, Adams, Lloyd, and Rau, *Phys. Rev.*, **72**: 724 (1947).

The first real electron *spectrum* from μ meson decay was measured by Leighton *et al.*[13] with a cloud chamber in a magnetic field of about 7000 gauss exposed to the cosmic radiation; 75 decay electron tracks were measured, and it was found that the electron spectrum extends from 9 to 55 Mev. The observed upper limit of the spectrum implies a μ meson mass of $217 \pm 4\ m_e$ assuming the decay scheme $\mu \rightarrow e + 2\nu$ (ν is a neutral particle of mass 0, presumably a neutrino) although it was not clear, in view of the experimental error, whether the spectrum at the upper limit had a finite or zero cutoff. The mean electron energy turned out to be about 35 Mev—about one-third of the μ meson rest mass—and therefore argued against more than two neutral particles (in addition to the electron).

Further evidence, though not so accurate as the cloud-chamber evidence, for a continuous electron spectrum was obtained more recently by Davies *et al.*[14] using photographic plates. These authors measured the energies of 81 decay electrons and obtained a peak in the energy distribution somewhere between 35 and 40 Mev. The observed spread of energies was definitely outside the statistical spread which would have resulted from a single decay energy. The upper limit of the spectrum was not so sharply defined as in the cloud-chamber experiment but nevertheless led to a reasonable mass for the μ meson, namely, $204 \pm 19m_e$. A second photographic measurement of the electron spectrum from μ decay has been made recently by Bramson and Havens;[15] their results, based on 117 decays, are shown in Fig. 1. If the average electron energy is taken as one-third of the total available energy, the mass of the μ meson can be inferred from Fig. 1 and turns out to be $209.3 \pm 2.2m_e$. The Columbia authors believe that their points imply a finite cutoff at the high-energy end (in disagreement with Sagane *et al.*[16]—cf. below), although the statistical nature of the multiple scattering measurements (by means of which the electron energies were determined) must make this conclusion questionable. The most recent and most accurately determined electron spectrum from μ^+ meson decay has been obtained by Sagane *et al.*,[16] using a spiral-orbit spectrometer in conjunction with the Berkeley cyclotron; their spectrum is shown in Fig. 2 including the corrections due to the finite resolution of the spectrometer. The salient features of the spectrum of Sagane *et al.* are: (1) the maximum energy = 53 ± 2 Mev, from which one derives a μ meson mass = $212 \pm 5\ m_e$; (2) the intensity is a maximum at $70 \pm 3 m_e c$ on a momentum scale; and (3) the intensity is zero[16a] at the upper limit of the spectrum within the experimental accuracy (10 per cent of the maximum intensity).

---

[13] Leighton, Anderson, and Seriff, *Phys. Rev.*, **75**: 1432 (1949); cf. R. W. Thompson, *Phys. Rev.*, **74**: 490 (1948); and J. Steinberger, *Phys. Rev.*, **75**: 1136 (1949).

[14] Davies, Lock, and Muirhead, *Phil. Mag.*, **40**: 1250 (1949).

[15] H. Bramson and W. Havens, *Phys. Rev.*, **83**: 861 (1951); cf. R. Levi-Setti and G. Tomasini, *Nuovo cimento*, **8**: 994 (1951).

[16] Sagane, Gardner, and Hubbard, *Phys. Rev.*, **82**: 557 (1951).

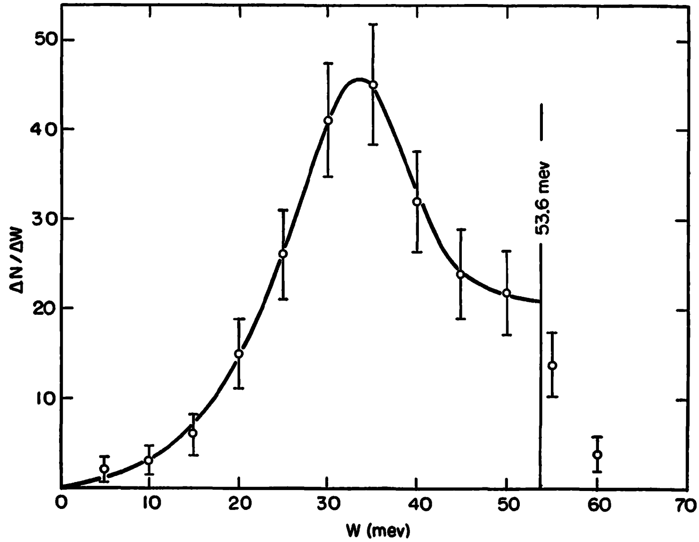

FIG. 1. Measured electron spectrum from μ^+ decay (Bramson and Havens); the solid curve represents the best fit to the experimental points.

We have referred to the charged particle resulting from the decay of a μ meson as an electron; this statement must be proved. The best demonstration that the charged decay particle indeed possesses electronic mass comes from an experiment by Hincks and Pontecorvo,[17] who investigated the penetration of the charged decay particles from μ mesons through various absorbers. They found two components in the decay radiation, one of which was more penetrating than the other. In a lead absorber, for example, the "soft" component was absorbed by 20 g/cm² while the "hard" component was still detected after 40 g/cm^2. The "soft" component is the charged particles whereas the "hard" component is the bremsstrahlung radiation associated with the charged particles constituting the "soft" component. The actual intensity of the "hard" component requires a mass[18] less than $2m_e$ for the charged decay particle. Further support for the electronic nature of the charged decay particle from the μ meson comes from an observation of the collision of one of the decay particles with an electron in a photographic emulsion and a measurement of the energies before and after the collision by means of the scattering method.[19] It turns out that the conservation law requires the charged decay particle to be an electron.

[16a] More recent than the experiment of Sagane *et al.* are some recent cloud-chamber experiments by A. Lagarrigue and C. Peyrou [*J. Phys. Radium*, **12**: 848 (1951)] and H. W. Hubbard (*UCRL* No. 1623) whose results can only with difficulty be reconciled with zero cutoff. A conclusive experiment still remains to be done.

[17] E. Hincks and B. Pontecorvo, *Phys. Rev.*, **77**: 102 (1950).

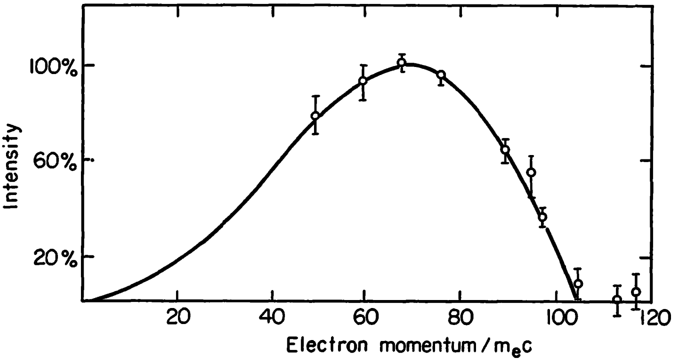

FIG. 2. Measured electron spectrum from μ^+ decay (Sagane *et al.*); the solid curve represents Eq. (9) in the text.

It is still necessary to fix the nature of the neutral particles resulting from the decay of a μ meson. It was known for a long time[20] from an analysis of the soft component of the cosmic radiation in equilibrium with the penetrating component that not all the μ meson energy is converted into soft component, *i.e.*, electrons and γ rays. Hincks and Pontecorvo,[21] however, performed a direct experiment (looking for coincidences between decay electrons and materialized γ rays) in order to decide definitely whether or not one of the neutral decay particles is a photon; their result was completely negative.

---

[18] Cf. D. Feer, *Phys. Rev.*, **75**: 731 (1949).

[19] U. Camerini and P. Fowler, quoted in C. F. Powell, *Reports on Progress in Physics*, **13**: 350 (1950).

[20] Cf. K. Greisen, *Phys. Rev.*, **61**: 121 (1942); the most recent proof was given by W. L. Kraushaar [*Phys. Rev.*, **76**: 1045 (1949)], who measured the number of electrons with energies greater than 10 Mev at sea level and showed that his value of 0.60×10^{-2} /cm^2 sec was consistent with at most 50 per cent conversion of meson energy into soft component.

[21] E. Hincks and B. Pontecorvo, *Phys. Rev.*, **73**: 257 (1948); cf. also R. Sard and E. Althaus, *Phys. Rev.*, **74**: 1364 (1948).

All the quoted experimental results lead to the following unique decay scheme for the μ meson (provided that we do not introduce any new neutral particles of small rest mass):

$$\mu^{\pm} \rightarrow e^{\pm} + 2\nu \tag{2}$$

where ν represents a neutrino. Equation (2) implies at once that the μ meson is a fermion. If one is willing to consider the possibility of a new neutral decay particle of small rest mass (we shall call it a neutretto and denote it by μ^0), then an alternative decay scheme would be

$$\mu^{\pm} \rightarrow e^{\pm} + \nu + \mu^0 \tag{3}$$

If μ^0 were a fermion, then μ would be a fermion; and if, further, the upper limit on the μ^0 mass is several electron masses (as seems to be indicated by the experimental data), then the various theoretical predictions (*e.g.*, the electron spectra) would be qualitatively the same as for the two-neutrino mode of decay. Hence, we shall disregard this possibility and consider scheme (3) only for a boson μ^0. If μ^0 is a boson, then Eq. (3) implies that the μ meson is a boson (possessing spin 0 rather than spin 1 or higher, as is required by the burst production experiments, cf. below). However, in order to explain the absence of visible star excitation energy, we would then have to assume that the absorption of a μ^- meson by a heavy nucleus involves the emission of a boson μ^0. Also, since the π meson is a boson, we would have to assume that the π decay scheme is $\pi^+ \rightarrow \mu^{\pm} + \mu^0$.. The decay scheme (3) appears to be excluded by the spectrum of Sagane *et al.*, as we shall see below.

2. *Theoretical predictions.* The various types of electron spectra which are predicted by theory for the decay scheme (2) were first investigated by Michel[22] and Tiomno *et al.*[23] These authors have worked out all possible spectra corresponding to decay scheme (2) without introducing derivatives of the spinor wave functions into the interaction Hamiltonian (in analogy with the theory of β decay). Despite this simplifying assumption, the calculations are complicated by the fact that the reaction may be assumed to proceed in three different ways, depending on whether the μ meson decays into an electron plus two neutrinos, one neutrino plus one antineutrino, or two antineutrinos. The decay scheme (3) has been investigated by Tiomno.[23a]

---

[22] L. Michel, *Nature,* **163**: 959 (1949).

[23] Tiomno, Wheeler, and Rau, *Rev. Mod. Phys*, **21**: 144 (1949); there are several numerical errors in this reference which have been corrected in L. Michel, *Proc. Phys. Soc.*, **63A**: 514 (1950).

[23a] J. Tiomno, *Phys. Rev.*, **76**: 856 (1949).

In nuclear β decay, only one neutral particle is emitted, and it may be a neutrino or an antineutrino; moreover, it is customary to couple the neutron and proton together in one covariant and the electron and neutrino or antineutrino in a second covariant, and to combine the two covariants in such a manner as to yield a scalar interaction Hamiltonian. In other words, one writes, for the interaction Hamiltonian,[24]

$$H_i = G_\beta(\psi_P^c C^{-1} O_i \psi_N)(\psi_e^c C^{-1} O_i \psi_\nu) \tag{I}$$

or

$$H_i = G_\beta(\psi_P^c C^{-1} O_i \psi_N)(\psi_e^c C^{-1} O_i \psi_\nu^c) \tag{II}$$

where the subscript notation is obvious, the superscript c denotes the charge conjugate spinor, and O_i is one of the five interaction operators: scalar, vector, tensor, axial vector, or pseudoscalar.[25] The two types of interaction Hamiltonians written out above are designated—for obvious reasons—as charge-exchange interactions; charge-exchange interaction (I) represents the process $N \rightarrow P + e^- + \bar{\nu}$, (II) the process $N \rightarrow P + e^- + \nu$. Since the physical consequences of the two charge-exchange interactions are identical for single β decay (this is not true for double beta decay—cf. below), it suffices to work with only one of them, and it is customary to choose the charge-exchange (I) formulation.

In the case of μ meson decay, not only do the two charge-exchange interactions lead to different electron spectra, but there is a third type of charge-exchange interaction which leads to a physically distinct result, namely,[26]

$$H_i = G_\mu(\psi_\mu C^{-1} O_i \psi_\nu^c)(\psi_e^c C^{-1} O_i \psi_\nu^c) \tag{III$'$}$$

It is understood, of course, that the two types of charge-exchange interactions listed above for nuclear β decay are transformed in the present instance into

$$H_i = G_\mu(\psi_\mu C^{-1} O_i \psi_\nu)(\psi_e^c C^{-1} O_i \psi_\nu) \tag{I$'$}$$

$$H_i = G_\mu(\psi_\mu C^{-1} O_i \psi_\nu)(\psi_e^c C^{-1} O_i \psi_\nu^c) \tag{II$'$}$$

Whereas in nuclear β decay, the shapes of the electron spectra do not differ for allowed transitions and pure couplings (forbidden transitions are another matter, of course[27]), it now turns out that, except for an accidental degeneracy, each coupling for each of the three types of interactions (I′), (II′), and (III′) leads to a different electron spectrum for μ meson decay. This is due to the fact that the decay of a μ meson leads to two particles of zero rest mass and to relativistic energies for all three final particles, unlike the situation in nuclear β decay where only one zero rest mass particle is emitted and one of the final particles is a slowly moving nucleon. Tiomno *et al.*[23] have computed the electron spectra corresponding to μ meson decay on the basis of the charge-exchange interactions (I′) and (II′); instead of working with charge-exchange interaction (III′), however, they chose to compute the electron spectra corresponding to the so-called charge-retention interaction (II):

---

[24] Cf. C. MacCallum and A. Wightman, Technical Report No. 7, Princeton University, 1951; the operator C is defined by $\psi^c = C\bar{\psi}$, $\bar{\psi} = \psi^*\gamma_4$. We follow the notation of these authors.

[25] Cf. W. Pauli, "Die allgemeinen Principien der Wellenmechanik," J. W. Edwards, 1946.

[26] The analogue to the charge-exchange interaction (III) in nuclear beta decay does not exist.

[27] Cf. E. J. Konopinski, *Rev. Mod. Phys.*, 15: 209 (1943).

$$H_i^{\text{II}} = G_\mu(\psi_\mu C^{-1}O_i\psi_e^c)(\psi_\nu^c C^{-1}O_i\psi_\nu) \tag{II}$$

However, instead of writing down the expressions obtained by Tiomno *et al.* for the electron spectra on the basis of the charge-exchange (I′) and (II′) and the charge-retention (II) interactions, we write down, following Michel[22] and MacCallum and Wightman,[24] expressions for the electron spectra predicted by the three forms of charge-retention theory, namely,

$$H_i^{\text{I}} = G_\mu(\psi_\mu C^{-1}O_i\psi_e^c)(\psi_\nu C^{-1}O_i\psi_\nu) \tag{I}$$
$$H_i^{\text{III}} = G_\mu(\psi_\mu C^{-1}O_i\psi_e^c)(\psi_\nu^c C^{-1}O_i\psi_\nu) \tag{III}$$

in addition to (II) above.

No generality is lost by working with the charge-retention formulations because any one of the five interactions in any one of the three charge-exchange formulations can be written as a linear combination of the five possible interactions in the corresponding formulation of charge-retention theory[27a]. Consequently, the most general electron spectrum which can result from the decay of the μ meson can be expressed as a linear combination of eleven interactions, five from charge-retention theory (II) and three each from charge-retention theories (I) and (III).[28] If we write the most general interaction in the form (the *d*'s are constants)

$$H_{\text{int}} = \sum_i (d_{i\text{I}}H_i^{\text{I}} + d_{i\text{II}}H_i^{\text{II}} + d_{i\text{III}}H_i^{\text{III}}),$$

[27a] There is one particular linear combination of interactions, $S - A + P$, first introduced by C. Critchfield and E. Wigner [*Phys. Rev.*, **60**: 412 (1941)], which is invariant under any permutation of the order of the four fermions; however, neither the μ decay nor β decay experiments support this choice (cf. below).

[28] The vector and tensor interactions from the charge-retention theories (I) and (III) vanish identically, thereby reducing the maximum possible number of interactions from 15 to 11. The vector and tensor interactions vanish identically because identical neutrino operates appear in H_i^{I} and H_i^{III} and the operators $C^{-1}O_V = C^{-1}\gamma_\mu$ and $C^{-1}O_T = C^{-1}\gamma_\mu\gamma_\nu$ are symmetric operators.

then the differential electron spectrum (per unit energy) is given by:

$$P(W)dW = \frac{G_\mu^2 W \sqrt{W^2 - 1}}{12\pi^3} \Big\{ 3[D_S^2 + 2(D_V^2 + D_T^2 + D_A^2) + D_P^2]\mu(W_0 - W) + 2(D_V^2 + 2D_T^2 + D_A^2)\frac{\mu}{W}(W^2 - 1) + 3(D_S^2 - 2D_V^2 + 2D_A^2 - D_P^2)\frac{\mu}{W}(W_0 - W) \Big\} dW \tag{4}$$

where
$$D_i^2 = d_{iI}^2 + \tfrac{1}{2}d_{iII}^2 + d_{iIII}^2 \qquad \text{for } i = S, A, P$$
$$= \tfrac{1}{2}d_{iII}^2 \qquad \text{for } i = V, T$$

In Eq. (4), W is the energy of the electron, μ the meson mass, and all coupling constants are given in units of $\hbar^2/m_ec^2$ and all energies in units of m_ec^2.

It is well known that in the Majorana theory of the neutrino,[29] the neutrino and antineutrino are treated as equivalent and the neutrino field is represented by a real quantized wave function. In terms of our earlier notation, the neutrino wave function U can be written as

$$U = \frac{1}{\sqrt{2}}(\psi_\nu + \psi_\nu^c) \tag{5}$$

and the nuclear β decay in the charge-exchange order as

$$H_i = G_\beta(\psi_P^c C^{-1} O_i \psi_N)(\psi_e^c C^{-1} O_i U) \tag{M}$$

The Majorana theory of β decay is identical with the Dirac theory which distinguishes between neutrino and antineutrino (this is not true for double β decay—cf. below). The Majorana μ decay interaction in charge-retention order would then be

$$H_i^M = G_\mu(\psi_\mu C^{-1} O_i \psi_e^c)(UC^{-1} O_i U) \tag{M}$$

The most general electron spectrum resulting from the decay of the μ meson on the basis of (M) is

$$P(W)dW = \frac{G_\mu^2 W \sqrt{W^2 - 1}}{12\pi^3} \Big[3(d_{SM}^2 + 2d_{AM}^2 + d_{PM}^2)\mu(W_0 - W) + 2d_{AM}^2 \frac{\mu}{M}(W^2 - 1) + 3(d_{SM}^2 + 2d_{AM}^2 - d_{PM}^2)\mu(W_0 - W) \Big] dW \tag{6}$$

where the subscripts on the constants refer to the five interactions as before (the V and T interactions vanish identically in the Majorana theory—cf. footnote 28).

---

[29] E. Majorana, *Nuovo cimento*, **14**: 171 (1937).

The alternative mode of decay of the μ meson represented by Eq. (3) with the boson μ^0 has been calculated by Tiomno.[23a] The only spectrum which is not in qualitative disagreement with experiment is[24]

$$P(W)dW \approx \sqrt{W^2 - 1}\,(\mu W - 2W^2 + 1)dW \tag{7}$$

In deriving Eq. (7), Tiomno assumes that both μ and μ^0 possess spin 0 and that the coupling is $\bar{\psi}_e\phi(\mu_0)[\partial\phi(\mu)/\partial x_\rho]\gamma_\rho\psi_\nu$.

It should be remarked that all the electron spectra from μ decay computed above are derived on the assumption that the μ meson decays at rest. This is certainly correct for the μ^+ meson since, in solid material, the μ^+ meson will decay at rest because the decay time is extremely long compared with the slowing-down time. However, a μ^- meson will be captured into the K shell of the appropriate mesic atom and in material of small Z ($\lesssim 10$) will decay from the K shell rather than undergo nuclear absorption (cf. Chap. 5). Porter and Primakoff[30] have shown that, because the μ^- meson decays from a K shell, the maximum momentum of the emitted electron will be shifted compared with what it would be if the μ^- meson decayed at rest by an amount depending on the charge of the nucleus. If p_0 is the maximum momentum the emitted electron would have if the μ^- meson decayed *in vacuo* and p is the maximum momentum for decay in matter, then $p = p_0\,(1 + \alpha Z)$ where α is the fine-structure constant. Hence, as much as a 15 per cent correction may have to be made to the upper-energy end of the electron spectrum from μ^- mesons (in order to compare with theory) unless the μ^- decay spectrum is measured *in vacuo*.

Let us now assume that the high-energy end point of the electron spectrum from μ decay has a zero cutoff in agreement with the experimental curve of Sagane *et al.*[16] (although one must remember that the experimental uncertainty is 10 per cent) and examine the theoretical consequences of this assumption. It follows immediately from Eq. (4) that

$$D_A^2 + 2D_T^2 + D_V^2 = 0 \tag{8}$$

Equation (8) would imply that only the scalar and pseudoscalar interactions for each of the three charge-retention theories are possible for "Dirac" neutrinos. It is to be noted, furthermore, that the last term in Eq. (4) is proportional to m_e/W so that it is negligible compared with the first term over most of the electron spectrum. Hence the theoretical "Dirac" spectrum attains the completely unique shape

$$P(W)dW = G_\mu^2\,\frac{W\sqrt{W^2 - 1}}{4\pi^3}\,(D_S^2 + D_P^2)\mu(W_0 - W)dW \tag{9}$$

---

[30] C. Porter and H. Primakoff, *Phys. Rev.*, **83**: 849 (1951).

Within experimental error, the experimental spectrum of Sagane *et al.* is in excellent agreement with the above uniquely predicted simple shape, although a more accurate experiment must be performed before it can be concluded that Eq. (9) represents the electron spectrum from μ decay.

The Majorana theory of μ decay leads to the same result as the theory involving "Dirac" neutrinos, *viz.*, only a linear combination of the scalar and pseudoscalar interactions is possible. In the Majorana theory, however, the vector and tensor interactions are already absent in Eq. (6) (because of the appearance of identical operators in the neutrino covariant), and taking the zero cutoff seriously only adds the axial vector interaction to the excluded list. Finally, as far as Tiomno's theory of μ decay in terms of a boson μ^0 is concerned, although Eq. (7) predicts the assumed zero cutoff, it is in poor agreement with the rest of the Sagane *et al.* spectrum.

Wightman[31] has evaluated the interaction constant for μ decay from the experimental spectrum of Sagane *et al.*; he finds

$$G_\mu \sqrt{D_S^2 + D_P^2} \left(\frac{\hbar}{m_e c}\right)^3 m_e c^2 = 2.2 \pm 0.5 \times 10^{-49} \text{ erg cm}^3 \tag{10}$$

where a mass of $210 m_e$ and a lifetime of 2.1×10^{-6} sec were used. The error given in Eq. (10) corresponds to the accuracy of the experimental spectrum. Strictly speaking, Eq. (10) does not determine the interaction constant G_μ, since D_s and D_p are as yet unknown and will depend on whether the decay of the μ meson leads to the emission of two neutrinos, one neutrino plus one antineutrino, or two antineutrinos [cf. Eq. (4)] and on what particular linear combination of scalar and pseudoscalar interactions in the charge-retention theories must be used. However, $\sqrt{D_s^2 + D_p^2}$ will be of the order of magnitude of unity, so that $G_\mu(\hbar/m_e c)^3 m_e c^2 \approx 10^{-49}$ erg cm^3. It is interesting to compare the μ decay constant with the β decay constant derived from the half life of the neutron,[32] namely, 12.5 ± 2.5 min. If a true Fermi-type interaction is assumed (scalar or vector), the β decay constant turns out to be

$$G_\beta \left(\frac{\hbar}{m_e c}\right)^3 m_e c^2 = 3.1 \pm 0.4 \times 10^{-49} \text{ erg cm}^3 \tag{11}$$

On the other hand, if a pure Gamow-Teller-type interaction is assumed (axial vector or tensor), the β decay constant is

$$G_\beta \left(\frac{\hbar}{m_e c}\right)^3 m_e c^2 = 1.8 \pm 0.2_5 \times 10^{-49} \text{ erg cm}^3 \tag{12}$$

---

[31] A. S. Wightman, Supplement to Technical Report No. 7, Princeton University, 1951.

[32] J. M. Robson, *Phys. Rev.*, **83**: 349 (1951).

While the exact value of the β decay constant again depends on the actual linear combination of interactions which holds, and while the interaction Hamiltonian corresponding to the β decay process is written in the charge-exchange form instead of the charge-retention form used for μ decay, the closeness of the values of the β and μ decay coupling constants is nevertheless an extremely striking fact, a fact noted by many authors.[33]

It is not only interesting to compare the magnitudes of the β and μ decay constants, but it is illuminating to inquire into the possibility of the same interaction Hamiltonian operating for both μ decay and β decay. Since the discussion of μ decay has proceeded in terms of charge-retention order for the spinor wave functions in the interaction Hamiltonian, and of β decay in terms of the charge-exchange order, it is necessary to translate the charge-retention interactions into appropriate linear combinations of the charge-exchange interactions. The connecting equations are

$$
\begin{aligned}
S &= \tfrac{1}{4}(S' + V' + T' + A' + P') && (13a)\\
V &= \tfrac{1}{4}(4S' - 2V' + 2A' - 4P') && (13b)\\
T &= \tfrac{1}{4}(6S' - 2T' + 6P') && (13c)\\
A &= \tfrac{1}{4}(4S' + 2V' - 2A' - 4P') && (13d)\\
P &= \tfrac{1}{4}(S' - V' + T' - A' + P') && (13e)
\end{aligned}
$$

where the unprimed quantities denote the charge-retention interactions and the primed quantities denote the charge-exchange interactions. Now the experimental data on nuclear β decay make certain requirements on the acceptable linear combinations of interactions in the charge-exchange order: (1) the shapes of forbidden β spectra from nuclei like Be^{10} and Y^{91} require Gamow-Teller selection rules,[34] *i.e.*, some admixture of the A' or T' interaction; (2) the shapes of the forbidden spectra from nuclei[35,36] like Cl^{36} and Cs^{137} and the β-γ correlation from a nucleus[37] like Rb^{86} are inconsistent with any linear combination of interactions not containing the T' interaction; (3) the allowed shape of the spectrum from He^6 excludes a linear combination of the T' and A' interactions;[38] (4) the allowed shapes of the spectra from the mirror nuclei exclude a linear combination of the S' and V' interactions;[38a] (5) the spectrum from RaE requires a linear combination[39] of T' and P' if a γ ray is absent.[40]

---

[33] Cf. O. Klein, *Nature*, **161**: 897 (1948); J. Tiomno and J. Wheeler, *Rev. Mod. Phys.*, **21**: 144 (1939).

[34] C. S. Wu, *Rev. Mod. Phys.*, **22**: 386 (1950).

[35] C. Wu and L. Feldman, *Phys. Rev.*, **76**: 693 (1949); **82**: 457 (1951); H. Fulbright and J. Milton, *Phys. Rev.*, **82**: 274 (1951).

[36] L. Langer and R. Moffat, *Phys. Rev.*, **82**: 635 (1951).

[37] C. S. Wu, private communication.

[38] M. Fierz, *Z. Physik*, **104**: 553 (1937).

[38a] O. Kofoed-Hansen and A. Winther, *Phys. Rev.*, **86**: 428 (1952).

The only possible β interactions which are consistent with the above experimental facts are linear combinations of the S', T', and P' interactions, or the V' and T' and P' interactions. On the other hand, if the zero cutoff of Sagane *et al.* for the electron spectrum from μ decay is accepted, the only possible μ interaction is a linear combination of the S and P interactions. If this statement is coupled with the assumption that μ decay leads to the emission of a neutrino plus an antineutrino, a unique prediction would follow for the β interaction if we postulate that the same interaction Hamiltonian holds for both μ and β decay [cf. Eq. (13)]. This prediction is $\frac{1}{2}(S' + T' + P')$ since the most general linear combination $(d_S S + d_P P)$ (d_S and d_P are constants) can be written $\{[d_S + d_P)/2](S + P) + [(d_S - d_P)/2](S - P)\}$ and

$$S + P = \tfrac{1}{2}(S' + T' + P') \tag{14a}$$
$$S - P = \tfrac{1}{2}(V' + A') \tag{14b}$$

On the other hand, if μ decay leads to the emission of two neutrinos or two antineutrinos, the V and T interactions vanish identically and the right-hand sides of Eqs. (13*b*) and (13*c*) must be added to $(d_S S + d_P P)$ with arbitrary coefficients; when this more general expression is examined, it turns out that the postulation of the same interaction for both μ and β decay, together with the assumption of zero cutoff at the upper end of the electron spectrum from μ decay, implies two possible linear combinations for β decay, namely,

$$d_1'T' + d_2'(S' + P') \tag{15a}$$

or

$$d_3'T' + d_4'(V' + 2P') \tag{15b}$$

where the d's are arbitrary coefficients. It should be possible to test these predictions by further β decay experiments, in particular by single β decay experiments involving forbidden transitions with unfavorable parity change, and by experiments on double β decay.

It should be remarked in connection with the double β decay experiments, that, if double β decay actually takes place,[41] this would imply either that (*a*) the neutrino is a Majorana particle and that the antineutrino does not exist or (*b*) the interaction allows the emission of either a neutrino or an antineutrino in the same process, *e.g.*, the decay of the neutron can take place by

---

[39] A. Petschek and R. Marshak, *Phys. Rev.*, **86**: 698 (1952).

[40] Cf. L. M. Langer, *Phys. Rev.*, **75**: 328 (1949); and R. Morrissey and C. Wu, *Phys. Rev.*, **75**: 1288 (1949).

[41] Cf. E. Fireman, Ph.D. Thesis, Princeton University, 1948; and J. Tiomno, Ph.D. Thesis, Princeton University, 1950. Fireman's original experiment on Sn^{124} has since been demonstrated to be incorrect by many authors, including Fireman himself [cf. E. Fireman and D. Schwarzer, *Phys. Rev.*, **86**: 451 (1952)]. Recently, J. A. McCarthy (*Phys. Rev.*, in press) has obtained some extremely preliminary evidence for the double beta decay of Zr^{96} (which has a much larger available energy than Sn^{124}).

$$N \rightarrow P + e^- + \nu$$

or

$$N \rightarrow P + e^- + \bar{\nu}$$

The simplest solution would be (*a*), and this would require, on the hypothesis of the same interaction Hamiltonian applying to both μ and β decay, the emission of identical particles in the decay of the μ meson and consequently the linear combinations (15*a*) or (15*b*) for β decay.

If further experiments do establish the identity of the μ and β interactions, strong impetus will be given to the idea of a universal Fermi interaction among all known spin $\frac{1}{2}$ particles: proton, neutron, μ meson, electron, neutrino (and possibly κ meson—cf. Chap. 9). Some support for the idea of a universal Fermi interaction among all spin $\frac{1}{2}$ particles is provided by the interaction constant evaluated from experiments on nuclear absorption of μ^- mesons, *i.e.*, the process $\mu^- + $ "P" $\rightarrow$ "N" $+ \nu$ (the quotes indicate that the nucleon is bound in a nucleus). It will be recalled (cf. Chap. 5) that treating μ^- absorption from the K shell of a mesic atom as equivalent to K-electron capture, and setting the transition probabilities for μ^- absorption and μ^- decay equal at $Z = 10$, the interaction constant comes out to be

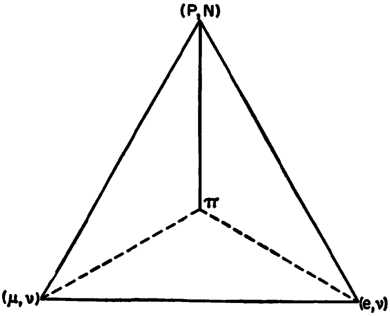

FIG. 3. Diagrammatic sketch representing the interactions of fermions with each other and with the π meson; the solid curves represent direct interactions, the dotted curves indirect interactions (see text).

$$G_{\mu^-\text{abs}}\left(\frac{\hbar}{m_e c}\right)^3 m_e c^2 \approx 1.3 \times 10^{-49} \text{ erg cm}^3$$

This value is certainly compatible with the nuclear β decay and μ meson decay coupling constants, considering the uncertainty of the nuclear matrix element for μ^- absorption. It is not possible to say anything very definite about the interaction Hamiltonian for the μ^- absorption process because of the complexity of the nucleus which absorbs the μ^- meson. It is certainly consistent with the existing experimental data to postulate the same direct interaction between (neutron, proton) and (electron, neutrino), between (neutron, proton) and (μ meson, neutrino), and between (μ meson, neutrino) and (electron, neutrino). The hypothesis of a universal Fermi interaction among (P, N), (μ, ν) and (e, ν) is represented pictorially in Fig. 3.

Several authors have considered a more general formulation of the universal Fermi interaction than the one considered above. They have assumed that there is a direct interaction with a unique coupling constant among all particles of spin $\frac{1}{2}$: ν, e, μ, P, N, and their antiparticles, and have inquired in what manner the requirements of charge conservation and Lorentz invariance forbid the processes not observed in nature and allow those which do take place. Caianiello,[42] in particular, has examined the behavior of the universal Fermi interaction under space and time inversion and has shown that, if the coefficients of the spinor products appearing in the Hamiltonian density transform like a tensor density, the only interactions which will exclude the unwanted processes must transform like a pseudoscalar under space inversion and like a pseudoscalar under time inversion or like a pseudoscalar under space inversion and like a scalar under time inversion. In this demonstration, cognizance is taken of the fact that a spinor wave function can be multiplied by $+1$, -1, i and $-i$ (in contrast to the two possible values $+1$ and -1 for bosons) under space and time inversions.[43] The two types of interactions of the desired character still allow the following processes to take place:

$$\begin{aligned} P + \bar{P} &\rightarrow 2\nu \\ N + \bar{N} &\rightarrow 2\nu \\ \mu + \bar{\mu} &\rightarrow 2\nu \\ e + \bar{e} &\rightarrow 2\nu \\ \nu + \bar{\nu} &\rightarrow 2\nu \end{aligned} \tag{16}$$

This is not an argument against the hypothesis of a generalized universal Fermi interaction because the above processes could take place with extremely small probability (*e.g.*, the relative probability of neutrino annihilation of pairs in matter with respect to photon annihilation is of the order of 10^{-7}).

Curiously enough, the interactions shown by Caianiello to be consistent with the hypothesis of a generalized universal Fermi interaction are all of the odd-coupling type in contrast to the ones considered earlier, which were of the even-coupling type. For example, a typical interaction would, for Caianiello, assume the form

$$H_i = (\psi_P^c C^{-1} O_i \psi_N)(\psi_e^c C^{-1} O_i \gamma_5 \psi_\nu) \tag{17}$$

---

[42] C. Yang and J. Tiomno, *Phys. Rev.*, **79**: 495 (1950); A. Gamba, *Nuovo cimento*, **7**: 919 (1950); and E. R. Caianiello, *Nuovo cimento*, **8**: 749 (1951).

[43] Cf. Yang and Tiomno, *loc. cit.;* a recent paper by Wick, Wightman, and Wigner (*Phys. Rev.*, in press) questions the essential correctness of classifying spinor wave functions into four categories under space and time inversions.

in contrast to the earlier formulation, namely,

$$H_i = (\psi_P^c C^{-1} O_i \psi_N)(\psi_e^c C^{-1} O_i \psi_\nu) \tag{18}$$

McCallum and Wightman[24] have shown that, as far as the experimental data on β decay and μ decay are concerned, the same arguments which apply to the even-coupling theories can be carried over without change to the odd-coupling theories. By adopting certain "plausible criteria of simplicity," Caianiello arrives at two mutually exclusive linear combinations of interactions in the charge-exchange order, namely, $(S' + T' + P')$ or $(V' + A')$. It is seen that one of them, $(S' + T' + P')$ is identical with the unique linear combination to which we were led in our earlier discussion on the assumption that μ decay leads to the emission of a neutrino plus an antineutrino. This agreement may be sheer coincidence, but it must be admitted that, if it turns out to be possible to derive a unique universal Fermi interaction in agreement with all known experimental data on clear, unequivocal theoretical grounds (and not just on the basis of "plausible criteria of simplicity"), a major triumph in elementary particle physics would surely be registered.

Even if a universal Fermi interaction exists among all spin $\frac{1}{2}$ particles, or fermions, the interesting question still remains as to the nature of the interactions between the boson particles (for example, π meson, τ meson, etc.—cf. Chap. 9) and the fermion particles. In particular, it is known that the pseudoscalar π meson interacts strongly with (P, N) and decays into (μ, ν), and it is interesting to speculate whether it is possible to explain the observed ratio of $\pi \rightarrow e$ decay to $\pi \rightarrow \mu$ decay (cf. Chap. 4) in terms of two-step processes based on direct interactions among all the spin $\frac{1}{2}$ particles and a direct interaction between the pseudoscalar π meson and the nucleons (cf. Fig. 3 where the direct interactions are represented by solid lines and the two indirect interactions by dotted lines). In other words, the two possible decays of the π meson are postulated to take place in accordance with the schemes

$$\pi^+ \rightarrow \left\{\begin{matrix} P + \bar{N} \\ \pi^+ + \bar{P} + N + \mu^+ + \nu \end{matrix}\right\} \rightarrow \mu^+ + \nu \tag{19}$$

$$\pi^+ \rightarrow \left\{\begin{matrix} P + \bar{N} \\ \pi^+ + \bar{P} + N + e^+ + \nu \end{matrix}\right\} \rightarrow e^+ + \nu \tag{20}$$

where the bar over P and N represents the antiparticle. Unfortunately, the calculations diverge and it is necessary to have recourse to cutoff procedures; however, the divergent integrals cancel out when the ratio between the probabilities for $\pi \rightarrow \mu$ decay and $\pi \rightarrow e$ decay is considered.

The results obtained by Ruderman and Finkelstein[44] for a pseudoscalar π meson are shown in Table 1; it is seen that, if the interaction operators for the three covariants (P, N), (μ, ν), and (e, ν) are chosen as scalar, vector, or tensor, the transitions are forbidden for both $\pi \rightarrow \mu$ and $\pi \rightarrow e$ decay. If the interaction is pseudoscalar, the ratio of $\pi \rightarrow e$ to $\pi \rightarrow \mu$ decay turns out to be 5.1 and if the interaction operator is axial vector, the ratio turns out to be 10^{-4}. Since the observed $\pi \rightarrow e$ to $\pi \rightarrow \mu$ decay probability ratio is less than $\frac{1}{1400}$ (cf. Chap. 4), and the experimental data on β decay and μ decay are in disagreement with a universal axial vector interaction, it appears that $\pi \rightarrow e$ decay and $\pi \rightarrow \mu$ decay cannot be explained on the basis of a universal Fermi interaction coupled with the interaction between a pseudoscalar π meson and the nucleon field. It is to be noted that an earlier attempt (cf. Chap. 4) to explain the processes

TABLE 1. THEORETICAL RATIOS OF $\pi \rightarrow e$ TO $\pi \rightarrow \mu$ DECAY

	Type of β decay				
	S'	V'	T'	A'	P'
$PS(PS)$ or $PS(PV)$	Forbidden	Forbidden	Forbidden	1.0×10^{-4}	5.1

$$\mu^- + P \rightarrow N + \nu \tag{21a}$$

$$N \rightarrow P + e^- + \nu \tag{21b}$$

in terms of direct interactions between π and (P, N) and π and (μ, ν) and π and (e, ν) also met failure. It was possible to explain the μ^- absorption process (21a) in terms of direct interactions between the π meson and the (μ, ν) and (P, N) fields; but it was not possible to explain the β decay process (21b) on the corresponding basis.

4. Spin of the μ Meson

The various decay and absorption phenomena in which the μ meson participates (its own decay into an electron plus two light neutral particles, its absorption by a proton in a nucleus giving rise to one light neutral particle, and its origin in the decay of the π meson) are all extremely suggestive of spin $\frac{1}{2}$ for the μ meson. In particular, the acceptance of zero cutoff at the high-energy end of the electron spectrum from μ decay as an experimental fact enables one to exclude spin $\frac{3}{2}$ for the μ meson. This is so because all direct couplings of a spin $\frac{3}{2}$ μ meson with a spin $\frac{1}{2}$

---

[44] M. Ruderman and R. Finkelstein, *Phys. Rev.*, **76**: 1458 (1949); cf. also L. I. Schiff, *Phys. Rev.*, **76**: 303 (1949).

electron and two spin $\frac{1}{2}$ neutrinos lead to electron spectra with finite cutoffs.[45] Spin 0 for the μ meson is also excluded since zero cutoff rules out all spin 0 theories except one, and the over-all shape of the electron spectrum from μ decay appears sufficient to exclude this one possibility (cf. above). These statements follow only if one believes the μ decay spectrum of Sagane *et al.*[16] If a finite cutoff turned out to be correct,[15] after all, spin $\frac{1}{2}$ would still be plausible but the μ decay experiment would not constitute a measurement of the μ meson spin.

The question still remains, therefore, whether there is any other type of experiment which yields a more direct determination of the μ meson spin. Christy and Kusaka[46] were the first to point out that a careful analysis of certain cosmic-ray experiments on the frequency of large bursts of ionization produced by very energetic μ mesons (the so-called "burst production" by the penetrating component of the cosmic radiation) would throw light on the μ meson spin. Christy and Kusaka argued that the electromagnetic interactions of the μ meson are responsible for the burst production and that the cross sections for these electromagnetic processes are strongly spin-dependent at high energies. Let us examine the argument.

The burst-production phenomena are very large bursts of ionization (greater than, say, 100 times the ionization of a singly charged relativistic particle) which are detected with counters under very great thicknesses of material, *e.g.*, lead or iron. These bursts of ionization consist of showers of electrons and positrons (similar to the showers produced in thin lead or iron plates by high-energy photons or electrons) and under large thicknesses of material (of the order of 20 radiation units) at sea level, cannot arise from the soft component of cosmic radiation, but only from the very penetrating radiation, *viz.*, the μ meson. This statement must be qualified to some extent; a fraction of the large bursts at sea level (up to one-third) may be produced by high-energy γ rays[47] arising from π^0 mesons created in a thick absorber by the high-energy tail of the N component, *i.e.*, nucleons or π mesons. We shall see below that at mountain altitudes the large majority of bursts are indeed due to the decay γ rays from π^0 mesons.[48]

Let us examine the mechanism whereby a cascade shower of electrons and positrons is generated by the passage of an energetic μ meson through a thick absorber. We have already pointed out that the interaction of the μ meson with the nucleon is extremely weak (cf. below), accounting for the great penetrating power of μ mesons. However, the μ meson is a charged particle and will interact electromagnetically with atomic nuclei or with atomic electrons. Consequently, a cascade shower may start with a γ ray resulting from the bremsstrahlung of a μ meson in the electric field of a nucleus or with a knock-on electron produced as a result of an elastic collision of the μ meson with an atomic electron. There are other electromagnetic processes possible, but at the high energies needed for burst production (10 to 1000 times the μ meson mass), photonic bremsstrahlung and knock-on electrons supply the chief mechanisms for large energy transfers.

---

[45] Cf. E. R. Caianiello, *Phys. Rev.*, **83**: 735 (1951).

[46] R. Christy and S. Kusaka, *Phys. Rev.*, **59**: 414 (1941).

[47] E. F. Fahy, *Phys. Rev.*, **83**: 413 (1951).

[48] Cf. H. Bridge and W. Hazen, *Phys. Rev.*, **74**: 579 (1948).

The possibility of determining the spin of the μ meson from a study of the frequency of burst production (as a function of energy or the number of particles in a burst) arises from the fact that the cross sections for photonic bremsstrahlung and knock-on electron production depend on the energy of the μ meson and on its spin. These cross sections have been calculated by Christy and Kusaka[49] for mesons of spin 0, $\frac{1}{2}$, and 1. The resulting formulas are listed in Table 2 in units of σ_0 where

TABLE 2. KNOCK-ON AND BREMSSTRAHLUNG CROSS SECTIONS FOR MESONS OF DIFFERENT SPIN

Spin	Cross Section, $\frac{\sigma(\epsilon_0, \eta)d\eta}{\sigma_0}$
Knock-on Electrons	
0	$\frac{2\pi\mu^2}{\alpha Z M\epsilon_0}\frac{d\eta}{\eta^2}\left(1 - \frac{\eta}{\eta_m}\right)$
$\frac{1}{2}$	$\frac{2\pi\mu^2}{\alpha Z M\epsilon_0}\frac{d\eta}{\eta^2}\left(1 - \frac{\eta}{\eta_m} + \frac{\eta^2}{2}\right)$
1	$\frac{2\pi\mu^2}{\alpha Z M\epsilon_0}\frac{d\eta}{\eta^2}\left[1 - \frac{\eta}{\eta_m} + \frac{\eta^2}{3} + \frac{m_e\epsilon_0\eta}{3\mu^2}\left(1 - \frac{\eta}{\eta_m} + \frac{\eta^2}{2}\right)\right]$
Bremsstrahlung	
0	$\frac{16(1 - \eta)d\eta}{3\eta}\left\{\log\left[\frac{2(1 - \eta)\epsilon_0}{\frac{5}{8}\mu Z^{\frac{1}{3}}\eta}\right] - \frac{1}{2}\right\}$
$\frac{1}{2}$	$\frac{16}{3}\left(\frac{3\eta}{4} + \frac{1 - \eta}{\eta}\right)d\eta\left\{\log\left[\frac{2(1 - \eta)\epsilon_0}{\frac{5}{8}\mu Z^{\frac{1}{3}}\eta}\right] - \frac{1}{2}\right\}$
1	$d\eta\left[\frac{\pi\epsilon_0}{5\mu Z^{\frac{1}{3}}}\left(\frac{2 - 2\eta + 7\eta^2}{12}\right) + 0(ln\ \epsilon_0)\right]$

$$\sigma_0 = \left[\left(\frac{e^2}{\mu c^2}\right)^2 \alpha Z^2\right] = Z^2 1.6 \times 10^{-32}\ \text{cm}^2 \tag{22}$$

with α the fine-structure constant and Z the charge on the nucleus. In Table 2 ϵ_0 is the energy of the incident meson, η is the fractional energy transfer to the electron or photon, and $\eta_m \sim (1 + \mu^2/2m_e\epsilon_0)^{-1} \approx \epsilon_0/(\epsilon_0 + 10^{10}$ ev) is the maximum fractional energy transfer in a single collision experienced by the μ meson (m_e and μ are the masses of the electron and meson, respectively). The last term in the last entry of Table 2 represents terms which increase no faster than logarithmically with ϵ_0. It is apparent that the bremsstrahlung cross sections, which go as $d\eta/\eta$, dominate over the knock-on cross sections, which go as $d\eta/\eta^2$, for very high energies, say, greater than 10^{10} ev.

---

[49] Christy and Kusaka, *loc. cit.;* cf. also W. Pauli, *Rev. Mod. Phys.*, **13**: 203 (1941); and D. C. Peaslee, *Nuovo cimento*, **9**: 56 (1952).

The first two bremsstrahlung cross sections in Table 2 are in error for large ϵ_0 because of the neglect of electron screening effects. This may be seen as follows: the matrix element for the interaction of a meson with the coulomb field of a nucleus contains the integral[60]

$$\int \frac{d\mathbf{r}}{r} e^{i(\mathbf{q}_0-\mathbf{q}-\mathbf{k})\cdot\mathbf{r}/\hbar} \tag{23}$$

where $\mathbf{q}_0$ is the initial momentum of the meson, $\mathbf{q}$ its final momentum, $\mathbf{k}$ the photon momentum, and the integral is taken over all space. If we write $\mathbf{P} = \mathbf{q}_0 - \mathbf{q} - \mathbf{k}$, then the major contribution to the above integral comes from distances of the order $r_0 \sim \hbar/P$ since for $r > r_0$, the integral oscillates rapidly and is small, and for $r < r_0$ the volume element $d\mathbf{r}$ is small. Now, using the Thomas-Fermi model for the atom, it can be shown that atomic screening comes into play at distances of the order of $r_0 \approx a_0/Z^{\frac{1}{3}}$, where a_0 is the Bohr radius of hydrogen. Furthermore, it is easy to show that $P \approx \mu^2\omega/2\epsilon_0\epsilon$ where ϵ is the final energy of the meson and ω is the photon energy; since $\omega/\epsilon \approx 1$, the incident energy at which screening becomes important is

$$\epsilon_0 \approx \frac{a_0}{2Z^{\frac{1}{3}}(\hbar/\mu c)}\,\mu c^2 \simeq 5 \times 10^{11} \text{ ev for lead} \tag{24}$$

Consequently, the bremsstrahlung formulas for spin 0 and spin $\frac{1}{2}$ mesons listed in Table 2 must be modified above the indicated energy for lead (and correspondingly for iron) in such a manner that the cross sections saturate.

The bremsstrahlung formula for a spin 1 meson listed in Table 2 is not valid above about 10^{10} ev, but for another reason: at relativistic energies, the electromagnetic interaction is dominated by the magnetic moment associated with the spin. As the incident energy of the meson increases, the magnetic interaction with the Coulomb field becomes very large and the perturbation treatment breaks down; hence Christy and Kusaka, in their calculations on burst production, used the formula in Table 2 for photon energies less than 137 μc^2 and suppressed all higher

---

[60] Cf. W. Heitler, "The Quantum Theory of Radiation," Oxford University Press, 1947.

Fourier components for larger incident energies. This procedure should underestimate the bremsstrahlung cross section for mesons[51] of spin 1. Moreover, it should be noted that the formulas in Table 2 refer to particles with normal magnetic moments although spin $\frac{1}{2}$ or spin 1 mesons may, of course, possess "anomalous" magnetic moments. Here also, Christy and Kusaka[52] and Peaslee[52] have shown that the bremsstrahlung cross sections derived without introducing anomalous magnetic moments are minimum cross sections.

In order to predict the frequency of burst production on the basis of the bremsstrahlung and knock-on cross sections listed in Table 2, it is necessary to know the relationship between the number of electrons observed in a burst and the energy of the incident μ meson. This relationship follows from the theory of cascade showers[52] wherein it is demonstrated that the average number of particles S in a shower is

TABLE 3. INTEGRAL NUMBER OF BURSTS WITH MORE THAN S PARTICLES PRODUCED IN 20 RADIATION UNITS OF IRON BY MESONS OF DIFFERENT SPIN

$S\xi \times 10^9$	Knock-on bursts (cm^{-2} sec^{-1})			Bremsstrahlung bursts (cm^{-2} sec^{-1})		
	Spin 0	Spin $\frac{1}{2}$	Spin 1	Spin 0	Spin $\frac{1}{2}$	Spin 1
1	2.1×10^{-7}	2.7×10^{-7}	3.8×10^{-7}	2.0×10^{-7}	3.2×10^{-7}	1.0×10^{-6}
2	4.1×10^{-8}	5.6×10^{-8}	1.0×10^{-7}	7.3×10^{-8}	1.2×10^{-7}	4.8×10^{-7}
4	7.2×10^{-9}	1.0×10^{-8}	2.5×10^{-8}	2.2×10^{-8}	3.8×10^{-8}	2.1×10^{-7}
8	1.1×10^{-9}	1.7×10^{-9}	6.6×10^{-9}	6.0×10^{-9}	1.0×10^{-8}	8.7×10^{-8}
16	1.6×10^{-10}	2.5×10^{-10}	1.8×10^{-9}	1.4×10^{-9}	2.5×10^{-9}	3.3×10^{-8}
32	2.2×10^{-11}	3.8×10^{-11}	4.7×10^{-10}	2.9×10^{-10}	5.1×10^{-10}	1.2×10^{-8}
64	3.0×10^{-12}	5.0×10^{-12}	1.2×10^{-10}	5.0×10^{-11}	9.0×10^{-11}	3.7×10^{-9}

$$S \approx \frac{E_0}{10\xi} \tag{25}$$

where E_0 is the energy of the initiating electron or photon and ξ is the critical energy, *i.e.*, the energy at which radiation loss becomes equal to ionization loss in a given material. The quantity ξ is 8 Mev for lead and 26 Mev for iron. Equation (25) is the connecting link which enables one to predict the frequency of bursts as a function of their size once the μ meson spectrum is specified.

The number of bursts as a function of $S\xi$ (the number of particles in the burst times the critical energy—this makes it possible to translate the numbers to other materials) predicted by the three theories are listed in Table 3 for an absorber consisting of 35 cm of iron (the experimental setup of Lapp[53] at sea level). A breakdown is given to show the relative contributions of the knock-on and bremsstrahlung processes. The numbers in Table 3 were computed by Lapp assuming a meson mass of $200m_e$ and a meson intensity at sea level of 0.01/cm^2/sec/ster. Recently, Fahy[47] has computed these numbers for spin 0 and spin $\frac{1}{2}$ theories, using improved values of the meson mass ($216m_e$) and of the meson intensity at sea level (8.8×10^{-3}/cm^2/sec/ster). His curves corresponding to the spin 0 and spin $\frac{1}{2}$ theories are plotted in Fig. 4; the old spin 1 curve is given since its disagreement with the experimental curve (*d*) of Lapp (also shown in Fig. 4) is so great that an improved calculation is unnecessary. It is evident that the sea-level curve of Lapp definitely rules out spin 1 for the μ meson (and presumably all higher spins because the magnetic interaction should always be at least as important as for spin 1) since the predicted number of bursts produced by μ mesons cannot be greater than the number observed (it can be less—cf. below). The burst production experiment of Lapp does not allow one to decide between spin 0 and spin $\frac{1}{2}$ because it is always possible to ascribe a somewhat ill-defined fraction of bursts to γ rays arising from π^0 mesons.

---

[51] Cf. J. R. Oppenheimer, *Phys. Rev.*, **59**: 462 (1941).

[52] B. Rossi and K. Greisen, *Rev. Mod. Phys.*, **13**: 240 (1941).

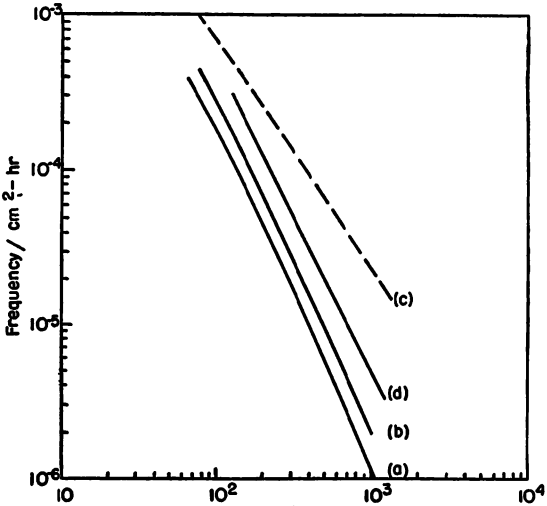

FIG. 4. Theoretical frequency-size distributions for burst production corresponding to different assumed spins for the μ meson; curve (*a*) corresponds to spin 0, (*b*) to spin $\frac{1}{2}$, (*c*) to spin 1. Curve (*d*) represents the experimental results of Lapp at sea level using a 35-cm iron absorber.

---

[53] R. E. Lapp, *Phys. Rev.*, **69**: 321 (1946).

Fahy has actually worked the argument the other way; assuming that the μ meson possesses spin $\frac{1}{2}$ (on the basis of the decay experiments), Fahy infers from a comparison of the theoretical spin $\frac{1}{2}$ curve and the (*d*) curve in Fig. 4 that 55 per cent of the large bursts under 35 cm of iron at sea level are produced by μ mesons. Since the theoretical spin $\frac{1}{2}$ curve is parallel to the experimental curve, it is reasonable to assume that the fractional contribution to burst production by μ mesons is roughly constant over the range of burst size given. It follows, therefore, from the slope of the experimental curve that the integral μ meson spectrum in the energy region 10^{10} to 10^{11} ev is of the form $d\epsilon/\epsilon^{1.7}$.

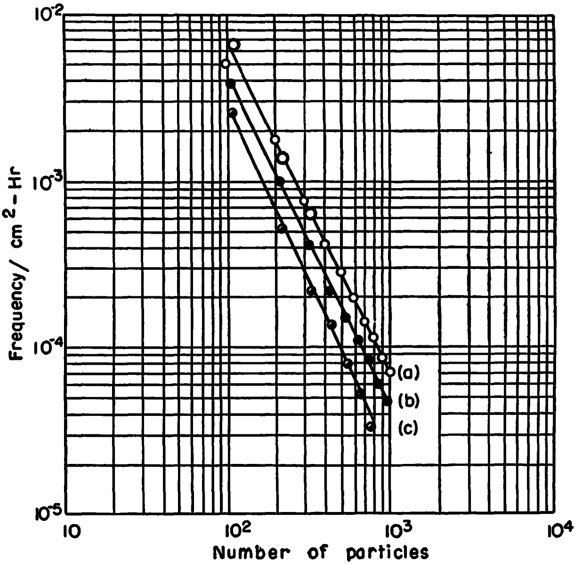

FIG. 5. Measured frequency-size distributions for burst production under different thicknesses of lead absorber and at two altitudes. Curve (*a*) corresponds to 10.7 cm of Pb at 3500 m, (*b*) to 26.7 cm of Pb on top and 10.7 cm of Pb on bottom at 3500 m, (*c*) to 10.7 cm of Pb at sea level.

Fahy[47] has measured the burst production rate at an altitude of 3500 m under thick absorbers consisting of (1) 10.7 cm of lead surrounding an ionization chamber and (2) 26.7 cm of lead surrounding the top hemisphere of the ionization chamber and 10.7 cm surrounding the bottom hemisphere. His integral size-frequency curves are shown in Fig. 5, together with the sea-level curves obtained by Lapp under 10.7 cm of lead.[53] It is seen that there is a factor of 8.5 between the sea-level and mountain-altitude rates under a 10.7-cm lead absorber and a factor of 1.6 at mountain altitude between the two thicknesses of lead absorber.

From the fact that 55 per cent of the burst production under 35 cm of iron at sea level is caused by μ mesons and the assumption that the remaining 45 per cent of the burst-producing radiation which does not consist of μ mesons is made up of a radiation whose cross section for burst production is proportional to $A^{\frac{2}{3}}$ (A is the atomic weight), it is possible to deduce that 68 per cent of the bursts observed at sea level under 10.7 cm of lead are produced by μ mesons. Accepting 68 per cent as the fractional contribution of the μ mesons at sea level, the three curves in Fig. 5 imply[47] that that part of the burst producing radiation which is not composed of μ mesons has an absorption mean free path of 346 ± 36 g/cm^2 in lead and 124 ± 8 g/cm^2 in air. An independent experiment by Stinchcomb[54] to determine the absorption mean free paths for the burst producing radiation not consisting of μ mesons led to a value in agreement with the above in lead, a value of 240 ± 20 g/cm^2 in iron, and a lower value, 74 ± 14 g/cm^2, in air.

5. Nuclear Interaction of μ Mesons

We now turn to the problem of the nuclear interaction of μ mesons. This problem, as it concerns the nuclear absorption of slow μ^- mesons, has been examined in Chap. 5. The experimental evidence cited in that chapter indicates an extremely weak coupling between slow μ mesons and nucleons. Two other types of experiment bear on the nuclear interaction of μ mesons: the nuclear (*i.e.*, large-angle) scattering of fast μ mesons and the penetration of cosmic rays (the vast majority of which are μ mesons) deep underground.

The scattering and the underground experiments are important for establishing the point that the μ meson is very weakly coupled to nucleons at all energies. What has been established by the slow μ^- absorption experiments is that the μ meson-neutrino field is very weakly coupled to the nucleon field. This deduction is consistent with the fact that no evidence has been obtained from accelerator experiments for the direct single production of μ mesons. Suppose, however, that a strong interaction exists between the μ meson-pair field and the nucleon field.[55] This would be reconcilable with the decay of μ^- mesons from the K shells of light elements since energy conservation would prohibit any nuclear reaction proceeding through the μ meson-pair field. However, a strong coupling between the μ meson-pair field and the nucleon field would require direct production of μ meson pairs when sufficient energy is available, sizable cross sections for nuclear scattering of fast μ mesons, and rapid absorption of the energetic penetrating component below sea level. The existing experimental evidence against the last two consequences of the μ meson pair theory (the first has not yet been disproved) eliminates the possibility of a strong coupling between the μ meson-pair field and the nucleons. Let us consider the scattering first.

---

[54] T. G. Stinchcomb, *Phys. Rev.*, **83**: 422 (1951).

[55] Cf. G. Wentzel, *Phys. Rev.*, **79**: 710 (1950); also P. A. Wolff, *Phys. Rev.*, **81**: 1056 (1951).

A. Scattering of μ Mesons by Nuclei. We have seen that the strong coupling of a single μ meson to a nucleon or of a single μ meson and a light neutral particle to a nucleon are definitely excluded. However, the possibility of a strong coupling of a μ meson pair to a nucleon still remains to be disproved. As long as a μ pair-nucleon coupling is postulated, it does not matter whether the μ meson possesses[56] spin $\frac{1}{2}$ or 0. Both spin $\frac{1}{2}$ and spin 0 pair theories have been investigated by various authors,[57] and the predictions of both types of theories agree in so far as nuclear scattering is concerned. The essential prediction of the pair theories is that nuclear scattering of mesons should be of the order of the geometrical cross section for a coupling constant chosen to fit the magnitude of nuclear forces. For example, the spin $\frac{1}{2}$ pair theory (with tensor coupling) predicts a scattering cross section[58]

$$\sigma = 64\pi^5 G^2 \mu^2 \left\{ \frac{q\epsilon(q + \epsilon/4)}{q + \epsilon/2} - \frac{\epsilon^2}{4} \ln \frac{2q + \epsilon}{\epsilon} \right\} \tag{26}$$

where ϵ is the energy of the μ meson, q is its momentum, and G is the coupling constant. Equation (26) is derived by calculating the diagonal matrix element of the interaction Hamiltonian

$$G(\bar{\Psi}\gamma_\alpha\gamma_\beta\Psi)(\bar{\psi}\gamma_\alpha\gamma_\beta\psi) \tag{27}$$

where Ψ is the nucleon wave function and ψ is the μ meson wave function (both assumed to satisfy the Dirac equation). This is to be compared with the cross section for nuclear scattering of π mesons where the calculation requires the π meson to pass through an intermediate state (cf. Chap. 7). Despite this difference, weak coupling meson theory predicts equally large cross sections for nuclear scattering of μ and π mesons for comparable values of the coupling constants.[59]

---

[56] Of course, if the μ meson possesses spin 0, it can be coupled singly to a nucleon; however, it is conceivable that nature would allow only pair coupling.

[57] Cf. R. E. Marshak, *Phys., Rev.*, **57**: 1101 (1940); R. Marshak and V. Weisskopf, *Phys. Rev.*, **59**: 130 (1941); J. Weinberg, *Phys. Rev.*, **59**: 776 (1941); O. Klein, *Arkiv. Mat. Astron. Fysik.*, **A30**: 1 (1943); and S. Noma, *Prog. Theor. Phys.*, **1**: 71 (1946); and **3**: 54 (1948).

[58] This formula differs from Eq. (15) in Marshak and Weisskopf, *loc. cit*, where a numerical error was made in evaluating the coupling constant [*i.e.*, the phase space factor $(2\pi)^6$ was omitted]; insertion of the correct numbers leads to the much larger cross section given here.

The experimental situation as regards nuclear scattering of μ and π mesons is totally different. Whereas the cross section for π meson scattering has been found to be geometrical (*i.e.*, 5×10^{-26} cm^2) at energies of several hundred Mev (cf. Chap. 7), experiments on μ meson scattering always yield cross sections at least two orders of magnitude smaller. Just as in the π meson scattering experiments, the μ meson scattering experiments consist in looking for large-angle scatterings in order to eliminate the effects of multiple Coulomb scattering which contributes at small angles. Some of the early μ meson scattering experiments were carried out by Code[60] and by Shutt.[61] Code observed 8 large-angle scatterings (> 8°) of penetrating particles in a cloud chamber operating in a magnetic field of 12,900 gauss; of these 8 tracks, 7 were positive and 1 negative. On the assumption that the tracks were due to μ mesons, Code deduced a cross section of 10^{-28} cm^2 per nucleon. This result is suspect because of the charge asymmetry of the eight tracks, and it is probable that the majority of the tracks are due to protons. Similarly, Shutt derived a cross section of less than 10^{-28} cm per nucleon.

More recently, Amaldi and Fidecaro[62] have studied the scattering of μ mesons with a counter-hodoscope setup. These authors have measured the large-angle scattering for fast μ mesons in iron and lead plates for two separate energy bands, *viz.*, from 200 to 320 Mev kinetic energy and from 320 Mev to infinity. About half a million incident μ mesons were counted; and, after correcting for multiple coulomb scattering and the contribution of protons present in the cosmic radiation at sea level, Amaldi and Fidecaro derived upper limits on the μ meson scattering cross section: 4.5×10^{-29} cm^2 per nucleon for the 200- to 320-Mev energy band and 2.3×10^{-30} cm^2 per nucleon for the > 320-Mev energy band. These numbers follow if the hypothetical nuclear scattering of μ mesons does not deviate too strongly from an isotropic distribution in the center-of-mass system. The fact that the most accurate μ meson scattering experiment places an upper limit on the cross section at least three orders of magnitude smaller than geometrical implies, of course, that the coupling of the μ meson-pair field to nucleons is weak and much smaller than nuclear forces would require [cf. Eq. (26)]. It appears, therefore, that the only nonelectric coupling of the μ meson to the nucleon occurs through the μ meson-neutrino field and we have already shown that this coupling is 10^{13} times weaker than the π meson coupling to the nucleon (cf. Chap. 5). Corresponding to such a weak coupling, the cross section for the nuclear scattering of μ mesons would be of the order of 10^{-38} cm^2 and therefore completely unobservable.

---

[59] A similar statement holds in the so-called "strong coupling" theories; cf. J. M. Blatt, *Phys. Rev.*, **69**: 292 (1946); and W. Pauli, "Meson Theory of Nuclear Forces," Interscience Publishers, 1946.

[60] F. L. Code, *Phys. Rev.*, **59**: 229 (1941).

[61] R. P. Shutt, *Phys. Rev.*, **61**: 6 (1942).

[62] E. Amaldi and G. Fidecaro, *Helv. Phys. Acta*, **23**: 93 (1950); and *Phys. Rev.*, **81**: 339 (1951). Cf. A. B. Sabiar, *Proc. Indian Acad. Sci.*, **34A**: 201 (1951).

B. Behavior of μ Mesons Underground. The second group of cosmic-ray experiments which indicate a weak coupling of μ mesons to nuclei is the set of experiments carried out deep underground. Cosmic rays have been detected at a depth of 1600 m.w.e. (by the Cornell group[63]), and there is every reason to believe that they penetrate much deeper.[64] What is the nature of these penetrating particles? They cannot be π mesons or protons since π mesons or protons would be very quickly absorbed in the earth in virtue of their strong interaction with nuclei. Similarly, any electronic component at sea level would be quickly absorbed. The obvious conjecture is that the cosmic rays which penetrate deep underground are chiefly μ mesons. If this supposition can be verified, we shall have still another proof that μ mesons interact weakly with nuclei.

One of the verifications consists in explaining the observed variation of cosmic-ray intensity with depth, for depths shallower than 300 m.w.e. exclusively in terms of electromagnetic interactions, chiefly ionization processes. We have already noted in our discussion of burst production by μ mesons (cf. Sec. 4 above) that the slope of the integral burst frequency curve which is observed at sea level implies an integral energy spectrum for μ mesons of the form $d\epsilon/\epsilon^{1.7}$ between 10^{10} and 10^{11} ev. If ionization processes constitute the chief mechanism for energy loss in the energy region 10^{10} to 10^{11} ev, then, to a first approximation, each meson has a fixed range proportional to its energy.[65] Hence, if k is the energy loss per g/cm^2, then at depth d, all mesons with energy greater than kd are still present and the energy spectrum $\epsilon^{-\gamma}$ ($\gamma \approx 1.7$) is transformed approximately into the absorption curve $d^{-\gamma}$.

The underground absorption law[66] $d^{-\gamma}$ holds for μ mesons between

---

[63] L. M. Bollinger, Ph.D. Thesis, Cornell University, 1951; cf. O. Tiffany and W. Hazen, *Phys. Rev.*, **77**: 849 (1950).

[64] Y. Nishina [*Phys. Rev.*, **59**: 401 (1941)] has detected cosmic rays at a depth of 3000 m.w.e.; however, his data are very rough and will not be discussed here.

[65] This is approximately true in the energy region under consideration because of the Fermi saturation effect (cf. W. Heisenberg, "Cosmic Radiation," Dover Publications, 1946), although there is still a tendency for a slow logarithmic increase of energy loss with energy.

[66] V. C. Wilson, *Phys. Rev.*, **53**: 337 (1938).

100 and 300 m.w.e.; at depths greater than 300 m.w.e. the absorption curve increases more rapidly, roughly as $d^{-2.5}$. At depths less than 100 m.w.e., the absorption curve decreases more slowly than the $d^{-1.7}$; from 0 to 10 m.w.e., the deviation is explained as a transition effect from air to solid material connected with the decay of the μ meson, while from 10 to 100 m.w.e. (corresponding to the energy range 10^9 to 10^{10} ev), the deviation is explained as a result of the variation in the energy spectrum of μ mesons at sea level. The explanation of the kink in the experimental absorption curve which appears[66] at depths greater than 300 m.w.e. is more subtle.

It was thought at first that the kink in the underground absorption curve in the neighborhood of 300 m.w.e. is caused by the additional bremsstrahlung and knock-on electron energy losses setting in for the more energetic (and hence more deeply penetrating) μ mesons. Careful calculations,[67] using the formulas of Table 2, of the expected intensity curve at depths below 1000 m.w.e. showed that these effects are too small for spin 0 or $\frac{1}{2}$ mesons to give a satisfactory explanation of the kink—despite the fact that μ mesons must possess energies $> 10^{11}$ ev to penetrate to depths as great as 1000 m.w.e. However, if the energy spectrum of μ mesons continues to obey the power law $d\epsilon/\epsilon^{1.7}$, some other mechanism must be invoked to explain the kink in the underground intensity curve. Greisen[67] has suggested that the steep increase in the underground absorption of μ mesons beyond 300 m.w.e. is explicable in terms of the energy dependence of the lifetime for $\pi \rightarrow \mu$ decay. Greisen argues that, since μ mesons are decay products of π mesons and π mesons are produced by the primary protons in the atmosphere at a height of about 20 km above sea level, a π meson must possess an energy $< 10^{11}$ ev in order to decay into a μ meson before being absorbed in the atmosphere or in the first few meters of earth. The majority of π mesons produced with energies $> 10^{11}$ ev will live sufficiently long, because of the time dilatation factor $\epsilon/\mu c^2$ [$\tau = \tau_0(\epsilon/\mu c^2)$ where τ is the lifetime in the laboratory system, $\tau_0 = 2.5 \times 10^{-8}$ sec is the lifetime for $\pi \rightarrow \mu$ decay in the rest frame of the π meson, ϵ is the π meson energy, and μ is the π meson rest mass] that they will quickly be absorbed by air nuclei or by earth nuclei before they decay into μ mesons. This accounts for an extra factor of approximately $1/d$ in the absorption curve for μ mesons below a depth d corresponding to about 300 m.w.e., that is, the change from a $d^{-1.7}$ to a $d^{-2.5}$ law.[66]

---

[67] K. Greisen, *Phys. Rev.*, **73**: 521 (1948); cf. also S. Hayakawa and S. Tomonoga, *Prog. Theor. Phys.*, **4**: 287, 496 (1949); S. Hayakawa, *Phys. Rev.*, **84**: 37 (1951); and D. C. Peaslee, *Nuovo cimento*, **9**: 61 (1952).

At depths greater than 1000 m.w.e., the μ mesons must lose energy not only by ionization but to some extent by bremsstrahlung, and it can be shown that at 1600 m.w.e. where Bollinger[63] has performed his measurements, the differential μ meson spectrum $d\epsilon/\epsilon^{\gamma+1}$ should be converted into an absorption curve $d^{-1.26(\gamma+1)} \approx d^{-3.5}$ for $\gamma \approx 1.7$. This expectation appears to be confirmed by Bollinger, who finds a variation of the form $d^{-3.5\pm0.2}$ between the depths 1570 and 2200 m.w.e. It is clear that the validity of any conclusions drawn from the depth variation is contingent upon our knowledge of the μ meson spectrum. In order to ensure even more reliable conclusions, it is desirable to measure the μ meson intensity not only as a function of the depth d but also as a function of the azimuthal angle θ (since more μ mesons should come from an inclined direction for the same amount of absorbing material). If the depth dependence is represented by d^{-n} and the azimuthal variation by $\cos^m \theta$, then it can be shown that, independent of the details of the energy spectrum of μ mesons, the $\pi \rightarrow \mu$ decay hypothesis would require that $n - m$ is equal to unity. The azimuthal measurement has also been carried out by Bollinger,[63] who finds $m = 2.8 \pm 0.15$ and therefore $n - m = 0.8 \pm 0.3$. This result is consistent with the $\pi \rightarrow \mu$ decay process as the explanation for the kink in the μ meson underground absorption curve. If this explanation is accepted, the value of the $\pi \rightarrow \mu$ decay lifetime which is implied is in agreement with the directly measured value.

C. Star Production Due to Energetic μ Mesons. We have seen that the behavior of the μ mesons up to underground depths of about 1600 m.w.e. can be explained reasonably well in terms of electromagnetic interactions; *i.e.*, the interaction mean free path of μ mesons with nuclei cannot be appreciably less than 1600 m.w.e. However, a cross section for nuclear interaction of energetic μ mesons of this order of magnitude is not excluded, and actually George and Evans[68] were the first to show that just such a cross section exists by exposing photographic emulsions for 6 to 12 months at depths up to 60 m.w.e. Table 4 lists the numbers and

TABLE 4. EXPERIMENTAL DATA ON NUCLEAR STAR PRODUCTION UNDERGROUND

Depth below ground, m.w.e.	Number of stars observed	Frequency/cm^3/day
0	383	1.46 ± 0.07
20	7	0.0066 ± 0.0025
34	13	0.0044 ± 0.0012
60	22	0.0050 ± 0.0010

---

[68] E. P. George and J. Evans, *Proc. Phys. Soc.*, 63A: 1248 (1950).

frequencies of stars observed at sea level and at three different underground depths by George and Evans. Despite the poor statistics, it is clear that there is a slow variation of the star production frequency with depth. This fact suggests that the underground stars are produced either directly or indirectly by fast μ mesons since the star-producing radiation above sea level, *viz.*, nucleons and π mesons, are absorbed too rapidly to account for the slow decrease. Actually, of the 42 underground stars observed, only 24 were detected in electron-sensitive plates and of these, 10 were initiated by charged primaries and 14 by neutral primaries. If the energies in the 10 stars are evaluated in accordance with the empirical relation

$$\epsilon\ (\text{Mev}) = 37N_h + 4N_h^2 \tag{27a}$$

where N_h is the number of heavy prongs, a correlation can be established between the angle of deflection of the charged primary (assuming it to be a μ meson undergoing an elastic collision with a nucleon in the nucleus) and the energy ϵ. The energies of the incident μ mesons so determined lie in the range 10^9 to 10^{10} ev, as they should. The 14 stars produced by neutral primaries are probably due to neutrons (themselves star products from fast μ meson disintegrations) and to photons in equilibrium with the μ mesons.

If it is assumed that the charged primaries producing the underground stars are μ mesons, one can deduce a nuclear interaction cross section which turns out to be about 5×10^{-30} cm^2 per nucleon. A cross section of this order cannot be due to the extremely weak interaction of the meson-neutrino field with nucleons (cf. above), and its origin must be sought elsewhere. A likely origin is found immediately if it is recalled that a virtual photon field[69] is associated with the high-energy charged μ meson and that the measured cross section for photon-initiated stars is 10^{-28} cm^2 per nucleon. This can be seen as follows: a high-energy particle of charge e, rest mass μ, and energy ϵ is equivalent to a beam of photons with a frequency distribution $N(\omega)$ given by[69]

$$N(\omega)d\omega = \frac{2\alpha}{\pi}\log\left[\frac{\epsilon}{\hbar\omega d(\mu c/\hbar)}\right]\frac{d\omega}{\omega} \tag{28}$$

where α is the fine-structure constant, d is the de Broglie wave length of the particle or the linear dimension of the structure with which the particle interacts, whichever is the larger (in the present instance $d \approx R$, the nuclear radius[70]). The photon spectrum extends to the frequency

---

[69] E. J. Williams, *Kgl. Danske Videnskab. Selskab.*, **13**: 4 (1935).

[70] Strictly speaking, $R = (\hbar/m_\pi c)A^{\frac{1}{3}}$ where m_π is the π meson mass and A is the mass number; we set $R = \hbar/\mu c$ (μ is the μ meson mass) since the entire calculation is only approximate.

$\omega_{\max} = \epsilon/\hbar$. Using Eq. (28), the cross section for star production by a μ meson of energy ϵ can be written

$$\sigma = \int_{\omega_{\min}}^{\omega_{\max}} \sigma(\omega) \frac{2\alpha}{\pi} \log\left(\frac{\epsilon}{\hbar\omega}\right) \frac{d\omega}{\omega} \tag{29}$$

where $\sigma(\omega)$ is the experimental cross section for photostar production at an energy $\hbar\omega$ and $\omega_{\min}$ is the threshold frequency for star production, say $\mu c^2/\hbar$.

Recent synchrotron experiments[71] yield photostar production cross sections comparable with photo-π meson production cross sections. Thus Miller[71] at Berkeley has made photographic exposures at synchrotron energies of 322, 242, and 161 Mev and measured the absolute yields of stars with two prongs and higher. Assuming that the star production cross sections are proportional to mass number, he finds a cross section of $9.8 \pm 1.2 \times 10^{-27}$ cm²/equivalent quantum for silver in the energy range 242 to 322 Mev and a cross section of $6.2 \pm 0.7 \times 10^{-27}$ cm² in the energy range 161 to 242 Mev. Since the cross sections for photomesic production in silver are comparable with these cross sections, it is likely that a sizable fraction of the photostars are associated with real meson production and most of the remainder with virtual meson production (*i.e.*, a π meson is produced and reabsorbed in the same nucleus knocking out several nucleons). We see that the photostar production cross section stays roughly constant, at about 10^{-28} cm² per nucleon. Assuming this value up to 10^{10} ev (a somewhat more dubious assumption although the result is insensitive to the exact variation because of the logarithmic variation of the number of light quanta), Eq. (29) leads to a cross section of about 4×10^{-30} cm²/nucleon[72] for star production by μ mesons having an energy of about 10^{10} ev, in good agreement with experiment.

George and Evans have also observed that 4 of the 10 stars produced by charged primaries contain showers of minimum ionization tracks, although none of the 14 stars initiated by neutral primaries contain shower particles. The stars containing showers presumably can also be explained in terms of the virtual photon field associated with an energetic μ meson which produces a fast proton or π meson which subsequently multiplies inside the nucleus (*i.e.*, plural production of shower particles). It is possible that a very energetic virtual photon may produce several π mesons in one elementary act (*i.e.*, multiple production), although it is likely that plural production is the dominant process for energies in the neighborhood of 10^{10} ev (cf. Chap. 8).

---

[71] Cf. S. Kikuchi, *Phys. Rev.*, **81**: 1060 (1951); R. D. Miller, *Phys. Rev.*, **82**: 260 (1951).

[72] If $\sigma(\omega)$ is assumed constant, Eq. (29) integrates to $\sigma = \sigma(\omega)(\alpha/\pi) \log^2 (\epsilon/\mu c^2)$; setting $\sigma(\omega) = 10^{-28}$ cm² and $\epsilon = 10^{10}$ ev yields $\sigma = 4 \times 10^{-30}$ cm².

Other authors have also obtained evidence for a small nuclear interaction of μ mesons deep underground; for example, George and Trent[73] have detected showers of penetrating particles underground which must have been produced by μ mesons, and Cocconi Tongiorgi[74] has detected groups of moderate-energy neutrons underground which must have had a similar origin. Most recently, Cocconi and Cocconi Tongiorgi[75] have measured the absorption curve in water (at depths up to 60 m) of the radiation producing nuclear disintegrations by recording the neutron showers produced in an absorber surrounded by BF_3 counters. In contrast to the photographic technique of George and Evans, the neutron method has the advantage of providing greater statistical accuracy because thick absorbers can be used. On the other hand, the interpretation of the neutron data is not so clearcut as the interpretation of the photographic results. Nevertheless, by carefully analyzing the absorption curve, Cocconi and Tongiorgi show that the N component produces the great majority of events at sea level and under the first few meters of water with an absorption length of about 160 g/cm², whereas, at greater depths, say from 10 m of water down to 60 m, neutron events are produced by the penetrating component of the cosmic radiation, *i.e.*, the μ mesons, with an absorption length of the order of 4000 g/cm². They show that the neutron events of low multiplicity (1 and 2) produced in a 4-in. lead absorber at 20 m water are caused chiefly by the capture of slow negative μ mesons and by photons in equilibrium with the μ mesons (this is no longer true of neutron events with a multiplicity greater than 2). After subtracting these contributions, the Cornell group finds that the total number of counts associated with the 4-in. lead absorber is 37 per hour and that the average neutron multiplicity is of the order of 15. Furthermore, the interaction cross section turns out to be $1 \pm 0.5 \times 10^{-29}$ cm²/nucleon corresponding to an average μ meson energy of about 6 Bev (*i.e.*, 20 m of water). A similar analysis of their 60-m water data (statistically less accurate than the 20-m data) leads the Cornell group to a similar cross section. Moreover, the ratio of frequencies of neutron events occurring in the 4-in. lead absorber at 20 and 60 m of water turns out to be 3.7, close to the ratio between the μ meson intensities at the two levels, which is 4. The almost constant cross section for nuclear interaction of μ mesons which is observed at the two levels (within the statistical error) is certainly consistent with the logarithmic variation predicted by Eq. (29). It is also interesting to note that the average energy loss corresponding to Eq. (29) is given by

---

[73] E. George and P. Trent, *Nature*, **164**: 838 (1949).

[74] V. Cocconi Tongiorgi, *Phys. Rev.*, **76**: 517 (1949).

[75] G. Cocconi and V. Cocconi Tongiorgi, *Phys. Rev.*, **84**: 29 (1951).

$$\frac{\Delta\epsilon}{\epsilon} = \frac{2}{\log^2(\epsilon/\mu c^2)} \tag{30}$$

which is only 11 per cent at $\epsilon = 10^{10}$ ev, a result which again is not inconsistent with the underground data.

In conclusion, it seems clear that, while the nuclear interaction of μ mesons is much stronger than is allowed by the coupling of the nucleon and the μ meson-neutrino field, it is much weaker than is required by any of the meson pair theories. The cross sections which are observed, *viz.*, of the order of 10^{-29} cm^2 per nucleon, can be completely understood in terms of the virtual photon field associated with the moving charge of the μ meson.

CHAPTER 7

NUCLEAR INTERACTION OF FAST π MESONS

1. Introduction

We have seen in the preceding chapter that the nuclear interaction of μ mesons is extremely weak and that the small nuclear interaction cross section which is observed (10^{-29} cm^2 per nucleon) can be explained completely in terms of the virtual photon field associated with the charge of the μ meson. This is not at all surprising since the coupling constant of the μ meson-neutrino field to the nucleon field is of the same order of magnitude as the β decay coupling constant, and it is known how extremely small the latter is. However, the coupling of the π meson to the nucleon field is many orders of magnitude greater than that of the μ meson, and the large value of the π meson coupling constant indicated by the many production experiments (discussed in Chaps. 1 and 2) implies that the π meson should interact strongly with nucleons and nuclear matter. In this chapter, we examine more thoroughly the present status of our knowledge concerning the nuclear interaction of fast π mesons. We break down the nuclear interaction phenomena into the processes of elastic and inelastic scattering of π mesons by nuclei, the absorption of π mesons by nuclei, and the reproduction of π mesons.

Some aspects of the problem of nuclear interaction of π mesons have been treated in considerable detail in preceding chapters. Thus, in Chap. 4, we considered the two competing processes which occur when π^- mesons arriving in the K shells of mesic-hydrogen atoms are absorbed by the hydrogen nuclei. One process, involving the emission of a single high-energy γ ray (called radiative absorption) competes on equal terms with a second, involving the emission of a slow π^0 meson (called mesic absorption), when the π^- mesons are bound. For π^- mesons in the continuum, a third process can occur, *viz.*, ordinary scattering of π^- mesons by protons, and it becomes of great interest to find out how the three processes—radiative absorption, charge-exchange scattering (which is a more correct designation than mesic absorption), and ordinary scattering compete as the energy of the π^- meson increases.

Again, in Chap. 4, the three competing processes, which can occur when π^- mesons arrive in the K shells of mesic-deuterium atoms and are absorbed by the deuterium nuclei, were treated. In deuterium, not only is a bound π^- meson capable of giving rise to a high-energy γ ray or a low-energy π^0 meson but it can also undergo genuine absorption (called neutron absorption) and not give rise to any new particles but merely convert the proton in the deuteron into a neutron which shares the rest mass energy of the π^- meson with the other neutron. The observed rates of the three slow π^- reactions in deuterium enabled us to rule out the scalar and vector fields for the charged π mesons. For π^- mesons in the continuum, two new reactions are added for deuterium, *viz.*, the ordinary elastic scattering, $\pi^- + D \rightarrow \pi^- + D$ and the ordinary inelastic scattering, $\pi^- + D \rightarrow \pi^- + N + P$, in addition to the three cited above. Again, the relative cross sections for the five competing reactions in deuterium become of great theoretical and experimental interest.

It should be noted that, while the bound meson reactions involve only the negative variety, all reactions can take place from the continuum for π^+ mesons as well: one need only substitute a proton for a neutron and conversely in all the equations. Of course, this statement must be qualified since free neutrons do not exist and, for hydrogen, π^+ mesons can be only scattered and not charge-exchange scattered or radiatively absorbed (unless doubly charged isobaric states of the proton exist—cf. Chap. 9). Now, one of the processes involving the nuclear interaction of fast π^+ mesons with deuterons was examined in Chap. 4 in connection with our discussion of the determination of the π meson spin. It was shown that the meson absorption reaction $\pi^+ + D \rightarrow P + P$ is related by detailed balancing to the production reaction $P + P \rightarrow \pi^+ + D$ and that measurement of the cross sections for both reactions, at appropriately related meson and proton energies, would yield the spin of the π^+ meson. It was the fulfillment of this program which led to spin zero for the charged π meson and to fixing the charged π meson as a pseudoscalar particle. However, the other four fast meson reactions in deuterium still remain to be properly discussed.

Finally, in Chap. 5, we treated the absorption of bound π^- mesons by nuclei heavier than deuterons. It was seen that, in a photographic emulsion, 73 per cent of the π^- absorptions gave rise to nuclear stars with one or more visible prongs. Independent experimental evidence was cited as proof that the remaining 27 per cent of the π^- absorptions were due chiefly to neutron stars with the possibility that not more than 1 to 2 per cent could represent radiative absorption. For π^- mesons in the continuum (and also for π^+ mesons), the possible modes of nuclear interaction of π mesons are increased to include not only genuine (star) absorption and radiative absorption, but also elastic scattering (including diffraction scattering), charge-exchange scattering, and inelastic scattering.

At extremely high π meson energies (available in the cosmic radiation), the nuclear interaction of the π meson can lead to the production of additional π mesons with or without nuclear stars. We shall discuss the experimental material bearing on all these possible modes of nuclear interaction of π mesons together with the theoretical interpretations which are at present available.

2. Interaction of π Mesons with Protons

As usual, our discussion begins with the nucleus of hydrogen. A study of the fast π meson reactions in hydrogen, in particular the scattering reactions, should yield some very important information concerning the π meson-nucleon interaction: the type of coupling and the magnitude and sign of the various coupling constants (g, g_N, and g_P or f, f_N, and f_P). Only four meson reactions can take place in hydrogen (as long as isobaric states of nucleons are not considered); they are

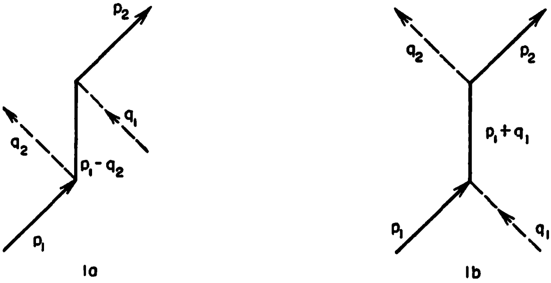

FIG. 1. Feynman diagrams for π meson scattering by nucleons (see text); the solid lines represent nucleons, the dotted lines π mesons.

$$\pi^+ + P \rightarrow \pi^+ + P \tag{I}$$
$$\pi^- + P \rightarrow \pi^- + P \tag{II}$$
$$\pi^- + P \rightarrow \pi^0 + N \tag{III}$$
$$\pi^- + P \rightarrow \gamma + N \tag{IV}$$

The first three reactions are the scattering reactions and have been calculated for pseudoscalar π mesons by many authors[1] in the lowest order of weak coupling theory.[2] The lowest order Feynman diagrams for the three types of scattering are shown in Fig. 1. In diagram 1*a* corresponding to scattering process (I), the final meson is emitted by the proton prior to the absorption of the initial meson since a proton can emit but not absorb a π^+ meson. (The Feynman diagram corresponding to the reaction $\pi^- + N \rightarrow \pi^- + N$ is identical with 1*a*.) In diagram 1*b*, corresponding to scattering process (II), the absorption of the initial meson precedes the emission of the final meson. (The Feynman diagram for the reaction $\pi^+ + N \rightarrow \pi^+ + N$ is identical with 1*b*.) It is evident that both Feynman diagrams 1*a* and 1*b* contribute to the charge-exchange scattering (III) and that the cross section for the charge-exchange reaction $\pi^+ + N \rightarrow \pi^0 + P$ is identical with that for (III). With each diagram goes a relativistically invariant matrix element which may be written down immediately in the characteristic Feynman fashion. The cross sections are then obtained by taking the absolute squares of the total matrix element, averaging over the spin of the initial nucleon, and summing over the spin of the final nucleon. The weak coupling differential cross section in the laboratory system for all three reactions can be written in the form[3]

---

[1] Cf. Ashkin, Simon, and Marshak, *Prog. Theor. Phys.*, **5**: 634 (1950); M. Jean and J. Prentki, *Compt. rend.*, **230**: 365 (1950); M. Peshkin, *Phys. Rev.*, **81**: 425 (1951); and M. Cini and L. Radicati, *Nuovo cimento*, **7**: 317 (1951).

[2] Some strong coupling calculations of meson scattering have also been carried out and will be discussed briefly below.

$$\frac{d\sigma_{\rm I,II,III}}{d\Omega} = \frac{Mq_2^2|H|^2_{\rm I,II,III}}{q_1q_2(M + \epsilon_1) - q_1^2\epsilon_2 \cos\theta} \tag{1}$$

where $(\mathbf{q}_1, \epsilon_1)$ and $(\mathbf{q}_2, \epsilon_2)$ are the momentum-energy four-vectors of the initial and final mesons, respectively (it is assumed for the purposes of the scattering calculation that the π^0 meson mass is identical with the charged π meson mass), θ is the angle of scattering, and $|H|^2_{\rm I,II,III}$ are the matrix elements corresponding to reactions (I), (II), and (III). Since the π meson is pseudoscalar, we record only the matrix elements for the *PS*(*PS*) and *PS*(*PV*) theories. They are[4]

PS(*PS*)

$$|H|^2_{\rm I} = \frac{g^4M^2A}{(2M\epsilon_2 - \mu^2)^2} \tag{2a}$$

$$|H|^2_{\rm II} = \frac{g^4M^2A}{(2M\epsilon_1 + \mu^2)^2} \tag{2b}$$

$$|H|^2_{\rm III} = g^2M^2A\left(\frac{g_N}{2M\epsilon_1 + \mu^2} + \frac{g_P}{2M\epsilon_2 - \mu^2}\right)^2 \tag{2c}$$

PS(*PV*)

$$|H|^2_{\rm I} = \frac{f^4M^2}{\mu^4}(E^2A + B - EC) \tag{3a}$$

$$|H|^2_{\rm II} = \frac{f^4M^2}{\mu^4}(D^2A + B + DC) \tag{3b}$$

$$|H|^2_{\rm III} = \frac{f^2M^2}{\mu^4}\{A(Df_N + Ef_P)^2 + B(f_N + f_P)^2 - C[Df_N^2 + (D + E)f_Nf_P + Ef_P^2]\} \tag{3c}$$

[3] The Coulomb interaction has been neglected in all calculations of meson scattering by hydrogen, a sufficiently good approximation at experimental energies provided the nuclear scattering cross section is not too low (cf. L. Van Hove, *Phys. Rev.*, in press).

[4] The scattering cross sections are all taken from Ashkin *et al.*, *loc. cit.*

where
$$A = \frac{\epsilon_1\epsilon_2}{M^2} - \frac{\mu^2}{2M^3}(\epsilon_1 - \epsilon_2)$$
$$B = 4 + \frac{2}{M}(\epsilon_1 - \epsilon_2)$$
$$C = \frac{2}{M}(\epsilon_1 + \epsilon_2)$$
$$D = \frac{4M^2 + \mu^2 + 2M\epsilon_1}{2M\epsilon_1 + \mu^2}$$
$$E = \frac{4M^2 + \mu^2 - 2M\epsilon_2}{2M\epsilon_2 - \mu^2}$$

and g, g_P, g_N, f, f_P, and f_N are the π meson coupling constants as usual.

It is useful to record in addition the equations relating the angles and energies in the laboratory system to the corresponding quantities in the center-of-mass system. If $\bar{\theta}$ is the angle of scattering of the meson and $\bar{\gamma}$ and $\bar{\Gamma}$ refer respectively to the energies of the meson and nucleon in units of their respective rest masses, all quantities in the center-of-mass system, it can be shown that

$$\epsilon_2 = \mu\bar{\gamma}\bar{\Gamma} + M(\bar{\Gamma}^2 - 1)\cos\bar{\theta} \tag{4a}$$
$$\mu\sqrt{\bar{\gamma}^2 - 1} = M\sqrt{\bar{\Gamma}^2 - 1} \tag{4b}$$
$$\bar{\Gamma} = \frac{\gamma + M/\mu}{\sqrt{1 + 2(M/\mu)\gamma + (M/\mu)^2}} \tag{4c}$$

where γ is the energy of the incident meson in the laboratory system in units of its rest mass, that is, $\gamma = \epsilon_1/\mu$. The quantity $\cos\bar{\theta}$ can be expressed in terms of $\cos\theta$ as follows:

$$\cos\bar{\theta} = \frac{\left[1 + 2\frac{M}{\mu}\gamma + \left(\frac{M}{\mu}\right)^2\right]\cos\theta\sqrt{1 - \left(\frac{\mu}{M}\right)^2\sin^2\theta} - \left[\gamma + \frac{\mu}{M}\right]\left[\gamma + \frac{M}{\mu}\right]\sin^2\theta}{\left[\gamma + \frac{M}{\mu}\right]^2 - (\gamma^2 - 1)\cos^2\theta} \tag{5a}$$

and therefore

$$J = \frac{d\cos\bar{\theta}}{d\cos\theta}$$
$$= \frac{\left[1 + \frac{2M}{\mu}\gamma + \left(\frac{M}{\mu}\right)^2\right]\left\{\left[\gamma + \frac{\mu}{M}\right]\cos\theta + \left[\gamma + \frac{M}{\mu}\right]\sqrt{1 - \left(\frac{\mu}{M}\right)^2\sin^2\theta}\right\}^2}{\sqrt{1 - \left(\frac{\mu}{M}\right)^2\sin^2\theta}\left\{\left[\gamma + \frac{M}{\mu}\right]^2 - (\gamma^2 - 1)\cos^2\theta\right\}^2} \tag{5b}$$

J represents the ratio of solid angle in the center of mass to the laboratory system and is a particularly useful quantity for translating the laboratory angular distribution into the corresponding center-of-mass angular distribution. Equations (4) and (5) can be used to compute the energy loss of a π meson resulting from the elastic scattering by a nucleon at rest as a function of the incident meson energy and the scattering angle (in the laboratory system); Table 1 lists some representative numbers in both the accelerator and cosmic-ray energy regions ($\mu = 276\ m_e$).

The weak coupling differential cross sections can be integrated exactly to yield the total cross sections; however, the results are rather complicated, and we give instead for each reaction the total cross section in the extreme nonrelativistic (N.R.) limit (sometimes called the Thomson limit in analogy with the scattering of photons by electrons) and in the extreme relativistic (E.R.) limit:

Reaction I
PS(*PS*)

$$\sigma_{\text{I}}(\text{N.R.}) = \pi\left(\frac{g^2}{M}\right)^2 \frac{1}{[1-(\mu/2M)]^2[1+(\mu/M)]^2} \tag{6a}$$

$$\sigma_{\text{I}}(\text{E.R.}) = \frac{\pi g^4}{2M\epsilon_1}\log\left(\frac{2\epsilon_1}{M}\right) \tag{6b}$$

PS(*PV*)

$$\sigma_{\text{I}}(\text{N.R.}) = \pi\left(\frac{f^2}{M}\right)^2 \frac{1}{[1-(\mu/2M)]^2[1+(\mu/M)]^2} \tag{7a}$$

$$\sigma_{\text{I}}(\text{E.R.}) = \pi\left(\frac{f}{\mu}\right)^4 M\epsilon_1 \tag{7b}$$

Reaction II
PS(*PS*)

$$\sigma_{\text{II}}(\text{N.R.}) = \pi\left(\frac{g^2}{M}\right)^2 \frac{1}{[1+(\mu/2M)]^2[1+(\mu/M)]^2} \tag{8a}$$

$$\sigma_{\text{II}}(\text{E.R.}) = \frac{\pi g^4}{4M\epsilon_1} \tag{8b}$$

PS(*PV*)

$$\sigma_{\text{II}}(\text{N.R.}) = \pi\left(\frac{f^2}{M}\right)^2 \frac{1}{[1+(\mu/2M)]^2[1+(\mu/M)]^2} \tag{9a}$$

$$\sigma_{\text{II}}(\text{E.R.}) = \frac{\pi f^4 M\epsilon_1}{\mu^4} \tag{9b}$$

TABLE 1. ENERGY LOST BY π MESON IN SCATTERING FROM NUCLEON AT REST (IN MEV)

Angle of scattering / Incident kinetic energy, Mev	10°	20°	30°	45°	60°	90°	120°	150°	180°
5	0.02	0.09	0.20	0.42	0.70	1.31	1.83	2.17	2.28
50	0.29	1.08	2.34	4.94	8.09	14.82	20.26	23.68	24.83
100	0.77	2.83	4.53	10.37	16.82	32.54	45.25	51.63	53.80
200	1.60	6.12	13.21	27.33	43.69	75.56	99.37	113.19	117.64
400	4.46	17.06	36.33	73.16	113.29	184.68	233.07	259.34	267.53
800	13.95	52.68	109.30	209.51	308.12	460.94	551.06	596.09	609.62
1,600	47.69	174.48	345.08	610.35	835.06	1,124.3	1,270.01	1,336.9	1,356.4
4,800	365.8	1,119.1	2,044.3	2,998.4	3,581.4	4,149.6	4,379.0	4,473.9	4,500.6
14,400	2,771.3	7,027.4	9,818.3	11,920.5	12,882.6	13,658.9	13,935.6	14,045.6	14,075.7
43,200	17,874.1	31,889.3	37,319.3	40,364.9	41,547.5	42,423.0	42,719.3	42,835.0	42,866.6

Reaction III

PS(*PS*)

$$\sigma_{\text{III}}(\text{N.R.}) = \pi\left(\frac{g}{M}\right)^2 \frac{1}{[1+(\mu/M)]^2[1-(\mu/M)]^2} \left[(g_N+g_P)^2 + \frac{\mu}{M}(g_P^2 - g_N^2) + \left(\frac{\mu}{2M}\right)^2 (g_N - g_P)^2\right] \tag{10a}$$

$$\sigma_{\text{III}}(\text{E.R.}) = \frac{\pi g^2 g_P^2}{2M\epsilon_1}\log\left(\frac{2\epsilon_1}{M}\right) \tag{10b}$$

PS(*PV*)

$$\sigma_{\text{III}}(\text{N.R.}) = \pi\left(\frac{f}{M}\right)^2 \frac{1}{[1+(\mu/M)]^2[1-(\mu/M)]^2} \left[(f_N+f_P)^2 + \frac{\mu}{M}(f_P^2 - f_N^2) + \left(\frac{\mu}{2M}\right)^2 (f_N - f_P)^2\right] \tag{11a}$$

$$\sigma_{\text{III}}(\text{E.R.}) = \frac{\pi f^2 (f_N - f_P)^2 M\epsilon_1}{\mu^4} \tag{11b}$$

Examination of the differential and total cross sections enumerated above shows some important differences in the predictions made by the *PS*(*PS*) and *PS*(*PV*) theories. Table 2 lists the total cross sections and the ratios of the differential cross sections in the laboratory system at

TABLE 2. WEAK COUPLING CROSS SECTIONS FOR THE SCATTERING OF π MESONS BY NUCLEONS (CM²)

	Meson kinetic energy, Mev			
	0	25	50	100
PS(*PS*)				
σ_{I}	1.2×10^{-27}	1.2×10^{-27}	1.2×10^{-27}	1.1×10^{-27}
$\sigma_{\text{I}}(0°):\sigma_{\text{I}}(90°):\sigma_{\text{I}}(180°)$	1:0.75:0.55	1:0.75:0.55	1:0.74:0.54	1:0.73:0.53
σ_{II}	8.9×10^{-28}	8.6×10^{-28}	8.2×10^{-28}	7.4×10^{-28}
$\sigma_{\text{II}}(0°):\sigma_{\text{II}}(90°):\sigma_{\text{II}}(180°)$	1:0.75:0.55	1:0.68:0.47	1:0.63:0 40	1:0.54:0.31
σ_{III}	2.4×10^{-29}	2.9×10^{-29}	3.4×10^{-29}	4.6×10^{-29}
$\sigma_{\text{III}}(0°):\sigma_{\text{III}}(90°):\sigma_{\text{III}}(180°)$	1:0.75:0.55	1:1.33:1.34	1:2.15:2.57	1:4.73:6.57
PS(*PV*)				
σ_{I}	1.2×10^{-27}	1.5×10^{-28}	5.2×10^{-26}	1.6×10^{-25}
$\sigma_{\text{I}}(0°):\sigma_{\text{I}}(90°):\sigma_{\text{I}}(180°)$	1:0.75:0.55	1:0.83:0.69	1:0.59:0 38	1:0.47:0.25
σ_{II}	8.9×10^{-28}	1.7×10^{-28}	5.4×10^{-26}	1.6×10^{-25}
$\sigma_{\text{II}}(0°):\sigma_{\text{II}}(90°):\sigma_{\text{II}}(180°)$	1:0.75:0.55	1:0.41:0.14	1:0.45:0.20	1:0 43:0.20
σ_{III}	2.4×10^{-29}	2.2×10^{-28}	7.5×10^{-26}	2.3×10^{-25}
$\sigma_{\text{III}}(0°):\sigma_{\text{III}}(90°):\sigma_{\text{III}}(180°)$	1:0.75:0.55	$1:4 \times 10^{-4}:0.31$	$1:2 \times 10^{-4}:0.27$	$1:1 \times 10^{-4}:0.23$

0, 90, and 180° corresponding to meson kinetic energies 0, 25, 50, and 100 Mev for all three types of scattering; the results are given in units of g^4 or f^4 for reactions (I) and (II) and in units of $g^2g_0^2$ or $f^2f_0^2$ for the charge-exchange scattering reaction (III) (it is assumed that $g_N = -g_P = g_0$ or $f_N = -f_P = f_0$—cf. below). We have not recorded the values of the cross sections for meson energies greater than 100 Mev because, while it is hoped that the qualitative features of the weak coupling predictions are significant below 100 Mev, it is certain that the theory breaks down at relativistic nucleon energies [if only because the *PS*(*PV*) cross sections increase indefinitely—already evident for the 100-Mev numbers in Table

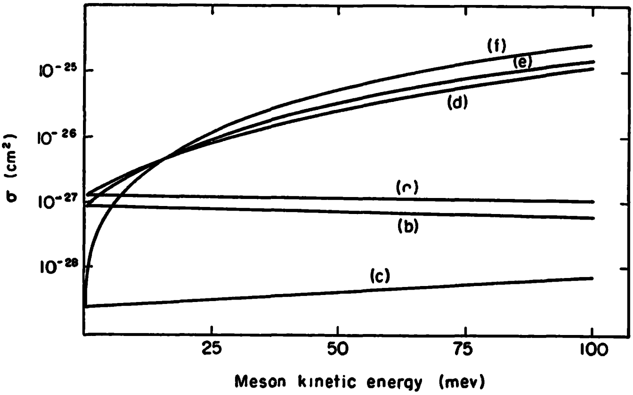

FIG. 2. Weak coupling total π meson scattering cross sections as a function of meson energy. Curve (*a*) corresponds to the *PS*(*PS*) theory for reaction (I), (*b*) to the *PS*(*PS*) theory for reaction (II), (*c*) to the *PS*(*PS*) theory for reaction (III) and $g_N = -g_P$, (*d*) to the *PS*(*PV*) theory for reaction (I), (*e*) to the *PS*(*PV*) theory for reaction (II), (*f*) to the *PS*(*PV*) theory for reaction (III) and $f_N = -f_P$; units same as for Table 2.

2—and must be cut down by the reaction of the meson field—cf. below]. In order to exhibit in a more striking fashion the differences between the *PS*(*PS*) and *PS*(*PV*) theories, we have plotted in Fig. 2 the variation of total cross section with energy from 0 to 100 Mev for all three reactions. It is seen from Fig. 2 (and from Table 2) that the cross sections for the ordinary scattering reactions (I) and (II) differ only slightly from each other as regards both absolute value and variation with energy; the angular distributions predicted for reactions (I) and (II) are also very similar, as can be seen from Table 2. The striking feature of curves (*a*) and (*b*) in Fig. 2 is the essentially constant cross section as a function of energy predicted by the *PS*(*PS*) theory in contrast to the rapidly increasing cross section predicted by the *PS*(*PV*) theory. The fact that the *PS*(*PV*) strong coupling theory leads to the same rapid increase of scattering cross section with energy (cf. below) as does the weak coupling theory underlines the characteristic behavior of a derivative coupling theory.

The cross section for the charge-exchange reaction (III) depends very sensitively on the relative signs of the π^0 meson coupling constant to the proton and neutron; if the two π^0 coupling constants have the same sign, the predicted cross sections are very similar to those for reactions (I) and (II) and are not given in Table 2 or plotted in Fig. 2. The curves and values which are given are those corresponding to opposite sign of the proton and neutron π^0 coupling constants (symmetrical theory) and differ markedly from the curves for reactions (I) and (II). The $PS(PS)$ curve for reaction (III) has the same shape as the $PS(PS)$ curves for reactions (I) and (II) but is reduced by a factor of about 50, whereas the $PS(PV)$ curve for reaction (III) starts out much lower than the $PS(PV)$ curves for reactions (I) and (II) but becomes almost identical with the latter two above about 15 Mev. There are some equally striking differences predicted by the $PS(PS)$ and $PS(PV)$ theories for the angular distribution of the scattered mesons, in particular for the charge-exchange reaction, as can be seen from Table 2. Moreover, it is interesting to note that the zero energy cross sections (*i.e.*, the Thomson limits) corresponding to PS and PV coupling are identical for equal values of the coupling constant. Also, the charge-exchange scattering cross section in the Thomson limit can be derived immediately from the calculation (cf. Chap. 4) of the transition probability for π^- mesic absorption from the K shell of the mesic-hydrogen atom by replacing the reciprocal volume of the meson-proton system by the number of protons per cubic centimeter. While the actual numbers in Table 2 cannot be taken seriously because of the importance of higher order effects[5] and the possible incorrect treatment of negative-energy states in weak coupling theory,[6] it is reasonable to hope that the qualitative differences will persist to an extent sufficient to discriminate between pseudoscalar and pseudovector coupling on the basis of scattering experiments.

The radiative absorption reaction in hydrogen, *viz.*, reaction (IV) listed above, is readily seen to be the inverse of the photomesic production process. Once this is recognized, it is possible to write down the cross section for reaction (IV) by starting with Eq. (16*a*) in Chap. 1 and applying the principle of detailed balancing. Since the equivalence theorem between pseudoscalar and pseudovector coupling holds for the photomesic production process in the lowest order of perturbation theory, it must of necessity hold for the radiative absorption process, and one finds the following differential cross section for reaction (IV) for pseudoscalar π mesons in the center-of-mass system:

---

[5] Cf. Ashkin, Simon, and Marshak, *loc. cit.;* and E. Corinaldesi and G. Field, *Phil. Mag.*, **40**: 1159 (1949); **41**: 364 (1950).

[6] Some indication of this trouble was already noted in Chap. 4 in connection with our discussion of the slow π^- meson reactions in hydrogen.

$$\left(\frac{d\sigma_{\text{IV}}}{d\Omega}\right)_{\text{c.m.}} = 2\left(\frac{k}{q}\right)^2\left(\frac{d\sigma^-}{d\Omega}\right)_{\text{c.m.}} \tag{12}$$

where $(d\sigma^-/d\Omega)_{\text{c.m.}}$ is the cross section for the production of π^- mesons and $\mathbf{q}$ and $\mathbf{k}$ are the π meson and photon momenta in the center-of-mass system and are related by the equation

$$\sqrt{\mu^2 + q^2} + \sqrt{M^2 + q^2} = \omega + \sqrt{M^2 + k^2} \tag{12a}$$

with ω the photon energy in the center-of-mass system. Figure 3 contains a graph of the theoretically predicted total cross section for reaction (IV) as a function of π^- meson kinetic energy (from 0 to 100 Mev). A direct measurement of the cross section for reaction (IV) would be extremely valuable because it would determine the cross section for the production of π^- mesons in photon-neutron collisions (by detailed balancing); the comparison of the latter cross section with the cross section for π^+ production in photon-proton collisions would then impose a stringent test on weak coupling theory (cf. Chap. 1).

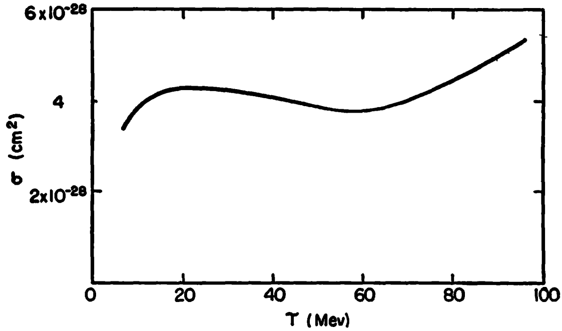

FIG. 3. Weak coupling $PS(PV)$ total cross section for reaction (IV) as a function of meson kinetic energy τ. The meson coupling constant is set equal to unity.

The relativistic weak coupling cross sections for reactions (I) to (IV) have been presented in order to exhibit the differences between the $PS(PS)$ and $PS(PV)$ formulations for the π meson field. If one restricts oneself to the $PS(PV)$ theory, it is helpful to write down the cross sections in the approximation of infinite nucleon mass in order to facilitate comparison with the strong coupling predictions. The weak coupling differential cross sections for the symmetrical choice of coupling constants (that is, $f_N = -f_P = f/\sqrt{2}$) are:

$$\frac{d\sigma_{\text{I}}}{d\Omega} = \frac{d\sigma_{\text{II}}}{d\Omega} = \frac{f^4q^4}{\mu^4\epsilon^2} \tag{3a',b'}$$

$$\frac{d\sigma_{\text{III}}}{d\Omega} = \frac{2f^4q^4}{\mu^4\epsilon^2}\cos^2\theta \tag{3c'}$$

$$\frac{d\sigma_{\text{IV}}}{d\Omega} = \frac{2e^2f^2\epsilon}{\mu^2q}\left[1 - \frac{\mu^2q^2\sin^2\theta}{2\epsilon^2(\epsilon - q\cos\theta)^2}\right] \tag{12'}$$

In contrast to Eqs. (3a') to (3c'), the cross sections predicted by the classical strong coupling theory are[7]:

$$\frac{1}{2}\left(\frac{d\sigma_{\text{I}}}{d\Omega} + \frac{d\sigma_{\text{II}}}{d\Omega}\right) = \frac{11}{25}\left(\frac{q}{\epsilon}\right)^4 a^2\left(1 + \frac{52}{11}\cos^2\theta\right) \tag{13a}$$

$$\frac{d\sigma_{\text{III}}}{d\Omega} = \frac{4}{25}\left(\frac{q}{\epsilon}\right)^4 a^2\left(1 + \frac{4}{3}\cos^2\theta\right) \tag{13b}$$

where a is the nucleon source size. Equation (13a) is the expression for the average of the cross sections corresponding to (I) and (II), since the classical strong coupling theory is incapable of separating between the two scattering processes. The classical strong coupling expression for $d\sigma_{\text{IV}}/d\Omega$ is identical with Eq. (12′) except for a factor $\frac{2}{3}$ since this is the factor which enters into $(d\sigma^-/d\Omega)$ [cf. Eq. (12) and Sec. 4 of Chap. 1].

It is seen that, just as in the case of photoproduction of π^0 mesons, the weak and classical strong coupling theories predict comparable absolute magnitudes,[7a] the same strong dependence on the meson momentum,[7b] and completely different angular distributions for the π meson scattering. The ratio of ordinary [defined by $\frac{1}{2}(\sigma_{\text{I}} + \sigma_{\text{II}})$] to charge-exchange scattering turns out to be much larger in the classical strong coupling than in the weak coupling theory. The quantum mechanical strong coupling scattering cross sections[7c] show a fairly close resemblance to the classical results, except that the angular distributions turn out to be $(1 + 3\cos^2\theta)$ for all three processes (I), (II), and (III) and the corresponding magnitudes are in the ratios[7d] 9:1:2.

---

[7] D. Feldman, *Phys. Rev.*, in press.

[7a] Again, strictly speaking, the strong coupling scattering cross section is the smaller of the two since it is assumed that $a\mu < f^2$; an intermediate coupling theory applied in the neighborhood of resonance with a metastable nucleon isobar will yield a larger cross section (cf. reference 7; also footnote 22a of Chap. 1).

[7b] This is due to the fact that in the $M \to \infty$ approximation the $PS(PV)$ theory requires the meson to be emitted into a p-state.

[7c] Cf. G. Wentzel, *Phys. Rev.*, **86**: 437 (1952).

[7d] These ratios follow from an implicit resonance with the $I = \frac{3}{2}$, $J = \frac{3}{2}$ nucleon

Relatively few measurements of the differential cross sections for π meson scattering in hydrogen have been carried out thus far. A crude diffusion cloud chamber experiment[8] with the Columbia cyclotron using 53 ± 10 Mev π^+ mesons led to an anisotropic angular distribution in the center-of-mass system, $d\bar{\sigma}_I/d\bar{\Omega} \approx (1 \pm 0.2)(1 + 2\cos^2\bar{\theta})$ mb/ster; the total cross section is therefore 20 ± 4 mb. At the higher meson energies available from the Chicago cyclotron and with the use of scintillation counters and liquid hydrogen targets, Anderson *et al.*[8a] have obtained the differential cross sections listed in Table 3*a*.

TABLE 3*a*. COEFFICIENTS FOR THE DIFFERENTIAL SCATTERING CROSS SECTIONS IN H

Laboratory meson energy, Mev	Process	*a*	*b*	*c*	Total cross section, mb
110	(I)	3.5 ± 0.6	−4.6 ± 0.8	7.2 ± 1.8	74.5 ± 5.4
135	(I)	3.8 ± 2.2	−6.8 ± 2.7	17.5 ± 6.6	121 ± 19
135	(II)	1.2 ± 0.2	−0.1 ± 0.3	0.3 ± 0.7	16.2 ± 2.3
135	(III)	1.1 ± 0.6	−2.5 ± 0.5	6.3 ± 1.9	40.6 ± 2.3

The coefficients *a*, *b*, and *c* in Table 3*a* are related to the differential cross section in the center of mass system by:

$$\frac{d\bar{\sigma}}{d\bar{\Omega}} = a + b\cos\bar{\theta} + c\cos^2\bar{\theta}\,\frac{\text{mb}}{\text{ster}} \tag{13c}$$

The total cross sections derived from Eq. (13*c*) are listed in the last column. It is interesting to note that there are pronounced backward maxima in the angular distributions for processes (I) and (III) (indicating interference between *s*- and *p*-waves), whereas the angular distribution for process (II) is approximately isotropic.

A fairly large number of transmission experiments through hydrogen have been performed with both π^+ and π^- mesons; these experiments determine the total cross section σ_I for π^+ mesons and the sum $(\sigma_{II} + \sigma_{III} + \sigma_{IV})$ for π^- mesons. The results are tabulated in Table 3*b*. It can

---

isobar predicted by the quantum strong coupling theory (cf. footnote 22*a* of Chap. 1; also the *Proceedings of the Rochester Conference on Meson Physics*, Jan. 11–12, 1952). The more general consequences of the constancy of isotopic spin for meson scattering processes are examined by W. Heitler [*Proc. Roy. Irish Acad.*, **51**: 33 (1946)] and K. A. Brueckner [*Phys. Rev.*, **86**: 109 (1952)].

[8] Fowler, Fowler, Shutt, Thorndike, and Whittemore, *Phys. Rev.*, **86**: 1053 (1952).

[8a] Anderson, Fermi, Nagle, and Yodh, *Phys. Rev.*, **86**: 793 (1952).

easily be shown that σ_{IV} only contributes 1–2 mb [cf. Eq. (12)] so that column 3 of Table 3*b* closely represents the sum $(\sigma_{II} + \sigma_{III})$.

TABLE 3*b*. TOTAL INTERACTION CROSS SECTIONS IN *H*

Meson energy, Mev	σ_I, mb	$(\sigma_{II} + \sigma_{III} + \sigma_{IV})$ (mb)	Reference
37	17 ± 4	....	Barnes *et al.*[9a]
55–58	20 ± 10	....	Anderson *et al.*[9b]
	27.8 ± 2.5	17.6 ± 2.2	Isaacs *et al.*[9c]
82–89	50 ± 13	21 ± 8	Anderson *et al.*[9b,9d]
	....	13.1 ± 1.1	Chedester *et al.*[9e]
112–118	91 ± 6	31 ± 9	Anderson *et al.*[9b,9d]
135–136	152 ± 14	52 ± 6	Anderson *et al.*[9b,9d]
176	....	66 ± 6	Anderson *et al.*[9b,9d]
217	....	60 ± 6	Anderson *et al.*[9b,9d]

The rapid increase of cross section exhibited in Table 3*b* for both π^+ and π^- mesons provides strong evidence for the *PS*(*PV*) theory (whether in the weak or strong coupling versions). The *PS*(*PS*) theory can only be reconciled with experiment if the higher order corrections make increasingly larger contributions to the cross section as the meson energy increases. The anisotropic angular distribution for processes (I) and (III) (cf. Table 3*a*) and the large σ_I to $(\sigma_{II} + \sigma_{III})$ ratios (cf. Table 3*b*) are more favorable to the strong coupling than to the weak coupling *PS*(*PV*) theory. However, the large absolute magnitudes and the pronounced backward maxima in the angular distributions for processes (I) and (III) (since *s*-waves are needed—cf., however, reference 7*c*) create difficulties for the strong coupling theory. Moreover, it is not evident that the cross sections σ_I, σ_{II}, σ_{III} are in the ratio 9:1:2 required by the quantum strong coupling theory. Further measurements are clearly necessary in order to decide whether the $I = \frac{3}{2}$, $J = \frac{3}{2}$ meson-nucleon state does indeed play a dominant role or even whether the charge independence hypothesis can at all be applied to meson scattering phenomena.

3. Interaction of π Mesons with Deuterons

Positive-energy π mesons can react with deuterons in five distinct ways if the possible existence of isobaric states of nucleons is neglected (*e.g.*, a reaction like $\pi^+ + D \rightarrow P^{++} + N$, where P^{++} is a doubly charged proton, could take place if isobaric states were admitted); they are

---

[9a] Barnes, Clark, Perry, and Angell, *Phys. Rev.*, in press.

[9b] Anderson, Fermi, Long, and Nagle, *Phys. Rev.*, **85**: 936 (1952).

[9c] Isaacs, Sachs, and Steinberger, *Phys. Rev.*, **85**: 803 (1952).

[9d] Anderson, Fermi, Long, Martin, and Nagle, *Phys. Rev.*, **85**: 934 (1952).

[9e] Chedester, Isaacs, Sachs, and Steinberger, *Phys. Rev.*, **82**: 958 (1951).

$$\pi^+ + D \rightarrow P + P \tag{I}$$
$$\pi^+ + D \rightarrow P + P + \gamma \tag{II}$$
$$\pi^+ + D \rightarrow P + P + \pi^0 \tag{III}$$
$$\pi^+ + D \rightarrow D + \pi^+ \tag{IV}$$
$$\pi^+ + D \rightarrow P + N + \pi^+ \tag{V}$$

where we have written down the π^+ reactions since they can be more easily detected. The π^- reactions are also five in number and can be derived from the above by interchanging P and N. The π^- analogues of the reactions (I) to (III) have been calculated by Tamor[10] for the bound case, and the results of his calculations were presented in Chap. 4. The methods employed by Tamor, *i.e.*, weak coupling theory, nonrelativistic expressions for the meson-nucleon interaction operators, assumption that the nucleon which absorbs the initial π^- meson also emits the final γ ray or π^0 meson (this is equivalent to the assumption that the characteristic time for the meson-nucleon interaction is much shorter than the characteristic period of the deuteron—called the impulse approximation by Chew[11]), etc., can be extended to positive energy π mesons for all five reactions, provided that the meson energy is small compared with the nucleon rest mass energy. These calculations have been carried out by Cheston[12] for pseudoscalar π mesons, and the results of his calculations for reaction (I) have been discussed in Chap. 4. We shall not repeat the discussion of reaction (I) here except to remark that the calculation of the cross section for reaction (I) is a first-order calculation in the sense of perturbation theory since the nucleon-nucleon potential is treated phenomenologically.

The deuteron reactions (II) to (V) are second-order reactions in the sense of perturbation theory. In calculating each of these four reactions it is assumed that the nucleons in the initial and final states obey the Dirac equation and that the deuteron wave function can be represented by a superposition of positive-energy solutions of Dirac's equation for two noninteracting particles.[13] The matrix element for any of these four reactions can be written in the form

$$M = \sum_{i=1}^{2} \int \Psi^*(\mathbf{r}_i, \boldsymbol{\sigma}_i, \boldsymbol{\tau}_i) \left(\frac{e^{-i\mathbf{q}\cdot\mathbf{r}_i}}{\sqrt{2\epsilon}}\, O\, \frac{e^{i\mathbf{q}_0\cdot\mathbf{r}_i}}{\sqrt{2\epsilon_0}} \right) \Psi_0(\mathbf{r}_i, \boldsymbol{\sigma}_i, \boldsymbol{\tau}_i)\, d\mathbf{r}_1\, d\mathbf{r}_2 \tag{14}$$

---

[10] S. Tamor, *Phys. Rev.*, **82**: 38 (1951).

[11] G. F. Chew, *Phys. Rev.*, **80**: 196 (1950); cf. also G. Chew and G. Wick, *Phys. Rev.*, **85**: 636 (1952).

[12] W. B. Cheston, *Phys. Rev.*, **85**: 952 (1952).

[13] L. Rosenfeld, "Nuclear Forces," North-Holland Publishing Co., 1948.

where Ψ_0 is the deuteron wave function, Ψ is the wave function for the two final nucleons, $\mathbf{r}_i$ is the position of the ith nucleon, $\boldsymbol{\sigma}_i$ is the spin of the ith nucleon, $\boldsymbol{\tau}_i$ is the isotopic spin of the ith nucleon, $(\mathbf{q}_0, \epsilon_0)$ is the momentum-energy four-vector of the initial meson, $(\mathbf{q}, \epsilon)$ is the momentum-energy four-vector of the final meson or γ ray. O is the interaction operator which transforms the initial two-nucleon state (deuteron) into the final state and represents the relativistic summation over intermediate states including negative-energy states for the nucleons, wherever necessary. It is only after this summation is carried out that the nonrelativistic approximation to the interaction operator is inserted to first order in v/c of the nucleon [the nonrelativistic approximation was introduced immediately in calculating the matrix element for the first-order reaction (I)]. Another approximation which is made before evaluating Eq. (13) for any of the reactions is to assume that the terms depending upon the momentum of the initial state neutron are negligible; this is called the "target at rest" approximation and is justified by the fact that the matrix element is usually a slowly varying function of the target momentum and the wave function of the deuteron has large Fourier amplitudes for zero momentum. One can now proceed to calculate with Eq. (13) by inserting the deuteron wave function for Ψ_0 and the appropriate final wave function for Ψ. For reaction (IV), it is clear that the final wave function is again a deuteron wave function. For reaction (II), plane waves can be used for the final two-nucleon wave functions if one is interested only in the total cross section (by taking advantage of the closure property). If angular distributions and energy spectra of the final quantum [γ, π^0, or π^+ for the reaction (II), (III), or (V), respectively] are desired, it is necessary to take account of the distortion of the plane wave by the nucleon-nucleon interaction. For not too high incident meson energies, it usually suffices to consider the distortion of the S part of the two-nucleon plane wave and to calculate the distortion on the basis of the shape-independent approximation for the N-P or P-P system. For reactions (II), (IV), and (V) [(IV) is obvious], the transitions to even-parity states are the most important for pseudoscalar π mesons. For the charge-exchange scattering reaction (III), it turns out that transitions to odd-parity states are as important as transitions to even-parity states.

After all these preliminary remarks, let us quote some of Cheston's results for the reactions (II) to (V). Cheston has evaluated the total cross section for reaction (II) corresponding to the $PS(PV)$ theory for a 25-Mev incident π^+ meson and obtains a value of $3.0(f^2/\hbar c)$mb. so that the ratio of the total cross sections for reactions (I) to (II) is 3.0 [cf. Eq. (23) of Chap. 4]. This ratio is to be compared with the theoretical ratio of approximately 2 for the transition probabilities

$$\frac{\pi^- \text{ (}K\text{ shell)} + D \rightarrow N + N}{\pi^- \text{ (}K\text{ shell)} + D \rightarrow N + N + \gamma} \tag{14a}$$

which agreed with the measured value (cf. Chap. 4). The near constancy of the ratio of nonradiative to radiative absorption of π mesons by deuterons on the basis of the $PS(PV)$ theory is due to the fact that no special angular momentum selection rules operate for the bound π^- meson and it is essentially the character of the meson-nucleon interaction in the $PS(PV)$ theory which suppresses the two-nucleon emission. On the other hand, it will be recalled that the $PV(PV)$ theory also predicts a ratio of 2 for bound π^- mesons; however, the $PV(PV)$ value is not obtained by comparing transition probabilities for nonradiative and radiative absorption as in the $PS(PV)$ case but derives from the operation of a selection rule against nonradiative absorption from the $J = 1$ substate of the π^- meson-deuteron system (cf. Chap. 4). When reactions (I) and (II) are examined for positive-energy pseudovector mesons, the selection rule no longer operates and it is necessary to calculate the ratio of the transition probabilities. It now turns out that the ratio is 130 rather than 3 as in the $PS(PV)$ theory. This striking difference would provide a sensitive method for discriminating between the pseudoscalar and pseudovector fields for the π meson if the field had not already been fixed by other methods, in particular the measurement of the ratio of the cross sections for reaction (I) and its inverse (cf. Chap. 4). The $PS(PS)$ theory for reaction (II) leads to results very similar to those of the $PS(PV)$ theory because the equivalence theorem holds approximately (the equivalence theorem does not hold exactly because conservation of energy does not hold for the reaction $\pi^+ + \text{“}N\text{”} \rightarrow \text{“}P\text{”} + \gamma$ when the neutron is part of the deuteron).

Just as for reaction (II), the charge-exchange scattering reaction (III) requires only the calculation of the matrix element for the neutron. The presence of the neutron in the deuteron and the fact that the two final protons obey the Pauli exclusion principle lead to a small matrix element in the forward direction for reaction (III). Thus, the charge-exchange scattering cross section for the deuteron will be extremely small compared with that for the free neutron in the forward direction. Actual calculation with the $PS(PV)$ theory at 25-Mev incident π^+ meson energy leads to the variation of the differential cross section with angle (in the laboratory system) shown in Table 4; also shown is the variation with angle of the charge-exchange scattering cross section for the neutron. For both the deuteron and the neutron it has been assumed that $f_N = -f_P$, the difference in mass between the π^+ and π^0 mesons has been taken into account and the values have been normalized to the neutron cross section at 180°. In the case of the *PS*(*PS*) theory, Cheston finds that the small value of the cross section for forward scattering remains unchanged. On the other hand, the precipitous drop in the cross section at 90° when use is made of the symmetrical choice of π^0 coupling constants, that is, $g_N = -g_P$, does not occur in the *PS*(*PS*) theory since the scattering from an individual nucleon does not exhibit the cancellation at 90° (cf. Sec. 2). Thus, while the absolute numbers may be incorrect (in view of the hydrogen scattering experiments—cf. above), the ratios between the deuteron and neutron cross sections probably give some indication of the effect of the presence of the proton in the deuteron.

TABLE 4. DIFFERENTIAL CROSS SECTION FOR CHARGE-EXCHANGE SCATTERING BY THE DEUTERON AND BY THE NEUTRON

Angle of scattering, degrees	Deuteron	Neutron
0	8.8×10^{-3}	1.2
30	0.31	0.76
60	0.23	0.45
90	1.6×10^{-3}	1.0×10^{-2}
120	0.41	0.59
180	1	1

Segall[14] has calculated the total weak coupling *PS*(*PV*) cross sections for the charge-exchange reaction (III) in deuterium for a range of energies with the results shown in Table 5; for comparison, the single nucleon cross sections are also given. In Table 5, a distinction is made between the cross section associated with a spin flip of the neutron (σ_A) or with no spin flip (σ_B); the *PS*(*PV*) theory contributes both types of terms—in its usual formulation—and the total cross section is ($\sigma_A + \sigma_B$) in each case.

TABLE 4*a*. TOTAL CROSS SECTIONS FOR CHARGE-EXCHANGE SCATTERING BY THE DEUTERON AND NEUTRON

Meson energy, Mev	Deuteron		Neutron	
	$\frac{\sigma_A \times 10^{27}\ \text{cm}^{-2}}{f^2(f_P + f_N)^2}$	$\frac{\sigma_B \times 10^{27}\ \text{cm}^{-2}}{f^2(f_P - f_N)^2}$	$\frac{\sigma_A \times 10^{27}\ \text{cm}^{-2}}{f^2(f_P + f_N)^2}$	$\frac{\sigma_B \times 10^{27}\ \text{cm}^{-2}}{f^2(f_P - f_N)^2}$
28	20	4.1	25	15
56	59	16	70	35
90	120	34	130	68

---

[14] B. Segall, *Phys. Rev.*, **83**: 1247 (1951).

Reactions (IV) and (V) in deuterium differ from reactions (I) to (III) in that there are now interference terms because both the neutron and proton in the deuteron can scatter the π^+ meson. The interference effects can readily be taken into account, however, and the resulting cross sections for reactions (IV) and (V) can be calculated.

The laboratory angular distributions for reaction (IV) corresponding to the *PS*(*PV*) and *PS*(*PS*) theories have been calculated by Cheston at an incident energy of 25 Mev, and his results are shown in Fig. 4. The total cross sections turn out to be

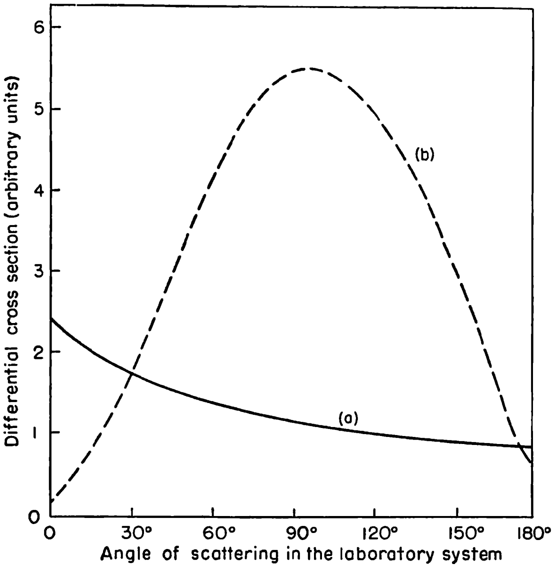

FIG. 4. Theoretical angular distributions of π mesons elastically scattered from deuterons at 25-Mev incident meson energy. Curve (*a*) corresponds to the *PS*(*PS*) theory, (*b*) to the *PS*(*PV*) theory.

$$\sigma_{PS(PV)}(D) = 2.4\left(\frac{f^2}{\hbar c}\right)^2 \times 10^{-26}\ \text{cm}^2 \tag{15a}$$

$$\sigma_{PS(PS)}(D) = 3.6\left(\frac{g^2}{\hbar c}\right)^2 \times 10^{-27}\ \text{cm}^2 \tag{15b}$$

to be compared with the total cross sections for a free neutron or a free proton:

$$\sigma_{PS(PV)}(N) = 1.7\left(\frac{f^2}{\hbar c}\right)^2 \times 10^{-26}\ \text{cm}^2 \tag{16a}$$

$$\sigma_{PS(PS)}(N) = 0.86\left(\frac{g^2}{\hbar c}\right)^2 \times 10^{-27}\ \text{cm}^2 \tag{16b}$$

$$\sigma_{PS(PV)}(P) = 1.5\left(\frac{f^2}{\hbar c}\right)^2 \times 10^{-26}\ \text{cm}^2 \tag{16c}$$

$$\sigma_{PS(PS)}(P) = 1.2\left(\frac{g^2}{\hbar c}\right)^2 \times 10^{-27}\ \text{cm}^2 \tag{16d}$$

The total $PS(PV)$ cross sections for reaction (IV) in deuterium have also been evaluated at 50 and 100 Mev; they are

$$\sigma_{PS(PV)}(D) = 6.2\left(\frac{f^2}{\hbar c}\right)^2 \times 10^{-26}\ \text{cm}^2 \tag{17a}$$

$$\sigma_{PS(PV)}(D) = 11\left(\frac{f^2}{\hbar c}\right)^2 \times 10^{-26}\ \text{cm}^2 \tag{17b}$$

Equations (17*a*) and (17*b*) reflect the rapid increase of the $PS(PV)$ scattering cross sections by the free nucleon (cf. Table 2). Cheston points out that, if the neutron and proton matrix elements were equal to each other and did not contain terms depending on the nucleon spin, the cross section for elastic scattering by the deuteron would be approximately four times the cross section for the elastic scattering by a free nucleon. Since this is only approximately true even in the $PS(PS)$ theory and the overlap integral is less than unity except in the forward direction, there is a reduction in this factor[15] of 4.

It is interesting to note that Cheston's results agree qualitatively with a phenomenological calculation carried out by Fernbach *et al.*[16] in which the elastic scattering cross section by the deuteron is expressed in terms of the free nucleon cross sections. The latter authors find

$$\frac{d\sigma_D}{d\Omega} = \left(\frac{d\sigma_P}{d\Omega} + \frac{d\sigma_N}{d\Omega}\right) H_1(\theta) + 2\cos\delta\sqrt{\frac{d\sigma_P}{d\Omega}\frac{d\sigma_N}{d\Omega}}\, H_2(\theta) \tag{18}$$

where $(d\sigma_P/d\Omega)$ and $(d\sigma_N/d\Omega)$ are the free particle cross sections, $\cos\delta$ is an unknown phase factor (Cheston specifies this phase factor by working with a specific form of the meson-nucleon interaction), and the weighting factors $H_1(\theta)$ and $H_2(\theta)$ are defined by

$$H_1(\theta) = \frac{1}{J_0}\int d\mathbf{p}J(\mathbf{p})\left\{\Psi_D\left[\mathbf{p} + \frac{1}{2}(\mathbf{q}(\mathbf{p}) - \mathbf{q}_0)\right]\right\}^2 \tag{19a}$$

$$H_2(\theta) = \frac{1}{J_0}\int d\mathbf{p}\Psi_D\left[\mathbf{p} + \frac{1}{2}(\mathbf{q}(\mathbf{p}) - \mathbf{q}_0)\right]\Psi_D\left[\mathbf{p} - \frac{1}{2}(\mathbf{q}(\mathbf{p}) - \mathbf{q}_0)\right] \tag{19b}$$

---

[15] Cheston's numbers do not agree with those of B. Ferretti and S. Gallone [*Phys. Rev.*, **77**: 153 (1950)], who have found that the cross section for meson scattering by a deuteron is down by a factor of 10 compared with a free nucleon at 25-Mev incident meson energy; cf. J. S. Blair, *Phys. Rev.*, **83**: 1246 (1951).

[16] Fernbach, Green, and Watson, *Phys. Rev.*, **82**: 980 (1951).

where $\mathbf{q}_0$ and $\mathbf{q}(\mathbf{p})$, as before, are the momenta of the incident and scattered mesons, respectively, $\mathbf{p}$ is the relative momentum of the two final nucleons, $J(\mathbf{p})$ is the volume of momentum space available to the scattered meson, and J_0 is the corresponding quantity for scattering by free nucleons. If one replaces $\mathbf{q}(\mathbf{p})$ and $J(\mathbf{p})$ by appropriate average values and integrates over all $\mathbf{p}$ space, there results the closure approximation according to which

$$H_1(\theta) = 1 \tag{20a}$$

and

$$H_2(\theta) = \left\langle \frac{\sin |\mathbf{q} - \mathbf{q}_0|r}{|\mathbf{q} - \mathbf{q}_0|r} \right\rangle_{\text{av}} \tag{20b}$$

where $\mathbf{q}$ is defined for a given θ by the free particle energy-momentum conservation laws and the average is taken over the square of the deuteron wave function Ψ_D. Figure 5 contains a plot of Eq. (20*b*) for scattering angles > 50° corresponding to an incident meson energy of 70 Mev. The quantity $H_2(\theta)$ can also be used to calculate the scattering angle beyond which the correlation effect, *i.e.*, the third term on the R.H.S. of Eq. (18), will be small for a given meson energy where the criterion of smallness is taken as $H_2 < \frac{1}{3}H_1$; the results are shown in Fig. 6. Figure 6

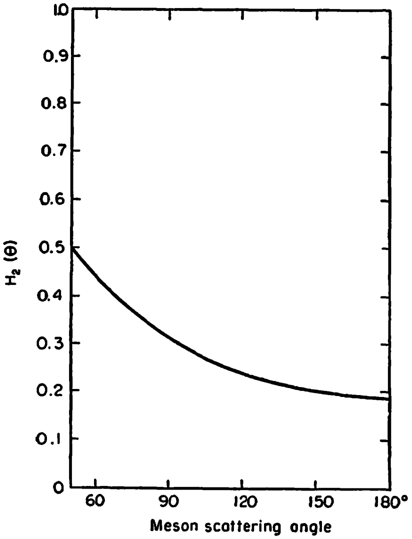

FIG. 5. Theoretical interference term in elastic π-D scattering based on the closure approximation as a function of meson scattering angle (see text).

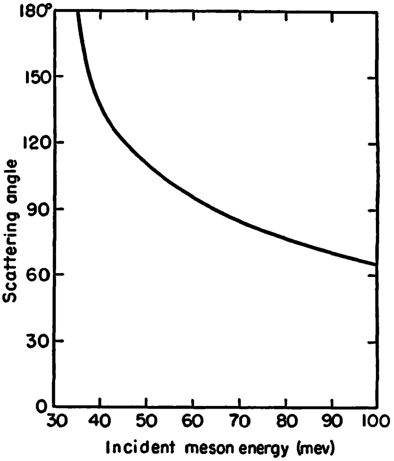

FIG. 6. Meson scattering angle in laboratory system beyond which correlation effects are small for elastic π-D scattering as a function of meson energy.

confirms Cheston's ratios for the deuteron to the free nucleon cross sections and not Ferretti and Gallone's.[15]

In an actual experiment, reaction (V) will compete with reaction (IV) because of the interaction between the two final nucleons (just as the reaction $P + P \rightarrow P + N + \pi^+$ competes with $P + P \rightarrow D + \pi^+$) and the same methods employed to calculate the cross section for reaction (IV) can be applied to reaction (V). The total cross sections calculated by Cheston at 25 Mev turn out to be

$$\sigma_{PS(PV)} = 1.6 \left(\frac{f^2}{\hbar c}\right)^2 \times 10^{-26} \text{ cm}^2 \tag{21a}$$

$$\sigma_{PS(PS)} = 2.4 \left(\frac{g^2}{\hbar c}\right)^2 \times 10^{-27} \text{ cm}^2 \tag{21b}$$

The elastic scattering cross sections are therefore somewhat larger than the inelastic scattering cross sections, a not unexpected result.

No strong coupling calculations of the π meson reactions in deuterium have been performed up to the present time.

The experimental data bearing on reaction (I) in deuterium have been discussed in Chap. 4. As far as reactions (II) to (V) are concerned, only transmission experiments which measure the sum of the total cross sections for processes (II) to (V) [in addition to (I)] have been carried out. The results obtained by Isaacs *et al.*[9b] for 58 Mev π^+ and π^- mesons [when the π^- meson is used P and N interchange roles on the R.H.S. of Eqs. (I) to (V)] are 38.3 ± 3.1 and 32.8 ± 3.1 mb, respectively. The more recent results of Anderson *et al.*[16a] are shown in Table 5. The observed total cross sections in deuterium are consistent with charge symmetry, are comparable in magnitude to the sum of all the cross sections in hydrogen, and exhibit a correspondingly rapid increase with

TABLE 5. TOTAL INTERACTION CROSS SECTIONS IN D

Meson energy, mev	$\sigma(\pi^+)$, mb	$\sigma(\pi-)$, mb
72	60 ± 9	
79	79 ± 15	54 ± 13
109	109 ± 16	103 ± 10
127	151 ± 21	129 ± 11
164	....	198 ± 12
179	....	234 ± 12
209	....	192 ± 26

[16a] Anderson, Fermi, Nagle, and Yodh, *Phys. Rev.*, **86**: 413 (1952).

energy. However, they are too preliminary to justify a detailed comparison with the theoretical considerations sketched above.

4. Interaction of π Mesons with Heavy Nuclei at Moderate Energies

For some time to come, experiments on fast π meson reactions in hydrogen and deuterium will be restricted to artificial sources of π mesons due to intensity considerations. This is no longer the case for heavier nuclei, and there exist some cosmic-ray data on π meson interactions. The cosmic-ray π mesons used to study nuclear interactions generally originate in local penetrating showers which are produced in either a lead plate or some other material placed inside a cloud chamber or in a photographic emulsion. Since cosmic-ray energies are appreciably higher than the energies available from present-day accelerators, the cosmic-ray studies

TABLE 6. DATA ON π^- INTERACTIONS WITH NUCLEI IN PHOTOGRAPHIC EMULSIONS (30 TO 110 MEV)

(*a*)

Energy, Mev	Track length scanned, cm	No. of stars	No. of stoppings	No. of elastic scatters > 30°	No. of inelastic scatters
30–50	2145 ± 21	49 (15)	8	8 (17)	2 (6)
70–80	1438 ± 14	44 (11)	4	4 (4)	7 (8)
60–90	1000 ± 50	19 (7)	44	3 (6)	6 (8)
100–110	2716 ± 28	76 (16)	18	15 (20)	22 (32)

(*b*)

Energy, Mev	Electrons in beam, per cent	μ mesons in beam, per cent	Corrected track lengths, cm	No. of mesons	λ_{geom}, cm	λ_{obs}, cm
30–50	3 ± 2	8 ± 4	1910 ± 100	80	15.6	24.0 ± 3.0
70–80	10 ± 2	9 ± 3	1165 ± 55	60	19.1	19.4 ± 2.6
60–90	10 ± 5	10 ± 5	800 ± 100	37	....	21.5 ± 4.2
100–110	2	5 ± 3	2610 ± 100	146	20.4	18.0 ± 1.3

(*c*)

Energy, Mev	Cross section for stars and stoppings	Cross section for elastic scatters > 30°	Cross section for inelastic scatters	Total cross section
30–50	0.62*b*	0.19*b*	0.06*b*	0.87*b*
60–90	0.76*b*	0.10*b*	0.19*b*	1.05*b*
100–110	0.75*b*	0.16*b*	0.25*b*	1.16*b*

provide the only source of information concerning the interaction of π mesons with nuclei at energies greater than approximately 200-Mev kinetic energy for the incident π meson. Before turning to the cosmic-ray experiments in the next section, we present in this section the experimental data obtained with artificially produced π mesons.

The first comprehensive work on the nuclear interaction of π mesons has been carried out by Bernardini *et al.*,[17] who exposed thick electron-sensitive nuclear emulsions to the external π^- meson beam of the Columbia cyclotron. These authors (by scanning along the π^- meson tracks) studied the types of events produced by π^- mesons in the energy range 30 to 110 Mev. Their results are shown in Tables 6*a* to 6*c*. In Table 6*a*, a star is defined as any event in which the prongs are other than mesons, a stopping as a disappearance in flight of the meson with no visible prongs, an elastic scattering as an event in which the incident and scattered π mesons differ in energy by less than 15 per cent (occasionally an elastic-scattering event may be accompanied by a short black prong or a slow electron of 10 to 100 kev at the vertex), and an inelastic scattering is defined as an event in which the scattered meson experiences an energy loss greater than 15 per cent of the incident energy. The bracketed figures in columns 5 and 6 indicate uncertain events in which the distinction between meson and proton could not be established, whereas the bracketed figures in column 3 give the number of stars having at least one proton of energy > 30 Mev. In Table 6*b*, columns 2 and 3 list the relative fractions of electrons and μ mesons in the different beams, column 4 the total lengths of π^- tracks observed (corrected for the admixture of electrons and μ mesons), column 5 the total number of mesons which are counted, column 6 the values for the geometrical mean free paths derived from the formula

$$\lambda_{\text{geom}}^{-1} = \sum_i N_i \pi \hbar^2 \left(\frac{A^{\frac{1}{3}}}{\mu c} + \frac{1}{q} \right)^2 \tag{22}$$

where the summation is taken over the constituents N_i of the photographic emulsion and the second term in the parentheses takes account of the finite size of the π meson wave packet (q is the meson momentum), and column 7 the observed mean free path. Comparison between the last two columns indicates that the observed mean free path is close to geometrical at the high energies but somewhat larger at the low energies (indicating a transparency of about 70 per cent). In Table 6*c*, the absolute cross sections for the various types of nuclear interactions are given in barns (*b*) as a function of energy. The stoppings are included with the stars because independent experiments by the same authors with π^+ mesons provide strong evidence that the stoppings are stars containing only neutron prongs (and not charge-exchange scatterings—cf. below). Table 6*c* shows clearly that there is a definite increase with energy of the relative frequency of the catastrophic types of interaction (*i.e.*, absorption and inelastic scattering) as compared with the elastic scatterings. The Columbia data also contain some very unusual results not shown in Tables 6*a* to 6*c*, namely, (1) large-angle scatterings are very probable for both the elastic and inelastic scattering events; (2) the average energy loss in inelastic scattering events is very large, greater than 50 per cent of the incident energy; some outgoing mesons have as little as 10 per cent of the incident energy; (3) the small-angle elastic scattering, less than 30°, can be explained completely in terms of single Coulomb scattering and diffraction scattering by the nuclei of the emulsion.

---

[17] Bernardini, Booth, and Lederman, *Phys. Rev.*, **83**: 1075 (1951); cf. also Bernardini, Booth, Lederman, and Tinlot, *Phys. Rev.*, **82**: 105 (1951).

It appears possible to explain some, though not all, of the features of the Columbia experiment by adopting the Fermi gas model for a heavy nucleus. The Fermi gas model implies that a scattering event will take place if the nucleon with which the meson interacts is imparted sufficient energy, greater than the Fermi energy. This would favor large-angle scattering since the recoil energy of the nucleon is greater the larger the angle of scattering of the meson. The Fermi gas model would also explain why some of the elastic scattering events contain outgoing mesons whose energies, corresponding to the observed scattering angles, are less than would be allowed by the momentum and energy conservation laws for nucleons at rest (cf. Table 1); for a given angle of scattering, the energy loss is greater if the colliding nucleon moves in the same direction as the incident meson. But the Fermi gas model cannot explain the extremely large energy losses in the inelastic scattering events unless, at the energies in question, there is more than one elastic collision inside a heavy nucleus of the emulsion as a consequence of the large $\pi^- - N$ scattering cross section (which follows, by charge symmetry, from the large cross section for $\pi^+ - P$ scattering—cf. Sec. 2). Another possibility, pointed out by Bernardini *et al.*,[18] is that in heavy nuclei the scattering of mesons is a many-body process which, in an as yet unknown manner, withdraws large amounts of energy.

Bernardini and Levy[19] have also studied the interaction of π^+ mesons with the nuclei of the photographic emulsion. As far as the elastic and inelastic scattering events are concerned, the π^+ meson behaves in a fairly similar fashion to the π^- meson. On the other hand, the π^+ mesons give rise to fewer stoppings and to stars with a larger average number of prongs. For example, in a group of 55 stars produced by a beam of 70-Mev π^+ mesons, the average number of prongs turned out to be 3.2 compared with 1.5 for π^- mesons of the same energy. Moreover, there was only 1 stopping compared with 6 for the π^- meson. Both these features can be explained by the fact that the absorption of a π^+ meson by a nucleus results in the conversion of a neutron into a proton (in contrast to the π^- case where a proton is converted into a neutron), thereby giving an initial bias in favor of visible prongs, *i.e.*, protons. It will be recalled from our discussion of slow π^- disintegrations (see Chap. 4) that a plausible mechanism for the absorption process was the conversion of most of the rest energy of the π^- meson into the kinetic energy of one high-energy nucleon, in that case a neutron. The subsequent collision of this high-energy neutron and the secondary protons and neutrons could explain the observed fraction of high-energy protons (> 30 Mev) and the average excitation energy. When a π^+ meson is absorbed, the high-energy nucleon which results is a proton, and it is clear that its subsequent history will favor protons rather than neutrons, thereby explaining the higher average number of prongs. It will also be recalled that, corresponding to the 10 per cent emission of high-energy protons, it was predicted that about 50 per cent of the π^- absorptions will give rise to high-energy neutrons. Qualitatively, this would explain another observation of the Columbia group, *viz.*, that 85 per cent of the π^+ stars contain one proton greater than 30 Mev and 30 per cent contain two protons, each with an energy greater than 30 Mev. These numbers are higher than the corresponding numbers of high-energy neutrons predicted for the slow π^- absorptions and are not unexpected in view of the 70-Mev kinetic energy carried by the π^+ mesons.

---

[18] Bernardini, Booth, and Lederman, *Phys. Rev.*, **83**: 1277 (1951).

[19] G. Bernardini and F. Levy, *Phys. Rev.*, **84**: 610 (1951).

It has been pointed out above that the inelastic scattering results of the Columbia group can be understood in terms of an independent nucleon model of the nucleus, provided more than one elastic collision takes place inside the same nucleus. The idea is that the finite nucleon momenta in the nucleus can lead to much greater energy losses per elastic collision than are allowed by the momentum-energy conservation laws for nucleons at rest (cf. Table 1); and if more than one collision occurs, the large average energy loss for the inelastically scattered mesons can be explained. Thus Johnson,[20] assuming a Fermi gas model for the nucleus, has derived the following formula for the differential cross section for the scattering of a π meson by a Fermi gas of nucleons assuming that the free nucleon cross section is a constant:

---

[20] M. H. Johnson, *Phys. Rev.*, **83**: 510 (1951).

$$d\sigma = \frac{3(\epsilon + M)\sigma_0\, d\mathbf{q}'}{4\pi q\epsilon M P_F^3|\mathbf{q} - \mathbf{q}'|} \left\{ \begin{array}{l} P_F^2 - \left[\dfrac{(\epsilon + M)}{2\epsilon|\mathbf{q} - \mathbf{q}'|}\left(\epsilon^2 - \epsilon'^2 - \dfrac{2\epsilon q^2}{\epsilon + M} + \dfrac{2\epsilon \mathbf{q}\cdot\mathbf{q}'}{\epsilon + M}\right)\right] \\ 2M(\epsilon - \epsilon') \end{array} \right. \tag{23}$$

where the lesser of the two terms in the brackets is always used. In Eq. (23), σ_0 is the constant free nucleon cross section, ($\mathbf{q}$, ϵ) and ($\mathbf{q}'$, ϵ') are, respectively, the momentum-energy four-vector of the meson before and after the collision with a nucleon of the Fermi gas and P_F is the maximum momentum of the Fermi gas of nucleons. Figure 7 shows the average energy loss as a function of energy for two angles of scattering, *i.e.*, 90° and 180°; the curves in Fig. 7 were calculated on the basis of Eq. (23), *i.e.*, the assumption of a constant scattering cross section in the center-of-mass system. However, any reasonable variation with energy of the cross section will not materially alter the result. It is seen that the average energy loss per collision can be sufficiently large so that the occurrence of two or more collisions in the same nucleus can account for large inelastic energy losses in meson scattering.

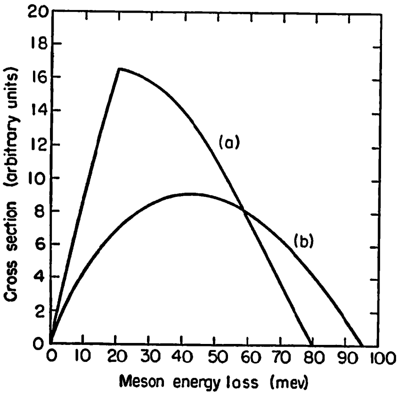

FIG. 7. Theoretical energy distributions of scattered π mesons from a Fermi gas of nucleons at an incident meson energy of 100 Mev. Curve (*a*) corresponds to a scattering angle of 90°, (*b*) to a scattering angle of 180°.

Experiments on the nuclear interaction of artificially produced π mesons have been carried out at several other laboratories besides Columbia. Thus Bradner and Rankin,[21] using 38-Mev π^- mesons from the Berkeley cyclotron, studied the absorption and scattering events in thick photographic emulsions. In a scan of about 10 m of track, they observed 11 one- and two-prong stars, 5 stoppings, and 26 scatterings of which 2 were inelastic, 10 were elastic between 30 and 50°, and the remainder were elastic greater than 50°. The relatively large number of elastic scatterings between 30 and 50° represent diffraction scattering events. However, even taking this feature into account, the Berkeley data do not agree too well with the Columbia data; the Berkeley workers find more scatterings than stars in contrast to the Columbia workers. This discrepancy, which appears to be outside the statistical uncertainties of the experiments, is difficult to understand.

---

[21] H. Bradner and B. Rankin, *Phys. Rev.*, **81**: 916 (1951).

Both Bernardini *et al.*[17] and Bradner and Rankin[21] found that the total interaction cross sections for π mesons with the nuclei of the emulsion were close to geometrical. These photographic measurements are confirmed by an independent experiment carried out by Chedester *et al.*,[9e] who measured the attenuation of the 85-Mev π^- meson beam of the Columbia cyclotron with liquid scintillation counters. Table 7 contains their results (including the cross section for hydrogen previously cited); the last column of Table 7 lists the values of the geometrical cross section computed with $R = 1.37 \times 10^{-13}A^{\frac{1}{3}}$ cm. It is seen that all cross sections, except the one for hydrogen, are close to geometrical, in agreement with the photographic results. Since the experimental setup of Chedester *et al.* was such that only the total attenuation was measured, no separation between absorption and scattering events could be made; however, the elastic diffraction scattering gave only a small contribution to the measured attenuation.[21a]

TABLE 7. TOTAL CROSS SECTIONS OF VARIOUS NUCLEI FOR 85-MEV π^- MESONS

Nucleus	Mean free path, g/cm²	Cross section, cm²	Nuclear area $\pi A^{\frac{2}{3}}\left(\frac{\hbar}{\mu c}\right)^2$, cm²
H	125 ± 10	$1.33 \pm 0.11 \times 10^{-26}$	6.1×10^{-26}
Li	48 ± 2	24.2 ± 1	22.6
Be	59 ± 4	25.3 ± 2	26.5
C	58 ± 2	34.4 ± 1.3	31.9
O	57 ± 2	46.6 ± 1.8	38.9
Al	72 ± 3	62.3 ± 2.5	55.1
Cu	106 ± 5	99 ± 5	98
Cd	117 ± 5	159 ± 7	142
Pb	143 ± 6	240 ± 11	214

A careful experiment has been carried out by Shapiro[22] at Cornell on the interaction of π mesons with carbon, using a Geiger counter-triggered cloud chamber and π^+ and π^- mesons produced by the 310-Mev γ ray beam of the Cornell synchrotron. The π mesons (both positive and negative) incident on the cloud chamber had an initial energy of 65 ± 5 Mev, and their energy inside the chamber was in the range 35 to 60 Mev, with an average of 48 Mev. Thin plates of carbon, $\frac{1}{8}$ in. in thickness, were placed inside the cloud chamber. The Cornell experiment has an advantage over the experiment of Chedester *et al.*,[9e] since scatterings and stars can be differentiated; and although the statistics are not so good as those of Bernardini *et al.*,[17] it is superior to the photographic experiments since it is possible to study the meson interaction cross section with a single type of nucleus. The Cornell results are tabulated in Table 8; columns 1 to 2 are obvious, column 3 lists the numbers of nuclear interactions which includes stars of 0 to 3 prongs and inelastic scatterings (scatterings involving energy losses > 15 Mev) and column 4 the corresponding cross sections, columns 5 and 6 list the number of elastic scatterings (scatterings with energy loss < 15 Mev) for the angular regions 20 to 75° and > 75° (75° is the angle for which the first zero of the diffraction scattering occurs for carbon), and column 7 the corresponding cross sections. Scatterings with angles < 20° are not included because they are chiefly due to Coulomb scattering and $\pi \rightarrow \mu$ decays in flight. All elastic scatterings are attributed to diffraction scattering, and if the angular distribution specified by Eq. (29) below is assumed to hold, the total diffraction cross section turns out to be 115 ± 25 mb.

[21a] Recently, Martin, Anderson, and Yodh [*Phys. Rev.*, **85**: 486 (1952)] have measured the attenuation of 109 and 133 Mev π^- meson beams in C, Al, Cu, Cd, Sn, and Pb, and have in all cases found geometric cross sections within the 15 per cent uncertainty of the experiment.

[22] A. M. Shapiro, *Phys. Rev.*, **84**: 1063 (1951); cf. also Camac, Corson, Littauer, Shapiro, Silverman, Wilson, and Woodward, *Phys. Rev.*, **82**: 745 (1951). A more recent experiment with a single carbon plate has been carried out by Byfield, Kessler, and Lederman [*Phys. Rev.*, **86**: 17 (1952)] with 62 Mev π^+ and π^- mesons with similar results.

TABLE 8. MEASURED INTERACTIONS OF π MESONS WITH C

Meson type	No. of traversals	No. of nuclear interactions	σ (nuclear interactions), mb	No. of elastic scatterings		σ (elastic scatterings > 20°), mb
				20–75°	> 75°	
π^+	6133	33	214 ± 37	11	2	78 ± 23
π^-	3310	20	240 ± 54	8	0	96 ± 34
$\pi^+ + \pi^-$	9443	53	223 ± 52	19	2	84 ± 19

Bethe and Wilson[23] have inquired into the significance of the Cornell measurements for the scattering of π mesons by free nucleons. Adopting the optical model for the nucleus, *i.e.*, the model in which the nucleus is treated as a sphere of uniform density with a refractive index and an absorption coefficient, these authors have deduced the cross section for the elastic scattering of a meson by a free nucleon. It will be seen that the conclusions of Bethe and Wilson are in conflict with the measurement of the scattering cross section in hydrogen (assuming the correctness of the Cornell numbers for carbon) unless the amplitudes for the scattering of the meson by a proton and neutron have opposite sign. It seems worth while to present Bethe and Wilson's argument in somewhat greater detail.

---

[23] H. Bethe and R. Wilson, *Phys. Rev.*, **83**: 690 (1951).

The optical model of the nucleus, in the hands of Fernbach *et al.*,[24] has had considerable success in explaining the nuclear interaction of neutrons at high energies, *i.e.*, at energies at which the de Broglie wave length of the neutron is small compared with the radius of the nucleus. The formulas of Fernbach *et al.* which state what happens when a neutron wave is scattered by a sphere of material characterized by an absorption coefficient K (K is the reciprocal mean free path for interaction with nuclear matter) and an index of refraction k_1 can be taken over with an obvious change of notation for the meson case provided that the meson wave length is small compared with the nuclear radius. If k is the wave number of the meson outside the nucleus, its wave number inside is defined as $(k + k_1)$ where

$$k_1 = k\left[\left(1 + \frac{V_0}{\tau}\right)^{\frac{1}{2}} - 1\right] \tag{24}$$

τ is the kinetic energy of the meson, and V_0 is the mean potential energy of the meson inside the nucleus. The absorption coefficient K in nuclear matter is equal to the particle density times the effective cross section σ_0 for interaction of the meson with a nucleon in the nucleus, namely,

$$K = \frac{3A\sigma_0}{4\pi R^3} \tag{25}$$

where $R = r_0A^{\frac{1}{3}}$ ($r_0 = 1.47 \times 10^{-13}$ cm) is the nuclear radius and A is the mass number. In terms of the meson-proton and meson-neutron cross sections, σ_P and σ_N, respectively, σ_0 can be written

$$\sigma_0 = \frac{Z\sigma_P + (A - Z)\sigma_N}{A} \tag{25a}$$

Now, the cross section for nuclear "absorption" (including stars, large-angle scatterings, and stoppings) σ_a is πR^2 times the probability that the meson collides with a nucleon in the nucleus. If refraction and reflection from the surface layer of the nucleus are neglected (*i.e.*, if it is assumed that k_1 and K attain their interior values in a distance larger than $1/k$), σ_a can easily be computed on the basis of geometrical optics with the result

$$\sigma_a = \pi R^2\left\{1 - \frac{1}{2K^2R^2}\left[1 - (1 + 2KR)e^{-2KR}\right]\right\} \tag{26}$$

---

[24] Fernbach, Serber, and Taylor, *Phys. Rev.*, **75**: 1352 (1949).

The diffraction or shadow scattering cross section σ_d is the elastic scattering arising from the disturbance of the incident meson wave by the nucleus; it can be similarly evaluated from geometrical optics and can be written

$$\sigma_d = \pi R^2 \left(1 + \frac{1}{2K^2R^2}[1 - (1 + 2KR)e^{-2KR}] - \frac{1}{\left(\frac{K^2}{4} + k_1^2\right)^2 R^2} \right.$$
$$\times \left\{ \left(\frac{K^2}{4} - k_1^2\right) + e^{-KR} \sin 2k_1R \left[2k_1R \left(\frac{K^2}{4} + k_1^2\right) + k_1K \right] \right.$$
$$\left.\left. - e^{-KR} \cos 2k_1R \left[\left(\frac{K^2}{4} - k_1^2\right) + KR \left(\frac{K^2}{4} + k_1^2\right) \right] \right\} \right) \tag{27}$$

An approximation to Eq. (27) which holds to an accuracy of 10 per cent for $O < 0.9$ ($O = \sigma_a/4\pi R^2$ is called the opacity of the nucleus) and $k_1/K < 1$ is

$$\sigma_d(K, k_1) = \sigma_d(K, O) \left[1 + 4 \left(\frac{k_1}{K}\right)^2 \left(1 - \frac{K^2R^2}{18} + \cdots \right) \right] \tag{27a}$$

Of particular interest in diffraction scattering is the angular distribution $f(\theta)$ of the scattered particle; an analytic expression has not been found for the angular intensity but has been expressed in terms of an integral, namely,

$$f(\theta) = k \int_0^R [1 - e^{-(K+2ik_1)\sqrt{R^2-\rho^2}}] J_0(k\rho \sin \theta)\rho \, d\rho \tag{28}$$

In the limit $KR \to \infty$, a fairly good approximation to the actual experimental conditions, Eq. (28) reduces to the well-known expression

$$\frac{d\sigma_d(\theta)}{d\Omega} = \frac{\sigma_d}{\pi} \left[\frac{J_1(kR \sin \theta)}{\sin \theta} \right]^2 \tag{29}$$

The diffraction scattering cross section σ_d is plotted in Fig. 8 as a function of the opacity of the nucleus for several values of k_1; the rectangular box represents the Cornell result for carbon taking account of the statistical errors. If it is recalled that σ_a for carbon is 223 mb, $(1/K)$ is found to be $3.7 \pm 0.7 \times 10^{-13}$ cm, corresponding to an interaction cross section σ_0 between meson and nucleon of 40 ± 8 mb. With the above value of K, Fig. 8 yields a value of $0.8 \pm 0.8 \times 10^{12}$ cm^{-1} for k_1 and therefore a value of 11 ± 11 Mev for V_0, the average potential in the nucleus.

Bethe and Wilson proceed to point out that the average potential in the nucleus is defined in terms of the potential of a meson in a field of one nucleon by

$$V_0 = \sum_{\text{nucleons}} \int \frac{V(r)dr}{4\pi R^3/3} \tag{30}$$

and that the same quantity V_0 is related to the forward scattering amplitudes a_P and a_N from the proton and neutron, respectively, by the equation (μ is the meson mass)

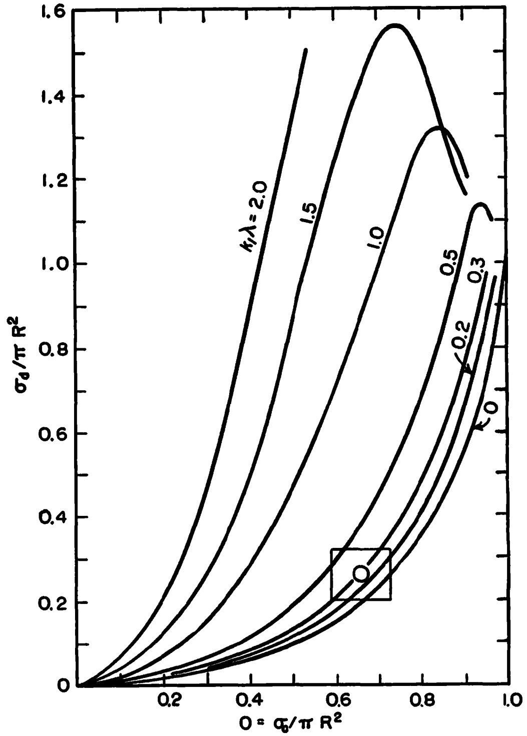

FIG. 8. Diffraction scattering cross section as a function of the nuclear opacity O for several values of the refractive index k_1; the rectangular box represents the Cornell result for carbon, and $\lambda = 1/k$.

$$V_0 = -\frac{3\hbar^2}{2\mu r_0^3 A}[Za_P + (A - Z)a_N] \tag{31}$$

If it is assumed that the scattering is isotropic, the total scattering cross section per nucleon becomes

$$\sigma_S = 0.735 r_0^6 V_0^2 \times 10^{-30} \text{ cm}^2 \tag{32}$$

where r_0 is measured in units of 10^{-13} cm and V_0 in Mev. Inserting $V_0 = 11 \pm 11$ Mev for V_0 into Eq. (32) yields [illegible]

Bethe and Wilson's value for σ_S at 50 Mev is much lower than the experimentally determined value of 28 ± 3 mb for the scattering of π^+ mesons by protons and of 18 ± 2 mb for the scattering of π^- mesons by protons.[9e] One possible explanation of the discrepancy may lie in the breakdown of the optical model for the interaction of 50-Mev mesons with carbon; this possibility is difficult to assess at the present time, although it should be pointed out that the meson wave length at 50 Mev is only one-half the radius of the carbon nucleus. Another possibility is that Isaacs *et al.*[9e] measured the sum of two cross sections, the ordinary scattering and the charge-exchange scattering of π^- mesons by protons, and that the latter gives by far the major contribution; this explanation retains the difficulty since the π^+ scattering experiment does not include a charge-exchange component. A third possibility is that the scattered amplitudes a_P and a_N from protons and neutrons have opposite signs and that, while the average potential in the nucleus is small [cf. Eq. (31)], the individual scattering amplitudes from neutron and proton are large in absolute magnitude, that is, $\sigma_S(P) = 4\pi a_P^2$ and $\sigma_S(N) = 4\pi a_N^2$ are both much larger than σ_S as defined by Eq. (32). Interestingly enough, the *PS*(*PV*) theory predicts an attractive potential between π^+ meson and proton and conversely for π^- mesons. The *PS*(*PS*) theory predicts a repulsive potential in all cases—between π^+ or π^- meson and proton or neutron—since transitions to intermediate negative-energy states play the dominant role in all the scattering processes.[25] Since the scattering amplitude is negative for a repulsive potential and positive for an attractive one, the experiments argue for the *PS*(*PV*) theory, in agreement with the conclusion drawn from the rapid increase with energy of the cross section for the scattering of π mesons by protons (cf. Sec. 2).

5. Interaction of π Mesons with Heavy Nuclei at High Energies

The data on the nuclear interaction of π mesons presented thus far have been gathered by experimentalists working with artificial sources of low-energy π mesons produced in the various types of accelerators. A considerable amount of cosmic-ray data exist on the nuclear interaction of high-energy π mesons produced as components of penetrating showers or nuclear stars. Penetrating showers are, of course, identical with nuclear stars, the two terms being generally used in connection with cloud-chamber and photographic experiments, respectively. The object of the cloud-chamber or photographic experiment is to measure the mean free path for nuclear interaction of the minimum ionization particles contained in the penetrating showers or nuclear stars. Unfortunately, the photographic experiments suffer from poor statistics and the inability to distinguish between π mesons and protons for energies greater than 1500 Mev. The latter difficulty is probably not serious, since it is likely that at least 80 per cent of the particles above 1500 Mev are π mesons; this follows from the fact that 80 per cent of the shower particles with grain density less than 1.5 times minimum are known to be π mesons (79 ± 6 per cent to be exact—of the remainder, 17 ± 3 per cent are protons and 4.0 ± 1.3 per cent are deuterons or tritons—cf. Camerini *et al.*[26]). The cloud-chamber experiments also suffer from the difficulty of distinguishing between π mesons and protons and in addition from the difficulty of determining the number of nuclear interaction events. That is to say, a shower particle cannot be followed and observed continuously in the cloud chamber because of the thicknesses of the plates of lead or other material which are interposed in order to ascertain the penetrating power of the particle; consequently, those nuclear interactions will be missed which are absorbed completely within the plate and a substantial correction must be applied. The results of some of the key cloud-chamber and photographic experiments are shown in Table 9; N_s in column 5 is the number of shower particles in the secondary interaction event.

---

[25] The identity of sign in the effective meson-nucleon potential (we can speak of a potential at all because meson scattering by nucleons is a second-order process) is due to the importance of the odd part of the *PS*(*PS*) interaction operator and therefore of negative-energy states for the nucleons. If, for some as yet unknown reason, the contribution of the negative-energy states is suppressed, the identity of sign would not occur.

It is seen from Table 9 that the *corrected* cloud-chamber experiments all lead to nuclear interaction cross sections within a factor of 2 of geometrical. Since the evidence is strong from other experiments that high-energy protons have a geometrical cross section for nuclear interaction, the interaction cross section of the π meson component cannot be appreciably less than geometrical.[27] However, in view of the fact that the so-called penetrating particle tracks observed in cloud chambers may possess up to two to three times minimum ionization (because of the inaccuracy of visual estimates), thereby increasing the admixture of protons (as a matter of fact, an appreciable fraction of the tracks less than three times minimum ionization—up to 50 per cent—may be due to protons), a tabulation of the various types of nuclear interaction events has not been attempted. This is not true for the photographic experiments where, at least below 1500 Mev, the particles are definitely identified. We therefore give in Table 10 a breakdown of the nuclear events produced by π mesons in the energy range 200 to 1100 Mev, which were

---

[26] Camerini, Fowler, Lock, and Muirhead, *Phil. Mag.*, **41**: 413 (1950); cf., however, the recent paper by Daniel, Davies, Mulvey, and Perkins [*Phil. Mag.*, **43**: 753 (1952)], where evidence is adduced for the presence of appreciable numbers of heavy mesons in high-energy stars.

[27] Cf. K. Greisen, *Phys. Rev.*, **77**: 713 (1951).

Table 9. Interaction Experiments with π Mesons

Author	Method	Result	Observed M.F.P. / Geom. value	Energy range of mesons
Fretter[28]	Cloud chamber with Pb plates at mountain altitudes	750 g/cm^2 Pb uncorrected	4.7	> 150 Mev ($N_s \geq 2$)
Lovati, Mura, Salvini, and Tagliaferri[29]	Cloud chamber with Pb plates at mountain altitudes	300 ± 100 g/cm^2 Pb corrected	1.9	> 150 Mev ($N_s \geq 2$)
Brown and McKay[30]	Cloud chamber with Pb plates at mountain altitudes	316 ± 70 g/cm^2 Pb corrected	2.0	> 150 Mev
Butler, Rosser, and Barker[31]	Cloud chamber with Pb plates at sea level	400 g/cm^2 Pb uncorrected 200 g/cm^2 Pb corrected	2.5 1.25	Average energy of shower ~ 7 Bev
Harding and Perkins[32]	Photographic plates exposed under ice	120 g/cm^2 ice	2.0	> 100 Mev
Camerini, Fowler, Lock, and Muirhead[26]	Electron-sensitive plates exposed at high altitudes	100 g/cm^2 emulsion	1.1	> 150 Mev
Harzler[32a]	Cloud chamber with Au plates at mountain altitudes	230 ± 60 g/cm^2	1.4 ± 0.3	500 Mev–10 Bev
Lovati, Mura, Succi, and Tagliaferri[32b]	Cloud chamber with Pb plates at mountain altitudes	200 ± 50 g/cm^2 Pb corrected	1.25	> 150 Mev ($N_s \geq 2$)
Gregory and Tinlot[32c]	Cloud chamber with Pb, Al plates at mountain altitudes	172 ± 30 g/cm^2 Pb 164 ± 50 g/cm^2 Al	1.1 2.0	$N_s \geq 3$ $N_s \geq 3$
Branch and Cocconi[33]	Cloud chamber with Pb plates at mountain altitudes	172 ± 29 g/cm^2 Pb corrected	1.1	> 2 Bev

---

[28] W. B. Fretter, *Phys. Rev.*, **76**: 511 (1949).

[29] Lovati, Mura, Salvini, and Tagliaferri, *Phys. Rev.*, **77**: 284 (1950).

[30] W. Brown and A. McKay, *Phys. Rev.*, **77**: 342 (1950).

[31] Butler, Rosser, and Barker, *Proc. Phys. Soc.*, **63A**: 145 (1950); **64A**: 4 (1951).

[32] J. Harding and D. Perkins, *Nature*, **164**: 285 (1949).

[32a] A. J. Harzler, *Phys. Rev.*, **82**: 359 (1951).

[32b] Lovati, Mura, Succi, and Tagliaferri, *Nuovo cimento*, **8**: 271 (1951).

[32c] B. Gregory and J. Tinlot, *Phys. Rev.*, **81**: 675 (1951).

[33] G. Branch and G. Cocconi, *Phys. Rev.*, **84**: 146 (1951).

observed by Camerini *et al.*[26,34] in photographic emulsions exposed at 68,000 ft. The statistics are too poor to draw any definite conclusions, but one is struck by the fact that, in those cases where a secondary meson emerges, the average energy loss is a very large fraction of the initial energy, in agreement with the results of Bernardini *et al.*[17] for much lower energy mesons. Moreover, there appears to be no simple correlation between the meson energy loss and the angle of scattering nor between the incident meson energy and the number of heavy prongs (N_h) in the star produced.

TABLE 10. OBSERVED INTERACTIONS OF HIGH-ENERGY π MESONS IN PHOTOGRAPHIC EMULSION

Kinetic energy of incident meson, Mev	Kinetic energy of outgoing meson, Mev	Angle of scattering, deg	N_h
252	180	62	4
340	28	28	1
375	85	19	6
460	310	26	1
640	39	18	7
670	110	22	9
755	70	167	6
755	450	15	6
785	56	96	6
825	17	125	5
900	29	43	6
960	225	17	3
1040	120	5	3
1050	120	90	4
1050	365 375	. . .	3

It is interesting to note that one nuclear interaction event in Table 10 contains two emerging low-energy mesons. The question arises whether this reproduction of the initial π mesons is to be attributed to the direct production of two mesons in a meson-nucleon collision or to an elastic scattering of the initial π meson by a nucleon plus one additional meson produced in the collision of the recoil nucleon with another nucleon in the nucleus. Since the initial meson has an energy of 1100 Mev, both explanations are possible on energetic grounds (cf. Table 1). Some independent evidence by Rosser and Swift[35] perhaps favors the direct

---

[34] Camerini, Davies, Fowler, Franzinetti, Muirhead, Lock, Perkins, and Yekutieli, *Phil. Mag.*, **42**: 1241 (1951); also Camerini, Davies, Franzinetti, Lock, Perkins, and Yekutieli, *Phil. Mag.*, **42**: 1261 (1951); and Lock and Yekutieli, *Phil. Mag.*, **43**: 231 (1952).

[35] W. Rosser and M. Swift, quoted in footnote 32.

production of several mesons by one π meson. These authors have exposed photographic emulsions at an altitude of 2860 m above and below 30 cm of lead and have found that, for showers with two or more shower particles, the ratio of charged primaries to neutral primaries is 0.86 ± 0.21 above the lead block and 1.76 ± 0.48 below the lead block. Since most of the penetrating particles must be π mesons, the increase is certainly due to the greater number of π mesons below the lead. Furthermore, since the ratios hold for showers with two or more shower particles, the mechanism of knock-on nucleons producing further mesons is unfavored. This follows because the average energy of a nucleon required to produce a penetrating shower with at least two shower particles is of the order of 4 Bev, and consequently the energy from the initiating π meson would have to be even higher; Rosser and Swift show that the number of such high-energy π mesons does not suffice to explain the magnitude of the observed effect. On the other hand, they can explain their results by assuming that π mesons of energies greater than 1 Bev multiply directly in collisions with nucleons with a cross section of the order of geometrical.

Kaplon[36] has examined the problem of the production of two π mesons in a π meson-nucleon collision within the context of weak coupling theory. He finds the same characteristic difference between the *PS*(*PS*) and *PS*(*PV*) theories just above threshold for the two-meson production which is found in the nucleon-nucleon production of one meson just above threshold (cf. Chap. 2), *i.e.*, a first-power momentum dependence for the *PS*(*PS*) theory and a third-power momentum dependence for the *PS*(*PV*) theory (the momentum refers to the meson, of course). This means that the *PS*(*PS*) cross section stays small compared with the meson-nucleon elastic scattering cross section even at energies high compared with the threshold for two-meson production. In the *PS*(*PV*) theory, the cross section builds up rapidly and reaches the geometrical value at several times the meson rest mass. These predictions are qualitatively interesting, although they certainly cannot be trusted because the very possibility of an appreciable cross section for double Compton scattering of π mesons depends on the fact that the π meson-nucleon coupling constant is not small. (For example, the cross section for the double Compton scattering of a photon by an electron is much smaller than the single Compton scattering cross section, by a factor of $e^2/\hbar c = \frac{1}{137}$.) The reproduction of mesons by mesons will be discussed further in Chap. 8 in connection with observations of large numbers of penetrating particles in the extensive air showers.

---

[36] M. F. Kaplon, Ph.D. Thesis, University of Rochester, 1951; cf. also M. Cini and L. Radicati, *Nuovo cimento*, **8**: 542 (1951).

CHAPTER 8

PRODUCTION OF π MESONS AT RELATIVISTIC NUCLEON ENERGIES

1. Introduction

In the preceding chapters, we have been concerned chiefly with the production of π mesons by artificial sources of photons and nucleons and with the properties and behavior of these artificially produced mesons. This emphasis was chosen deliberately so that the more clear-cut accelerator experiments[1] would receive proper attention and enable a comparison to be made with theoretical predictions whose qualitative features could at least be trusted. Indeed, this enterprise has been so successful that we are now in a position to state rather unequivocally that the π meson is a pseudoscalar particle and is coupled to the nucleon field through gradient (pseudovector) coupling. [It is possible that there is an admixture of direct (pseudoscalar) coupling, but pseudovector coupling must surely play a role.[1a]] Many experiments have been cited which lead to this conclusion, but the particular series of experiments[1] which, in our opinion, offers the most convincing demonstration of the above statement is (1) the experiment on the absorption of slow π^- mesons by deuterium, which rules out the scalar and vector fields for the charged π meson; (2) the measurements of the cross sections for the reactions $\pi^+ + D \leftrightarrows P + P$, which requires spin 0 for the charged π meson; (3) the rapid increase of cross section with energy for the scattering of π mesons by hydrogen, which strongly favors gradient coupling; (4) the observation of the two-photon decay of the π^0 meson, which eliminates spin 1 for the π^0 meson; (5) the experiment on the absorption of slow π^- mesons by hydrogen, which requires the π^0 meson to possess the same parity as the π^- meson (once the pseudoscalar field is fixed for the π^- meson); (6) the measurement of the cross section for the photoproduction of π^0 mesons in hydrogen, which favors gradient coupling for the π^0 meson.

Once it has been established that the *PS*(*PV*) field description applies to the π meson, it becomes of great interest to examine the existing cosmic-ray data with a view toward understanding the meson production phenomena which take place at relativistic nucleon energies. Such energies are beyond the range of the accelerators now in operation and, in some cases, completely beyond the range of the largest accelerator under construction (*i.e.*, the Berkeley bevatron, which is expected to yield 6-Bev protons). If it is recalled that the average cosmic-ray energy, say at mountain altitudes, is of the order of 10 Bev and that incontrovertible evidence exists for energies as high as 10^{15} ev per nucleon in the primary cosmic radiation, it is seen that an enormous energy range still remains to be covered. While some cosmic-ray experiments have been performed over the entire energy range, they become increasingly more difficult with increasing energy because of rapidly diminishing intensities. Even at the low end of the cosmic-ray energy spectrum, decisive experiments are rare because of the intensity problem. Nevertheless, we shall present the results of the important cosmic-ray experiments as they bear on the problem of high-energy meson production.

---

[1] Cf. R. E. Marshak, *Rev. Mod. Phys.*, **23:** 137 (1951).

[1a] However, it must be borne in mind that the *PS*(*PS*) theory may exhibit many of the desirable features of the *PS*(*PV*) theory when a proper (*i.e.*, nonweak coupling) treatment is achieved.

The fact that the π meson field is $PS(PV)$ has consequences which are just the reverse of the situation in quantum electrodynamics. In quantum electrodynamics, the strength of the electron-photon interaction decreases with increasing energy, thereby ensuring the convergence of the radiative cross sections (*e.g.*, Compton scattering, photonic bremsstrahlung, etc.) at high energies. Another feature which leads to finite cross sections in quantum electrodynamics in the relativistic limit is the small value of the coupling constant $\alpha = e^2/\hbar c \approx \frac{1}{137}$ which characteristizes the electron-photon interaction. The small value of the coupling constant and the decrease in the matrix element with energy justifies the use of weak coupling theory and the application of standard perturbation methods even at relativistic electron energies. It is easy to show, and this has been done by Heitler,[2] that if, for example, σ_c is the cross section for the Compton scattering of a photon by an electron, then $(\alpha^{n-1}\sigma_c)$ is the approximate cross section for the production of $(n - 1)$ quanta in addition to the scattered photon. Similarly, if σ_b is the cross section for the production of one photon by an electron interacting with the Coulomb field of a nucleus, the cross section for the production of n light quanta is approximately $(\alpha^{n-1}\sigma_b)$ provided that the emitted quanta are not of low frequency. These statements imply that single photon emission is much more probable than the emission of many photons in the elementary act. On the other hand, it is well known that multiple photon processes occur at very low frequencies (infrared catastrophe!) as a result of the increasing electron-photon interaction with decreasing energy. Despite the fact that the coupling constant still retains its small value, the matrix element is no longer small, and the weak coupling perturbation methods are no longer applicable. Fortunately, the occurrence of the divergence in the low-frequency limit enables one to make a perfectly legitimate approximation and to apply a rigorous method—the so-called Bloch-Nordsieck method,[3] to the solution of radiation problems.

---

[2] W. Heitler, "Quantum Theory of Radiation," Oxford University Press, 1947.

The situation is just the reverse in π meson theory (unless otherwise stated, we restrict ourselves to π mesons—heavy mesons constitute only a small fraction of the meson component except possibly at the highest energies—cf. Chap. 9) where, because of gradient coupling, the meson-nucleon interaction increases with increasing energy. When this fact is combined with the intrinsically larger π meson-nucleon coupling constant ($f_\pi^2/\hbar c$ is about $\frac{1}{4}$ compared with $\frac{1}{137}$ in quantum electrodynamics), it would appear to follow that, at high energies, multiple meson processes should occur with appreciably probability and the perturbation-theoretic methods should break down. (There is no infrared catastrophe in meson theory because of the finite rest mass of the meson quantum.) These consequences become especially evident when it is recalled that the cross section for the scattering of π mesons by nucleons attains its geometrical value at a meson kinetic energy of about 100 Mev and that, in the weak coupling approximation, the matrix element continues to increase without limit beyond this energy. The onset of multiple meson processes would mean that, at sufficiently high energies, a meson scattered by a nucleon would lead to the production of more than one meson, more than one meson would be produced in a nucleon-nucleon collision, and so on (the first process is the analogue of double and higher Compton scattering in quantum electrodynamics, and the second is the analogue of photonic bremsstrahlung). In Sec. 3, we shall discuss several representative theories which have been proposed to describe the process of multiple meson production in nucleon-nucleon collisions.

While it seems natural to expect multiple meson processes to take place at sufficiently high energies (and we shall see that the experimental material supports this expectation), it is conceivable that the increasing damping effect resulting from the reaction of the meson field on the nucleon source may cut down, in a very significant way, the matrix element at high energies. It is even possible that the meson-nucleon interaction may be inhibited to such a degree that multiple meson processes are suppressed compared with single meson processes. On this basis, some authors have argued that the observation of large numbers of mesons in penetrating showers does not necessarily imply that more than one meson is created in the elementary act. Instead, it is proposed that only one meson is created in the primary nucleon-nucleon collision responsible for the penetrating shower and that the observation of many π mesons merely implies that the primary and secondary nucleons suffer additional collisions during the course of their traversal of a nucleus. This explanation of the multiplicity of π meson production in penetrating showers is termed the plural meson hypothesis—in contrast to the multiple meson hypothesis which accepts the possibility that more than one π meson can be produced in a single nucleon-nucleon encounter. We shall discuss the predictions of the plural theory in the next section before we turn to the multiple meson theories in Sec. 3.

---

[3] Cf. F. Bloch and A. Nordsieck, *Phys. Rev.*, **52**: 54 (1937).

In Sec. 4 we summarize briefly the kinematical formulas which make possible a comparison of the experimental quantities which are measured in the laboratory system and the theoretical numbers which are given in the center-of-mass system. The experimental evidence in favor of plural meson production will be presented in Sec. 5 and the data supporting multiple meson production in Sec. 6. Finally, Sec. 7 contains a discussion of extensive air (Auger) showers as they bear on the problem of π meson production at relativistic nucleon energies.

2. Theory of Plural Production of π Mesons

The plural theory of π meson production has been espoused chiefly by Heitler and Janossy,[4] who have investigated the possibility of explaining the experimental data on penetrating showers in terms of a plural production mechanism. In order to judge the success of the plural production hypothesis, it is necessary to enumerate some of its characteristic predictions, in particular as regards the size-frequency distribution of penetrating showers, the ratio of nucleons to π mesons in a penetrating shower, etc.

The first calculations with the plural theory were carried out by Heitler and Janossy[4] on the basis of the following assumptions: (*a*) The primary nucleon which initiates a shower of n mesons suffers n collisions during its traversal of a target nucleus and emits only one meson per collision. (*b*) In each inelastic nucleon-nucleon collision, the incoming nucleon loses energy to the meson via a process similar to photonic bremsstrahlung, viz., in accordance with the law

$$\sigma(E', E)dE' = \sigma\left(\frac{E'}{E}\right)\frac{dE'}{E} \tag{1}$$

where $\sigma(E', E)$ is the probability that a nucleon with energy E will retain an energy E' after one collision ($E - E'$ = energy of the created meson plus the energy of the recoil nucleon). This assumption is equivalent to the statement that the total cross section for meson production is independent of the energy of the incident nucleon. This assumption can evidently be correct only above a certain critical energy E_c which must lie appreciably above the threshold energy for meson production in nucleon-nucleon collisions—which is approximately $2\mu c^2$ (μ is the meson mass) for π meson production. (*c*) The individual acts of meson emission are statistically independent, *i.e.*, the nucleus is undisturbed by any one act of meson creation. This appears to be a plausible assumption since, at the high energies under consideration, it seems reasonable to regard the nucleons in the target nucleus as free and acting independently of one another. (*d*) Secondary processes are neglected, *i.e.*, the production of mesons by recoil nucleons and the reproduction of mesons by mesons are neglected. It is evident that the number of π mesons predicted will be increased by taking account of secondary processes. This improvement has been attempted by Clementel[5] and will be noted after we state the results of Heitler and Janossy. (*e*) The integral energy spectrum of the incident nucleons has the form of a power law (dE/E^γ) ($\gamma \approx 1.5$). Heitler and Janossy[4] have shown that a power law spectrum retains its form at any depth below the top of the atmosphere provided that primary nucleons lose energy in inelastic collisions with other nucleons in accordance with Eq. (1). It is therefore self-consistent to assume a power law spectrum for the nucleons producing penetrating showers.

---

[4] W. Heitler and L. Janossy, *Proc. Phys. Soc. London*, **62**: 669 (1949); cf. also *Helv. Phys. Acta.*, **23**: 417 (1950).

On the basis of assumptions (*a*) to (*e*), it is possible to write down an exact expression for the probability for the creation of *n* mesons resulting from the passage of a fast nucleon through a given nucleus. If one writes

$$\sigma\left(\frac{E'}{E}\right)\frac{dE'}{E} = \sigma_0\omega\left(\frac{E'}{E}\right)\frac{dE'}{E}; \qquad \int_0^E \omega\left(\frac{E'}{E}\right)\frac{dE'}{E} = 1 \tag{2}$$

then the probability P_n for the production of n mesons by a nucleon of energy E is given by

$$\begin{aligned} P_n = \bar{\omega}^{n-1}\left[\Gamma_n(a_A) - \frac{n(n+1)}{a_A^2}\Gamma_{n+2}(a_A)\right] \\ - \bar{\omega}^n\left[\Gamma_{n+1}(a_A) - \frac{(n+1)(n+2)}{a_A^2}\Gamma_{n+3}(a_A)\right] \end{aligned} \tag{3}$$

where
$$\bar{\omega} = \int_0^E \omega\left(\frac{E'}{E}\right)\left(1 - \frac{E'}{E}\right)^\gamma \frac{dE'}{E}, \qquad a_A = \sigma_0\rho d_A$$

$$\Gamma_m(a) = \int_0^a \frac{x^{m-1}}{(m-1)!}e^{-x}\,dx \qquad \text{(incomplete } \Gamma \text{ function)}$$

with ρ the density of nuclear matter and d_A the nuclear diameter corresponding to atomic weight A. It is seen that the distribution function

---

[5] E. Clementel, *Nuovo cimento*, **7**: 109 (1950).

P_n depends on two constants: the total cross section

$$\sigma_0 = \int_0^E \sigma \left(\frac{E'}{E}\right)\left(\frac{dE'}{E}\right)$$

and a weighted average of the differential cross section over the energy spectrum of the incident nucleons, namely, $[1 - (E'/E)]^\gamma$. In principle, both of these constants could be determined from the observed size-frequency distribution of penetrating showers. However, experiment indicates that σ_0 is the geometrical cross section, and this leaves only one adjustable parameter in the theory.

Equation (3) is not in a form directly suitable for comparison with the experimental data on penetrating showers since, in most experiments, only charged particles are observed. It is plausible to assume that, at least in the large penetrating showers, half of the nucleons emitted are unobserved neutrons. There is also some experimental evidence (compare Sec. 6 below) that at high energies the number of π^0 mesons created is approximately one-half the total number of charged π mesons (positive and negative) produced. Moreover, under assumptions (*a*) to (*e*) above, approximately one recoil nucleon should be produced per meson. In other words, if n mesons are produced, we expect, on the basis of these considerations, that on the average $(7n/6)$ shower particles are visible (*i.e.*, charged). However, in order not to prejudge the matter, Heitler and Janossy[4] have generalized formula (3) to allow for the more general situation where a π meson emitted in an individual creation act has a probability δ of being neutral and a charged shower particle has a probability ξ of being a π meson [$(1 - \xi)$ of being a proton], independently of how many particles there are in the shower. They find, for the probability P_N for the emission of N charged shower particles,

$$P_N = \chi \left\{ \bar{\omega}'^{N-1} \left[\Gamma_N(a'_A) - \frac{N(N+1)}{a'^2_A} \Gamma_{N+2}(a'_A) \right] - \bar{\omega}'^{N} \left[\Gamma_{N+1}(a'_A) - \frac{(N+1)(N+2)}{a'^2_A} \Gamma_{N+3}(a'_A) \right] \right\} \quad (4)$$

where $a'_A = a_A \dfrac{[\xi + \bar{\omega}(1 - \delta - \xi)]}{\xi}$, $\quad \bar{\omega}' = \dfrac{(1 - \delta)\bar{\omega}}{\xi + \bar{\omega}(1 - \delta - \xi)}$

$$\chi = \frac{(1 - \delta\bar{\omega})}{\xi(1 - \bar{\omega}) + (1 - \delta)\bar{\omega}}$$

Table 1 contains the predictions of Eq. (4) for several values of a'_A and $\bar{\omega}'$. It is plausible to assume geometrical cross section for σ_0 so that a'_A will be a function of A, δ, and ξ. It is also plausible that $\bar{\omega}$ is greater than 0.4

since, even for a constant $\omega(E'/E)$ and $\gamma = 1.5$, $\bar{\omega}$ would be 0.4; furthermore, $\bar{\omega}$ must be less than 1. For comparison with experiment, a reasonable value of $\bar{\omega}$ seems to be something intermediate between 0.4 and 1, say $\frac{2}{3}$, and $\bar{\omega}'$ becomes a function of δ and ξ. A choice of δ and ξ will then fix a'_A and $\bar{\omega}'$. It is interesting to note in Table 1 how relatively rapidly the frequency for large showers drops off for small a'_A, that is, the light nuclei, and the appreciable probability for relatively large showers in the heavy nuclei.

We have already remarked that one of the assumptions underlying Heitler and Janossy's calculations leads to an underestimate of the shower size, *viz.*, the neglect of secondary production processes. Strictly speaking, the reproduction of π mesons by π mesons should be excluded in the context of a pure plural theory. That is to say, if it is considered legitimate to allow for the production of two π mesons in a π meson-nucleon collision (*i.e.*, "double Compton scattering"), by the same token, it should be possible for two nucleons to produce two π mesons per collision; but this would contradict the underlying assumption of the plural production hypothesis. Consequently, a π meson-nucleon collision should not be regarded as a further source of mesons but merely as a mechanism for altering the initial angle of the π meson ("ordinary Compton scattering"). It is consistent, however, for the plural theory to take into account the π meson production resulting from collisions of the recoil nucleons with the nucleons of the target nucleus.

Evidently, the efficacy of the recoil nucleon production mechanism and the possibility of developing a small nucleonic cascade depends upon the energy of the primary nucleon and the fractional energy transfer to the meson per inelastic nucleon-nucleon collision. Clementel[6] has made a preliminary attempt to take cognizance of the effects of the recoiling nucleons on the generation of penetrating showers. In Clementel's treatment, the need for using the experimental ratio of π mesons to protons is eliminated, and it is possible instead to predict this ratio. Clementel's argument is as follows: assume that the probability for a nucleon of energy E to create a π meson in the energy interval between ϵ and $\epsilon + d\epsilon$ in a volume element between x and $x + dx$ within the nucleus, the target nucleon recoiling with an energy between E' and $E' + dE'$ can be written in the form

$$\begin{aligned}\sigma(\epsilon, E'; E)\,d\epsilon\,dE'\,dx &= f(\epsilon, E)g(E', E)\,d\epsilon\,dE'\,dx \\ &= k\left(1 - \frac{\epsilon}{E}\right)^{\alpha}\left(1 - \frac{E'}{E}\right)^{\beta}\frac{d\epsilon}{E}\,\frac{dE'}{E}\,dx \qquad (5)\end{aligned}$$

where k, α, and β are constants. If $S(E, x)$ is defined as the number of nucleons in the volume element between x and $x + dx$ whose energy is

TABLE 1. RELATIVE FREQUENCY (PER CENT) OF SHOWERS P_N WITH N CHARGED PARTICLES* (PLURAL THEORY WITHOUT RECOIL NUCLEONS)

$\bar{\omega}' = 0.6$

a'_A \ N	1	2	3	4	5	6	7	8	9	10
2.5	49	21	5.5	1.5	0.4	0.1	0	0	0	0
4	46	24	11	4.3	1.5	0.46	0.13	0	0	0
7	43	25	14	7.3	3.6	1.6	0.70	0.28	0.10	0
11	41	25	14	8.2	4.6	2.5	1.3	0.69	0.34	0.16

$\bar{\omega}' = 0.7$

a'_A \ N	1	2	3	4	5	6	7	8	9	10	11–12	13–14	15–16
3	43	23	10	4.0	1.3	0.36	0.09	0	0	0	0	0	0
5	38	25	15	8.1	3.9	1.7	0.66	0.24	0.08	0	0	0	0
9	33	23	16	10	6.7	4.1	2.4	1.3	0.67	0.33	0.2	0	0
14	31	22	15	11	7.2	4.7	3.2	2.1	1.3	0.85	0.73	0.25	0.07

$\bar{\omega}' = 0.8$

a'_A \ N	1	2	3	4	5	6	7	8	9	10	11–12	13–14	≥15
3	37	24	13	5.5	2.1	0.67	0.19	0	0	0	0	0	0
5	30	24	17	11	6.0	3.0	1.4	0.56	0.21	0.07	0	0	0
9	23	19	16	12	9.2	6.6	4.4	2.8	1.7	1.0	0.9	0.3	0
14	22	18	14	11	8.9	7.0	5.4	4.0	3.0	2.2	2.5	1.1	0.58
20	21	17	13	11	8.5	6.9	5.3	4.2	3.3	2.5	3.4	1.9	1.9

$\bar{\omega}' = 0.9$

a'_A \ N	1	2	3	4	5	6	7	8	9	10	11–12	13–14	15–16	17–18	≥19
3	31	24	15	7.3	3.1	1.2	0.4	0.11	0	0	0	0	0	0	0
5	22	21	18	13	8.5	4.9	2.5	1.2	0.50	0.20	0	0	0	0	0
9	14	14	14	13	11	9.4	7.4	5.4	3.8	2.4	2.3	0.4	0	9	0
14	12	11	10.5	10	9.2	8.2	7.5	6.5	5.4	5.0	6.9	3.9	1.9	0.75	0.37
20	11	10	9.3	8.4	8.0	7.1	6.5	5.7	5.4	4.6	7.8	5.8	4.1	2.7	3.0

* The probabilities are normalized to 100 including P_0.

between E and $E + dE$, then the diffusion equation for the nucleons is

$$\frac{\partial S}{\partial x}(E, x) = -S(E, x) \int_0^E f(\epsilon, E)d\epsilon \int_0^{E-\epsilon} g(E', E)dE' + \int_0^\infty S(\bar{E}, x)d\bar{E} \int_0^{\bar{E}-E} f(\epsilon, \bar{E})g(E, \bar{E})d\epsilon$$
$$+ \int_0^\infty S(\bar{E}, x)d\bar{E} \int_0^{\bar{E}-E} f(\epsilon, \bar{E})g(\bar{E} - E - \epsilon, \bar{E})d\epsilon \qquad (E \geq E_c) \quad (6a)$$

$$\frac{\partial S}{\partial x}(E, x) = \int_{E_c}^{E_0} S(\bar{E}, x)d\bar{E} \int_0^{\bar{E}-\epsilon} f(\epsilon, \bar{E})[g(E, \bar{E}) + g(\bar{E} - E - \epsilon, \bar{E})]d\epsilon \qquad (E < E_c) \quad (6b)$$

where E_0 is the energy of the primary nucleon and E_c is the critical energy below which it is assumed that meson production ceases (*i.e.*, the meson production cross section is assumed to be a discontinuous function of the energy with the transition point at $E = E_c$ with E_c to be specified later). The first term on the R.H.S. of Eq. (6*a*) is the number of nucleons which are removed from the given energy interval by collisions, the second term represents those nucleons which are added to the energy interval due to a gain in energy from collisions, and the third term gives the contribution of those nucleons which are added to the energy interval because of a loss of energy from collisions. If $\omega(\epsilon, E)d\epsilon = d\epsilon \int_0^{E-\epsilon} \sigma(\epsilon, E'; E)dE'$ defines the probability of creating a meson with energy between ϵ and $\epsilon + d\epsilon$ by a nucleon within the nucleus with energy E, the diffusion equation for the meson distribution function $R(\epsilon, x)$ is

$$\frac{\partial R}{\partial x}(\epsilon, x) = \int_\epsilon^{E_0} S(E, x)\omega(\epsilon, E)dE \qquad (\epsilon \geq E_c) \qquad (7a)$$

$$\frac{\partial R}{\partial x}(\epsilon, x) = \int_{E_c}^{E_0} S(E, x)\omega(\epsilon, E)dE \qquad (\epsilon < E_c) \qquad (7b)$$

If Eqs. (6) and (7) are integrated over the diameter of the nucleus (that is, $2x\,dx$), the expressions for S and R are then averaged over the spectrum of incoming primaries [that is, $(dE_0/E_0^{\gamma+1})$, $\gamma \approx 1.5$], and the resulting quantities are finally integrated over all energies above cutoff (cutoff means the energy below which the particles are no longer regarded as shower particles, say 30 Mev for π mesons and 200 Mev for protons), it is possible to predict the average multiplicity of charged π mesons and protons. Table 2 lists the results for two representative nuclei of the emulsion, *viz.*, oxygen and silver, assuming $E_c = 3.5 \times 10^9$ ev. If the assumption is then made that the individual acts of emission are statistically independent, then the average multiplicity obtained above may be associated with a Poisson distribution. Carrying out the identifications indicated by Table 2, the size-frequency distribution for shower particles resulting for O and Ag is shown in Table 3.

TABLE 2. AVERAGE NUMBER OF CHARGED SHOWER PARTICLES FROM O AND AG (PLURAL THEORY WITH RECOIL NUCLEONS)

	O	Ag
Average number of mesons..............	1.35	1.74
Average number of protons..............	1.21	1.28
Total number = N....................	2.56	3.02

TABLE 3. POISSON DISTRIBUTION CORRESPONDING TO TABLE 2

N	3	4	5	6	7	8
O	34	21	11	4.5	1.6	0.5
Ag	34	26	15	7.7	3.4	1.4

3. Theories of Multiple Production of π Mesons

Heisenberg[6] was the first to argue that multiple meson processes, *e.g.*, production of many mesons in a single nucleon-nucleon collision, should play an important role at relativistic nucleon energies. He considered the analogy with the electromagnetic field where the sudden deflection of an electrically charged particle leads, at the moment of deflection, to a discrepancy between the electromagnetic fields surrounding the particle before and after the deflection; the difference between the electromagnetic fields becomes in a certain sense detached and wanders into space as electromagnetic radiation. The radiation spectrum is the well-known bremsstrahlung spectrum $d\omega/\omega$, that is, the mean number dn_γ of light quanta in the frequency interval $d\omega$ is given by

$$dn_\gamma \approx \frac{e^2}{\hbar c}\frac{d\omega}{\omega} \tag{8}$$

Equation (8) leads to the well-known infrared catastrophe, *i.e.*, an infinite number of very low energy light quanta.

Heisenberg argued that, in analogy with the electromagnetic case, the sudden deflection of a very energetic nucleon should lead to a discrepancy between the associated meson fields before and after the collision and that this difference between the meson fields would become detached and wander into space as meson radiation. If one postulates that the meson spectrum again has the bremsstrahlung form, one would write (ϵ is now the energy of the meson including its rest mass)

---

[6] W. Heisenberg, *Z. Physik*, **113:** 61 (1939).

$$dn_\pi \approx \frac{f^2}{\hbar c}\frac{d\epsilon}{\epsilon} \tag{9}$$

where $(f^2/\hbar c)$ is now the meson-nucleon coupling constant (of the order of $\frac{1}{4}$). Because of the finite rest mass of the meson, Eq. (9) does not lead to an infrared catastrophe, but the much larger value of the coupling constant shows that the multiplicity can exceed one when the energy is not too excessive [$n_\pi > 1$ when $\epsilon > \mu c^2 \exp\,(\hbar c/f^2) \approx 50\mu c^2$ for $f^2/\hbar c \approx \frac{1}{4}$]. However, it is not clear why the bremsstrahlung spectrum should hold for meson production, and Heisenberg[7] has recently recognized that the characteristic feature of the meson-nucleon interaction is its increasing strength with increasing energy in contrast to the electromagnetic case. Heisenberg's recent interpretation of the increasing meson-nucleon interaction is that in a very high-energy nucleon-nucleon collision, nonlinear effects enter which cause a kind of turbulent meson mixing of the nucleonic wave packet; when the nucleonic wave packet spreads out to a sufficient degree, the nonlinear terms lose their significance. In the course of this turbulent mixing, the Fourier meson spectrum of the nucleonic wave packet undergoes a displacement toward low frequencies signifying the creation of many low-energy mesons. Heisenberg makes no explicit attempt to spell out the quantitative predictions of his nonlinear theory[7a] but is content merely to state the qualitative consequences, namely, (1) a penetrating shower should, usually, contain many more low-energy than high-energy mesons; (2) the mean number of mesons produced should increase with the available primary nucleonic energy; (3) the form of the meson spectrum should depend only slightly on the primary energy; and (4) the angular distribution of the mesons should be isotropic in the center-of-mass system (in analogy with the isotropic distribution of the small turbulences which are discarded by a turbulent fluid). The Heisenberg production spectrum is usually taken, for purposes of comparison with experiment, as

$$n_\pi(\bar\epsilon, \bar\theta)d\bar\epsilon\, d\bar\Omega = k\frac{d\bar\epsilon}{\bar\epsilon^m}\, d\bar\Omega \tag{10}$$

---

[7] W. Heisenberg, *Nature*, **164**: 65 (1949); *Z. Physik*, **126**: 569 (1949). Cf. also G. Wataghin, *Phys. Rev.*, **74**: 975 (1948).

[7a] A recent paper by W. Heisenberg (to be published as a chapter in a revised edition of "Cosmic Radiation," edited by W. Heisenberg) contains more quantitative considerations, *e.g.*, the dependence of the degree of inelasticity of the collision on the impact parameter, the magnitude of the deviations from an isotropic angular distribution associated with the high energy tail of the meson spectrum, etc. Cf. also W. Heisenberg, *Naturwiss.*, **39**: 69 (1952).

where $\bar{\theta}$ is the angle of emission of the meson (in the center-of-mass system) and k and m are constants ($m = \frac{5}{3}$ in the theory of isotropic turbulence but can be left arbitrary provided that it is taken greater than unity[7b]).

The second major attempt to develop a theory of multiple meson production was made by Lewis *et al.*[8] who pushed even further the analogy between the meson radiation and electromagnetic radiation problems. We have already pointed out that perturbation methods break down in quantum electrodynamics in the limit of zero frequency and that Bloch and Nordsieck showed how a rigorous calculation of the photon emission could, nevertheless, be performed despite the inapplicability of perturbation theory. The assumptions underlying the Bloch-Nordsieck method are: (*a*) the collision time is short compared with the period of the emitted radiation, (*b*) the recoil effect of the emitted radiation on the source can be neglected, and (*c*) only those components of the radiation field need be considered which satisfy (*a*) and (*b*). It can readily be demonstrated that these assumptions are true for the electromagnetic case and that the emitted radiation spectrum can be derived as the difference between the quasi-static fields before and after collision. The Bloch-Nordsieck method also leads to the result that the total collision cross section is unaltered even though collisions are now accompanied by the emission of radiation. It is the Bloch-Nordsieck method which, with suitable modifications, Lewis *et al.* apply to the π meson production problem.

It would appear, at first sight, that the increasing strength of the π meson-nucleon interaction with increasing energy would invalidate the assumptions underlying the Bloch-Nordsieck method. Lewis *et al.* argue, however, that a strong meson-nucleon interaction at high energies does not necessarily imply a completely inelastic collision and that, if only a small fraction of the available nucleonic energy is transferred to the mesons and the collision is not accompanied by large momentum changes of the nucleons (although accompanied by large changes in the spins and isotopic spins), then assumptions (*a*) to (*c*) can still be maintained. The changes in the nucleonic charges and spins produce a discrepancy between the meson fields initially and finally present around the nucleons which is treated by Lewis *et al.* along the lines of the Bloch-

---

[7b] In turbulence theory, the $m = \frac{5}{3}$ law holds only for intermediate values of the wave number.

[8] Lewis, Oppenheimer, and Wouthuysen, *Phys. Rev.*, **73**: 127 (1948); cf. also B. D'Espagnat, Thèse, Université de Paris, 1950; H. Fukuda and G. Takeda, *Prog. Theor. Phys.*, **5**: 957 (1950); E. Clementel and N. Dallaporta, *Nuovo cimento*, **5**: 298 (1948).

Nordsieck method. If a law of force between the nucleons is then chosen and if it is assumed that the reaction of the meson field affects the cross sections corresponding to different meson multiplicities in the same way, it is possible to derive relative production cross sections. Calculations were carried out by Lewis *et al.* for both the symmetric scalar (with scalar coupling) and symmetric pseudoscalar (with pseudovector coupling) meson theories. They obtained the following expressions for the cross section σ (n) for the production of n mesons in a single collision and the average multiplicity $\bar{n}$ of meson emission ($\bar{\epsilon}_m$ in units of M):

Symmetric scalar

$$\sigma(n) \approx \sigma_s \left[\frac{4g^2/\hbar c(\Delta\tau)^2}{\pi}\right]^n \frac{1}{n!}\left[\ln\left(\frac{\bar{\epsilon}_m}{\bar{\gamma}}\right)\right]^n \tag{11a}$$

$$\bar{n} \approx \frac{4g^2/\hbar c(\Delta\tau)^2}{\pi} \ln\left(\frac{\bar{\epsilon}_m}{\bar{\gamma}}\right) \tag{11b}$$

Symmetric pseudoscalar

$$\sigma(n) \approx \sigma_P \left(\frac{f^2/\hbar c}{\pi}\right)^n \frac{\bar{\epsilon}_m^{2n}}{(n!)^3} (\Delta\tau\sigma)^{2n} \tag{12a}$$

$$n \approx \left[\frac{f^2}{\pi\hbar c} (\Delta\tau\sigma)^2 \bar{\epsilon}_m^2\right]^{\frac{1}{3}} \tag{12b}$$

where σ_s and σ_p are the undetermined constants of the theory, g or f is the meson-nucleon coupling constant, $\bar{\epsilon}_m$ is the maximum energy available in the center-of-mass system for meson production, $\bar{\gamma} = (1 - \bar{\beta}^2)^{-\frac{1}{2}}$ ($\bar{\beta}$ is the velocity of the center of mass), $\Delta\tau$ is the change in isotopic spin due to the collision in the scalar theory, and $\Delta(\tau\sigma)$ is the change in spin and isotopic spin due to the collision in the pseudoscalar theory.

Examination of Eqs. (11) and (12) reveals two interesting points which are not really independent: (1) scalar mesons can be radiated by a change in the isotopic spin of the nucleonic source and pseudoscalar mesons by a change in either the ordinary or isotopic spin; (2) the average multiplicity of scalar meson emission is essentially independent of energy, whereas the multiplicity in the pseudoscalar theory increases as $\bar{\epsilon}_m{}^{\frac{2}{3}}$, corresponding to an $E_0{}^{\frac{1}{3}}$ increase where E_0 is the energy of the incoming nucleon in the laboratory system. The energy-dependent multiplicity in the pseudoscalar theory arises from the gradient coupling in the meson-nucleon interaction, which gradient coupling is associated with the nucleon spin. There are two other differences between the scalar and pseudoscalar theories not shown in Eqs. (11) and (12): (3) the pseudoscalar theory predicts an isotropic angular distribution of emitted mesons in the center-of-mass system, whereas the scalar theory predicts maxima in the forward and backward directions in the center-of-mass system; and (4) the total cross section in the scalar theory is large, of the order of $(\hbar/\mu c)^2$, whereas the pseudoscalar theory predicts a relatively small cross section since impact parameters of the order of $\hbar/Mc$ enter into this theory. Since we now know that the pseudoscalar field applies to the π meson, the predictions of Lewis *et al.* for showers of π mesons would be: multiplicity varying as the cube root of the incident nucleon energy, small cross section, and isotropic emission in the center-of-mass system. These conclusions will be altered if the singularity in the pseudoscalar meson-nucleon interaction is "cut off" and if the recoil nucleon effect on the preexisting meson spectrum is taken into account. Both modifications would tend to decrease the multiplicity, increase the cross section, and concentrate the emissions forward and backward in the center-of-mass system.[8a]

A third type of multiple meson theory has been developed by Fermi,[9] who takes his lead from Heisenberg's notion that a very high energy collision between two nucleons sets the meson "fluids" surrounding the two nucleons in some sort of turbulent motion by the impact. Whereas Heisenberg is willing to stop with this turbulent state, which is the beginning of an approach to thermal equilibrium, Fermi argues that the meson-nucleon interaction becomes so strong and the processes of meson creation and destruction operate so fast at high energies that statistical equilibrium is actually reached before the nucleons separate. That is to say, Fermi pictures a high-energy collision between two nucleons as taking place in a time long compared with the time required for the loading of the intermingled meson "fluids" surrounding the two nucleons with the available energy. If Fermi's assumption is correct (and this contrasts with the short-collision-time assumption of the Lewis *et al.* theory), the available energy should be rapidly distributed among the various degrees of freedom present in the volume occupied by the two nucleons and their meson "fluids" in accordance with statistical laws. The probability for any particular process may be computed, just as in Bohr's theory of the compound nucleus, by finding the number of statistically independent states corresponding to the process in question. It would appear that the probability should be maximized by this type of statistical calculation so that, for example, Fermi's theory would be expected to provide an upper limit on the multiplicity of meson production. However, this would be true only provided that no appreciable meson production takes place during the course of dissolution of the meson-nucleon structure, and it is not self-evident that this should be the case. At any rate, the absence of "postequilibrium" production is assumed in the Fermi theory. It should also not be too surprising if Fermi's theory were to break down for relatively low energy nucleon-nucleon collisions where the final states are reached in only a small number of ways and statistical equilibrium may not be established sufficiently rapidly.

[8a] H. W. Lewis (*Rev. Mod. Phys.*, in press) has recently shown that a more careful treatment of the fundamental phase space integral of the pseudoscalar theory [in the formulation of Lewis *et al.* (see footnote 8)] leads to an unphysical (and experimentally incorrect) forward *or* backward angular distribution of mesons depending on whether the incident or target nucleon emits the mesons.

[9] E. Fermi, *Prog. Theor. Phys.*, **5**: 570 (1951).

The statistical theory, applied to meson production, implies that the cross section for the production of a given number of mesons is proportional to the probability that the given number of mesons will be contained at the same time inside the small volume occupied by the meson-nucleon structure and into which the energy has been concentrated. Of course, it is understood that the statistical weight which measures this probability is compatible with the conservation laws of energy, momentum, charge, angular momentum, etc. We have spoken of the volume occupied by the two nucleons and their meson "fluids" or clouds; the question now arises as to what size to choose for this volume since the statistical weight of any process will depend upon the volume. Fermi ultimately chooses, apart from the Lorentz contraction, a sphere of radius $R = (\hbar/\mu c)$ (where μ is the π meson mass); however, for the present, let us denote the volume by Ω. Since, in the multiple meson production process, the two nucleons approach each other with very high energy in their center-of-mass system, their surrounding meson clouds will be Lorentz-contracted and the volume in which the energy is concentrated will be correspondingly reduced by the Lorentz factor $(2M/\bar{E})$ where $\bar{E}$ is the total energy of the two colliding nucleons in their center-of-mass system and M is the nucleon mass. Once the relevant volume Ω is specified, the statistical model states that, for a state which describes n completely independent particles with momenta $p_1, p_2, \ldots, p_n$, the cross section is proportional to

$$\sigma(n) \sim \left(\frac{\Omega}{V}\right)^n \left[\frac{V}{(2\pi\hbar)^3}\right]^n \frac{dQ(\bar{E})}{d\bar{E}} \tag{13}$$

where V is the normalization volume and $Q(\bar{E})$ is the volume of momentum space corresponding to the total energy $\bar{E}$. The first term on the R.H.S. of Eq. (13) expresses the fact that the square of the matrix element for the emission of n completely independent particles is proportional to the nth power of the ratio of the volume to the large normalization volume V, whereas the remaining terms represent the number of states per unit energy interval. Equation (13) holds for n completely independent particles; in an actual situation, the positions and momenta of only $(n - 1)$ of the n particles characterizing the state are independent variables so that the exponent of Ω should be $(n - 1)$ instead of n and $Q(\bar{E})$ should be $(3n - 3)$-dimensional instead of $3n$-dimensional. Moreover, Eq. (13), as it stands, does not take into account the statistical weights associated with the spins of the particles and the fact that some of the particles may be identical; these deficiencies can easily be remedied. A deficiency which is somewhat more difficult to correct for—although it can be done—arises from the fact that the conservation of angular momentum restricts the statistical equilibrium attained in a given collision to states with angular momentum equal to that of the two colliding nucleons. Since one is dealing with highly energetic collisions, the de Broglie wave length $\lambda\!\!\!^{-}$ is small compared with the radius R of the sphere of action, and it is necessary to consider separately collisions with different values of the classical impact parameter b (b is the perpendicular distance between the two trajectories along which the nucleons move just before colliding). The cross section for an event of a specified multiplicity is then obtained by adding the contributions of the various l values ($l\hbar$ is the angular momentum) where l is related to the impact parameter b by the usual relation

$$l \sim \frac{b}{\lambda\!\!\!^{-}} \tag{14}$$

We shall see that taking cognizance of the conservation of angular momentum is extremely important for determining the angular distribution of the emitted mesons in the center-of-mass system.

Fermi first applies his statistical theory to the problem of determining the ratio of the cross section for the production of a single meson in a nucleon-nucleon collision just above threshold to the elastic-scattering cross section for the two nucleons. Taking account of momentum and energy conservation, but disregarding all other effects (*e.g.*, spin, charge, etc.), he finds that the cross section for elastic scattering is proportional to

$$\sigma_{\text{el}} \sim \frac{\Omega M^{\frac{3}{2}}}{4\pi^2\hbar^3}\sqrt{\bar{T}} \tag{15}$$

where $\bar{T}$ is the total kinetic energy of the two nucleons in their center-of-mass system. The cross section for the production of one π meson turns out to be proportional to

$$\sigma_{\text{inel}} \sim \frac{\Omega^2 M^{\frac{3}{2}}\mu^{\frac{3}{2}}}{32\sqrt{2}\,\pi^3\hbar^6}(\bar{T} - \mu c^2)^2 \tag{16}$$

The ratio of σ_{inel} to σ_{el} is

$$\frac{\sigma_{\text{inel}}}{\sigma_{\text{el}}} \approx \frac{1}{6\sqrt{2}}\left(\frac{\bar{T}}{\mu c^2} - 1\right)^2 \tag{17}$$

In Eq. (17) the volume Ω has been replaced by the uncontracted volume $\Omega_0 = (4\pi/3)R^3$ ($R \approx \hbar/\mu c$) since the Lorentz contraction factor is close to unity just above threshold for single meson production. Inserting numbers into Eq. (17)—140 Mev for the π meson mass and 340 Mev for the energy of the nucleon in the laboratory system—the formula yields 0.004 for $\sigma_{\text{inel}}/\sigma_{\text{el}}$. Considering the omissions, this value is in good agreement with the ratio of π^+ production cross section in proton-proton collisions[10] to the cross section for elastic scattering, *viz.*, 0.008. However, it will be recalled from Chap. 2 that the cross section for π^0 production in *P-P* collisions is down by more than a factor 10 compared with π^+ production, and this means that Fermi's theory cannot account for π^0 production in proton-proton collisions, even when proper account is taken of spins, charges, etc. It was pointed out earlier that disagreement of Fermi's statistical theory with experiment at low energies does not necessarily invalidate the theory at high energies; at low energies, relatively few states are involved and statistical equilibrium may not be attained, as indeed seems to be indicated by the π^0 production experiment. It is reasonable to expect the cross section to depend upon the character of the meson-nucleon coupling, and it is gratifying that the pseudoscalar theory (at least with pseudovector coupling) can explain the small relative cross section for π^0 to π^+ production in proton-proton collisions just above threshold (cf. Chap. 2).

Fermi's theory should be more reliable at energies far above the meson production threshold. Equation (13) can now be applied to derive a formula for the relative probability for the emission of different numbers of π mesons, namely,

$$P_n = \frac{[(251/\bar{W})(\bar{W} - 2)^3]^n}{\frac{3}{2} \times \frac{5}{2} \times \cdots \times (6n + 1)/2} \tag{18}$$

where $\bar{W} = \bar{E}/Mc^2$ is the energy of the two nucleons in the center-of-mass system in units of Mc^2. Table 4 lists the probabilities for the production of different multiplicities of π mesons calculated in accordance with Eq. (18). The first column lists $\bar{W}$, the second W, the energy of the primary nucleon in the laboratory system in units of $Mc^2 (W = \bar{W}^2/2 + 1)$, the next eight columns the numbers of π mesons produced in percentage figures, and the last column the average number of π mesons produced at each energy. The most probable multiplicity, according to Eq. (18) is

$$\frac{2.1(\bar{W} - 2)}{\bar{W}^{\frac{1}{3}}} \tag{19}$$

---

[10] We have used a total cross section of 2×10^{-28} cm^2 for the π^+ production (cf. Chap. 2) and an isotropic differential cross section of 4 mb/ster for the proton-proton scattering [cf. Chamberlain, Segrè, and Wiegand, *Phys. Rev.*, **83**: 923 (1951)].

Table 4 shows that, for a laboratory bombarding kinetic energy of about 1 Bev, the relative probability for an elastic nucleon-nucleon collision is down to 50 per cent and decreases rapidly, dropping below 1 per cent, for bombarding nucleon kinetic energies above 5 Mev. As the bombarding energy of the nucleon increases, the relative probability for inelastic meson production increases and the average multiplicity increases slowly, reaching the value 3.5 at 10-Bev kinetic energy.

The numbers in Table 4 should not be taken too literally since conservation of angular momentum and statistical correlations have been neglected. Instead of making the angular momentum and correlation corrections to Eq. (18) and complicating the analysis, Fermi proceeds to simplify the calculations by means of a thermodynamical treatment of the meson-nucleon structure in statistical equilibrium within the volume Ω. The thermodynamical treatment is especially convenient at extremely high[11] energies ($> 5 \times 10^{12}$ ev) since relativistic thermodynamics can be applied to both mesons and nucleons, thereby introducing great simplifications into the thermodynamical relations. Since π mesons are bosons (like photons), Stefan's law for π mesons will be identical with the ordinary Stefan's law for black-body radiation except for a factor $\frac{3}{2}$. This factor must be introduced because the π meson carries a statistical weight of 3 because of its three varieties of charge (not because of its spin which is zero) whereas the photon possesses a statistical weight of 2 due to its two polarizations. Thus the energy density associated with π mesons is[12]

TABLE 4. FERMI'S PREDICTIONS FOR THE MULTIPLICITY OF π MESON PRODUCTION

$\bar{W}$	W	$n = 0$	1	2	3	4	5	6	7	$\bar{n}$
2.5	2.1	49	47	4						0.6
3	3.5	9	59	30	2					1.2
3.5	5.1	2	31	46	18	3				1.9
4	7.0		13	40	33	11	2			2.5
5	11.5		2	15	34	31	14	3	1	3.5

$$u_\pi = \frac{\pi^2 (kT')^2}{10\hbar^3 c^3} \tag{20}$$

where k is the Stefan-Boltzmann constant and T' is the temperature. The contribution of the nucleons to the energy density is given by a similar formula except that the nucleons are fermions and the statistical weight of each nucleon is 2 (because its spin is $\frac{1}{2}$). In the extreme relativistic case, the energy density of nucleons is[12]

---

[11] In the energy region 10^{10} to 5×10^{12} ev, nonrelativistic thermodynamics can in principle be applied, although the numerical work is considerable.

[12] R. C. Tolman, "The Principles of Statistical Mechanics," Oxford University Press, 1938.

$$u_{\mathfrak{N}} = \frac{2 \times 11.364}{\pi^2 \hbar^3 c^3} (kT')^4 \tag{21}$$

In the above expression, the factor 2 takes account of the possibility of the creation of antiprotons and antineutrons; unless otherwise stated, we shall assume the existence of antinucleons in the following considerations, as does Fermi.[13]

The temperature of the meson-nucleon structure is now obtained by equating the total available energy $\bar{E}$ in the center-of-mass system to the product of the volume Ω and the sum of the two energy densities; one finds

$$(kT')^4 = 0.152 \frac{\hbar^3 c^3 \bar{E}^2}{Mc^2 \Omega_0} \tag{22}$$

The same statistical-mechanical arguments which lead to Stefan's formula also yield expressions for the number densities of π mesons and nucleons (plus antinucleons), namely,

$$n_\pi = 0.367 \left(\frac{kT'}{\hbar c}\right)^3, \qquad n_{\mathfrak{N}} = 0.855 \left(\frac{kT'}{\hbar c}\right)^3 \tag{23}$$

The total numbers of π mesons and nucleons are derived by multiplying Eq. (23) by the volume Ω, substituting in the resulting equation the temperature calculated from Eq. (22), and correcting for the failure to take into account the conservation of angular momentum. It turns out that angular momentum conservation merely has the effect of reducing the total number of π mesons and nucleons by a factor of 0.51. Hence the total number of π mesons is

$$0.54 \sqrt{\frac{\bar{E}}{Mc^2}} \tag{24}$$

and the total number of nucleons (plus antinucleons) is

$$1.3 \sqrt{\frac{\bar{E}}{Mc^2}} \tag{25}$$

assuming, as before, that $\Omega_0 = (4\pi R^3/3)(R \approx \hbar/\mu c)$. It is interesting to note that the theory predicts the production of comparable numbers of

---

[13] We shall not, however, take into account the possibility of the production of mesons heavier than π mesons (that is, τ mesons, etc.); the production of heavy mesons should compete unfavorably with the production of π mesons except at very high energies.

π mesons, nucleons, and antinucleons at very high energies. If it is furthermore assumed than two-thirds of the π mesons and one-half of the nucleons are charged, it follows that the total number of charged particles which should emerge, on the average, from a collision of a nucleon having an energy E in the laboratory system with a nucleon at rest is

$$1.2\left(\frac{E}{Mc^2}\right)^{\frac{1}{4}} \tag{26}$$

It is now possible to deduce a value of the critical energy above which Eqs. (22) and (23) can be expected to hold; let us rewrite Eq. (22) in the form

$$\left(\frac{kT'}{Mc^2}\right) = 0.105\sqrt{\frac{\bar{E}}{Mc^2}} \tag{27}$$

It is clear that $(kT') \approx Mc^2$ when $\bar{E}$ is greater $\bar{E}_c = 100Mc^2$; this value of $\bar{E}_c$ corresponds to a value of $E_c = 5 \times 10^{12}$ ev. Consequently, above $E_c = 5 \times 10^{12}$ ev, Fermi's relativistic thermodynamical theory should hold; below E_c, the number of nucleon-antinucleon pairs formed will decrease very rapidly since a minimum energy of $2Mc^2$ in the center-of-mass system is required for nucleon pair production. If one disregards the possibility of nucleon pair production, one can apply relativistic thermodynamics to a calculation of the multiplicity of meson production below E_c. The total energy density is now given by Eq. (20), and by replacing $\bar{E}$ by $(\bar{E} - 2Mc^2)$ (since the energy of the two colliding nucleons does not contribute to the energy of the π meson gas), the total number of π mesons becomes

$$\frac{1.34(\bar{W} - 2)^{\frac{3}{2}}}{\bar{W}} \tag{28}$$

Equation (28) gives somewhat lower meson multiplicities at energies below E_c than does Table 4, which was based on a formula [Eq. (18)] which did not take into account the statistical correlation between various types of π mesons and the conservation of angular momentum [in contrast to Eq. (28)].

The effect of the conservation of angular momentum on the numbers of mesons and nucleons predicted by the thermodynamical model is not very serious; it merely introduces a numerical factor of about ½ in all formulas. On the other hand, its effect on the angular distribution of the emitted particles is much more critical, the more so the larger the impact parameter b. Large values of the impact parameter imply large values of the angular momentum and since, even at the critical energy E_c, the de Broglie wave length of a nucleon in the center-of-mass system is $\frac{1}{300}$ as large as the radius of the sphere of action ($R \approx \hbar/\mu c$), it is seen that angular momenta as high as 300 can enter the picture. Since angular momentum must be conserved between the initial and final states, the outgoing particles (π mesons, nucleons, and antinucleons) must carry away the large amounts of angular momenta associated with the two initial nucleons whenever the two nucleons experience a collision with a large impact parameter (comparable with R). It is readily seen that the particles emitted in the direction of either the incident nucleon or the target nucleon in the center-of-mass system will carry away the largest amount of angular momentum. In this fashion, forward and backward emission in the center-of-mass system will be favored and the angular distribution of the emitted particles will be anisotropic, the anisotropy increasing with increasing impact parameter.

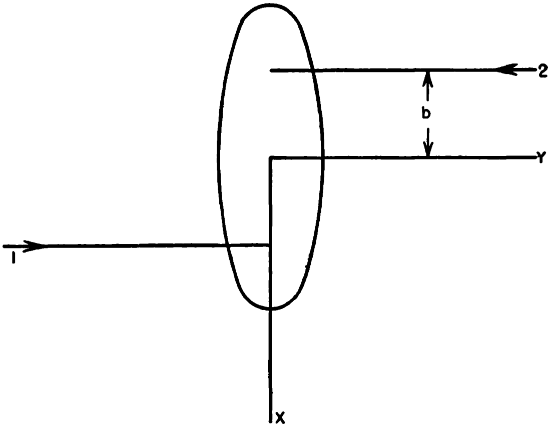

FIG. 1. Trajectories and Lorentz-contracted sphere of action of nucleons 1 and 2 in the center-of-mass system on the basis of Fermi's theory; b is the impact parameter.

A quantitative estimate of the anisotropy can be obtained as follows:[14] the average number of particles emitted with an energy E and a z component of the total angular momentum (the z axis is taken perpendicular to the plane of the two colliding nucleons) equal to M_z is given by the expression

$$\bar{n} = \frac{3}{e^{\frac{E-\lambda M_z}{kT'}} - 1} + \frac{8}{e^{\frac{E-\lambda M_z}{kT'}} + 1} \tag{29}$$

where the constants T' ("temperature") and λ in Eq. (29) must be adjusted in such a way that $E = \bar{E}$ and $M_z = \bar{E}b/c$. The number of particles emitted between x and $x + dx$ (cf. Fig. 1), momentum between

---

[14] E. Fermi, *Phys. Rev.*, **81**: 684 (1951); cf. also Hazen, Heineman, and Lennox, *Phys. Rev.*, **86**: 198 (1952).

p and $p + dp$, and $\eta = \cos\bar{\theta}$ ($\bar{\theta}$ is the angle of emission in the center-of-mass system) between η and $\eta + d\eta$, is given by the expression

$$dn = \frac{Mc^2}{2\pi\hbar^3 E}[3F_-(\zeta) + 8F_+(\zeta)](R^2 - x^2)dx\,p^2\,dp\,d\eta \tag{30}$$

where

$$F_-(\zeta) = (e^\zeta - 1)^{-1}, \qquad F_+(\zeta) = (e^\zeta + 1)^{-1},$$

$$\zeta = \xi p\left(1 - \frac{\rho\eta x}{R}\right), \qquad \xi = \frac{c}{kT'}, \qquad \rho = \frac{\lambda R}{c}$$

Integrating Eq. (30) with respect to all variables, the total number N of emitted particles follows immediately:

$$N = \frac{(3a_+ + 8a_-)Mc^2R^3}{2\pi E\hbar^3\xi^3} f_1(\rho) \tag{31}$$

where

$$f_1(\rho) = \left[\frac{(1 + \rho^2)}{\rho^3}\ln\left(\frac{1 + \rho}{1 - \rho}\right) - \frac{2}{\rho^2}\right], \qquad a_+ = 2\sum_1^\infty \frac{1}{m^3} = 2.413,$$

$$a_- = 2\sum_1^\infty \frac{(-)^{m+1}}{m^3} = 1.803$$

The total energy of the emitted particles is

$$E = \frac{(3a'_+ + 8a'_-)Mc^3R^3}{3\pi E\hbar^3\xi^4} f_2(\rho) \tag{32}$$

where

$$f_2(\rho) = \left[\frac{1}{\rho}\ln\left(\frac{1 + \rho}{1 - \rho}\right) + \frac{2}{1 - \rho^2}\right], \qquad a'_+ = 6\sum_1^\infty \frac{1}{m^4} = 6.494,$$

$$a'_- = 6\sum_1^\infty \frac{(-)^{m+1}}{m^4} = 5.682$$

and the total z component of the angular momentum is

$$M_z = \frac{(3a'_+ + 8a'_-)Mc^2R^4}{2\pi E\hbar^3\xi^4} f_3(\rho) \tag{33}$$

where

$$f_3(\rho) = \left[\frac{2}{\rho^3} + \frac{4}{3\rho(1 - \rho^2)} - \frac{(3 + \rho^2)}{3\rho^4}\ln\left(\frac{1 + \rho}{1 - \rho}\right)\right]$$

Instead of working with Eq. (33), it is more convenient to work with the ratio M_z/E; setting $M_z/E = b/c$ (the value for the two initial nucleons—cf. Fig. 1), one obtains

$$\frac{b}{R} = \frac{3}{2}\frac{f_3(\rho)}{f_2(\rho)} \tag{33a}$$

Equation (30) can be used to find the angular distribution of the emitted particles (mesons plus nucleons plus antinucleons) independent of energy and the energy spectrum independent of angle. If Eq. (30) is integrated with respect to all variables except η, the resulting expression is the angular distribution

$$\frac{dn}{d\eta} = \frac{(3a_+ + 8a_-)Mc^2R^3}{2\pi E\hbar^3\xi^3} f_4(\rho\eta) \tag{34}$$

where $$f_4(\rho) = \left[\frac{2}{\rho^2(1-\rho^2)} - \frac{1}{\rho^3}\ln\left(\frac{1+\rho}{1-\rho}\right)\right]$$

If Eq. (30) is integrated with respect to all variables except p, the resulting expression is the energy spectrum

$$\frac{dn}{d(\xi p)} = \frac{4}{\rho^2 f_1(\rho)} \sum_{m=1}^{\infty} \left\{\left[\frac{3}{a_+} + \frac{8(-)^{m+1}}{a_-}\right]\frac{e^{-m\xi p}}{m^2} \left[\frac{\sinh(m\xi p\rho)}{m\xi p\rho} - \cosh(m\xi p\rho) + m\xi p\rho \operatorname{Shi}(m\xi p\rho)\right]\right\} \tag{35}$$

where $$\operatorname{Shi} y = \int_0^y \frac{\sinh t}{t}\,dt$$

A good approximation to Eq. (35) is

$$\frac{dn}{d(\xi p)} \approx (\xi p)^2 \left[\frac{3}{a_+(e^{\xi p} - 1)} + \frac{8}{a_-(e^{\xi p} + 1)}\right] \qquad (\xi p \le 1) \tag{35a}$$

and $$\frac{dn}{d(\xi p)} \approx \frac{4}{\rho^2 f_1(\rho)} e^{-\xi p}\left(\frac{3}{a_+} + \frac{8}{a_-}\right) \left[\frac{\sinh(\xi p\rho)}{\xi p\rho} - \cosh(\xi p\rho) + \xi p\rho \operatorname{Shi}(\xi p\rho)\right] \qquad (\xi p > 1) \tag{35b}$$

Actually, Eq. (35) reduces to Eq. (35a) for all values of p when $\rho = 0$.

Table 5 lists the functions $f_1(\rho)$, $f_2(\rho)$, $f_3(\rho)$, $\frac{3}{2}f_3(\rho)/f_2(\rho)$, and $f_4(\rho)$ as a function of ρ. The same functions result if antinucleons do not exist; only different numerical coefficients would enter Eqs. (31) to (34) (that is, $a_- \equiv 0$, $a'_- \equiv 0$). It is clear that, for an impact parameter $b = 0$, that is, for a perfectly centered collision, $\rho = 0$, the angular dependence in the distribution law (34) disappears, the multiplicity N is a maximum, and the average energy is a minimum (for a given E). For an impact parameter close to the maximum (that is, R), ρ is close to unity, the angular distribution is strongly anisotropic, and the average energy is increased (for the same E). The impact parameter will, of course, vary from collision to collision and will range in value from 0 to R; the median value of the impact parameter is $R/\sqrt{2}$. It is interesting to exhibit graphically the angular distributions and energy spectra associated with four values of the impact parameter. Figures 2 and 3 contain, respectively, the predicted angular distributions and energy spectra for four values of ρ: $\rho = 0, 0.5, 0.9, 0.99$ corresponding, respectively, to $b/R = 0$, 0.160, 0.528, 0.876. It is worth remarking that, for a given impact parameter, Fermi's theory predicts angular distributions and energy spectra independent of the incident nucleon energy [the latter provided (cp) is expressed in units of $(\xi/c)^{-1} = kT'$].

Table 5. The Fermi Functions

ρ	$f_1(\rho)$	$f_2(\rho)$	$f_3(\rho)$	$b/R = \frac{3}{2}f_3/f_2$	$f_4(\rho)$
0	2.000	4.000	0.000	0.000	1.33
0.1	2.680	4.027	0.059	0.022	1.35
0.2	2.711	4.111	0.132	0.048	1.40
0.3	2.767	4.261	0.250	0.088	1.53
0.4	2.857	4.499	0.369	0.123	1.63
0.5	2.986	4.864	0.519	0.160	1.88
0.6	3.173	5.436	0.739	0.204	2.26
0.7	3.454	6.400	1.152	0.270	2.95
0.8	3.913	8.302	2.036	0.368	4.39
0.9	4.842	13.798	4.857	0.528	8.96
0.92	5.173	16.476	6.305	0.574	11.3
0.94	5.619	20.880	8.825	0.634	15.3
0.96	6.283	29.564	13.994	0.710	23.3
0.98	7.484	55.193	29.951	0.814	47.7
0.99	8.8	105.85	61.816	0.876	97.0
1.0	∞	∞	∞	1.000	∞

4. Kinematics of Multiple Meson Production

Before turning to the experimental material, we present a synopsis of the essential kinematical transformation formulas which enable one to relate the experimentally measured quantities in the laboratory system to the theoretically predicted quantities in the center-of-mass system. Since our interest is in nucleon-nucleon collisions which lead to the production of more than one π meson, relativistic nucleon energies will necessarily be involved, and relativistic expressions for all particles (nucleons as well as mesons) must be employed. It is important to keep these transformation formulas clearly in mind since the high incident nucleon energies will always tend to project the mesons into the forward hemisphere in the laboratory system, and discrimination between theories will depend upon subtle distinctions among the observed quantities translated back into the center-of-mass system.

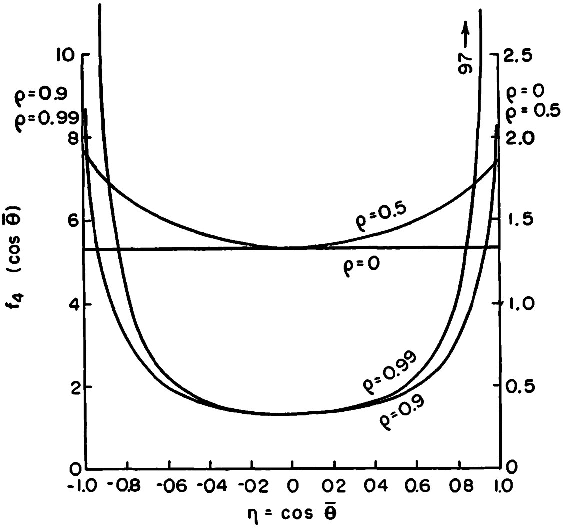

FIG. 2. Angular distributions in Fermi's theory corresponding to four different values of the parameter ρ.

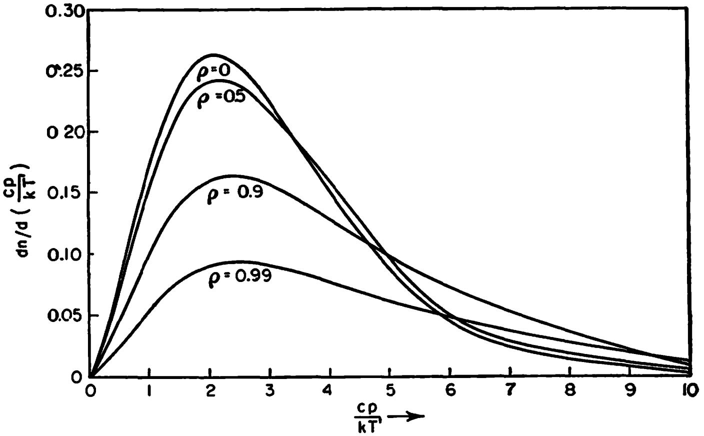

FIG. 3. Energy spectra in Fermi's theory corresponding to four different values of the parameter ρ.

We first catalogue the notation to be used:[15]

L system refers to the laboratory system.

C system refers to the center-of-mass system, *i.e.*, the system in which the total momentum of all the particles (nucleons and mesons) is zero.

---

[15] Cf. Bradt, Kaplon, and Peters, *Helv. Phys. Acta* **23**: 24 (1950).

$\beta = v/c$ is the velocity of the incident nucleon in units of the velocity of light.

$\gamma = (1 - \beta^2)^{-\frac{1}{2}}$ is the energy of the incident nucleon in units of its rest energy.

$p = \sqrt{\gamma^2 - 1}$ is the corresponding momentum.

θ is the polar angle with respect to the direction of the incoming nucleon in the L system.

$\bar{\beta}$, $\bar{\gamma}$, $\bar{p}$, $\bar{\theta}$ are the corresponding quantities in the C system.

Without subscripts, these symbols refer to the incoming nucleon; with zero subscripts, they refer to π mesons of mass μ.

$m = \bar{\beta}/\bar{\beta}_0$ is the ratio of the velocity of the nucleon to the velocity of the meson in the C system.

$\alpha = \bar{\gamma} \tan \theta$ is a convenient parameter characterizing the angular distribution of mesons in the L system.

N is the multiplicity, *i.e.*, the number of mesons produced in the nucleon-nucleon collision.

$K(0 \leq K \leq 1)$ is the fraction of the available energy in the C system converted into mesons and is defined by $2K(\bar{\gamma} - 1) = \sum_{i=1}^{N} \mu \bar{\gamma}_{0i}$.

$N_m = [2K(\bar{\gamma} - 1)]/\mu$ is the largest number of mesons which could be produced if all the mesons were produced at rest in the C system; it is also the maximum energy available in the C system in units of μc^2.

$\Gamma_0 = N_m - N + 1$ is the largest energy in units of the rest mass μc^2 with which a meson can be produced in the C system.

$\theta_{\frac{1}{2}}$ is the half width of the angular distribution of mesons in the L system.

θ_T is the total width of the angular distribution of mesons in the L system.

A_i is a four-vector in the L system which transforms via a Lorentz transformation into a four-vector $\bar{A}_i$ in the C system by means of the formula

$$\bar{A}_i = \sum_j a_{ij} A_j \tag{36}$$

where a_{ij} represents the matrix

$$\begin{vmatrix} \bar{\gamma} & 0 & 0 & i\bar{\beta}\bar{\gamma} \\ 0 & 1 & 0 & 0 \\ 0 & 0 & 1 & 0 \\ -i\bar{\beta}\bar{\gamma} & 0 & 0 & \bar{\gamma} \end{vmatrix} \tag{36a}$$

In Eq. (36*a*), $\bar{\beta}$ is the velocity of the C system in units of c and

$$\bar{\gamma} = 1/\sqrt{1 - \bar{\beta}^2}$$

where it is assumed that the first component of the four-vector is in the direction of the velocity of the C system.

Let γ be the energy of the incoming nucleon in the L system and let γ' be the energy of the incoming and therefore also the target nucleon in the C system, then their momenta will be, respectively, $\sqrt{\gamma'^2 - 1}$ and $-\sqrt{\gamma'^2 - 1}$ in the direction of the incoming nucleon. Transforming the energy-momentum four-vector in accordance with Eqs. (36) and (36*a*) and solving the resulting equations for $\bar\beta$, we find

$$\bar\beta = \frac{\gamma - 1}{\gamma + 1}$$

or

$$\gamma = 2\bar\gamma^2 - 1 \tag{37}$$

also

$$\gamma' = \bar\gamma \tag{38}$$

Thus the energy of the incoming nucleon in the L system is related to the energy in the C system, γ', by Eq. (37) with $\bar\gamma = \gamma'$.

The components of momenta and energy of a meson in the C system may be transformed to the L system of Eqs. (36) and (36*a*) using the energy-momentum four-vector

$$(\mu\sqrt{\bar\gamma_0^2 - 1}\cos\theta,\ \mu\sqrt{\bar\gamma_0^2 - 1}\sin\theta,\ 0,\ \mu\bar\gamma_0)$$

Thus

$$\bar\gamma\tan\bar\theta = \frac{\sin\theta}{\cos\theta - \bar\beta/\beta_0} \tag{39}$$

or

$$\alpha = \frac{\sin\bar\theta}{\cos\bar\theta + m} \tag{40}$$

and

$$\bar\gamma_0 = \gamma_0\bar\gamma - \sqrt{\gamma_0^2 - 1}\sqrt{\bar\gamma^2 - 1}\cos\theta \tag{41}$$

or

$$\gamma_0 = \bar\gamma_0\bar\gamma + \sqrt{\bar\gamma_0^2 - 1}\sqrt{\bar\gamma^2 - 1}\cos\bar\theta \tag{42}$$

From Eq. (40)

$$\cos\bar\theta = -\frac{m\alpha^2 \pm \sqrt{1 - (m^2 - 1)\alpha^2}}{\alpha^2 + 1}$$

Inserting this into Eq. (42)

$$\gamma_0 = \frac{\bar\gamma_0(\bar\gamma^2 + \alpha^2)/\bar\gamma \pm \sqrt{\bar\gamma^2 - 1}\sqrt{\bar\gamma_0^2 - 1}\sqrt{1 - (m^2 - 1)\alpha^2}}{\alpha^2 + 1} \tag{43}$$

The origin of the double-valuedness of γ_0 can be seen by considering the graphical interpretation of Eq. (39) (cf. Figs. 4*a* and 4*b*). Secants to a unit circle are drawn from a point A distant m from the center and making an angle δ with AO. The angle δ is defined by $\tan\delta = \bar\gamma\tan\theta = \alpha$ and θ_i is the angle made by the line joining the intercept of the circle with the secant and the line AO. If $m > 1$ $(\bar\beta_0 < \bar\beta)$, there are two values of $\bar\theta$ corresponding to a given angle θ; in Eq. (43), there are two different energies in the L system corresponding to these two possible angles in the

C system. If $m \leq 1$ $(\bar{\beta}_0 \geq \bar{\beta})$, the plus sign applies if $\theta < \pi/2$ and the minus sign applies if $\theta > \pi/2$ and θ may vary from 0 to π. For $m > 1$, θ is less than $\pi/2$ and the largest value of θ, θ_c, occurs when a tangent to the circle is drawn from A where θ_c is defined by

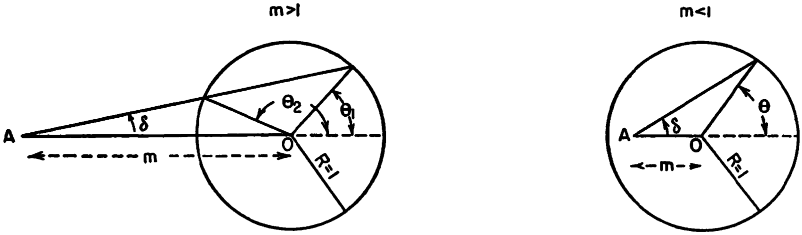

FIG. 4. Relations between the angles in the center-of-mass and the laboratory systems (see text).

$$\sin \delta_c = \frac{1}{m} \tag{44}$$

or

$$\sin \theta_c = \sqrt{\frac{\bar{\gamma}_0^2 - 1}{\bar{\gamma}^2 - 1}}. \tag{45}$$

At a given angle $\theta < \theta_c$,

$$\sqrt{m^2 - 1} < \frac{1}{\alpha} \tag{46}$$

or

$$\bar{\gamma}_0 > \cos \theta \sqrt{\alpha^2 + 1} \tag{47}$$

Hence at an angle $\theta < \theta_c$, the energy of the emitted meson is bounded below.

Now let $F(\bar{\theta}, \bar{\gamma}_0)d\bar{\Omega}\, d\bar{\gamma}_0$ denote the number of mesons emitted in the C system between $\bar{\Omega}$ and $\bar{\Omega} + d\bar{\Omega}$ and between $\bar{\gamma}_0$ and $\bar{\gamma}_0 + d\bar{\gamma}_0$, then the distribution of the mesons in the L system is given by

$$N(\theta, \gamma_0)d(\cos \theta)d\gamma_0 = F[\bar{\theta}(\theta, \gamma_0), \bar{\gamma}_0(\theta, \gamma_0)]Jd(\cos \theta)d\gamma_0$$

where $J = \dfrac{\partial(\cos \bar{\theta}, \bar{\gamma}_0)}{\partial(\cos \theta, \gamma_0)} = \dfrac{\sin \bar{\theta}}{\sin \theta}$. For many purposes, the quantity of interest is the angular distribution of the mesons in the L system, $N(\theta)d(\cos \theta)$, independent of their energy. $N(\theta)d(\cos \theta)$ can most simply be obtained from the relation

$$N(\theta)d(\cos \theta) = 2\pi \int d\bar{\gamma}_0 F[\bar{\theta}(\theta, \bar{\gamma}_0), \bar{\gamma}_0]Jd(\cos \theta) \tag{48}$$

where $J = \left.\dfrac{\partial \cos \bar{\theta}}{\partial \cos \theta}\right|_{\bar{\gamma}_0}$. If $m \leq 1$, F and J are single-valued and the lower limit of $\bar{\gamma}_0$ is $\bar{\gamma}$ and the upper limit $\bar{\Gamma}_0$, the highest energy with which mesons can be produced in the C system. If $m > 1$, F and J are doublevalued, the lower limit of $\bar{\gamma}_0$ is $(\cos\theta\sqrt{\alpha^2+1})$ and the upper limit is $\bar{\gamma}$. Evaluating $J = \left.\dfrac{\partial \cos\bar{\theta}}{\partial\cos\theta}\right|_{\bar{\gamma}_0}$ gives

$$J = \frac{\bar{\gamma}^2[m \pm \sqrt{1-(m^2-1)\alpha^2}]^2}{\cos^3\theta\,(\alpha^2+1)^2\sqrt{1-(m^2-1)\alpha^2}} \tag{49}$$

The (±) signs in Eq. (49) apply as in Eq. (43).

We shall now apply the above transformation formula (48) to find the angular distribution of mesons in the L system corresponding to several assumed distributions in the C system, roughly approximating the distributions predicted by the three theories discussed in Sec. 3.

Case I. Let the mesons be distributed isotropically with a common energy in the C system; this is the simplest distribution to consider and could be taken as a representation of the theory of Lewis *et al.*[15] We write

$$F(\bar{\theta},\bar{\gamma}_0)d\bar{\Omega}\,d\bar{\gamma}_0 = \frac{N}{4\pi}\,\delta(\bar{\gamma}_0-\bar{\gamma}_0')d\bar{\Omega}\,d\bar{\gamma}_0 \tag{50}$$

where $N = \int F(\bar{\theta},\bar{\gamma}_0)d\bar{\Omega}\,d\bar{\gamma}_0$
For $m > 1$, $N(\theta)$ is the sum of two terms corresponding to the two possible energy values of Eq. (43), namely,

$$N(\theta) = \frac{N\bar{\gamma}\alpha}{\cos^2\theta\,(\alpha^2+1)^2}\,\frac{m^2+1-(m^2-1)\alpha^2}{\sqrt{1-(m^2-1)\alpha^2}} \tag{51}$$

For $m \leq 1$, $N(\theta)$ is single-valued, namely,

$$N(\theta) = \frac{N\bar{\gamma}\alpha[m+\sqrt{1-(m^2-1)\alpha^2}]^2}{2\cos^2\theta\,(\alpha^2+1)^2\sqrt{1-(m^2-1)\alpha^2}} \tag{52}$$

The distribution of $[\cos^2\theta\,N(\theta)]$ vs. $\alpha = \bar{\gamma}\tan\theta$ for several values of $m > 1$ is shown in Fig. 5. For large $\bar{\gamma}$, a cone of angular width $\theta_T = 3/\bar{\gamma}$ contains all the mesons if $m \geq \sqrt{10}/3$; if $1 < m < \sqrt{10}/3$, the point A in Fig. 4*a* lies slightly outside the unit circle. If mesons are projected outside the cone defined by $\alpha = 3$, which from Fig. 4*a* corresponds in the C system to $\bar{\theta} = 2\delta$, then $\cos\bar{\theta} < -0.8$. The fraction of the total number of mesons outside the cone $\alpha = 3$ is therefore

$$\frac{\int_{-1}^{-0.8} d(\cos\theta)}{\int_{-1}^{1} d(\cos\theta)} = \frac{1}{10}$$

so that at least 90 per cent of all mesons are within $\theta < 3/\bar{\gamma}$, whatever the energy with which the mesons are produced in the L system. If $\bar{\gamma}_0$

is also large so that m is close to unity, then for not too large α,

$$N(\theta) = \frac{N\bar{\gamma}m\alpha}{2\cos^2\theta\,(\alpha^2+1)^2} \tag{53}$$

and $N(\theta)$ reaches a maximum value at $\theta_m = 0.58/\bar{\gamma}$ and drops to one-half its maximum value at $\theta_{\frac{1}{2}} = 1.34/\bar{\gamma}$.

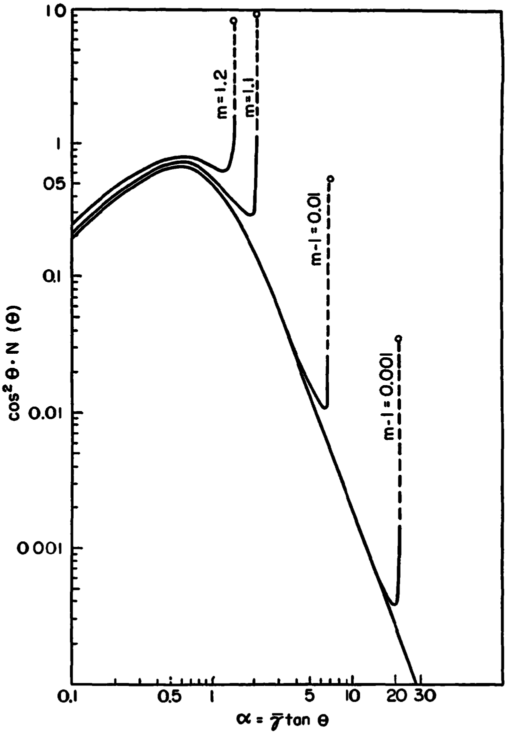

FIG. 5. Laboratory angular distribution functions corresponding to an isotropic and uniform energy distribution of mesons in the center-of-mass system for several values of $m > 1$ (see text).

Consequently, the energy of the incident nucleon can be derived directly from the maximum or half width of the meson distribution provided that both the incident nucleon and the meson in the C system possess relativistic velocities and the mesons have an isotropic angular distribution. Under these assumptions, the total width of the showers can never be more than about twice the half width of the peak in the forward direction, namely,

$$\theta_T \leq 2.2\theta_{\frac{1}{2}}$$

The multiplicity of meson production is related to the degree of inelasticity K by

$$N \approx 9.2 \frac{K\gamma^{\frac{1}{4}}}{\bar{\gamma}_0'} \tag{54}$$

where we have substituted $\sqrt{\gamma/2}$ for $\bar{\gamma}$ and 6.65 for M/μ (the ratio of the nucleon to the π meson mass).

Case II. Case I was a particularly simple illustration since it was assumed that the mesons are produced in the C system both isotropically and with constant energy. If the isotropic distribution is still maintained, but it is assumed that the mesons are created in the C system with a smoothly varying and not too extreme energy spectrum, the angular distribution in the L system turns out to be not very different from what it was in Case I. As an illustration of a smoothly varying energy spectrum, the following form is chosen:

$$F(\bar{\theta}, \bar{\gamma}_0)\,d\bar{\Omega}\,d\bar{\gamma}_0 = \frac{A}{4\pi} \frac{\sqrt{\bar{\gamma}_0^2 - 1}}{\bar{\gamma}_0^3}\,d\bar{\Omega}\,d\bar{\gamma}_0 \tag{55}$$

which is proportional to the volume of momentum space at low energy and falls off as the inverse square of the energy at high energies. This spectrum can serve as an illustration of the Heisenberg theory. The angular distribution in the L system now becomes

$$N(\theta) = \frac{A}{2} \int_{\bar{\gamma}}^{\bar{\Gamma}_0} d\bar{\gamma}_0 \frac{\sqrt{\bar{\gamma}_0^2 - 1}}{\bar{\gamma}_0^3} \frac{\bar{\gamma}^2 \sin\theta[m + \sqrt{1 - (m^2 - 1)\alpha^2}]^2}{\cos^2\theta\,(\alpha^2 + 1)^2 \sqrt{1 - (m^2 - 1)\alpha^2}} \tag{56}$$

where the constant A is determined by the normalization

$$A \int_1^{\bar{\Gamma}_0} d\bar{\gamma}_0 \frac{\sqrt{\bar{\gamma}_0^2 - 1}}{\bar{\gamma}_0^3} = N \tag{57}$$

A is now a function of $\bar{\Gamma}_0$, the largest energy (in units of μc^2) with which a meson can be produced in the C system; in order to evaluate $\bar{\Gamma}_0$, we use the expression for the available energy converted into mesons in the C system, namely,

$$A \int_1^{\bar{\Gamma}_0} \frac{d\bar{\gamma}_0 \sqrt{\bar{\gamma}_0^2 - 1}}{\bar{\gamma}_0^2} = N_m \tag{58}$$

Solving Eq. (58) for $\bar{\Gamma}_0$, one finds

$$N = \frac{N_m}{2} \left(\frac{\tan^{-1}\sqrt{\bar{\Gamma}_0^2 - 1} - \sqrt{\bar{\Gamma}_0^2 - 1}/\bar{\Gamma}_0^2}{\cosh^{-1}\bar{\Gamma}_0 - \sqrt{\bar{\Gamma}_0^2 - 1}/\bar{\Gamma}_0} \right) \tag{59}$$

which for large values of $\bar{\Gamma}_0$ reduces to

$$\bar{\Gamma}_0 = N_m \left\{ 1 - \frac{\pi}{4[1 - \ln 2\bar{\Gamma}_0]} \right\} \tag{60}$$

Hence A is determined. It is interesting to plot the relation between the multiplicity N and the energy of the incident nucleon γ as determined by Eq. (59); this is done in Fig. 6a where N is actually plotted as a function of γK^2. In the same figure are shown two curves for Case I assuming unique meson energies in the C system, namely, $\bar{\gamma}_0' = 10$ and $\bar{\gamma}_0' = 100$ (corresponding to Figs. 6b and 6c, respectively).

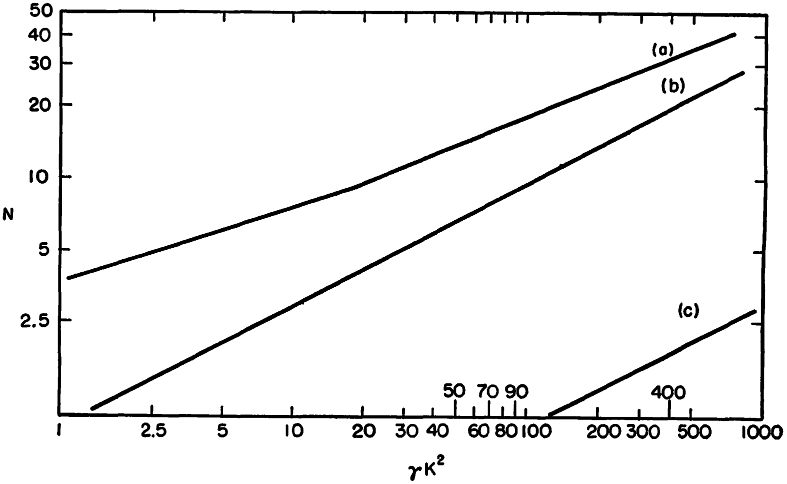

FIG. 6. Multiplicity as a function of γK^2 (defined in text) corresponding to an isotropic angular distribution and nonuniform and uniform meson energy distributions in the center-of-mass system. Curve (a) corresponds to Case II of text, (b) to Case I $\bar{\gamma}_0' = 10$, (c) to Case I, $\bar{\gamma}_0' = 100$.

We now proceed to evaluate $N(\theta)$; using the proper Jacobian in Eq. (56), $N(\theta)$ becomes:

$$N(\theta) = \frac{A\bar{\gamma}\alpha}{\cos^3\theta\,(\alpha^2+1)^2}\left[\int_a^{\bar{\gamma}}\left(\bar{\beta}^2\cos^2\theta + 1 - \frac{a^2}{\bar{\gamma}_0^2}\right)\frac{d\bar{\gamma}_0}{\bar{\gamma}_0\sqrt{\bar{\gamma}_0^2 - a^2}} \right.$$
$$\left. + \int_{\bar{\gamma}}^{\bar{\Gamma}_0}\frac{\bar{\beta}\cos\theta}{\bar{\gamma}_0^2}\,d\bar{\gamma}_0 + \frac{1}{2}\int_{\bar{\gamma}_-}^{\bar{\Gamma}_0}\left(\bar{\beta}^2\cos^2\theta + 1 - \frac{a^2}{\bar{\gamma}_0^2}\right)\frac{d\bar{\gamma}_0}{\bar{\gamma}_0\sqrt{\bar{\gamma}_0^2 - a^2}}\right] \tag{61}$$

where $a = \cos\theta\sqrt{\alpha^2+1}$. Equation (61) evaluates into

$$N(\theta) = \frac{A\bar{\gamma}\alpha(2\bar{\beta}^2\cos^2\theta + 1)}{4\cos^4\theta(\alpha^2+1)^{\frac{5}{2}}}\left[\cos^{-1}\left(\frac{a}{\bar{\gamma}}\right) + \cos^{-1}\left(\frac{a}{\bar{\Gamma}_0}\right)\right]$$
$$+\frac{A\bar{\gamma}\alpha}{2\cos^3\theta\,(\alpha^2+1)^2}\left[\frac{2(\bar{\Gamma}_0 - \bar{\gamma})}{\bar{\Gamma}_0\bar{\gamma}}\,\bar{\beta}\cos\theta - \frac{\sqrt{\bar{\Gamma}_0^2 - a^2}}{\bar{\Gamma}_0^2} - \frac{\sqrt{\bar{\gamma}^2 - a^2}}{\bar{\gamma}^2}\right] \tag{62}$$

The second term in Eq. (62) may be neglected for high energies since it is less than the first term by a factor $1/\bar{\gamma}$ or $1/\bar{\Gamma}_0$. We may also replace

$\cos^{-1}(a/\bar{\gamma})$ and $\cos^{-1}(a/\bar{\Gamma}_0)$ by $\pi/2$ if we confine ourselves to values of $\alpha < 3$, which, as shown earlier, account for at least 90 per cent of all mesons. Then the angular distribution for high energies reduces to

$$N(\theta) = \frac{\pi A \bar{\gamma} \alpha (2 \cos^2 \theta + 1)}{4 \cos^4 \theta \, (\alpha^2 + 1)^{\frac{5}{2}}} \tag{63}$$

which has a maximum value at $\theta_m = 0.5/\bar{\gamma}$ and drops to half maximum at $\theta_{\frac{1}{2}} = 1.1/\bar{\gamma}$.

Thus Cases I and II lead to similar angular distributions in the L system. In either case, the primary energy can be determined from the observed half angle of the meson distribution in the L system.

Case III. Thus far, we have given two examples of isotropic emission in the C system. As the last case, we treat an illustration of anisotropic emission which reproduces some of the essential features of Fermi's theory. We assume that the mesons are emitted with a common energy $\bar{\gamma}_0'$ in the C system and with an angular distribution varying as $\cos^{2n} \bar{\theta}$; hence we write

$$F(\bar{\theta}, \bar{\gamma}_0)\, d\bar{\Omega}\, d\bar{\gamma}_0 = \frac{(2n+1)N}{4\pi} \cos^{2n} \bar{\theta}\, \delta(\bar{\gamma}_0 - \bar{\gamma}_0')\, d\bar{\Omega}\, d\bar{\gamma}_0 \tag{64}$$

where N is a constant. $N(\theta)$ again takes on two different forms, depending on whether $m \leq 1$ or $m > 1$. For $m > 1$, we find

$$\begin{aligned} N(\theta) = {} & \frac{(2n+1) N \bar{\gamma} \alpha}{2 \cos^2 \theta \, (\alpha^2 + 1)^{2n+2}} \\ & \left\{ \frac{[m + \sqrt{1 - (m^2 - 1)\alpha^2}]^2 [-m\alpha^2 + \sqrt{1 - (m^2 - 1)\alpha^2}]^{2n}}{\sqrt{1 - (m^2 - 1)\alpha^2}} \right. \\ & \left. + \frac{[m - \sqrt{1 - (m^2 - 1)\alpha^2}]^2 [-m\alpha^2 - \sqrt{1 - (m^2 - 1)\alpha^2}]^{2n}}{\sqrt{1 - (m^2 - 1)\alpha^2}} \right\} \end{aligned} \tag{65}$$

for $m \leq 1$, we get

$$\begin{aligned} N(\theta) = {} & \frac{(2n+1) N \bar{\gamma} \alpha}{2 \cos^2 \theta \, (\alpha^2 + 1)^{2n+2}} \\ & \left\{ \frac{[m + \sqrt{1 - (m^2 - 1)\alpha^2}]^2 [-m\alpha^2 + \sqrt{1 - (m^2 - 1)\alpha^2}]^{2n}}{\sqrt{1 - (m^2 - 1)\alpha^2}} \right\} \end{aligned} \tag{66}$$

If $m \approx 1$, Eqs. (65) and (66) both reduce to

$$N(\theta) \approx \frac{2(2n+1) N \bar{\gamma} \alpha (\alpha^2 - 1)^{2n}}{\cos^2 \theta \, (\alpha^2 + 1)^{2n+2}} \tag{67}$$

which reaches a maximum value for α satisfying the equation

$$\alpha_m^2 = \frac{2(2n+1) \pm \sqrt{4(2n+1)^2 - 3}}{3} \tag{68}$$

Equation (68) shows that there are two peaks—the first peak occurring for $n > 1$ at $\alpha_m^- = 0.5/\sqrt{2n+1}$ or

$$\theta_m^- = \frac{0.5}{\bar{\gamma}\sqrt{2n+1}} \tag{69}$$

and the second peak occurring at $\alpha_m^+ = \dfrac{2\sqrt{2n+1}}{\sqrt{3}}$ or

$$\theta_m^+ = \frac{2\sqrt{2n+1}}{\sqrt{3}\,\bar{\gamma}} \tag{70}$$

The existence of two peaks in the L system is characteristic of an anisotropic meson distribution in the C system which is symmetric about $\bar{\theta} = 90°$. This is seen more clearly in Fig. 7, where $\cos^2 \theta N(\theta)$ is plotted as a function of $\alpha = \bar{\gamma} \tan \theta$ for $m = 1.01$ and $n = 0, 1, 2$. Compared with the isotropic case, a $\cos^{2n} \bar{\theta}$ angular distribution in the C system yields a forward peak in the L system which is appreciably narrower; this means that, for an observed half width $\theta_{\frac{1}{2}}$ of the narrow core of a shower, the value of $\bar{\gamma}$ which will be deduced (and therefore of γ, the incident nucleon energy) will be smaller the larger the exponent n. To compensate for the narrower forward peak, there now exists a second peak (cf. Fig. 7) which, as we shall see below, may be identified with the diffuse core of extremely energetic showers.

It is also interesting to note that there is a limit to the degree of anisotropy which can be postulated for a meson shower of known multiplicity and average energy in the L system. Thus it follows from Eq. (42) that

$$\langle\gamma_0\rangle = \bar{\gamma}\langle\bar{\gamma}_0\rangle$$

The multiplicity is given by

$$N = \frac{2K(\bar{\gamma} - 1)}{\mu\langle\gamma_0\rangle} \approx \frac{3K}{\langle\gamma_0\rangle(2n+1)(\theta_m^-)^2} \tag{71}$$

The quantity $\bar{\gamma}$ has been eliminated in the last equation by means of Eq. (69). Hence, if θ_m^- of the narrow core of the shower as well as $\langle\gamma_0\rangle$ and N are known, an increase in the assumed anisotropy (*i.e.*, larger n) requires an increasing degree of inelasticity K. But since K must be less than or equal to unity, n must be bounded, and this is the conclusion we seek.

Recently, Kaplon and Ritson[16] have computed the angles in the laboratory system containing specified fractions of the total number of mesons produced. If the angular distribution in the C system has the form

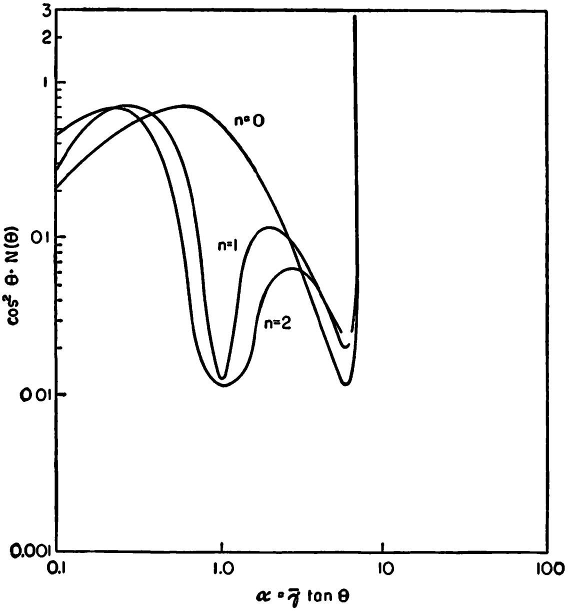

FIG. 7. Laboratory angular distribution functions corresponding to an anisotropic and uniform energy distribution of mesons in the center-of-mass system for $m = 1.01$ and several values of n (see text).

$\cos^{2n} \bar{\theta}$, and f denotes the fraction of mesons produced, then one can write (assuming that m is close to unity)

$$\alpha_f = \frac{C_f(n)}{\sqrt{2n+1}}, \qquad \alpha_{2f} = C_{2f}(n)\sqrt{2n+1} \tag{72}$$

where the C's depend only on n and f; the case $n = 0$ has to be treated separately. Several characteristic values of $C_f(n)$ and $C_{2f}(n)$ are given in Table 6. Kaplon and Ritson[16] have also shown that the assumptions of $m \approx 1$ and symmetric production of mesons about the 90° plane in the center-of-mass system lead to a simple relation between any arbitrary angle θ_f and θ_{1-f} in the laboratory system, namely,

$$\theta_f \theta_{1-f} = \frac{1}{\bar{\gamma}^2} \tag{72a}$$

---

[16] M. Kaplon and D. Ritson, private communication.

Equation (72a) follows immediately from Eq. (40) (assuming $m = 1$) and provides a simple method for estimating $\bar{\gamma}$, and therefore γ, independent of n.

TABLE 6. ANGLES OF NARROW AND DIFFUSE SHOWERS

f	$C_f(n)$	$C_{2f}(n)$	$C_f\ (n = 0)$
0.40	0.895	1.96	0.817
0.425	0.969	2.37	0.857
0.45	1.07	2.98	0.905
0.475	1.215	4.3	0.95

5. Experimental Evidence for Plural Production of π Mesons

Before it is possible to establish whether the experimental data on penetrating showers can be explained by a plural theory of meson production, it is necessary to know the cross section for single meson production in nucleon-nucleon collisions as a function of energy. The highest laboratory energy at which this cross section has been measured has been 381 Mev (protons); at this energy, the cross section for π^+ production is about 7×10^{-28} cm^2 for proton collisions in hydrogen.[17] This cross section is almost 100 times smaller than geometrical, and although there is every indication that the meson production cross section increases rapidly with energy, it is desirable to have a direct determination of this cross section. Unfortunately, the cosmic-ray evidence at higher energies is not so accurate as one would like, but it does appear that the cross section for meson production in nucleon-nucleon collisions is close to geometrical at sufficiently high nucleon energies, say greater than 5 Bev.

Evidence for an approximately geometrical cross section for the production of penetrating showers comes from several sources. There was first the pioneer counter experiment of Schein *et al.*[18] where coincidences due to the production of penetrating showers in paraffin were observed and it was concluded that the production cross section in carbon is close to geometrical. More recently, Cocconi and Greisen[19] made a counter study of the dependence of the number of penetrating showers initiated by primary nucleons on the atomic number of the absorbing material and found that the number of penetrating showers was 1.58 ± 0.07 times greater from a carbon absorber than from a lead absorber for the same thickness in g/cm^2. This result shows that the cross section for shower production per nucleus increases less strongly than with A and more like $A^{\frac{2}{3}}$, the geometrical area. Similar experiments have been carried out by other authors[20]: Cocconi found an interaction mean free path λ_I for the production of penetrating showers of 160 g/cm² in Pb (geometrical is 156) and 100 g/cm² in C (geometrical is 60). Walker found the decrease in the interaction mean free path with increasing shower size shown in Table 7. Sitte found λ_I (Pb) $= 196 \pm 13$ g/cm² for secondaries which penetrate 100 g/cm² of lead absorber and λ_I (Pb) $= 162 \pm 10$ g/cm² for secondaries which penetrate 200 g/cm² of lead absorber. Finally, Walker *et al.* have measured the mean free paths for the production of penetrating showers containing at least three particles; results were obtained for charged and neutral primaries in both Pb and C as follows:[20a]

---

[17] Passman, Block, and Havens, *Phys. Rev.*, **83**: 167 (1951).

[18] Schein, Iona, and Tabin, *Phys. Rev.*, **64**: 253 (1943).

[19] G. Cocconi and K. Greisen, *Phys. Rev.*, **74**: 62 (1948).

TABLE 7. INTERACTION M.F.P. AS FUNCTION OF SHOWER SIZE IN PB

Number of shower particles.......	3	4, 5	>5	>7
λ_I (Pb), g/cm²..................	208	180 ± 10	150 ± 8	140 ± 10

$$\begin{aligned}
\lambda_I \text{ (Pb) (charged primaries)} &= 157 \pm 12 \text{ g/cm}^2 \\
\lambda_I \text{ (Pb) (neutral primaries)} &= 164 \pm 15 \text{ g/cm}^2 \\
\lambda_I \text{ (C) (charged primaries)} &= 82 \pm 8 \text{ g/cm}^2 \\
\lambda_I \text{ (C) (neutral primaries)} &= 80 \pm 7 \text{ g/cm}^2
\end{aligned}$$

From all these experiments, we can conclude that: (1) charged and neutral primaries (*i.e.*, protons and neutrons) have very similar cross sections for the production of penetrating showers; (2) the production cross section is closer to geometrical for Pb than it is for C for the same size of penetrating shower; and (3) the cross section increases and approaches its geometrical value for the more energetic penetrating showers; this is true for Pb, but presumably it will also be true for C at somewhat higher primary energies.

The approximately geometrical cross sections for the production of penetrating showers observed in cosmic-ray experiments lead to the expectation that some sort of nucleonic cascade process will take place in the earth's atmosphere and give rise to an attenuation mean free path λ_A (defined as the thickness of absorber in g/cm² which reduces the

---

[20] G. Cocconi, *Phys. Rev.*, **76**: 984 (1949); W. D. Walker, *Phys. Rev.*, **77**: 686 (1950); K. Sitte, *Phys. Rev.*, **78**: 714 (1950); Walker, Walker, and Greisen, *Phys. Rev.*, **80**: 546 (1950).

[20a] Recently, H. Boehmer and H. Bridge [*Phys. Rev.*, **85**: 863 (1952)] found for neutral primaries and events of the highest multiciplicity (in their setup),

$$\lambda_I(\text{Pb}) = 143 \pm 30 \text{ g/cm}^2 \text{ and } \lambda_I(\text{C}) = 85 \pm 12 \text{ g/cm}^2.$$

intensity by a factor of $1/e$) which is larger than the interaction mean free path discussed above. This is borne out by experiment. Thus Tinlot,[21] using a coincidence counter arrangement, measured the rate of increase of local penetrating showers with height up to 9000 m and found an exponential variation corresponding to an attenuation mean free path in air of 118 ± 2 g/cm². A similar result can be deduced from the photographic experiments of Brown *et al.*[22] and Camerini *et al.*[23] These authors measured the numbers of nuclear stars of various types at 11,000 and 70,000 ft, respectively; from the ratio of these numbers, attenuation mean free paths for the nucleonic component of the cosmic radiation can be inferred for various star sizes. Because the angular distribution of the primaries becomes much more isotropic at high altitudes, it is necessary to use the Gross transformation in order to infer λ_A from the observed variation with altitude. The Gross transformation is

$$I = I_0\left(e^{-x/\lambda_A} - \frac{x}{\lambda_A}\int_{x/\lambda_A}^{\infty} \frac{e^{-y}}{y}\,dy\right)$$

in contrast to the exponential variation $I = I_0 e^{-x/\lambda_A}$ with the distance x. The attenuation mean free paths obtained in this manner are listed in Table 8 for all stars ($N_s \geq 0$), stars with at least 3 shower particles ($N_s \geq 3$), and finally stars with at least 6 shower particles ($N_s \geq 6$); for comparison, the attenuation mean free paths derived on the basis of an assumed exponential variation with altitude are also listed. The Gross values are more reliable and the value of λ_A for the largest stars agrees well with Tinlot's value of 118 g/cm². It is interesting to note the decrease in the attenuation mean free path in air as the collisions become more energetic and the fact that the attenuation mean free path even at the highest energies is still greater than the interaction mean free path. Both features of the observations are easily understood in terms

TABLE 8. ATTENUATION M.F.P. AS FUNCTION OF STAR SIZE

Star type	λ_A (Gross value), g/cm²	λ_A (exponential value), g/cm²
$N_s \geq 0$	170	130
$N_s \geq 3$	135	105
$N_s \geq 6$	120	95

---

[21] J. H. Tinlot, *Phys. Rev.*, **73**: 1476 (1948); **74**: 1197 (1948).

[22] Brown, Camerini, Fowler, Heitler, King, and Powell, *Phil. Mag.*, **40**: 862 (1949).

[23] Camerini, Coor, Davies, Fowler, Lock, Muirhead, and Tobin, *Phil. Mag.*, **40**: 1073 (1949).

of the approximately geometrical value for the interaction cross section and the degradation in energy of the N component (nucleons and π mesons) during the course of several successive collisions with air nuclei between 10,000 and 70,000 ft.

It is clear that, if several collisions can take place in different air nuclei over distances of several mean free paths, then occasionally plural collisions should take place in the same air nucleus. This is obvious if one computes the interaction mean free path in nuclear matter corresponding to a geometrical cross section; λ_1 is 1.5×10^{-13} cm when one takes the radius of a nucleus to be $r_0 A^{\frac{1}{3}}$ ($r_0 \approx 1.5 \times 10^{-13}$ cm, A is the atomic weight). We can therefore anticipate that plural collisions will play some role in the generation of penetrating showers, particularly in the heavy nuclei. It is the purpose of the remainder of this section to spell out the precise extent to which an exclusively plural production mechanism can account for the observed properties of penetrating showers, such as multiplicity and angular distribution.

The evidence in favor of the plural production mechanism has been supplied chiefly by experiments with cloud chambers and photographic plates. Many cloud-chamber experiments have been performed to investigate the properties of penetrating showers by suitable triggering of the cloud chamber with Geiger-Müller counters arranged above and below the chamber; a sufficient amount of absorber is interposed between the cloud chamber and the lower set of counters to ensure that the penetrating shower contains one or more penetrating particles. One of the cloud-chamber experiments, carried out by Fretter[24] at 10,000 ft, which bears on the present problem was partly discussed in Chap. 3 in connection with the cosmic-ray evidence for the production of π^0 mesons in nucleon-nuclei collisions. The interesting result for our present purposes is Fretter's numbers on the frequency of different multiplicities of penetrating particles (a penetrating particle is defined as a lightly ionizing track—less than three times minimum ionization—which penetrates at least one ½-in. lead plate without producing secondaries) present in penetrating showers emerging from lead plates. A carbon experiment was carried out with the same apparatus by Green[25] at 12,000 ft; the comparison between Fretter's and Green's results is shown in Table 9*a*.

TABLE 9*a*. SIZE-FREQUENCY DISTRIBUTION OF PENETRATING SHOWERS IN C AND PB[24,25]

Number of penetrating particles N_s	2	3	4	5	6	7	8	9	≥10
C	200	138	47	34	13	15	2	2	2
Pb	45	63	33	15	10	6	4	2	1

[24] W. B. Fretter, *Phys. Rev.*, **76**: 511 (1949).

[25] J. R. Green, *Phys. Rev.*, **80**: 832 (1950).

A similar cloud-chamber experiment was performed by Lovati *et al.*[26] with the results shown in Table 9*b*. Although the statistics are not very good in either experiment and appreciable corrections must be made for the different detection efficiencies of the carbon and lead experiments (see footnote 26), the trend, on the whole, seems to be toward greater average multiplicity of the penetrating showers produced in lead as compared with those produced in carbon. A similar conclusion follows from a recent cloud-chamber experiment by Gregory and Tinlot,[27] who find evidence that high-energy neutrons produce, on the average, penetrating showers of greater multiplicity in lead than in aluminum. All these experiments favor the operation of a plural production mechanism since a pure multiple production mechanism should lead to the same average multiplicity in both light and heavy nuclei. Of course, the cloud-chamber experiments do not rule out the possibility of a pluro-multiple production mechanism in the generation of penetrating showers.

TABLE 9*b*. SIZE-FREQUENCY DISTRIBUTION OF PENETRATING SHOWERS IN C AND Pb[26]

N_s	2	3	4	5	6	7	8	9	≥10
C	8	6	9	3	4	2	1	0	0
Pb	20	15	16	12	9	0	1	0	5

Much stronger support for the occurrence of plural processes in the generation of penetrating showers comes from recent photographic experiments. One of these experiments, carried out by Feld *et al.*,[28] consisted in the exposure of electron-sensitive plates to the cosmic radiation at 90,000 ft at three latitudes—31° (Cuba), 48° (Pennsylvania), and 57° (Minnesota). The emulsions were surveyed for nuclear stars containing at least four minimum ionization tracks (a minimum track is defined as one with grain density corresponding to a singly charged particle of kinetic energy greater than its rest mass). The results of the MIT group for 17 stars are shown in Table 10. The 17 stars divide naturally into two groups (for reasons given below): 6 which can be attributed to disintegrations of the light nuclei contained in the emulsion (CNO) and 11 to the heavy nuclei (Br, Ag). Column 1 of Table 10 indicates this separation, column 2 contains the number of minimum tracks observed in each star, and column 3 the average angular spread of the shower particles with respect to the shower axis taken as the center of gravity of the minimum tracks. Column 4 contains the number of near-minimum tracks (a near-minimum track is defined as one with a grain density from minimum to 5 times minimum), and column 5 their average angular spread. Column 6 contains the number of heavy tracks in each star (a heavy track is defined as one whose grain density is greater than 5 times minimum), and column 7 the minimum charge in the heavy tracks. By making simultaneous measurements of the multiple Coulomb scattering and grain density on a number of long near-minimum tracks, Feld *et al.* have shown that most near-minimum tracks are due to high-energy protons. The heavy tracks are presumably due to low-energy protons, α particles, and nuclear fragments, and a clear separation into two groups of values for $Z_{\min}$ justifies the earlier statement that the first 6 stars are produced in light nuclei and the last 11 in the heavy nuclei of the emulsion. Column 8 of Table 10 contains values of $Z_{\min}$ including the near-minimum tracks, and column 9 the total minimum observable charge, *i.e.*, including the minimum tracks. Since the values of $Z_{\min}$ in column 8 already equal or exceed the charges of the light nuclei, column 9 implies that most of the minimum tracks are due to mesons. Finally, column 10 indicates the character of the particle producing the nuclear event and

---

[26] Lovati, Mura, Salvini, and Tagliaferri, private communication from Dr. Salvini.

[27] B. Gregory and J. Tinlot, *Phys. Rev.*, **81**: 667 (1951). Cf. also Walker, Duller, and Sorrels, *Phys. Rev.*, **86**: 865 (1952).

[28] Feld, Lebow, and Osborne, *Phys. Rev.*, **77**: 731 (1950) and L. S. Osborne, *Phys. Rev.*, **81**: 239 (1951). Cf. S. Biswas and V. Hopper, *Phys. Rev.*, **86**: 209 (1952).

TABLE 10. SUMMARY OF DATA ON SHOWERS IN PHOTOGRAPHIC PLATES

Star	Minimum tracks		Near-minimum tracks		Heavy tracks		$Z_{\min}$ including near-minimum tracks	Total observable charge	Incoming minimum track?	$(\pi - \theta)$ for incoming track
	Number	θ_{av}	Number	θ_{av}	Number	$Z_{\min}$				
L1	6	34°	2	30°	4	4	6	12	Yes	10°
L2	7	35	3	85	4	4	7	14	Yes	10
L3	9	17.5	5	43	2	2	9	18	?	
L4	10	16.5	4	68	3	3	7	17	No	
L5	10	20	5	31	5	5	9	19	No	
L6	13	17	5	7	4	4	9	22	No	
H1	5	45	9	65	14	27	36	41	Yes?	65?
H2	5	40	10	54	18	26	36	41	Yes	15
H3	9	44	6	72	20	28	34	43	Yes	20
H4	10	43	8	74	17	24	32	42	No	
H5	11	35.5	1	(137)	11	15	16	27	Yes	20
H6	12	32	6	38	15	18	24	36	Yes	18
H7	12	22	6	59	11	17	23	35	α particle	9
H8	13	37	8	87	17	19	27	40	No	
H9	14	9	5	50	22	43	48	62	?	
H10	15	32	4	55	11	22	26	41	Yes	19
H11	20	25.5	19	65	15	19	38	58	Yes	10

column 11 the angle between the backward projection of the shower axis (for definition see above) and the direction of the charged particle producing the star; it is seen that in no case does this angle definitely exceed 20°.

Two aspects of Table 10 lend support to the plural production hypothesis: (1) The average multiplicity of minimum tracks is greater for heavy than for light nuclei, being 12.6 for the former and 9.1 for the latter; this effect is more definite than in the cloud-chamber experiments. (2) The large number of near-minimum tracks (presumed to be chiefly protons) with forward collimation indicates the occurrence of more than one nucleon-nucleon collision inside the nucleus, even in the light nuclei. However, an even stronger argument for the operation of plural processes comes from the measured angular distributions of the minimum and near-minimum tracks from light and heavy nuclei shown in Fig. 8. The

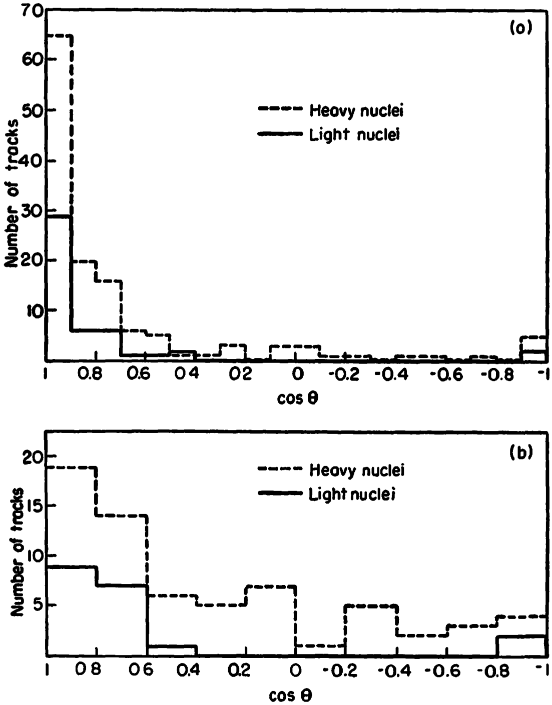

Fig. 8. Measured angular distribution with respect to their shower axes (at 90,000 ft) of (*a*) all minimum tracks (kinetic energy > rest mass) and (*b*) all near-minimum tracks (kinetic energy between 0.08 and 0.6 times the rest mass) from the light and heavy nuclei of the photographic emulsion (Feld *et al.*).

angular distributions from the heavy nuclei are significantly broader for both minimum and near-minimum tracks and indicate a greater angular spread, for the same multiplicity of meson production, compared with the light nuclei. A plural production mechanism can readily account for these observations.

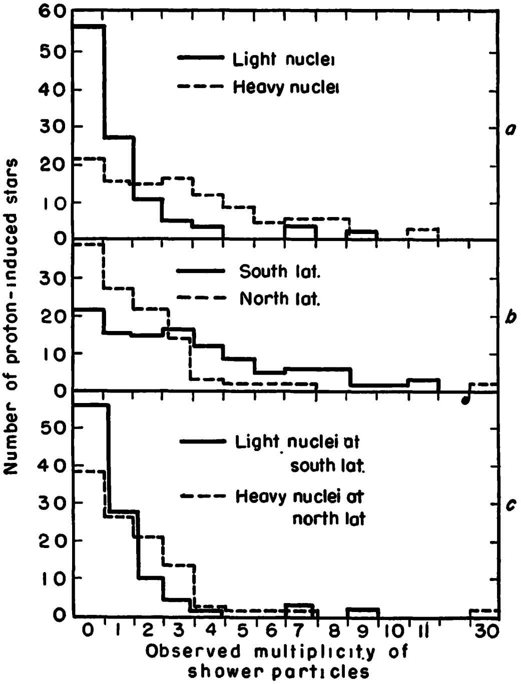

FIG. 9. Histograms of the observed multiplicities associated with proton-induced stars in photographic emulsions exposed at 90,000 ft (Salant *et al.*). *a* represents the histograms of frequency vs. multiplicity from the light and heavy nuclei at the southern latitude, *b* the histograms of frequency vs. multiplicity from the heavy nuclei at the northern and southern latitudes, *c* the histograms of frequency vs. multiplicity from the heavy nuclei at the northern latitude and from the light nuclei at the southern latitude.

Another photographic experiment lending support to the plural production mechanism was carried out by Salant *et al.*[29] Electron-sensitive plates were again exposed at 90,000 ft at the Cuba and Minnesota latitudes (as a matter of fact, the plates used by Feld *et al.* came from the same flight as these plates). The Brookhaven authors concentrated their attention on measuring the multiplicities of minimum ionization tracks (defined by them as tracks with grain densities less than 1.3 times minimum) as a function of star size (defined as the number of heavy tracks —greater than 1.3 times minimum—in the star) produced by protons at the two latitudes. Their histograms are shown in Fig. 9: Fig. 9*a* contains a plot of the frequency vs. multiplicity at the southern latitude for heavy nuclei (defined as stars with at least 9 heavy prongs) and light nuclei (defined as nuclei with 5 heavy prongs or less); the intermediate cases are not presented (6 to 8 heavy prongs) since they may arise from either the light or the heavy nuclei. Figure 9*b* shows a histogram for the heavy nuclei at the northern and southern latitudes and Fig. 9*c* a histogram for the heavy nuclei at northern latitudes and the light nuclei at the southern latitudes. The cutoff energies are 1 Bev at the northern latitude and 8 Bev at the southern latitude. The results of Salant *et al.* are presented in a more concise form in Table 11 where the mean multiplicities of shower particles $\bar{N}_0$ ($\bar{N}_0$ is defined as the total number of minimum tracks divided by the total number of stars including stars with no shower particles) and $\bar{N}_1$ ($\bar{N}_1$ is defined as the total number of minimum tracks divided by the total number of stars excluding events with no shower particle) are listed for light nuclei (2 to 5N_h—N_h stands for the number of heavy prongs), light-heavy nuclei (6 to 8N_h), and heavy nuclei ($> 9N_h$). The first row represents the southern latitude, the second row the northern latitude, and the third row the difference between the two corresponding to proton energies between 1 and 8 Bev [the mean multiplicity in the third row is calculated from the relation $\frac{1}{4}$ $(5\bar{N}_{\text{north}} - \bar{N}_{\text{south}})$].

---

[29] Salant, Hornbostel, Fisk, and Smith, *Phys. Rev.*, **79**: 184 (1950).

TABLE 11. MEAN MULTIPLICITIES OF SHOWER PARTICLES IN LIGHT AND HEAVY NUCLEI[29]

	2–5N_h $\bar{N}_0$	6–8N_h $\bar{N}_0$	$\geq 9N_h$ $\bar{N}_0$	2–5N_h $\bar{N}_1$	6–8N_h $\bar{N}_1$	$\geq 9N_h$ $\bar{N}_1$
31°	1.4 ± 0.3	2.4 ± 0.4	4.2 ± 0.3	3.0 ± 0.5	3.4 ± 0.4	5.2 ± 0.4
57°	1.4 ± 0.2	1.7 ± 0.3	2.0 ± 0.3	2.6 ± 0.3	2.7 ± 0.5	3.2 ± 0.4
1–8 Bev	1.3 ± 0.3	1.5 ± 0.4	1.5 ± 0.4	2.5 ± 0.4	2.4 ± 0.6	2.7 ± 0.5

Figure 9*a* and the first row in Table 11 show that the multiplicity increases appreciably at the southern latitude in going from the light to the heavy nuclei. This is evidence for plural production of the shower particles in the heavy nuclei. Column 2 of Table 11 indicates that the mean multiplicity in the light nuclei does not vary with the incident proton energy, within the statistical error; such an energy-insensitivity would be consistent with the idea that the greater available energy of the proton does not lead to a marked increase in the multiplicity of meson

production in a single proton-nucleon encounter but rather to the transfer of a greater amount of energy to the single meson produced. On the other hand, Fig. 9*b* and Table 11 imply that the higher proton energies raise the multiplicities of shower particles resulting from heavy nuclei; this again favors the cascade production of mesons in heavy nuclei since there was no recognizable increase of multiplicity with energy from the light nuclei. Finally, Fig. 9*c* and Table 11 show that heavy nuclei struck by 1- to 8-Bev protons (median energy 2.5 Bev) yield as high mean multiplicities as do light nuclei struck by protons with energies greater than 8 Bev (median energy 14 Bev); again, this is evidence for plural production.[29a]

The most comprehensive study of penetrating showers with the photographic technique has been carried out by Camerini *et al.*,[30] who exposed photographic plates at 68,000 ft. These workers examined 87 cm^3 of emulsion, observed 15,000 stars, and made multiple scattering and grain-density measurements on 2000 tracks associated with these stars. In addition, they measured the grain density and angle of emission of 3070 shower particle tracks (a shower particle in the present experiment is defined as one having a grain density less than or equal to 1.5 times minimum, and the number of such particles in a given star is denoted by N_s) and 1508 gray tracks (a gray track is defined as one with a grain density between 1.5 and 7 times minimum, and the number is denoted by N_g—a black track is then one with a grain density greater than 7 times minimum and the number is denoted by N_b). Finally, all stars produced by primary particles, of sufficient track length for their energies to be determined, were analyzed in detail. We shall not do justice here to this extensive work but merely quote some of the salient results as they bear on the problem of plural π meson production; Table 12 gives the breakdown of the 15,300 stars in terms of N_s and $N_h = N_g + N_b$.

Of the 2000 tracks whose grain density and scattering were measured, 470 turned out to be shower particles. Of this 470, 60 per cent were mesons with kinetic energies ranging from 80 to 1100 Mev, 17 per cent were protons with energy between 500 and 800 Mev, and the remaining 23 per cent could not be definitely identified. Table 13 lists the average energies (including the rest mass) of the 280 or so identifiable mesons

---

[29a] In a recent private communication, Dr. Hornbostel has emphasized the importance of subtracting out the contribution of secondary protons from the data presented in Fig. 9 and Table 11. This correction may weaken considerably the arguments for plural production based on Fig. 9 and Table 11.

[30] Camerini, Davies, Fowler, Franzinetti, Lock, Perkins, and Yekutieli, *Phil. Mag.*, **42**: 1241 (1951); and Camerini, Davies, Franzinetti, Lock, Perkins, and Yekutieli, *Phil. Mag.*, **42**: 126 (1951).

TABLE 12. ANALYSIS OF 15,300 STARS OBSERVED IN PLATES FLOWN AT 68,000 FT

N_s \ N_h	3	4	5	6	7	8	9	10	11	12	13	14	15	16	17	18	19	20	21	22	23	24	25	26	27	28	29	⩾30	Totals
0 *n*	2499	2132	1499	938	576	367	238	169	124	100	89	67	47	37	29	14	18	11	7	3	4	1	1	3	2	1		1	8977
p	225	310	356	305	204	137	116	92	75	45	49	53	32	32	22	12	10	11	9	8	3	2	4	1	2	1	1		2117
1 *n*	133	194	195	199	128	97	88	63	51	53	28	34	23	13	25	15	18	3	8	1	2	1	1	2	1	1		1	1378
p	91	146	151	135	96	79	52	50	44	36	28	25	24	15	15	18	11	6	10	5	1	8	6	3	2	3		3	1063
2 *n*	33	36	44	51	37	26	26	23	20	17	16	27	17	15	15	9	3	4	2	7		1	2		1		2	3	437
p	24	42	28	49	32	24	29	29	22	15	20	23	20	10	13	7	7	7	3	8	1	2	3	2	1		1	2	424
3 *n*	9	5	8	7	6	10	5	4	4	5	2	2	5	2		1	2		1		2		1		2				83
p	13	15	25	17	14	14	12	12	18	10	11	16	12	7	1	7	4	5	2	1	6	2	2	1	1			1	229
4 *n*	3	6	7	6	7	2	6	2	2	2	1	4		2		3	1		2	1	1	1			1	1			61
p	3	11	15	11	11	9	9	10	5	4	6	2	5	6	8	1	4	5	4	2	5	4	2	1	3		1	1	148
5 *n*	3	2	1	4	3	1	1	5	1	4	2		1			4	1	1	1					2					37
p	8	5	8	9	7	5	6	6	5	5	2	4	4	4	3	2	1	2	2	1	1	3	1	1	1	1			97
6 *n*		2		3	4	1	3	1	1		5	1				1			1	2		2		1					28
p	5	5	3	7	5	2	5	2	2	5	2	6	2	1	3	4	1	1	1	3	1	1		1					68
7 *n*				1								1	1		2		1												6
p	1	2	1	2	2	1	3	4		5		2	6		1	1			1	2				2			1	2	39
8 *n*				1		2											1												4
p			2	1	4		1	3	3	3		1	1	2	1	2	1		1	2	3	2			1				34
9 *n*	1	1	1			1								1											1				6
p		1	1	2		1	1			1				2				1						3				1	14
10 *n*							1					1		1			1												4
p		2	1		2						1	1		1					1	1	2		1						13
11 *n*																													0
p					1			3					1			1													6
12 *n*																													0
p					1								1							1									3
13 *n*																													0
p				1		1	1					2		1		1				1		1							9
14 *n*										1																			1
p																													0
15 *n*																1			2										3
p			1	1		1								2		1	1		1	1	1	1							11

Grand total 15.300

TABLE 13. AVERAGE KINETIC ENERGY OF IDENTIFIED π MESONS AS FUNCTION OF N_h AND N_s

N_s $\bar{T}$	1 385 ± 40 Mev	2–4 340 ± 35 Mev	≥ 5 395 ± 40 Mev
N_h $\bar{T}$	3–8 385 ± 45 Mev	9–14 360 ± 40 Mev	≥ 15 360 ± 30 Mev

which were observed; there seems to be no significant dependence on either N_h or N_s. The angular distributions of the shower particles with respect to the primary particles were determined for more than 1000 stars, and the resulting distributions are shown in Figs. 10 and 11. The median angle of the distribution as a function of the multiplicity is plotted in Fig. 12. The significance of these figures—the slow increase of half width with N_s in Fig. 10 and the near constancy of median angle as a function of multiplicity in Fig. 12—for the plural production mechanism will be discussed below. Another 250 tracks whose grain density and scattering were measured were identified as primaries of stars; Fig. 13 shows the variation of the average multiplicity of shower particles $\bar{N}_s$,

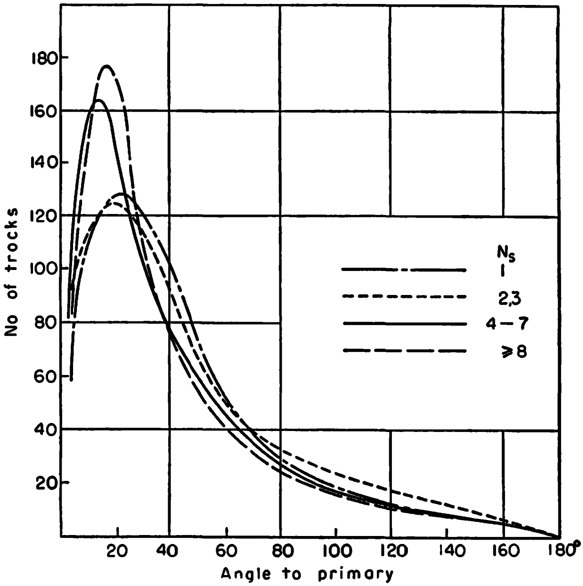

FIG. 10. The measured angular distributions in the laboratory system of shower particles observed in photographic emulsions at 68,000 ft for different ranges of multiplicity (Camerini *et al.*).

average number of gray tracks $\bar{N}_g$, and average number of heavy tracks $\bar{N}_h$, as a function of the primary energy of the shower particle (which are separated into π mesons, nucleons, and "uncertain particles" by appropriate symbols). There is a definite increase of all types of tracks with energy, the greatest increase taking place for the shower particles, although a closer breakdown would show a wide spread of multiplicity of shower particles at a given energy. No primaries were identified with energies greater than 20 Bev and very few above 10 Bev. Knowledge of the energies of the primaries, together with a measurement of the energies of the secondaries—wherever possible—enable Camerini *et al.* to deduce the ratio of neutral to charged π mesons emitted from the stars; their result is 1.0 ± 0.3 corresponding to an average primary energy of 2700 ± 150 Mev. This ratio is to be compared with the value derived by Gregory and Tinlot[31] from a cloud chamber experiment in which they observed the cascade showers produced by the decay γ rays from the π^0 mesons and compared this number with the number of charged penetrating particles; Gregory and Tinlot's value for the ratio of neutral to

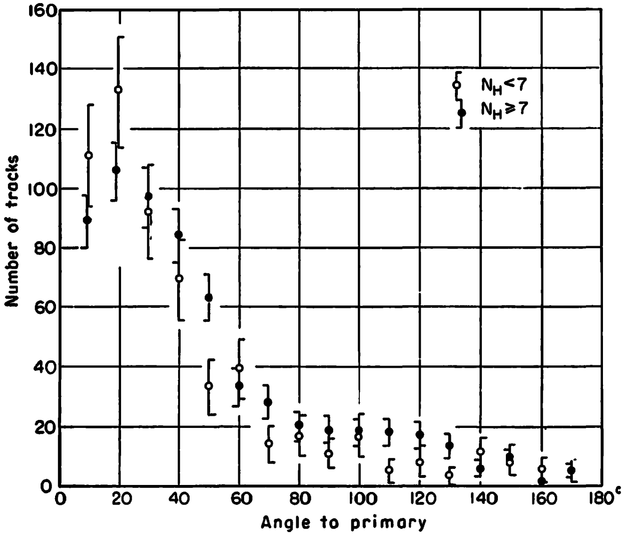

FIG. 11. The measured angular distributions of shower particles associated with stars of $N_h < 7$ and $N_h \geq 7$ (Camerini *et al.*).

---

[31] B. Gregory and J. Tinlot, *Phys. Rev.*, **81**: 675 (1951); cf. also Lovati, Mura, and Tagliaferri, *Nuovo cimento* **9**: 205 (1952) who found 0.3 — 0.5 for the ratio.

charged π mesons turned out to be 0.3; the discrepancy is somewhat difficult to understand since the energies are not too different.

Camerini *et al.* compare their experimental data with the predictions of the plural theory of Heitler and Janossy in its simplest version, *i.e.*, neglecting meson production by the recoil nucleons and meson reproduction. The simple plural theory leads to the following expression (cf. Sec. 3) for the average multiplicity of mesons $\bar{N}_\pi$ as a function of energy:

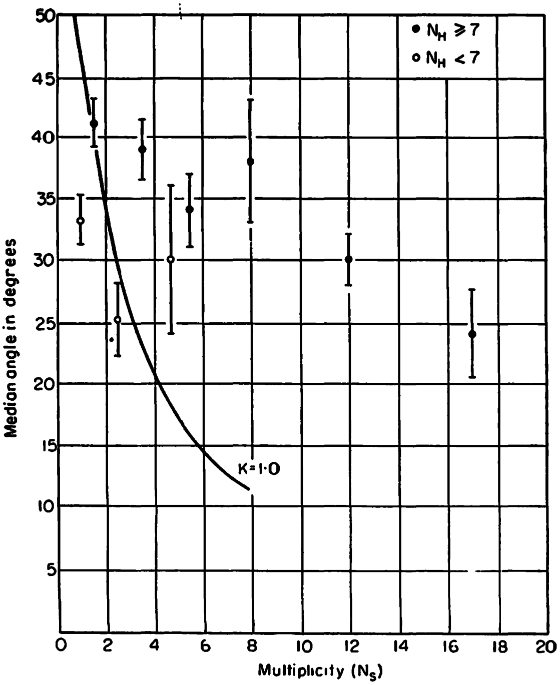

FIG. 12. The measured variation of the median angle of the showers with the multiplicity for stars of $N_h \geq 7$ and $N_h < 7$ (Camerini *et al.*). The solid curve shows the variation expected on the assumption of multiple isotropic production in a single completely inelastic ($K = 1.0$) nucleon-nucleon collision (see text).

$$\bar{N}_\pi = \frac{\log [(\gamma - 1)/(\gamma_c - 1)]}{- \log \bar{\omega}} + 1 \tag{73}$$

where γ is the energy of the incident nucleon in the laboratory system in units of Mc^2, γ_c is the cutoff energy (in the same units) below which the primary nucleon is assumed not to produce further mesons, and $\bar{\omega}$ is the constant fractional kinetic energy remaining to the primary after each collision. To calculate the cutoff energy, it is recalled that the definition of a shower particle is such that $\gamma_s > 1.7$; hence

$$\left(\frac{M}{\mu}\right)(\gamma_c - 1)(1 - \bar{\omega} - \delta) = 1.7 \tag{74}$$

where δ is the constant fraction of the primary energy taken off by the recoil nucleon. Camerini *et al.* choose $\bar{\omega} = \frac{3}{4}$, $\delta = \frac{1}{8}$ so that $\gamma_c = 3.1$.

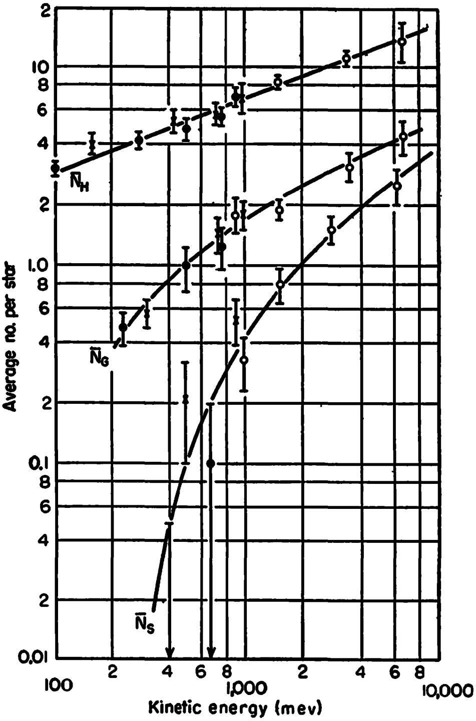

FIG. 13. The measured variation of $\bar{N}_h$, $\bar{N}_g$, and $\bar{N}_s$ with the kinetic energy of the primary particle; × stars produced by π mesons, ● proton-initiated stars, ○ stars initiated by unidentified particles (Camerini *et al.*).

If, in addition, it is assumed that the average number of charged π mesons is $\frac{2}{3}\bar{N}_\pi$, it is possible to plot the number of charged mesons (taken as the observed shower particles) as a function of $\bar{\gamma}$ (and therefore of γ); this curve is shown in Fig. 14 together with the experimental data. At sufficiently high primary energies, the recoil nucleons can themselves produce further mesons and the average number in the second generation is $\bar{N}'_\pi(\bar{N}'_\pi - 1)/2$ where

$$\bar{N}'_\pi = \frac{\log(\gamma - 1) - \log(\gamma_c - 1)\log\delta}{-\log\bar{\omega}} + 1 \tag{75}$$

The effect of the second generation is shown as the dotted curve in Fig. 14 starting at $\gamma = 15$ Bev.

The average multiplicity vs. energy criterion is not a good one for distinguishing between plural and multiple theories; a reasonable fit with the experimental data could also be achieved with a multiple type of theory. A better way of discriminating between the two types of theories is to examine the angular distributions of the shower particles shown in Figs. 10 to 12; Fig. 12, in particular (where the solid curve shows the prediction of one of the characteristic multiple production theories), provides evidence for plural processes as against a pure multiple process in a single nucleon-nucleon encounter. On the other hand, there are difficulties with the simple plural theories. The appreciable backward fraction of shower particles which is observed,[32] even at high multiplicities, appears to require the additional assumption that the mesons which are created inside the nucleus suffer elastic scatterings with nucleons (this is not unreasonable—cf. Chap. 7) and frequently suffer large-angle deflections. A further difficulty is revealed by the fact[33] that the number of gray and black tracks increases too slowly with increasing number of

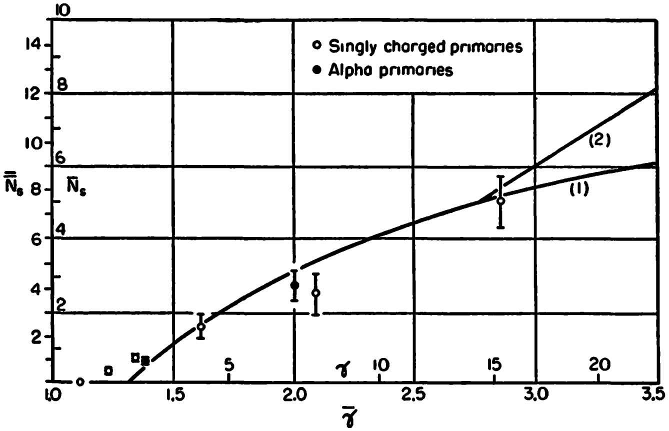

FIG. 14. The measured variation of the average multiplicity of shower particles with primary energy; for α particles, the multiplicity per nucleon is plotted against energy per nucleon. The solid curves represent the predictions of the plural theory: (1) takes account only of the first generation (see text), (2) includes the second generation. $\bar{\bar{N}}_s$ represents the sum of the charged shower particles $\bar{N}_s$ plus the π^0 mesons.

---

[32] Cf. Fig. 5 of Camerini *et al.* (footnote 30).

[33] Cf. Fig. 6 of Camerini *et al.* (footnote 30).

shower particles at high multiplicity (an increase of 0.5 nucleons per charged π meson or 0.3 per π meson including charged and neutral). This contradicts the simple plural theory which predicts roughly one nucleon per π meson. However, Heitler and Terreaux[34] have recently shown that a simple extension of the plural theory will reduce the number of recoil nucleons per shower particle. They argue that at sufficiently high energies several recoil nucleons will all be incident on the same nucleon, thereby giving rise to several mesons with the addition of only one more recoil nucleon. After m such stages there will be $[m(m+1)]/2$ mesons associated with only $(m+1)$ recoil nucleons. On the basis of this assumption, Heitler and Terreaux show that it is possible to reconcile the experimental findings referred to above.

6. Experimental Evidence for Multiple Production of π Mesons

It has been demonstrated that the plural production theory, with reasonable modifications, can explain much of the experimental data on penetrating showers, possibly even with shower multiplicities as large as 20. On the other hand, a pure multiple production theory was shown to be incapable of explaining certain features of the penetrating-shower data. It must be remembered, however, that all the data presented thus far were gathered under normal cosmic-ray conditions, *i.e.*, at average nucleon energies of the order of 10 Bev. It is quite conceivable that, at sufficiently high energies, say greater than 10^{12} ev, the multiple production mechanism will begin to operate with full force; and, while plural effects will undoubtedly enter, the multiple production mechanism will determine the chief features of penetrating showers. It thus appears that a study of the extremely energetic showers, rare though they be, may shed more light on the multiple production mechanism than a statistical analysis of the lower energy events. The Auger showers provide another means of studying extremely high energy meson production processes and will be treated separately in Sec. 7.

The first extremely high energy event which was thoroughly analyzed was the R star,[35] observed in a stack of electron-sensitive plates exposed to the cosmic radiation at an altitude of 90,000 ft. We have already mentioned the R star in connection with our discussion of the lifetime of the π^0 meson (cf. Chap. 4). For our present purposes, the R star is of interest because it was produced by an alpha particle having an energy between 10^{12} and 10^{13} ev and contains 56 shower particles, of which about half are concentrated in a narrow core of half width 1.7° and the remainder are spread out over an angular interval of 60°. In addition, there are 18 gray and 5 black tracks representing a minimum charge of 27 so that the total observed minimum charge is 81; this definitely proves that most of the shower particles are not protons and are π mesons [or a mixture[35a] of π mesons, τ and heavier mesons, etc. (cf. Chap. 9)] since the heaviest nucleus in the emulsion is silver with an atomic number of 47. Another important feature of the *R* star is that the careful alignment of adjacent photographic plates made it possible to trace the narrow core through three emulsions[35] and to observe a sizable multiplication of charged particles in the core of the shower. It can be shown that this multiplication is due to the creation of electron pairs by high-energy γ rays arising from the decay of neutral π mesons created simultaneously with the charged π mesons. Assuming zero lifetime for the π^0 meson, it can furthermore be shown from the known amount of stopping material (glass and emulsion) that the γ rays in the core must number at least 35. This number rules out a possible bremsstrahlung origin for the γ rays associated with the creation of the charged π mesons since the fraction of the incident charged meson energy that can be given off in the form of γ radiation is at least a factor of 100 too small for the spin 0 π meson.[36] With at least 35 γ rays observed in the core, the number of neutral mesons in the core must be at least one-half of the number of charged π mesons. The energies of the γ rays in the core and therefore of the π^0 mesons can be estimated from the angular separations of the electron pairs seen within the core in the second and third emulsions (only one electron pair is observed in the first emulsion where the star is produced). It turns out that 15 to 20 Bev is a reasonable estimate for the average energy of the π^0 mesons (and presumably the charged π mesons) in the core of the *R* star.

---

[34] Private communication quoted in Camerini *et al.* (footnote 30); cf. C. Terreaux, *Helv. Phys. Acta*, **24**: 551 (1951).

[35] Kaplon, Peters, and Bradt, *Phys. Rev.*, **76**: 1735 (1949); cf. also Bradt, Kaplon, and Peters, *Helv. Phys. Acta*, **23**: 24 (1950). The R star has been traced through a third emulsion (private communication from the authors).

The question now arises as to the mechanism whereby an incident alpha particle of very high energy produces a well-defined shower core of about 40 mesons (neutral and charged) with an average energy of 15 to 20 Bev and a diffuse shower of comparable intensity. Three explanations are possible: (*a*) The 80 or so mesons were produced as a result of a large number of collisions between the nucleons of the incoming alpha particle and the nucleons of the target nucleus (pure plural theory). (*b*) The 80 or so mesons were produced as a result of single encounters between the nucleons of the incoming alpha particle and the nucleons of the target nucleus (pure multiple theory). (*c*) Only the narrow core of the shower was produced as a result of single nucleon-nucleon collisions, whereas the diffuse part resulted from a large number of secondary collisions (pluro-multiple theory). Let us examine each of these hypotheses in turn. Hypothesis (*a*) seems very unlikely for the following reasons: (1) The probability that there will be 80 nucleon-nucleon collisions inside a silver nucleus is extremely small; the radius of a silver nucleus is only 5 times the mean free path (assumed geometrical). (2) If the recoil nucleons have made appreciable contributions to the shower, one should see a larger number of gray and black tracks than one actually sees (multiplying the total number of gray and black tracks by 2 to take account of the neutrons, there is still only 0.5 nucleon per meson) unless one accepts the hypothesis of Heitler and Terreaux.[34] However, even accepting this hypothesis, one would expect a more continuous angular distribution of the shower particles than is actually observed (cf. Fig. 15) and not such a clear-cut separation between the narrow core and the diffuse shower. Hypothesis (*b*) is no more promising if one believes in a theory which predicts an isotropic production in the center-of-mass system (*i.e.*, Heisenberg's theory or the published version of the theory of Lewis *et al.*); one cannot then explain the simultaneous production of the narrow core and the diffuse shower. However, if one adopts a multiple meson theory like Fermi's which predicts considerable anisotropy in the center-of-mass system, the comparable meson intensities in the narrow core and diffuse core of the *R* star can be explained. The solid curve in Fig. 15 shows the angular distribution of the mesons

---

[35a] In a recent paper, Daniel, Davies, Mulvey, and Perkins [*Phil. Mag.*, **43**: 753 (1952)] claim to have evidence that, above 50 Bev, heavy mesons are produced with a frequency comparable to that of π mesons.

[36] Cf. L. I. Schiff, *Phys. Rev.*, **76**: 89 (1950); cf. also R. E. Marshak, *Phys. Rev.*, **76**: 1736 (1951).

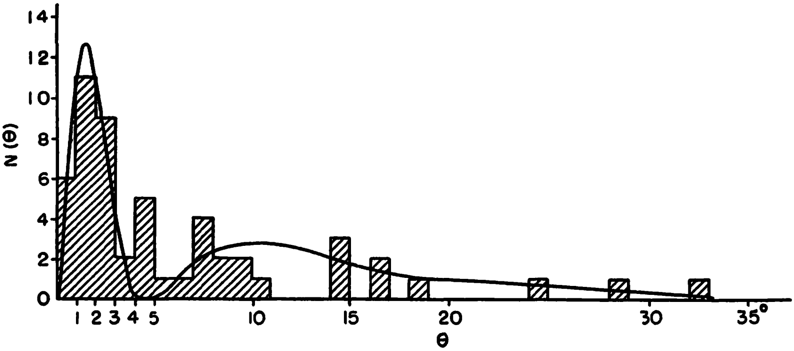

FIG. 15. Measured angular distribution of the shower particles in the *R* star; the solid curve represents the predictions of the anisotropic production theory with $n = 1$ (see text).

in the laboratory system predicted under the assumption of a $\cos^2 \bar{\theta}$ distribution for the mesons in the center-of-mass system and equal energies for all mesons (Case III of Sec. 4 with $n = 1$) and $\langle \gamma_0 \rangle = 120$ (corresponding to an average meson energy in the laboratory system of about 20 Bev); the agreement is fairly good. The $\cos^2 \bar{\theta}$ distribution and $\langle \gamma_0 \rangle = 120$ leads to an energy of 0.3×10^{12} ev per nucleon, assuming that all four nucleons of the incoming alpha particle contribute equally to the production of the meson shower (*i.e.*, assuming a multiplicity of about 20 per nucleon). At this energy, Fermi's theory predicts a multiplicity of 6, which is too low. Hence the *R* star cannot be readily explained by any of the pure multiple theories discussed in Sec. 3.

The most plausible explanation of the *R* star is hypothesis (*c*), which states that the narrow core of the shower is due to a multiple production mechanism whereas the diffuse part arises from plural processes. Unfortunately, it is then not possible to discriminate among the various theories since a suitable choice of parameters can explain the narrow core on any of the theories. This is seen in Table 14 where the parameters required by the three characteristic theories discussed in Sec. 4 are listed. Line 1 of Table 14 lists the average observed meson energy in the laboratory system (of the order of 20 Bev) except for Case II where the observed multiplicity (taken as 9 per nucleon) and the width of the narrow core determine $\bar{\gamma}$ and therefore $\langle \gamma_0 \rangle$; in view of the experimental uncertainties, the value of 82 listed for Case II is still possible. The remaining rows are self-explanatory and are all derived on the assumption that $N_s = 9$, $\theta_m = 1.5°$ and $\langle \gamma_0 \rangle = 120$. It is interesting to note that a $\cos^4 \bar{\theta}$ distribution is the largest anisotropy of meson production in the center-of-mass system which can be assumed since otherwise the inelasticity of the collision would have to be greater than its maximum value unity for the

TABLE 14. ANALYSIS OF *R* STAR

	Case I (isotropy and uniform energy)	Case II [isotropy and $F = (A/4\pi)(\sqrt{\bar{\gamma}_0^2 - 1}/\bar{\gamma}_0^3)$]	Case III [uniform energy and anisotropy $F(\bar{\theta})$]	
			$F(\bar{\theta}) \sim \cos^2 \bar{\theta}$	$\sim \cos^4 \bar{\theta}$
$\langle \gamma_0 \rangle$	120	82	120	120
$\bar{\gamma}$	30	20	12	10
γ	1800	800	290	200
$E_\alpha = 4\gamma Mc^2$ (in 10^{12} ev)	7.2	3.2	1.2	0.8
$\langle \bar{\gamma}_0 \rangle = \langle \gamma_0 \rangle / \bar{\gamma}$	4.0	4.1	10.0	12.0
K	0.1	0.15	0.6	1.0

above choice of N_s, θ_m, and $\langle\gamma_0\rangle$ (cf. Sec. 4 for notation). Thus, the narrow core of the *R* star can certainly be explained by a pure multiple theory. The diffuse part of the *R* star can be explained by a pure plural theory, as shown by calculations of Bradt *et al.* Hence, the total *R* star is probably a good illustration of pluro-multiple meson production.[37]

Another extremely high energy event which gives even more definitive evidence for multiple meson production was observed by Lord *et al.*;[38] we shall term this event the *S* star. The *S* star was produced in an electron-sensitive emulsion by a primary proton at an altitude of 90,000 ft. It consists of a shower of 15 minimum ionization particles, of which 7 are in an extremely narrow core of 0.003 radian half width (that is, $\theta_{\frac{1}{2}} = 0.006$) and the remaining 8 are in a diffuse core of only 0.13 radian half width (that is, $\theta_T = 0.26$). There are only two nonshower particles in the *S* star; this is strong evidence that the 15 shower particles are due to a single collision of the primary proton with one of the nucleons near the edge[38a] of a nucleus in the emulsion. Relative scattering measurements of the minimum ionization tracks enabled Lord *et al.* to determine lower limits on the energies of the 7 shower particles in the core, with the result that most of the particles in the core have energies greater than 250 Bev. The energies of the particles in the diffuse core are much lower—of the order of several Bev. The high average energy of the shower particles in the narrow core and the presence of two cores rule out any multiple meson production theory which predicts an isotropic distribution of mesons in the center-of-mass system but are consistent with a theory which predicts an anisotropic meson distribution in the center-of-mass system. Using the method developed by Kaplon and Ritson (cf. Sec. 3), one can deduce the energy of the incident proton responsible for the *S* star from the relation $\bar{\gamma}^2 = 1/\theta_{\frac{1}{2}}^2$ [cf. Eq. (72*a*)]; $\bar{\gamma}$ turns out to be 165, and therefore the incident proton energy is 5×10^{13} ev.[39] This value is probably correct to a factor of 4 if the assumption is indeed correct that all the shower particles in the S star were produced in a single nucleon-nucleon encounter. None of the multiple meson production theories can explain quantitatively all the features of the S star. On Fermi's theory, the observed angular distribution of the shower particles in the laboratory system requires a value of ρ of 0.9975 and therefore a value of the impact parameter close to unity (cf. Table 5). For this value of the impact parameter and an energy of 5×10^{12} ev, Fermi's theory predicts a multiplicity of 4, which is much too low (the observed multiplicity of 15 should be increased to about 25—to include π^0 mesons and neutron-antineutron pairs—in order to be compared with the figure 4). The theories of Heisenberg and Lewis *et al.* predict much higher multiplicities which can be reconciled with what is actually observed in the S star.

---

[37] Cf. LePrince-Ringuet, Bousser, Tchang Fong, Jauneau, and Morellet, *Phys. Rev.*, **76**: 1273 (1949); cf. also P. Freier and E. Ney, *Phys. Rev.*, **77**: 337 (1950).

[38] Lord, Fainberg, and Schein, *Phys. Rev.*, **80**: 970 (1950). An event very simliar to the *S* star has recently been detected at 11,500 ft by Gerosa and Levi-Setti [*Nuovo cimento* **8**: 601 (1951)] in so far as the shower particles are concerned; however, the number of heavy prongs is much larger.

[38a] It is impossible that the *S* star resulted from a collision with a hydrogen nucleus because of the presence of an *even* number of shower particles. Kaplon and Ritson (private communication) have found a nuclear star with 16 shower particles and no nonshower particles produced by a proton with an energy of 10^{13} ev. At lower energies ($\sim 5 \times 10^{10}$ cv) M. Teucher [*Naturwiss.*, **39**: 68 (1952)] has observed a star with 20 shower particles and no nonshower particles.

[39] This value is larger than the 3×10^{13} ev deduced by the authors on the basis of Fermi's theory.

A third very energetic multiple meson event which has been detected in photographic emulsions and subjected to a careful analysis is the T star discovered by Kaplon *et al.*[40] and already cited in Chap. 4. The T star was produced by a proton in a 3-mm brass plate constituting part of a stack of alternating brass plates (each 3 mm thick) and photographic emulsions (each 100 microns thick)—a total of 20 of each—exposed to the cosmic radiation at 95,000 ft. The T star contains 36 charged shower particles with angular widths of the narrow and diffuse cores comparable with those of the S star; values of the angles in the laboratory system containing different fractions of the total number of charged shower particles are listed in Table 15. Values of the product $\theta_f \times \theta_{1-f}$ are also listed in Table 15 as $(\bar{\gamma})^{-2}$ [cf. Eq. (72*a*)] as well as values of the quotient θ_{1-f}/θ_f. If all the shower particles were produced in a single nucleon-nucleon collision, then the product should be strictly constant provided that m is close to unity (*i.e.*, the mesons are produced with kinetic energies in the center-of-mass system at least equal to their rest energies). The variation of $(\bar{\gamma})^{-2}$ by a factor 2 which is evident in Table 15 is not a

TABLE 15. OBSERVED ANGLES IN THE T STAR

f	θ_f	θ_{1-f}	$\theta_f\theta_{1-f} \equiv (\bar{\gamma})^{-2}$	$\dfrac{\theta_{1-f}}{\theta_f}$
0.1	3×10^{-3}	2×10^{-1}	6×10^{-4}	67
0.25	5×10^{-3}	1.1×10^{-1}	5.5×10^{-4}	22
0.5	1.8×10^{-2}	1.8×10^{-2}	3.24×10^{-4}	1

---

[40] Kaplon, Peters, and Ritson, *Phys. Rev.*, **85**: 900 (1952). Recently, Lal, Pal, Peters, and Swami (*Proc. Indian Acad. Sci.*, in press) have examined in detail a nuclear star containing 207 shower particles produced in glass by a primary magnesium nucleus with an energy of 2×10^{14} ev.

decisive argument in favor of plural meson production since the statistical errors are so large especially for small f. The most statistically significant value of $\bar{\gamma}$ is the one corresponding to $f = 0.5$, and this yields an energy of 6.5×10^{12} ev for the primary proton, a value which is uncertain by a factor of 4 either way, assuming the Poisson law for fluctuations.

In the case of the T star, it is possible to derive an independent estimate of the primary energy by actually measuring the energy in the π^0 component of the T star and by determining the ratio of charged to neutral π mesons. The first part is accomplished by studying the multiplication of the electron cascade showers arising from the decay γ rays of the π^0 mesons produced in the initial event. Since the T star is produced in the sixth brass plate from the top at an angle of 60° to the vertical, and there are 14 brass plates of 3 mm each and 14 glass plates (the glass plates hold the emulsions) of 1.4 mm each below the sixth glass plate, the total corresponding to about 5 radiation lengths, the electron showers undergo considerable multiplication. The electron showers enabled Kaplon *et al.* to detect π^0 mesons with energies of $3 \pm 1 \times 10^{12}$ ev, $1.5 \pm 1 \times 10^{12}$ ev, $7 \pm 1 \times 10^{11}$ ev, $3 \pm 1 \times 10^{11}$ ev (4 of these) in the central core and about 10 π^0 mesons with an average energy of about 5×10^{10} ev in the diffuse shower. The energies of the two most energetic π^0 mesons were verified by taking advantage of the presence of double cores of electron cascades with angular apertures of 1.35×10^{-4} and 2×10^{-4} radians, respectively. From these angles and the ratios of energies in the two components of the double cores, energies of 2.4×10^{12} and 1.6×10^{12} ev were deduced for the π^0 mesons. (These values of the energy and the distances from the T star at which the electron cascades originate, which turn out to be 2.4 and 7 cm, respectively, yield a π^0 lifetime of about 1×10^{-14} sec—cf. Chap. 4). The number of π^0 mesons is found from the charged particle multiplication in the first two emulsions (for the less energetic π^0 mesons), the observed number of electron cascades (for the more energetic π^0 mesons), the π^0 lifetime and the cross section for pair production by photons; the number turns out to 20 ± 7. The minimum total energy in the π^0 component of the T star is thus 6×10^{12} ev, and the total energy in both charged and neutral components 1.7 to 2.2×10^{13} ev, depending on whether or not it is assumed that all 36 charged shower particles are charged π mesons or only one-half are (the remainder being antiprotons in accordance with Fermi's theory). The value of the incident proton energy deduced in this way is within the statistical error of the kinematical value.

Table 15 permits one to deduce a reasonably accurate value of the impact parameter in Fermi's theory (provided always that the T star originated in a single nucleon-nucleon encounter). All three values of θ_{1-f}/θ_f

are consistent with $\rho = 0.99$ and an impact parameter $(b/R) = 0.876$. With this value of the impact parameter and $\bar{\gamma} = 100$ (corresponding to 2×10^{13} ev), Fermi's theory predicts a multiplicity of 10, which is again much too small (to be compared with a multiplicity of 55); the discrepancy is a factor 5, as in the case of the S star. This discrepancy can be removed, of course, by increasing the radius R of the sphere of action in Fermi's theory by a factor of about 10; however, this would require $R \approx 10\hbar/\mu c \sim 10^{-12}$ cm—a completely unreasonable value. Fermi's theory appears to be in further trouble in connection with the ratio of neutral to charged π mesons if antinucleons actually exist. Fermi's theory would then predict that, of the 36 charged shower particles in the T star, 13 are charged π mesons and the remainder protons and antiprotons so that the $\pi^0/(\pi^+ + \pi^-)$ ratio is 1.5 ± 0.5. Despite the large error, this cannot be regarded as confirmation of Fermi's prediction of 0.5. If most of the 36 charged particles in the T star are charged π mesons, the $\pi^0/(\pi^+ + \pi^-)$ ratio is 0.6 ± 0.2, which is in much better agreement with Fermi's preduction and with the charge independence hypothesis.[40a]

The discrepancies with Fermi's theory are disagreeable especially since, for the T star at least, the energy spectrum of the π^0 mesons (and presumably, therefore, of the charged shower particles) and the angular distribution of the charged shower particles agree reasonably well with the predictions of the theory (cf. Figs. 2 and 3). It appears, therefore, that, while Fermi's theory makes reasonably self-consistent predictions of the angular distribution and the energy spectrum of the mesons in the center-of-mass system, it does not fare so well in so far as the multiplicity is concerned. This may be due to the fact that mesons continue to be produced after the nucleon-nucleon assemblage is dissolved or, what is certainly possible, that plural processes contribute significantly to both the S and T stars. The theories of Heisenberg and Lewis *et al.* can again explain the high multiplicity observed in the T star but not much more.

Despite the strong evidence of the R, S, and T stars in favor of multiple meson production in nucleon-nucleon collisions, it would still be desirable to establish this fact unequivocally by working with pure hydrogen. Unfortunately, to date, this has not been possible, although Fretter[41] has attempted to arrive at a conclusive answer by studying the production of penetrating showers in a lithium block placed above a cloud chamber. The cloud chamber containing $\frac{1}{4}$-in. Pb plates was operated at sea level (Berkeley) and was triggered to respond to relatively large penetrating showers. The penetrating showers which Fretter observed are listed in Table 16. Column 2 of Table 16 lists the numbers of charged particles in each penetrating shower, column 3 the minimum number of penetrating particles (identified by their passage through two $\frac{1}{4}$-in. lead plates without interaction), and column 4 the number of electron showers starting from the first lead plate (presumably caused by the decay of π^0 mesons into γ rays). Since the maximum number of nucleon-nucleon interactions in a lithium nucleus is 7, and since, even assuming that only charged mesons are produced in each interaction (which is certainly not true in view of the observed electron showers and other independent evidence), Table 16 (in particular events 1, 5, 6, and 8) argues for the production of more than one meson in a single nucleon-nucleon encounter.

[40a] The charge independence hypothesis for mesons and nucleons applied to multiple π meson production predicts that the collisions of nucleons with nuclei consisting of equal numbers of protons and neutrons will produce on the average one-half as many neutral π mesons as charged π mesons [cf. K. M. Watson, *Phys. Rev.*, **85**: 852 (1952); and Van Hove, Marshak, and Pais, *Phys. Rev.*, in press].

[41] W. B. Fretter, *Phys. Rev.*, **80**: 921 (1950). Recently, M. Vidale and M. Schein [*Phys. Rev.*, **84**: 593 (1951)] performed an experiment with liquid hydrogen and a counter array at 90,000 ft. in which they found evidence for multiple events originating

TABLE 16. MULTIPLICITY OF PENETRATING SHOWERS FROM LITHIUM

Event No.	Charged particles traceable to point of origin	Identified penetrating particles	Electron showers starting from first lead plate
1	10	3	>3
2	2	2	1
3	2	2	3
4	2	2	0
5	10	5	>2
6	13	10	6
7	4	4	2
8	12	7	4
9	2	2	0
10	5	4	0
11	6	6	0
12	4	3	2
13	7	5	3
14	7	5	>2

To sum up: the evidence is strong that the multiple meson production mechanism operates at sufficiently high energies and with increasing

---

in the hydrogen. The authors ascribe these events to multiple meson production in proton-proton collisions, although the possibility that the less abundant heavy nuclei colliding with the hydrogen nuclei are responsible for the observations is not ruled out.

multiplicity.[41a] No theory of multiple meson production proposed thus far appears capable of explaining all features of very energetic penetrating showers, at least if it is assumed that the events are produced in single nucleon-nucleon encounters. It is to be expected from the approximately geometrical cross section for the production of penetrating showers that plural processes will take place, the more so the heavier the nucleus. In the energy region 5×10^9 to 5×10^{11} ev the plural mechanism seems to be chiefly responsible for the sizable multiplicities observed, at least from heavy nuclei. At energies greater than 10^{11}, or better 10^{12}, the multiple production mechanism assisted by the plural mechanism apparently determines the characteristic features of penetrating showers.

7. Auger Showers

In this final section, we consider Auger showers which, under a different guise, must, in the light of recent knowledge, be nothing more than the latest stage in the development of the most energetic penetrating showers produced by the primary cosmic radiation. The initial investigations of the extensive air showers, or Auger showers, as they are called, were carried out by Auger and his collaborators.[42] In experiments carried out with trays of counters separated by many meters and operating in coincidence, Auger *et al.* were able to establish the existence of extensive air showers with the following characteristics: (1) extension over many hundreds of meters; (2) extremely large total numbers of particles having the properties of the soft component of the cosmic radiation, *i.e.*, electrons and photons; and (3) large amounts of energy in the shower derived on the basis of the well-established cascade theory of electron-photon shower development.[43] More recent experiments have[44] shown that an Auger shower contains a small percentage of charged penetrating particles—of the order of 1.5 to 2.5 per cent depending on the energy of the shower—the ratio slowly increasing by a factor of 2 with increasing distance from the core of the Auger shower. It has also been shown that the penetrating particles consist of both μ mesons and N component (nucleons and π mesons), the former becoming more prevalent at the larger distances.

[41a] Recent systematic work on meson production at high energies covering the range $10^{11} - 10^{13}$ ev [cf. E. Pickup and L. Voyvodic, *Phys. Rev.*, **84**: 1190 (1951) and M. Kaplon and D. Ritson, *Phys. Rev.*, **85**: 932 (1952)] indicates that the multiplicity increases as the one-fourth power of the incident nucleon energy.

[42] Auger, Maze, and Grivet-Meyer, *Compt. rend.*, **206**: 1721 (1938).

[43] B. Rossi and K. Greisen, *Rev. Mod. Phys.*, **13**: 240 (1941).

[44] J. Treat and K. Greisen, *Phys. Rev.*, **74**: 414 (1948); Cocconi, Tongiorgi, and Greisen, *Phys. Rev.*, **75**: 1063 (1949); **76**: 1020 (1949); J. Ise and W. Fretter, *Phys. Rev.*, **76**: 933 (1949); W. Brown and A. McKay, *Phys. Rev.*, **76**: 1034 (1949); C. McCusker and D. Millar, *Proc. Phys. Soc.*, **64A**: 915 (1951); G. M. Branch, *Phys. Rev.*, **84**: 147 (1951).

Any hypothesis concerning the origin of Auger showers must explain not only the above features but also the lateral structure of Auger showers (*i.e.*, the variation of soft component and penetrating particle density with distance from the shower axis), dependence of shower characteristics upon the altitude of observation, etc. These tests are quite stringent and serve to rule out several of the original hypotheses invented to explain the origin of Auger showers. Thus one of the original hypotheses concerning the origin of Auger showers was that they are initiated by a small admixture of electrons in the primary cosmic radiation. However, Hulsizer[45] found that less than 1 per cent of the particles of the primary cosmic radiation, energetic enough to be responsible for Auger showers, are of electronic nature. In addition, Feenberg and Primakoff[46] have shown that, even if electrons were primary cosmic-ray particles, if they were of extragalactic origin, they would be sufficiently reduced in energy by collisions with photons in intergalactic space to be effectively removed from the primary cosmic-ray beam. Finally, Mills[47] has shown that a plot of the frequency of extensive air showers vs. altitude of observation reaches a maximum at too low an altitude compared with experiment[48] on the assumption that the initiating particle of an Auger shower is an electron. Similar arguments can be applied against a photonic origin of Auger showers.

Even if it is granted that the primary protons and, to some extent, the primary heavy nuclei are responsible for Auger showers, the question still remains by what mechanism. It can readily be shown that the generation of Auger showers by protons via a bremsstrahlung mechanism —through either the charge acceleration of the proton[49] or the production of charged π mesons[50]—cannot work. Since the R and T stars have shown that large numbers of γ rays and therefore of π^0 mesons are produced in nuclear collisions (in addition to large numbers of penetrating particles) at energies of 10^{12} to 10^{13} ev and since many experiments[51] have shown that every large shower of penetrating particles in air is accompanied by extensive showers of photons and electrons, it is natural to conclude that Auger showers originate in collisions of the most energetic protons and heavy nuclei of the primary cosmic radiation with air nuclei.

---

[45] R. Hulsizer, *Phys. Rev.*, **73**: 1252 (1948); cf. also Critchfield, Ney and Oleska, *Phys. Rev.*, **85**: 461 (1952) and M. Kaplon and D. Ritson, *Phys. Rev.* in press.

[46] E. Feenberg and H. Primakoff, *Phys. Rev.*, **73**: 449 (1948).

[47] M. M. Mills, *Phys. Rev.*, **74**: 155(A) (1948), also Ph.D. Thesis, California Institute of Technology, 1948; cf. also J. R. Oppenheimer, *Phys. Rev.*, **71**: 462 (1947).

[48] Cf. H. Kraybill, *Phys. Rev.*, **73**: 632 (1948).

[49] S. Hayakawa, *Phys. Rev.*, **75**: 1759 (1949).

[50] Schiff, *loc. cit.*

[51] Cf. Cocconi, Loverdo, and Tongiorgi, *Phys. Rev.*, **70**: 852 (1946).

On this explanation, the soft component of an Auger shower is the electron-photon cascade of the decay γ rays arising from the π^0 mesons[47] produced in the initial nuclear collision at the top of the atmosphere, and the penetrating component is the result of a nucleonic cascade of the charged π mesons and nucleons produced in the same event.

The hypothesis that an Auger shower represents a late stage in the development of a very energetic penetrating shower can account for all the qualitative features which are observed: the numbers of particles and energies, the lateral structure, etc. Thus this hypothesis can account for the findings of Blatt,[52] who notes that the decoherence function observed at distances[53] of 2 to 20 m (defined as the coincidence counting rate for two ionization chambers as a function of their separation) rises less steeply than the cascade theory of Moliere,[54] based on the assumption that one electron or photon initiates the Auger shower at the top of the atmosphere, would predict. Blatt's suggestion that the discrepancy between theory and experiment is due to an underestimate of the age of the shower as it reaches the ionization chambers would be in line with the idea that a sizable multiplicity of π^0 mesons and therefore of γ rays are responsible for the Auger shower. The π^0 meson hypothesis would yield, by a similar argument, better agreement between Mills's theoretical calculations and the experimental evidence on the variation of the frequency of extensive air showers with altitude. Since Mills underestimated the age of the showers in his calculations, so the argument would go, the maximum in the plot of the frequency of extensive air showers vs. altitude should occur at a higher altitude than that predicted by Mills, and this is actually observed. The experiment of Williams[53] would, at first sight, appear to provide evidence against the π^0 meson hypothesis, since multiple cores (associated with the multiple origin of the π^0 mesons produced in the initial nuclear interaction) are not detected in Auger showers (at mountain altitudes) at counter separations greater than 1 m. Further reflection soon convinces one, however, that the large multiple Coulomb scattering of the electrons in Auger showers observed at mountain altitudes under the conditions of Williams's experiment will wash out any multiple-core effects which may exist in the high atmosphere. As a matter of fact, the *T* star discussed earlier gives definite evidence for the existence of multiple cores in Auger showers having energies of 10^{13} to 10^{14} ev and even shows how the multicore structure is washed out after several radiation lengths.

---

[52] J. M. Blatt, *Phys. Rev.*, **75**: 1584 (1949).

[53] R. W. Williams, *Phys. Rev.*, **74**: 1689 (1948). Cf. also W. E. Hazen, *Phys. Rev.*, **85**: 455 (1952); and I. Campbell and J. Prescott, *Proc. Phys. Soc.*, **65A**: 258 (1952).

[54] G. Moliere, Chap. 3 of "Cosmic Radiation," ed. by W. Heisenberg, Dover Publications, 1946.

We have stated that the penetrating component of Auger showers can be explained as a nucleonic cascade of the initially produced π mesons and nucleons. Since Auger showers have been observed with as many as 10^8 electrons (deduced on the basis of the Moliere structure function which also predicts a corresponding minimum energy of 10^{17} ev), the observation of 1.5 to 2.5 per cent penetrating particles implies that there are as many as $10^6 \mu$ mesons, π mesons, and nucleons in the largest Auger showers. Such a high multiplicity of meson production in the initial encounter with the air nucleus, even at an energy of 10^{17} ev, is very unlikely, and it seems reasonable to assume that the initially produced nucleons and π mesons multiply during the course of their traversal through the atmosphere. It is easy to understand a cascade multiplication (by both nucleons and π mesons) of the magnitude required, assuming geometrical interaction cross sections for both π mesons and nucleons. It should be noted that the nucleonic cascade will be disrupted at π meson energies of approximately 10^{11} ev, since below this energy, π mesons will preferentially decay into μ mesons rather than suffer further nuclear collisions; this transition energy is arrived at by setting the mean free path for decay equal to the geometrical mean free path, that is, $c\tau_0 \mu c^2/\epsilon \approx \lambda_{\text{geom}}$, where ϵ is the energy of the π meson, μ its rest mass, and $\tau_0 = 2.5 \times 10^{-8}$ sec, its lifetime for decay at rest. In this fashion, the presence of μ mesons, π mesons, and nucleons in Auger showers can be understood qualitatively, although no precise quantitative calculations have as yet been performed. The hypothesis that an Auger shower is a late stage in the development of a very energetic penetrating shower may also account for the fact that the ratio of the number density in the penetrating component to that in the soft component increases with increasing distance from the shower axis if the π mesons are produced with a large anisotropy in the center-of-mass system. A strong anisotropy results in narrow cores and diffuse showers of neutral and charged π mesons. The diffuse shower will contain the lower energy π^0 mesons, and the electron showers initiated by the decay γ rays from these lower energy π^0 mesons will not reach the point of observation of the Auger showers, whereas the penetrating particle cascade will. As a result, only the relatively narrow electron showers within the central core of the original nuclear star will be observed in the Auger shower, whereas both the narrow and wide penetrating showers will be detected. It should be possible to test this auxiliary hypothesis and to establish whether multiple meson production is strongly anisotropic at the highest energies available in the primary cosmic radiation.

CHAPTER 9

NEW PARTICLES AND NEW PROCESSES

1. Introduction

In the preceding chapters we focused our attention on the two types of mesons whose existence has been established beyond doubt. The π meson (both charged and neutral), in particular, has been the central object of our study. As we considered one type of experiment after another in which the π meson was involved, we were able to sharpen our conclusions, and we can now say that the π meson is strongly coupled to the nucleon, that the field describing it is pseudoscalar, and that its coupling to the nucleon is probably of the gradient type.[1] This much seems clear; although no self-consistent $PS(PV)$ theory has been developed, the theoretical concepts which were employed in our effort to understand the experimental material appear to give relatively correct qualitative answers at nonrelativistic nucleon energies. At relativistic nucleon energies, these theoretical concepts are certainly inadequate, and no alternative theory which is fully convincing has as yet been propounded. The μ meson turned out to be weakly coupled to nucleons, π mesons, and electrons and to possess all the properties of a Dirac particle.

For both π and μ mesons, the picture which emerged out of our discussion contained many elements of clarity, and it seemed not overly optimistic to hope that we were at least on our way toward a deeper understanding of nuclear forces and of the nature of elementary particles. The illusoriness of this hope has been underlined by several recent cosmic-ray discoveries which have added several types of heavy mesons (τ, κ, χ, ζ, etc.) and at least one type of particle with mass intermediate between the proton and the deuteron (the so-called V particle) to the list of elementary particles. Both the heavy mesons and the V particle will probably become indispensable components of the meson story—the mesons playing an essential role in the future correct theory of nuclear forces and the V particle revealing in a decisive fashion the character of the couplings which characterize meson-nucleon interactions. We have theoretical indications for the existence of a third new class of particles, *viz.*, the antinucleons, although no clear-cut experimental evidence for

[1] Cf. footnote 1*a* of Chap. 8.

their existence has been obtained as yet. We shall first treat the antinucleons, then the heavy mesons, and finally the *V* particles.

2. Production and Annihilation of Antinucleons

Almost all the meson-theoretic calculations discussed in the preceding chapters were based on the assumption that the proton and neutron are particles obeying the Dirac equation.[1a] This assumption, in analogy with electron-positron theory, implies the existence—in real as in virtual states—of antiprotons and antineutrons. Especially in a theory like the *PS*(*PS*) theory for the π meson-nucleon interaction, the negative-energy states of the Dirac equation for the nucleon play an essential role since the operator in the interaction Hamiltonian is odd and couples positive- and negative-energy states. In the *PS*(*PV*) theory, the dominant term in the interaction is even and it can be argued, without changing the qualitative predictions for most processes,[2] that the negative-energy states are nonexistent. However, one process which was discussed in Chap. 4, *viz.*, the rapid decay of the neutral π meson into two γ rays, offers a striking qualitative argument in support of the existence of virtual antinucleons even though the agreement between the experimentally measured lifetime of the π^0 meson and the theoretically predicted value is not especially impressive (cf. Chap. 4). The assumption that the π^0 meson decays through the virtual creation of a proton-antiproton pair which subsequently annihilate with the emission of two γ rays seems to provide a natural interpretation of this particular process. Thus the evidence for the existence of antinucleons is indirect and cannot be regarded as conclusive—putting aside for the moment all theoretical arguments based on the symmetry of nature, etc.[3] It is therefore of interest to consider the production mechanism for antinucleons and their characteristic properties once they are produced which would make their direct detection possible.

Similar to the case of electron-pair production by photons, an antinucleon will be produced when a nucleon in a Dirac negative-energy state is raised to a positive-energy state leaving a hole, *i.e.*, an antinucleon; this means that the production of an antinucleon will simultaneously lead to the production of its nucleon counterpart, *i.e.*, a proton and an antiproton, a neutron and an antineutron. The most promising mechanism for the production of nucleon-antinucleon pairs is nucleon-nucleon collisions, whether in the cosmic radiation or in the future Berkeley bevatron. When a nucleon-antinucleon pair is produced in a nucleon-nucleon collision, the final state will consist of four particles each possessing mass M. In order to calculate the threshold energy at which nucleon-antinucleon pair production can take place, it is necessary to have recourse to Eq. (37) of Chap. 8. If γM (M is the nucleon mass) is the energy of the incident nucleon in the laboratory system (including its rest mass), $\sqrt{(\gamma + 1)/2}$ is the energy of each nucleon in the center-of-mass system; at threshold, the nucleon-antinucleon pair has zero kinetic energy[4] so that $\sqrt{(\gamma + 1)/2} = 2$ and $\gamma = 7$. In other words, the incident nucleon must possess a kinetic energy[5] of at least $6\ M = 5.6$ Bev in order to produce a nucleon-antinucleon pair in a collision with a target nucleon at rest. Because of the high threshold energy, the finite nucleon momenta in a complex nucleus will not appreciably lower the threshold as was the case in π meson production [where the threshold energy was decreased by a factor of 2—cf. Eq. (1) of Chap. 3]; thus using the Fermi energy of 22 Mev for a nucleon and assuming the most favorable circumstances, *i.e.*, the 22-Mev nucleon moving in an equal and opposite direction to the incident nucleon, the threshold is reduced to 4.6 Bev.

[1a] From this point of view, the anomalous magnetic moments of the proton and neutron are ascribed to virtual meson currents (for which a correct quantitative theory is still absent) or are treated phenomenologically in accordance with Pauli's formulation (cf. Chap. 1).

[2] *E.g.*, the slow π^- meson reactions in hydrogen and deuterium appear to require the existence of virtual negative-energy states, at least in the weak coupling theory, since the even part of the *PS*(*PV*) operator vanishes at zero energy. However, it will be recalled that the weak coupling theory is quantitatively least successful in explaining these particular reactions (cf. Chap. 4).

[3] Cf. H. J. Bhabha, *Rev. Mod. Phys.*, **17**: 200 (1945).

Apart from the fact that the production of nucleon-antinucleon pairs in nucleon-nucleon collisions is a fourth-order process (in the perturbation-theoretic sense) and very complicated to calculate even in the weak coupling approximation,[6] the high threshold energy makes the applicability of weak coupling theory very dubious. It seems more appropriate to quote the predictions of Fermi's simple statistical theory[7] for the process in question. At energies above 5.7 Bev, Fermi's statistical theory for multiple π meson production (cf. Chap. 8) should be equally applicable to nucleonic pair formation. Fermi finds the following expression for the probability of nucleon pair creation accompanied by n π mesons:

---

[4] Cf. H. Feshbach and L. Schiff, *Phys. Rev.*, **72**: 254 (1947).

[5] The threshold energies in photon-nucleon and π meson-nucleon collisions are $4M = 3.7$ Bev and $2(2M + \mu) = 4.0$ Bev (μ is the π meson mass), respectively, which are lower than in nucleon-nucleon collisions. However, the intensities in the cosmic radiation of γ rays and π mesons of appropriate energies and at suitable altitudes (cf. below) are much lower than the intensity of the nucleonic component.

[6] Cf. C. W. Helstrom, *Phys. Rev.*, **78**: 88 (1950); and M. Taketani and S. Machida, *Prog. Theor. Phys.*, **6**: 559 (1951).

[7] E. Fermi, *Prog. Theor. Phys.*, **5**: 570 (1951).

$$P_{\text{pair}}(n) = \frac{105}{\bar{W}}\left[6.3\,\frac{(\bar{W}-4)}{\bar{W}^{\frac{1}{3}}}\right]^{3n+\frac{7}{2}}\frac{\exp\left[-6.3(\bar{W}-2)/\bar{W}^{\frac{1}{3}}\right]}{(3n+\frac{7}{2})!} \tag{1}$$

Table 1 lists the probabilities of nucleon pair formation accompanied by the emission of up to four π mesons, neglecting statistical correlations and conservation of angular momentum (cf. Table 4 of Chap. 8). However, the qualitative features of Table 1 would not be modified by the more accurate treatment, and it is seen that, even at nucleon energies as high as 20 Bev, the probability of nucleon pair formation is only 0.005; since at this energy probably an average of two or three π mesons are also created, it follows that the ratio of the number of antinucleons to the number of π mesons at normal cosmic-ray energies is less than 10^{-3}. At extremely high energies, say greater than 5×10^{12} ev, Fermi's theory predicts a much more favorable ratio for the number of antinucleons compared with the number of π mesons. As a matter of fact, we have seen in Chap. 8 that, at sufficiently high energies where the relativistic thermodynamic model can be used for both nucleons and π mesons, Fermi's theory predicts a somewhat larger number of antinucleons than of π mesons (because of the greater statistical weight of the spin $\frac{1}{2}$ nucleons and antinucleons compared with the spin 0 π mesons). Unfortunately, the primary cosmic radiation contains a very small intensity of extremely high energy nucleons so that the outlook for observing the hypothetical antinucleon in the stratosphere is not too hopeful. One may have to await the completion of the Berkeley bevatron before it will be possible to establish the existence or nonexistence of the elusive antinucleons.

TABLE 1. FERMI'S PREDICTIONS FOR THE PRODUCTION OF ANTINUCLEONS TOGETHER WITH π MESONS
(Columns 3 to 7 inclusive $\times 10^{-4}$)

$\bar{W}$	W	$n = 0$	$n = 1$	$n = 2$	$n = 3$	$n = 4$	Total
$4 + \delta$	7.0	$1000\delta^{\frac{7}{2}}$					$0.1\delta^{\frac{7}{2}}$
4.5	9.1	14	0.6				15×10^{-4}
5.0	11.5	27	8	0.7			36×10^{-4}
5.5	14.3	21	21	5	0.5		47×10^{-4}
6.0	16.9	12	25	14	3	0.3	54×10^{-4}

Supposing that an antinucleon is produced in a nucleon-nucleon collision, the question still remains as to its mode of detection. Of course, one way of detecting the charged antinucleon, *i.e.*, the negative proton as it is called, is to measure its mass and charge (*e.g.*, using a cloud chamber in a magnetic field); this is extremely difficult to accomplish in a cosmic-ray experiment because of the extremely low intensities expected, although it may be possible with the bevatron. Moreover, there should be very little difference in the behavior of the nucleon and the antinucleon with respect to collision processes in which the total number of nucleons does not change. Fortunately, there is one essential difference between the nucleon and antinucleon which should make feasible the detection of the antinucleon, *viz.*, the antinucleon can initiate an annihilation event in combination with a nucleon. It is well known that a positron will annihilate a free electron (or one which is loosely bound) and produce two γ rays. If the positron traverses ordinary matter it will be slowed down to essentially zero energy before it will be annihilated, and consequently positron-electron annihilation will lead to the creation of two γ rays moving in equal and opposite directions, each with an energy m_ec^2. Single γ emission will occur with only appreciable probability when the electron is strongly bound to a nucleus with a binding energy comparable with the electron rest energy, *e.g.*, an electron in the K shell of a heavy element. The emission of three or more γ rays will be much less probable than the emission of two γ rays because of the small value of the fine-structure constant.

The annihilation of an antinucleon by a nucleon has some features in common with positron-electron annihilation but there are also significant differences. The nucleons have strong interactions with the π meson field, much stronger than with the electromagnetic field, and consequently the annihilation process should give rise to a pair of π mesons rather than to a pair of γ rays. The following annihilation reactions should take place between protons, antiprotons, neutrons, and antineutrons:

$$P + \bar{P} \rightarrow \pi^+ + \pi^- \tag{I}$$
$$P + \bar{P} \rightarrow 2\pi^0 \tag{II}$$
$$N + N \rightarrow \pi^+ + \pi^- \tag{III}$$
$$N + N \rightarrow 2\pi^0 \tag{IV}$$
$$P + \bar{N} \rightarrow \pi^+ + \pi^0 \tag{V}$$
$$N + \bar{P} \rightarrow \pi^0 + \pi^- \tag{VI}$$

Reaction (II) has perhaps the closest correspondence to positron-electron annihilation, but the other reactions are also possible because of the existence of two types of nucleons and three varieties of π mesons (positive, negative, and neutral). A simple estimate indicates that the binding of a nucleon in a nucleus is not sufficiently strong to make one-meson annihilation a serious competitor to two-meson annihilation. It is somewhat more difficult to make a positive assertion about the relative probability of three- and higher-meson annihilation compared with two-meson annihilation, although it is perhaps safe to say that two-meson annihilation would not be greatly overbalanced by multiple-meson annihilation since, as we have seen in Chap. 8, a small multiplicity for π meson production in nucleon-nucleon collisions is indicated at normal cosmic-ray energies. In contrast to electron-pair annihilation, nucleon-pair annihilation may take place with sufficient cross section (perhaps close to geometrical) at finite kinetic energies so as to make annihilation in flight compete on favorable terms with annihilation at rest.

It is possible to calculate the cross section for nucleon-pair annihilation in flight in the weak coupling approximation using the *PS*(*PV*) theory for the π meson field.[8] However, the expressions turn out to be very complicated and are almost certainly unreliable since the π mesons are emitted with such high energies. We shall not record these cross sections here but merely note two kinematical features of the nucleon-pair annihilation in flight which are of particular interest: first, it follows from momentum conservation that, if the nucleon with which an antinucleon annihilates is at rest, the momenta of the antinucleon and the final two π mesons will all lie in the same plane. Secondly, since the velocity of the two π mesons in the center-of-mass system of the nucleon pair will, in general, be greater than the velocity of the center-of-mass system itself with respect to the laboratory system, the chances are excellent that one of the mesons resulting from the annihilation process will be emitted backward in the laboratory system. Both these kinematical features will provide, except for some qualifications, fairly clear-cut criteria for distinguishing the antinucleon from an ordinary nucleon, particularly antiprotons annihilating with protons in photographic emulsions. The qualifications are: the binding of the proton in one of the complex nuclei of the emulsion destroys to some extent the coplanar relationship which should otherwise exist among the tracks of the incident antiproton and the two emergent charged π mesons; an estimate indicates that the deviation from coplanarity due to this effect is on the average $< 5°$. Nucleon-pair annihilation events in the photographic emulsion may also be complicated by the presence of a small evaporation star arising from the excitation of the residual nucleus after the sudden removal of one of its protons; however, the excitations, of the order of 30 Mev, which would result in this way would not lead to any sizable stars. Finally, it should be remarked that the large cross section for nuclear interaction of the two outgoing π mesons will make it quite difficult to distinguish annihilations in flight from other events in which several mesons are produced.

A more promising method for detecting antiprotons, at least in photographic emulsions, is to look for annihilation events initiated by very low energy antiprotons, *i.e.*, annihilation at rest. Such events would be characterized by the presence of a slow singly charged particle suddenly changing into two minimum ionization tracks (representing two 931-Mev π mesons) moving in opposite directions [reaction (I)]. It can readily be shown (at least in weak coupling theory, although the qualitative predictions probably have more general validity) that the annihilation reactions (I) and (III) have cross sections varying as $1/v$ in the limit of zero velocity for the antinucleon. In the same limit, the cross sections for reactions (II) and (IV) vanish because of a cancellation of matrix elements; this cancellation does not occur in positron annihilation at rest[9] because the photon possesses spin 1 (in contrast to the π^0 meson, which possesses spin 0). For the annihilation reactions (V) and (VI), the cross sections vanish or vary as $1/v$, depending on the relative signs of the neutral mesic charges of neutron and proton. The $PS(PV)$ weak coupling expressions for the annihilation cross sections (I) to (VI) (cf. above) are so simple that we write them down[8]

---

[8] Cf. Ashkin, Auerbach, and Marshak, *Phys. Rev.*, **79**: 266 (1951).

$$\sigma\ (\mathrm{I,\ III}) \rightarrow \frac{\pi}{v}\left(\frac{Mf^2}{\mu^2}\right)^2 \tag{2}$$

$$\sigma\ (\mathrm{II,\ IV}) \rightarrow 0 \tag{3}$$

$$\sigma\ (\mathrm{V,\ VI}) \rightarrow 0 \qquad (f_P = f_N) \tag{4a}$$

$$\sigma\ (\mathrm{V,\ VI}) \rightarrow \frac{4\pi f_P^2 f^2 M^2}{v\mu^4} \qquad (f_P = -f_N) \tag{4b}$$

$$\sigma(P + \bar{P} \rightarrow 2\gamma) \rightarrow \frac{\pi e^4}{vM^2} \tag{5}$$

We have also recorded the cross section (in the limit of zero velocity) for the annihilation of a proton pair with the emission of two γ rays. Hence, while the annihilation of proton-antiproton pairs and neutron-antineutron pairs with π^0 emission will be dominated by γ ray emission in the limit of zero velocity, this is not the case for charged π emission, contrary to a statement by McConnell.[10]

Since the cross section for reaction (I) varies as $1/v$ at low velocities, the lifetime for annihilation is independent of the velocity and becomes

$$\frac{1}{\tau} = \frac{N\pi f^4 M^2}{\mu^4} \tag{6}$$

---

[9] Cf. W. Heitler, "The Quantum Theory of Radiation," Oxford University Press, 1947.

[10] J. McConnell [*Proc. Roy. Irish Acad.*, **50A**: 189 (1945); **51**: 173 (1947)], using Heitler's method of radiation damping finds the contrary result; the discrepancy cannot be a consequence of the neglect of radiation damping, which should become unimportant at low energies, and McConnell's results must be incorrect (cf. reference 8 and Taketani and Machida, footnote 6).

where N is the number of protons per unit volume. For a photographic emulsion, N is of the order of $10^{24}/\text{cm}^3$ and if we set $f^2/\hbar c \approx 0.3$, $\tau \approx 2 \times 10^{-10}$ sec; this is to be compared with 10^{-10} sec [cf. Eq. (2) of Chap. 5], the time taken by an antiproton to be slowed down from an energy of about 5 Mev, say, to its eventual capture in an orbit about some nucleus. The annihilation lifetime is longer, and we would therefore expect that most antiprotons reaching low energies would be annihilated after being captured in orbits because the lifetime for annihilation from the K shell of carbon, say, can easily be shown to be 2×10^{-24} sec, by inserting for N in Eq. (6) the reciprocal volume of a sphere of radius equal to that of the K shell multiplied by the number of protons in the given nucleus. However, it should be realized that the lifetime given in Eq. (6) depends on a high power of the π meson-nucleon coupling constant and that the weak coupling theory is probably unreliable even in the limit of zero velocity; it is therefore quite possible that most antiprotons would be annihilated before capture in atomic orbits. Fortunately, the visible aspects of the annihilation event would remain unchanged, independent of whether the annihilation takes place from an orbit or while in flight at low energies; in either case, we would have an annihilation at rest.

To sum up, we can say that present-day theory and some indirect experimental evidence (*i.e.*, the π^0 decay) argue for the existence of antinucleons. All reasonable estimates indicate extremely small cross sections for nucleon-antinucleon pair production, except at very high energies (of the order of 10^{12} to 10^{13} ev) where the cosmic-ray intensities are extremely small. Antinucleons will therefore be rare objects. However, if antinucleons actually do exist, their detection should be possible in cloud chambers through a measurement of their mass and charge or in photographic emulsions through an observation of their characteristic annihilation processes, either in flight or at rest.

3. Heavy Mesons

Ever since the existence of two types of mesons was established, and even before,[11] claims have been made for the existence of mesons with masses intermediate between the π meson and the proton. The claims were generally based on the observation of one or two peculiar tracks[12] either in a cloud chamber or in a photographic emulsion. Thus, LePrince-Ringuet and Lheritier[11] observed an unusual scattering of a cosmic-ray particle by an electron in a cloud chamber operated in a magnetic field and deduced a mass of 990 ± $120m_e$ for the particle. Later, LePrince-Ringuet[13] noticed one particle which appeared to come to rest in a photographic emulsion and to end in a nuclear star containing one π^- meson (identified by the star it produced) and five other prongs; the inferred mass of the particle was $> 700m_e$. A similar event, *i.e.*, an especially large star (containing one emerging meson) produced by a particle allegedly coming to rest in a photographic emulsion, was observed by Forster.[14] Another type of observation was made by Wagner and Cooper[15] in which they measured the grain density vs. residual range of particles emerging from nuclear stars and found evidence for three particles with an average mass of 725 ± $40m_e$.

---

[11] L. LePrince-Ringuet and M. Lheritier, *Compt. rend.*, **219**: 618 (1944).

[12] More systematic counter evidence for the existence of many kinds of heavy mesons (called varitrons) has been presented by Alichanian, Alichanov, and Weissenberg [*J. Expl. Theoret. Phys. U.S.S.R.*, **18**: 301 (1948)]. The arguments against this evidence are given in C. F. Powell, *Reports on Progress in Physics*, **13**: 350 (1950).

The diversity of the phenomena with which a presumed heavy meson appeared to be associated and the fact that at first a systematic study of the masses of particles emitted from nuclear stars failed to reveal any masses intermediate between the π meson and the proton[16] placed the isolated pieces of evidence for a heavy meson on a very uncertain footing. However, recently a total of five self-consistent examples of a heavy particle disintegrating into three ionizing particles have been found in photographic emulsions by three independent groups of workers, which argues strongly for the existence of at least one charged heavy meson (designated the τ meson). Table 2 lists the pertinent data for four of these five elements: column 1 the observer, columns 2 to 4 the measured masses of the three decay particles in units of m_e, column 5 the total kinetic energy (Q value) carried by the three decay particles, column 6 the deduced mass of the τ meson assuming that the decay products are all π mesons and using the Q value of column 5, and column 7 the mass of the τ meson which is directly measured by grain density and scattering. The average value of the τ meson mass derived from column 6 of Table 2 is 974 ± $10m_e$ (assuming $m_\pi = 276m_e$—cf. Chap. 4) and is in satisfactory agreement with the less accurate direct measurements of the τ meson mass. All four events considered in Table 2 have the common property that the tracks corresponding to the decay particles a, b, and c are all coplanar and are all consistent with a decay into three π mesons. There is no direct evidence for the sign of charge of the τ meson, although it is probably positive. A lower limit for the lifetime of the τ^+ meson

---

[13] L. LePrince-Ringuet, *Rev. Mod. Phys.*, **21**: 42 (1949); cf. also LePrince-Ringuet, Fong, Jauneau, and Morellet, *Compt. rend.*, **226**: 1897 (1948).

[14] H. Forster, *Phys. Rev.*, **77**: 733 (1950).

[15] N. Wagner and D. Cooper, *Phys. Rev.*, **76**: 449 (1949).

[16] P. H. Fowler, *Phil. Mag.*, **41**: 169 (1950); cf. also C. Franzinetti, *Phil. Mag.*, **41**: 86 (1950).

TABLE 2. DATA ON THE τ MESON

Observer	Masses of the decay particles			Q value, Mev	Mass of τ meson	
	(a)	(b)	(c)		Q value	Direct measure
Brown *et al.*[17]	276*	280 ± 30	$m_c/m_b = 1.02 \pm 0.10$	65 ± 8	955 ± 17	990 ± 270‡ 1080 ± 16§
Harding[18]	1	1.1 ± 0.15	1 ± 0.1	85 ± 15	995 ± 31	
Fowler *et al.*[19]	285 ± 20†	0.88 ± 0.11	1.03 ± 0.05	75 ± 5	975 ± 11	1015 ± 280‡ 910 ± 220§
Hodgson[20]	....	....	....	73.5 ± 7	972 ± 15	

* Identified as a π^- meson by the star it produces.
† From grain density and scattering.
‡ From scattering and range.
§ From grain density and range.

can be derived from the fact that the τ^+ meson decays at rest[20a] and that the slowing-down time is of the order of 5×10^{-11} sec [cf. Eq. (2) of Chap. 5]; from considerations of the frequency of occurrence of τ mesons,[21] it is likely that the lifetime is as high as 10^{-9} sec. The event observed by LePrince-Ringuet[13] in a photographic emulsion, *viz.*, the disintegration of a nucleus with the emission of one π^- meson by what appears to be a negative particle with mass intermediate between the π meson and the proton, may be an illustration of what happens to a τ^- meson when it comes to rest in matter. No real measurements of the relative abundance of τ and π mesons exist as yet, although it would be surprising if this figure turns out to be greater than 1 per cent at normal cosmic-ray energies ($\sim$ 10 Bev).

What is strange at first sight about the τ meson is not that it exists—after all there is no a priori principle which dictates that only one meson strongly coupled to the nucleon field, *viz.*, the π meson, should exist in nature and from the point of view of a satisfactory meson theory of nuclear forces the τ meson may serve an indispensable function (cf. Chap. 2)—but rather that it decays into three π mesons rather than into two π mesons or into one π meson and one ray. Since the τ meson decays into three π mesons, it must be a boson, and it is plausible to assume that it is strongly coupled to the nucleon field. If a meson is strongly coupled to nucleons and if the explanation of the decay of the π^0 meson into two γ rays lies in the virtual creation of a proton-antiproton pair which subsequently annihilate to produce the two γ rays, then a similar mechanism should lead to the decay of a τ meson into a charged and neutral π meson (I) or into a charged π meson and a γ ray (II) unless selection rules intervene (cf. below). Now, the measured lifetime of the π^0 meson is 10^{-14} sec (its theoretically predicted value is even shorter—cf. Chap. 4), and it would be expected[22] that the lifetimes of decay processes (I) or (II) would be at least as short (even granting that f_τ^2 is of the order of $(1/100)f_\pi^2$ which must be a lower limit since the threshold for τ meson production is higher than for π meson production—cf. above).

---

[17] Brown, Camerini, Fowler, Muirhead, Powell, and Ritson, *Nature*, **163**: 82 (1949).

[18] J. B. Harding, *Phil. Mag.*, **41**: 405 (1950).

[19] Fowler, Menon, Powell, and Rochat, *Phil. Mag.*, **42**: 1040 (1951).

[20] P. E. Hodgson, *Phil. Mag.*, **42**: 1060 (1951).

[20a] Recently, two τ mesons have been observed to decay in flight inside a cloud chamber [R. Leighton and S. Wanlass, *Phys. Rev.*, **86**: 426 (1952)]; the mass is deduced to be $975m_e$ and the lifetime $\gtrsim 10^{-9}$ sec—in agreement with the photographic experiments.

[21] C. O'Ceallaigh [*Phil. Mag.*, **42**: 1032 (1951)] has observed 1 τ meson in a volume of emulsion in which 750 π mesons were recorded.

The above statement is true, provided that no parity and angular momentum selection rules enter to restrict the decay possibilities of the τ meson. Thus suppose the parities of the τ and π mesons are opposite, then process (I) would be completely forbidden. On the other hand, process (II) can be completely forbidden by a suitable choice of the spin of the τ meson. Indeed, since the π meson is known to be pseudoscalar, a pseudoscalar field for the τ meson would forbid both processes (I) and (II), and this is a unique assignment. Although a pseudoscalar field for the τ as well as the π meson would forbid the two-particle decay processes, the three-particle decay processes would be allowed, namely,

$$\tau \rightarrow 3\pi \tag{III}$$
$$\tau \rightarrow \pi + 2\gamma \tag{IV}$$

Calculations[22] of the theoretical lifetimes associated with the three-particle decay processes (III) and (IV) are all consistent, within the theoretical uncertainties (there are divergences and some form of cutoff procedure must be used), with the observed lower limit of the τ meson lifetime, namely, 5×10^{-11} sec. The theoretical calculations do not unequivocally predict that process (IV) will be less probable than process (III), although the observations indicate that this is the case. Moreover, neither theory nor experiment yields a very accurate value of the

---

[22] Cf. S. Power, *Phys. Rev.*, **76**: 865 (1949); C. B. Van Wyck, *Proc. Phys. Soc.* **62A**: 697 (1949); **63**: 350 (1950); S. Osaki, *Prog. Theor. Phys.*, **5**: 373 (1950); Fukuda, Hayakawa, and Miyamoto, *Prog. Theor. Phys.*, **5**: 282; **5**: 352 (1950); Sasaki, Oneda, and Ozaki, *Prog. Theor. Phys.*, **5**: 25; **5**: 165 (1950).

τ meson-nucleon coupling constant. However, the restriction on the character of the τ meson field (*i.e.*, that it is pseudoscalar) constitutes an important piece of theoretical information.

It should be remarked that no direct experimental evidence for the existence of a neutral τ meson, *i.e.*, a neutral meson with a mass between 900 and 1000 electron masses which decays into three π mesons (three neutral or two charged plus one neutral), has been found;[22a] this is not surprising, since a pseudoscalar τ^0 meson should decay rapidly into 2γ rays, like the pseudoscalar π^0 meson, and this process would be difficult to detect with the low cosmic-ray intensities available.

Recently, evidence has been accumulating for the existence of two superheavy mesons, *i.e.*, mesons with masses intermediate between that of the τ meson and the proton. This evidence is not so conclusive as the evidence for the τ meson, but it does seem convincing nevertheless. Several events (a half-dozen or so) have been found[23] in photographic emulsions exposed to the cosmic radiation which appear to represent the decay of a charged particle possessing a mass of approximately 1100 electron masses (called a κ meson). Two of the events are particularly favorable for experimental analysis; one κ meson decays at rest into a μ meson of 6.9 Mev which subsequently decays into an electron (which decay actually provides the means for identifying the μ meson). It will be recalled that the $\pi \rightarrow \mu \rightarrow e$ sequence of decays is a well-known phenomenon, and it might be thought that this event represents a $\pi \rightarrow \mu$ decay in flight; however, such an interpretation is excluded by the fact the μ meson is ejected backward and not forward as it should be if it represents a $\pi \rightarrow \mu$ decay in flight. The view that one is dealing with a new type of particle is supported by a measurement of the mass of the decaying particle with the usual scattering technique combined with range; the mass of the κ meson turns out to be $1125 \pm 140m_e$. The second κ meson decays at rest into a μ meson of 34 Mev and its mass is consistent with that of the first, namely $1000 \pm 150m_e$. It is possible that some of the so-called S particles[24] observed to come to rest in the lead plates of a cloud chamber and to decay into charged secondaries of mesonic mass are κ mesons.

If it is assumed that all the κ mesons are identical (an assumption which is certainly not forced by the available experimental data), one is led to the plausible decay scheme

---

[22a] Recently, some indirect evidence for the possible existence of τ^0 has been furnished by observations on the χ meson—cf. below.

[23] Cf. C. O'Ceallaigh, *Phil. Mag.*, **42**: 1032 (1951), Crussard, Mabboux, Morellet, Trembley, and Orkin-Lecourtois, *Compt. rend.*, **234**: 84 (1952); and "Report of the International Physics Conference" (Copenhagen, June 3–17, 1952).

[24] Cf. Rossi, Bridge, and Annis, *Rend. Lincei*, **11**: 73 (1951); and Annis, Bridge, Courant, Olbert, and Rossi, *Phys. Rev.*, in press. The majority of S particles are probably χ mesons—cf. below.

$$\kappa \rightarrow \mu + 2\nu \tag{7}$$

Equation (7) is plausible because it allows the μ meson to take on a continuum of kinetic energies from 0 to 200 Mev, a possibility which is consistent with the experimental data. Moreover, Eq. (7) says that the κ meson is a fermion which decays into three lighter fermions in analogy with the decay of the μ meson, which emits the three lighter fermions, $e + 2\nu$. If it is furthermore assumed that the decay of the κ meson is governed by the requirements of the universal Fermi interaction, the predicted lifetime for process (7) is approximately 10^{-9} sec[25]—in accord with the experimental lower limit 5×10^{-11} sec. The universal Fermi interaction hypothesis is not in contradiction to another implication which follows therefrom, *viz.*, that the κ meson should also decay in accordance with the scheme

$$\kappa \rightarrow e + 2\nu \tag{7a}$$

The operation of the universal Fermi interaction would imply that the relative probabilities for μ emission and electron emission are essentially determined by the phase space available to the μ meson and electron, respectively. A simple calculation shows that these phase space factors are roughly comparable and that μ emission and e emission should therefore compete on favorable terms with each other. This is certainly consistent with the meager experimental data. It should be noted that if the decay scheme (7) is correct, the κ meson is a fermion and cannot be produced alone in nucleon-nucleon collisions. It must either be produced together with another fermion or it may be the decay product of a heavier boson, *e.g.*, the χ meson (cf. below).

The second type of superheavy meson which appears to have a fairly definite existence is the so-called χ meson. The Bristol group[25a] has seen three examples of the χ meson in which a particle of mass 1470 $\pm$ $100m_e$ decays into a π meson of unique energy 150 ± 10 Mev. This implies the decay scheme

$$\chi^{\pm} \rightarrow \pi^{\pm} + N^0 \tag{8}$$

where N^0 is a neutral particle with a rest mass of 890 $\pm$ $100m_e$ and may actually represent the neutral counterpart of the τ meson (cf. above). It is possible to set 5×10^{-10} sec as the lower limit on the lifetime of the

---

[25] A. M. L. Messiah, Rochester Report NYO-3036 (1951); cf. also L. Michel and R. Stora, *Compt. rend.*, **234**: 1257 (1952).

[25a] C. F. Powell, "Report of the International Physics Conference" (Copenhagen, June 3–17, 1952).

χ meson. The unique kinetic energy of the π meson resulting from the χ decay corresponds to a unique momentum of 250 Mev/c, and it must be significant that the majority of the secondaries from the S particles possess this momentum[24] as do the secondaries in the rest system of the charged V particles[25b] (cf. Sec. 4). It is also likely that most of the superheavy mesons found[25c] in nuclear interactions above 50 Bev are χ, not κ, mesons. Indeed, it is possible that the less abundant κ meson is an occasional decay product of the χ meson in accordance with the scheme

$$\chi^{\pm} \longrightarrow \kappa^{\pm} + \nu \tag{8a}$$

The apparent copious production of χ mesons at high energies and their subsequent weak interaction through a decay scheme of the form (8a) would create no new theoretical problem; an explanation could be given along the lines of the old two-meson hypothesis[25d] developed for the π-μ case. However, the long lifetime ($> 5 \times 10^{-10}$ sec) associated with the decay of the χ meson into two bosons [Eq. (8)] interacting strongly with nucleons is much more difficult to reconcile with its copious production.[25e]

To confuse the picture even further, there is increasing evidence for the existence of sub-heavy mesons, *i.e.*, mesons with masses intermediate between that of the π meson and the τ meson. There is first the v^0 meson which appears to decay into two charged π mesons and will be discussed in Sec. 4 under V particles. Then there is the ζ meson which occasionally shows up (five cases thus far) as a shower particle in an energetic nuclear interaction[25a,25c] with a mass in the neighborhood of $500m_e$. One such track appears to deviate through 1° after which it continues as a π meson; this particular track leads to a Q value of about 1 Mev and a lifetime $> 10^{-10}$ sec assuming the decay scheme

$$\zeta^{\pm} \longrightarrow \pi^{\pm} + \pi^0 \tag{8b}$$

Leighton and Wanlass[20a] have also seen several particles (three cases) in penetrating showers whose measured masses (by means of curvature and ionization) are in the range 400 to $650m_e$ and are perhaps to be identified with the ζ meson. Unless large statistical fluctuations have occurred in both sets of measurements, the existence of the charged ζ meson seems to be established. On the other hand, claims have also been made for the existence of a ζ^0 meson which decays into two π mesons of opposite charge with a Q value ~ 2 Mev and a lifetime $< 10^{-14}$ sec.

[25b] Cf. Armenteros, Barker, Butler, Cachon, and York, *Phil. Mag.*, in press.

[25c] Daniel, Davies, Mulvey, and Perkins, *Phil. Mag.*, **43**: 753 (1952).

[25d] R. Marshak and H. Bethe, *Phys. Rev.*, **72**: 506 (1947).

[25e] Cf. A. Pais, *Phys. Rev.*, **86**: 663 (1952).

These claims[25f] are based on apparent angular correlations between pairs of π mesons emitted at large angles in nuclear stars of moderate energy (characterized by $2 \leq N_s \leq 6$). These correlations have not been found in nuclear stars of higher energy[25g] and may represent the effects of a strong interaction between the two emerging π mesons in the lower energy region.[25h] It seems more likely that the v^0 meson rather than the ζ^0 is the neutral counterpart of the charged ζ meson.

To sum up: There exist at least four classes of unstable charged mesons with masses greater than that of the π meson and with lifetimes greater than 5×10^{-11} sec. Of the four, three—the ζ, τ, and χ mesons—appear to be bosons and to consist in some sense of complexes of 2, 3, and 4π mesons respectively. The fourth charged heavy meson—the κ meson—appears to be a fermion and to belong to the class of fermions exemplified by the μ meson and the electron. There is experimental evidence for the direct production of the ζ and χ mesons but none as yet for the τ and κ. As regards heavy mesons of the neutral variety, at least two types have been observed—v^0 and N^0—which may be the neutral counterparts of ζ and τ. The κ^0 meson will be as difficult to detect as the μ^0 (cf. Chap. 6) and it is not surprising that the χ^0 meson has escaped observation thus far since its mode of decay may coincide with that of the π^0.

4. *V* Particles

We have already pointed out that the ζ^0 meson may correspond to one class of *V* particles. Actually, the distinction between heavy mesons and *V* particles is purely phenomenological at the present time and is determined chiefly by the experimental technique which is employed. If a photographic emulsion is used, the unstable particle has an excellent chance of coming to rest before decaying, while a cloud chamber favors decay in flight (provided, of course, that the lifetime is in the appropriate range). Decay in flight of a neutral unstable primary favors a small angle between the two charged secondaries, whereas the decay of a charged primary favors a large angle between it and the charged secondary; in both cases the result is the appearance of a *V* track.

The first experimental evidence for the existence of *V* particles was obtained in 1947 by Rochester and Butler,[26] who observed two events in a cloud chamber which appeared to originate in the gas of the chamber and which they interpreted as the decay of one neutral and one charged particle. The first event appeared to represent the decay of an electrically neutral particle, since designated as V^0, into at least two charged particles of opposite sign (a third neutral particle was not excluded). The second event apparently represented the decay of a positively charged particle, since designated as V^+, into at least one lighter positively charged particle. Rochester and Butler invoked the decay hypothesis in order to explain the fact that the two types of events were not observed to emerge from the 3-cm lead plate (present in the cloud chamber) with much greater probability (in the ratio of the density of lead to the density of the argon gas in the chamber), as would befit collision processes. Moreover, if the two events represented collision processes in the gas, recoil argon nuclei should have been visible in the cloud chamber, and they were not. From measurements of the momentum p and specific ionization I of the tracks of the decay particles, it was possible to say that the three decay particles (the two from the V^0, the one from the V^+) all possessed masses at least equal to that of the μ meson.

[25f] Cf. Danysz, Lock, and Yekutieli, *Nature*, **169**: 364 (1952).

[25g] M. Kaplon and D. Ritson, *Phys. Rev.*, in press.

[25h] K. A. Brueckner, *Phys. Rev.*, in press.

[26] D. Rochester and C. Butler, *Nature*, **160**: 855 (1947).

After a lapse of several years, Rochester and Butler's work was confirmed by Seriff *et al.*,[27] who operated a cloud chamber in a magnetic field of 6500 gauss with a 2-cm lead plate in the median plane and a 20-cm block above the chamber. The California group observed $6V^0$ particles in 3000 photographs taken at 750 ft elevation and $24V^0$ particles and 4 charged V particles in 8000 photographs taken at 10,500 ft elevation. The angles θ between the two charged decay products of the $30V^0$ particles were found to vary from 3.5 to 126° (less than 40° in 17 cases), and in 12 cases the plane of the decay particles could be shown to pass, within experimental error, through the origin of the nuclear explosion. In 6 cases out of the 30, it was possible to show that the mass of one of the decay particles was less than nucleonic and in 10 traversals by decay particles of the 2-cm lead plate, 2 nuclear interactions were observed. The first set of observations indicates that the decay products of the V^0 particle are two in number and the second set that at least one of the decay particles is a π meson. From observations of the numbers of V^0 particles above and below the 2-cm lead plate, it was possible to deduce an approximate value of the lifetime which turned out to be $3 \pm 2 \times 10^{-10}$ sec. The number of charged V particles observed was insufficient to draw even approximate conclusions except to provide evidence for the existence of a new type of unstable charged particle.

Since the experiment of Seriff *et al.*, several V particle experiments have been performed with cloud chambers operated under different conditions and at different altitudes. Thus, Bridge and Annis[28] have observed $4V^0$ and 4 charged V particles in a large multiple-plate cloud chamber operated at 700 g/cm^2 atmospheric depth. For 2 of the V^0 particles, it was possible to say from ionization, range, and scattering measurements that one of the decay particles was a meson. Thompson *et al.*[29] operated a cloud chamber in a magnetic field of 3100 gauss at sea level and observed $9V^0$ particles. In 2 of these cases, the positive decay product was identified as a proton and the negative decay product as a particle with a mass not much heavier than a π meson. Table 3 gives the essential data on these two events and the deduced Q values and V^0 masses on the assumption that each event represents the disintegration of a V^0 particle into a proton and a π^- meson. In 1 of the 9 cases, Thompson *et al.* find that the positive decay particle cannot be much heavier than a π^+ meson; unfortunately, the negative decay particle could not be identified. If the negative decay particle were of nucleonic mass, this would establish the existence of the antiproton, and the event would therefore represent the decay of an anti-V^0 particle. On the other hand, if the negative decay particle in this particular event is a π^- meson, this would imply the existence of a new type of V^0 particle or possibly of a τ^0 meson which decays via the decay scheme $\tau^0 \rightarrow \pi^+ + \pi^- + \pi^0$. These alternatives will be discussed more fully below.

---

[27] Seriff, Leighton, Hsiao, Cowan, and Anderson, *Phys. Rev.*, **78**: 290 (1950).

[28] H. Bridge and M. Annis, *Phys. Rev.*, **82**: 445 (1951); also Bridge, Courant, and Rossi, *Phys. Rev.*, **85**: 159 (1952).

TABLE 3. DATA OF THOMPSON *et al.* ON V° PARTICLES

p_+, Bev/c	$I_+/I_{\min}$	p_-, Bev/c	$I_-/I_{\min}$	θ,°	Q, Mev	Mass, m_e
0.75 ± 0.11	2–4	0.24 ± 0.02	1	23.8	28 ± 10	2165 ± 20
1.2 ± 0.2		0.22 ± 0.01		28.6	31 ± 5	2170 ± 10

More recently, Leighton *et al.*[30] have observed nine new examples of the decay of V^0 particles in two cloud chambers operating in magnetic fields and arranged to respond to cosmic-ray penetrating showers. The data which they obtained on these nine V^0 particles are listed in Table 4. It is seen that all the negative decay products are mesons, whereas most of the positive decay products are much heavier than mesons. The Q values in the last column of Table 4 are calculated from the formula

$$Q = (m_+ + m_-)\left[\left(1 + \frac{2\bar{Q}}{m_+ + m_-}\right)^{\frac{1}{2}} - 1\right] \tag{9}$$

where m_+ and m_- are the rest masses of the two decay particles and

$$\bar{Q} = \frac{E_+E_- - m_+m_- - p_+p_- \cos\theta}{m_+ + m_-} \tag{10}$$

---

[29] Thompson, Cohn, and Flum, *Phys. Rev.*, **83**: 175 (1951).

[30] Leighton, Wanlass, and Alford, *Phys. Rev.*, **83**: 843 (1951).

The quantity Q is a good approximation to $\bar{Q}$ when $Q \ll (m_+ + m_-)$. In Eq. (10), θ is the angle between the two decay products and (p_+, E_+), (p_-, E_-) are the momentum-energy four-vectors of the two decay particles. All the Q values in Table 4 have been calculated on the assumption of a two-body decay of the V^0 particle; and, if this assumption is correct, there is an indication from the table that there are two types of V^0 particles decaying in accordance with the decay schemes

TABLE 4. DATA OF LEIGHTON *et al.* ON V^0 PARTICLES

p_+, Mev/c	$I_+/I_{\min}$	m_+, m_e	p_-, Mev/c	$I_-/I_{\min}$	m_-, m_e	θ,°	Q, Mev
700 ± 200	1.7 ± 0.3	1500 ± 700	47 ± 2	6 ± 2	280 ± 60	157	65 ± 20
172 ± 10	8 ± 3	1200 ± 300	136 ± 5	1.5 ± 0.3	260 ± 60	96	55 ± 10
178 ± 25	>15	>1500	172 ± 25	1.7 ± 0.3	340 ± 150	37	50 ± 20
620 ± 100	1.3 ± 0.2	870 ± 600	117 ± 5	1.5 ± 0.3	225 ± 70	44	21 ± 5* 130 ± 30†
370 ± 50	2.5 ± 1	1100 ± 500	180 ± 20	1.3 ± 0.2	250 ± 100	52	53 ± 10
475 ± 75	1.8 ± 0.7	1100 ± 600	101 ± 5	2.0 ± 0.5	260 ± 50	70	32 ± 5
350 ± 100	5 ± 2	1800 ± 900	65 ± 10	3.5 ± 1.5	260 ± 70	134	32 ± 5
500 ± 100	<1.3	<850	216 ± 20	<1.3	<320	39	93 ± 20†
850 ± 200	<1.3	<1500	125 ± 25	1.7 ± 0.5	270 ± 120	71	63 ± 20

* Calculated for $\pi^- + P$ decay.
† Calculated for $\pi^+ + \pi^-$ decay.

$$V^0 \rightarrow P + \pi^- \tag{11}$$

$$v^0 \rightarrow \pi^+ + \pi^- \tag{12}$$

The Q value seems to be about twice as large for the v^0 particle as compared with the V^0 particle. As far as the data of Leighton *et al.* are concerned, all nine cases can also be fitted by a single three-body decay process involving the emission of one nucleon and two π mesons; such a decay scheme would be consistent with a single Q value.

Fretter[31] has also obtained some data on the V particles, having observed 37V^0 particles and 8 charged V particles in a multiplate cloud chamber operated at sea level. A careful study was made of the 26 of the 37V^0 events which were ascertained to be coplanar with the initial nuclear explosion, and it turned out that the assumption of a single type of V^0 particle decaying into a proton and a π^- meson could not easily be reconciled with the observed angular distribution of the decay products. Fretter suggests a possible three-body decay process such as $V^0 \rightarrow P + \mu^- + \nu$ where μ is the μ meson and ν is the neutrino. However, apart from the fact that this decay scheme leads to too long a lifetime[32]—10^{-7} sec instead of 10^{-10} sec, assuming that the coupling constant is the same as the β coupling constant—the postulation of a second type of V^0 particle decaying into two π mesons [cf. Eq. (12)] would also explain the distortion of the angular distribution observed by Fretter.

---

[31] W. B. Fretter, *Phys. Rev.*, **83**: 1053 (1951); also W. Fretter and M. May, *Phys. Rev.*, **85**: 773 (1952).

The most comprehensive experiment on V particles thus far reported is the one by Armenteros *et al.*;[33] these authors have observed $70V^0$ particles in a cloud chamber operated in a magnetic field of 7500 gauss at an elevation of 2867 m. Nine heavily ionizing decay particles were particularly suitable for mass determination, and the results are shown in Table 5. It is seen that all positively charged particles have a mass consistent with the proton mass, whereas all negatively charged particles have a mass consistent with the π^- meson mass. No identifiable negative protons were found nor were any slow positive mesons observed among the decay products. The reason for believing the negatively charged particles of mesic mass to be π^- mesons is that 1 of the 4 slow negative decay particles appears to decay in flight into a negative μ meson. Another reason is that 4 nuclear interactions of the secondary particles with the lead plate placed inside the cloud chamber were observed—produced by the decay particles of mesic mass as well as those of protonic mass. The Manchester group carried out momentum measurements on 43 negative decay particles and on 34 positive decay particles with the results shown in Fig. 1; the contributions of the heavily ionizing particles are indicated by the shaded areas. Figure 1 shows that some of the

TABLE 5. DATA OF ARMENTEROS *et al.* ON V^0 PARTICLES

Momentum, 10^8 ev/c	Estimated ionization, $I_{\min}$	Mass range, m_e	Calculated ionization for proton, $I_{\min}$	Calculated ionization for π meson, $I_{\min}$
2.42 ± 0.2	8–15	1550–2400	9.3	
4.8 ± 0.5	3–4	1700–2400	3.1	
3.5 ± 0.35	4–6	1450–2300	5.0	
4.50 ± 0.45	3–4	1600–2250	3.3	
6.0 ± 0.6	2–3	1450–2500	2.3	
1.05 ± 0.05	2–3	270–430		2.0
0.80 ± 0.04	2–4	210–380		2.7
0.78 ± 0.14	3–4	290–370		2.8
0.74 ± 0.04	2.5–3.5	230–330		3.0

---

[32] Contrary to a statement in Fretter, footnote 31.

[33] Armenteros, Barker, Butler, and Cachon, *Phil. Mag.*, **42**: 1113 (1951); cf. also Armenteros, Barker, Butler, Cachon, and Chapman, *Nature*, **167**: 501 (1951).

Pure Mathematical Physics

secondary decay particles must be positive mesons since all protons with a momentum less than 7×10^8 ev/c should appear heavily ionizing whereas there is a sizable number of particles with minimum ionization below this momentum. On the other hand, the fact that the average momentum of the negative decay particles (see Fig. 1*b*) is much less than the average momentum of the positive decay particles (see Fig. 1*a*) indicates that a large fraction of the positive decay particles are much heavier than the negative decay particles, *i.e.*, protons as compared with π^- mesons.

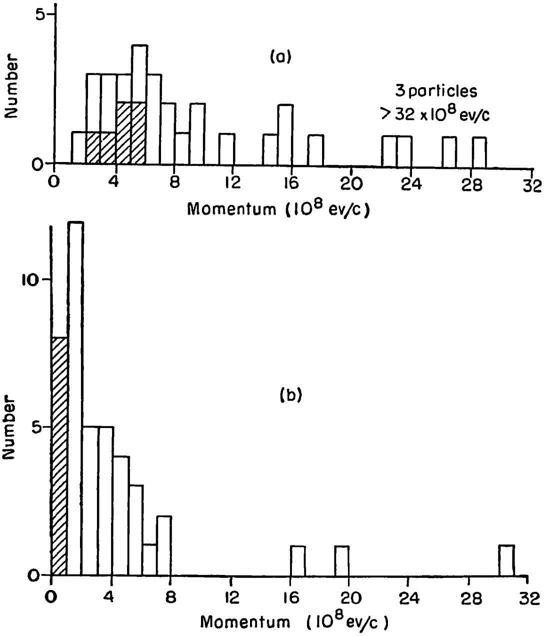

Fig. 1. Frequency distribution of the measured momenta of the decay products of the V^0 particles (Armenteros *et al.*). Histogram (*a*) corresponds to the positive secondaries, (*b*) to the negative. The identified slow protons and mesons are indicated by the shaded regions.

The Manchester group also searched for neutral particles among the decay products of the V^0 particles both by looking for deviations from coplanarity in the case of V^0 particles decaying below the lead plate inside the cloud chamber and by looking for soft component showers (produced by γ rays or π^0 mesons which decay into γ rays) associated with V^0 decays just above the lead plate. In no case was any evidence found for a third neutral particle, although the statistics are too poor to draw any final conclusions. If one assumes that the V^0 particles studied by Armenteros *et al.* decay into only two particles, it is evident from the data presented above that there must be two types of V^0 particles decaying in accordance with the decay schemes given by Eqs. (11) and (12). The mass values and Q values of $12V^0$ particles and $8v^0$ particles are given in Table 6. The average mass for the V^0 particle turns out to be 2203 ± 12m_e and the average Q value 46 ± 6 Mev,[33a] whereas the average mass of the v^0 particle is 796 ± 27m_e and the average Q value 122 ± 13 Mev, always assuming that the particles of mesic mass are charged π mesons. The numbers given in Table 6 are representative of the relative numbers of V^0 and v^0 particles which occur in the Manchester experiment. It is interesting to note that the Q value for the v^0 particle is approximately twice that of the V^0 particle. The statistics are still not sufficiently good—as regards both the detection of the π^0 meson and the absence of low-momentum v^0 particles—to rule out the possibility that the V^0 particle is actually a single particle and decays in accordance with the unique decay scheme

TABLE 6. MASS AND Q VALUE DETERMINATIONS OF V^0 AND v^0 PARTICLES

V^0		v^0	
Mass value, m_e	Q value, Mev	Mass value, m_e	Q value, Mev
2277 ± 40	82 ± 20	796 ± 130	122 ± 65
2228 ± 40	58 ± 20	883 ± 50	165 ± 25
2186 ± 20	37 ± 10	872 ± 50	160 ± 25
2218 ± 10	53 ± 5	841 ± 60	144 ± 30
2228 ± 10	58 ± 5	820 ± 50	134 ± 25
2160 ± 20	24 ± 10	700 ± 30	74 ± 15
2183 ± 20	36 ± 10	675 ± 100	61 ± 50
2181 ± 10	40 ± 5	785 ± 30	116 ± 15
2188 ± 10	38 ± 5		
2157 ± 30	23 ± 15		
2169 ± 10	29 ± 5		
2256 ± 50	72 ± 25		

$$V^0 \rightarrow \text{nucleon} + 2\pi \text{ mesons} \qquad (13)$$

The decay schemes (11) and (12) would then become special cases of the three-particle decay process (13).

The experimental data on the V particles can be summed up as follows: (1) slow positive particles of protonic mass and slow negative particles of mesic mass have been identified among the decay products of V^0 particles. The fact that some of the mesic decay particles undergo nuclear interactions implies that they are π^- mesons. In addition, several positive particles of mesic mass have been seen, and the indications are that the companion negative particles are also of mesic mass and not negative protons. (2) In many cases, the plane of the decay particles passes through the origin of the initial event (within experimental error) in which the V^0 particles were produced; in other cases, coplanarity is not conspicuously present. The presence of coplanarity does not necessarily exclude three-particle decay if one of the decay particles is heavy[33b] nor does its absence imply three-particle decay because of the experimental difficulties of making a decision and the possibility that the V^0 particles were produced in some other part of the apparatus and were not necessarily associated with the penetrating shower which tripped the cloud chamber. (3) No evidence has been found for neutral partners to the charged decay products of V^0 particles; this applies to neutral particles like γ rays or π^0 mesons which rapidly decay into γ rays. Neutrinos or neutral μ mesons would not be excluded nor would some as yet unknown neutral particle which does not decay into γ rays. (4) The most plausible explanation of the experimental data is to assume two types of V^0 particles, decaying in accordance with the decay schemes (11) and (12). If this interpretation is correct, the mass of the V^0 particle is approximately 2200 electron masses and the mass of the v^0 particle is approximately 800 electron masses. The abundance of the V^0 particles is greater than that of the v^0 particles, which may be due to a difference in lifetime and/or the experimental setup.[33c] It is also possible that a different mechanism of production is operative for the V^0 and v^0 particles; *e.g.*, π^- meson-proton collisions may be chiefly responsible for the creation of the former in contrast to nucleon-nucleon collisions for the latter. (5) The lifetime for decay of the V^0 particle is $3\text{–}5 \times 10^{-10}$ sec.[33d] (6) There is no positive evidence for the existence of anti-V^0 particles, *i.e.*, particles which decay into anti (negative) protons and π^+ mesons. This may be due to the mechanism of production (cf. point 4 above) or to the higher threshold energy associated with a conservation law for nucleons and V^0 particles.[33e] (7) The charged V particles are much less abundant than the neutral V particles, and no real indication of the mechanism of their decay is available at the present time except that evidence for the existence of charged V particles heavier than the nucleon is conspicuously absent.[33f]

[33a] In its latest experiments the Cal. Tech. group has measured up the Q values of more than 50 V^0 particles and has found them to group at 35 and 75 Mev (C. D. Anderson, private communication).

[33b] Particularly if the primary momentum is high; cf. K. Brueckner and R. Thompson, *Phys. Rev.*, **87**: 390 (1952).

[33c] Thus, the Cal. Tech. group places an upper limit of 15 per cent on the ratio of v^0 to V^0 in its latest experiments, whereas the Manchester ratio is more like 35 per cent (cf. above). The method of selection of penetrating showers is somewhat different for the two groups.

[33d] The latest Manchester value is 5×10^{-10} sec, whereas the Cal. Tech. value is $2.8\text{–}3.4 \times 10^{-10}$ sec for the low Q (35 Mev) group and $1.8\text{–}2.4 \times 10^{-10}$ sec for the high Q (75 Mev) group (cf. footnote 33*a*); the latter distinction is not statistically significant as yet.

5. Theoretical Interpretation of the V Particles

While many details remain to be cleared up, the experimental work on V particles shows clearly that there exists one type of neutral unstable particle which is more massive than the sum of the nucleon and π meson masses. It is tempting to regard this neutral particle as a metastable isobaric state of the neutron and to look to strong coupling meson theory[34] for an elucidation of the properties of such a state. Here, one meets with what at first appears to be a pleasant surprise in that the scalar strong coupling theory does not predict the existence of metastable isobaric states, whereas the pseudoscalar strong coupling theory does[35] and it is known that the π meson is a pseudoscalar particle. This at first sight satisfactory result for the pseudoscalar theory is quickly vitiated by the fact that the same theory predicts an extremely short lifetime for the metastable state, a lifetime 10^{13} times shorter than the observed lifetime. Both these statements can be proved in a simple fashion: the implicit equations for the excitation energy[36] ΔE corresponding to bound isobaric states of nucleons in the symmetric $S(S)$ and neutral[37] $PS(PV)$ theory can be shown to be

$$S(S)\text{ (symmetric)}: \quad \Delta E = Cg^2\{\mu^2 - [\mu^2 - (\Delta E)^2]^{\frac{1}{2}}\} \tag{14}$$

$$PS(PV)\text{ (neutral)}: \quad \Delta E = \frac{2C}{3} f_0^2 \left\{\frac{(\Delta E)^2}{a} - \mu^3 + [\mu^2 - (\Delta E)^2]^{\frac{3}{2}}\right\} \tag{15}$$

[33e] Cf. L. I. Schiff, *Phys. Rev.*, **85**: 374 (1952); also E. P. Wigner, *Proc. Nat. Acad. Sci.* (May, 1952).

[33f] The Manchester group (reference 25*b*) has recently analyzed 21 cases of charged V particle decay and found it possible to attribute all 21 events to the decay of superheavy mesons (cf. Sec. 3).

[34] Cf. W. Pauli, "Meson Theory of Nuclear Forces," Interscience Publishers, 1946; and G. Wentzel, *Rev. Mod. Phys.*, **19**: 1 (1947).

[35] Cf. S. Tomonaga, *Prog. Theor. Phys.*, **2**: 6 (1947); also R. E. Marshak, *Phys. Rev.*, **78**: 346 (1950); and Y. Fujimoto and H. Miyazawa, *Prog. Theor. Phys.*, **5**: 1052 (1950).

[36] Strictly speaking, ΔE is not the excitation energy but is equal to $\hbar\omega$, where ω is the precession angular velocity of the spin or isotopic spin vector about the z axis. For large quantum numbers the two become equal, while for small quantum numbers the errors introduced do not alter any of the qualitative conclusions (cf. footnote 34).

[37] The symmetric $PS(PV)$ theory brings in the isotopic as well as the ordinary spin and yields an expression—though somewhat more complicated—similar to that of the neutral $PS(PV)$ theory (D. Feldman, private communication).

where g and f_0 are the $S(S)$ and neutral $PS(PV)$ coupling constants, respectively, μ is the π meson mass, a is the size of the nucleon source and is introduced in order to make the $PS(PV)$ theory convergent, and C is the z component of the isotopic spin in the symmetric scalar theory and the z component of the ordinary spin in the neutral pseudoscalar theory. Equations (14) and (15) are derived by a classical treatment taking account of the inertial reaction of the meson field on the nucleon source; however, they are closely analogous to the equations which result on the basis of quantum-mechanical considerations.[34] If it is assumed that the meson field is very strongly coupled to the nucleon field, that is, $g^2/\hbar c > 1$ and $f^2/\hbar c > 1$ (actually in the pseudoscalar theory it suffices to assume that $f^2/\hbar c > a\mu c/\hbar$—cf. below), one obtains the so-called strong coupling limits to Eqs. (14) and (15), namely,

$$S(S): \qquad \Delta E = \frac{2\mu}{g^2 C} \tag{16}$$

$$PS(PV): \qquad \Delta E = \frac{3a}{2f_0^2 C} \tag{17}$$

It is evident from Eqs. (16) and (17) that in the strong coupling limit the excitation energy is smaller than the meson rest mass and the isobaric state is therefore bound—in agreement with the original hypothesis. Suppose, however, that $\Delta E > \mu$, corresponding to a situation where the coupling constant is not so large; then Eqs. (14) and (15) must be rewritten in the form

$$S(S): \qquad \Delta E = Cg^2\{\mu + i[(\Delta E)^2 - \mu^2]^{\frac{1}{2}}\} \tag{18}$$

$$PS(PV): \quad \Delta E = \frac{2C}{3} f_0^2 \left\{\frac{(\Delta E)^2}{a} - \mu^3 + i[(\Delta E)^2 - \mu^2]^{\frac{3}{2}}\right\} \tag{19}$$

The isobaric state is now unbound, and if it is to be metastable, a solution of Eq. (18) or (19) must exist of the form

$$\Delta E = \Delta E_0 + i\lambda \qquad (\lambda \ll \Delta E_0) \tag{20}$$

where ΔE_0 essentially fixes the energy of the isobaric state and λ^{-1} is the reciprocal lifetime (in units where $\hbar = c = 1$) of the metastable state. It can easily be shown that no solution of this form exists for Eq. (18) but that one does exist for Eq. (19) wherein

$$\lambda = \frac{a}{\Delta E_0} [(\Delta E_0)^2 - \mu^2]^{\frac{3}{2}} \tag{21}$$

If the Q value of the V^0 particle is now inserted into Eq. (21), that is, $\Delta E_0 = \mu + Q$ and the nucleonic source size a is chosen as the nucleon Compton wave length, λ^{-1} turns out to be 5×10^{-23} sec. We see, therefore, that a simple application of the strong coupling meson theory cannot explain the long lifetime of the V^0 particle.

long to be reconciled with the customary formulation of strong coupling pseudoscalar theory. The long lifetime of the v^0 particle also finds no straightforward theoretical interpretation. If the v^0 particle decays into a pair of charged π mesons, it must be a scalar particle (since the π meson is pseudoscalar); but a neutral scalar particle should decay—through the virtual creation of a proton-antiproton pair—into two γ rays with its lifetime as short as that of the pseudoscalar π^0 meson (somewhat shorter because of its greater mass) and we know that the π^0 meson has a lifetime of 10^{-14} sec. It is therefore not clear why the v^0 particle chooses to decay into a pair of charged π mesons with a lifetime of the order of 10^{-10} sec, to say nothing of the much shorter lifetime which would be expected for decay into a pair of π mesons. One possible solution to the dilemma has been suggested by Noyes,[38] who has found that adding a term of the form $A\phi^3$ (A is a constant, ϕ is the v^0 wave function) to the interaction Hamiltonian between the v^0 and the nucleon field not only makes the theory renormalizable[39] for a scalar v^0 but introduces an additional parameter which can be chosen in such a manner as to reduce appreciably the lifetimes for decay both into a pair of two photons and into a pair of charged π mesons. However, it is difficult to believe that the accidental cancellation which can be achieved in this manner and which derives from a special relation between the v^0 and π coupling constants is really responsible for the long lifetime of the v^0 particle.

If one does not accept the two-particle decay schemes of the V^0 particles, but argues instead for a unique V^0 particle with the decay scheme (13), the situation is not happier. One then appears to have a metastable isobaric state of a nucleon with an excitation energy appreciably greater than that of the V^0 particle and with a preference for emitting two π mesons rather than one. No theory exists to explain such a phenomenon.

Quite a few theoretical attempts have recently been made to explain the longevity of the V particles (as of the heavy mesons of boson type—cf. Sec. 3) either by invoking new kinds of selection rules,[40] requiring production in pairs,[25e] or by postulating complex structures[41] for the new unstable particles. However, none of these theories has shown itself capable of coping with the rapidly changing experimental situation, and discussion of the relative merits of the various theories is postponed to some more auspicious occasion.

---

[38] H. P. Noyes, *Phys. Rev.*, **87**: 344 (1952).

[39] A. Salam, *Phys. Rev.*, **82**: 217 (1951).

[40] Cf. the extensive series of papers by Japanese authors in *Prog. Theor. Phys.* since 1949.

[41] Cf. R. G. Sachs, *Phys. Rev.*, **84**: 305 (1951).

There are other difficulties with explaining the V^0 particle in terms of a strong coupling treatment of the π meson field. The lifetime argument discussed above was based on the strong coupling theory of the π^0 meson field and it was indicated (cf. footnote 37) that a similar difficulty would be encountered when the charged π meson field is included (after all, the decay product of the V^0 particle is not a π^0 meson but a π^- meson). However, if the charged and neutral π meson fields are coupled to the nucleon, the strong coupling theory predicts the existence not only of neutral isobaric states but also of doubly charged and negatively charged isobaric states of nucleons. In particular, if the symmetrical *PS*(*PV*) theory is adopted (since all the experimental facts point in this direction), the formula for the isobaric excitation energy becomes

$$\Delta E = \frac{3[j(j+1) - \frac{3}{4}]a\mu^2}{2f^2} \tag{22}$$

where j is the spin of the isobaric state and the only restriction is $|n| \leq j$ with $(n + \frac{1}{2})$ the charge of the isobaric state. It is seen from Eq. (22) that $j = \frac{1}{2}$ corresponds to the ordinary neutron ($n = -\frac{1}{2}$) and proton states ($n = \frac{1}{2}$) of the nucleon, whereas $j = \frac{3}{2}$ would predict equal excitation energies for the charged states 2, 1, 0, -1. Thus far, no experimental evidence exists for doubly or negatively charged isobaric states although, according to strong coupling theory, they should not be rarer than neutral isobaric nucleons. Furthermore, it is not clear why the V^0 particle, identified as a neutral isobaric nucleon, which according to formula (22) must possess a spin greater than $\frac{1}{2}$, does not decay by γ emission to the ground state, *i.e.*, the ordinary neutron, in an extremely short time. For example, if the V^0 particle were to possess spin $\frac{3}{2}$, the γ decay should proceed by magnetic dipole radiation with a lifetime given by the formula

$$\tau_\gamma^{-1} \approx (\Delta E_0)^3 |M_{\frac{3}{2}\to\frac{1}{2}}|^2 \tag{23}$$

where $|M_{\frac{3}{2}\to\frac{1}{2}}|$ is the magnetic moment matrix element and ΔE_0 the excitation energy of the isobaric state [defined by (22)]; taking $|M_{\frac{3}{2}\to\frac{1}{2}}| \sim \frac{e\hbar}{Mc}$ (M is the nucleon mass) and $\Delta E_0 \approx 200$ Mev, one finds $\tau_\gamma \approx 3 \times 10^{-20}$ sec. This lifetime is much shorter than the observed lifetime of the V^0 particle. These are serious objections to an explanation of the V^0 particle in terms of a straightforward application of strong coupling theory to the π meson field.

Several other features of the experimental data on V particles are difficult to understand on theoretical grounds. We have seen that, while the V^0 particle possesses many of the properties which would characterize a metastable isobaric state of a nucleon, its lifetime is much too

NAME INDEX

A

Aamodt, R. L., 132*n.*, 159*n.*, 171*n.*
Adams, R. V., 204*n.*
Adelman, F., 182, 186, 190
Aidzu, K., 149*n.*
Alford, W. L., 353*n.*
Alichanian, A. I., 344*n.*
Alichanov, A. I., 344*n.*
Al-Salam, S. G., 187, 188
Althaus, E., 207*n.*
Alvarez, L. W., 204
Amaldi, E., 228
Anderson, C. D., 202, 204, 205*n.*, 248, 352*n.*
Anderson, H. L., 248, 249, 257, 263*n.*
Angell, C. E., 249*n.*
Annis, M., 348*n.*, 352
Araki, G., 5*n.*, 13*n.*, 15*n.*, 167
Armenteros, R., 350*n.*, 355, 356, 357
Ashkin, J., 123*n.*, 238*n.*, 239, 245*n.*, 342
Auerbach, T., 342*n.*
Auger, P., 333
Austern, N., 160*n.*

B

Barkas, W. H., 73, 79, 131, 132, 136, 203
Barker, K. H., 270, 350*n.*, 355*n.*
Barnes, S. W., 249
Basri, S., 159*n.*
Benoist-Guental, P., 5*n.*, 15*n.*
Berger, M. J., 200*n.*
Bernardini, G., 259, 260, 263, 264, 271
Bethe, H., 134, 195*n.*, 264–266, 268, 350*n.*
Birge, R. W., 190*n.*
Birnbaum, M., 131
Bishop, A., 32*n.*, 101
Biswas, S., 312*n.*
Bjorklund, R., 119, 120, 140
Blair, J. S., 255*n.*
Blatt, J. M., 159*n.*, 335
Bloch, F., 275*n.*, 284
Block, M., 66*n.*, 82*n.*, 113*n.*, 308*n.*
Boehmer, H., 309*n.*
Bohr, N., 222, 286
Bollinger, L. M., 229*n.*, 231
Booth, E. T., 136*n*, 203*n*, 259*n*, 260*n.*
Bousser, F., 328*n.*
Bradner, H , 116, 262, 263
Bradt, H., 140, 297*n.*, 324*n.*, 328
Bramson, H., 138, 205
Branch, G. M., 270, 333*n.*
Bridge, H., 127*n.*, 220*n.*, 309*n.*, 348*n.*, 352
Brode, R. B., 203
Brown, R. H., 310, 346
Brown, W. W., 270, 333*n.*
Brueckner, K. A., 5*n.*, 24*n.*, 26*n.*, 47*n.*, 53*n.*, 56, 58*n.*, 60, 146*n.*, 248*n.*, 351*n.*, 358*n.*
Bruno, B., 189*n.*
Budini, P., 180*n.*
Butler, C. C., 270, 350*n.*, 351*n.*, 352*n.*, 355*n.*
Byfield, H., 136*n.*, 203*n.*, 263*n.*

C

Cachon, A., 350*n.*, 355*n.*
Caianiello, E. R., 140, 159*n.*, 217, 218, 220*n.*
Camac, M., 178*n.*, 263*n.*
Camerini, U., 119, 134*n.*, 207*n.*, 269, 270, 271, 310, 317, 319–323*n.*, 324, 346*n.*
Campbell, I., 335*n.*
Carlson, A. G., 128, 129, 132, 141
Cartwright, W. F., 64, 65, 67, 131*n.*, 132
Case, K. M., 5*n.*, 10*n.*, 174*n.*, 176*n.*
Chamberlain, O., 135, 289*n.*
Chang, C., 203*n.*
Chang, W. Y., 179
Chao, C. Y., 125*n.*
Chapman, A. H., 355*n.*
Chedester, C., 249, 263, 264
Cheston, W. B., 60, 145*n.*, 161, 182, 186, 250, 251, 253–255, 257*n.*
Chew, G. F., 70, 84*n.*, 96, 250
Christian, R., 56*n.*
Christy, R., 220–223
Cini, M., 238*n.*, 272*n.*
Clark, D. L., 118, 162, 249*n.*
Clementel, E., 188, 277, 279, 284*n.*
Cocconi, G., 37*n.*, 38*n.*, 234, 270, 308, 309, 333*n.*, 334*n.*
Code, F. L., 228
Cohn, H. O., 353*n.*

Conforto, A., 200
Conversi, M., 191, 193, 202
Cook, L. J., 32*n.*
Cooper, D., 345
Coor, J., 310*n.*
Corinaldesi, E., 245*n.*
Corson, D. R., 263*n.*
Cosyns, M. G. E., 171, 179
Courant, H., 348*n.*, 352*n.*
Cowan, E. W., 352*n.*
Crandall, W. E., 119*n.*, 140*n.*
Crawford, F. S., 67*n.*
Critchfield, C. L., 210*n.*, 334*n.*
Crouch, M., 200
Crowe, K. M., 67*n.*
Crussard, J., 348*n.*
Cuer, P., 189*n.*

D

Daitch, P., 82
Dalitz, R. H., 141*n.*
Dallaporta, N., 284*n.*
Daniel, R. R., 127*n.*, 141*n.*, 269*n.*, 325*n.*, 350*n.*
Danysz, M., 351*n.*
Davies, J. H., 127*n.*, 141*n.*, 205, 269*n.*, 271*n.*, 310*n.*, 317*n.*, 325*n.*, 350*n.*
D'Espagnat, B., 139, 284*n.*
Dilworth, C. C., 171*n.*
Dirac, P. A. M., 8, 211, 212, 337, 338
Drell, S. D., 5*n.*, 27
Duller, N. M., 312*n.*
Durbin, R., 163, 164
Dyson, F. J., 155

E

Eguchi, T., 138*n.*
Epstein, S. T., 193*n.*
Evans, J., 198, 199, 231, 232–234

F

Fahy, E. F., 220*n.*, 224, 225
Fainberg, J., 141*n.*, 328*n.*
Feenberg, E., 177*n.*, 334
Feer, D., 11*n.*, 160, 207*n.*
Feld, B. T., 312–315
Feldman, D., 247*n.*
Feldman, L., 214*n.*
Fermi, E., 59*n.*, 146, 167–171, 179, 195, 248*n.*, 249*n.*, 257*n.*, 286–292, 296, 297, 305, 326–328*n.*, 329–331, 339, 340
Fernbach, S., 98*n.*, 255, 265
Ferretti, B., 167*n.*, 255*n.*, 257
Feshbach, H., 91–93, 100, 339
Feynman, R. P., 6*n.*, 7, 10, 47, 239
Fidecaro, G., 228
Field, G., 245*n.*
Fierz, M., 214*n.*
Finkelstein, R. J., 143*n.*, 193*n.*, 219
Fireman, E., 215*n.*
Fisk, C. B., 315*n.*
Flum, R. S., 353*n.*
Foldy, L. L., 13*n.*, 55, 60
Fong, H. T., 328*n.*, 345*n.*
Forster, H., 345
Fowler, E. C., 248*n.*
Fowler, P. H., 119*n.*, 127, 207*n.*, 269*n.*, 270, 271, 310*n.*, 317*n.*, 345*n.*, 346
Fowler, W. B., 248*n.*
Francis, N., 21, 36
Franzinetti, C., 171*n.*, 188*n.*, 271*n.*, 317*n.*, 345*n.*
Freier, P., 328*n.*
Fretter, W. B., 125*n.*, 126, 270, 311, 331*n.*, 332, 333*n.*, 354, 355
Friedman, H., 134
Frohlich, H., 170*n.*
Fry, W. F., 138, 171*n.*, 180*n.*, 198*n.*
Fujimoto, Y., 5*n.*, 27*n.*, 149*n.*, 188, 359*n*
Fukuda, H., 89*n.*, 149*n.*, 284*n.*, 347*n.*
Fulbright, H., 214*n.*

G

Gallone, S., 255*n.*, 257
Gamba, A., 217*n.*
Gardner, W. L., 131*n.*, 205*n.*
George, E. P., 198, 199, 231–234
Gerosa, A., 328*n.*
Gilbert, W. S., 99*n.*
Goldberger, M. L., 70*n.*, 84*n.*, 189
Goldfarb, L., 145*n.*, 182, 186
Green, J. R., 311
Green, T. A., 255*n.*
Gregory, B. P., 125*n.*, 270, 312, 320
Greisen, K., 134*n.*, 207*n.*, 223*n.*, 230, 269*n.*, 308*n.*, 309*n.*, 333*n.*
Grivet-Meyer, T., 333*n.*
Groetzinger, G., 200
Gunn, J. C., 60*n.*

H

Hadley, J., 132*n.*, 171*n.*, 189*n.*
Hales, R. W., 67*n.*, 125*n.*
Hamlin, D., 117
Harding, J., 270, 346
Harrison, F. B., 194
Hart, E., 5*n.*, 56*n.*

Hartsough, W., 28*n*.
Harzler, A. J., 270
Havens, W., 66*n*., 82*n*., 113*n*., 138*n*., 205, 308*n*.
Hayakawa, S., 89–92, 100, 104, 106, 230*n*., 334*n*., 347*n*.
Hazen, W. E., 220*n*., 229*n*., 293*n*., 335*n*.
Heckrotte, W., 21*n*.
Heidmann, J., 189*n*.
Heineman, R. E., 293*n*.
Heisenberg, W., 229*n*., 282, 283, 286, 303, 326, 331, 335*n*.
Heitler, H., 310*n*.
Heitler, W., 5*n*., 45*n*., 222*n*., 248*n*., 274*n*., 276–279, 321, 324, 326, 343*n*.
Helstrom, C. W., 339*n*.
Henley, E. M., 82, 86
Henri, V. P., 135*n*.
Henrich, L. R., 21*n*.
Hilberry, N., 204*n*.
Hildebrand, R. H., 67*n*., 125*n*.
Hill, M., 28*n*.
Hincks, E., 206, 207
Hoag, J. B., 204*n*.
Hodgson, P. E., 346
Hooper, J. E., 128*n*., 132*n*.
Hopper, V. D., 312*n*.
Hornbostel, J., 315*n*., 317*n*.
Hsiao, C., 352*n*.
Hubbard, H. W., 205*n*., 206*n*.
Huddleston, R., 82, 86
Hulsizer, R., 334

I

Iloff, E., 64*n*.
Inoue, T., 195*n*.
Iona, M., 308*n*.
Isaacs, P. J., 249, 257*n*., 268
Ise, J., 333*n*.
Ittner, W. B., 200*n*.

J

Jackson, J., 159*n*.
Jakobson, M. J., 102, 103, 117*n*., 135
Janossy, L., 276–279, 321
Jauneau, L., 328*n*., 345*n*.
Jean, M., 238*n*.
Johnson, M. H., 161, 261
Jones, S. B., 110, 182
Jungerman, J., 187*n*.

K

Kaplon, M. F., 5*n*., 16, 18, 20, 31, 47*n*., 124*n*., 140*n*., 141, 160, 272, 297*n*., 307, 324*n*., 328–330, 333*n*., 351*n*.
Kelly, E., 189*n*.
Kessler, J., 136*n*., 203*n*., 263*n*.
Keuffel, J. W., 194*n*.
Kikuchi, S., 102*n*., 233*n*.
King, D. T., 128*n*., 132*n*., 310*n*.
Klein, O., 214*n*., 227*n*.
Knable, N., 67,125
Kofoed-Hansen, O., 214*n*.
Konopinski, E. J., 209*n*.
Kraushaar, W. L., 135, 207*n*.
Kraybill, H., 334*n*.
Kruse, U. F., 190*n*.
Kusaka, S., 220–223

L

Lagarrigue, A., 206*n*.
Lal, D., 329*n*.
Langer, L. M., 214*n*., 215*n*.
Lapp, R. E., 224
Latter, R., 139*n*., 196, 197
Lattes, C. M. G., 130*n*., 134, 136, 203
Lawson, J., 120
Lax, M., 91–93, 100
Lebow, I. L., 312*n*.
LeCouteur, K. J., 188*n*.
Lederman, L., 136, 203, 259*n*., 260*n*., 263*n*.
Leighton, R. B., 205, 346, 350, 352*n*.–354
Leith, C., 189*n*.
Lennox, E. S., 293*n*.
Lepore, J. V., 21*n*.
LePrince-Ringuet, L., 189*n*., 328*n*., 344–346
Levi-Setti, R., 205*n*., 328*n*.
Levy, F., 260
Lewis, H. W., 284–286, 301, 326, 329, 331
Lheritier, M., 344
Littauer, R., 35, 104, 263*n*.
Lloyd, E., 204*n*.
Loar, H., 163*n*.
Lock, W. O., 119*n*., 205*n*., 269*n*–271 310*n*., 317*n*., 351*n*.
Long, E. A., 249*n*.
Longacre, A., 204*n*.
Lord, J. J., 141, 328
Lovati, A., 270, 312, 320*n*.
Loverdo, A., 334*n*.

M

Mabboux, C., 348*n*.
MacCallum, C., 209*n*., 210, 218
McCarthy, J. A., 215*n*.
McClure, G., 200*n*.
McConnell, J., 343

McCusker, C., 333n.
McGuire, A., 178n.
Machida, S., 339n., 343n.
McKay, A. S., 270, 333n.
McMillan, E. M., 98, 161
McMillan, W., 72, 79, 80
Majorana, E., 211, 213n.
Marshak, R. E., 21n., 55, 123n., 134, 145n., 149n., 154n., 161n., 178n., 195n., 215n., 227n., 238n., 245n., 325n., 331n., 342n., 350n., 359n.
Marshall, J., 68n.
Marshall, L., 68n.
Martin, R., 249n., 263n.
Martinelli, E., 135
Matthews, P. T., 143n.
May, M., 354n.
Maze, R., 333n.
Medicus, H. A., 35n., 104
Menon, M. G. K., 182, 184, 185n., 190, 346n.
Merritt, J., 117n.
Messiah, A. M. L., 63, 95n., 138n., 159, 174n., 176n., 178n., 349n.
Michel, L., 208, 210, 349n.
Millar, D., 333n.
Miller, R. D., 102n., 233
Mills, M. M., 334
Milton, J., 214n.
Miyamoto, Y., 347n.
Miyazawa, H., 5n., 27n., 359n.
Molière, G., 335, 336
Moller, C., 197
Morand, M., 189n.
Morellet, D., 328n., 345n.
Morette, C., 47n., 55n.
Morrat, R., 214n.
Morrissey, R., 215n.
Mott, N. F., 170n.
Moyer, B. J., 67n., 119n., 124n., 125n., 140n.
Mozley, R. F., 101, 109n., 135n.
Muirhead, H., 119n., 134n., 182n., 205n., 269–271, 310n., 346n.
Mulvey, J. H., 127n., 141n., 269n., 325n., 350n.
Mura, A., 270, 312, 320n.

N

Nagahara, Y., 154n.
Nagle, D. E., 248n., 249n., 257n.
Neddermeyer, S., 202
Nedzel, V. A., 68n.
Nereson, N., 204
Ney, E., 328n., 334n.
Nishina, Y., 229n.
Noma, S., 227n.
Nordsieck, A., 275n., 284
Noyes, H. P., 115n., 362

O

Occhialini, G. P. S., 119, 130, 171n., 203n.
O'Ceallaigh, C., 137, 346n., 348n.
O'Connell, D. J., 116n.
Ogawa, S., 154n.
Ogren, V. G., 204n.
Okayama, T., 168n.
Olbert, S., 348n.
Oleska, S., 334n.
Oneda, S., 347n.
Oppenheimer, J. R., 193n., 223n., 284n., 334n.
Orkin-Lecourtois, A., 348n.
Osaki, S., 347n.
Osborne, L. S., 312n.
Owen, B., 199n.
Ozaki, S., 347n.

P

Page, N., 171n.
Pais, A., 331n., 350n.
Pal, Y., 329n.
Pancini, E., 191n., 193, 202n.
Panofsky, W. K. H., 36n., 107n., 109, 132, 135, 157, 171, 181, 182
Passman, S., 66n., 82, 86, 87, 89, 113, 115, 308n.
Pauli, W., 5n., 18, 143n., 145n., 209n., 221n., 338, 359n.
Peaslee, D. C., 142n., 221n., 223, 230n.
Perkins, D. H., 127n., 141n., 171n., 182, 269, 270, 317n., 325n., 350n.
Perry, J. P., 249n.
Peshkin, M., 238n.
Peters, B., 140n., 141n., 297n., 324n., 329n.
Peterson, J. M., 99–101
Peterson, V. Z., 64, 65, 98n., 161
Petschek, A., 215n.
Peyrou, C., 206n.
Phillips, R., 159n.
Piccioni, O., 137n., 191n., 193, 201, 202n., 203n.
Pickup, E., 333n.
Platt, J., 178n.
Pontecorvo, B., 197, 206, 207
Porter, C., 212
Powell, C. F., 119n., 130, 134n., 161, 203n., 207n., 310n., 344n., 346, 349n.

Powell, W. M., 28*n*.
Power, E. A., 60*n*.
Power, S., 347*n*.
Prentki, J., 5*n*., 15*n*., 238*n*.
Prescott, J., 335*n*.
Primakoff, H., 144, 188*n*., 194*n*., 212, 334
Puppi, G., 188

R

Radicati, L., 238*n*., 272*n*.
Rainwater, J., 134
Ramsey, N. F., 190*n*.
Rankin, B., 116*n*., 262
Ratier, J., 5*n*., 15*n*.
Rau, R. R., 204*n*., 208*n*.
Retallack, J., 203*n*.
Reynolds, G. T., 194*n*.
Richardson, J. R., 135
Richman, C., 64, 65, 70*n*., 110, 113
Ritson, D., 134*n*., 141*n*., 307, 328, 329*n*., 333*n*., 346*n*., 351*n*.
Roberts, A., 162*n*.
Robson, J. E., 213*n*.
Rochat, O., 182*n*., 346*n*.
Rochester, D., 351, 352
Rosenblueth, M. N., 197
Rosenfeld, L., 21*n*., 51*n*., 250*n*.
Rosser, W. G. V., 270–272
Rossi, B., 125*n*., 127*n*., 204, 223*n*., 333*n*., 348*n*., 352*n*.
Ruderman, M., 219

S

Sabiar, A. B., 228*n*.
Sachs, A. M., 147*n*., 249*n*.
Sachs, R. G., 362*n*.
Sagane, R., 205, 206, 208, 212, 213, 215, 220
Sakata, S., 143, 195*n*.
Salam, A., 5*n*., 362*n*.
Salant, E. O., 315, 316
Salvini, G., 270, 312
Sands, M., 119
Sard, R., 200, 207*n*.
Sasaki, S., 347*n*.
Schein, M., 127*n*., 141*n*., 308, 328*n*., 331*n*.
Schiff, L. I., 219*n*., 325*n*., 334*n*., 339, 359*n*.
Schoenberg, M., 171*n*.
Schrödinger, E., 178
Schulte, H., 178*n*.
Schulz, A., 117*n*., 135*n*.
Schwarzer, D., 215*n*.
Schwinger, J., 143*n*.
Segall, B., 253
Segrè, E., 189*n*., 289*n*.
Seifert, A. M., 138*n*.
Serber, R., 5*n*., 21*n*., 80*n*., 98*n*., 146*n*., 187, 265*n*.
Seriff, A. J., 205*n*., 352
Serpe, J., 89*n*.
Shanley, T. J. B., 179
Shapiro, A. M., 263
Sherman, D., 64*n*.
Shutt, R. P., 228, 248*n*.
Silverman, A., 36–38*n*., 263*n*.
Simon, A., 123*n*., 176*n*., 238*n*., 245*n*.
Sitte, K., 309
Smith, F. M., 131*n*.
Smith, J. E., 315*n*.
Sorrels, J. O., 312*n*.
Stearns, M., 36, 37
Steinberger, J., 32*n*., 36*n*., 70*n*., 96, 101, 107, 135*n*., 143*n*., 147, 163*n*., 205*n*., 249*n*.
Steller, J., 36*n*., 107*n*., 109
Stevenson, E., 202
Stevenson, M. L., 67*n*.
Stinchcomb, T. G., 226
Stora, R., 349*n*.
Street, J. C., 198*n*., 202
Stuart, R., 159
Succi, C., 270
Swami, M. S., 329*n*.
Swift, M., 271, 272

T

Tagliaferri, G., 270, 312*n*., 320
Takayanagi, K., 149*n*.
Takeda, G., 89*n*., 149*n*., 284*n*.
Taketani, M., 339*n*., 343*n*.
Tamor, S., 146, 149*n*., 154, 155*n*., 180*n*., 189, 190, 250
Tanikawa, Y., 143
Taylor, T. B., 80, 82, 98*n*., 265*n*.
Teller, E., 72, 79, 80, 146, 167–171, 179
Ter Haar, D., 80
Terreaux, C., 324, 326
Teucher, M., 328*n*.
Thomas, J. E., 135*n*.
Thomas, R. E., 204*n*.
Thompson, R. W., 205*n*., 353, 358*n*.
Thorndike, A. M., 248*n*.
Ticho, H. K., 193, 194
Tiffany, O., 229*n*.
Tinlot, J. H., 125*n*., 259*n*., 270, 310, 312, 320
Tiomno, J., 197*n*., 208, 210, 212–214*n*., 215*n*., 217*n*.

Tobin, J., 308*n.*
Tobin, N., 310*n.*
Tolman, R. C., 290*n.*
Tomasini, G., 205*n.*
Tomonaga, S., 5*n.*, 167, 230*n.*, 359*n.*
Tongiorgi, V. C., 234, 333*n.*
Touschek, B., 60*n.*
Treat, J., 333*n.*
Trembley, J., 348*n.*
Trent, P., 234

U

Uhlenbeck, G., 203*n.*

V

Valley, G. E., 193, 194
Van Hove, L., 239*n.*, 331*n.*
Van Wyck, C. B., 347*n.*
Vidale, M., 331*n.*
Villars, F., 143*n.*
Voorhees, H. G., 198*n.*
Voyvodic, L., 333*n.*

W

Wagner, N., 345
Walker, D., 35, 104
Walker, S. P., 309*n.*
Walker, W. D., 309, 312*n.*
Wanlass, S., 346*n.*, 350*n.*, 353*n.*
Warshaw, S., 68*n.*
Wataghin, G., 283*n.*
Watson, K., 5*n.*, 58*n.*, 70*n.*, 146*n.*, 159, 255*n.*, 331*n.*
Weinberg, J., 227*n.*
Weissbluth, M., 110
Weissenberg, A., 344*n.*
Weisskopf, V., 167*n.*, 183, 200, 227*n.*
Wentzel, G., 9*n.*, 160*n.*, 174*n.*, 226*n.*, 247*n.*, 359*n.*
Wheeler, J. A., 167*n.*, 172, 174, 175, 177, 180, 197*n.*, 208*n.*, 214*n.*
White, R. S., 98*n.*, 99*n.*, 110, 161*n.*
Whitehead, W., 64, 65
Whittemore, W. L., 248*n.*
Wick, G., 217*n.*, 250*n.*
Wiegand, C. E., 135*n.*, 189*n.*, 289*n.*
Wightman, A., 146, 149*n.*, 209*n.*, 210, 213, 217*n.*, 218
Wigner, E. P., 210*n.*, 217*n.*, 359*n.*
Wilcox, H., 64, 110, 113
Williams, E. J., 232*n.*
Williams, R. W., 335
Wilson, J., 199*n.*
Wilson, R., 123*n.*, 162*n.*
Wilson, R. R., 263*n*, 264-266, 268
Wilson, V. C., 229*n.*
Winther, A., 214*n.*
Wolff, P. A., 226*n.*
Woodward, W. M., 263*n.*
Wouthuysen, S., 60, 284*n.*
Wright, S., 187*n.*
Wu, C. S., 214*n.*, 215*n.*

Y

Yamada, E., 154*n.*
Yamaguchi, Y., 149*n.*, 188
Yang, C. N., 70*n.*, 142*n.*, 164, 165, 217*n.*
Yekutieli, G., 271*n.*, 317*n.*
Yodh, G. B., 248*n.*, 257*n.*, 263*n.*
York, C. M., 350*n.*
York, H. F., 84, 119*n.*, 140, 189*n.*
Yukawa, H., 140, 168*n.*, 202

SUBJECT INDEX

Absorption, nuclear (*see* Nuclear absorption)
Absorption mean free path, 226, 234
  (*See also* Nuclear absorption)
Air showers, 272, 276, 324, 333–336
  lateral spread of, 334–335
  multiple cores in, 335–336
  origin of, 334
  penetrating particles in, 272, 333–336
Alpha particle, model, 96, 103, 189, 201
  nuclear γ rays due to, 122
  as star-producing radiation, 141, 323–325, 327
  from stars, 313
  (*See also* Helium)
Alpha to proton ratio, 171, 183, 188
Aluminum, absorber, 65, 120
  decay of μ^- mesons in, 193–195
  interaction of π mesons in, 263, 270
  mesic X rays from, 179
  nucleonic production of π mesons in, 117–118
  penetrating showers from, 312
  photomesic production in, 101–102, 105–106, 109
Angular distribution, of charged π mesons produced, in nucleon-nucleon collisions, 44, 51, 55, 61–70
    in nucleon-nucleus collisions, 78, 80, 109
    in photon-nucleon collisions, 26–30, 32
    in photon-nucleus collisions, 78
  of neutral π mesons produced, in nucleon-nucleon collisions, 55
    in photon-nucleon collisions, 31
  of shower particles in nuclear stars, 319, 329, 331
Annihilation, of electron-positron pairs, 217, 341, 343
  of μ meson pairs, 217
  of neutrino pairs, 217
  of nucleon pairs, 143, 217, 341–343, 347
Anomalous magnetic moment (*see* Magnetic moment)
Anti-V particle (*see* V particle)
Antimony, decay of μ^- mesons in, 194
Antineutrino (*see* Neutrino)
Antineutron (*see* Antinucleon)
Antinucleon, 218, 291–294, 329, 331, 337–343, 355, 358, 362
  (*See also* Annihilation; Pair production)
Attenuation mean free path, 309–310
Auger showers (*see* Air showers)
Auger transitions, 167, 169, 172, 177–179

B

Beryllium, interaction of π mesons in, 263
  nucleonic production of π mesons in, 118–120, 122, 125, 135
  photomesic production in, 35, 36, 101–102, 105–107, 109
  proton bremsstrahlung from, 123
Beta decay, 97, 138, 208–211, 215, 218–219
  coupling constant in, 197, 213–214, 216
  double, 209, 215
  electron spectrum from, 209–211
  selection rules in, 213–215
  types of interaction in, 209, 215
  Yukawa's scheme for, 140, 195*n*., 202–203
  (*See also* Universal Fermi interaction)
Beta-gamma correlation, 214
Betatron, 2
Bevatron, 274, 339, 341
Bismuth, fission of, 187
  photomesic production in, 105
Black-body radiation, 290–291
Black tracks, 259, 313–317, 320, 323, 325
Blob, 182, 191
Bloch-Nordsieck calculation, 27, 275, 284
Boron, nucleonic production of π mesons in, 125
  photomesic production in, 101
Bose statistics, 145, 218
  of χ meson, 350–351
  of π meson, 8, 144–147, 166, 186
  of τ meson, 347, 351
  of ζ meson, 351
  of neutretto, 208, 212–213
Bosons (*see* Bose statistics)
Bremsstrahlung, cross section for, 221–224
  from electron, 44, 54, 123, 274–276

Bremsstrahlung, internal, 138
  from μ meson, 207, 221, 230–231
  from π meson, 283, 328, 334
  from proton, 122–123, 334
  spectrum of photons, 3, 27–28, 32–33, 90, 92, 98–105, 282–283
Bursts, 208, 220–226, 229
  (*See also* Electron showers)

C

Cadmium, interaction of π mesons in, 263
Calcium, absorption of μ^- mesons by, 200–201
  photomesic production in, 104–106
Capture of negative mesons, 146, 167, 171–172, 179
Carbon, π^- absorption in, 183–185
  antiproton annihilation in, 344
  decay of μ^- mesons in, 191
  interaction of π mesons in, 263–264, 267–268
  mesic X rays from, 178*n.*
  nucleonic production of π mesons in, 64, 68, 75, 88, 110–121, 123, 125, 135
  penetrating showers from, 308–312
  photomesic production in, 36, 90–92, 98–109
  proton bremsstrahlung from, 123
  slowing down in, 168–172
Cascade showers (*see* Electron showers)
Catastrophic transition, 7, 9–10, 13, 15, 24, 26, 39
Cerenkov radiation, 131
Charge-exchange interaction, 209–211, 214, 218
  (*See also* Universal Fermi interaction)
Charge-exchange scattering of π mesons, by deuterons, 237, 250–252
  by heavy nuclei, 260
  by nucleons, 236–239, 244–245, 252, 268
Charge independence hypothesis, 63*n.*, 95*n.*, 124*n.*, 249, 331
Charge-retention interaction, 210–214
  (*See also* Universal Fermi interaction)
Charge symmetry, 257, 260
Chew-Goldberger distribution of nucleon momenta, 83–95
Chi meson, 337, 348*n.*–351
Chlorine, π^- absorption in, 181
Closure approximation, 251, 256
Cloud chamber, 125, 136, 203–205, 228, 248, 258, 264, 268–270, 311–312, 314, 332, 341, 345, 346*n.*, 348, 351–358
Coincidence experiments, 35, 36, 108–109, 119, 147, 165, 207
Competing reactions for meson production, 74, 76
Compton scattering, 272, 274–275, 279
Compton wave length, 15, 21, 360
Conservation, of angular momentum, 58, 148, 153*n.*, 287–293, 340
  of charge, 217, 287
  of energy and momentum, 25, 38, 92, 126, 137, 147, 152, 207, 226, 252, 256, 260–261, 287–288, 342
  of nucleons, 359
  of parity, 58, 148
Coplanarity of tracks, 342, 345, 354, 356, 358
Copper, absorber, 65
  decay of μ^- mesons in, 194–195
  interaction of π mesons in, 263
  nucleonic production of π mesons in, 117–118
  photomesic production in, 101–102, 109
Cosmic rays, components of, hard, 204, 207, 234
    N, 128, 234, 311, 333
    soft, 114, 207, 333, 335
  energy spectrum of, 274, 277
  intensity of, 224
  primary, 334
  zenith angle dependence of, 204
Coulomb barrier, 97, 102, 116, 171, 183, 188
Coulomb effects, 112, 115
Coulomb-oscillator potential, 174, 177
Coulomb potential, 44–45, 54, 72, 78, 97, 111, 119, 122, 144, 167, 174*n.*, 222
Coulomb scattering, 239*n.*, 260, 264
  multiple, 228, 313, 335
    (*See also* Photographic emulsion)
Coulomb wave function, 148, 197
Coupling, of electrino-neutrino, to μ meson, 213
    to nucleon, 211–214, 236, 355
  of heavy meson to nucleon, 348, 362
  of μ meson to nucleon, 1, 177, 194–197, 216, 220, 226–229, 232–236, 337
  of π meson, to μ meson, 138–139, 161
    to nucleon, 5, 9, 23, 35, 47*n.*, 54, 68–72, 140, 143–144, 147, 151, 155, 177, 195–197, 202, 236, 238, 245, 252, 272, 283, 289, 337, 344, 346, 362
  of photons, to electron, 5, 38, 40, 149, 221, 232, 274, 341
    to π meson, 144, 157*n.*
    to nucleon, 143

- Critical energy, 223, 276, 281, 292
- Cyclotron, 67, 68*n.*, 110, 116–119, 125, 135, 162–163, 187, 248, 259, 263

D

- de Broglie wave length, 73, 97, 232, 265, 288
- Decay, of charged π meson, 130, 134, 142, 181, 218–219
    - lifetime for, 130, 134–136, 168, 196, 230
    - products from, 131, 134, 136–138
  - of μ meson, 181, 191–195, 202–203, 210, 218, 226, 230
    - lifetime for, 168, 191–196, 203–204
    - products from, 171, 192, 196–197, 201–208
  - of neutral π meson, 8, 20, 36, 108, 124, 126, 127*n.*, 130, 132, 140–144, 164–165, 273, 325, 338, 347
    - lifetime for, 98, 130, 140–144, 324–325, 330, 338, 347
    - products from, 132, 141*n.*, 145
- Degree of inelasticity, 283*n.*, 303, 306, 327
  - (*See also* Kinematics)
- Dependence on atomic number, of nucleonic production of π mesons, 109, 117–118
  - of photomesic production, 101–102, 105, 109
- Depolarization effects, 161
- Detailed balancing, 7, 161, 245–246
- Deuterium, π meson interaction in, 250–254, 257–258
  - nucleonic production of π mesons in, 68, 114–115, 125
  - photomesic production in, 21, 35–38, 105, 106, 109
  - (*See also* Elastic scattering; Inelastic scattering; Nuclear absorption)
- Deuteron, mass of, 337
  - pickup, 84, 269
  - wave function of, 60, 62, 70, 250–251
  - (*See also* Deuterium)
- Diffraction scattering of π mesons, 237, 260, 262–267
- Dineutron, 159
- Diproton, 62
- Dirac equation, 174–175, 227, 250, 338
- Dirac δ function, 22, 35
- Dirac operators, 8, 9, 54
- Distribution, Gaussian, of nucleon momenta, 83–88
  - (*See also* Angular distribution)
- Divergence difficulties, 218, 274
- Doppler shift, 121–122, 133–134
- Double beta decay, 209, 215

E

- Efficiency for meson production, 93–96, 101
- Elastic scattering, of μ mesons, 195*n.*, 202, 227–229
  - of π mesons, by deuterons, 237, 250–251, 254–257
    - by heavy nuclei, 236, 258–266, 271–272, 288
    - by nucleons, 236, 238–244, 268, 273, 275, 323
    - (*See also* Nucleon-nucleon scattering)
- Electromagnetic interaction, of μ meson, 172, 203, 220–222, 229, 231
  - of π meson, 8, 172
- Electron, from π meson, 127*n.*, 138, 141*n.*
- Electron production of π mesons, 38–40
  - (*See also* Beta decay; Bremsstrahlung; Electron showers; Pair production)
- Electron showers, double cores of, 126, 142
  - fluctuations in, 127
  - production of, by μ mesons, 220
    - by π^0 mesons, 126–127, 141, 320, 330, 332, 336, 356
    - by *N* component, 220
  - theory of, 223, 333, 335
- Elementary particle, 203, 218, 337
  - (*See also* specific particles)
- Emulsion cloud chamber, 141
  - (*See also* Photographic emulsion)
- Energy, critical, 223, 276, 281, 292
  - threshold (*see* Threshold energy)
- Energy spectrum, of alpha particles from π^- stars, 182, 185
  - of charged π mesons produced, 28, 33
    - in nucleon-nucleon collisions, 2, 44
    - in nucleon-nucleus collisions, 80–82, 85–88, 109–115, 119
    - in photon-nucleus collisions, 90–92, 99–105, 109
  - of cosmic rays, 274, 277
  - of electrons from μ meson decay, 205–208, 211–215, 219–220
  - of μ mesons, 223, 225, 229–231
  - of π mesons in nuclear stars, 331
  - of neutral π mesons produced, 31, 33, 36

Energy spectrum, of neutral π mesons produced, in nucleon-nucleon collisions, 64, 67
  in nucleon-nucleus collisions, 78, 124, 128–129
  in photon-nucleus collisions, 78, 108
 of protons from π^- stars, 182–190, 198
 of γ rays from π^- absorption, 133, 157–159
Equivalence theorem, 10*n.*, 38, 48*n.*, 51, 143–144, 150–151, 155, 196*n.*, 245, 252
Equivalent photon, 33, 99–100, 233
Evaporation model of nucleus, 183, 188
 (*See also* Nucleus)
Evaporation nucleons, 185, 188, 190
Evaporation star, 189, 342
Exchange forces (*see* Nuclear forces)
Excitation function, for nucleonic production of π mesons, 63, 78, 109–110, 116, 123
 for photomesic production, 4, 34, 37–38
Extensive air showers (*see* Air showers)

F

Fermi gas model of nucleus, 73, 79–92, 110, 188–189, 198, 200–201, 260–262, 339
Fermi statistics, 145, 218, 291
 of κ meson, 349–351
 of μ meson, 187, 208, 216
Fermion (*see* Fermi statistics)
Feynman diagrams, for decay of neutral π meson, 143
 for electron production of π mesons, 39
 for π meson scattering, 238–239
 for nucleonic production of π mesons, 45–46, 54
 for photomesic production, 6, 10, 18
 for radiative π^- absorption in hydrogen, 148
Field (*see* Coupling; specific fields)
Fine structure constant (*see* Coupling)
Finite charge distribution of nucleus, 173, 177
 (*See also* Mesic X rays)
Fission, 187
Fluorine, photomesic production in, 105–106
Fourier components, of electromagnetic radiation, 223
 of wave function, 62, 85, 91, 251
Fourier meson spectrum, 283
Fourier transform of force, 70–71

G

Gamma rays, from μ^- absorption, 201
 from antiproton annihilation, 343
 Doppler effect for, 121–122, 133–134
 from μ meson decay, 207
 from π^0 meson decay, 128, 356
 as star-producing radiation, 232–234
 (*See also* Bremsstrahlung; Decay; Nuclear absorption)
Gauge invariance, 7, 9, 24, 47*n.*, 54, 95, 143
Gaussian distribution of nucleon momenta, 83–88
Geiger-Muller counter, 264, 311
Geometric mean free path, definition of, 259
Gold, interaction of π mesons in, 270
Gray tracks, 312–317, 320, 323–328
Gross transformation, 310

H

Hammer track, 184
Harmonic potential, 173–174, 180
Heavy mesons, 8, 275, 291*n.*, 325, 337–338, 344–345, 362
Heavy nuclei, nucleonic production of π mesons in, 72, 93, 95, 97, 109, 118, 125, 166
 photomesic production in, 72, 89, 93–94, 97–98, 101–102, 106, 118, 144, 166
Helium, π^- absorption in, 182
 nucleonic production of π mesons, in, 72, 75
 photomesic production in, 102, 104
Higher order corrections, in π meson scattering, 245
 in nucleonic production of π mesons, 69
 in photomesic production, 2
Hulthen wave function, 85
Hydrogen, π meson scattering in, 248–249, 253, 257–258, 263
 molecular ion, 146
 nucleonic production of π mesons in, 64–68, 125
 photomesic production in, 32, 35–37, 101–105, 109, 273
 (*See also* Elastic scattering; Slowing down)
Hydrogenic approximation, 180

I

Impact parameter, 283*n.*, 288, 292–296, 329–331
 (*See also* Multiple production)

Impulse approximation, 250
Inelastic scattering of π mesons, by deuterium, 250, 254, 257
  by nuclei, 236–237, 258–264
Infrared catastrophe, 274–275, 282–283
Insulators, Brillouin gaps in, 170
  (*See also* Slowing down)
Interaction mean free path, for μ mesons, 231
  for π mesons, 98
  for shower particles, 309–311
Interference effects in deuterium, 254–256
Intermediate coupling theory, of π meson scattering, 247*n*.
  of photomesic production, 27*n*.
  (*See also* Coupling)
Invariant matrix element, 89, 239
Inverse reaction, 20, 161, 252
Iodine, Z_{eff} for, 180
Ionization chamber, 225
Ionization loss, 168, 229, 231
  Fermi saturation effect for, 229*n*.
Iron, absorption by, of μ^- mesons, 191
    of π mesons, 226
  bursts under, 220–225
  mesic X rays from, 179
  nucleonic production of π mesons in, 117
  scattering of μ mesons in, 228
  slowing down in, 169–170
Isobaric states, of π mesons, 122
  of nucleons, 26, 27*n*., 109, 122, 237–238, 247*n*., 248*n*., 249–250, 359*n*.
  and V particles, 359–362
Isotopic spin of nucleon, 5, 21, 251
  and π meson scattering, 248*n*., 249
  and nuclear forces, 51, 53, 54
  and nucleonic production of π mesons, 60, 95, 284
  and photomesic production, 26, 27*n*., 93
  and V particles, 359*n*., 360–361

J

Jacobian, 44, 300–301, 304

K

K-electron capture, 197, 216
Kappa meson, 166*n*., 337, 348–350
Kinematics, of π meson scattering, 240–242
  of multiple meson production, 276, 296–308
  of single meson production, in nucleon-nucleon collisions, 41, 44
    in nucleon-nucleus collisions, 72, 77
    in photon-nucleon collisions, 3
    in photon-nucleus collisions, 75, 77
  of two-photon decay of π^0 meson, 36, 108, 126
  of V-particle decay, 353–354
  (*See also* Threshold energy)
Klein-Gordon equation, 174, 176
Knock-on electrons, cross section for, 221–224
  from μ mesons, 230

L

Lead, absorption by, of μ^- mesons, 200, 234
    of π mesons, 120, 226
  bursts under, 220, 222–225
  interaction of π mesons in, 263, 270
  mesic X rays from, 177, 179
  nucleonic production of π mesons in, 110*n*., 111–118
  penetrating showers from, 258, 308–312
  photomesic production in, 101–102, 109
  scattering of μ mesons in, 228
  V particles from, 352, 355–356
  Z_{eff} for, 180
Lead converter, 107, 127
Lead filter, 200
Liquid-drop model of nucleus, 188
Lithium, π^- absorption in, 182
  interaction of π^- mesons in, 263
  penetrating showers from, 332
  photomesic production in, 101–102, 109
  slowing down in, 171–172, 178*n*.
Lorentz contraction, 287, 289, 293
Lorentz invariance, 217
Lorentz transformation, 75, 77, 298

M

Magnesium, absorption of μ^- mesons by, 200–201
  decay of μ^- mesons in, 194–195
  as star-producing radiation, 329*n*.
Magnetic moment, of μ meson, 175–176, 222–223
  of nucleon, 7, 12, 15–16, 20, 23–25, 38, 143, 148–149, 338
  Pauli expression for, 18
Majorana operator, 56
Mass, of charged π meson, 130–132, 145, 203, 232
  of μ meson, 203, 205, 224, 232

Mass, of neutral π meson, 124, 130–134, 145
  (*See also* Heavy mesons)
Maximum kinetic energy of π mesons, in nucleon-nucleon collisions, 42–43, 47
  in nucleon-nucleus collisions, 75, 80, 96, 117, 125
  in photon-nucleus collisions, 77
Mesic absorption (*see* Nuclear absorption)
Mesic atoms, 167–168, 178, 180
  Bohr orbits of, 167, 169, 170, 172, 191, 194, 197, 212, 216
  energy levels of, 173, 175, 177
  ionization potentials of, 175
  Z_{eff} for, 180, 191
Mesic charge, 152
Mesic-deuterium atom, 153–154, 194, 236, 252
Mesic-hydrogen atom, 132, 145–149, 152*n.*, 172, 236, 245
Mesic X rays, 167, 169, 171–179
Meson production (*see* Multiple production; Nucleonic production; Photoproduction; Plural production)
Meson theory of nuclear forces, 2, 52, 55–56, 228, 347
Mixed showers, 126
Mu meson, altitude variation of, 119
  discovery of, 202
  (*See also* Cosmic rays; Nuclear absorption; Nuclear interaction; specific properties; Underground)
Multinucleon model for π^- absorption, 189–191
Multiple Coulomb scattering, 228, 313, 335
  (*See also* Photographic emulsion)
Multiple production, of π mesons, 233, 274–275, 282, 323, 326, 331–333, 336
    angular distribution in, 288, 323
    backward fraction in, 323
    energy spectrum in, 44*n.*, 118
    Fermi theory of, 287–297, 331, 339
    multiplicity in, 127, 286, 342
    neutral to charged ratio in, 331
  of photons, 274–275

N

N^0 particle, 349, 351
Negative-energy states, 12, 36*n.*, 51, 53*n.*, 54, 60*n.*, 68, 106, 143, 149, 152, 245, 251, 268, 338
Negative mesons, capture of, 146, 167, 171–172, 179
Negative proton (*see* Antinucleon)
Neutral μ meson, 203
Neutral π meson, 21, 122–124
  (*See also* specific properties)
Neutral to positive π meson ratio, in nucleonic production, 55, 69
  in photoproduction, 12, 13, 16
Neutretto, 208
Neutrino, 203, 218
  in beta decay, 209, 210*n.*, 215–216
  Dirac theory of, 211–213
  from heavy mesons, 349, 350
  Majorana theory of, 211, 213, 215
  from μ meson absorption, 197
  from π meson absorption, 147
  from μ meson decay, 202, 204, 208
  from π meson decay, 131, 137–138
  from V particles, 354, 358
Neutron-neutron interaction, 156, 158–159, 190
Neutron-proton interaction, 123
Neutron-proton scattering, 56, 66, 189*n.*, 190
Neutrons, from μ meson stars, 200–201, 234
  as star-producing radiation, 232
Nitrogen, π^- absorption in, 181, 183–185
Nonlinear effects, 283
  (*See also* Multiple production)
Nonrenormalizable theory, 143*n.*
Nuclear absorption, 167
  of μ mesons, 137, 166, 186, 191–201, 204, 208, 216, 226
  of π mesons, 99–103, 111, 125, 131, 145–146, 166, 178, 198, 236–237
    in deuterium, mesic, 153, 156, 158, 181, 236
      nucleon, 152–158, 162–164, 181, 236–237, 252, 273, 338*n.*
      radiative, 153–158, 181, 236–237
    in heavy elements, 180–181, 191, 237
    in hydrogen, mesic, 132–133, 145–155, 164, 171, 180–181, 236
      radiative, 132–133, 145, 147–157, 171, 180–181, 196*n.*, 236, 245, 246, 252, 273, 338*n.*
    by nuclei of photographic emulsion, 182–183, 185*n.*, 187
    by tritium, 159
    (*See also* specific elements)
Nuclear fission, 187
Nuclear forces, 45, 51, 54, 59, 69–71, 87, 123, 250–251, 337
  central, 51, 55, 70
  charge independence of, 51–56
  exchange character of, 189–190

Nuclear forces, meson theory of, 2, 52, 55–56, 228, 347
  range of, 44, 202
  spin dependence of, 52, 54, 70, 71
  tensor character of, 51, 54, 56, 70
Nuclear interaction, of μ mesons, 203, 226, 234–236
  of π mesons, 32, 65, 78, 97–98, 101–102, 105, 109, 117, 249, 264–271, 358
  of nucleons, 112, 265
  (*See also* specific elements)
Nuclear stars, 269*n*., 270, 310, 351–354
  angular distribution of shower particles in, 319, 329, 331
  energy spectrum of π mesons in, 331
  frequency-size distribution of, 310, 316
  neutral to charged meson ratio in, 320, 325, 330–331
  nucleon to meson ratio, 326
  production of, by μ mesons, 198–199, 231–233
    by π mesons, 176, 182, 237, 258–265, 268, 336
    by nucleons, 328*n*.
  prong number of, 199
  (*See also* Penetrating showers; Photographic emulsion)
Nucleon-nucleon interaction, 332
  (*See also* Nuclear forces)
Nucleon-nucleon scattering, 290
  shape-independent approximation in, 159, 251
  (*See also* Neutron-proton scattering; Proton-proton scattering)
Nucleonic cascade, 279, 309, 335–336
Nucleonic production, of charged π mesons, 41, 52, 55–58, 63, 68–69, 72, 130, 196, 288–289
  of neutral π mesons, 41, 52, 57–58, 63, 67–69, 72, 130, 144, 164, 289
  (*See also* specific nucleui)
Nucleus, compound, 286
  excitation energy of, 188–190, 197–200, 208, 261
  radius of, 97–98, 174–177, 265, 311
  temperature of, 188, 190
  transparency of, 259
  (*See also* specific models)

O

Optical model of nucleus, 264–268
Optical transitions (*see* Mesic X rays)
Oxygen, π^- absorption in, 183–185
  interaction of π mesons in, 263
  nucleonic production of π mesons in, 125, 281–282
  photomesic production in, 105–106

P

Pair production, 362
  of electron-positron, 107, 127, 137, 141, 145, 165, 325, 330, 338
  of μ mesons, 1
  of nucleon-antinucleon, 143, 338–340, 347, 362
Pair spectrometer, 120, 132
Parity, of charged π meson, 8, 41, 130, 144, 147, 151–160, 196, 273
  of neutral π meson, 41, 68*n*., 130, 142, 144, 147, 151–152, 164, 273
Pauli exclusion principle, 52, 58, 62–63, 68, 72, 78, 87, 92, 96, 97, 101–103, 109, 152–154, 159, 169, 181, 252
Pauli moment, 18
Penetrating particles (*see* Penetrating showers)
Penetrating showers, 126–127, 228, 268–276, 283, 311, 324, 332–333, 350, 358*n*.
  multiplicity of, 312
  nucleons in, 276
  size-frequency distribution of, 278–279, 309
  V particles in, 353, 358
Perturbation-theoretic method (*see* Weak coupling theory)
Phase space, 78, 109, 227*n*., 286, 349
Photodisintegration of deuteron, 16
Photoelectric transition, 7, 10, 13, 15
Photographic emulsion, 125, 134, 311
  antiprotons in, 342–344
  black tracks in, 259, 313–317, 320, 323, 325
  blobs in, 182, 191
  detection of mesons in, 64, 98, 101–102, 110, 119, 135–138
  electron-sensitive, 205, 232, 259, 270, 312, 315, 324, 328
  gelatin, 170–171, 183–184, 190, 199
  grain density in, 119, 127, 130, 269, 312–313, 317, 345, 346*n*.
  gray tracks in, 312–317, 320, 323–328
  heavy fragments in, 184, 313
  heavy mesons in, 348, 351
  nuclear stars in, 119, 182, 184, 198, 231, 234, 237, 258, 260, 263–264, 268–272, 310–318, 329, 345
  range in, 131, 346, 348

Photographic emulsion, scattering measurements in, 119, 127, 130, 205, 207, 317, 328, 345, 346*n.*, 348
  shower particles in, 128, 141, 312–316, 320, 323
  silver bromide in, 170–171
Photons, multiple production of, 274–275
  (*See also* Gamma rays)
Photoproduction, of charged π mesons, 2, 41, 130, 134, 140, 160, 196
    theoretical cross sections for, 10, 14–17, 23–24, 245–246
  classical theory of, 21–26
  of μ mesons, 1
  of τ mesons, 1
  of neutral π mesons, 41, 130, 144, 247, 273
    theoretical cross sections for, 14, 18–20, 23, 27*n.*, 30
Pi meson (*see* specific properties or specific processes)
Pi meson-nucleon interaction (*see* Coupling)
Plane wave approximation, in absorption of π mesons, 251
  in nucleonic production of π mesons, 56–59, 62–63, 65, 70
Plural production, 279, 282, 312–325, 328–333
  of π mesons, 118, 276, 321
  nucleon to meson ratio in, 324
  of shower particles, 233–234, 281, 311
  size-frequency in, 280, 321
Pluro-multiple production, 312, 326, 328
Poisson law, 282, 330
Polarization, of mesons, 10, 11, 49, 51, 160–161
  of photons, 10, 23, 25, 164–165, 290
Pole of radiation from π^- absorption, in deuterium, 154–155
  in hydrogen, 148–149
Positive to negative π meson ratio, in electron production, 40
  in nucleonic production, 109, 115–117
  in photoproduction, 12–13, 24–26, 35, 36*n.*, 91, 94, 101, 104, 106
Positron, 97
  (*See also* Annihilation; Decay; Pair production)
Production, pluro-multiple, 312, 326, 328
  postequilibrium, 287, 331
  (*See also* Multiple production; Nucleonic production; Pair production; Photoproduction; Plural production)
Proton-proton interaction, 159
Proton-proton scattering, 56, 70, 190, 289*n.*
Protons (*see* specific processes)
Pseudoscalar, 217
Pseudoscalar field, 26, 34–35, 41, 57–58, 130, 149, 153–160, 164–165, 180–181, 218–219, 237–238, 245–246, 250–255, 286, 337–338, 347–348, 359, 362
  with pseudoscalar coupling, 5*n.*, 9, 18–20, 31, 33, 38, 41, 47–48, 51, 53, 54, 59, 68, 142–144, 149–156, 219, 249, 268, 272–273
  with pseudovector coupling, 9–20, 23, 29, 31, 33, 36*n.*, 38–41, 48, 51–63, 66–71, 80*n.*, 106, 130, 143–144, 150–156, 196*n.*, 219, 245–255, 268, 272–275, 285, 289, 337–338, 342–343, 359–360
Pseudovector field, 26, 34–35, 41, 57–58, 62, 130, 145, 149, 153–154, 157–158, 161
  with dual tensor coupling, 9, 160
  with pseudovector coupling, 9–17, 30–31, 35, 48–51, 54–55, 60–63, 66–69, 80*n.*, 150, 153*n.*, 155–156, 160, 252

Q

Quantum electrodynamics, 274–275

R

R star, 140, 324–328, 334
  (*See also* Nuclear stars)
Radiation, Cerenkov, 131
Radiation damping, 343*n.*
Radiation length, 330, 336
Radiative absorption (*see* Nuclear absorption)
Range, 203
  in cloud chambers, 204
  (*See also* Photographic emulsion)
Range-energy relation, 130
Reaction of meson field, 6, 26, 360
Recoil nucleons, and π meson production, 277–278, 282, 321–322, 324, 326
  and π meson scattering, 260
  and photomesic production, 3, 7, 25, 36–37, 89
Regulator methods, 143*n.*
Relativistic thermodynamics, 290, 292, 340
Renormalization, 5, 362
Reproduction of π mesons, 236, 271–272, 277, 279, 321, 336

S

S particles, 348, 350
S star, 328–329, 331
  (*See also* Nuclear stars)
Scalar field, 26, 32, 34, 57–58, 62, 149, 153–154, 158, 165, 237, 273, 359, 362
  with scalar coupling, 5*n*., 9–17, 21, 29, 31, 35, 39–40, 48, 52, 54–55, 59–63, 66, 68, 80*n*., 139, 142–144, 149–151, 155–156, 359–360
  with vector coupling, 9, 38
Scattering, Compton, 272, 274–275, 279
  Coulomb, 239*n*., 260, 264
    multiple, 228, 313, 335
  elastic (*see* Elastic scattering)
  of μ mesons in lead, 228
  of π mesons, charge-exchange (*see* Charge-exchange scattering of π mesons)
    diffraction, 237, 260, 262–270
    inelastic (*see* Inelastic scattering of π mesons)
  neutron-proton, 56, 66, 189*n*., 190
  nucleon-nucleon (*see* Nucleon-nucleon scattering)
  Thomson limit for, 149, 241, 245
Scintillation counter, 32, 36, 102, 135, 162, 194, 204, 248, 263
Screening effects, 173, 222
Shaking-off transition, 7–8, 10, 12, 15
Silver, nucleonic production of π mesons in, 117–118, 281–282
Slowing down, of antiprotons, 344
  of heavy mesons, 346
  in insulators, 170
  of mesons, 167, 169
    in heavy elements, 166–170
    in hydrogen, 146, 167–168
Sodium fluoride, decay of μ^- mesons in, 194–195
Space inversion, invariance under, 217
  (*See also* Parity)
Spin, of charged π meson, 8, 130, 144–147, 151–163, 167, 176, 196, 273
  of κ meson, 349
  of μ meson, 167, 196, 203, 219–222
  of τ meson, 347
  of neutral π meson, 36, 130, 142–147 152, 273
  of nucleon, 5, 23, 26, 27*n*.
Spin inertia, 26
Spin-orbit interaction, 174
Spiral-orbit spectrometer, 206
Stars (*see* Nuclear stars)
Statistical correlations, 290, 292, 340
Statistical equilibrium, 287, 289
Statistical factor, 87
Statistical independence, 277, 281, 286
Statistical theory of nuclei, 183, 200–201
Statistical weight, 157, 287–288
Stefan's law, 290–291
Stefan-Boltzmann constant, 290
Stoppings, 258–261, 265
Straggling of μ meson range, 136, 138
Strong coupling theory, 5, 26, 228
  of π meson scattering, 238*n*., 244–249, 257
  of photomesic production, 2, 21–23, 27, 32, 38
  and *V* particles, 359–363
  (*See also* Coupling)
Subheavy mesons, 350
  (*See also* Heavy mesons)
Sulphur, decay of μ^- mesons in, 194–195
  photomesic production in, 105–106
Superheavy mesons, 348, 359*n*.
  (*See also* Heavy mesons)
Symmetric meson theory, 21, 26, 32, 56, 71, 245, 247, 253, 285, 359*n*.
  (*See also* Charge independence hypothesis; Nuclear forces)
Synchrotron, 2, 35–36, 98, 102, 107, 135, 233, 264

T

T star, 141, 329–331, 334
  (*See also* Nuclear stars)
Target-at-rest approximation, 251
Tau meson, 166*n*., 291*n*., 325, 337, 345–348, 351, 353
Thermodynamics, relativistic, 290, 292, 340
Thomas-Fermi model, for atom, 169, 222
Thomson limit for scattering, 149, 241, 245
Thorium fission, 187
Threshold energy, for heavy meson production, 347
  for multiple meson production, 289
  for nucleon pair production, 339
  for single meson production, in nucleon-nucleon collisions, 41, 277
    in nucleon-nucleus collisions, 72–74, 78–80, 110, 124
    in photon-nucleon collisions, 3
    in photon-nucleus collisions, 76, 78
  for *V* particle production, 359
Time inversion, invariance under, 217
Tin, decay of μ^- mesons in, 194–195
  interaction of π mesons in, 263*n*.

Tin, photomesic production in, 101–102
Transitions, Auger, 167, 169, 172, 177–179
  catastrophic, 7, 9–10, 13, 15, 24, 26, 39
  photoelectric, 7, 10, 13, 15
  shaking-off, 7–8, 10, 12, 15
Triton, 269
Turbulent mixing, 283–286
  (*See also* Multiple production)
Two-meson hypothesis, 195, 350
Two-nucleon model for π^- absorption, 189–190

U

Underground, azimuthal variation, 231
  depth-intensity relation, 134, 229–231
  nuclear stars produced, by μ mesons, 198–200, 232
    by π mesons, 199
  penetration of μ mesons, 202, 226–230
Universal Fermi interaction, 215–219, 349
Uranium, fission of, 187
  as mesic atom, 173

V

v^0 particle, 350–351, 354, 356, 358, 362
V particle, 337–338, 351
  charged, 350, 352, 359
  neutral, 352–361
Varitrons, 344*n.*
Vector field, 32, 34, 57–58, 140, 145, 149, 153–154, 158, 237, 273
  with tensor coupling, 9, 160
  with vector coupling, 9–17, 30–31, 35, 48–49, 51, 54–55, 59–63, 66, 68*n.*, 69, 80*n.*, 150, 153*n.*, 155–157, 160
Virtual photon field, 39, 44–45, 232–236
Virtual processes, and anomalous magnetic moment, 27, 38, 338*n.*
Virtual processes, and nucleon-nucleon interaction, 2, 45
  and nucleonic production of π mesons, 44, 46, 54, 69
  and star production by μ mesons, 233

W

Water, decay of μ^- mesons in, 194–195
Weak coupling theory, 5, 16, 274–175, 338*n.*
  of μ^- absorption, in deuterium, 153*n.*, 154, 156
    in hydrogen, 148–150, 152*n.*, 154
    in tritium, 159
  of electromagnetic processes, 5
  of electron production of π mesons, 38
  of μ meson scattering, 227
  of π meson scattering, 238–246, 249–250, 253
  of nucleonic production, 44–46, 71
    field-theoretic method, 44–45, 54–56, 66, 68–69
    phenomenological method, 44–45, 53–56, 60, 63, 66, 68–70
  of nucleon-pair annihilation, 342–344
  of nucleon-pair production, 338–339
  (*See also* Coupling)
W.K.B. method, 174–175

Y

Yukawa potential, 22, 156
Yukawa's scheme for beta decay, 140, 195*n.*, 202–203

Z

Z law for meson capture in mixtures, 170–172, 194
Zeta meson, 350–351

Catalogue of Dover
SCIENCE BOOKS

DIFFERENTIAL EQUATIONS
(ORDINARY AND PARTIAL DIFFERENTIAL)

INTRODUCTION TO THE DIFFERENTIAL EQUATIONS OF PHYSICS, L. Hopf. Especially valuable to engineer with no math beyond elementary calculus. Emphasizes intuitive rather than formal aspects of concepts. Partial contents: Law of causality, energy theorem, damped oscillations, coupling by friction, cylindrical and spherical coordinates, heat source, etc. 48 figures. 160pp. 5⅜ x 8. S120 Paperbound $1.25

INTRODUCTION TO BESSEL FUNCTIONS, F. Bowman. Rigorous, provides all necessary material during development, includes practical applications. Bessel functions of zero order, of any real order, definite integrals, asymptotic expansion, circular membranes, Bessel's solution to Kepler's problem, much more. "Clear . . . useful not only to students of physics and engineering, but to mathematical students in general," Nature. 226 problems. Short tables of Bessel functions. 27 figures. x + 135pp. 5⅜ x 8. S462 Paperbound $1.35

DIFFERENTIAL EQUATIONS, F. R. Moulton. Detailed, rigorous exposition of all non-elementary processes of solving ordinary differential equations. Chapters on practical problems; more advanced than problems usually given as illustrations. Includes analytic differential equations; variations of a parameter; integrals of differential equations; analytic implicit functions; problems of elliptic motion; sine-amplitude functions; deviation of formal bodies; Cauchy-Lipshitz process; linear differential equations with periodic coefficients; much more. Historical notes. 10 figures. 222 problems. xv + 395pp. 5⅜ x 8. S451 Paperbound $2.00

PARTIAL DIFFERENTIAL EQUATIONS OF MATHEMATICAL PHYSICS, A. G. Webster. Valuable sections on elasticity, compression theory, potential theory, theory of sound, heat conduction, wave propagation, vibration theory. Contents include: deduction of differential equations, vibrations, normal functions, Fourier's series. Cauchy's method, boundary problems, method of Riemann-Volterra, spherical, cylindrical, ellipsoidal harmonics, applications, etc. 97 figures. vii + 440pp. 5⅜ x 8. S263 Paperbound $2.00

ORDINARY DIFFERENTIAL EQUATIONS, E. L. Ince. A most compendious analysis in real and complex domains. Existence and nature of solutions, continuous transformation groups, solutions in an infinite form, definite integrals, algebraic theory. Sturmian theory, boundary problems, existence theorems, 1st order, higher order, etc. "Deserves highest praise, a notable addition to mathematical literature," Bulletin, Amer. Math. Soc. Historical appendix. 18 figures. viii + 558pp. 5⅜ x 8. S349 Paperbound $2.55

ASYMPTOTIC EXPANSIONS, A. Erdélyi. Only modern work available in English; unabridged reproduction of monograph prepared for Office of Naval Research. Discusses various procedures for asymptotic evaluation of integrals containing a large parameter; solutions of ordinary linear differential equations. vi + 108pp. 5⅜ x 8. S318 Paperbound $1.35

LECTURES ON CAUCHY'S PROBLEM, J. Hadamard. Based on lectures given at Columbia, Rome, discusses work of Riemann, Kirchhoff, Volterra, and author's own research on hyperbolic case in linear partial differential equations. Extends spherical cylindrical waves to apply to all (normal) hyperbolic equations. Partial contents: Cauchy's problem, fundamental formula, equations with odd number, with even number of independent variables; method of descent. 32 figures. iii + 316pp. 5⅜ x 8. S105 Paperbound $1.75

NUMBER THEORY

INTRODUCTION TO THE THEORY OF NUMBERS, L. E. Dickson. Thorough, comprehensive, witn adequate coverage of classical literature. Not beyond beginners. Chapters on divisibility, congruences, quadratic residues and reciprocity, Diophantine equations, etc. Full treatment of binary quadratic forms without usual restriction to integral coefficients. Covers infinitude of primes, Fermat's theorem, Legendre's symbol, automorphs, Recent theorems of Thue, Siegal, much more. Much material not readily available elsewhere. 239 problems. 1 figure. viii + 183pp. 5⅜ x 8. S342 Paperbound **$1.65**

ELEMENTS OF NUMBER THEORY, I. M. Vinogradov. Detailed 1st course for persons without advanced mathematics; 95% of this book can be understood by readers who have gone no farther than high school algebra. Partial contents: divisibility theory, important number theoretical functions, congruences, primitive roots and indices, etc. Solutions to problems, exercises. Tables of primes, indices, etc. Covers almost every essential formula in elementary number theory! "Welcome addition . . . reads smoothly," Bull. of the Amer. Math. Soc. 233 problems. 104 exercises. viii + 227pp. 5⅜ x 8. S259 Paperbound **$1.60**

PROBABILITY THEORY AND INFORMATION THEORY

SELECTED PAPERS ON NOISE AND STOCHASTIC PROCESSES, edited by Prof. Nelson Wax, U. of Illinois. 6 basic papers for those whose work involves noise characteristics. Chandrasekhar, Uhlenback and Ornstein, Uhlenbeck and Ming, Rice, Doob. Included is Kac's Chauvenet-Prize winning "Random Walk." Extensive bibliography lists 200 articles, through 1953. 21 figures. 337pp. 6⅛ x 9¼. S262 Paperbound **$2.35**

A PHILOSOPHICAL ESSAY ON PROBABILITIES, Marquis de Laplace. This famous essay explains without recourse to mathematics the principle of probability, and the application of probability to games of chance, natural philosophy, astronomy, many other fields. Translated from 6th French edition by F. W. Truscott, F. L. Emory. Intro. by E. T. Bell. 204pp. 5⅜ x 8. S166 Paperbound **$1.25**

MATHEMATICAL FOUNDATIONS OF INFORMATION THEORY, A. I. Khinchin. For mathematicians, statisticians, physicists, cyberneticists, communications engineers, a complete, exact introduction to relatively new field. Entropy as a measure of a finite scheme, applications to coding theory, study of sources, channels and codes, detailed proofs of both Shannon theorems for any ergodic source and any stationary channel with finite memory, much more. "Presents for the first time rigorous proofs of certain fundamental theorems . . . quite complete . . . amazing expository ability," American Math. Monthly. vii + 120pp. 5⅜ x 8. S434 Paperbound **$1.35**

VECTOR AND TENSOR ANALYSIS AND MATRIX THEORY

VECTOR AND TENSOR ANALYSIS, G. E. Hay. One of clearest introductions to increasingly important subject. Start with simple definitions, finish with sure mastery of oriented Cartesian vectors, Christoffel symbols, solenoidal tensors. Complete breakdown of plane, solid, analytical, differential geometry. Separate chapters on application. All fundamental formulae listed, demonstrated. 195 problems. 66 figures. viii + 193pp. 5⅜ x 8. S109 Paperbound **$1.75**

APPLICATIONS OF TENSOR ANALYSIS, A. J. McConnell. Excellent text for applying tensor methods to such familiar subjects as dynamics, electricity, elasticity, hydrodynamics. Explains fundamental ideas and notation of tensor theory, geometrical treatment of tensor algebra, theory of differentiation of tensors, and a wealth of practical material. "The variety of fields treated and the presence of extremely numerous examples make this volume worth much more than its low price," Alluminio. Formerly titled "Applications of the Absolute Differential Calculus." 43 illustrations. 685 problems. xii + 381pp. S373 Paperbound **$1.85**

VECTOR AND TENSOR ANALYSIS, A. P. Wills. Covers entire field, from dyads to non-Euclidean manifolds (especially detailed), absolute differentiation, the Riemann-Christoffel and Ricci-Einstein tensors, calculation of Gaussian curvature of a surface. Illustrations from electrical engineering, relativity theory, astro-physics, quantum mechanics. Presupposes only working knowledge of calculus. Intended for physicists, engineers, mathematicians. 44 diagrams. 114 problems. xxxii + 285pp. 5⅜ x 8. S454 Paperbound **$1.75**

DOVER SCIENCE BOOKS

PHYSICS, ENGINEERING

MECHANICS, DYNAMICS, THERMODYNAMICS, ELASTICITY

MATHEMATICAL ANALYSIS OF ELECTRICAL AND OPTICAL WAVE-MOTION, H. Bateman. By one of century's most distinguished mathematical physicists, a practical introduction to developments of Maxwell's electromagnetic theory which directly concern the solution of partial differential equation of wave motion. Methods of solving wave-equation, polar-cylindrical coordinates, diffraction, transformation of coordinates, homogeneous solutions, electromagnetic fields with moving singularities, etc. 168pp. 5⅜ x 8. S14 Paperbound $1.60

THERMODYNAMICS, Enrico Fermi. Unabridged reproduction of 1937 edition. Remarkable for clarity, organization; requires no knowledge of advanced math beyond calculus, only familiarity with fundamentals of thermometry, calorimetry. Partial Contents: Thermodynamic systems, 1st and 2nd laws, potentials; Entropy, phase rule; Reversible electric cells; Gaseous reactions: Van't Hoff reaction box, principle of LeChatelier; Thermodynamics of dilute solutions: osmotic, vapor pressures; boiling, freezing point; Entropy constant. 25 problems. 24 illustrations. x + 160pp. 5⅜ x 8. S361 Paperbound $1.75

FOUNDATIONS OF POTENTIAL THEORY, O. D. Kellogg. Based on courses given at Harvard, suitable for both advanced and beginning mathematicians, Proofs rigorous, much material here not generally available elsewhere. Partial contents: gravity, fields of force, divergence theorem, properties of Newtonian potentials at points of free space, potentials as solutions of LaPlace's equation, harmonic functions, electrostatics, electric images, logarithmic potential, etc. ix + 384pp. 5⅜ x 8. S144 Paperbound $1.98

DIALOGUES CONCERNING TWO NEW SCIENCES, Galileo Galilei. Classic of experimental science, mechanics, engineering, as enjoyable as it is important. Characterized by author as "superior to everything else of mine." Offers a lively exposition of dynamics, elasticity, sound, ballistics, strength of materials, scientific method. Translated by H. Grew, A. de Salvio. 126 diagrams. xxi + 288pp. 5⅜ x 8. S99 Paperbound $1.65

THEORETICAL MECHANICS; AN INTRODUCTION TO MATHEMATICAL PHYSICS, J. S. Ames, F. D. Murnaghan. A mathematically rigorous development for advanced students, with constant practical applications. Used in hundreds of advanced courses. Unusually thorough coverage of gyroscopic baryscopic material, detailed analyses of Corilis acceleration, applications of Lagrange's equations, motion of double pendulum, Hamilton-Jacobi partial differential equations, group velocity, dispersion, etc. Special relativity included. 159 problems. 44 figures. ix + 462pp. 5⅜ x 8. S461 Paperbound $2.00

STATICS AND THE DYNAMICS OF A PARTICLE, W. D. MacMillan. This is Part One of "Theoretical Mechanics." For over 3 decades a self-contained, extremely comprehensive advanced undergraduate text in mathematical physics, physics, astronomy, deeper foundations of engineering. Early sections require only a knowledge of geometry; later, a working knowledge of calculus. Hundreds of basic problems including projectiles to moon, harmonic motion, ballistics, transmission of power, stress and strain, elasticity, astronomical problems. 340 practice problems, many fully worked out examples. 200 figures. xvii + 430pp. 5⅜ x 8. S467 Paperbound $2.00

THE THEORY OF THE POTENTIAL, W. D. MacMillan. This is Part Two of "Theoretical Mechanics." Comprehensive, well-balanced presentation, serving both as introduction and reference with regard to specific problems, for physicists and mathematicians. Assumes no prior knowledge of integral relations, all math is developed as needed. Includes: Attraction of Finite Bodies; Newtonian Potential Function; Vector Fields, Green and Gauss Theorems; Two-layer Surfaces; Spherical Harmonics; etc. "The great number of particular cases . . . should make the book valuable to geo-physicists and others actively engaged in practical applications of the potential theory," Review of Scientific Instruments. xii + 469pp. 5⅜ x 8. S486 Paperbound $2.25

DYNAMICS OF A SYSTEM OF RIGID BODIES (Advanced Section), E. J. Routh. Revised 6th edition of a classic reference aid. Partial contents: moving axes, relative motion, oscillations about equilibrium, motion. Motion of a body under no forces, any forces. Nature of motion given by linear equations and conditions of stability. Free, forced vibrations, constants of integration, calculus of finite differences, variations, procession and mutation, motion of the moon, motion of string, chain, membranes. 64 figures. 498pp. 5⅜ x 8. S229 Paperbound $2.35

THE DYNAMICS OF PARTICLES AND OF RIGID, ELASTIC, AND FLUID BODIES: BEING LECTURES ON MATHEMATICAL PHYSICS, A. G. Webster. Reissuing of classic fills need for comprehensive work on dynamics. Covers wide range in unusually great depth, applying ordinary, partial differential equations. Partial contents: laws of motion, methods applicable to systems of all sorts; oscillation, resonance, cyclic systems; dynamics of rigid bodies; potential theory; stress and strain; gyrostatics; wave, vortex motion; kinematics of a point; Lagrange's equations; Hamilton's principle; vectors; deformable bodies; much more not easily found together in one volume. Unabridged reprinting of 2nd edition. 20 pages on differential equations, higher analysis. 203 illustrations. xi + 588pp. 5⅜ x 8. S522 Paperbound $2.35

PRINCIPLES OF MECHANICS, Heinrich Hertz. A classic of great interest in logic of science. Last work by great 19th century physicist, created new system of mechanics based upon space, time, mass; returns to axiomatic analysis, understanding of formal, structural aspects of science, taking into account logic, observation, a priori elements. Of great historical importance to Poincaré, Carnap, Einstein, Milne. 20 page introduction by R. S. Cohen, Wesleyan U., analyzes implications of Hertz's thought and logic of science. 13 page introduction by Helmholtz. xlii + 274pp. 5⅜ x 8. S316 Clothbound **$3.50**
S317 Paperbound **$1.75**

MATHEMATICAL FOUNDATIONS OF STATISTICAL MECHANICS, A. I. Khinchin. A thoroughly up-to-date introduction, offering a precise and mathematically rigorous formulation of the problems of statistical mechanics. Provides analytical tools to replace many commonly used cumbersome concepts and devices. Partial contents: Geometry, kinematics of phase space; ergodic problem; theory of probability; central limit theorem; ideal monatomic gas; foundation of thermodynamics; dispersion, distribution of sum functions; etc. "Excellent introduction . . . clear, concise, rigorous," Quarterly of Applied Mathematics. viii + 179pp. 5⅜ x 8. S146 Clothbound **$2.95**
S147 Paperbound **$1.35**

MECHANICS OF THE GYROSCOPE, THE DYNAMICS OF ROTATION, R. F. Deimel, Prof. of Mechanical Engineering, Stevens Inst. of Tech. Elementary, general treatment of dynamics of rotation, with special application of gyroscopic phenomena. No knowledge of vectors needed. Velocity of a moving curve, acceleration to a point, general equations of motion, gyroscopic horizon, free gyro, motion of discs, the damped gyro, 103 similar topics. Exercises. 75 figures. 208pp. 5⅜ x 8. S66 Paperbound **$1.65**

MECHANICS VIA THE CALCULUS, P. W. Norris, W. S. Legge. Wide coverage, from linear motion to vector analysis; equations determining motion, linear methods, compounding of simple harmonic motions, Newton's laws of motion, Hooke's law, the simple pendulum, motion of a particle in 1 plane, centers of gravity, virtual work, friction, kinetic energy of rotating bodies, equilibrium of strings, hydrostatics, sheering stresses, elasticity, etc. Many worked-out examples. 550 problems. 3rd revised edition. xii + 367pp. S207 Clothbound **$3.95**

A TREATISE ON THE MATHEMATICAL THEORY OF ELASTICITY, A. E. H. Love. An indispensable reference work for engineers, mathematicians, physicists, the most complete, authoritative treatment of classical elasticity in one volume. Proceeds from elementary notions of extension to types of strain, cubical dilatation, general theory of strains. Covers relation between mathematical theory of elasticity and technical mechanics; equilibrium of isotropic elastic solids and aelotropic solid bodies; nature of force transmission, Volterra's theory of dislocations; theory of elastic spheres in relation to tidal, rotational, gravitational effects on earth; general theory of bending; deformation of curved plates; buckling effects; much more. "The standard treatise on elasticity," American Math. Monthly. 4th revised edition. 76 figures. xviii + 643pp. 6⅛ x 9¼. S174 Paperbound **$2.95**

NUCLEAR PHYSICS, QUANTUM THEORY, RELATIVITY

MESON PHYSICS, R. E. Marshak. Presents basic theory, and results of experiments with emphasis on theoretical significance. Phenomena involving mesons as virtual transitions avoided, eliminating some of least satisfactory predictions of meson theory. Includes production study of π mesons at nonrelativistic nucleon energies contracts between π and μ mesons, phenomena associated with nuclear interaction of π mesons, etc. Presents early evidence for new classes of particles, indicates theoretical difficulties created by discovery of heavy mesons and hyperons. viii + 378pp. 5⅜ x 8. S500 Paperbound **$1.95**

THE FUNDAMENTAL PRINCIPLES OF QUANTUM MECHANICS, WITH ELEMENTARY APPLICATIONS, E. C. Kemble. Inductive presentation, for graduate student, specialists in other branches of physics. Apparatus necessary beyond differential equations and advanced calculus developed as needed. Though general exposition of principles, hundreds of individual problems fully treated. "Excellent book . . . of great value to every student . . . rigorous and detailed mathematical discussion . . .. has succeeded in keeping his presentation clear and understandable," Dr. Linus Pauling, J. of American Chemical Society. Appendices: calculus of variations, math. notes, etc. 611pp. 5⅝ x 8⅜. T472 Paperbound **$2.95**

WAVE PROPAGATION IN PERIODIC STRUCTURES, L. Brillouin. General method, application to different problems: pure physics—scattering of X-rays in crystals, thermal vibration in crystal lattices, electronic motion in metals; problems in electrical engineering. Partial contents: elastic waves along 1-dimensional lattices of point masses. Propagation of waves along 1-dimensional lattices. Energy flow. 2, 3 dimensional lattices. Mathieu's equation. Matrices and propagation of waves along an electric line. Continuous electric lines. 131 illustrations. xii + 253pp. 5⅜ x 8. S34 Paperbound **$1.85**

THEORY OF ELECTRONS AND ITS APPLICATION TO THE PHENOMENA OF LIGHT AND RADIANT HEAT, H. Lorentz. Lectures delivered at Columbia Univ., by Nobel laureate. Unabridged, form historical coverage of theory of free electrons, motion, absorption of heat, Zeeman effect, optical phenomena in moving bodies, etc. 109 pages notes explain more advanced sections. 9 figures. 352pp. 5⅜ x 8. S173 Paperbound $1.85

SELECTED PAPERS ON QUANTUM ELECTRODYNAMICS, edited by J. Schwinger. Facsimiles of papers which established quantum electrodynamics; beginning to present position as part of larger theory. First book publication in any language of collected papers of Bethe, Bloch, Dirac, Dyson, Fermi, Feynman, Heisenberg, Kusch, Lamb, Oppenheimer, Pauli, Schwinger, Tomonoga, Weisskopf, Wigner, etc. 34 papers: 29 in English, 1 in French, 3 in German, 1 in Italian. Historical commentary by editor. xvii + 423pp. 6⅛ x 9¼. S444 Paperbound $2.45

FOUNDATIONS OF NUCLEAR PHYSICS, edited by R. T. Beyer. 13 of the most important papers on nuclear physics reproduced in facsimile in the original languages; the papers most often cited in footnotes, bibliographies. Anderson, Curie, Joliot, Chadwick, Fermi, Lawrence, Cockroft, Hahn, Yukawa. Unparalleled bibliography: 122 double columned pages, over 4,000 articles, books, classified. 57 figures. 288pp. 6⅛ x 9¼. S19 Paperbound $1.75

THE THEORY OF GROUPS AND QUANTUM MECHANICS, H. Weyl. Schroedinger's wave equation, de Broglie's waves of a particle, Jordon-Hoelder theorem, Lie's continuous groups of transformations, Pauli exclusion principle, quantization of Mawell-Dirac field equations, etc. Unitary geometry, quantum theory, groups, application of groups to quantum mechanics, symmetry permutation group, algebra of symmetric transformations, etc. 2nd revised edition. xxii + 422pp. 5⅜ x 8. S268 Clothbound $4.50
S269 Paperbound $1.95

PHYSICAL PRINCIPLES OF THE QUANTUM THEORY, Wernor Heisenberg. Nobel laureate discusses quantum theory; his own work, Compton, Schroedinger, Wilson, Einstein, many others. For physicists, chemists, not specialists in quantum theory. Only elementary formulae considered in text; mathematical appendix for specialists. Profound without sacrificing clarity. Translated by C. Eckart, F. Hoyt. 18 figures. 192pp. 5⅜ x 8. S113 Paperbound $1.25

INVESTIGATIONS ON THE THEORY OF THE BROWNIAN MOVEMENT, Albert Einstein. Reprints from rare European journals, translated into English. 5 basic papers, including Elementary Theory of the Brownian Movement, written at request of Lorentz to provide a simple explanation. Translated by A. D. Cowper. Annotated, edited by R. Fürth. 33pp. of notes elucidate, give history of previous investigations. 62 footnotes. 124pp. 5⅜ x 8. S304 Paperbound $1.25

THE PRINCIPLE OF RELATIVITY, E. Einstein, H. Lorentz, M. Minkowski, H. Weyl. The 11 basic papers that founded the general and special theories of relativity, translated into English. 2 papers by Lorentz on the Michelson experiment, electromagnetic phenomena. Minkowski's "Space and Time," and Weyl's "Gravitation and Electricity." 7 epoch-making papers by Einstein: "Electromagnetics of Moving Bodies," "Influence of Gravitation in Propagation of Light," "Cosmological Considerations," "General Theory," 3 others. 7 diagrams. Special notes by A. Sommerfeld. 224pp. 5⅜ x 8. S93 Paperbound $1.75

STATISTICS

ELEMENTARY STATISTICS, WITH APPLICATIONS IN MEDICINE AND THE BIOLOGICAL SCIENCES, F. E. Croxton. Based primarily on biological sciences, but can be used by anyone desiring introduction to statistics. Assumes no prior acquaintance, requires only modest knowledge of math. All basic formulas carefully explained, illustrated; all necessary reference tables included. From basic terms and concepts, proceeds to frequency distribution, linear, nonlinear, multiple correlation, etc. Contains concrete examples from medicine, biology. 101 charts. 57 tables. 14 appendices. iv + 376pp. 5⅜ x 8. S506 Paperbound $1.95

ANALYSIS AND DESIGN OF EXPERIMENTS, H. B. Mann. Offers method for grasping analysis ot variance, variance design quickly. Partial contents: Chi-square distribution, analysis of variance distribution, matrices, quadratic forms, likelihood ration tests, test of linear hypotheses, power of analysis, Galois fields, non-orthogonal data, interblock estimates, etc. 15pp. of useful tables. x + 195pp. 5 x 7⅜. S180 Paperbound $1.45

FREQUENCY CURVES AND CORRELATION, W. P. Elderton. 4th revised edition of standard work on classical statistics. Practical, one of few books constantly referred to for clear presentation of basic material. Partial contents: Frequency Distributions; Pearsons Frequency Curves; Theoretical Distributions; Standard Errors; Correlation Ratio—Contingency; Corrections for Moments, Beta, Gamma Functions; etc. Key to terms, symbols. 25 examples. 40 tables. 16 figures. xi + 272pp. 5½ x 8½. Clothbound $1.49

HYDRODYNAMICS, ETC.

HYDRODYNAMICS, Horace Lamb. Standard reference work on dynamics of liquids and gases. Fundamental theorems, equations, methods, solutions, background for classical hydrodynamics. Chapters: Equations of Motion, Integration of Equations in Special Gases, Vortex Motion, Tidal Waves, Rotating Masses of Liquids, etc. Excellently planned, arranged, Clear, lucid presentation. 6th enlarged, revised edition. Over 900 footnotes, mostly bibliographical. 119 figures. xv + 738pp. 6⅛ x 9¼. S256 Paperbound $2.95

HYDRODYNAMICS, A STUDY OF LOGIC, FACT, AND SIMILITUDE, Garrett Birkhoff. A stimulating application of pure mathematics to an applied problem. Emphasis is on correlation of theory and deduction with experiment. Examines recently discovered paradoxes, theory of modelling and dimensional analysis, paradox and error in flows and free boundary theory. Classical theory of virtual mass derived from homogenous spaces; group theory applied to fluid mechanics. 20 figures, 3 plates. xiii + 186pp. 5⅜ x 8. S22 Paperbound $1.85

HYDRODYNAMICS, H. Dryden, F. Murhaghan, H. Bateman. Published by National Research Council, 1932. Complete coverage of classical hydrodynamics, encyclopedic in quality. Partial contents: physics of fluids, motion, turbulent flow, compressible fluids, motion in 1, 2, 3 dimensions; laminar motion, resistance of motion through viscous fluid, eddy viscosity, discharge of gases, flow past obstacles, etc. Over 2900-item bibliography. 23 figures. 634pp. 5⅜ x 8. S303 Paperbound $2.75

ACOUSTICS AND OPTICS

PRINCIPLES OF PHYSICAL OPTICS, Ernst Mach. Classical examination of propagation of light, color, polarization, etc. Historical, philosophical treatment unequalled for breadth and readability. Contents: Rectilinear propagation, reflection, refraction, dioptrics, composition of light, periodicity, theory of interference, polarization, mathematical representation of properties, etc. 279 illustrations. 10 portraits. 324pp. 5⅜ x 8. S170 Paperbound $1.75

THE THEORY OF SOUND, Lord Rayleigh. Written by Nobel laureate, classical methods here will cover most vibrating systems likely to be encountered in practice. Complete coverage of experimental, mathematical aspects. Partial contents: Harmonic motions, lateral vibrations of bars, curved plates or shells, applications of Laplace's functions to acoustical problems, fluid friction, etc. First low-priced edition of this great reference-study work. Historical introduction by R. B. Lindsay. 1040pp. 97 figures. 5⅜ x 8.
S292, S293, Two volume set, paperbound $4.00

THEORY OF VIBRATIONS, N. W. McLachlan. Based on exceptionally successful graduate course, Brown University. Discusses linear systems having 1 degree of freedom, forced vibrations of simple linear systems, vibration of flexible strings, transverse vibrations of bars and tubes, of circular plate, sound waves of finite amplitude, etc. 99 diagrams. 160pp. 5⅜ x 8. S190 Paperbound $1.35

APPLIED OPTICS AND OPTICAL DESIGN, A. E. Conrady. Thorough systematic presentation of physical and mathematical aspects, limited mostly to "real optics." Stresses practical problem of maximum aberration permissible without affecting performance. Ordinary ray tracing methods; complete theory ray tracing methods, primary aberrations; enough higher aberration to design telescopes, low powered microscopes, photographic equipment. Covers fundamental equations, extra-axial image points, transverse chromatic aberration, angular magnification, similar topics. Tables of functions of N. Over 150 diagrams. x + 518pp. 5⅜ x 8⅝. S366 Paperbound $2.98

RAYLEIGH'S PRINCIPLE AND ITS APPLICATIONS TO ENGINEERING, G. Temple, W. Bickley. Rayleigh's principle developed to provide upper, lower estimates of true value of fundamental period of vibrating system, or condition of stability of elastic system. Examples, rigorous proofs. Partial contents: Energy method of discussing vibrations, stability. Perturbation theory, whirling of uniform shafts. Proof, accuracy, successive approximations, applications of Rayleigh's theory. Numerical, graphical methods. Ritz's method. 22 figures. ix + 156pp. 5⅜ x 8. S307 Paperbound $1.50

OPTICKS, Sir Isaac Newton. In its discussion of light, reflection, color, refraction, theories of wave and corpuscular theories of light, this work is packed with scores of insights and discoveries. In its precise and practical discussions of construction of optical apparatus, contemporary understanding of phenomena, it is truly fascinating to modern scientists. Foreword by Albert Einstein. Preface by I. B. Cohen, Harvard. 7 pages of portraits, facsimile pages, letters, etc. cxvi + 414pp. 5⅜ x 8. S205 Paperbound $2.00

ON THE SENSATIONS OF TONE, Hermann Helmholtz. Using acoustical physics, physiology, experiment, history of music, covers entire gamut of musical tone: relation of music science to acoustics, physical vs. physiological acoustics, vibration, resonance, tonality, progression of parts, etc. 33 appendixes on various aspects of sound, physics, acoustics, music, etc. Translated by A. J. Ellis. New introduction by H. Margenau, Yale. 68 figures. 43 musical passages analyzed. Over 100 tables. xix + 576pp. 6⅛ x 9¼.
S114 Clothbound **$4.95**

ELECTROMAGNETICS, ENGINEERING, TECHNOLOGY

INTRODUCTION TO RELAXATION METHODS, F. S. Shaw. Describes almost all manipulative resources of value in solution of differential equations. Treatment is mathematical rather than physical. Extends general computational process to include almost all branches of applied math and physics. Approximate numerical methods are demonstrated, although high accuracy is obtainable without undue expenditure of time. 48pp. of tables for computing irregular star first and second derivatives, irregular star coefficients for second order equations, for fourth order equations. "Useful. . . . exposition is clear, simple . . . no previous acquaintance with numerical methods is assumed," Science Progress. 253 diagrams. 72 tables. 400pp. 5⅜ x 8. S244 Paperbound **$2.45**

THE ELECTROMAGNETIC FIELD, M. Mason, W. Weaver. Used constantly by graduate engineers. Vector methods exclusively; detailed treatment of electrostatics, expansion methods, with tables converting any quantity into absolute electromagnetic, absolute electrostatic, practical units. Discrete charges, ponderable bodies. Maxwell field equations, etc. 416pp. 5⅜ x 8. S185 Paperbound **$2.00**

ELASTICITY, PLASTICITY AND STRUCTURE OF MATTER, R. Houwink. Standard treatise on rheological aspects of different technically important solids: crystals, resins, textiles, rubber, clay, etc. Investigates general laws for deformations; determines divergences. Covers general physical and mathematical aspects of plasticity, elasticity, viscosity. Detailed examination of deformations, internal structure of matter in relation to elastic, plastic behaviour, formation of solid matter from a fluid, etc. Treats glass, asphalt, balata, proteins, baker's dough, others. 2nd revised, enlarged edition. Extensive revised bibliography in over 500 footnotes. 214 figures. xvii + 368pp. 6 x 9¼. S385 Paperbound **$2.45**

DESIGN AND USE OF INSTRUMENTS AND ACCURATE MECHANISM, T. N. Whitehead. For the instrument designer, engineer; how to combine necessary mathematical abstractions with independent observations of actual facts. Partial contents: instruments and their parts, theory of errors, systematic errors, probability, short period errors, erratic errors, design precision, kinematic, semikinematic design, stiffness, planning of an instrument, human factor, etc. 85 photos, diagrams. xii + 288pp. 5⅜ x 8. S270 Paperbound **$1.95**

APPLIED HYDRO- AND AEROMECHANICS, L. Prandtl, O. G. Tietjens. Presents, for most part, methods valuable to engineers. Flow in pipes, boundary layers, airfoil theory, entry conditions, turbulent flow, boundary layer, determining drag from pressure and velocity, etc. "Will be welcomed by all students of aerodynamics," Nature. Unabridged, unaltered. An Engineering Society Monograph, 1934. Index. 226 figures. 28 photographic plates illustrating flow patterns. xvi + 311pp. 5⅜ x 8. S375 Paperbound **$1.85**

FUNDAMENTALS OF HYDRO- AND AEROMECHANICS, L. Prandtl, O. G. Tietjens. Standard work, based on Prandtl's lectures at Goettingen. Wherever possible hydrodynamics theory is referred to practical considerations in hydraulics, unifying theory and experience. Presentation extremely clear. Though primarily physical, proofs are rigorous and use vector analysis to a great extent. An Engineering Society Monograph, 1934. "Still recommended as an excellent introduction to this area," Physikalische Blätter. 186 figures. xvi + 270pp. 5⅜ x 8. S374 Paperbound **$1.85**

GASEOUS CONDUCTORS: THEORY AND ENGINEERING APPLICATIONS, J. D. Cobine. Indispensable text, reference, to gaseous conduction phenomena, with engineering viewpoint prevailing throughout. Studies kinetic theory of gases, ionization, emission phenomena; gas breakdown, spark characteristics, glow, discharges; engineering applications in circuit interrupters, rectifiers, etc. Detailed treatment of high pressure arcs (Suits); low pressure arcs (Langmuir, Tonks). Much more. "Well organized, clear, straightforward," Tonks, Review of Scientific Instruments. 83 practice problems. Over 600 figures. 58 tables. xx + 606pp. 5⅜ x 8. S442 Paperbound **$2.75**

PHOTOELASTICITY: PRINCIPLES AND METHODS, H. T. Jessop, F. C. Harris. For engineer, specific problems of stress analysis. Latest time-saving methods of checking calculations in 2-dimensional design problems, new techniques for stresses in 3 dimensions, lucid description of optical systems used in practical photoelectricity. Useful suggestions, hints based on on-the-job experience included. Partial contents: strain, stress-strain relations, circular disc under thrust along diameter, rectangular block with square hold under vertical thrust, simply supported rectangular beam under central concentrated load, etc. Theory held to minimum, no advanced mathematical training needed. 164 illustrations. viii + 184pp. 6⅛ x 9¼. S137 Clothbound **$3.75**

7 Pure Mathematical Physics

MICROWAVE TRANSMISSION DESIGN DATA, T. Moreno. Originally classified, now rewritten, enlarged (14 new chapters) under auspices of Sperry Corp. Of immediate value or reference use to radio engineers, systems designers, applied physicists, etc. Ordinary transmission line theory; attenuation; parameters of coaxial lines; flexible cables; tuneable wave guide impedance transformers; effects of temperature, humidity; much more. "Packed with information . . . theoretical discussions are directly related to practical questions," U. of Royal Naval Scientific Service. Tables of dielectrics, flexible cable, etc. ix + 248pp. 5⅜ x 8.
S549 Paperbound $1.50

THE THEORY OF THE PROPERTIES OF METALS AND ALLOYS, H. F. Mott, H. Jones. Quantum methods develop mathematical models showing interrelationship of fundamental chemical phenomena wtih crystal structure, electrical, optical properties, etc. Examines electron motion in applied field, cohesion, heat capacity, refraction, noble metals, transition and di-valent metals, etc. "Exposition is as clear . . . mathematical treatment as simple and reliable as we have become used to expect of . . . Prof. Mott," Nature. 138 figures. xiii + 320pp. 5⅜ x 8. S456 Paperbound $1.85

THE MEASUREMENT OF POWER SPECTRA FROM THE POINT OF VIEW OF COMMUNICATIONS ENGINEERING, R. B. Blackman, J. W. Tukey. Pathfinding work reprinted from "Bell System Technical Journal." Various ways of getting practically useful answers in power spectra measurement, using results from both transmission and statistical estimation theory. Treats: Autocovariance, Functions and Power Spectra, Distortion, Heterodyne Filtering, Smoothing, Decimation Procedures, Transversal Filtering, much more. Appendix reviews fundamental Fourier techniques. Index of notation. Glossary of terms. 24 figures. 12 tables. 192pp. 5⅝ x 8⅝. S507 Paperbound $1.85

TREATISE ON ELECTRICITY AND MAGNETISM, James Clerk Maxwell. For more than 80 years a seemingly inexhaustible source of leads for physicists, mathematicians, engineers. Total of 1082pp. on such topics as Measurement of Quantities, Electrostatics, Elementary Mathematical Theory of Electricity, Electrical Work and Energy in a System of Conductors, General Theorems, Theory of Electrical Images, Electrolysis, Conduction, Polarization, Dielectrics, Resistance, much more. "The greatest mathematical physicist since Newton," Sir James Jeans. 3rd edition. 107 figures, 21 plates. 1082pp. 5⅜ x 8. S186 Clothbound $4.95

CHEMISTRY AND PHYSICAL CHEMISTRY

THE PHASE RULE AND ITS APPLICATIONS, Alexander Findlay. Covers chemical phenomena of 1 to 4 multiple component systems, the "standard work on the subject" (Nature). Completely revised, brought up to date by A. N. Campbell, N. O. Smith. New material on binary, tertiary liquid equilibria, solid solutions in ternary systems, quinary systems of salts, water, etc. Completely revised to triangular coordinates in ternary systems, clarified graphic representation, solid models, etc. 9th revised edition. 236 figures. 505 footnotes, mostly bibliographic. xii + 449pp. 5⅜ x 8. S92 Paperbound $2.45

DYNAMICAL THEORY OF GASES, James Jeans. Divided into mathematical, physical chapters for convenience of those not expert in mathematics. Discusses mathematical theory of gas in steady state, thermodynamics, Bolzmann, Maxwell, kinetic theory, quantum theory, exponentials, etc. "One of the classics of scientific writing . . . as lucid and comprehensive an exposition of the kinetic theory as has ever been written," J. of Institute of Engineers. 4th enlarged edition, with new material on quantum theory, quantum dynamics, etc. 28 figures. 444pp. 6⅛ x 9¼. S136 Paperbound $2.45

POLAR MOLECULES, Pieter Debye. Nobel laureate offers complete guide to fundamental electrostatic field relations, polarizability, molecular structure. Partial contents: electric intensity, displacement, force, polarization by orientation, molar polarization, molar refraction, halogen-hydrides, polar liquids, ionic saturation, dielectric constant, etc. Special chapter considers quantum theory. "Clear and concise . . . coordination of experimental results with theory will be readily appreciated," Electronics Industries. 172pp. 5⅜ x 8.
S63 Clothbound $3.50
S64 Paperbound $1.50

ATOMIC SPECTRA AND ATOMIC STRUCTURE, G. Herzberg. Excellent general survey for chemists, physicists specializing in other fields. Partial contents: simplest line spectra, elements of atomic theory; multiple structure of line spectra, electron spin; building-up principle, periodic system of elements; finer details of atomic spectra; hyperfine structure of spectral lines; some experimental results and applications. 80 figures. 20 tables. xiii + 257pp. 5⅜ x 8. S115 Paperbound $1.95

TREATISE ON THERMODYNAMICS, Max Planck. Classic based on his original papers. Brilliant concepts of Nobel laureate make no assumptions regarding nature of heat, rejects earlier approaches of Helmholtz, Maxwell, to offer uniform point of view for entire field. Seminal work by founder of quantum theory, deducing new physical, chemical laws. A standard text, an excellent introduction to field for students with knowledge of elementary chemistry, physics, calculus. 3rd English edition. xvi + 297pp. 5⅜ x 8. S219 Paperbound $1.75

KINETIC THEORY OF LIQUIDS, J. Frenkel. Regards kinetic theory of liquids as generalization, extension of theory of solid bodies, covers all types of arrangements of solids; thermal displacements of atoms; interstitial atoms, ions; orientational, rotational motion of molecules; transition between states of matter. Mathematical theory developed close to physical subject matter. "Discussed in a simple yet deeply penetrating fashion . . . will serve as seeds for a great many basic and applied developments in chemistry," J. of the Amer. Chemical Soc. 216 bibliographical footnotes. 55 figures. xi + 485pp. 5⅜ x 8.
S94 Clothbound **$3.95**
S95 Paperbound **$2.45**

ASTRONOMY

OUT OF THE SKY, H. H. Nininger. Non-technical, comprehensive introduction to "meteoritics" —science concerned with arrival of matter from outer space. By one of world's experts on meteorites, this book defines meteors and meteorites; studies fireball clusters and processions, meteorite composition, size, distribution, showers, explosions, origins, much more. viii + 336pp. 5⅜ x 8.
T519 Paperbound **$1.85**

AN INTRODUCTION TO THE STUDY OF STELLAR STRUCTURE, S. Chandrasekhar. Outstanding treatise on stellar dynamics by one of greatest astro-physicists. Examines relationship between loss of energy, mass, and radius of stars in steady state. Discusses thermodynamic laws from Caratheodory's axiomatic standpoint; adiabatic, polytropic laws; work of Ritter, Emden, Kelvin, etc.; Stroemgren envelopes as starter for theory of gaseous stars; Gibbs statistical mechanics (quantum); degenerate stellar configuration, theory of white dwarfs; etc. "Highest level of scientific merit," Bulletin. Amer. Math. Soc. 33 figures. 509pp. 5⅜ x 8.
S413 Paperbound **$2.75**

LES MÉTHODES NOVELLES DE LA MÉCANIQUE CÉLESTE, H. Poincaré. Complete French text of one of Poincaré's most important works. Revolutionized celestial mechanics: first use of integral invariants, first major application of linear differential equations, study of periodic orbits, lunar motion and Jupiter's satellites, three body problem, and many other important topics. "Started a new era . . . so extremely modern that even today few have mastered his weapons," E. T. Bell. 3 volumes. Total 1282pp. 6⅛ x 9¼.
Vol. 1 S401 Paperbound **$2.75**
Vol. 2 S402 Paperbound **$2.75**
Vol. 3 S403 Paperbound **$2.75**
The set **$7.50**

THE REALM OF THE NEBULAE, E. Hubble. One of the great astronomers of our time presents his concept of "island universes," and describes its effect on astronomy. Covers velocity-distance relation; classification, nature, distances, general field of nebulae; cosmological theories; nebulae in the neighborhood of the Milky way; etc. 39 photos, including velocity-distance relations shown by spectrum comparison. "One of the most progressive lines of astronomical research," The Times, London. New Introduction by A. Sandage. 55 illustrations. xxiv + 201pp. 5⅜ x 8.
S455 Paperbound **$1.50**

HOW TO MAKE A TELESCOPE, Jean Texereau. Design, build an f/6 or f/8 Newtonian type reflecting telescope, with altazimuth Couder mounting, suitable for planetary, lunar, and stellar observation. Covers every operation step-by-step, every piece of equipment. Discusses basic principles of geometric and physical optics (unnecessary to construction), comparative merits of reflectors, refractors. A thorough discussion of eyepieces, finders, grinding, installation, testing, etc. 241 figures, 38 photos, show almost every operation and tool. Potential errors are anticipated. Foreword by A. Couder. Sources of supply. xiii + 191pp. 6¼ x 10.
T464 Clothbound **$3.50**

BIOLOGICAL SCIENCES

THE BIOLOGY OF THE AMPHIBIA, G. K. Noble, Late Curator of Herpetology at Am. Mus. of Nat. Hist. Probably most used text on amphibia, most comprehensive, clear, detailed. 19 chapters, 85 page supplement: development; heredity; life history; speciation; adaptation; sex, integument, respiratory, circulatory, digestive, muscular, nervous systems; instinct, intelligence, habits, economic value classification, environment relationships, etc. "Nothing comparable to it," C. H. Pope, curator of Amphibia, Chicago Mus. of Nat. Hist. 1047 item bibliography. 174 illustrations. 600pp. 5⅜ x 8.
S206 Paperbound **$2.98**

THE ORIGIN OF LIFE, A. I. Oparin. A classic of biology. This is the first modern statement of theory of gradual evolution of life from nitrocarbon compounds. A brand-new evaluation of Oparin's theory in light of later research, by Dr. S. Margulis, University of Nebraska. xxv + 270pp. 5⅜ x 8.
S213 Paperbound **$1.75**

THE BIOLOGY OF THE LABORATORY MOUSE, edited by G. D. Snell. Prepared in 1941 by staff of Roscoe B. Jackson Memorial Laboratory, still the standard treatise on the mouse, assembling enormous amount of material for which otherwise you spend hours of research. Embryology, reproduction, histology, spontaneous neoplasms, gene and chromosomes mutations, genetics of spontaneous tumor formations, of tumor transplantation, endocrine secretion and tumor formation, milk influence and tumor formation, inbred, hybrid animals, parasites, infectious diseases, care and recording. "A wealth of information of vital concern. . . . recommended to all who could use a book on such a subject," Nature. Classified bibliography of 1122 items. 172 figures, including 128 photos. ix + 497pp. 6⅛ x 9¼.
S248 Clothbound **$6.00**

THE TRAVELS OF WILLIAM BARTRAM, edited by Mark Van Doran. Famous source-book of American anthropology, natural history, geography, is record kept by Bartram in 1770's on travels through wilderness of Florida, Georgia, Carolinas. Containing accurate, beautiful descriptions of Indians, settlers, fauna, flora, it is one of finest pieces of Americana ever written. 13 original illustrations. 448pp. 5⅜ x 8. T13 Paperbound **$2.00**

BEHAVIOUR AND SOCIAL LIFE OF THE HONEYBEE, Ronald Ribbands. Outstanding scientific study; a compendium of practically everything known of social life of honeybee. Stresses behaviour of individual bees in field, hive. Extends von Frisch's experiments on communication among bees. Covers perception of temperature, gravity, distance, vibration; sound production; glands; structural differences; wax production; temperature regulation; recognition, communication; drifting, mating behaviour, other highly interesting topics. "This valuable work is sure of a cordial reception by laymen, beekeepers and scientists," Prof. Karl von Frisch, Brit. J. of Animal Behaviour. Bibliography of 690 references. 127 diagrams, graphs, sections of bee anatomy, fine photographs. 352pp. S410 Clothbound **$4.50**

ELEMENTS OF MATHEMATICAL BIOLOGY, A. J. Lotka. Pioneer classic, 1st major attempt to apply modern mathematical techniques on large scale to phenomena of biology, biochemistry, psychology, ecology, similar life sciences. Partial contents: Statistical meaning of irreversibility; Evolution as redistribution; Equations of kinetics of evolving systems; Chemical, inter-species equilibrium; parameters of state; Energy transformers of nature, etc. Can be read with profit by even those having no advanced math; unsurpassed as study-reference. Formerly titled "Elements of Physical Biology." 72 figures. xxx + 460pp. 5⅜ x 8.
S346 Paperbound **$2.45**

TREES OF THE EASTERN AND CENTRAL UNITED STATES AND CANADA, W. M. Harlow. Serious middle-level text covering more than 140 native trees, important escapes, with information on general appearance, growth habit, leaf forms, flowers, fruit, bark, commercial use, distribution, habitat, woodlore, etc. Keys within text enable you to locate various species easily, to know which have edible fruit, much more useful, interesting information. "Well illustrated to make identification very easy," Standard Cat. for Public Libraries. Over 600 photographs, figures. xiii + 288pp. 5⅝ x 6½. T395 Paperbound **$1.35**

FRUIT KEY AND TWIG KEY TO TREES AND SHRUBS (Fruit key to Northeastern Trees, Twig key to Deciduous Woody Plants of Eastern North America), W. M. Harlow. Only guides with photographs of every twig, fruit described. Especially valuable to novice. Fruit key (both deciduous trees, evergreens) has introduction on seeding, organs involved, types, habits. Twig key introduction treats growth, morphology. In keys proper, identification is almost automatic. Exceptional work, widely used in university courses, especially useful for identification in winter, or from fruit or seed only. Over 350 photos, up to 3 times natural size. Index of common, scientific names, in each key. xvii + 125pp. 5⅝ x 8⅜. T511 Paperbound **$1.25**

INSECT LIFE AND INSECT NATURAL HISTORY, S. W. Frost. Unusual for emphasizing habits, social life, ecological relations of insects rather than more academic aspects of classification, morphology. Prof. Frost's enthusiasm and knowledge are everywhere evident as he discusses insect associations, specialized habits like leaf-rolling, leaf mining, case-making, the gall insects, boring insects, etc. Examines matters not usually covered in general works: insects as human food; insect music, musicians; insect response to radio waves; use of insects in art, literature. "Distinctly different, possesses an individuality all its own," Journal of Forestry. Over 700 illustrations. Extensive bibliography. x + 524pp. 5⅜ x 8.
T519 Paperbound **$2.49**

A WAY OF LIFE, AND OTHER SELECTED WRITINGS, Sir William Osler. Physician, humanist, Osler discusses brilliantly Thomas Browne, Gui Patin, Robert Burton, Michael Servetus, William Beaumont, Laennec. Includes such favorite writing as title essay, "The Old Humanities and the New Science," "Books and Men," "The Student Life," 6 more of his best discussions of philosophy, literature, religion. "The sweep of his mind and interests embraced every phase of human activity," G. L. Keynes. 5 photographs. Introduction by G. L. Keynes, M.D., F.R.C.S. xx + 278pp. 5⅜ x 8. T488 Paperbound **$1.50**

THE GENETICAL THEORY OF NATURAL SELECTION, R. A. Fisher. 2nd revised edition of vital reviewing of Darwin's Selection Theory in terms of particulate inheritance, by one of greatest authorities on experimental, theoretical genetics. Theory stated in mathematical form. Special features of particulate inheritance are examined: evolution of dominance, maintenance of specific variability, mimicry, sexual selection, etc. 5 chapters on man's special circumstances as a social animal. 16 photographs. x + 310pp. 5⅜ x 8.
S466 Paperbound **$1.85**

THE AUTOBIOGRAPHY OF CHARLES DARWIN, AND SELECTED LETTERS, edited by Francis Darwin. Darwin's own record of early life; historic voyage aboard "Beagle;" furore surrounding evolution, his replies; reminiscences of his son. Letters to Henslow, Lyell, Hooker, Huxley, Wallace, Kingsley, etc., and thoughts on religion, vivisection. We see how he revolutionized geology with concepts of ocean subsidence; how his great books on variation of plants and animals, primitive man, expression of emotion among primates, plant fertilization, carnivorous plants, protective coloration, etc., came into being. 365pp. 5⅜ x 8.
T479 Paperbound **$1.65**

ANIMALS IN MOTION, Eadweard Muybridge. Largest, most comprehensive selection of Muybridge's famous action photos of animals, from his "Animal Locomotion." 3919 high-speed shots of 34 different animals, birds, in 123 types of action; horses, mules, oxen, pigs, goats, camels, elephants, dogs, cats guanacos, sloths, lions, tigers, jaguars, raccoons, baboons, deer, elk, gnus, kangaroos, many others, walking, running, flying, leaping. Horse alone in over 40 ways. Photos taken against ruled backgrounds; most actions taken from 3 angles at once: 90°, 60°, rear. Most plates original size. Of considerable interest to scientists as biology classic, records of actual facts of natural history, physiology. "Really marvelous series of plates," Nature. "Monumental work," Waldemar Kaempffert. Edited by L. S. Brown, 74 page introduction on mechanics of motion. 340pp. of plates. 3919 photographs. 416pp. Deluxe binding, paper. (Weight: 4½ lbs.) 7⅛ x 10⅝.
T203 Clothbound **$10.00**

THE HUMAN FIGURE IN MOTION, Eadweard Muybridge. New edition of great classic in history of science and photography, largest selection ever made from original Muybridge photos of human action: 4789 photographs, illustrating 163 types of motion: walking, running, lifting, etc. in time-exposure sequence photos at speeds up to 1/6000th of a second. Men, women, children, mostly undraped, showing bone, muscle positions against ruled backgrounds, mostly taken at 3 angles at once. Not only was this a great work of photography, acclaimed by contemporary critics as work of genius, but it was also a great 19th century landmark in biological research. Historical introduction by Prof. Robert Taft, U. of Kansas. Plates original size, full of detail. Over 500 action strips. 407pp. 7¾ x 10⅝. Deluxe edition.
7204 Clothbound **$10.00**

AN INTRODUCTION TO THE STUDY OF EXPERIMENTAL MEDICINE, Claude Bernard. 90-year old classic of medical science, only major work of Bernard available in English, records his efforts to transform physiology into exact science. Principles of scientific research illustrated by specified case histories from his work; roles of chance, error, preliminary false conclusion, in leading eventually to scientific truth; use of hypothesis. Much of modern application of mathematics to biology rests on foundation set down here. "The presentation is polished . . . reading is easy," Revue des questions scientifiques. New foreword by Prof. I. B. Cohen, Harvard U. xxv + 266pp. 5⅜ x 8. T400 Paperbound **$1.50**

STUDIES ON THE STRUCTURE AND DEVELOPMENT OF VERTEBRATES, E. S. Goodrich. Definitive study by greatest modern comparative anatomist. Exhaustive morphological, phylogenetic expositions of skeleton, fins, limbs, skeletal visceral arches, labial cartilages, visceral clefts, gills, vascular, respiratory, excretory, periphal nervous systems, etc., from fish to higher mammals. "For many a day this will certainly be the standard textbook on Vertebrate Morphology in the English language," Journal of Anatomy. 754 illustrations. 69 page biographical study by C. C. Hardy. Bibliography of 1186 references. Two volumes, total 906pp. 5⅜ x 8. Two vol. set S449, 450 Paperbound **$5.00**

EARTH SCIENCES

THE EVOLUTION OF IGNEOUS BOOKS, N. L. Bowen. Invaluable serious introduction applies techniques of physics, chemistry to explain igneous rock diversity in terms of chemical composition, fractional crystallization. Discusses liquid immiscibility in silicate magmas, crystal sorting, liquid lines of descent, fractional resorption of complex minerals, petrogen, etc. Of prime importance to geologists, mining engineers; physicists, chemists working with high temperature, pressures. "Most important," Times, London. 263 bibliographic notes. 82 figures. xviii + 334pp. 5⅜ x 8. S311 Paperbound **$1.85**

GEOGRAPHICAL ESSAYS, M. Davis. Modern geography, geomorphology rest on fundamental work of this scientist. 26 famous essays present most important theories, field researches. Partial contents: Geographical Cycle; Plains of Marine, Subaerial Denudation; The Peneplain; Rivers, Valleys of Pennsylvania; Outline of Cape Cod; Sculpture of Mountains by Glaciers; etc. "Long the leader and guide," Economic Geography. "Part of the very texture of geography . . . models of clear thought," Geographic Review. 130 figures. vi + 777pp. 5⅜ x 8.
S383 Paperbound **$2.95**

URANIUM PROSPECTING, H. L. Barnes. For immediate practical use, professional geologist considers uranium ores, geological occurrences, field conditions, all aspects of highly profitable occupation. "Helpful information . . . easy-to-use, easy-to-find style," Geotimes. x + 117pp. 5⅜ x 8. T309 Paperbound **$1.00**

DE RE METALLICA, Georgius Agricola. 400 year old classic translated, annotated by former President Herbert Hoover. 1st scientific study of mineralogy, mining, for over 200 years after its appearance in 1556 the standard treatise. 12 books, exhaustively annotated, discuss history of mining, selection of sites, types of deposits, making pits, shafts, ventilating, pumps, crushing machinery; assaying, smelting, refining metals; also salt alum, nitre, glass making. Definitive edition, with all 289 16th century woodcuts of original. Biographical, historical introductions. Bibliography, survey of ancient authors. Indexes. A fascinating book for anyone interested in art, history of science, geology, etc. Deluxe Edition. 289 illustrations. 672pp. 6¾ x 10. Library cloth. S6 Clothbound **$10.00**

INTERNAL CONSTITUTION OF THE EARTH, edited by Beno Gutenberg. Prepared for National Research Council, this is a complete, thorough coverage of earth origins, continent formation, nature and behaviour of earth's core, petrology of crust, cooling forces in core, seismic and earthquake material, gravity, elastic constants, strain characteristics, similar topics. "One is filled with admiration . . . a high standard . . . there is no reader who will not learn something from this book," London, Edinburgh, Dublin, Philosophic Magazine. Largest Bibliography in print: 1127 classified items. Table of constants. 43 diagrams. 439pp. 6⅛ x 9¼. S414 Paperbound **$2.45**

THE BIRTH AND DEVELOPMENT OF THE GEOLOGICAL SCIENCES, F. D. Adams. Most thorough history of earth sciences ever written. Geological thought from earliest times to end of 19th century, covering over 300 early thinkers and systems; fossils and their explanation, vulcanists vs. neptunists, figured stones and paleontology, generation of stones, dozens of similar topics. 91 illustrations, including Medieval, Renaissance woodcuts, etc. 632 footnotes, mostly bibliographical. 511pp. 5⅜ x 8. T5 Paperbound **$2.00**

HYDROLOGY, edited by O. E. Meinzer, prepared for the National Research Council. Detailed, complete reference library on precipitation, evaporation, snow, snow surveying, glaciers, lakes, infiltration, soil moisture, ground water, runoff, drought, physical changes produced by water hydrology of limestone terranes, etc. Practical in application, especially valuable for engineers. 24 experts have created "the most up-to-date, most complete treatment of the subject," Am. Assoc. of Petroleum Geologists. 165 illustrations. xi + 712pp. 6⅛ x 9¼. S191 Paperbound **$2.95**

LANGUAGE AND TRAVEL AIDS FOR SCIENTISTS

SAY IT language phrase books

"SAY IT" in the foreign language of your choice! We have sold over ½ million copies of these popular, useful language books. They will not make you an expert linguist overnight, but they do cover most practical matters of everyday life abroad.

Over 1000 useful phrases, expressions, additional variants, substitutions.

Modern! Useful! Hundreds of phrases not available in other texts: "Nylon," "air-conditioned," etc.

The ONLY inexpensive phrase book **completely indexed.** Everything is available at a flip of your finger, ready to use.

Prepared by native linguists, travel experts.

Based on years of travel experience abroad.

May be used by itself, or to supplement any other text or course. Provides a living element. Used by many colleges, institutions: Hunter College; Barnard College; Army Ordinance School, Aberdeen; etc.

Available, 1 book per language:

- **Danish** (T818) 75¢
- **Dutch** (T817) 75¢
- **English (for German-speaking people)** (T801) 60¢
- **English (for Italian-speaking people)** (T816) 60¢
- **English (for Spanish-speaking people)** (T802) 60¢
- **Esperanto** (T820) 75¢
- **French** (T803) 60¢
- **German** (T804) 60¢
- **Modern Greek** (T813) 75¢
- **Hebrew** (T805) 60¢
- **Italian** (T806) 60¢
- **Japanese** (T807) 75¢
- **Norwegian** (T814) 75¢
- **Russian** (T810) 75¢
- **Spanish** (T811) 60¢
- **Turkish** (T821) 75¢
- **Yiddish** (T815) 75¢
- **Swedish** (T812) 75¢
- **Polish** (T808) 75¢
- **Portuguese** (T809) 75¢

DOVER SCIENCE BOOKS

MONEY CONVERTER AND TIPPING GUIDE FOR EUROPEAN TRAVEL, C. Vomacka. Purse-size handbook crammed with information on currency regulations, tipping for every European country, including Israel, Turkey, Czechoslovakia, Rumania, Egypt, Russia, Poland. Telephone, postal rates; duty-free imports, passports, visas, health certificates; foreign clothing sizes; weather tables. What, when to tip. 5th year of publication. 128pp. 3½ x 5¼. T260 Paperbound 60¢

NEW RUSSIAN-ENGLISH AND ENGLISH-RUSSIAN DICTIONARY, M. A. O'Brien. Unusually comprehensive guide to reading, speaking, writing Russian, for both advanced, beginning students. Over 70,000 entries in new orthography, full information on accentuation, grammatical classifications. Shades of meaning, idiomatic uses, colloquialisms, tables of irregular verbs for both languages. Individual entries indicate stems, transitiveness, perfective, imperfective aspects, conjugation, sound changes, accent, etc. Includes pronunciation instruction. Used at Harvard, Yale, Cornell, etc. 738pp. 5⅜ x 8. T208 Paperbound $2.00

PHRASE AND SENTENCE DICTIONARY OF SPOKEN RUSSIAN, English-Russian, Russian-English. Based on phrases, complete sentences, not isolated words—recognized as one of best methods of learning idiomatic speech. Over 11,500 entries, indexed by single words, over 32,000 English, Russian sentences, phrases, in immediately useable form. Shows accent changes in conjugation, declension; irregular forms listed both alphabetically, under main form of word. 15,000 word introduction covers Russian sounds, writing, grammar, syntax. 15 page appendix of geographical names, money, important signs, given names, foods, special Soviet terms, etc. Originally published as U.S. Gov't Manual TM 30-944. iv + 573pp. 5⅜ x 8. T496 Paperbound $2.75

PHRASE AND SENTENCE DICTIONARY OF SPOKEN SPANISH, Spanish-English, English-Spanish. Compiled from spoken Spanish, based on phrases, complete sentences rather than isolated words—not an ordinary dictionary. Over 16,000 entries indexed under single words, both Castilian, Latin-American. Language in immediately useable form. 25 page introduction provides rapid survey of sounds, grammar, syntax, full consideration of irregular verbs. Especially apt in modern treatment of phrases, structure. 17 page glossary gives translations of geographical names, money values, numbers, national holidays, important street signs, useful expressions of high frequency, plus unique 7 page glossary of Spanish, Spanish-American foods. Originally published as U.S. Gov't Manual TM 30-900. iv + 513pp. 5⅝ x 8⅜. T495 Paperbound $1.75

SAY IT CORRECTLY language record sets

The best inexpensive pronunciation aids on the market. Spoken by native linguists associated with major American universities, each record contains:

14 minutes of speech—12 minutes of normal, relatively slow speech, 2 minutes of normal conversational speed.

120 basic phrases, sentences, covering nearly every aspect of everyday life, travel—introducing yourself, travel in autos, buses, taxis, etc., walking, sightseeing, hotels, restaurants, money, shopping, etc.

32 page booklet containing everything on record plus English translations easy-to-follow phonetic guide.

Clear, high-fidelity recordings.

Unique bracketing systems, selection of basic sentences enabling you to expand use of SAY IT CORRECTLY records with a dictionary, to fit thousands of additional situations.

Use this record to supplement any course or text. All sounds in each language illustrated perfectly—imitate speaker in pause which follows each foreign phrase in slow section, and be amazed at increased ease, accuracy of pronounciation. Available, one language per record for

French
Italian
Japanese
Polish
Spanish
Dutch
Russian
Swedish
German
Modern Greek
Portuguese
Hebrew
English (for German-speaking people)
English (for Spanish-speaking people)

7″ (33 1/3 rpm) record, album, booklet. $1.00 each.

SPEAK MY LANGUAGE: SPANISH FOR YOUNG BEGINNERS, M. Ahlman, Z. Gilbert. Records provide one of the best, most entertaining methods of introducing a foreign language to children. Within framework of train trip from Portugal to Spain, an English-speaking child is introduced to Spanish by native companion. (Adapted from successful radio program of N.Y. State Educational Department.) A dozen different categories of expressions,. including greeting, numbers, time, weather, food, clothes, family members, etc. Drill is combined with poetry and contextual use. Authentic background music. Accompanying book enables a reader to follow records, includes vocabulary of over 350 recorded expressions. Two 10″ 33 1/3 records, total of 40 minutes. Book. 40 illustrations. 69pp. 5¼ x 10½. T890 The set $4.95

LISTEN & LEARN language record sets

LISTEN & LEARN is the only extensive language record course designed especially to meet your travel and everyday needs. Separate sets for each language, each containing three 33 1/3 rpm long-playing records—1 1/2 hours of recorded speech by eminent native speakers who are professors at Columbia, New York U., Queens College.

Check the following features found only in LISTEN & LEARN:

Dual language recording. 812 selected phrases, sentences, over 3200 words, spoken first in English, then foreign equivalent. Pause after each foreign phrase allows time to repeat expression.

128-page manual (196 page for Russian)—everything on records, plus simple transcription. Indexed for convenience. Only set on the market completely indexed.

Practical. No time wasted on material you can find in any grammar. No dead words. Covers central core material with phrase approach. Ideal for person with limited time. Living, modern expressions, not found in other courses. Hygienic products, modern equipment, shopping, "air-conditioned," etc. Everything is immediately useable.

High-fidelity recording, equal in clarity to any costing up to $6 per record.

"Excellent . . . impress me as being among the very best on the market," Prof. Mario Pei, Dept. of Romance Languages, Columbia U. "Inexpensive and well done . . . . ideal present," Chicago Sunday Tribune. "More genuinely helpful than anything of its kind," Sidney Clark, well-known author of "All the Best" travel books.

UNCONDITIONAL GUARANTEE. Try LISTEN & LEARN, then return it within 10 days for full refund, if you are not satisfied. It is guaranteed after you actually use it.

6 modern languages—FRENCH, SPANISH, GERMAN, ITALIAN, RUSSIAN, or JAPANESE *—one language to each set of 3 records (33 1/3 rpm). 128 page manual. Album.

Spanish	the set $4.95	**German**	the set $4.95	**Japanese***	the set $5.95
French	the set $4.95	**Italian**	the set $4.95	**Russian**	the set $5.95

* Available Oct. 1959.

TRÜBNER COLLOQUIAL SERIES

These unusual books are members of the famous Trübner series of colloquial manuals. They have been written to provide adults with a sound colloquial knowledge of a foreign language, and are suited for either class use or self-study. Each book is a complete course in itself, with progressive, easy to follow lessons. Phonetics, grammar, and syntax are covered, while hundreds of phrases and idioms, reading texts, exercises, and vocabulary are included. These books are unusual in being neither skimpy nor overdetailed in grammatical matters, and in presenting up-to-date, colloquial, and practical phrase material. Bilingual presentation is stressed, to make thorough self-study easier for the reader.

COLLOQUIAL HINDUSTANI, A. H. Harley, formerly Nizam's Reader in Urdu, U. of London. 30 pages on phonetics and scripts (devanagari & Arabic-Persian) are followed by 29 lessons, including material on English and Arabic-Persian influences. Key to all exercises. Vocabulary. 5 x 7½. 147pp. Clothbound **$1.75**

COLLOQUIAL ARABIC, DeLacy O'Leary. Foremost Islamic scholar covers language of Egypt, Syria, Palestine, & Northern Arabia. Extremely clear coverage of complex Arabic verbs & noun plurals; also cultural aspects of language. Vocabulary. xviii + 192pp. 5 x 7½. Clothbound **$1.75**

COLLOQUIAL GERMAN, P. F. Doring. Intensive thorough coverage of grammar in easily-followed form. Excellent for brush-up, with hundreds of colloquial phrases. 34 pages of bilingual texts. 224pp. 5 x 7½. Clothbound **$1.75**

COLLOQUIAL SPANISH, W. R. Patterson. Castilian grammar and colloquial language, loaded with bilingual phrases and colloquialisms. Excellent for review or self-study. 164pp. 5 x 7½. Clothbound **$1.75**

COLLOQUIAL FRENCH, W. R. Patterson. 16th revised edition of this extremely popular manual. Grammar explained with model clarity, and hundreds of useful expressions and phrases; exercises, reading texts, etc. Appendixes of new and useful words and phrases. 223pp. 5 x 7½. Clothbound **$1.75**

COLLOQUIAL PERSIAN, L. P. Elwell-Sutton. Best introduction to modern Persian, with 90 page grammatical section followed by conversations, 35 page vocabulary. 139pp. Clothbound $1.75

COLLOQUIAL CZECH, J. Schwarz, former headmaster of Lingua Institute, Prague. Full easily followed coverage of grammar, hundreds of immediately useable phrases, texts. Perhaps the best Czech grammar in print. "An absolutely successful textbook," JOURNAL OF CZECHOSLOVAK FORCES IN GREAT BRITAIN. 252pp. 5 x 7½. Clothbound $2.50

COLLOQUIAL RUMANIAN, G. Nandris, Professor of University of London. Extremely thorough coverage of phonetics, grammar, syntax; also included 70 page reader, and 70 page vocabulary. Probably the best grammar for this increasingly important language. 340pp. 5 x 7½. Clothbound $2.50

COLLOQUIAL ITALIAN, A. L. Hayward. Excellent self-study course in grammar, vocabulary, idioms, and reading. Easy progressive lessons will give a good working knowledge of Italian in the shortest possible time. 5 x 7½. Clothbound $1.75

MISCELLANEOUS

TREASURY OF THE WORLD'S COINS, Fred Reinfeld. Finest general introduction to numismatics; non-technical, thorough, always fascinating. Coins of Greece, Rome, modern countries of every continent, primitive societies, such oddities as 200-lb stone money of Yap, nail coinage of New England; all mirror man's economy, customs, religion, politics, philosophy, art. Entertaining, absorbing study; novel view of history. Over 750 illustrations. Table of value of coins illustrated. List of U.S. coin clubs. 224pp. 6½ x 9¼. T433 Paperbound $1.75

ILLUSIONS AND DELUSIONS OF THE SUPERNATURAL AND THE OCCULT, D. H. Rawcliffe. Rationally examines hundreds of persistent delusions including witchcraft, trances, mental healing, peyotl, poltergeists, stigmata, lycanthropy, live burial, auras, Indian rope trick, spiritualism, dowsing, telepathy, ghosts, ESP, etc. Explains, exposes mental, physical deceptions involved, making this not only an exposé of supernatural phenomena, but a valuable exposition of characteristic types of abnormal psychology. Originally "The Psychology of the Occult." Introduction by Julian Huxley. 14 illustrations. 551pp. 5⅜ x 8. T503 Paperbound $2.00

HOAXES, C. D. MacDougall. Shows how art, science, history, journalism can be perverted for private purposes. Hours of delightful entertainment, a work of scholarly value, often shocking. Examines nonsense news, Cardiff giant, Shakespeare forgeries, Loch Ness monster, biblical frauds, political schemes, literary hoaxers like Chatterton, Ossian, disumbrationist school of painting, lady in black at Valentino's tomb, over 250 others. Will probably reveal truth about few things you've believed, will help you spot more easily the editorial "gander" or planted publicity release. "A stupendous collection . . . and shrewd analysis," New Yorker. New revised edition. 54 photographs. 320pp. 5⅜ x 8. T465 Paperbound $1.75

YOGA: A SCIENTIFIC EVALUATION, Kovoor T. Behanan. Book that for first time gave Western readers a sane, scientific explanation, analysis of yoga. Author draws on laboratory experiments, personal records of year as disciple of yoga, to investigate yoga psychology, physiology, "supernatural" phenomena, ability to plumb deepest human powers. In this study under auspices of Yale University Institute of Human Relations, strictest principles of physiological, psychological inquiry are followed. Foreword by W. A. Miles, Yale University. 17 photographs. xx + 270pp. 5⅜ x 8. T505 Paperbound $1.65

Write for free catalogs!

Indicate your field of interest. Dover publishes books on physics, earth sciences, mathematics, engineering, chemistry, astronomy, anthropology, biology, psychology, philosophy, religion, history, literature, mathematical recreations, languages, crafts, art, graphic arts, etc.

Write to Dept. catr
Dover Publications, Inc.
180 Varick St., N. Y. 14, N. Y.

Pure Mathematical Physics

MESON PHYSICS

ROBERT E. MARSHAK

This book is intended for research workers in meson physics, or as a primary or secondary text in a course on meson or high energy physics. It presupposes a course in quantum mechanics and some familiarity with the quantum theory of radiation and the quantum theory of fields. The basic theory of meson physics is traced in detail in Chapters 1 and 2, so that the reader becomes acquainted at the start with some of the characteristic methods and limitations of present-day meson field theory. The remainder of the book explicitly presents the results of meson experiments through 1952, including many of the indisputable facts concerning both π and μ mesons which were established since the discovery of the π meson in 1947. Throughout, particular emphasis has been laid on the theoretical significance of the new findings. However, by restricting itself to real meson processes and omitting nuclear phenomena which involve mesons only as virtual transitions, the book eliminates some of the most speculative and least satisfactory predictions of meson theory.

The first four chapters elucidate the behavior of charged and neutral π mesons at nonrelativistic nucleon energies, with special attention being given to the accelerator experiments which were increasingly more incisive in their determination of the properties of the π mesons. Chapters 5 and 6 focus on the striking contrasts between π and μ mesons. Chapter 7 delineates the characteristic problems associated with the nuclear interaction of π mesons. Chapter 8 discusses π meson production phenomena at relativistic nucleon energies. Chapter 9 presents the early evidence for new classes of particles and indicates the theoretical difficulties created by the discovery of heavy mesons and hyperons.

With the rapid development of meson physics during the past few years, and with the development of new meson-producing accelerators, this volume should become increasingly useful not only as an introduction to the field, but as a historical and research guide to one of the most exciting areas in modern physics.

Name index. Subject index. viii + 378pp. 5⅜ x 8.

Paperbound $1.95

THIS DOVER EDITION IS DESIGNED FOR YEARS OF USE

THE PAPER is chemically the same quality as you would find in books priced $5.00 or more. It does not discolor or become brittle with age. Not artificially bulked, either; this edition is an unabridged full-length book, but is still easy to handle.

THE BINDING: The pages in this book are SEWN in signatures, in the method traditionally used for the best books. These books open flat for easy reading and reference. Pages do not drop out, the binding does not crack and split (as in the case with many paperbooks held together with glue).

THE TYPE IS LEGIBLE: Margins are ample and allow for cloth rebinding.